ANALYTICA CHIMICA ACTA
Vol. 70 (1974)

ANALYTICA CHIMICA ACTA

International monthly devoted to all branches of analytical chemistry
Revue mensuelle internationale consacrée à tous les domaines de la chimie analytique
Internationale Monatsschrift für alle Gebiete der analytischen Chemie

ELSEVIER SCIENTIFIC PUBLISHING COMPANY
AMSTERDAM

Anal. Chim. Acta, Vol. 70 (1974)

PRINTED IN THE NETHERLANDS

Analytica Chimica Acta, 70 (1974) 1–15

DETERMINATION OF FOURTEEN ELEMENTS IN PURE IRON BY DESTRUCTIVE NEUTRON ACTIVATION ANALYSIS

C. DE WISPELAERE, J. P. OP DE BEECK and J. HOSTE

Institute for Nuclear Sciences, Rijksuniversiteit Gent, Proeftuinstraat, Ghent (Belgium)

(Received 13th October 1973)

Neutron activation analysis by means of NaI(Tl) γ-ray spectrometry has been widely used for the destructive and non-destructive determination of impurities in iron[1–9]. Recently, two papers have been published dealing with the instrumental determination of trace impurities in pure iron by Ge(Li) γ-spectrometry and computer techniques[10].

For the determination of some elements which show very low sensitivity or are present at very small concentrations, a destructive technique with chemical separations is necessary. After a reactor irradiation, the matrix activity consists mainly of the isotopes ^{59}Fe and ^{56}Mn, produced by the reactions ^{58}Fe(n, γ)^{59}Fe and ^{56}Fe(n, p)^{56}Mn. The most important step in a destructive technique therefore is the removal of the iron matrix. The isotope ^{56}Mn with its 2.582-h half life can be allowed to decay practically completely within a period of 1 to 2 days.

Danielsson and Ekström[11,12] have described a method, based on an ion exchange procedure in hydrofluoric acid medium, in order to separate large amounts of iron from a large number of elements. The distribution constant of iron in a 1 *M* hydrofluoric acid medium on anion- and cation-exchange resins is very low ($K_D < 1$), whereas this value for many of the elements is high for one or both types of resins As a result, a simple and fast separation of these elements from the iron matrix is possible.

Nuclear data and interferences

In Table I, the nuclear data[13–15] relevant to the iron matrix are summarized. The most important activities arising from nuclear reactions with the iron matrix, come from the isotopes ^{56}Mn, ^{59}Fe, ^{54}Mn and ^{51}Cr.

For the determination of manganese and chromium by means of the isotopes ^{56}Mn and ^{51}Cr, interferences from the reactions ^{56}Fe(n, p)^{56}Mn and ^{54}Fe(n, α)^{51}Cr must be considered. The apparent manganese and chromium concentrations can be determined experimentally by means of the double irradiation technique with and without a cadmium cover[16].

Alternatively, this apparent concentration can be calculated after a preliminary experimental determination of the thermal, epithermal and fast neutron flux during the irradiation[18].

TABLE I

NUCLEAR DATA FOR THE ISOTOPES PRODUCED IN THE IRON MATRIX

Isotope	% *Abundance*	*Reaction*	*Produced isotope*	*Cross-section (barn)*	*Half-life*	*Decay mode*
^{54}Fe	5.82	(n, γ)	^{55}Fe	2.3	2.7 y	e.c.
		(n, p)	^{54}Mn	$53 \cdot 10^{-3}$	313 d	e.c., γ
		(n, α)	^{51}Cr	$0.74 \cdot 10^{-3}$	27.8 d	e.c., γ
		(n, 2n)	^{53}Fe	$0.0032 \cdot 10^{-3}$	8.4 min	β^+, e.c., γ
^{56}Fe	91.66	(n, γ)	^{57}Fe	2.6	stable	
		(n, p)	^{56}Mn	$0.87 \cdot 10^{-3}$	2.582 h	β^-, γ
		(n, α)	^{53}Cr	$0.35 \cdot 10^{-3}$	stable	
		(n, 2n)	^{55}Fe	$0.07 \cdot 10^{-3}$	2.7 y	e.c.
^{57}Fe	2.19	(n, γ)	^{58}Fe	2.5	stable	
		(n, p)	^{57}Mn	$0.4 \cdot 10^{-3}$	1.7 min	β^-, γ
		(n, α)	^{54}Cr	$3.5 \cdot 10^{-3}$	stable	
		(n, 2n)	^{56}Fe	$3.0 \cdot 10^{-3}$	stable	
^{58}Fe	0.33	(n, γ)	^{59}Fe	1.2	45 d	β^-, γ
		(n, p)	^{58}Mn	$0.01 \cdot 10^{-3}$	1.1 min	β^-, γ
		(n, α)	^{55}Cr	$0.01 \cdot 10^{-3}$	3.53 min	β^-, γ
		(n, 2n)	^{57}Fe	$0.2 \cdot 10^{-3}$	stable	

EXPERIMENTAL

Sampling

The pure iron samples were obtained from an iron bar of 90 kg with a length of 6.8 m, which was part of a batch of 200 kg of pure iron prepared for the Verein Deutscher Eisenhüttenleute. Four discs of 43.5-mm diameter and 30-mm thickness, cut from the bar at different positions, were available. For the destructive analysis, samples of *ca.* 1.5 g were machined out of these discs. They were etched several times in a (1+1) mixture of 12 *M* hydrochloric acid and 50% hydrofluoric acid with dropwise addition of 30% hydrogen peroxide.

Preparation of the standards

In order to avoid self-shielding effects, amounts of 10 μg–1 mg of the elements to be determined were irradiated as standards together with the samples. These standards were prepared by pipetting a known amount of a stock solution, containing these elements, into quartz tubes (2-mm diameter, 4-cm length). The solutions were evaporated to dryness, by means of an i.r. lamp at a temperature of $\pm 75°$. After irradiation, the tubes were carefully broken and the standards were redissolved. They were separated from the bits of quartz by several washing and decantation steps. The recovery yield of the standards was checked by means of integral γ-ray counting, and turned out to be practically 100%.

Irradiation conditions

The samples and standards were irradiated either for 6 h in the Thetis reactor at the University of Ghent, at a thermal flux of $5 \cdot 10^{11}$ n cm^{-2} s^{-1}, or during one week in the BR-2 reactor of the C.E.N. at Mol (Belgium) at a thermal neutron flux of 10^{14} n cm^{-2} s^{-1}, when very long-lived isotopes were being determined.

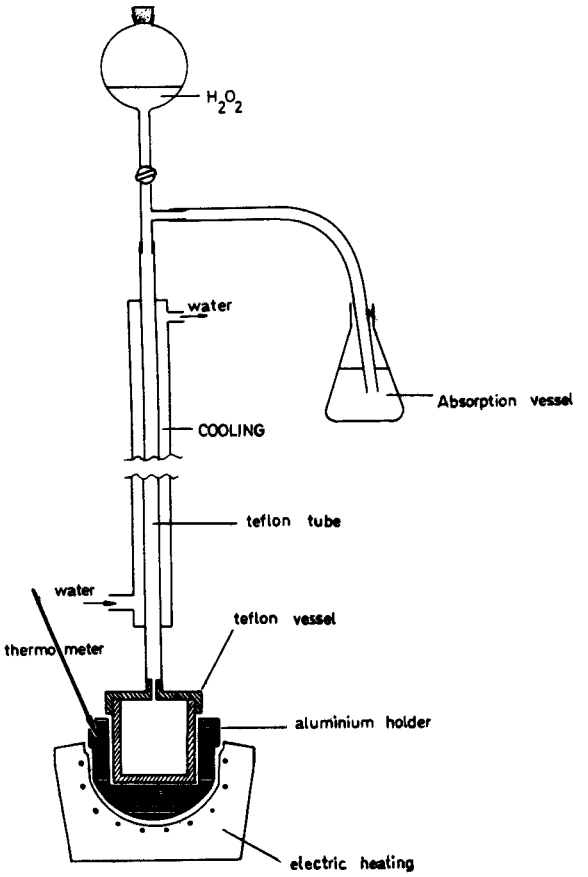

Fig. 1. Apparatus for the destruction of the iron samples.

Dissolution of the samples

For the destruction of the samples, the apparatus shown in Fig. 1 was used. A 1-g iron sample together with 30 mg of carrier for the elements arsenic and antimony was placed in the teflon vessel containing 3 ml of 40% hydrofluoric acid and 10 ml of water. During the dissolution, 10 ml of 30% hydrogen peroxide was added dropwise through the reflux cooler. Subsequently the temperature of the aluminium mantle was raised to 140–150°, in order to decompose the excess of peroxide. A complete destruction of any peroxide complexes that might have formed, was necessary in order to obtain complete adsorption on the resin for certain elements. During the dissolution step, only for mercury was a slight volatilization observed in spite of the cooling device. All other elements were completely recovered. The solution finally obtained had the exact hydrofluoric acid concentration required for a neat separation of iron from most other elements by means of exchange resins.

Preparation of exchange resins

As resins, Dowex 50W-X8 cation exchanger and Dowex 1-X8 anion exchanger, both sieved to 100–200 mesh particle size, were used. After equilibration with a 1 *M* hydrofluoric acid solution, the resin was placed in a teflon tube of 9-mm diameter.

The height of the resin column was adjusted to 10 cm. The use of teflon material is absolutely necessary, because other plastics show an important adsorption of some elements to the tube walls.

Removal of the iron matrix

After dissolution, the sample was passed through the anion or cation exchange

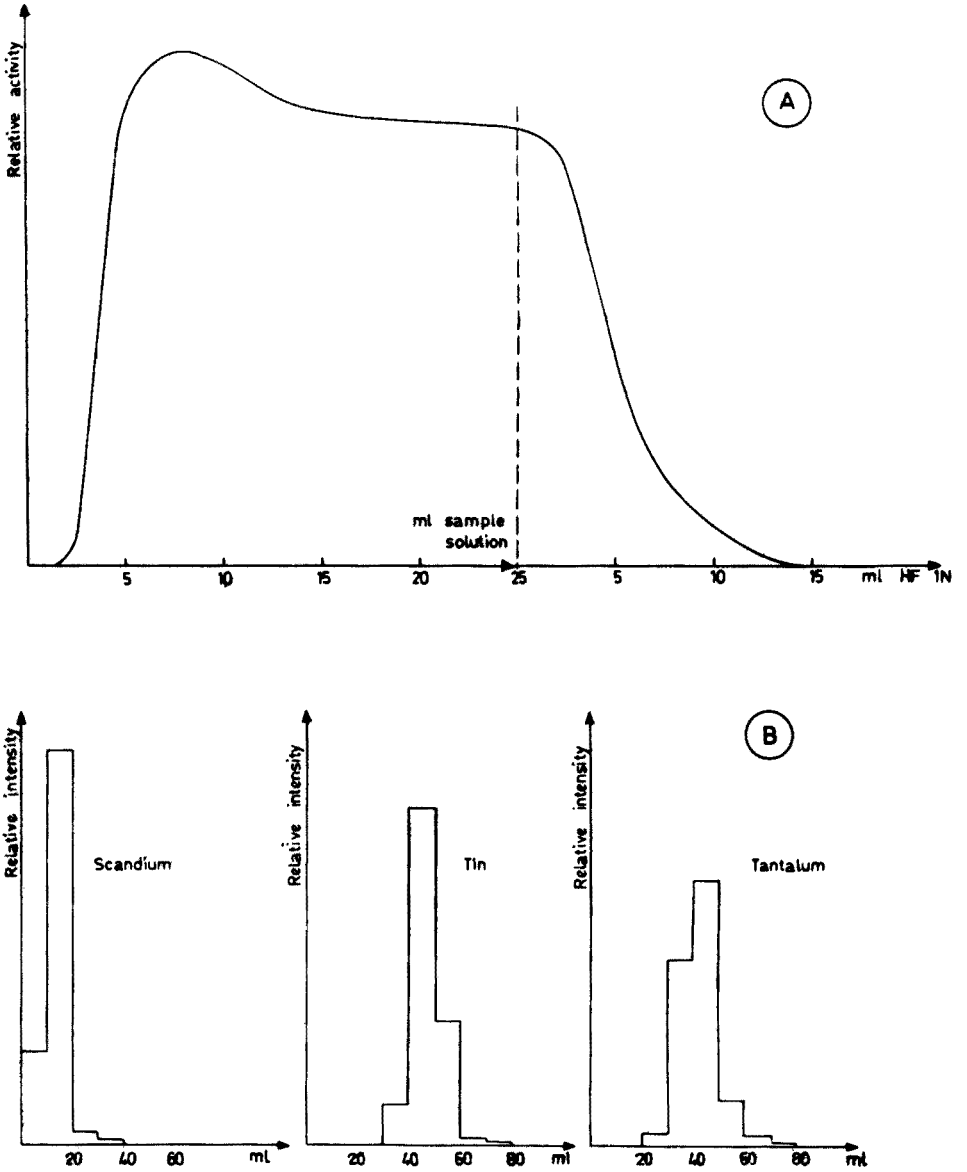

Fig. 2. Elution curves for the anion-exchange column: (A) Removal of the iron matrix in 1 *M* HF; (B) Elution of Sc and Sn with 22 *M* HF and Ta with 6 *M* HCl.

column. Elution curves were recorded for ^{59}Fe as a radioactive tracer with an integral γ-ray counting method. A total volume of 25 ml of 1 *M* hydrofluoric acid in excess added to the sample solution appeared to be sufficient for a complete removal of the iron from both resins.

The elution curves are shown in Figs. 2A and 3A. The elution rate during these experiments was kept at 1 drop every 4 s.

Separation of gallium, chromium, arsenic and nickel

For gallium, chromium and arsenic, which could not be easily separated from the iron matrix, special separation procedures were required. The initial solutions for the procedures outlined below were the eluates containing the iron matrix as described for the anion- and cation-exchange procedures. Nickel was separated completely individually in separate iron samples without any ion-exchange procedure being used.

Gallium. The solution was evaporated nearly to dryness and redissolved in 7.5 *M* hydrochloric acid. Iron was completely reduced to iron(II) by means of tin(II) chloride, and gallium was extracted with isopropyl ether. Before the extraction 30 mg of gallium carrier was added.

Chromium. The solution was evaporated and redissolved in 70% perchloric acid. Subsequently chromium was distilled as chromyl chloride[17]

Arsenic. To the solution 0.5 g of thioacetamide was added, and the mixture was heated at 100° until arsenic sulfide was completely precipitated. After cooling, the precipitate was filtered off on a porcelain filter.

Nickel. A 1-g iron sample, together with 30 mg of nickel carrier and 30 mg of manganese hold-back carrier, was dissolved in a mixture of 60 ml of 6 *M* hydrochloric acid and 10 ml of 7 *M* nitric acid. The solution was diluted with 200 ml of warm water and 25 ml of a 25% citric acid solution was added. By means of 14 *M* ammonia solution, the pH was adjusted to 3–4, and the solution was heated to 80°, before addition of 20 ml of alcoholic 1% dimethylglyoxime solution and neutralization with 6 *M* ammonia solution. The red precipitate was filtered off on a porcelain filter crucible. The yield was *ca.* 100%.

Counting equipment

All measurements for the analyses were carried out with a 35-cm^3 (Ortec) or a 40-cm^3 (Canberra) Ge(Li) detector connected to an Intertechnique DIDAC 4000 multichannel analyser. The energy resolution was 2.3 keV for the 1332.5-keV transition of ^{60}Co. In order to avoid errors from pulse pile-up effects, the dead-time of the system was kept below 10%. After each measurement, the spectrum was stored on IBM compatible magnetic tape. All spectra were transferred to a Digital PDP-9 computer for spectral analysis and further interpretation[19,20].

For the tracer experiments, all countings were done with a 3 × 3-in. NaI(Tl) detector coupled to a single-channel or a 400-channel analyser.

ADSORPTION CHARACTERISTICS OF THE IMPURITIES IN IRON

The complete adsorption on cation- and anion-exchange resins was checked by means of tracer experiments. A known amount of a radioactive tracer of the

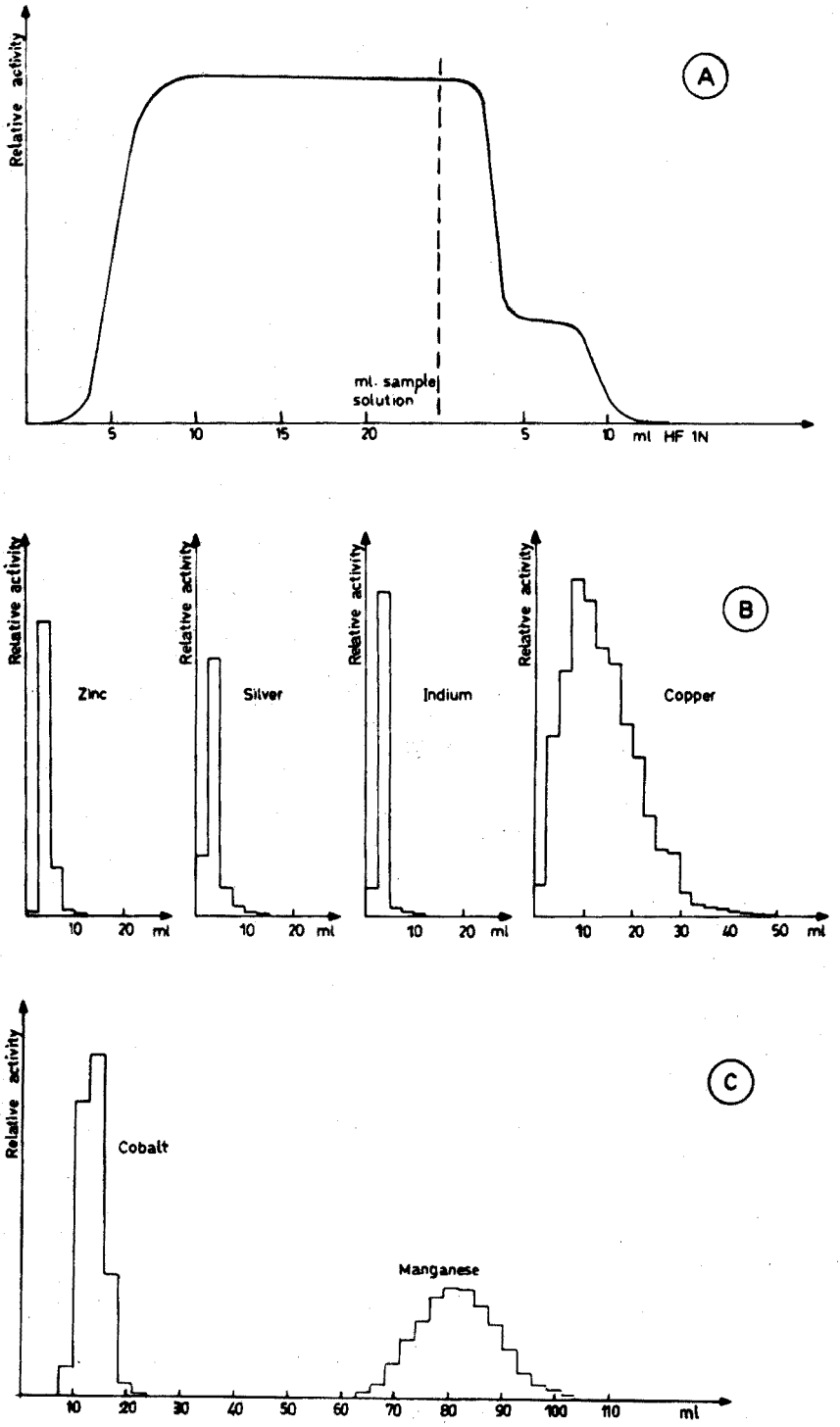

Fig. 3. Elution curves for the cation exchange column: (A) Removal of the iron matrix in 1 *M* HF; (B) Elution of Ag, Zn, In and Cu with a mixture of 10% 1.5 *M* HBr and 90% acetone; (C) Elution of Co and Mn with a mixture of 20% 5.5 *M* HCl and 80% acetone.

element in question was added to the iron sample just before the dissolution step. After the sample solution had been passed through one of the ion-exchange columns and after an additional elution with 25 ml of 1 *M* hydrofluoric acid, the resin was extruded from the column and both resin and eluate were counted. The activity in each fraction was determined. In order to check for possible losses by evaporation or by adsorption on the walls of the vessels or the column container, the measurements were always referred to the original amount of tracer added. The average results for three tracer experiments for every isotope are summarized in Table II. For three important impurities, gallium, arsenic and chromium, no complete adsorption either on anion- or on cation-exchange resin could be obtained.

TABLE II

ADSORPTION CHARACTERISTICS OF THE IMPURITIES IN IRON ON AN ION-EXCHANGE COLUMN IN 1 *M* HYDROFLUORIC ACID

Element	*Resin*	*% Activity on the resin*	*% Activity in the eluate*
Ta	Dowex 1-X8	98.8	0.034
W		99.3	0.03
Sn		98.3	0.02
Mo		101.2	0.4
Sb		99.1	0.1
Sc		99.7	0.016
Ag		99.3	0.05
In	Dowex 50W-X8	99.6	0.04
Na		99.3	0.14
Zn		99.2	0.07
Co		99.0	0.21
Cu		99.9	0.06
Ni		100.4	0.25
La		99.8	0.17

Anion-exchange separation scheme

The separation scheme with an anion-exchange resin, is shown in Fig. 4. As and after an additional elution with 25 ml of 1 *M* hydrofluoric acid, the resin was Dowex 1-X8 resin in this medium. Arsenic is partially adsorbed, and gold, although strongly adsorbed on the resin, cannot be determined in this fraction because of losses by adsorption on the walls of the destruction vessel and the column.

If necessary, Sn and Sc can be completely removed from the resin by an elution with 22 *M* hydrofluoric acid, while Sb and Ta remain strongly adsorbed. By a subsequent elution with 6 *M* hydrochloric acid, tantalum is removed from the column. Because antimony remains strongly adsorbed, a separation from tantalum is obtained. The elution curves are shown in Fig. 2B.

As gallium and chromium are completely present in the eluate containing the iron matrix, these elements can be determined in this fraction.

Cation-exchange separation scheme

The separation scheme with a cation-exchange resin, is also shown in Fig. 4. As can be seen from Table II, Co, Cu, Ni, Na, Zn, Mn, Ag, In as well as the rare

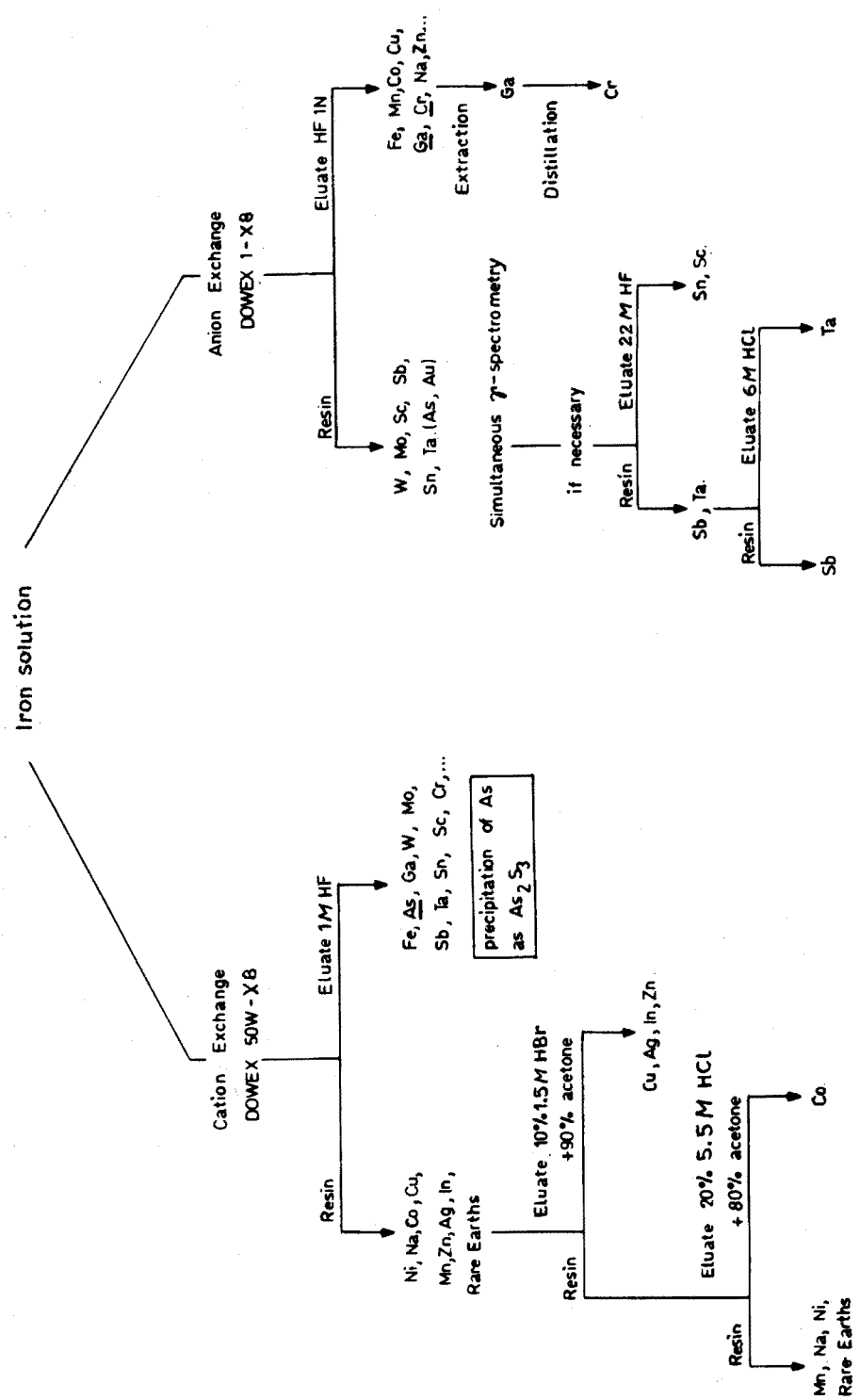

Fig. 4. General separation scheme.

earth metals, are strongly adsorbed in a 1 *M* hydrofluoric acid medium. A further separation of these elements can be obtained by two consecutive elution steps. In the first step, Cu, Ag, Zn and In are removed from the column by means of a mixture of 10% 1.5 *M* hydrobromic acid and 90% acetone. The elution curves are shown in Fig. 3B. In a second step, Co and Mn can be removed from the column as well as separated from each other with a mixture of 20% 5.5 *M* hydrochloric acid and 80% acetone, as shown by the elution curves presented in Fig. 3C. The rare earths and sodium remain strongly adsorbed on the resin.

Arsenic can be completely recovered from the eluate containing the iron matrix. This element is separated selectively by precipitation as the sulfide.

RESULTS AND DISCUSSION

The final results for all analyses carried out are summarized in Table III. The concentrations mentioned are averages of several determinations. The number of determinations and the standard deviation for a single determination are also indicated. For certain elements, only upper limits were calculated.

TABLE III

FINAL RESULTS FOR THE DETERMINATION OF TRACE IMPURITIES IN IRON

Element	*Concentration in p.p.m.*	*No. of analyses*
W	1.42 ± 0.08	8
Co	80.3 ± 1.1	8
Ga	6.70 ± 0.30	8
As	8.55 ± 0.35	8
Cu	40.1 ± 1.6	8
Mo	64.2 ± 1.0	8
Ni	864 ± 5	5
Ta	$(0.87 \pm 0.05) \cdot 10^{-3}$	4
Sn	3.5 ± 0.2	4
Sb	0.39 ± 0.02	4
Cr	6.2 ± 1.0	3
Ag	$< 10^{-3}$	4
Zn	$< 7.10^{-3}$	4
Sc	$< 3.10^{-5}$	4

For the calculations of the results several FORTRAN programs developed by Op de Beeck were used. By means of a spectral analysis program[19], the energies and peak areas were calculated. This program was used when only one or two isotopes were present in the spectrum.

For more complex spectra, a total activation analysis program[20] was used to calculate directly the concentrations and upper limits of the different elements. Manganese was not determined destructively although a measurement of the cation-exchange resin after a separation immediately after the irradiation would allow an easy and very sensitive determination. This element, however, can be determined non-destructively much faster, as has already been described[10].

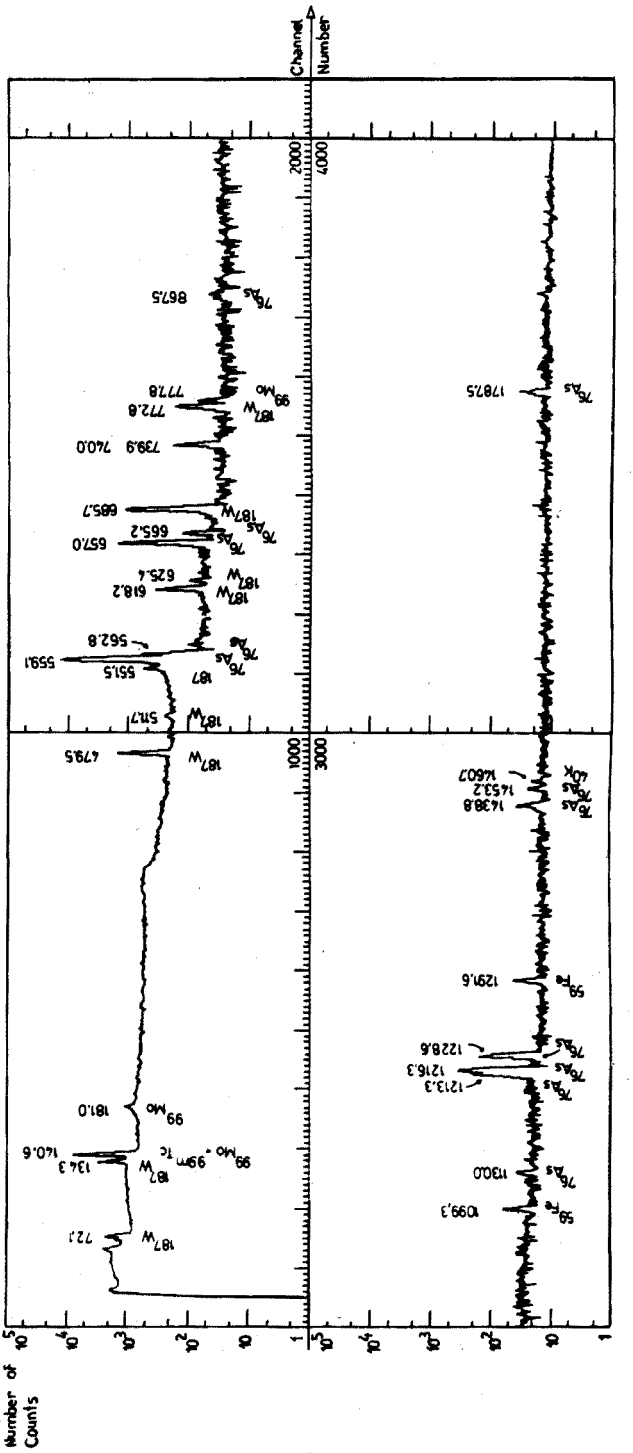

Fig. 5. Ge(Li) γ-spectrum of the anion-exchange resin group 3 days after irradiation.

Tungsten and molybdenum

These elements were determined after an irradiation in the Thetis reactor. The isotopes ^{99}Mo–^{99m}Tc and ^{187}W were measured on the resin fraction. Tungsten was determined by means of the peaks at 479.5 and 685.7 keV. For molybdenum, the 140.6-keV peak of the ^{99m}Tc daughter was used. In order to allow ^{99}Mo and ^{99m}Tc to reach their equilibrium ratio, the measurements were done at least 44 h after the end of the chemical separation. A typical Ge(Li) γ-spectrum of this fraction is shown in Fig. 5.

Tantalum, tin, antimony and scandium

Ta, Sn, Sb and Sc can be determined on the anion-exchange resin fraction containing W and Mo. For the determination of these elements, the samples were irradiated in BR-2 during one week at a thermal flux of 10^{14} n cm^{-2} s^{-1}. In Fig. 6 a typical spectrum of this fraction is shown, measured 30 days after the end of the irradiation. For the determination of tantalum, several peaks such as those at 67.7, 100.1 and 1221.4 keV can be used. For antimony, the 602.1-keV peak was preferred. For tin, the 391.4-keV peak of ^{113m}In, the daughter of ^{113}Sn, was used. As no peaks of ^{46}Sc could be detected, the upper limit was calculated according to the criterion of Currie[21].

Gallium

Gallium was determined after an irradiation in the Thetis reactor. In addition to peaks of ^{72}Ga, only very small peaks of ^{198}Au, ^{76}As and ^{59}Fe appeared in the Ge(Li) spectrum of this fraction. For the determination of gallium, the peak at 834.0 keV was used. Trace experiments showed that manganese, whose ^{54}Mn isotope might interfere with the gallium determination because it gives a peak at very nearly the same energy, was not extracted at all.

Chromium

Chromium could be determined after an irradiation for one week in BR-2. As the distillation of chromium as chromyl chloride is very selective (only Tc can interfere in the perchloric acid medium), the ^{51}Cr activity can be measured on a NaI(Tl) detector with a very high efficiency. The apparent chromium concentration, arising from the interfering reaction ^{54}Fe(n, α)^{51}Cr after an irradiation of one week in the BR-2 reactor, was calculated. An apparent concentration of 8.40 p.p.m. was obtained and taken into account.

Arsenic

Arsenic was determined after an irradiation in the Thetis reactor. The Ge(Li) γ-spectrum of this fraction showed that only molybdenum was partially coprecipitated. The presence of ^{99}Mo–^{99m}Tc in the spectrum did not interfere with the determination of arsenic.

Under the experimental circumstances of this work, copper was also precipitated when present, but as this element had already been adsorbed on the cation-exchange resin, no peaks of ^{64}Cu were observed in the spectrum.

Copper and cobalt

In Fig. 7 a typical Ge(Li) γ-spectrum of the cation-exchange resin fraction

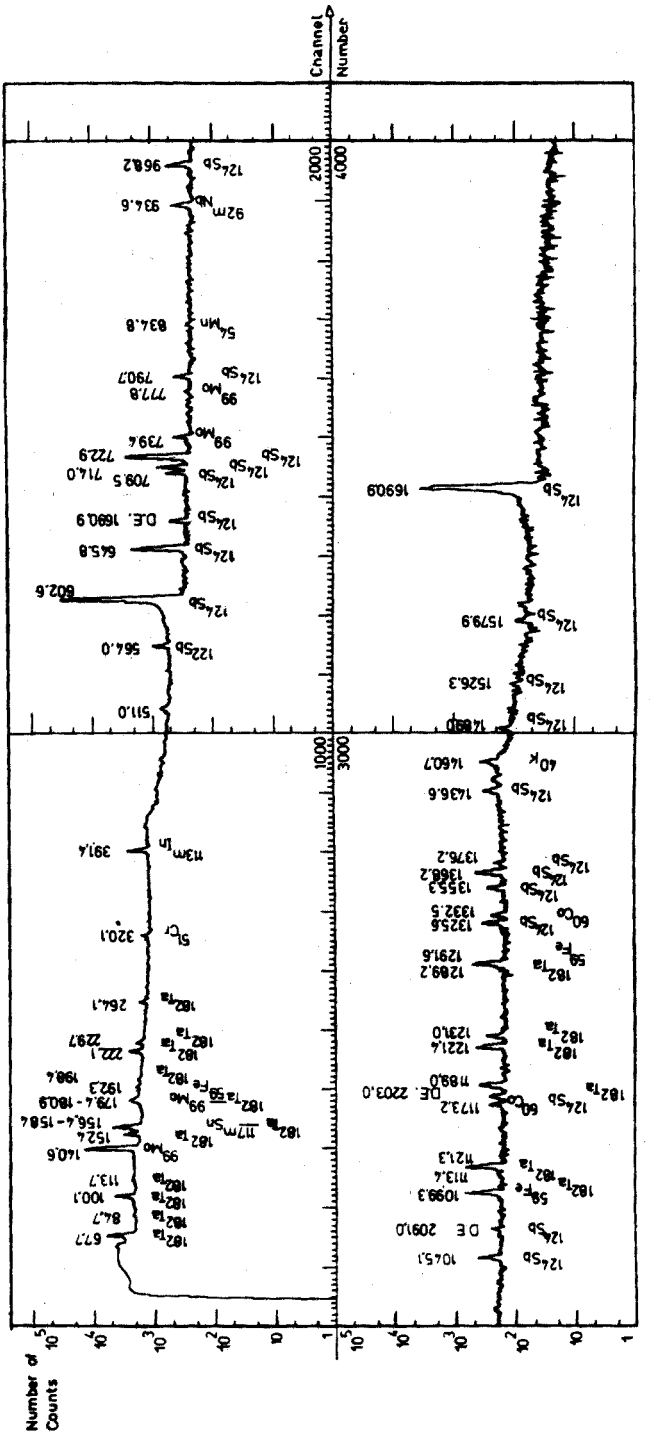

Fig. 6. Ge(Li) γ-spectrum of the anion-exchange resin group 30 days after irradiation.

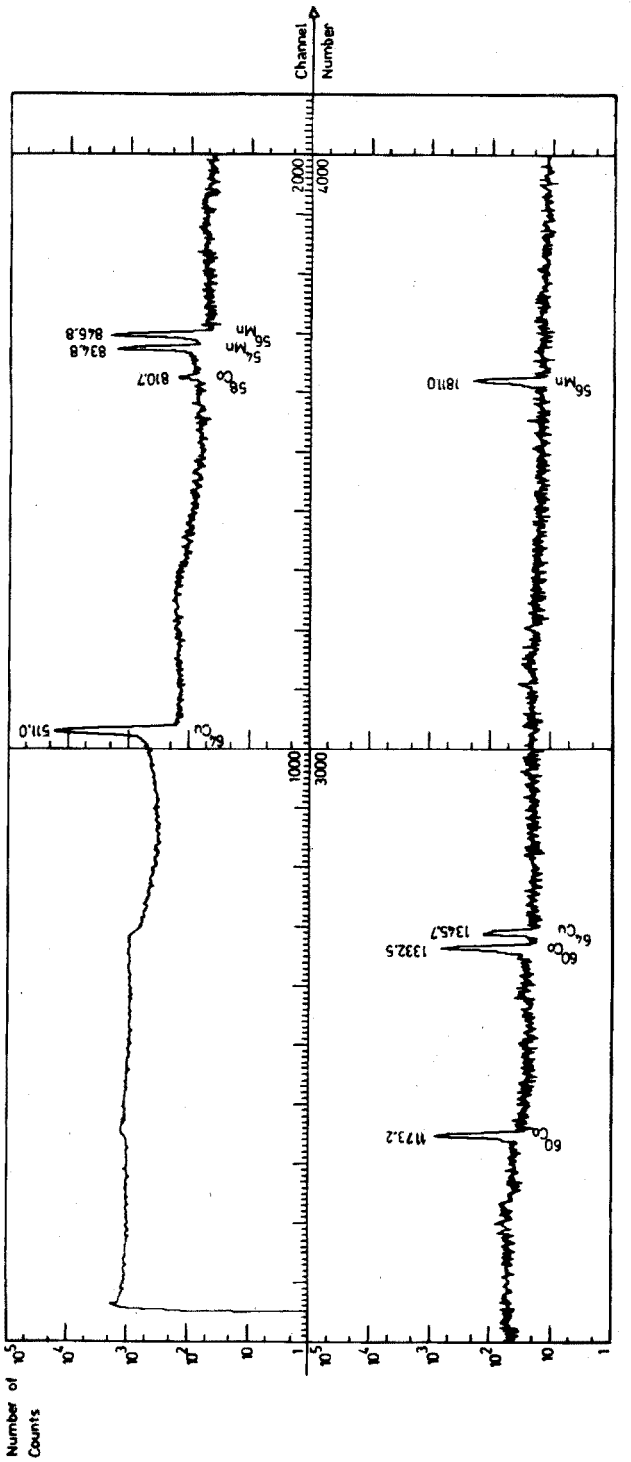

Fig. 7. Ge(Li) γ-spectrum of the total cation-exchange resin group 2 days after irradiation.

after the removal of the iron matrix is presented. As only peaks of ^{64}Cu, ^{58}Co, ^{60}Co and ^{56}Mn and ^{54}Mn can be detected one day after the end of the irradiation in the Thetis reactor, cobalt and copper were measured without further separations.

Zinc and silver

For these elements, a one-week irradiation in the BR-2 reactor was carried out at a flux of 10^{14} n cm^{-2} s^{-1}. After an elution of the cation-exchange resin with a hydrobromic acid–acetone mixture, the silver- and zinc-containing eluate was counted for 24 h on a 40-cm^3 Ge(Li) detector but no peaks of ^{110m}Ag or ^{65}Zn were detected. Upper limits were calculated.

Nickel

Nickel can be determined by means of the isotope ^{65}Ni with a half-life of 2.65 h. As mentioned above, nickel can be separated from the iron matrix by means of a cation-exchange resin. However, manganese, whose isotope ^{56}Mn has approximately the same half-life as ^{65}Ni and is formed from a relatively large amount of manganese impurity present as well as by a (n, p) reaction on the iron matrix, gives rise to a rather intense activity. Moreover, it appears in the same fraction as nickel in the general separation scheme, so that an additional Mn–Ni separation would be absolutely necessary. However, because of the short half-life of the ^{65}Ni isotope, a time-consuming separation procedure would considerably reduce the sensitivity of the determination. For this reason, a selective direct separation of nickel was preferred.

Nickel was determined after irradiation in the Thetis reactor. In the Ge(Li) γ-spectrum of the nickel precipitate, peaks of ^{64}Cu and ^{56}Mn were detected, besides the peaks of ^{65}Ni. They did not prevent the determination of nickel.

Thanks are due to Prof. Dr. W. Koch, Dr. H. Wünsch and Dr. K. Willmer for providing the pure iron samples. The partial financial support of the I.W.O.N.L. and the I.I.K.W. is also gratefully acknowledged.

SUMMARY

A method is presented for the determination of fourteen elements in pure iron by means of destructive thermal neutron activation analysis. By means of an anion- and cation-exchange procedure in 1 *M* hydrofluoric acid, the iron matrix is separated from a large number of elements, which are further separated in groups. W, Mo, Ta, Sn, Sb and Sc are found and measured as one group on the anion-exchange resin. Cu and Co, and Zn and Ag, are two groups obtained from the cation exchange procedure. For the elements Ga, Ni, Cr and As which cannot be included in the general group separation scheme, special individual methods are described.

REFERENCES

1 G. Aubouin and J. Laverlochère, *Rep. C.E.A. DR/AR/G/63-13*, May 1963.
2 W. J. Ross, *Anal. Chem.*, 36 (1964) 1114.
3 J. W. Mc Millan, *Analyst (London)*, 89 (1964) 594.

4 R. Malvano and P. Grosso, *Anal. Chim. Acta*, 34 (1966) 253.
5 D. A. Hilton and D. Reed, *Analyst (London)*, 90 (1965) 541.
6 J. C. Ricq, *J. Radioanal. Chem.*, 1 (1968) 443.
7 P. Albert, *Mem. Sci. Rev. Met.*, LXV (1968) 1.
8 B. A. Thompson and P. D. La Fleur, *Anal. Chem.*, 41 (1969) 852.
9 N. Deschamps and M. Fedoroff, *Z. Anal. Chem.*, 247 (1969) 221.
10 C. De Wispelaere, J. P. Op de Beeck and J. Hoste, *Anal. Chem.*, 45 (1973) 547; *Anal. Chim. Acta*, 64 (1973) 321.
11 L. Danielsson and T. Ekström, *Acta Chem. Scand.*, 20 (1966) 2402, 2415.
12 L. Danielsson, *Ark. Kemi*, 27 (1967) 453, 467.
13 J. C. Roy and J. J. Hawton, *AECL-1181 (CRC-1003)*, December 1960.
14 J. W. Boldeman, *J. Nucl. Energy, Parts A/B*, 18 (1964) 417.
15 N. E. Holden and F. W. Walker, *Chart of the Nuclides*, 11th Ed., Gen. Electric Co., Schenectady, N.Y., 1972.
16 R. De Neve, D. De Soete and J. Hoste, *Radiochim. Acta*, 5 (1966) 188.
17 *Annual Book of A.S.T.M. Standards*, E262-70; E264-70; E26ᵕ
18 F. De Corte, A. Speecke and J. Hoste, *J. Radioanal. Chem.*, 8 (1971) 287.
19 J. P. Op de Beeck, to be published.
20 J. P. Op de Beeck, *J. Radioanal. Chem.*, 11 (1972) 283.
21 L. A. Currie, *Anal. Chem.*, 40 (1968) 586.

Analytica Chimica Acta, 70 (1974) 17–24

CHARACTERIZATION OF A D.C. ARC PLASMA JET IN ARGON AS AN ATOMIZATION AND EXCITATION SOURCE FOR ATOMIC SPECTROSCOPY

PHILIP MERCHANT, JR* and CLAUDE VEILLON

Department of Chemistry, University of Houston, Houston, Texas 77004 (U.S.A.)

(Received 5th October 1973)

Renewed interest in d.c. arc plasmas as atomization and excitation sources has occurred in recent years. The high plasma temperatures and inert atmosphere offer important advantages for emission spectrometry, such as efficient atomization, a high degree of excitation, reduced compound formation, and decreased quenching of excited species by molecules. In addition, aqueous solutions can be handled directly, although it is frequently desirable to desolvate the sample aerosol before introduction into the plasma device in order to improve the stability of the discharge. Most plasma devices suffer from two limitations: the high background emission from the plasma necessitates the use of a high-dispersion monochromator, and the problem of getting most of the sample into the high-temperature plasma region is difficult. The first, of course, applies to any emission technique where high background emission is present, while the second appears to be a problem with most plasmas having a well defined high-temperature boundary which the sample aerosol particles must penetrate.

If an arc plasma is forced to pass through an orifice, the outer layers of the plasma near the orifice wall are cooled. This cooling decreases ionization and causes the cross-sectional area of the plasma to decrease, increasing the current density (and effective temperature) within the arc. With the d.c. arc plasma jet, this thermal pinch effect can increase the plasma temperature at relatively low overall arc current, which simplifies the power supply required. Practical applications of these devices for spectrochemical analysis have been described by Margoshes and Scribner[1,2] and Korolev and Vainshetin[3]. Owen[4] modified the Margoshes and Scribner design for improved stability. More recently, Valente and Schrenk[5] described a novel design for a plasma jet and gave relative emission intensity and detection limit data for several elements. Marinkovic and Vickers[7] described a long-path stabilized d.c. arc device and reported radial atomic distributions and detection limits for several refractory elements. Elliott[7] described the design and performance of a commercially available low-current plasma jet, and reported temperatures in the plasma core and the flame-like region above the horizontal cathode.

The purpose of this investigation was to characterize the d.c. arc plasma jet, or rather one version of it, as completely as possible. The high apparent

* Present address: Exxon Chemical Co., Houston, Texas 77029.

temperatures reported in the literature for these devices and the inert atmosphere used suggest that the atomization and excitation efficiency would make this an ideal emission source for spectrochemical analysis, especially for refractory elements which are not easily determined in chemical flames. Many of the parameters investigated in this study, such as the effect of gas flow rate, ionization, the effect of arc current, electron density, etc., gave results that were predictable or expected. Two studies, namely of apparent temperatures and relative atomic concentrations, gave results that were somewhat surprising. A sharp drop in apparent temperature in the plasma tail-flame region above the cathode was observed, and it appears that only a relatively small fraction of the sample aerosol particles penetrates the plasma boundary and undergo atomization.

EXPERIMENTAL

Apparatus

The main components of the plasma jet are shown schematically in Fig. 1. The cross-hatched components are the graphite anode, cathode and orifice ring. The dark portion is a phenolic plastic (Bakelite) insulator, and the remainder is constructed of brass. The water-cooled anode and cathode are made from 6.35 and 3.18-mm o.d. graphite rod, respectively, while the orifice ring is made from 12.7-mm o.d. graphite rod drilled to form a 6.35-mm i.d. orifice. Argon and desolvated sample aerosol enter the electrically isolated chamber tangentially and exit through the orifice. The plasma was initiated and maintained by a 0–15 A, d.c. arc power supply (Model 3020, Tomorrow Enterprises, Portsmouth, Ohio). The cathode center was 10 mm above the top of the orifice ring and the tip of the cathode was about 3 mm from the anode axis. A vertical plasma column of about 2 mm o.d. extended above the orifice ring, then sharply bent toward the cathode, forming a very low intensity "flame" extending vertically above the bend.

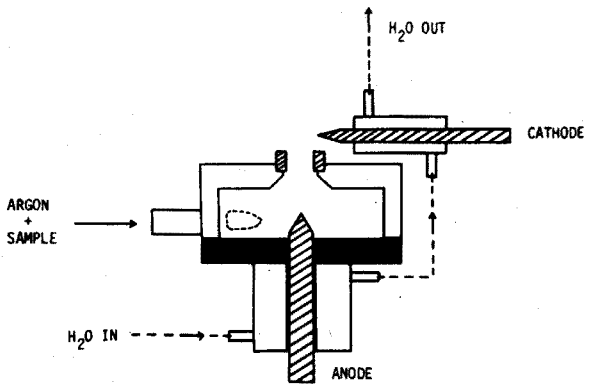

Fig. 1. Schematic diagram of the d.c. arc plasma jet.

An unmagnified image of the plasma was focused onto the entrance slit of the monochromator by a 50-mm diameter, 200-mm focal length fused silica lens. Entrance and exit slit width was 0.020 mm, and to localize the region viewed, the entrance slit height was stepped down to 1 mm. The monochromator

used was a Czerney–Turner type, with 250-mm focal length mirrors and an $f/4$ aperture. A 1200 grooves mm^{-1}, 52×52 mm ruled-area grating blazed for 300.0 nm was employed, resulting in a reciprocal linear dispersion of 3.2 nm mm^{-1}. An EMI 9783B photomultiplier was employed, and the signal was amplified by a phase-sensitive amplifier tuned to 330 Hz (Model 120, Princeton Applied Research Corporation, Princeton, New Jersey). A mechanical chopper modulated the radiation from the plasma jet (emission measurements) or the external source (absorption measurements) at 330 Hz, and also generated the reference signal for the amplifier with the circuit described previously[8]. Output from the synchronous amplifier was displayed on a 25-cm strip-chart recorder.

Plasmas generally tend to become unstable when appreciable quantities of water are introduced into them, such as in the form of aqueous sample aerosol particles. To minimize this effect, a desolvation system was used to introduce the sample as dry aerosol particles. This system consisted of a pneumatic nebulizer spraying into a heated chamber and followed by a condenser, and has been described previously[9]. The nebulizer was operated at an argon pressure of 2.8 kg cm^{-2}, which resulted in a gas flow rate of 3 l min^{-1} and a sample solution uptake rate of 1.9 ml min^{-1}. The measured overall efficiency of this sample introduction system was 33%, so that the net rate of sample introduction into the plasma jet device was 0.63 ml min^{-1}. No OH band emission was observed from the plasma.

Measurements

In the characterization of this d.c. arc plasma jet, various parameters were investigated as a function of the region of the plasma viewed. Unless otherwise specified, an arc current of 9A was used. The optical arrangement described earlier allowed measurements from small volumes of the plasma which corresponded to areas of about 0.02×1 mm and horizontally as thick as the plasma. In order to observe these various regions, the entire jet assembly was displaced horizontally and vertically by an adjustable mount. In addition to apparent temperature measurements as a function of plasma region and argon flow rate, similar measurements were made for the degree of ionization, electron density and relative line intensities. Measurements of atomic emission and absorption were also made.

RESULTS AND DISCUSSION

Temperatures

Reif *et al.*[10] have critically reviewed spectroscopic temperature measurements and have shown that the values obtained depend on the method employed, the energy states used, temperature gradients and the concentration distribution of the thermometric species. They found that the values observed correspond to an apparent temperature and not to an average temperature within the measured volume. Significant errors and uncertainties are possible, depending on the method used and the source of data for the various parameters needed in the temperature calculation. As discussed by Reif *et al.*[10], different apparent temperatures would be measured when lines arising from different electronic levels are used.

Therefore, for present purposes, the temperatures shown are apparent temperatures measured by the methods described below and they may not be directly comparable to temperatures measured by others in plasmas.

In order to determine the apparent excitation temperature in various plasma regions, the line-pair, intensity-ratio method[11] was employed. The argon 415.86 and 425.94 nm atomic lines, and the 434.81, 437.97 and 457.94 nm argon ion lines were used. Statistical weights and transition probabilities for these lines were obtained from Olson[12]. When the effective temperature along the plasma axis was measured vertically from the orifice, the results shown in Fig. 2 were obtained, where the data points represent the average values of the apparent temperatures calculated from the relative intensity measurements of the argon atomic and ion lines. The 415.86 and 425.94 nm atomic line pair gave one set of values for apparent temperature, and the ion line combinations 434.81/437.97, 434.81/457.94 and 437.97/457.94 nm, gave three sets of apparent temperatures. The relative intensities at each wavelength were corrected for differences in monochromator transmission and detector response. The four apparent temperatures thus obtained agreed within about 300 K and the averages were used for the data represented in Fig. 2.

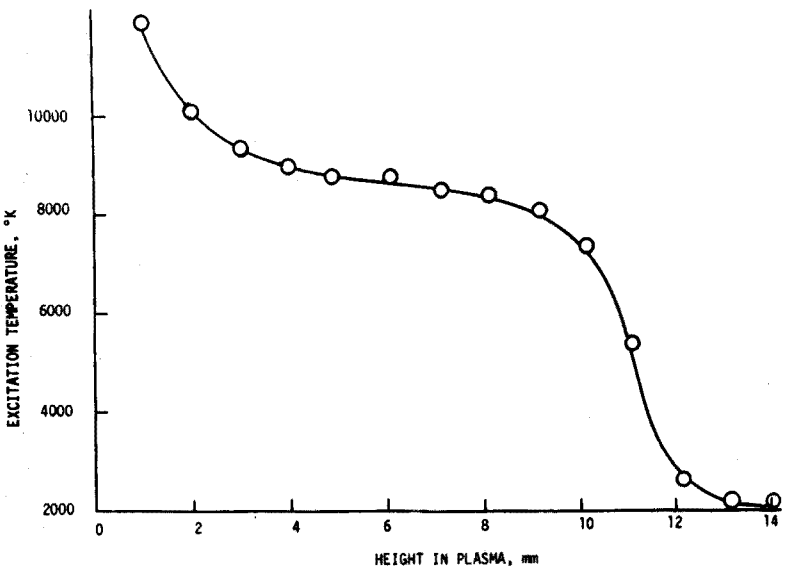

Fig. 2. Excitation temperature distribution in the plasma at 9 A and 3 l min^{-1} argon flow.

One observes in Fig. 2 that the apparent temperature is quite high near the orifice ring, perhaps owing to a higher current density, then becomes relatively constant up to the cathode position at 10 mm, then rapidly decreases above this point in the "flame" above the cathode. A schematic representation of the actual appearance of the plasma, its bending toward the cathode and the "flame" above this region is illustrated in Fig. 3. This very rapid drop in apparent temperature of about 5000 K immediately above the cathode region is in sharp contrast

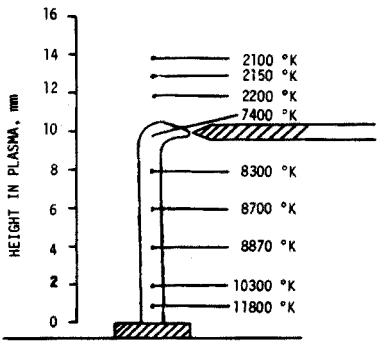

Fig. 3. Illustration of the plasma core, bending toward the cathode, and the flame-like region above the cathode.

with the temperatures reported by Elliott[7] for a similar plasma device. Our apparent temperatures in the plasma agree quite well with those of Elliott, yet in the flame-like region above the cathode Elliott reports a much slower temperature drop with vertical distance, decreasing to a temperature of about 4000 K well above the cathode region. Because the conditions and dimensions used in both devices are similar, these vastly different apparent temperatures in the region above the cathode must be due to the different electrode sizes, materials and gas sheathing of the electrodes, and to differences in the apparent temperature measurement procedures in these two cases. The work of Reif *et al.*[10] would indicate that the latter reason is probably the most significant in the differences observed. Elliott's data were based on measurements of Ti, V, Cd and Fe lines, and it was indicated that the plasma was not in local thermal equilibrium near the cathode. While the data presented in Fig. 2 agree reasonably well with those of de Galan[13] for plasmas in air, an increase in temperature near the cathode was not observed, presumably because of increased radial diffusion in the bent arc[6].

In the cathode region (10 mm), the apparent excitation temperature was also measured by using the relative intensities (corrected for wavelength difference) of the 610.4 and 670.7-nm lithium atomic lines, transition probabilities from Corliss and Bozman[14] and statistical weights obtained from data given by Moore[15] The resulting apparent temperature was almost 1000 K higher than the 7400 K measured when the argon lines were used, the discrepancy probably being due in part to the different sources of data and different atmospheres used. Reif *et al.*[10] have shown that differences of this magnitude (13% in this case) can easily occur and in many cases are very much larger. Above the cathode region, the apparent temperatures measured with the lithium atomic lines were within 200 K of those obtained with argon, while in the plasma region below the cathode reliable relative intensity measurements of the lithium lines could not be made owing to the intense plasma background emission in this wavelength region.

At a height above the orifice of 8 mm, the apparent plasma temperature as a function of argon flow rate is shown in Fig. 4. Up to a flow rate of about 3 l min^{-1}, the apparent temperature is constant, then decreases at higher flows. Presumably this is due to a simple cooling effect at the high flow rates, as

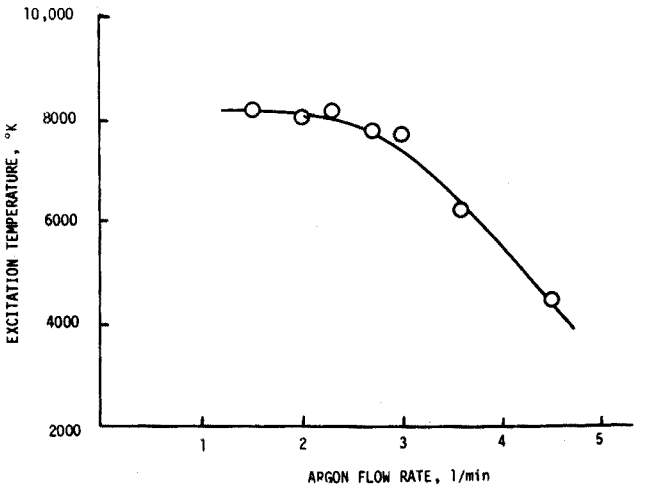

Fig. 4. Effect of gas flow rate on excitation temperature in the plasma (8mm).

is also evidenced by the very similar curve obtained for the degree of ionization as a function of flow rate shown in Fig. 5 for the 10 mm region near the cathode. The degree of ionization was calculated from the Saha equation[11] and the relative intensities of the 425.94-nm argon atomic line, the 434.81-nm argon ion line, statistical weights and transition probabilities from Olson[12], and by assuming the ion and atomic partition functions to be approximately equal.

The relative intensity of the 425.94-nm argon atomic line is directly proportional to the arc current for currents above 7 A. The same effect was observed for temperature, electron density and degree of ionization as a function of arc current.

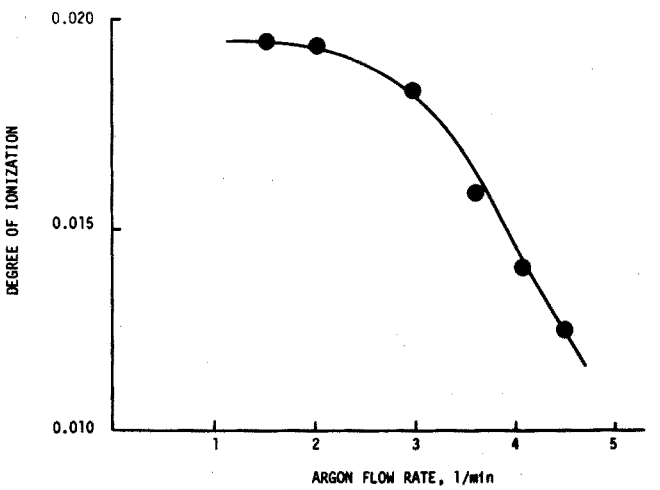

Fig. 5. Effect of gas flow rate on ionization in the plasma.

Emission measurements

One of the limitations cited earlier for the plasma jet is the high background emission from the high temperature plasma region, which makes a high-dispersion monochromator necessary to achieve good line-to-background ratios in emission measurements. For example, Valente and Schrenk[5] used a 3.4-m Ebert monochromator having a reciprocal linear dispersion of 0.25 nm mm^{-1}, Marinkovic and Vickers[6] used a 1-m Czerney–Turner monochromator in the second order (0.4 nm mm^{-1}), and Elliott[7] used an extremely high-dispersion echelle spectrometer (*ca.* 0.05 nm mm^{-1}). The low-dispersion monochromator employed in this investigation resulted in the best line-to-background ratios being obtained in the flame-like region above the cathode, but the relatively low apparent temperatures observed in this region resulted in relatively low sensitivity (and high detection limits in this case) by atomic emission. The minimum detectable concentrations (based on $S/N=2$) obtained for several elements by atomic emission are shown in Table I.

TABLE 1

DETECTION LIMITS AT 12-mm HEIGHT IN PLASMA

(Effective temperature 2200 K)

Element	*Wavelength (nm)*	*Detection limit ($\mu g\ ml^{-1}$)*	
		Emission	*Absorption*
Al	396.2	3.8	2.1
Au	267.6	2.2	1.0
B	249.7	4.1	2.1
Bi	306.8	1.5	1.5
Cu	324.7	1.0	0.3
In	303.9	1.2	0.5
Li	670.8	0.5	0.6
Mo	390.3	3.3	0.9

Absorption measurements

Even with the relatively low apparent temperatures in the region above the cathode, one would at first expect that the sample atomic concentration might be appreciable, owing to the atomization capabilities of the plasma region, the efficiency of the sample introduction system used and the inert atmosphere, which would result in good analytical sensitivity by atomic absorption spectrometry. Determinations of these same eight elements by atomic absorption (Table I) resulted in detection limits comparable or slightly better than those in emission, indicating that perhaps very little of the sample is present in this region. Similar absorption measurements within the plasma core (at 2 and 8 mm heights) supported this observation. Apparently, only a small fraction of the dry sample aerosol particles penetrates the plasma boundary and experiences the high temperatures therein. While these results are not conclusive, especially since absolute atomic concentrations are very difficult to measure, they support similar observations and conclusions by Marinkovic and Vickers[6] and Dickinson and Fassel[16]. It would

then appear that the very good detection limits reported by others[5–7] are largely due to the use of high-dispersion spectrometers, and not necessarily to the high overall atomization efficiency of these devices. An intense background emission does not *per se* degrade the *S/N* ratio and thus the detection limit. However, when a weak line emission is superimposed on an intense continuum, the analytical sensitivity is a function of the dispersion of the monochromator. In this case, the lower sensitivity will frequently result in poorer detection limits as well.

Atomic absorption measurements outside, but adjacent to, the plasma core did not give measurable absorption signals, indicating that any dry sample aerosol particles not penetrating the plasma boundary are not atomized to any appreciable extent. Clearly, further study is needed on these devices to determine the fraction of sample actually entering the plasma and undergoing atomization, and to establish means of increasing the atomic concentration within the plasma and region above the cathode.

The work was supported in part by the National Science Foundation and in part by the Robert A. Welch Foundation.

SUMMARY

A low-current d.c. arc plasma jet in argon is characterized. Apparent temperatures observed in the plasma flame region are considerably lower than those reported previously by other workers with similar devices. It appears that much of the sample aerosol does not enter the high-temperature plasma region.

REFERENCES

1 M. Margoshes and B. F. Scribner, *Spectrochim. Acta*, 15 (1959) 138.
2 M. Margoshes and B. F. Scribner, *J. Res. Nat. Bur. Stand.*, 67A (1963) 561.
3 V. V. Korolev and E. E. Vainshtein, *J. Anal. Chem. USSR*, 15 (1959) 731.
4 L. E. Owen, *Appl. Spectros.*, 15 (1961) 150.
5 S. E. Valente and W. G. Schrenk, *Appl. Spectros.*, 24 (1970) 197.
6 M. Marinkovic and T. J. Vickers, *Appl. Spectros.*, 25 (1971) 319.
7 W. G. Elliott, *American Laboratory*, August, 1971, p. 45.
8 C. Veillon and M. Margoshes, *Spectrochim. Acta*, 23B (1968) 503.
9 C. Veillon and M. Margoshes, *Spectrochim. Acta*, 23B (1968) 553.
10 I. Reif, V. A. Fassel and R. N. Kniseley, *Spectrochim. Acta*, 28B (1973) 105.
11 P. W. J. M. Boumans, *Theory of Spectrochemical Excitation*, Plenum Press, New York, 1966, p. 106.
12 H. N. Olson, *J. Quant. Spectros. Radiat. Transfer*, 3 (1963) 305.
13 L. deGalan, *J. Quant. Spectros. Radiat. Transfer*, 5 (1966) 735.
14 C. H. Corliss and W. R. Bozman, *N. B. S. Monograph 53*, U.S. Government Printing Office, Washington, D.C., 1962, p. 180.
15 C. E. Moore, *N. B. S. Circular No. 467*, Vol. I, 1949, p. 20.
16 G. W. Dickinson and V. A. Fassel, *Anal. Chem.*, 41 (1969) 1021.

Analytica Chimica Acta, 70 (1974) 25–33

DETERMINATION OF CADMIUM IN AIR PARTICULATES BY FLAMELESS ATOMIC ABSORPTION SPECTROMETRY WITH A GRAPHITE TUBE

M. JANSSENS and R. DAMS

Institute for Nuclear Sciences, Ghent University, Ghent (Belgium)

(Received 1st November 1973)

The determination of lead in atmospheric particulates has been of importance for some time and now there is increasing interest in the determination of cadmium. Several methods have already been described, such as x-ray fluorescence[1], neutron activation analysis[2], atomic absorption[3–5], anodic stripping voltammetry[6,7] and mass spectrometry[8], each with its own merits and disadvantages. A comparative study of these methods seems to indicate that flameless atomic absorption spectrometry should be preferred as a routine method for cadmium determinations in such a complex matrix as an aerosol because of its rapidity, sensitivity, selectivity and precision. The greatest problem is the pretreatment of the sample. A wet-ashing procedure is described by Beyer[4]. Kometani *et al.*[5] analysed air particulate matter collected on cellulose and glass-fibre filters by wet- and dry-ashing procedures; they found that no significant losses occur in dry-ashing cellulose filters at 500°C when the metal salts have previously been converted to the sulphates. Losses with glass-fibre filter dry-ashing were ascribed to the formation of insoluble metal silicates. Low-temperature ashing was used by Thompson *et al.*[3] and Colovos *et al.*[7]. A comparison of the percentage recovery for several elements, when a muffle oven (550°C) and a low-temperature asher were used, has been given by Morgan and Homan[9]; cadmium recoveries were only 53% with the muffle oven and 92% with the low-temperature asher.

In the present paper, a procedure for particulate removal from the filter is described, by means of ultrasonic treatment with an eluting acid. The results are compared with those obtained by low-temperature ashing. This procedure has the additional advantage that the impurity levels of the filter itself are less critical. It is further shown that a cadmium determination can be performed in optimal conditions starting from the same filter solution as used for the lead determination described previously[10]. Compared to lead, the normal cadmium levels in atmospheric aerosols are about fifty times lower, but fortunately, flameless atomic absorption spectrometry is about fifty times more sensitive for cadmium than for lead.

EXPERIMENTAL

Apparatus and reagents

A Branson ultrasonic cleaner, consisting of an ultrasonic generator Model LG-150 and an ultrasonic tank-type transducer LTH-60, and a Tracerlab low-temperature asher LTA-600 were used.

The atomic-absorption spectrometer (Perkin-Elmer Model 303) was equipped with an Intensitron cadmium hollow-cathode lamp, deuterium background corrector, HGA-70 graphite furnace and Hitachi-Perkin Elmer recorder Model 159.

A stock standard solution of cadmium (1.000 mg Cd ml^{-1}) was prepared by dissolving 2.7445 g of reagent-grade cadmium nitrate in 0.1 *M* nitric acid and diluting to 1 l. This solution was standardized by comparison to a standard solution of cadmium metal (*p.a.*) in 0.1 *M* nitric acid.

The working standard solutions were prepared weekly in the range 0.25–10 μg Cd l^{-1}. They were kept in polyethylene containers, prechecked for the absence of cadmium to avoid contamination effects. All dilutions were made with 0.1 *M* suprapure nitric acid (Merck). A week of ageing appeared to be acceptable, even for the lowest concentrations.

Sampling and procedure

Aerosols were collected by pumping air through a 10-cm diameter Whatman No. 41 cellulose filter. During a 24-h period about 400 m^3 of air was sampled. The complete sampling system is described by Dams and Heindryckx[11]. After the determination of the total suspended particulate, a one-eighth sector of the filter was cut out and transferred to a beaker containing 50 ml of 0.1 *M* nitric acid. This was vibrated for 10 min in the ultrasonic cleaner, the solution was decanted into a 100-ml volumetric flask, and the ultrasonic treatment was repeated for another 5 min with 30 ml of fresh 0.1 *M* nitric acid. The two solutions were combined and made up to 100 ml. With Eppendorf micropipettes, 10, 20 or 50 μl of the solution were injected into the graphite tube. The following optimal apparatus settings were used: lamp current 10 mA, slit 4, program 4 and atomization voltage of 9 V (*i.e.* drying at 100°C, charring at 330°C, atomization at about 2400°C). Peak heights were measured at 228.8 nm. After subtraction of the blank value, the concentration was determined from a calibration curve.

Influence of the acidity

The influence of the acidity can be twofold: on the measurement and on the quantitative character of the removal of particulate matter from the filter into the solution.

A standard solution of 5 μg Cd l^{-1} in different nitric acid concentrations was measured at the optimal apparatus settings. No other acids were checked because lead has also to be extracted in this medium. Equal fractions of a single filter were also eluted with different acidities. Results for standard and filter solutions are shown in Table I. An acid concentration of 0.1 *M* gave the highest net readings. It appears that high acid content lowers the net absorbances, while water fails to remove the cadmium quantitatively.

Ultrasonic treatment

Equal sectors of a single filter were treated ultrasonically with 50 ml of 0.1 *M* nitric acid for increasing times varying from 5 to 30 min, and the solutions were decanted. All sectors were subjected to a second ultrasonic treatment with fresh 0.1 *M* nitric acid for 5 min. Each fraction was made up to 100 ml with 0.1 *M* nitric acid and the cadmium contents were measured.

TABLE I

INFLUENCE OF THE ACIDITY ON MEASUREMENT OF PEAK HEIGHTS AND COMPLETENESS OF ELUTION

(Net absorbances normalized to net absorbances in 0.1 *M* nitric acid, taken as 100)

Acidity (M HNO_3)	*Standard solution (5 μg Cd l^{-1}), rel. absorbance*	*Filter solution, rel. absorbance*
2	70	63
1	80	81
0.5	95	—
0.1	100	100
0.005	99	—
0	—	74

TABLE II

TIME-DEPENDENCE OF THE ULTRASONIC TREATMENT

(Results compared with low-temperature ashing)

First fraction			*Second fraction (5 min)*		*Combined fractions, ultrasonic treatment (10 min+5 min) μg/100 ml*	*Low-temperature ashing μg/100 ml*
Time (min)	*Absorbance*	*μg/100 ml*	*Absorbance*	*μg/100 ml*		
5	0.1070	250	0.0128	15	295	280
10	0.1057	240	0.0164	20	295	275
15	0.1026	235	0.0146	20	265	280
20	0.1027	235	0.0114	15	275	285
25	0.1113	265	0.0182	20	290	280
30	0.1081	255	0.0272	30	275	280
					265	
					265	
Mean		247		20	278	280
s on one determination (%)		4.9		—	4.8	1.3

Equal filter sectors were also treated twice, once for 10 min and once for 5 min, the solutions were combined and the cadmium contents were measured. Table II summarises the results of these experiments. A time dependence cannot be distinguished but a second elution appears to yield an additional amount of cadmium. Although the net reading on the second fraction is only of the order of the blank reading, the combined fractions give significantly larger values than the first fraction.

HGA-70 operating program

The optimal furnace operating program was checked with standard cadmium solutions and afterwards also with a real sample. With Eppendorf micropipettes, 20-μl volumes were injected into the graphite tube at each possible combination of program setting (2–7) and atomization voltage (4–10 V). Charring the

sample was found to be necessary to avoid interfering signals. Ashing at temperatures higher than 500°C, however, resulted in irreproducible results, owing to losses by volatilization. Programs 3, 4 and 5 gave the most sensitive signal at an atomization voltage of 8–10 V. At 10 V, a too fast atomization caused less reproducible peak heights. As the best compromise, program 4 at 9 V was used for the measurements, *i.e.* drying at 100°C, charring at 330°C, atomization at about 2400°C.

Standardization and precision

In order to avoid errors from inter-element interferences, which could be encountered in such a complex matrix as airborne dust, the method of standard additions was preferred. This method was, however, not applied for routine purposes as it is rather lengthy.

For analysing large numbers of samples, the best practical standardization involved running a set of standard solutions before and after measuring a series of samples. The mean absorbances of the standards were plotted against the amounts introduced into the furnace. The calibration curve was linear from 0.01 ng to 0.12 ng of cadmium. Deviations from linearity occurred for concentrations higher than 0.12 ng. The curve could, however, be used up to 0.20 ng of cadmium. The calibration curve fitted by the method of least squares had the equation (a): $A = 1.2787\,c + 0.0197$. The regression line of the concentration c on the absorbance A followed the equation (b): $c = 0.7776\,A - 0.0150$. The two lines, cutting each other at the point $c = 0.0547$, $A = 0.0897$, were nearly coincident, which is an indication that the data are very well described by a linear relationship. The deviation from (a) to (b) was 1.31% at a concentration of 0.01 ng Cd and 0.16% at the level of 0.10 ng Cd.

Routinely, 20-μl amounts were injected. In replicate runs, this volume could be adapted in order to obtain peak heights between 20 and 70% absorption. In a series, the same volume was injected both for standards and unknowns.

RESULTS AND DISCUSSION

Sensitivity

When 20 μl of a 5 μg Cd l^{-1} standard solution was injected, an absorbance value of 0.1550 or 30% absorption was obtained. Therefore, the sensitivity, expressed as the amount of cadmium required to give 1% absorption was 0.003 ng. More realistic and useful would be the "determination limit" or value at which the given procedure is sufficiently precise to yield a satisfactory quantitative estimate. Currie[12] proposed taking 14.1 times the standard deviation on a blank determination, and this criterion results in a determination limit for cadmium of 0.04 ng. With 20-μl volumes, an amount of 0.2 μg should be contained in 100-ml solution. Because a one-eighth fraction of a 24-h filter corresponded to *ca.* 50 m^3 air and was dissolved in 100 ml, the lowest accurately determinable atmospheric cadmium concentration was 4 ng m^{-3}. If lower concentrations are encountered, a larger filter fraction, *e.g.* a half, could be used, the solution could be diluted to 50 ml and a 50-μl amount injected. This procedure would reduce the limit of accurate determination to 0.2 ng m^{-3} which is sufficient for samples collected in very clean areas. At a total suspended particulate level of 100 μg m^{-3}, typical for urban areas, this corresponds to only 2 p.p.m., while typical cadmium concentrations of airborne dust are around 100

p.p.m. If required, sampling times can of course also be increased, resulting in even higher sensitivities per volume of air.

During the investigations, it was found that some plastic bottles used to store the solutions, released easily detectable amounts of cadmium. Since these amounts increased on ageing, the type of plastic containers used must be selected carefully.

Reproducibility

The reproducibility of the whole procedure, including fractionation of the filter, preparation of the sample, measurement of the percentage absorption and calculation of the concentration, was investigated with 8 equal fractions of a single filter. A reproducibility, expressed as the standard deviation on one measurement, of 4.8% was obtained (Table II, column 6). However, after low-temperature ashing, the agreement between the results obtained from equal filter fractions was even better (Table II, column 7), the standard deviation being reduced to 1.3%. This indicates that the larger spread on the results is mainly due to the eluting procedure. Important is the very good agreement between the mean results of the two procedures. As a consequence, the much faster ultrasonic cleaning should be preferred for most routine analyses. The results also show that there were no significant inhomogeneities over the filter.

Selectivity

Each air sample is a unique and complex mixture of components varying in concentration from aerosol to aerosol. Simulating the aerosol composition in a standard is obviously very difficult. Therefore those elements which have an absorption line near the cadmium resonance line of 228.8 nm, were checked for interferences; 20-μl volumes of standard solutions of Sb, Ni, Sn, I, Na and Cl were injected in concentrations at least five times higher than those generally found in urban aerosols. No absorptions at 228.8 nm were recorded for Sn, I, Na and Cl. However, contributions to the cadmium absorption peak by nickel and antimony became serious at the unusually high concentration level of 8 μg Ni m^{-3} of air and at 500 ng Sb m^{-3}. Recordings with and without deuterium background corrector did not result in different readings for the samples checked.

Accuracy

The accuracy of the results is more difficult to assess. However, the agreement between the results with ultrasonic cleaning and low-temperature ashing, the reproducibility of the procedure, and the relative freedom from interference suggest a good accuracy.

A synthetic filter sample prepared by IAEA in Vienna was analysed for cadmium; results of 3.05 μg/filter and 3.10 μg/filter were obtained while the spotted amount was 3.06 μg/filter[13].

APPLICATION

Cadmium concentrations were measured on two different days at 14 various residential and industrial stations in Belgium. Information about the stations is given in Table III. Figures 1 and 2 show the concentration levels of cadmium and total

TABLE III

SAMPLING SITES IN BELGIUM

Name	*Symbol*	*Description*
Antwerp residential	AR	Residential area (large city)
Ghent residential	GR	Residential area (large city)
Brussels residential	BR	Residential area (large city)
Liège residential	LR	Residential area (large city)
Charleroi	CH	Residential area (large city)
Antwerp industrial	AI	Industrial area
Ghent industrial	GI	Industrial area
Liège industrial	LI	Industrial area
Mechelen	ME	Center of medium-sized city
Houffalize	HF	Village in the Ardennes
Mol	ML	Semi-rural area
Ploegsteert	PL	Agricultural area
Zeebrugge	ZB	At the sea-coast
Dourbes	DB	Remote area in the Ardennes

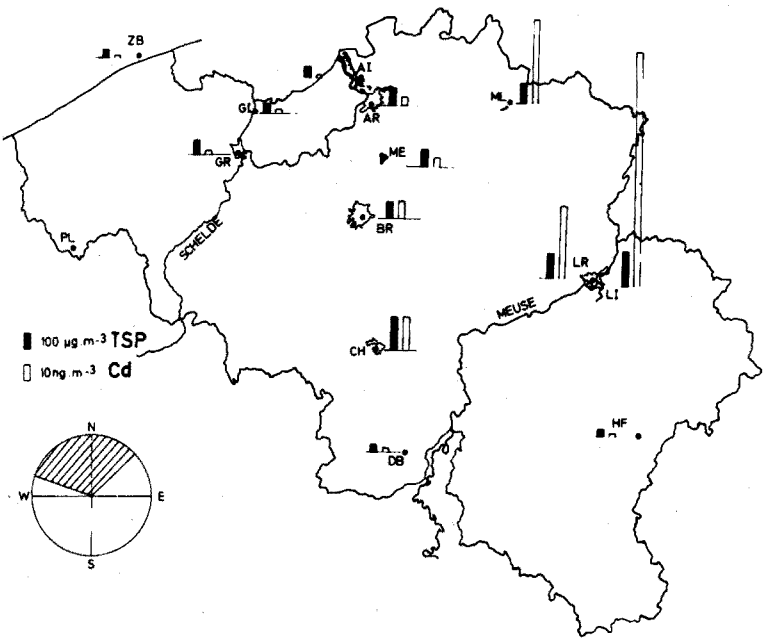

Fig. 1. Cadmium and TSP concentrations at 13 stations and wind-direction on 19.10.1972.

suspended particulate (TSP) at the locations of the stations on 19.10.1972 and 18.12.1972. The nationwide distribution differs from day to day but at the stations in Liège and Mol, the aerosols are always enriched in cadmium.

On 19 October 1972, the TSP showed typical values for Belgium, ranging from 50 to 220 $\mu g\ m^{-3}$, the concentrations of cadmium having much larger

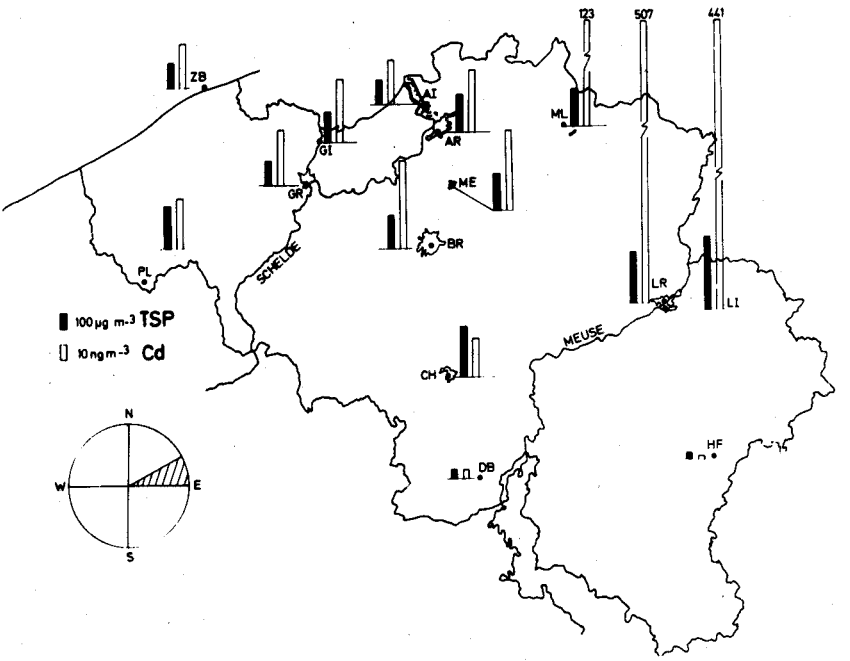

Fig. 2. Cadmium and TSP concentrations at 14 stations and wind-direction on 18.12.1972.

ranges. The highest values were detected at Liège and Mol. On 18 December 1972 the concentration levels of total suspended particulate and most elements were higher than on 19 October 1972. The range of cadmium concentrations was still much larger than on the first day. The second day was in a period of east winds, which brought highly polluted continental air over Belgium. By coincidence, the same east winds caused very high cadmium values in Liège, to the east of which are important metallurgical industries. This coincidence resulted locally in extremely high cadmium values.

There is another non-ferrous metallurgical industry just south of Antwerp. When the winds come from the south or south-southwest, the plume from this factory is blown over the Antwerp residential station (AR), and the concentration of the cadmium is increased by a factor of 10 or more. This effect is shown in Fig. 3, where concentrations of cadmium as parts per million of the total particulate (p.p.m.) collected at station AR are plotted as a function of wind direction.

CONCLUSION

Flameless atomic absorption spectrometry can readily be used for the determination of cadmium in atmospheric aerosols collected on a paper filter. The earlier procedure for ultrasonic removal of lead from the filters in 0.1 *M* nitric acid is also appropriate for the quantitative elution of cadmium. Although the cadmium levels in urban air are one or two orders of magnitude lower than lead, this is compensated by the fact that the sensitivity for cadmium by flameless atomic

absorption spectrometry is one to two orders better than for lead. Thus the same solution can be used for both measurements. Selectivity, reproducibility and sensitivity were found to be entirely satisfactory. Since only a small fraction of the filter is used, most of the filter sample is still available for other chemical analyses. An application has shown the potential interest of cadmium determinations in pollution aerosols.

The authors are indebted to Prof. J. Hoste for his continuous interest and helpful suggestions during the work and to Miss M. Helsen for technical assistance. Thanks are due to Prof. F. Verbeek and Prof. A. Claeys, respectively for the use of the atomic absorption and ashing equipment. This work was supported in part by the "Nationaal Centrum voor de Studie van Luchtverontreiniging door Verbranding".

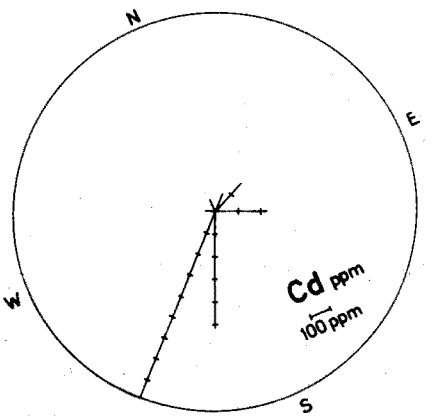

Fig. 3. Cadmium concentrations (p.p.m.) in the aerosol at AR as a function of prevailing wind-directions.

SUMMARY

A sensitive and selective determination of cadmium in aerosols by flameless atomic absorption spectrometry is described. By two successive treatments in 0.1 *M* suprapure nitric acid, the cadmium is removed from the paper filter on which the particulates have been collected. Routinely 10–50 μl of the 100-ml solution are injected into a graphite oven and the % absorption at 228.8 nm is measured. If half a 24-h filter (400 m^3 air) is used, the dilution is made to 50 ml and 50 μl is injected, an unusually low concentration of 0.20 ng m^{-3} can be determined quantitatively with a relative standard deviation of 10%. The reproducibility of the complete procedure is 4.8%. An interlaboratory comparison indicated that the accuracy is very good. The same solution can also be used for lead determination mostly without any further dilution. As an application, the cadmium concentrations were measured on two different days at 14 stations of the nationwide sampling network, and the influence of nonferrous industries on the cadmium levels is shown.

REFERENCES

1 A. Minderhoud and J. P. Boogerd, *Proceedings of the European Colloqium on the Problems of the Contamination of Man and his Environment by Mercury and Cadmium*, Luxembourg, July 1973.
2 *Study of National Air Pollution by Combustion, Progress Report, 1972*, Inst. Nucl. Wet. (Univ. Gent); Lab. Toxicol. (Univ. Liège).
3 R. J. Thompson, G. B. Morgan and L. J. Purdue, *At. Absorption Newslett.*, 9 (1970) 53.
4 M. Beyer, *At. Absorption Newslett.*, 8 (1969) 23.
5 T. Y. Kometani, J. L. Bove, B. Nathanson, S. Siebenberg and M. Magyar, *Environ. Sci. Technol.*, 6 (1972) 617.
6 P. R. Harrison, W. R. Matson and J. W. Winchester, *Atmos. Environ.*, 5 (1971) 613.
7 G. Colovos, G. S. Wilson and J. Moyers, *Anal. Chim. Acta*, 64 (1973) 457.
8 R. Brown, M. L. Jacobs and H. E. Taylor, *Int. Lab.*, 1 (1973) 32.
9 G. B. Morgan and R. E. Homan, Pittsburgh Analytical Conference, Cleveland, Ohio, (1968).
10 M. Janssens and R. Dams, *Anal. Chim. Acta*, 65 (1973) 41.
11 R. Dams and R. Heindryckx, *Atmos. Environ.*, 7 (1973) 319.
12 L. A. Currie, *Anal. Chem.*, 40 (1968) 586.
13 L. Gorski, Int. Atom. Energy Agency, Vienna, private communication.

Analytica Chimica Acta, 70 (1974) 35–39

APDC–MIBK EXTRACTION SYSTEM FOR THE DETERMINATION OF COPPER AND IRON IN 1 CM^3 OF SEA WATER BY FLAMELESS ATOMIC-ABSORPTION SPECTROMETRY

K. KREMLING and H. PETERSEN

Institut für Meereskunde, Düsternbrooker Weg 20, 23 Kiel (Germany)

(Received 1st October 1973)

In spite of the increasing attention that trace metals in sea water have received in recent years, our knowledge of their role in the biochemical and geochemical cycles of the oceans, and of their horizontal, vertical and seasonal variations is only fragmentary. Many of these efforts have been hindered or prevented by difficulties in analytical techniques.

One of the modern instrumental methods promising more success in this field is flameless atomic-absorption spectrometry. The development of atomizers such as the graphite tube furnaces of Massmann[1] and L'vov[2] has made it possible to determine very much smaller amounts than can be done by conventional atomic-absorption techniques. The smaller samples required need only small containers which are more convenient for cleaning, sampling and preventing contamination.

This paper describes the development of a method for the determination of copper and iron in 1-cm^3 samples of oceanic waters based on the chelation of the metals with ammonium pyrrolidinedithiocarbamate (APDC) and extraction of the chelates into methyl isobutyl ketone (MIBK). The method was first applied to sea water by Brooks *et al.*[3] and improved by Brewer *et al.*[4]; the two procedures required volumes of about 750 and 400 cm^3 of sea water, respectively.

This technique was selected for further study in view of the advantage of simultaneous extraction of several metals and the sensitivity of flameless atomic-absorption spectrometry, although the concentrations of trace metals reported by this method represent only that available to the chelation–solvent extraction process. With a phase ratio of nearly 1 (volume ratio of the aqueous to the organic phase), the extraction proceeds completely and a second extraction becomes unnecessary[3]. The standard addition method[4] is employed for evaluation of the measurements, thus eliminating interferences from different chemical compositions of samples.

Attempts to analyze for trace metals by direct atomization of sea water were shown by Segar and Gonzales[5] to be unsatisfactory, owing to scattering interferences by the major components.

EXPERIMENTAL

Reagents

Ammonium pyrrolidinedithiocarbamate (APDC). Prepare a 2% solution (w/v)

by dissolving 1 g of APDC (Merck) in 50 cm^3 of distilled water, add 10 cm^3 of MIBK and shake for 10 min in a funnel to purify the reagent. After separation run off the aqueous layer into a quartz vessel. The solution must be prepared daily.

Methyl isobutyl ketone (MIBK). Redistil the commercial-grade reagent (Riedel-de-Haen AG) very slowly and carefully in a quartz still; no blank value for copper and iron should then be detected. Store the MIBK in a quartz vessel. Test the solvent before starting the extraction process.

Hydrochloric acid. Redistil from purified hydrochloric acid ("Suprapur", Merck), standardize and dilute to a 0.01 *N* solution.

Standard metal solution. Prepare a standard stock solution (pH 2) of 1000 p.p.m. copper and 1000 p.p.m. iron (Titrisol, Merck). From this stock solution, prepare daily a 0.1 p.p.m. working standard (pH 2) by dilution.

Instrumentation

A Perkin-Elmer Model 403 atomic absorption spectrophotometer equipped with a Rikadenki Kogyo Model Mark II recorder, a deuterium arc background corrector and a Perkin-Elmer HGA-72 heated graphite atomizer was employed. The instrumentation has been fully described by Welz[6]. For better precision and higher sensitivity, the special grooved graphite tube was used. A simple modification was made to the spectrophotometer for balancing the energies of the copper cathode lamp and the deuterium arc corrector. For this purpose, a shutter (diam. 7 mm) was installed behind the cathode lamp to lower its energy flow. Argon was used as the purging gas with a flow rate of 1.7 $dm^3\ min^{-1}$. All measurements were made in air-filtered rooms.

Extractions were carried out in quartz tubes (length 7 cm, diam. 0.7 cm). The stoppers were of polypropylene, which however remained untouched by solvent during the mixing and extraction processes. The tubes were cleaned with an APDC–MIBK mixture, rinsed with MIBK and dried with purified acetone. If this cleaning process is well done, no blank value should be detected after shaking with MIBK.

All additions of reagents and sample injections were made with Eppendorf microlitre pipettes. Their plastic tips must be cleaned in the same manner as described for the quartz tubes, otherwise large contamination effects can be observed.

The mixing and extraction process was done with an Eppendorf rotating mixer Model 3300 which allowed the simultaneous handling of 24 tubes.

Procedure

To each quartz tube, add 1.000 cm^3 of sea water, 0.1 cm^3 of 0.01 *M* hydrochloric acid, 0.050 cm^3 of APDC solution; and 0, 0.030, 0.060 and 0.090 cm^3 of the working standard solution. The chelation proceeds at pH 3–4. After mixing for 2 min, add 1.000 cm^3 MIBK to the tube, and mix for 3 min.

Allow the phases to separate (about 10 min), and start measurement of the metal content by the atomic absorption spectrophotometer with the temperature programme described in Table 1. For stability of complexes, iron should be measured within 3 h after the extraction process, whereas the copper

TABLE I

PROGRAMME FOR THE HGA-72 FURNACE

	Fe (248.3 nm) after 10 min – 3 h				*Cu (324.7 nm) after 2–22 h*			
Step	(1)[a]	(2)[b]	(3)[c]	(4)[d]	(1)[a]	(2)[b]	(3)[c]	(4)[d]
Temp. (°)	100	1400	2200	–	100	900	2200	–
Times (s)	90	60	10	60	90	240	10	60

[a] Evaporation of MIBK (3×0.10 cm^3).
[b] Heat combustion of organic material.
[c] Atomization (with GAS STOP).
[d] Cooling period.

complex is stable for about 22 h without any loss of absorbance. This is in good agreement with the results of Brooks *et al.*[3].

Inject the MIBK solvent with a 0.100 cm^3 pipette and evaporate by step (1). To obtain higher absorbance, the metal quantity in the graphite tube is enriched by repeating this step 3 times, so that the overall volume needed is 0.300 cm^3.

The temperature programmes for iron and copper differ in the heat combustion step (2). A lower temperature is necessary for copper because it starts to atomize above 950°; therefore more time is needed for complete removal of the organic material. The atomization step (3) is carried out with the GAS STOP programme, which provides an increased sensitivity of nearly 100%. Because of the higher impedance of the grooved furnace, its maximum temperature is limited to about 2200°. Step (4) is provided for cooling the tube with which about 100 measurements may be made.

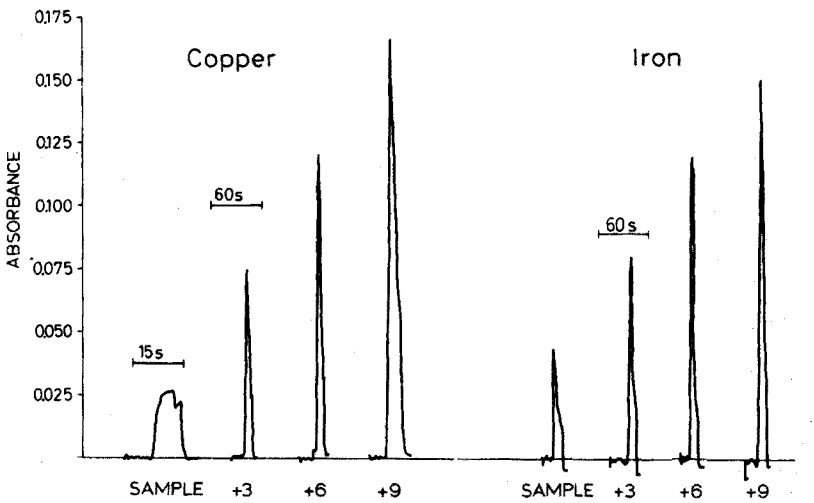

Fig. 1. A set of atomization peaks (with deuterium arc corrector) for copper and iron. The second peak of the copper "Sample" probe indicates the furnace emission. The numbers on the horizontal axis represent the metal added in μg dm^{-3}.

A typical set of recorded curves is shown in Fig. 1. The recorder speed was normally 2 cm min^{-1}; but, to separate the atomization peak for copper clearly from the emission signal of the heated graphite tube, a speed of 8 cm min^{-1} was used for the copper "Sample" probe. Optical modifications recently made to Perkin-Elmer double-beam spectrophotometers seem to overcome the emission problem[7].

CALCULATIONS

The calculation of the metal concentrations is illustrated in Fig. 2. The measured absorbance values and the quantity of standard in nanograms, added to each 1-cm^3 aliquot of sea water, are plotted as coordinates. The linear regression lines are fitted by the method of least squares. The intercept gives the amount of metals in 1 cm^3 of seawater, which equals the concentration in μg dm^{-3}.

The precision of the method was tested by 10 replicate measurements of a filtered sample (0.4 μm Nuclepore filter) with mean concentrations of 3.5 μg Fe dm^{-3} and 1.6 μg Cu dm^{-3}. The standard deviations of the whole procedure were found to be 17 and 14%, respectively.

Some results for sea water are shown in Table II. The samples were obtained from the area of upwelling of the tropical north-east Atlantic Ocean during Cruise 26 of the R.V. "Meteor" in 1972. The copper and iron concentrations measured are in the same range as found by Riley and Taylor[8] in this area, despite the different filtration and pre-concentration steps used in the two investigations. Although the locations are nearly identical, substantial variations can be observed from station to station. This fact is, as yet, unexplained, but seems to be mainly caused by adsorption processes.

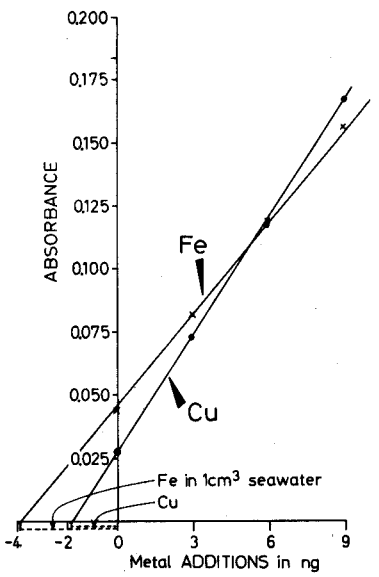

Fig. 2. Method of calculation of results.

TABLE II

ANALYSIS OF SEA WATER FROM THE TROPICAL NORTH-EAST ATLANTIC OCEAN

Location	*Depth (m)*	*Concentration ($\mu g\ dm^{-3}$)*	
		Fe	*Cu*
19°10'N	0	5.5	1.9
16°54'W	7	1.3	2.2
	15	8.5	1.8
	30	3.2	1.2
	200	3.9	3.0
	300	1.6	3.5
	400	3.1	2.8
19°04'N	0	2.6	1.4
16°50'W	15	6.6	4.2
	30	4.8	2.8
	75	2.6	0.7
	200	3.7	1.2
	300	4.1	2.3
	400	3.0	1.3
19°06'N	0	5.1	2.9
16°52'W	11	3.7	2.0
	23	3.9	2.0
	75	8.1	3.4
	200	2.8	3.1

The authors acknowledge the financial support of Deutsche Forschungsgemeinschaft.

SUMMARY

A micro APDC–MIBK extraction method is described for the simultaneous determination of copper and iron in 1-cm^3 samples of sea water by flameless atomic-absorption spectrometry with a HGA-72 graphite atomizer. Replicate analyses of Atlantic sea water with mean concentrations of 1.6 μg Cu dm^{-3} and 3.5 μg Fe dm^{-3} showed standard deviations of 14% and 17%, respectively.

REFERENCES

1 H. Massmann, *Spectrochim. Acta*, 23B (1968) 215.
2 B. V. L'vov, *Spectrochim. Acta*, 24B (1969) 53.
3 R. R. Brooks, B. J. Presley and I. R. Kaplan, *Talanta*, 14 (1967) 809.
4 P. G. Brewer, D. W. Spencer and C. L. Smith, *Atomic Absorption Spectroscopy*, ASTM/STP 443, American Society for Testing and Materials, 1969, p. 70.
5 D. A. Segar and J. G. Gonzales, *Anal. Chim. Acta*, 58 (1972) 7.
6 B. Welz, *CZ-Chemie-Technik*, 1 (1972) 455.
7 J. D. Kerber, A. J. Russo, G. E. Peterson and R. D. Ediger, *At. Absorption Newslett.*, 12 (1973) 106.
8 J. P. Riley and D. Taylor, *Deep-Sea Res.*, 19 (1972) 307.

Analytica Chimica Acta, 70 (1974) 41–47

MERCURY CONCENTRATIONS IN FISH FROM THE GREAT SMOKY MOUNTAINS NATIONAL PARK

JOHN W. HUCKABEE, CYRUS FELDMAN and YAIR TALMI

Environmental Sciences Division and Analytical Chemistry Division, Oak Ridge National Laboratory, Oak Ridge, Tennessee 37830 (U.S.A.)

(Received 17th September 1973)

Mercury occurs ubiquitously at low concentrations in the environment, but the discharge of various mercurial compounds has had detrimental ecological and epidemiological effects[1,2]. Fish especially tend to concentrate mercury in their tissues, and mercury concentrations in fish ostensibly due to pollution have been well documented[2–7]. Mercury concentrations in fish tissue exceeding 1.0 p.p.m. (Sweden) or 0.5 p.p.m. (United States) are considered to be dangerous for human consumption. Based on government standards, thousands of pounds of commercial fish have been found unfit for eating[8,9].

The natural background concentrations of mercury in fish—concentrations probably harmless to consumers—have not been well defined. Naturally-occurring mercury is widely but unevenly distributed as mercury(II) sulfide in sandstones and other clastic sedimentary rocks[10]. Magmatic and metamorphic rocks usually contain smaller concentrations of mercury than sedimentaries. Because of this inhomogeneity of mercury distribution, the background mercury concentrations in fish and other organisms should vary from region to region[11]. Mean background values reported for natural mercury concentrations in fish range from 0.2 to 0.02 p.p.m.[2,12]. These values are based on extrapolations from the literature, on composite samples, or on small sample sizes.

Natural background concentrations of mercury are difficult to determine because few areas are free from all sources of mercury pollution. Even in areas distant from pollution sources, mercury is introduced into the environment through the impingement of mercury vapor and the fallout of fly ash derived from the burning of mercury-containing coal[1,4,13–15].

In order to obtain data of mercury concentrations in fish at or near natural background levels, 198 fish of five species were collected from three high-altitude streams remote from pollution sources in the Great Smoky Mountains National Park (83° 25′–50′ west longitude by 35° 30′–35′ north latitude) during May and June 1972. A second collection of fish of the same species was made from Hazel Creek in May 1973 in order to validate the 1972 data and to extend the analyses to methylmercury. Although most of the mercury reported in fish tissue is in the methyl form[3,16,17], the site of methylation is in doubt. Jensen and Jernelov[18] found that bacteria in sediments could methylate other forms of mercury, but Spangler *et al.*[19] demonstrated that demethylation processes by microbes in sediments probably reduce some or all of the methyl form to metallic mercury. Indeed, very

little methylmercury has been discovered in sediments or the overlying water.

The section of the Park in which the study streams are located is incompletely mapped geologically, but the bedrock on which the streams flow is probably the partially metamorphosed clastic sediments of the Precambrian Ocoee Series. There are some abandoned copper mines in the study area (near Hazel Creek) in which the ore was the sulfide minerals of Cu and Fe, with some Zn and traces of Pb, Co, and As[20]. No cinnabar (HgS) was detected.

Sampling techniques

The study streams are located in remote sections of the park and are accessible only on foot or horseback. Since the trails down each drainage end at the waters of Fontana Reservoir, there is little horse traffic. Historically the area was heavily logged, but all commercial activity was phased out in 1926. In 1972 rainbow trout (*Salmo gairdneri*) and stonerollers (*Campostoma anomalum*) were collected at 550-m elevation in all three streams. Rainbow trout were collected at 580 m in Hazel Creek and at 850 and 1225 m in Forney Creek. Eastern brook trout (*Salvelinus fontinalis*) were collected at elevations between 1150 and 1225 m in all three streams. Rosyside dace (*Clinostomus funduloides*) and banded sculpin (*Cottus carolinae*) were collected at 550 m in Hazel Creek.

Examination of the variance of the 1972 data indicated that the 1973 collection should contain at least 20 fish. Based upon this estimate four stonerollers, two rosyside dace, five banded sculpin, seven rainbow trout, and three brook trout were collected in Hazel Creek in May 1973. The brook trout were taken at 1225 m; the other species at 550 m. The fish sampled represent two trophic levels: trout, dace, and sculpins are predators, and stonerollers feed on periphyton. None of the streams are stocked with hatchery fish; the rainbow trout were introduced approximately 50 years ago. Sediment samples were also collected in 1972 at 550 m in each of the three streams.

Most of the fish collecting was done by electroshocking, but the discharge and gradient of the streams at the lower reaches were too great for this method to be effective on the trout. Trout collections in the lower reaches were by angling. All fish samples were immediately frozen in Dewar flasks containing Dry Ice for transport to the laboratory. The gastrointestinal tracts were removed from all the stonerollers to avoid the possibility of prejudicing the analyses with mercury-containing sediment or food organisms. Comparative analyses of trout samples were made with the gastrointestinal tract present and removed. A comparison was also made of mercury content in trout by dissolving separately for analysis the whole fish and a strip of axial muscle tissue. Under conditions of chronic exposure to mercury, the muscle tissue of fish contains the greatest percent of the total mercury body burden[21].

EXPERIMENTAL

Total mercury

The cold-vapor atomic absorption method is the most sensitive method currently available for the determination of total mercury. The procedure involves the conversion of all mercury compounds to inorganic mercury(II), reduction, and

sparging elemental mercury into an atomic absorption cell. However, it is necessary first to destroy all organic compounds present.

The procedure finally adopted was a modification of the perchloric–nitric acid procedure[22], with air-cooled and water-cooled condensers connected in series over the reaction vessel. This apparatus will wet-ash fish samples up to 5 g without losing mercury, but the condenser and stopcock arrangement is too complicated for the wet-ashing of many (*e.g.* 20) samples simultaneously. A simplified apparatus was developed, taking advantage of the fact that volatile mercury(II) compounds have lower vapor pressures than nitric acid, water or the higher perchloric acid hydrates.

Apparatus. The reaction flask was a 250-ml volumetric flask, of the wide-bottomed (Kimax) design. Each flask was fitted with an air condenser consisting of a male 19/38 standard taper borosilicate glass joint, the exposed part of which was enclosed in a suitable length of 7/8-in. woven asbestos tubing. This tubing was held in place by wrapping with Teflon sealing tape. The overall height of the assembly was 42 cm.

Procedure. Transfer each sample (5 g or less) to a flask which has been baked overnight at 450°. Add *ca.* 20 mg of potassium dichromate, 10–15 ml of concentrated nitric acid and 15 ml of 60% perchloric acid. Fit with the air condenser, and heat for 30 min on a hotplate with a surface temperature of 230° 30 min at a surface temperature of 250°, and then at a surface temperature of 340° until the solution (originally brown or tan, and then green) turns orange. Cool, rinse the condenser into the flask, remove, and fill the flask to the mark with demineralized water. This solution was then analyzed by the cold-vapor atomic absorption method.

Recovery of added organic and inorganic compounds of mercury by this procedure averaged 96–102%. A thoroughly homogenized and freeze-dried sample of tuna was analyzed by the above procedure, by neutron activation analysis (with chemical isolation of carrier added after irradiation), and by isotope dilution mass spectrometry[23]; excellent agreement was found among the three analyses (0.425, 0.45, and 0.45 p.p.m., respectively). Since the last two procedures have essentially no inherent risk of error from loss of mercury during analysis, the agreement indicates that mercury also was not lost during the present wet-ashing procedure.

Methylmercury

The analytical detection system for organomercurials consisted of a gas chromatograph equipped with a microwave emission spectrometric detector. This system[24–26] provides better sensitivity and selectivity than any other chromatograph system available with the possible exception of the g.c.–m.s. system. The microwave emission detector sensitivity is generally independent of the molecular structure of the mercurial analyzed in contrast to the widely used electron capture detector. Thus, the detectability of the system for either CH_3HgCl or $(CH_3)_2Hg$ is at the 3–8 pg range.

Procedure. Homogenize the fish tissue, and weigh 0.5–1.0 g of it into a centrifuge tube. Add 1 ml of concentrated hydrochloric acid and 2 ml of water to the sample before it is thoroughly mixed (3 min). Add 3–5 ml of benzene to the centrifuge tube, shake vigorously for 5 min, and then centrifuge. Inject 1–20 μl of the

dried (over anhydrous sodium sulfate) benzene layer into the g.c. column, and monitor the emission intensity at the 253.7-nm Hg spectral line.

Calculate concentrations of CH_3HgCl by comparing the emission intensity (peak height) to a standard curve resulting from chromatography of pure standard.

Since it was found that the extraction efficiency is in the 75–90% range, the extraction procedure should be repeated.

The excellent selectivity provided by the g.c.–microwave emission system eliminates the need for the tedious and time-consuming cleanup procedures of the organic extract. Also, the extracts can be injected at the rate of 30–50 per h compared to 1–2 per h with conventional systems. Typical accuracy values at the 10–40 p.p.b. CH_3HgCl in fish were 4–12%; reproducibility, expressed as relative standard deviation, was 3–10%.

RESULTS AND DISCUSSION

There was very little difference in the total mercury content of three sediment samples taken at 550 m in all three streams. Samples from Hazel Creek had 0.004 p.p.m. mercury; from Eagle Creek, 0.004 p.p.m.; and from Forney Creek 0.005 p.p.m. Almost all reports of analyses for mercury in fish and other organisms show wide variability of mercury concentration in tissue. The actual amounts —nanograms and less—are very small, so that a large percentage variation actually involves only a small quantity of mercury. The known heterogeneity of mercury distribution in rocks could easily account for the observed differences in mercury concentrations for fish from a single stream[1].

TABLE I

TOTAL MERCURY CONCENTRATIONS IN FISH FROM HIGH ALTITUDE STREAM IN GREAT SMOKY MOUNTAINS

Species	*Stream*	*Elevation (m)*	*n*	$\bar{x}$ *(p.p.m.)*	*(Range)*	*±1 SE*
Salmo gairdneri (Rainbow trout)	Hazel Creek	550	15	0.023	(0.006–0.147)	0.009
		580	12	0.060	(0.016–0.177)	0.013
	Eagle Creek	550	11	0.014	(0.008–0.020)	0.001
	Forney Creek	550	17	0.040	(0.003–0.097)	0.006
		850	12	0.042	(0.024–0.061)	0.003
		1225	8	0.042	(0.030–0.056)	0.002
	Total, all streams		75	0.036	(0.003–0.177)	0.003
Salvelinus fontinalis (Eastern brook trout)	Hazel Creek	1225	9	0.019	(0.014–0.030)	0.001
	Eagle Creek	1150	7	0.002	(0.0007–0.005)	0.0003
	Forney Creek	1220	3	0.053	(0.046–0.064)	0.005
	Total, all streams		19	0.018	(0.0007–0.064)	0.004
Campostoma anomalum (Stoneroller)	Hazel Creek	550	18	0.031	(0.015–0.070)	0.003
	Eagle Creek	550	9	0.059	(0.031–0.076)	0.004
	Forney Creek	550	6	0.033	(0.009–0.083)	0.011
	Total, all streams		33	0.039	(0.009–0.083)	0.003
Clinostomus funduloides (Rosyside dace)	Hazel Creek	550	44	0.044	(0.026–0.129)	0.002
Cottus carolinae (Banded sculpin)	Hazel Creek	550	27	0.025	(0.006–0.105)	0.003

Table I shows the mercury concentrations in fish from Hazel Creek, Eagle Creek, and Forney Creek. Two-way analysis of variance and Scheffe's Multiple-Comparison test showed that the difference in mercury concentration in rainbow trout from each of the three streams was significant at the 0.05 level, and the differences in brook trout and stonerollers from each of the three streams were significant at the 0.01 level.

Within one stream (Hazel Creek), the mercury concentrations of brook trout and sculpin were not statistically distinct from each other, but mercury concentrations in brook trout–sculpin, rainbow trout, stonerollers and rosyside dace were significantly different from all other species at the 0.05 level. In Hazel Creek, the order of mercury concentration (p.p.m.) from highest to lowest was: rosyside dace (0.044) > rainbow trout (0.040) > stoneroller (0.031) > brook trout (0.019)–sculpin (0.025); rosyside dace and sculpin were not found in Eagle and Forney Creek. There was no systematic change in mercury concentration in the fish along the elevational gradient sampled. No differences (normalized to weight) were detected when the whole fish was analyzed or when only axial musculature was analyzed, nor when the whole fish or fish with gastrointestinal tracts removed were analyzed.

Table II shows that the total mercury concentration of the 1973 collection was very similar to the 1972 collection. Comparison of the mean values of all observations in both collections shows that the total mercury concentration in 1972 averaged 0.035 ± 0.001, and in 1973 averaged 0.036 ± 0.003. Methylmercury determinations showed that 93 ± 2.6 % of the mercury present in the fish tissue was in the methyl form, in agreement with a recent report on fish methylmercury levels[17].

The relative importance of direct uptake of mercury and food chain uptake of mercury by fish is not clear. Hannerz[27] conducted a series of experiments which indicated that direct uptake of mercury was more significant than food chain uptake to total body burden of mercury in fish, but he warned that his data were preliminary. He found no evidence of trophic level magnification of mercury. Wobeser *et al.*[7] analyzed 81 fish of 10 species from the Saskatchewan River and found no evidence of varying mercury concentration with trophic level. The results of the present study also indicate no clear trophic level concentration since the predatory trout and sculpin had lower mean tissue mercury concentrations than the stonerollers (primary consumer) taken at the same sampling station (Table I). The highest mercury concentrations were found in the predatory rosyside dace.

The brook trout, which were collected at the highest altitude and the greatest distance ($\geqslant$25 km) from the industrialized Appalachian Valley, had the lowest mean concentrations of mercury, but this could be a species difference rather than a geographical difference. Mercury concentrations have been measured in brook and rainbow trout before. Zitko *et al.*[28] analyzed seven brook trout in Canada and found a range from 0.08 to 0.13 p.p.m. (wet weight) methylmercury. In Idaho, Gebhards *et al.*[29] measured mercury concentrations by neutron activation analysis in wild and hatchery-reared rainbow trout. The 16 wild fish had a mean of 0.31 p.p.m. (wet weight) mercury with a range of <0.008–0.6 p.p.m., and the hatchery fish had a mean mercury concentration of 0.10 p.p.m. with a range of 0.05–0.17 p.p.m.

TABLE II

MERCURY AND METHYLMERCURY CONCENTRATIONS IN FISH FROM A HIGH ALTITUDE STREAM (HAZEL CREEK) IN GREAT SMOKY MOUNTAINS NATIONAL PARK IN 1973

Species	*Wt (g)*	*Total mercury*[a] *(p.p.m.)*	*Methylmercury*[b] *(p.p.m.)*	*Methylmercury (%)*
Campostoma anomalum	6.78	0.055	0.055	100
(Stoneroller)	5.43	0.031	0.030	96
	7.07	0.029	0.022	75
	3.93	0.018	0.016	88
Clinostomus funduloides	5.64	0.037	0.040	108
(Rosyside dace)	4.78	0.025	0.025	100
Cottus carolinae	4.74	0.023	0.020	86
(Banded sculpin)	3.91	0.020	0.021	105
	3.39	0.017	0.015	88
	4.86	0.017	0.014	82
	7.12	0.037	0.033	89
Salmo gairdneri	17.7	0.038	0.029	76
(Rainbow trout)	16.0	0.029	0.032	110
	54.9	0.098	0.083	84
	30.5	0.043	0.048	111
	11.2	0.036	0.035	97
	9.4	0.032	0.029	90
	13.5	0.041	0.033	80
Salvelinus fontinalis	11.4	0.039	0.030	81
(Brook trout)	11.5	0.039	0.045	115
	11.1	0.041	0.035	85
	$\bar{x} \pm 1$ SE	0.035 ± 0.003	0.033 ± 0.003	93 ± 2.6

[a] By cold vapor atomic absorption.
[b] By gas chromatography.

When compared with the meager literature, it appears that the mercury concentrations reported here may be close to the minimum that can be expected in nature for these fish species, but species differences in mercury concentrations are detectable, although very small. It also appears that most of the mercury in fish tissue is present as methylmercury.

This survey was conducted with the permission and cooperation of the U.S. National Park Service. Paul F. McCrary, Chief of Interpretation, was instrumental in making the work possible. Ronald D. Jones, Fisheries Management Biologist, Bureau of Sport Fisheries and Wildlife, his staff, and his equipment were essential in the planning and collecting phases of the study. This research was sponsored by the U.S. Atomic Energy Commission and the National Science Foundation under contract with the Union Carbide Corporation.

SUMMARY

Excessive mercury concentrations ostensibly due to pollution have been widely

reported in fish tissue. The concentrations of mercury occurring naturally in fish tissue have not been well defined. A collection for mercury analysis of 198 fish of five species was made in 1972 in three high altitude streams in the Great Smoky Mountains, 20–25 km from the nearest pollution source. Mercury concentrations were (means, p.p.m.): rainbow trout (*Salmo gairdneri*), 0.036; brook trout (*Salvelinus fontinalis*), 0.018; banded sculpin (*Cottus carolinae*), 0.025; rosyside dace (*Clinostomus funduloides*), 0.044; stoneroller (*Campostoma anomalum*), 0.039. There was no significant difference in mercury concentration among fish analyzed whole, with gastrointestinal tract removed, or a strip of axial musculature. There was a significant ($P > 0.05$) difference in mercury concentration among species in one stream and in three species from different streams. A second collection of fish of the same species in 1973 verified the 1972 results. Methylmercury constituted $93 \pm 2.6\%$ of total mercury. These results indicate that all fish acquire about the same tissue concentrations of mercury at chronic exposure to very low levels.

REFERENCES

1 M. Fleischer, *U.S. Geol. Surv., Pap.*, 713 (1970) 6.
2 R. A. Wallace, W. Fulkerson, W. D. Shultz and W. S. Lyon, USAEC Rpt. ORNI-NSF-EP-1, Oak Ridge National Laboratory, Oak Ridge, Tennessee, 1971.
3 C. A. Bache, W. H. Gutenmann and D. J. Lisk, *Science*, 172 (1971) 951.
4 A. G. Johnels and T. Westermark in M. W. Miller and G. G. Berg (Eds.), *Chemical Fallout*, Thomas, Springfield, Ill., 1968, p. 221.
5 N. Fimreite, W. N. Holsworth, J. A. Keith, P. A. Pearce and I. M. Gruchy, *Can. Field Nat.*, 85 (1971) 211.
6 Ronald J. Evans, Jack D. Bails and Frank M. D'Itri, *Technical Report*, No. 22, Institute of Water Research, Michigan State University, 1972.
7 G. Wobeser, N. O. Nielsen and R. H. Dunlop, *J. Fish. Res. Board Can.*, 27 (1970) 830.
8 J. F. Uthe and E. G. Bligh, *J. Fish. Res. Board Can.*, 28 (1971) 786.
9 N. Nelson, *Environ. Res.*, 4 (1971) 1.
10 V. M. Goldschmidt, *Geochemistry*, Oxford University Press, London, 1958, pp. 4, 725.
11 A. P. Pierce, J. M. Botbol and R. E. Learned, *U.S. Geol. Surv., Prof. Pap.*, 713 (1970) 14.
12 R. C. Harriss, *Biological Conservation*, 3 (1971) 279.
13 K. K. Bertine and E. D. Goldberg, *Science*, 173 (1971) 233.
14 O. I. Joensuu, *Science*, 172 (1971) 1027.
15 J. W. Huckabee, *Atmospheric Environment*, 7 (1973) 749.
16 L. R. Kamps, R. Carr and H. Miller, *Bull. Environ. Contam. Toxicol.*, 8 (1972) 273.
17 G. Westoo, *Science*, 181 (1973) 567.
18 S. Jensen and A. Jernelov, *Nature*, 223 (1969) 753.
19 W. J. Spangler, J. L. Spigarelli, J. M. Rose and H. M. Miller, *Science*, 180 (1973) 192.
20 G. H. Espenshade, *Geol. Ser. Bull.*, 1142-I, U.S. Government Printing Office, Washington D.C., 1963.
21 A. Jernelov and H. Lann, *Oikos*, 22 (1971) 403.
22 G. F. Smith, *Anal. Chim. Acta*, 8 (1953) 397.
23 C. Feldman, J. A. Carter and L. C. Bate, *Environment*, 14 (1972) 48.
24 A. J. McCormack, S. C. Tong and W. D. Cook, *Anal. Chem.*, 37 (1965) 1470.
25 C. A. Bache and D. J. Lisk, *Anal. Chem.*, 37 (1965) 1477; 40 (1968) 2224.
26 Y. Talmi and R. Crossmun, *Ecology and Analysis of Trace Contaminants*, ORNL-NSF-EATC-1, 1973.
27 L. Hannerz, *Inst. Freshwater Drottingholm*, 48 (1968) 120.
28 V. Zitko, B. J. Finlayson, D. J. Wildish, J. M. Anderson and A. C. Kohler, *J. Fish. Res. Board Can.*, 28 (1971) 1285.
29 S. Gebhards, J. E. Cline, F. Shields and L. Pearson, *J. Idaho Acad. Sci.*, Special Research Issue No. 2, 1971, p. 44.

Analytica Chimica Acta, 70 (1974) 49–56

DETERMINATION OF STABILITY CONSTANTS OF COMPLEXES FROM SPECTROPHOTOMETRIC DATA WITH A DIGITAL COMPUTER

M. C. CHATTOPADHYAYA and R. S. SINGH
Chemistry Department, Indian Institute of Technology, Powai, Bombay 400076 (India)
(Received 11th September 1973)

Spectrophotometric methods have been widely used for determining the stability constants of metal complexes. With the increasing use of computers, several methods have been suggested which do not involve any approximation in the calculations[1–3]. Gans and Irving[4] have recently described a method for calculation of stability constants of weak complexes from spectrophotometric data. In the present paper, a method is described for the calculation of the stability constant as well as the molar absorptivity of complexes of the type ML_n, where $n = 1, 2, 3, \ldots$.

MATHEMATICAL EXPRESSIONS

Consider the formation of a 1:1 species. The stability constant for the complex can be expressed as

$$\beta_1 = \frac{[ML]}{(M^0 - [ML])(L^0 - [ML])} \tag{1}$$

where M^0 and L^0 are the analytical concentrations of metal ion and ligands, respectively. If metal ion, ligand, and complex absorb light in the region of study, the absorbance, for unit path, can be expressed as

$$A = (M^0 - [ML])\varepsilon_m + [ML]\varepsilon_c + (L^0 - [ML])\varepsilon_l \tag{2}$$

where ε_m, ε_c and ε_l are the molar absorptivities of the species M, ML and L, respectively.

The value of [ML] can be calculated from eqn. (2) provided that ε_m, ε_c and ε_l are known. The direct evaluation of ε_m and ε_l is often possible, but the direct evaluation of ε_c is not always possible. The addition of excess of ligand for the determination of ε_c may result in the formation of higher complexes, or if the complex is very weak, complete conversion of metal ion into ML may not be possible. To avoid this, solutions can be prepared by mixing metal ion and ligand in a 1:1 ratio at different concentrations, and their absorbance measured at a suitable wavelength. The value of ε_c can be calculated as follows.

From eqns. (1) and (2):

$$\frac{M^0 L^0}{A - \varepsilon} - \frac{M^0 + L^0}{\varepsilon_0} + \frac{A - \varepsilon}{\varepsilon_0^2} = \frac{1}{\varepsilon_0 \beta_1} = \text{constant} \tag{3}$$

where

$$\varepsilon = \varepsilon_m M^0 + \varepsilon_l L^0 \tag{4}$$

and

$$\varepsilon_0 = \varepsilon_c - \varepsilon_m - \varepsilon_l \tag{5}$$

For two solutions with different amounts of metal ion and ligand, we can write

$$\left(\frac{M_1^0 L_1^0}{A_1 - \varepsilon_1} - \frac{M_2^0 L_2^0}{A_2 - \varepsilon_2}\right)\varepsilon_0^2 + (M_2^0 + L_2^0 - M_1^0 - L_1^0)\varepsilon_0 + A_1 - \varepsilon_1 - A_2 + \varepsilon_2 = 0 \tag{6}$$

The quadratic eqn. (6) can be solved to give two values for ε_0. The conditions for ε_0 to be positive and real are:

$$b^2 > 4ac\,, \tag{7}$$

and

$$[-b + (b^2 - 4ac)^{\frac{1}{2}}] > 0 \tag{8}$$

where

$$b = (M_2^0 + L_2^0) - (M_1^0 + L_1^0) \tag{9}$$

$$a = \frac{M_1^0 L_1^0}{A_1 - \varepsilon_1} - \frac{M_2^0 L_2^0}{A_2 - \varepsilon_2} \tag{10}$$

and

$$c = A_1 - \varepsilon_1 - A_2 + \varepsilon_2 \tag{11}$$

To account for the statistical fluctuations, a number of solutions could be prepared with different metal ion and ligand concentrations. If n such solutions are prepared, n_{C_2} pairs could be formed and hence $(n-1)n/2$ quadratic equations could be solved for ε_0. The average of all these values will give the desired ε_0. Knowing ε_c, ε_m and ε_l, one can calculate [ML] from eqn. (2) and then substitute the value of [ML] in eqn. (1) to obtain the value of β_1. If a digital computer is available, the value of n can be kept as high as 9 or 10 and 36 or 45 quadratic equations can be solved. The value of ε_c can also be found at different wavelengths and all these values should give the same value of β_1.

If the complex is the only absorbing species, eqn. (6) simplifies to:

$$\left(\frac{M_1^0 L_1^0}{A_1} - \frac{M_2^0 L_2^0}{A_2}\right)\varepsilon_c^2 + (M_2^0 + L_2^0 - M_1^0 - L_1^0)\varepsilon_c + A_1 - A_2 = 0\,. \tag{12}$$

The above concept can be extended to a 1:2 complex for which the stability constant can be written as

$$\beta_2 = \frac{[ML_2]}{\{M^0 - [ML_2]\}\{L^0 - 2[ML_2]\}^2} \tag{13}$$

If metal ion, ligand, and complex all absorb light in the region of interest and if the concentration of the intermediate complex (1:1) is negligible, the absorbance, for unit path length, can be expressed as

$$A = (M^0 - [ML_2])\varepsilon_m + (L^0 - 2[ML_2])\varepsilon_l + [ML_2]\varepsilon_2 \tag{14}$$

From eqns. (13) and (14):

$$\frac{M^0(L^0)^2}{A-\varepsilon}\varepsilon_p^3-\{4M^0L^0-(L^0)^2\}\varepsilon_p^2+ \\ +4(A-\varepsilon)(M^0+L^0)\varepsilon_p-4(A-\varepsilon)^2=\varepsilon_p^2/\beta_2=\text{constant} \quad (15)$$

where

$$\varepsilon=\varepsilon_m M^0+\varepsilon_l L^0 \quad (16)$$

and

$$\varepsilon_p=\varepsilon_2-2\varepsilon_l-\varepsilon_m \quad (17)$$

For two solutions having different values of M^0 and L^0, we can write

$$\left\{\frac{M_1^0(L_1^0)^2}{A_1-\varepsilon_1}-\frac{M_2^0(L_2^0)^2}{A_2-\varepsilon_2}\right\}\varepsilon_p^3+\{4M_2^0L_2^0-(L_2^0)^2-4M_1^0L_1^0+(L_1^0)^2\}\varepsilon_p^2+ \\ +\{4(A_1-\varepsilon_1)(M_1^0+L_1^0)-4(A_2-\varepsilon_2)(M_2^0+L_2^0)\}\varepsilon_p+ \\ +4\{(A_2-\varepsilon_2)^2-(A_1-\varepsilon_1)^2\}=0 \quad (18)$$

Equation (18) is cubic in ε_p and can be solved readily with a computer, by means of the Newton–Raphson iteration method. From a set of n data, n_{C_2} different combinations are possible and hence $(n-1)n/2$ values of ε_p can be calculated. The average of all ε_p values will take into account the statistical fluctuations. Once ε_p is known, β_2 can be calculated from eqn. (15).

By similar considerations, a quartic equation for a 1:3 complex can be derived, which could be solved for real roots with the help of a computer by Brown's method.

APPLICATIONS

To compare the values of the molar absorptivity and stability constant (or apparent equilibrium constant) of 1:1 complexes, calculated by this method, with the values reported in the literature, several systems were studied.

Iron(III)–salicylate system

Salicylic acid and its various derivatives give an intense violet colour with iron(III) in acidic solution. The colour formation has long been used[5] for the photometric determination of iron(III). The colour is due to the formation of a 1:1 complex[6–12]. If we represent salicylic acid and its various derivatives as H_2L, the equilibrium reaction can be represented as

$$Fe^{3+}+H_2L \rightleftarrows FeL^+ + 2H^+ \quad (19)$$

At constant pH, the apparent equilibrium constant, K_1, can be written as

$$K_1=\frac{[FeL^+]}{[Fe^{3+}][H_2L]}. \quad (20)$$

In the present work, the K_1 and ε_c values were calculated for the iron(III) complexes of the following acids: salicylic acid, 5-nitrosalicylic acid, and 5-sulfosalicylic acid.

TABLE I

MOLAR ABSORPTIVITIES AND EQUILIBRIUM CONSTANTS OF VARIOUS METAL–SALICYLATE SYSTEMS

Working wave-length (nm)	*Tempera-ture (°)*	*Molar absorptivity*			*Log equilibrium constant*		*Medium*	*Reference*
		ε_m	ε_l	ε_c	K_1	β_1[a]		
Iron(III) complex with salicylic acid[b]								
525	15	—	—	1630		16.35	$I=0.0$	6
530	25	—	—	1619		17.44[c]	$I=0.05$	7
530	25	—	—	1745		17.40[c]	$I=0.123$	7
530	20–25	—	—	2000		15.64	0.05 *M* acetate, pH 2.04	10
530	20–25	—	—	1720		15.17	0.05 *M* acetate, pH 2.81	10
530		—	—	1630				11
530	25	—	—	1530	4.73[d]		$I=0.5$ ($NaClO_4$)	12
530	25±2	—	—	1660	4.70	16.17 (17.52)[c]	$I=0.1$ ($NaClO_4$), pH 2.35±0.05	This work
Iron(III) complex with nitrosalicylic acid[b]								
499	25	—	—	2255		14.34[c]	$I=0.123$	8
496	25±2	—	—	2097	5.14	12.81 (14.16)[c]	$I=0.1$ ($NaClO_4$), pH 2.35±0.05	This work
Iron(III) complex with 5-sulfosalicylic acid[b]								
480	25–28	—	—	1830		14.05	0.05 *M* acetate, pH 2.2	9
510	25	—	—	1866	5.39[d]		$I=0.5$ ($NaClO_4$)	12
510	25	—	—	2008	5.18[d]		$I=0.5$ (KNO_3)	12
505	25	—	—	1880	5.12[d]		$I=0.5$ (KNO_3)	12
506	25±2	—	—	1931	5.06	14.96 (16.98)[c]	$I=0.1$ ($NaClO_4$), pH 2.35±0.05	This work

Beryllium complex with 5-sulfosalicylic acid[a]								
317[e]	25	—	660	3480	4.92	11.47	$I=0.1$ ($NaClO_4$), pH 5.2	14
315[e]	28–32	—	984	3996	4.18		$I=0.1$, pH 4.5	15
315[e]	29.5	—	1030	3757	3.67		$I=0.1$, pH 4.0	16
317[e]	25±2	—	850	3305	4.69	11.59	$I=0.1$ ($NaClO_4$), pH 5.0	This work
320[e]	25±2	—	600	2991	4.66	11.56 (12.91)[c]	$I=0.1$ ($NaClO_4$), pH 5.0	This work
Copper(II) complex with 5-sulfosalicylic acid								
630[f]	25	—	—	16			pH 5.0	17
					2.70			
700[f]	25	—	—	33			pH 5.0	17
390[b]	25	—	—	102.5	1.97	10.03	$I=0.2$, pH 4.03	18
390[b]	25	—	—	175.3	2.66	9.65.	$I=0.2$, pH 5.1	18
390[b]	25	—	—	228.0	2.90	9.49	$I=0.2$, pH 5.5	18
750[f]	28	—	—	33.65	2.50		$I=0.08$ ($NaClO_4$), pH 4.5	19
750[f]	34	—	—	36.57	2.03		$I=0.2$ ($NaClO_4$)	19
750[f]	25±2	9	—	41	2.72	9.62 (10.97)[c]	$I=0.1$ ($NaClO_4$), pH 5.0	This work

[a] $\beta_1 = K_1\phi$, where $\phi = 1 + ([H^+]/K_{\text{phenolic}}) + ([H^+]^2/K_{\text{phenolic}}K_{\text{carboxyl}})$.
[b] Only the complex is an absorbing species.
[c] Thermodynamic values obtained by making activity corrections on the basis of Davies equation.
[d] These values were calculated at pH 2.35 from the constant defined as $K = [ML][H^+]^2/[M][H_2L]$.
[e] Both complex and ligand absorb.
[f] Both metal and complex absorb.

Solutions were prepared by mixing iron(III) chloride and the organic acid in a 1:1 ratio. The pH was adjusted to 2.35 ± 0.05 by adding perchloric acid and the ionic strength was maintained at 0.1 with sodium perchlorate solution. For each system a set of 6 or 7 solutions was prepared, and the absorbance of each solution was recorded at the wavelength of maximum absorbance. As the metal ion and ligands do not absorb at the wavelength used, the molar absorptivity of the complex, ε_c, was calculated from eqn. (12) for each pair of points. The apparent equilibrium constant was then calculated from the following expression:

$$K_1 = \frac{A\varepsilon_c}{(\varepsilon_c M^0 - A)(\varepsilon_c L^0 - A)}. \tag{21}$$

From a set of 6 or 7 solutions, as many as 15–21 different combinations can be formed, and 15–21 values of ε_c and K_1 can be calculated. It was considered justifiable to reject those values of ε_c and K_1 which differed by 10% or more from the mean of all the values. This reduced the number of useful estimates of ε_c and K_1, and minimized the scatter. The values of ε_c and K_1 for all the three systems are given in Table I. It can be seen from the table that there is a good agreement between the present values and some of the values reported in the literature.

TABLE II

DETERMINATION OF STABILITY CONSTANT AND MOLAR ABSORPTIVITY OF THE $(FeSCN)^{2+}$ COMPLEX

$[Fe^{3+}]$ (M)	$[SCN^-]$ (M)	Absorbance (A)						
		400 nm	420 nm	440 nm	450 nm	460 nm	480 nm	500 nm
0.001	0.0003	0.0998	0.1408	0.1601	0.1617	0.1570	0.1332	0.1020
0.002	0.0003	0.1953	0.2650	0.3040	0.3060	0.2990	0.2540	0.1922
0.002	0.0003	0.1807	0.2435	0.2820	0.2845	0.2770	0.2370	0.1812
0.003	0.0003	0.2505	0.3390	0.3915	0.3940	0.3833	0.3260	0.2500
0.003	0.0003	0.2450	0.3320	0.3840	0.3860	0.3760	0.3210	0.2470
0.005	0.0003	0.3550	0.4740	0.5510	0.5529	0.5350	0.4580	0.3480
0.008	0.0003	0.4600	0.6240	0.7200	0.7250	0.7030	0.6080	0.4560
0.008	0.0003	0.4510	0.6100	0.7050	0.7075	0.6920	0.5875	0.4480
ε_c		3406 (3003)[a]	3937 (3981)	4675 (4642)	4639 (4685)	4547 (4512)	3784 (3914)	2912 (2920)
β_1		143 (134)[a]	154 (138)	148 (136)	150 (135)	151 (137)	147 (134)	147 (139)

[a] The values given in brackets are those of Frank and Oswalt.

Beryllium(II)–sulfosalicylate system

Meek and Banks[13] found that 5-sulfosalicylic acid can be used for the spectrophotometric determination of beryllium. This method is based on the fact that the absorption maximum of 5-sulfosalicylic acid is displaced appreciably towards longer wavelengths by the presence of beryllium. Banks and Singh[14]

reported the formation of a 1:1 complex of beryllium(II) with 5-sulfosalicylic acid at about pH 5.0, determined the ε_l and ε_c values directly at 317 nm, and from these values, calculated K_1 at pH 5.2. Das and Aditya[15,16] used a similar procedure to calculate ε_c, ε_l and K_1 at two different pH values (4.0 and 4.5).

In the present study of the complex, solutions were prepared by mixing beryllium sulfate and 5-sulfosalicylic acid in a 1:1 ratio and the pH values of these solutions were adjusted to 5.0 with acetate buffer; all the solutions were 0.1 *M* in sodium perchlorate. Absorbance of each solution was measured at 317 and 320 nm. The results are summarized in Table I.

Copper(II)–sulfosalicylate system

Copper(II) forms a 1:1 complex with 5-sulfosalicylic acid [17,18,19]in the pH range 4–6. In this case, solutions were prepared by mixing copper sulfate with the reagent in a 1:1 ratio, the pH being maintained at 5.0. All these solutions were 0.1 *M* in sodium perchlorate. The greenish coloured complex thus formed absorbs light in the wavelength region 650–750 nm. In this region, copper(II) also absorbs, hence ε_m was also determined. By means of eqn. (6), ε_c values were calculated and for each ε_c value, the corresponding K_1 value was calculated. The mean ε_c along with the mean K_1 is given in Table I.

Iron(III)–thiocyanate system

Frank and Oswalt[20] have studied the formation of the $Fe(SCN)^{2+}$ complex by a spectrophotometric method. They used a slope–intercept method for the calculation of molar absorptivity and stability constant. Their data were used here to calculate ε_c and β_1 at different wavelengths (Table II). It can be seen that there is good agreement in the two results.

Bis[di(*p*-tolyl)dithiophosphinato]nickel(II) forms a weak 1:1 complex with α-picoline. The elimination method was also found to be applicable to this system.

We are grateful to Mr. M. D. Zingle and Mr. M. S. Venkateshan for their help. One of us (M.C.C.) expresses his gratitude to the Director, I.I.T. Bombay for the award of a fellowship.

SUMMARY

A method for the calculation of the stability constants of complexes from spectrophotometric measurements is presented. The method is based on the elimination of one of the two unknowns and is applicable to both weak and stable complexes. A few examples illustrate the practicability of the method.

REFERENCES

1 K. Conrow, G. D. Johnson and R. E. Bowen, *J. Amer. Chem. Soc.*, 86 (1964) 1025.
2 R. W. Ramette, *J. Chem. Educ.*, 44 (1967) 647.
3 J. R. Siefker, *Anal. Chim. Acta*, 52 (1970) 545.
4 P. Gans and H. M. N. H. Irving, *J. Inorg. Nucl. Chem.*, 34 (1972) 1885.
5 F. J. Welcher, *Organic Analytical Reagents*, Vol. II, Van Nostrand, New York, 1949, p. 118.

6 C. Bertin-Batsch, *Ann. Chim. (Paris)*, 7 (1952) 481.
7 Z. L. Ernst and J. Menashi, *Trans. Faraday Soc.*, 59 (1963) 1794.
8 Z. L. Ernst and J. Menashi, *Trans. Faraday Soc.*, 59 (1963) 2838.
9 K. Ogawa and N. Tobe, *Bull. Chem. Soc. Jap.*, 39 (1966) 223.
10 K. Ogawa and N. Tobe, *Bull. Chem. Soc. Jap.*, 39 (1966) 227.
11 G. Ackermann and D. Hesse, *Z. Anorg. Allg. Chem.*, 375 (1970) 77.
12 W. A. E. McBryde, J. L. Rohr, J. S. Penciner and J. A. Page, *Can. J. Chem.*, 48 (1970) 2574.
13 H. V. Meek and C. V. Banks, *Anal. Chem.*, 22 (1950) 1512.
14 C. V. Banks and R. S. Singh, *J. Amer. Chem. Soc.*, 81 (1959) 6159.
15 R. C. Das and S. Aditya, *J. Indian Chem. Soc.*, 38 (1961) 19.
16 R. C. Das and S. Aditya, *J. Indian Chem. Soc.*, 41 (1964) 765.
17 S. E. Turner and R. C. Anderson, *J. Amer. Chem. Soc.*, 41 (1949) 912.
18 V. S. K. Nair, *Trans. Faraday Soc.*, 57 (1961) 1988.
19 R. C. Das, R. K. Nanda and S. Aditya, *J. Indian Chem. Soc.*, 42 (1965) 307.
20 H. S. Frank and R. L. Oswalt, *J. Amer. Chem. Soc.*, 69 (1947) 1321.

Analytica Chimica Acta, 70 (1974) 57–63

THE USE OF THE FIRST-DERIVATIVE CURVES OF ABSORPTION SPECTRA IN QUANTITATIVE ANALYSIS

A. M. WAHBI

Pharmaceutical Analytical Chemistry Department, Faculty of Pharmacy, University of Alexandria, Alexandria (Egypt)

S. EBEL

Fachbereich Pharmazie und Lebensmittelchemie der Philipps-Universität Marburg, Abteilung Analytische Chemie (BRD)

(Received 3rd October 1973)

Dual-wavelength spectrophotometry[1] for two-component analysis[2,3] depends in principle upon the selection of two wavelengths, λ_1 and λ_2, where ΔA_{12} is zero for one compound, so that the other can then be determined without the need for solving simultaneous equations[4]. Such an approach is equivalent to the correction of a constant interference in spectrophotometric analysis[5]. Accurate results can be obtained only when the mixture is prepared from the reference compounds; hence, the presence of a variable interference of unknown origin and shape as may arise from batch-to-batch differences or during the preparation of the final solutions will certainly lead to erroneous results.

The direct recording of first-derivative curves of electronic spectra[6,7] has been introduced in order to solve the problem of band overlap and to facilitate the detection and the determination of impurities in drugs and chemicals, and food additives as well as industrial wastes[8,9]. Shibata *et al.*[10] recently used a dual-wavelength spectrophotometer (Hitachi 356) both for qualitative and quantitative analysis. The present paper is mainly concerned with introducing first-derivative absorption curves, first to correct for interferences of higher order (*e.g.* quadratic irrelevant absorption), and secondly for the determination of a single substance in the presence of another with overlapping spectra. Furthermore, the proposed methods can be applied with a manual spectrophotometer when the double-wavelength variety is not available.

EXPERIMENTAL

Reagents

Phenol, atropine sulphate and phenylmercury(II) nitrate were of high purity. Solutions were prepared in 0.05 *M* sulphuric acid.

Apparatus

A Carl-Zeiss PMQ II photoelectric spectrophotometer with 1-cm quartz cells was used.

Absorbances

Throughout this work, an absorbance measurement was the mean of the second and third readings, each involving a prior resetting of the wavelength scale.

RESULTS AND DISCUSSION

The correction of quadratic irrelevant absorption

Among the methods used to deal with the problem of irrelevant absorption in spectrophotometric analysis are the mathematical methods. The complexity of the latter depends on the shape of the irrelevant absorption curve. The procedures followed to correct for quadratic irrelevant absorption depend mainly on the use of orthogonal polynomials[11–14], a set of absorbances measured at equally spaced wavelengths being used. However, first-derivative absorption curves can offer a simple solution to the same problem.

The key property of first-derivative absorption curves lies in the fact that the first differential of a quadratic curve is a straight line. Correction of the latter can easily be carried out either graphically or algebraically. Thus, according to Beer's Law, the absorbance of a pure compound, A, measured in a 1-cm cell at a given wavelength λ_i, is expressed as follows:

$$A_i = \alpha_i c_a \tag{1}$$

where α is the absorptivity and c is the concentration. In the presence of a quadratic irrelevant absorption:

$$A_i' = \alpha_i c_a + t + u\lambda_i + v\lambda_i^2 \tag{2}$$

where A_i' is the gross absorbance of the contaminated sample; t, $u\lambda_i$ and $v\lambda_i^2$ are the constant, linear and quadratic components of the irrelevant absorption, respectively. Differentiation of eqn. (2) with respect to λ yields:

$$dA_i'/d\lambda = c_a(d\alpha_i/d\lambda) + u + w\lambda_i \tag{3}$$

The term $(u+w\lambda_i)$ is a linear equation where u and w are the intercept and the slope, respectively. In practice, eqn. (3) can be written as follows:

$$\Delta A_i'/\Delta\lambda = c_a(\Delta\alpha_i/\Delta\lambda) + u + w\lambda_i \tag{4}$$

where $\Delta\lambda$ can be arranged to be 1 to 3 nm, according to the analytical problem[10]

In support of the above discussion, Fig. 1a shows the absorption curve of 0.0071% (w/v) phenol in 0.05 M sulphuric acid and a proposed quadratic curve, Z. The first-derivative curves, $\Delta A/\Delta\lambda$ and $\Delta Z/\Delta\lambda$ *versus* the mean wavelength, λ ($\Delta\lambda = 2$ nm) are shown in Fig. 1b. The absorption curve of phenol developed maxima and minima in its first-derivative curve whereas the quadratic curve, Z, changed to a straight line, z, when similarly treated. Apart from the possible correlation between the first-derivative curve and the molecular structure of phenol, the problem of eliminating the contribution of the resultant line z to the phenol first-derivative curve will now be discussed.

The correction of a linear interference can be carried out graphically or algebraically.

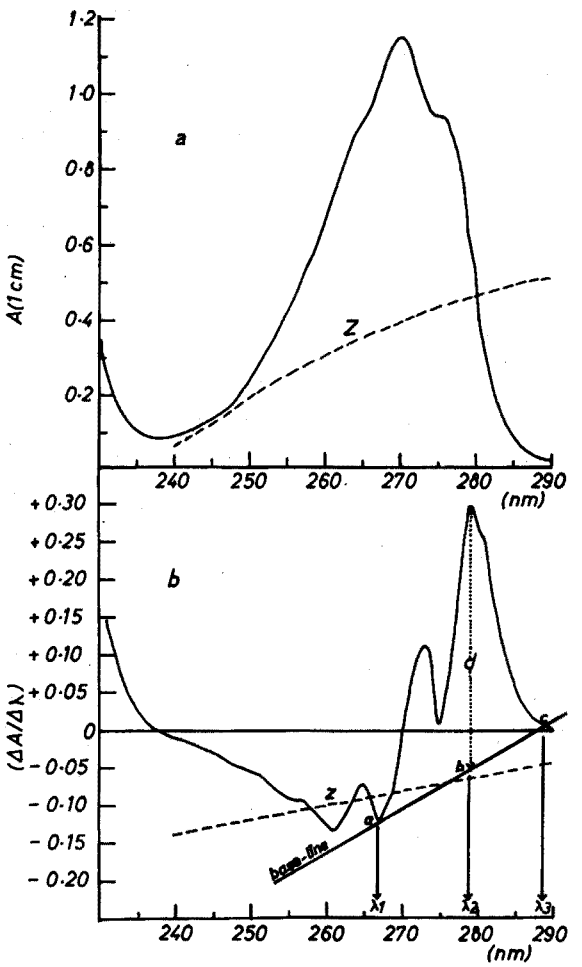

Fig. 1. (a) The absorption curve of 0.0071% (w/v) phenol in 0.05 *M* sulphuric acid (—) and a proposed quadratic interference curve *Z* (---). (b) The first-derivative curves of Fig. 1(a) where $\Delta\lambda = 2$nm. Phenol, (—); linear interference, *z* (---).

The graphical correction of the line *z* (Fig. 1b) can be done by Wright's base-line technique[15] which is used to correct for linear irrelevant absorption in infra-red spectrophotometric analysis. Thus, a straight line is drawn through the ΔA curve at points a and c, which correspond to the mean wavelengths λ_1 and λ_3, respectively, on either side of the peak of ΔA at the mean wavelength, λ_2 (Fig. 1b). A perpendicular, intersecting the first derivative curve at ΔA_2 and the base-line at b, is drawn at λ_2. c_a is then proportional to the distance between the intersections, d, which is independent of constant and linear components of both the irrelevant absorption and the original ΔA curves. A calibration curve can be constructed correlating d and the concentration of pure compound for the purpose of analysis.

Although ultraviolet spectroscopists prefer algebra to graphical construction,

for instrumental causes, the introduction of high-performance ultraviolet spectrophotometers could in fact lead to graphical corrections of the same order of accuracy as those obtained algebraically from results produced on a manual instrument.

The algebraic version of the base-line technique[16,17] can be used both for recording double-wavelength and manual spectrophotometers. Thus, in the present case, eqn. (4) can be written at the three mean wavelengths λ_1, λ_2 and λ_3:

$$\Delta A'_1/\Delta\lambda = c_a(\Delta\alpha_1/\Delta\lambda)+u+w\lambda_1 \quad (5)$$

$$\Delta A'_2/\Delta\lambda = c_a(\Delta\alpha_2/\Delta\lambda)+u+w\lambda_2 \quad (6)$$

$$\Delta A'_3/\Delta\lambda = c_a(\Delta\alpha_3/\Delta\lambda)+u+w\lambda_3 \quad (7)$$

When Cramer's rule[18,19] is used to solve a determinant for c_a:

$$c_a = \frac{\Delta A'_1(\lambda_2-\lambda_3)-\Delta A'_2(\lambda_1-\lambda_3)+\Delta A'_3(\lambda_1-\lambda_2)}{\Delta\alpha_1(\lambda_2-\lambda_3)-\Delta\alpha_2(\lambda_1-\lambda_3)+\Delta\alpha_3(\lambda_1-\lambda_2)} \quad (8)$$

If both the numerator and denominator of eqn. (8) are divided by $(\lambda_1-\lambda_3)$ followed by simple arrangement and substitution of h for $(\lambda_2-\lambda_3)/(\lambda_1-\lambda_3)$:

$$c_a = \frac{\Delta A'_2-h\Delta A'_1-(1-h)\Delta A'_3}{\Delta\alpha_2-h\Delta\alpha_1-(1-h)\Delta\alpha_3} \quad (9)$$

Equation (9) can be used to eliminate linear interferences during the spectrophotometric determination of an absorbing compound. In the present case of phenol (Fig. 1b), the selected mean wavelengths are $\lambda_1=267$ nm, $\lambda_2=279$ nm and $\lambda_3=289$ nm, respectively, hence the value of ΔA_{279} corrected for a linear interference [hereafter called ΔA(corr.)] can be obtained as follows:

$$\Delta A(\text{corr.})_{279} = \Delta A_{279}-(5/11)\Delta A_{267}-(6/11)\Delta A_{289} \quad (10)$$

In order to check the linearity of ΔA[10] and ΔA(corr.) with concentration, eight solutions of phenol in 0.05 M sulphuric acid (covering the range $A_{max}=$ 0.3–1.1) were prepared by accurate dilution of a strong phenol solution in the same solvent. The absorbances were measured at the following pairs of wavelengths: 266, 268nm, 278, 280nm, 288, 290nm and at 270 nm, respectively. Graphs of ΔA_{279} and $\Delta A(\text{corr.})_{279}$ were found to show excellent linearity and passed through the origin by comparison with A_{270} against concentration. The percentage fits for each graph[20] were found to be 99.85, 99.83, and 99.90%, respectively.

The determination of a single substance in the presence of another with overlap spectra

When properly applied, the modified Vierordt method[4] gives excellent results in analysing a mixture of two absorbing compounds, provided that the two spectra are sufficiently separated and irrelevant absorption is completely absent. In practice, however, certain groups of compounds may possess similar and overlapping spectra. For example atropine, phenylmercury(II) nitrate, ephedrine, amphetamine, etc. form a group of compounds in which the benzenoid structure constitutes the main feature of their absorption spectra[21]. In such a case, the analysis of a combination of any two of these compounds by the modified Vierordt method may

give erroneous results. Moreover, the presence of irrelevant absorption of non-specific origin will certainly increase the severity of the problem. In support of this argument, the percentage error obtained during the determination of atropine sulphate in the presence of phenylmercury(II) nitrate was reported[22] to be about 7%, when the two-component spectrophotometric method of analysis was used.

Such problems can be solved by the use of first-derivative curves to distinguish between apparently similar absorption curves and to correct for quadratic irrelevant absorption. The combination of atropine sulphate (0.1% w/v) and the bactericide phenylmercury(II) nitrate (0.003% w/v), which may be found in injection solutions[4], was chosen to demonstrate the advantage of the first-derivative curves in quantitative spectrophotometric analysis. Moreover, in view of their low absorptivity ($A_{1\,cm}^{1\%}=6$ in 0.05 *M* sulphuric acid), such injection solutions when measured in the ultraviolet region usually suffer from non-specific interferences. The latter has been described to be a linear[23] or at the most a quadratic[24] function of wavelengths. Figure 2a shows the absorption curves of 0.12% (w/v) atropine sulphate and 0.05% (w/v) phenylmercury(II) nitrate in 0.05 *M* sulphuric acid. It is apparent that the two spectra are quite similar and overlap considerably. However, the first derivative curves of the two spectra (Fig. 2b) for

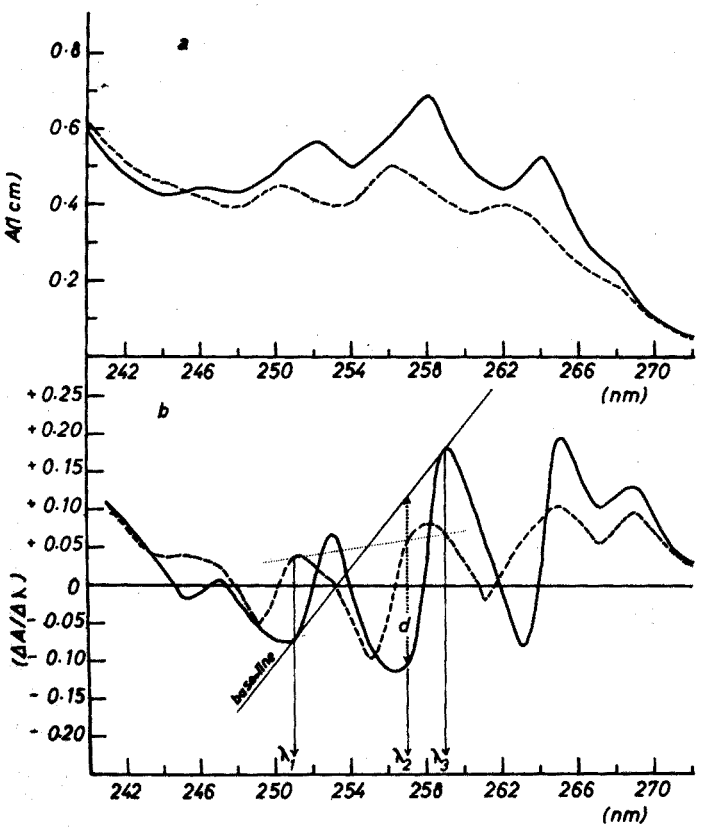

Fig. 2. (a) The absorption curves of 0.12% (w/v) atropine sulphate (—) and 0.05% (w/v) phenylmercury(II) nitrate (---) in 0.05 *M* sulphuric acid. (b) The first-derivative curves of Fig. 2 (a) where $\Delta\lambda=2$ nm.

$\Delta\lambda = 2$ nm, show significant differences which cannot be observed in the ordinary absorption spectra. It may be stressed that the present investigation is only concerned with the use of derivative curves as a tool for quantitative analysis and not for qualitative analysis.

It is obvious, of course, that a quadratic or a linear irrelevant absorption in atropine sulphate injections (which is usually the case) will change to a linear or a constant curve, respectively, when the first derivative curves are drawn. The correction of such a derivative irrelevant absorption curve can be easily carried out graphically or algebraically as previously discussed. Figure 2b shows that ΔA for phenylmercury(II) nitrate at the mean wavelengths 251, 257 and 259 nm occur on a straight line, whereas ΔA for atropine has a maximum at 257 nm. Accordingly, if a base-line is drawn between 251 and 259 nm through the first-derivative curve of a mixture of the two compounds, and then the distance between the points of intersection at 257 nm is measured (d in Fig. 2b), a direct estimate of atropine sulphate can be obtained; the non-specific irrelevant absorption originating during the preparation of the injection solution and the added phenylmercury(II) nitrate are simultaneously corrected for. Alternatively, an equation of the form:

$$\Delta A(\text{corr.})_{257} = \Delta A_{257} - 0.25\Delta A_{251} - 0.75\Delta A_{259} \qquad (11)$$

can be used to construct a calibration curve between $\Delta A(\text{corr.})_{257}$ and concentration of pure atropine sulphate.

The results obtained by means of eqn. (11) for the determination of atropine sulphate in the presence of phenylmercury(II) nitrate are given in Table I. These results are of course superior to those previously reported[4,22].

TABLE I

THE DETERMINATION OF ATROPINE SULPHATE IN THE PRESENCE OF PHENYLMERCURY(II) NITRATE BY THE FIRST DERIVATIVE METHOD

Exp. no.	*mg added per 100 ml*[a]	*% recovery*
1	73.6	100.8
2	86.0	100.6
3	98.0	98.3
4	110.4	99.0
5	122.6	98.3
6	140.8	98.3
7	62.0	99.0

[a] Each sample contained 10 mg of phenylmercury(II) nitrate to test the efficiency of the method under severe conditions.

Sources of error in the present method originate mainly from overall shifts in the wavelength calibration which affect absorbances made on steep slopes of the absorption curves. Such errors can be eliminated by keeping the instrument in a constant-temperature laboratory.

This work was sponsored by the "Deutsche Forschungsgemeinschaft" and the "Fonds der Chemischen Industrie". A. M. Wahbi is very grateful to the "Alexander von Humboldt Stiftung" for the award of a grant.

SUMMARY

The first-derivative curves of u.v.–visible spectra ($\Delta E/\Delta\lambda$) are useful in quantitative analysis. A base-line technique and its algebraic version are reported for (i) the correction of quadratic irrelevant absorption, and (ii) the determination of a substance in the presence of another with overlapping spectra. The method is illustrated by the determination of atropine sulphate in the presence of phenylmercury(II) nitrate. The results obtained suggest that the method warrants careful study over a wide field of applications.

REFERENCES

1 S. Shibata, M. Furukawa and K. Goto, *Anal. Chim. Acta*, 46 (1969) 271.
2 S. Shibata, M. Furukawa and K. Goto, *Anal. Chim. Acta*, 53 (1971) 369.
3 S. Shibata, K. Goto and Y. Ishiguro, *Anal. Chim. Acta*, 62 (1972) 305.
4 A. L. Glenn, *J. Pharm. Pharmacol.*, 12 (1960) 595.
5 *American Society for Testing of Materials, Rec. Practices for General Techniques of Ultraviolet Quantitative Analysis*, E169 Book of Standards, 1964, Part 31, p. 439.
6 A. T. Giese and C. S. French, *Appl. Spectrosc.*, 9 (1955) 78.
7 L. J. Saidel, *Arch. Biochem. Biophys.*, 54 (1955) 185.
8 *UV/Fluorescence Product Department, Technical Memo Number 4 (1970)*, Instrument Division, Perkin-Elmer Corporation, Norwalk, Conn. U.S.A., p. 1.
9 T. J. Porro, *Anal. Chem.*, 44 (1972) 93A.
10 S. Shibata, M. Furukawa and K. Goto, *Anal. Chim. Acta*, 65 (1973) 49.
11 G. C. Ashton and J. P. R. Tootill, *Analyst*, 81 (1956) 225, 232.
12 C. Daly, *Analyst*, 86 (1961) 129.
13 R. F. Rekker, *Pharm. Weekbl.*, 100 (1965) 933.
14 A. M. Wahbi and H. Abdine, *J. Pharm. Pharmacol.*, 25 (1973) 69.
15 N. Wright, *Ind. Eng. Chem., Anal. Ed.*, 13 (1941) 1.
16 F. W. Banes and L. T. Eby, *Anal. Chem.*, 18 (1946) 535.
17 F. J. Mulder F. J. Spruit and K. J. Keuning, *Pharm. Weekbl.*, 98 (1963) 745.
18 A. Frank, *Theory and Problems of Matrices*, Schaum, New York, 1962, p. 21.
19 H. D. C. Rapson, unpublished work, Chelsea College of Science and Technology, University of London.
20 O. L. Davis and P. Goldsmith, *Statistical Methods in Research and Production*, Oliver & Boyd, Edinburgh, 4th edn., 1972, p. 178.
21 I. Sunshine, *Handbook of Analytical Toxicology*, The American Rubber Co., Cleveland, p. 252.
22 M. Ismail, Ph.D. Thesis, University of London, 1964.
23 Van der Pol and R. F. Rekker, *Pharm. Weekbl.*, 94 (1959) 845.
24 I. U. Agwu and A. L. Glenn, *J. Pharm. Pharmacol.*, 19 (1967) 76S.

Analytica Chimica Acta, 70 (1974) 65–76

o-DIKETONEDIOXIME COMPOUNDS AS ANALYTICAL REAGENTS FOR THE SPECTROPHOTOMETRIC DETERMINATION OF NICKEL

SATORU KUSE, SHOJI MOTOMIZU and KYOJI TÔEI

Department of Chemistry, Faculty of Science, Okayama University, Tsushima, Okayama-shi 700 (Japan)

(Received 1st October 1973)

Since dimethylglyoxime was first used for the gravimetric determination of nickel by Tschugaeff[1], many analytical studies of dioxime compounds have been carried out. At present, dimethylglyoxime, α-furildioxime, α-benzildioxime and nioxime (1,2-cyclohexanedionedioxime) are often used as analytical reagents for nickel. Yamasaki[2] and Banks *et al.*[3] synthesized many dioxime compounds and studied the reactions with some metal ions.

The present authors have previously examined the coloration of some metal ions with sixteen *o*-diketonedioxime compounds and reported that these dioxime compounds generally show high sensitivity for nickel and cobalt[4]. In the work described here, the sensitivity for nickel of some new dioximes was examined, and compared with the sensitivity of well known dioximes in aqueous solution and in some organic solvents. Furthermore, synergic effects were examined for the improvement of sensitivity, and the compositions of the nickel dioximes were also examined.

The sixteen dioximes used are shown in Fig. 1. These reagents were classified from Group I to Group III according to their structure. Six of these reagents (asterisked in Fig. 1) are new compounds, and analytical studies of the nickel complexes of most of the others have received little attention. The reagent numbers used in the following Figures and Tables correspond to that of Fig. 1.

EXPERIMENTAL

Reagents

Dioxime compound solutions. All the dioxime compounds used were synthesized as previously reported[4]. Results of elemental analyses, melting points and references for the dioximes used are shown in Table I.

Dioximes [1], [3] and [13] were dissolved in distilled water and the other dioximes [2], [4]–[12] and [14]–[16], were dissolved in alcohol. Each dioxime solution was prepared to give 10^{-2} or 10^{-3} mol l^{-1}.

Buffer solutions. The pH was adjusted with the following solutions: hydrochloric acid (pH 2–3), acetic acid–sodium acetate (pH 4–5), potassium dihydrogenphosphate–disodium hydrogenphosphate (pH 6–7), ammonium chloride–ammonia (pH 8–10), sodium carbonate–sodium hydrogencarbonate (pH 11) and potassium hydroxide (pH 12–14).

Metal ion solutions. Nickel sulfate hexahydrate, cobalt nitrate hexahydrate,

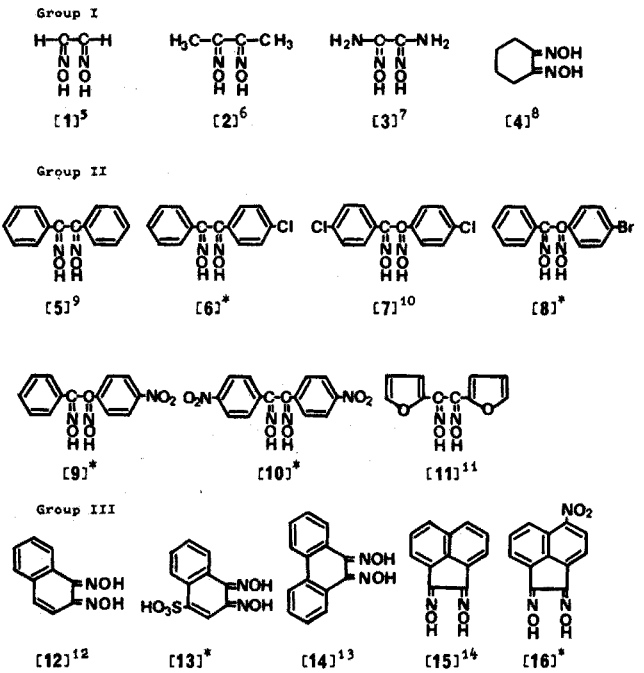

Fig. 1. *o*-Diketonedioxime compounds examined. Group I, [1]–[4]; Group II, [5]–[11]; Group III, [12]–[16]; asterisks indicate new compounds.

TABLE I

ELEMENTAL ANALYSIS OF DIOXIME COMPOUNDS USED

Reagent	*Found (calcd.)*			*M.p., °C found (lit.)*	*Ref.*
	C %	*H %*	*N %*		
[1] $C_2H_4N_2O_2$	26.8(27.3)	4.4(4.6)	31.0(31.8)	178–181(178)	5
[2] $C_4H_8N_2O_2$	41.1(41.4)	6.6(6.9)	23.9(24.1)	238–240(238–240)	6
[3] $C_2H_6N_4O_2$	20.5(20.3)	5.1(5.1)	47.5(47.4)	202–203(203)	7
[4] $C_6H_{10}N_2O_2$	51.2(50.7)	7.2(7.1)	19.6(19.7)	186–188(186–188)	8
[5] $C_{14}H_{12}N_2O_2$	69.7(70.0)	4.9(5.0)	11.5(11.7)	235–238(235–237)	9
[6] $C_{14}H_{11}N_2O_2Cl$	61.0(61.2)	4.3(4.0)	10.1(10.2)	229–231	
[7] $C_{14}H_{10}N_2O_2Cl_2$	54.1(54.4)	3.3(3.3)	9.3(9.1)	226(226)	10
[8] $C_{14}H_{11}N_2O_2Br$	52.8(52.7)	3.4(3.5)	8.6(8.8)	228–229	
[9] $C_{14}H_{11}N_3O_4$	58.8(59.0)	4.2(3.9)	15.0(14.7)	228–230	
[10] $C_{14}H_{10}N_4O_6$	50.6(50.9)	3.0(3.1)	16.9(17.0)	254–256	
[11] $C_{10}H_8N_2O_4 \cdot H_2O$	50.4(51.1)	4.2(4.1)	11.8(11.3)	83–85(84–85)	11
[12] $C_{10}H_8N_2O_2$	63.5(63.8)	4.2(4.3)	14.8(14.9)	142–144(149)	12
[13] $C_{10}H_8N_2O_5S \cdot 2H_2O$	39.1(39.5)	4.5(4.0)	9.3(9.2)	244–246	
[14] $C_{14}H_{10}N_2O_2$	71.6(70.6)	4.3(4.2)	10.7(11.7)	208–210(200)	13
[15] $C_{12}H_8N_2O_2$	67.1(67.9)	3.9(3.8)	12.4(13.2)	221–222(222)	14
[16] $C_{12}H_7N_3O_4$	54.4(56.0)	2.6(2.7)	15.4(16.3)	205–209	

Mohr's salt, iron(III) ammonium sulfate and copper(II) sulfate pentahydrate were used. Each metal solution contained 10^{-3} or 10^{-4} mol l^{-1}. Hydroxyammonium chloride (1% w/w) was added to the iron(II) solution.

Zephiramine. Zephiramine (tetradecyldimethylbenzylammonium chloride) (zeph) was dissolved in distilled water to give a 10^{-2} mol l^{-1} solution.

Other reagents. Chloroform, nitrobenzene, benzene, 1,2-dichloroethane, carbon tetrachloride and cyclohexane were used as extracting solvents. Pyridine, dioxane, methylamine and tri-n-butyl phosphate (TBP) were examined as synergic reagents. All the reagents used were of analytical-reagent grade.

Apparatus

A Shimadzu model QV-50 spectrophotometer and a Hitachi model EPS-3T recording spectrophotometer were used for measuring the absorbance in 10-mm quartz cells. A Hitachi–Horiba model F-5ss pH meter equipped with a combined electrode (6026-05T), and an Iwaki model KM shaker were used.

Determination of molar absorptivities

Aqueous solutions. The molar absorptivities of the metal complexes of four dioxime compounds ([1], [3], [4] and [13]), which form water-soluble chelate compounds, were measured in aqueous solution. Buffer solution (3 ml) at the optimal pH for coloration with metal ions, metal ion solution, and dioxime solution were pipetted into a test tube in this order, and distilled water was finally added to give a total amount of 5 ml. After mixing thoroughly, the absorbance was measured.

Solvent extraction. The molar absorptivities of the complexes of thirteen dioximes ([2], [4]–[12] and [14]–[16]), which do not form water-soluble chelate compounds, were measured in extracting solvents. Buffer solution (3 ml), metal ion solution and dioxime solution were pipetted into a stoppered 25-ml test tube, and then distilled water was added to give a total amount of 5 ml. Finally, 5 ml of extracting solvent was pipetted into the tube. After shaking for 20 min, the mixture was allowed to stand for 30 min and then the absorbance of the organic phase was measured. All the specified extracting solvents were examined in the case of nickel(II) ion; chloroform, nitrobenzene, benzene and dichloroethane were examined in the case of the other metal ions. The complex of dioxime [13] (1,2-naphthoquinonedioxime-4-sulfonic acid), which forms a water-soluble chelate compound, was extracted as a ternary complex in chloroform by adding zephiramine solution. Though the procedure was the same as that used for extracting the water-insoluble chelate compounds, 1 ml of zephiramine solution (10^{-2} mol l^{-1}) was added before the chloroform.

Effect of organic solvent (synergic effect)

Aqueous solution. Dioximes [1], [3] and [13], which form water-soluble chelates with nickel(II), were examined with regard to the synergic effects of organic solvents in aqueous solution. Buffer solution (3 ml), nickel(II) solution, dioxime solution and organic solvent were pipetted into a test tube, in this order, and distilled water was added to give a total volume of 5 ml. After mixing thoroughly, the solution was allowed to stand for 20 min and the absorbance

was then measured. Pyridine, dioxane and methylamine were used as organic solvent.

Solvent extraction. Dioximes [2], [4]–[12] and [14]–[16], which form water-insoluble chelate compounds, were examined with regard to the synergic effects of organic solvents in an extracting solvent. Buffer solution (3 ml), nickel(II) solution, dioxime solution and organic solvent (pyridine, dioxane, methylamine or TBP) were pipetted into a stoppered 25-ml test tube, in this order. Then distilled water was added to give a total volume of 5 ml and finally 5 ml of extracting solvent was pipetted in. After shaking for 20 min, the mixture was allowed to stand for 30 min and then the absorbance of the organic phase was measured. Here chloroform, nitrobenzene, benzene, 1,2-dichloroethane, carbon tetrachloride and cyclohexane were examined as the extracting solvent. As reagent [13] could be extracted as a ternary complex of metal–[13]–zephiramine, this reagent also was examined.

Determination of composition

The composition ratio of the nickel–reagent complex was determined by the mole ratio method and the continuous variations method. The compositions of the water-soluble chelates of [1], [3] and [13] were determined in aqueous solution, and those of the other reagents, [2] and [4]–[16], in organic solvents. As the metal chelate of reagent [13] was extracted in chloroform as a ternary complex with zephiramine and the chelate of the reagent [16] was extracted into nitrobenzene in the presence of TBP. each composition was also determined in each solvent.

RESULTS AND DISCUSSION

Molar absorptivities of metal chelate complexes

Molar absorptivities in aqueous solution. The optimal pH, the wavelengths of the absorption maxima and the molar absorptivities are shown in Table II.

TABLE II

MOLAR ABSORPTIVITIES IN AQUEOUS SOLUTION

Reagent	Ni^{2+}		Co^{2+}		Fe^{2+}		Fe^{3+}		Cu^{2+}	
	λ_{max} (nm)	ε ($\cdot 10^4$)	λ_{max} (nm)	ε ($\cdot 10^4$)	λ_{max} (nm)	ε ($\cdot 10^4$)	λ_{max} (nm)	ε ($\cdot 10^4$)	λ_{max} (nm)	ε ($\cdot 10^4$)
[1]	(pH 11)		(pH 9)		—		—		(pH 11)	
	319	0.88	265	2.06					304	1.12
[3]	(pH 9)		(pH 9)		—		—		(pH 11)	
	347	1.32	277	1.70					295	0.52
[4]	Pptn.		(pH 10)		(pH 4)		(pH 9)		(pH 10)	
			261	1.94	460	0.50	240	0.41	276	1.01
[13]	(pH 6)		(pH 6)		(pH 4)		(pH 5)		(pH 6)	
	301	2.06	307	4.80	230	3.66	234	2.57	303	2.36
	476	1.10	366	2.35	294	2.87	295	2.18	358	1.03
			522	1.29	330	2.26	444	0.94	500	1.06
					444	1.12	720	1.58		
					720	2.06				

Molar absorptivities in organic solvents. The best extracting solvent, the optimal pH, the wavelengths of the absorption maxima and the molar absorptivities are shown in Table III. Each value for dioxime [13] was determined when it was extracted as a ternary complex of metal–[13]–zephiramine. The molar absorptivities of Tables II and III were determined by preparing a calibration curve at each wavelength of maximal absorption; only the reproducible values are shown in Tables II and III.

Table III shows that the metal chelates were generally extracted into chloroform under ammonium-alkaline conditions. Comparison of the molar absorptivities of the nickel chelates of benzildioxime derivatives shows that those with most substituent groups had the largest molar absorptivities. As the iron chelates of the benzildioxime derivatives were scarcely extracted, and furthermore only the nickel chelate had an absorption maxima in the visible region, benzildioxime derivatives are good colorimetric reagents for nickel.

The absorption spectra of the nickel chelates of six benzildioxime derivatives, [5]–[10], are shown in Figs. 2 and 3.

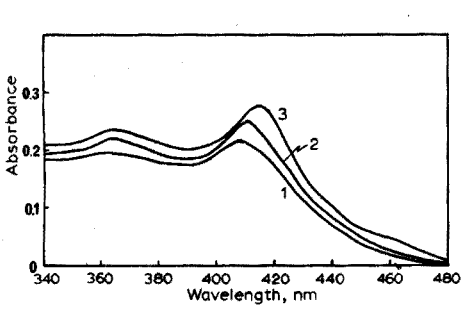

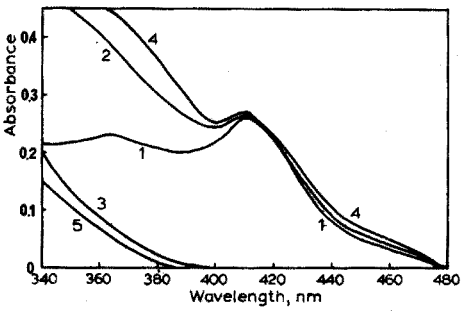

Fig. 2. Absorption spectra of the nickel chelates of benzildioxime derivatives. $[R]=2\cdot10^{-4}$ *M*; $[Ni^{2+}]=2\cdot10^{-5}$ *M*; reference solvent, chloroform. Curves: 1, reagent [5] (benzildioxime), pH 10; 2. reagent [6] (4-chlorobenzildioxime), pH 9; 3, reagent [7] (4,4′-dichlorobenzildioxime), pH 9.

Fig. 3. Absorption spectra of the nickel chelates of benzildioxime derivatives. $[R]=2\cdot10^{-4}$ *M*; $[Ni^{2+}]=2\cdot10^{-5}$ *M*; reference solvent, chloroform. Curves: 1, reagent [8] (4-bromobenzildioxime), pH 9; 2. reagent [9] (4-nitrobenzildioxime), pH 8; 3, reagent blank (reagent [9]), pH 8; 4, reagent [10] (4,4′-dinitrobenzildioxime), pH 10; 5, reagent blank (reagent [10]), pH 10.

As a representative example of the chelates, the absorption spectra of some other metal chelate complexes of [7] (4,4′-dichlorobenzildioxime) are shown in Fig. 4.

Synergic effect of organic solvent

Synergic effect in aqueous solution. The effects of dioxane, pyridine and methylamine were tested, and dioxane was found to be the best. The effect of the volume of dioxane added is shown in Fig. 5; 1 ml sufficed to give maximal effect. The molar absorptivities of the nickel complexes of three dioximes, [1], [3] and [13], at each absorption maximum, on adding 1 ml of dioxane, are shown in Table IV.

TABLE III

MOLAR ABSORPTIVITIES IN EXTRACTING SOLVENT[a]

Reagent	Ni^{2+}	Co^{2+}	Fe^{2+}	Fe^{3+}	Cu^{2+}
	λ_{max} (nm) ε ($\cdot 10^4$)	λ_{max} (nm) ε ($\cdot 10^4$)	λ_{max} (nm) ε ($\cdot 10^4$)	λ_{max} (nm) ε ($\cdot 10^4$)	λ_{max} (nm) ε ($\cdot 10^4$)
[2]	(pH 9)DCE	—	—	—	—
	261 2.42				
	330 0.46				
	374 0.36				
[4]	(pH 8)CF		—	—	(pH10)CF
	265 2.38				288 1.28
	335 0.50				
	385 0.38				
[5]	(pH 10)CF	(pH 8)CF	—	—	(pH 7)CF
	275 3.83	280 2.30			279 2.96
	362 0.99	(pH 8)DCE			(pH 7)B
	408 1.08	272 3.00			280 3.80
[6]	(pH 9)CF	(pH 9)CF	—	—	(pH 9)CF
	279 4.20	270 2.22			283 3.32
	364 1.12		(pH 11)DCE		(pH 9)B
	410 1.27		260 3.30		282 4.47
[7]	(pH 9)CF	(pH 10)CF	—	—	(pH 9)CF
	283 3.90	270 1.50			289 3.99
	366 1.19	320 0.80			(pH 9)DCE
	414 1.42				287 4.50
[8]	(pH 9)CF	(pH 9)CF	—	—	(pH 10)CF
	280 3.86	295 2.26			284 3.84
	364 1.17		(pH 11)DCE		(pH 10)B
	411 1.33		260 1.50		284 4.32
[9]	(pH 8)CF	(pH 7)CF	—	—	(pH 6)CF
	278 2.07	329 2.13			311 2.26
	360 1.56				
	412 1.33				

The absorption spectrum of the nickel chelate of [13] on adding 1 ml of dioxane is shown in Fig. 6. And the absorption spectra of some metal chelates of [13] are shown in Fig. 7. In the case of reagent [13] in aqueous solution, the molar absorptivity showed an increase of about 40% on addition of dioxane, and was also reproducible.

Synergic effect in organic solvent. None of the dioximes, except [16] (5-nitroacenaphthenequinonedioxime) showed any synergic effects in organic solvents. For reagent [16], pyridine, dioxane, methylamine and TBP were examined and TBP was found most effective. Nitrobenzene was a better extractant than carbon tetrachloride and cyclohexane. The effect of the volume of TBP added in nitrobenzene is shown in Fig. 8; 1 ml of TBP in 5 ml of nitrobenzene solution provided maximal absorbance. Though the nickel chelate of [16] was scarcely extracted without TBP, it was extracted quantitatively and showed a molar absorptivity of $1.48 \cdot 10^4$ at 546 nm on adding TBP. The extractability of the complex was increased by coordination of TBP.

Reagent	Ni^{2+}		Co^{2+}		Fe^{2+}		Fe^{3+}		Cu^{2+}	
	λ_{max} *(nm)*	ε $(\cdot 10^4)$	λ_{max} *(nm)*	ε $(\cdot 10^4)$	λ_{max} *(nm)*	ε $(\cdot 10^4)$	λ_{max} *(nm)*	ε $(\cdot 10^4)$	λ_{max} *(nm)*	ε $(\cdot 10^4)$
[10]	(pH 10)CF		—[b]		—		—		(pH 9)CF	
	279	4.62							313	0.62
	412	1.36							(pH 9)DCE	
									293	3.01
[11]	(pH 10)CF		(pH 9) CF		—		—		—[c]	
	296	4.42	296	1.28					(pH 8)B	
	390	1.28							345	1.81
	436	1.81							480	0.43
[12]	(pH 8)CTC		(pH 6)CTC		(pH 5)CTC		—		—[d]	
	324	3.33	313	2.65	310	2.14				
	464	1.76	414	1.17	448	0.98			(pH 8)B	
			(pH 6)NB		(pH 5)NB		(pH 5)NB		298	4.09
			430	1.38	430	1.14	430	0.47	410	1.01
[13][e]	(pH 8)CF		(pH 8)CF		(pH 8)CF		(pH 5)CF		(pH 8)CF	
	307	5.12	312	6.21	297	4.20	299	3.51	307	3.68
	480	2.03	370	3.79	432	1.50	446	1.05	476	1.97
			534	1.62	710	2.18	710	1.94		
					(pH 8)NB					
					710	2.27				
[14]	(pH 10)NB		(pH 7)NB		(pH 5)NB		—		(pH 12)NB	
	456	2.49	420	0.88	430	0.70	(pH 5)DCE		430	0.59
					490	0.65	335	0.32		
							408	0.89		
[15]	(pH 12)CF		(pH 8)CF		—		—		(pH 5)CF	
	374	0.46	370	1.28					300	3.04
									364	1.49
[16]	—		(pH 10)NB		(pH 8)NB		—		(pH 10)NB	
			490	0.67	470	0.57			456	0.97

[a] CF, chloroform; NB, nitrobenzene, B, benzene; DCE, 1,2-dichloroethane; CTC, carbon tetrachloride.
[b] Though this metal complex absorbs at about 280 nm in chloroform (pH 11), it is not reproducible.
[c] Though this metal complex absorbs at about 300 nm in chloroform (pH 8), it is not reproducible.
[d] Though this metal complex absorbs at about 310 nm in carbon tetrachloride (pH 8), it is not reproducible.
[e] This metal complex was extracted as a ternary complex of metal–[13]–zephiramine.
[f] This metal chelate complex is very insoluble and exists at the boundary of the extracting solvent and the aqueous solution as a precipitate.

The absorption spectra of some metal chelates of [16] on adding 1 ml of TBP at the optimal pH are shown in Fig. 9.

The composition of nickel–dioxime complexes

The composition ratio of nickel and some dioximes has been reported as 1:2, 1:3 (ref. 15) and 1:4 (ref. 16). The ratios of nickel and reagents [1], [3] and [13] were determined by the mole ratio method and the continuous variations method in aqueous solution, and the ratios of nickel and reagents [2] and [4]–[16], were determined in the extracting solvent. The results are shown in Table V.

As reagent [13] was extracted as a ternary complex of nickel–[13]–zephiramine, it was examined not only in aqueous solution but also in the organic

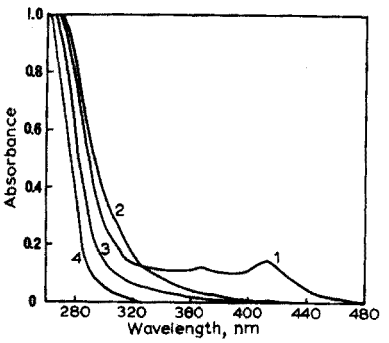

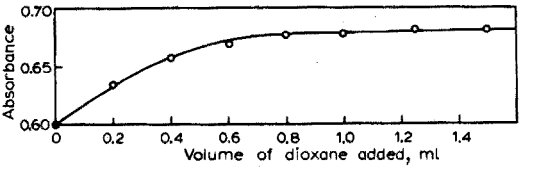

Fig. 4. Absorption spectra of some metal chelates of [7] (4,4'-dichlorobenzildioxime), [R]= $1 \cdot 10^{-4}$ *M*; [M]= $1 \cdot 10^{-5}$ *M*; pH 9–10; reference solvent, chloroform. Curves: 1, nickel(II); 2, copper(II); 3, cobalt(II); 4, reagent blank.

Fig. 5. Effect of dioxane. Reagent: [13], (1,2-naphthoquinonedioxime-4-sulfonic acid); [Ni^{2+}]= $2 \cdot 10^{-5}$ *M*; [R]= $2 \cdot 10^{-4}$ *M*; pH 6; wavelength, 476 nm; reference solvent, distilled water. The total amount of aqueous solution was 5 ml.

TABLE IV

EFFECT OF DIOXANE IN AQUEOUS SOLUTION

Reagent	*No dioxane*		*Adding 1 ml of dioxane*	
	λ_{max} *(nm)*	ε *(l mole^{-1} cm^{-1})*	λ_{max} *(nm)*	ε *(l mole^{-1} cm^{-1})*
[1]	319	$8.77 \cdot 10^3$	319	$1.5 \cdot 10^{4}$ [a]
[3]	347	$1.32 \cdot 10^4$	348	$1.37 \cdot 10^4$
[13]	301	$2.06 \cdot 10^4$	303	$2.90 \cdot 10^4$
	476	$1.10 \cdot 10^4$	476	$1.46 \cdot 10^4$

[a] Though the molar absorptivity almost doubles, it is not reproducible.

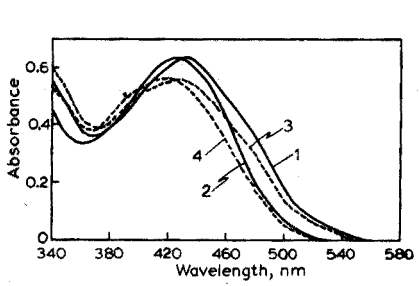

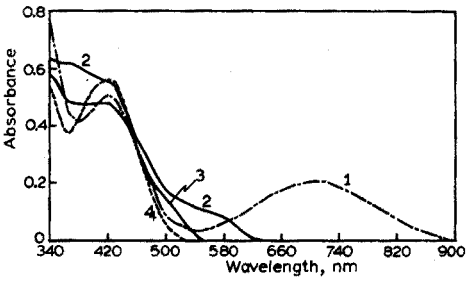

Fig. 6. Absorption spectrum of the nickel chelate of [13] on adding 1 ml of dioxane. Reagent: [13] (1,2-naphthoquinonedioxime-4-sulfonic acid); [R]= $1 \cdot 10^{-4}$ *M*; [M]= $1 \cdot 10^{-5}$ *M*; pH 6; reference solvent, distilled water. Curves: 1, Ni^{2+} + reagent + buffer solution + dioxane; 2, reagent + buffer solution + dioxane; 3, Ni^{2+} + reagent + buffer solution; 4, reagent + buffer solution.

Fig. 7. Absorption spectra of some metal chelates of [13] in aqueous solution. Reagent: [13] (1,2-naphthoquinonedioxime-4-sulfonic acid); [R]= $1 \cdot 10^{-4}$ *M*; [M]= $1 \cdot 10^{-5}$ *M*; pH 6, reference solvent, distilled water. Curves: 1, iron(II); 2, cobalt(II); 3, copper(II); 4, reagent blank.

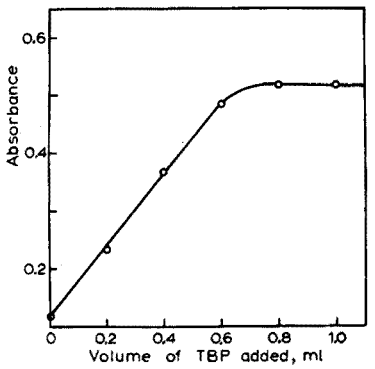

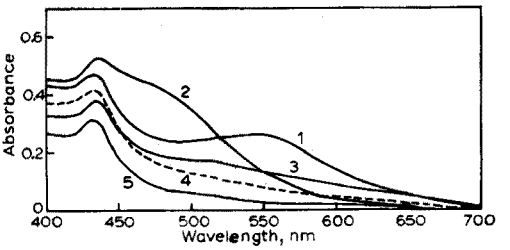

Fig. 8. Effect of increased volume of TBP. Reagent: [16] (5-nitroacenaphthenequinonedioxime); $[Ni^{2+}] = 4 \cdot 10^{-5}$ *M*; $[R] = 4 \cdot 10^{-4}$ *M*; pH 10; wavelength, 546 nm; reference solvent, nitrobenzene. The total amount of organic phase was 6 ml.

Fig. 9. Absorption spectra of some metal chelate complexes of [16] on adding 1 ml of TBP. Reagent: [16] (5-nitroacenaphthenequinonedioxime); $[M] = 1.67 \cdot 10^{-5}$ *M*; $[R] = 1.67 \cdot 10^{-4}$ *M*; pH 8–10; reference solvent, nitrobenzene. The total amount of organic phase was 6 ml (1 ml TBP + 5 ml NB). Curves: 1, nickel(II); 2, copper(II); 3, cobalt(II); 4, iron(II); 5, reagent blank (reagent [16]).

TABLE V

COMPOSITION RATIO OF NICKEL AND DIOXIME

Reagent[a]	*Mole ratio method* *Ni:R*	*Continuous variations method* *Ni:R*
$[1]_{aq.}$	1:1.0	1:1.0
$[2]_{DCE}$	1:2.1	1:2.0
$[3]_{aq.}$	1:3.0	1:3.0
$[4]_{CF}$	1:2.0	1:2.0
$[5]_{CF}$	1:2.1	1:2.0
$[6]_{CF}$	1:2.2	1:2.0
$[7]_{CF}$	1:2.0	1:2.0
$[8]_{CF}$	1:2.1	1:2.0
$[9]_{CF}$	1:2.2	1:2.0
$[10]_{CF}$	1:2.0	1:2.0
$[11]_{CF}$	1:5.9	1:6.1
$[12]_{CTC}$	1:3.0	1:3.2
$[13]_{aq.}$	1:3.0	1:3.0
$[13]_{CF}$	1:3.1	1:3.2
$[13]_{DO}$	1:4.0	1:3.8
$[14]_{NB}$	1:5.8	1:6.0
[15]	—	—
$[16]_{TBP}$	1:3.9	1:4.0

[a] Aq., aqueous solution; DCE, 1,2-dichloroethane; CF, chloroform; CTC, carbon tetrachloride; NB, nitrobenzene; DO, aqueous solution on adding 1 ml of dioxane; TBP, nitrobenzene on adding 1 ml of tri-n-butyl phosphate.

solvent. And, as the nickel chelate of [16] was scarcely extracted by the solvent alone, 1 ml of TBP was added.

The ratio of nickel and reagent [11] or [14] was about 1:6. The reason for this result is that the α-isomer and another isomer were probably mixed. As the nickel chelate of [15] was insoluble in aqueous solution and in organic solvents, the composition could not be determined. Though [16] is similar to [15], it can be extracted by adding TBP and the composition of [16] in Table V was obtained by adding TBP.

From Tables IV and V, it can be seen that though the molar absorptivity of the nickel chelate of [1] increased on adding dioxane, the reproducibility decreased; the reason for this is that only one molecule of reagent [1] coordinates to the nickel ion and several dioxane molecules coordinate irregularly to the remaining positions of nickel(II). The molar absorptivity of the nickel chelate of reagent [3] scarcely changed on adding dioxane, presumably because three molecules of the reagent coordinate strongly to the nickel ion so that the dioxane cannot coordinate. The molar absorptivity of the nickel chelate of reagent [13] increased 1.4 times by adding dioxane. As can be understood from Table V, this increase is due to the increase of the coordination number of reagent [13]. The nickel chelate of [13] may possess an octahedral configuration, and the reagent coordinated to the ion cannot form hydrogen bonds. Accordingly, it cannot form a stable complex, and so the ratio of nickel and [13] becomes 1:4 on adding dioxane.

The ratio of nickel and [16] was 1:4 in the presence of TBP. The behavior of this complex is probably the same as that of [13]. Unless TBP is present, three molecules of reagent [16] coordinate to the nickel ion, to form an anionic form of the nickel chelate, which scarcely dissolves in extracting solvents, as well as in aqueous solutions; the complex then appears at the water–solvent boundary.

As examples of the determination of the composition, results for reagents [1] (1:1), [10] (1:2), [13] (1:3) and [16] (1:4), by the mole ratio method and the continuous variations method are shown in Figs. 10 and 11.

CONCLUSION

The nickel complexes of the Group I reagents ([1]–[4]) show very little absorption in the visible region, and therefore the reagents are not suitable as color reagents for nickel. Those of Group II ([5]–[11]) can be extracted into organic solvents and furthermore show absorption maxima in the visible region with only the nickel ion. The molar absorptivities are $1.1–1.4 \cdot 10^4$ at 408–414 nm for reagents [5]–[10], which have the benzene ring, and $1.8 \cdot 10^4$ at 436 nm for [11] which has the furan ring. The reagents of Group III ([12]–[16]) react not only with the nickel ion but also with several metal ions such as cobalt, iron(II), iron(III) and copper ions. The nickel complexes and the other metal complexes are extracted into organic solvents under the same conditions, and the complexes have relatively large absorptivities in the visible region. Therefore, the Group III compounds are not selective spectrophotometric reagents for nickel. But the molar absorptivity of the ternary complex (Ni^{2+}–[13]–zephiramine) of [13] (1,2-naphthoquinonedioxime-4-sulfonic acid) was $2.03 \cdot 10^4$ at 480 nm, and that of the nickel

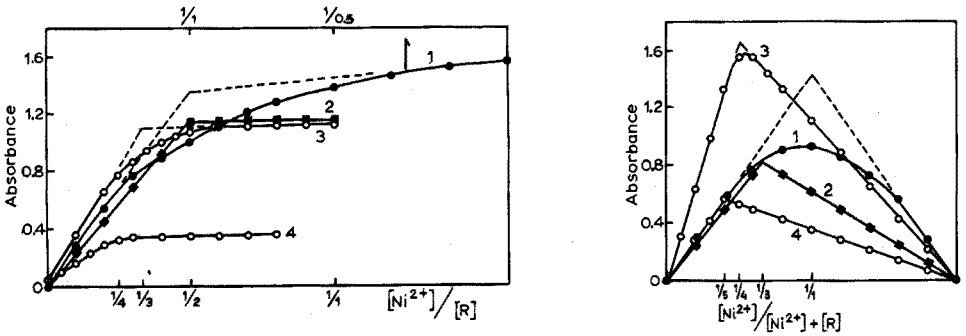

Fig. 10. Mole ratio method. Curves: 1, reagent $[1]_{aq.}$ (glyoxime), $[1] = 1 \cdot 10^{-3}$ *M* (319 nm); 2, reagent $[6]_{CF}$ (4-chlorobenzildioxime), $[6] = 2 \cdot 10^{-4}$ *M* (410 nm); 3, reagent $[13]_{aq.}$ (1,2-naphthoquinonedioxime-4-sulfonic acid), $[13] = 2 \cdot 10^{-3}$ *M* (510 nm); 4. reagent $[16]_{TBP}$ (5-nitroacenaphthenequinonedioxime), $[16] = 8.33 \cdot 10^{-5}$ *M* (546 nm). Aq., aqueous solution; CF, chloroform; TBP, nitrobenzene on adding 1 ml of tri-n-butyl phosphate.

Fig. 11. Continuous variations method. Curves: 1, reagent $[1]_{aq.}$, $[Ni^{2+}] + [1] = 2 \cdot 10^{-3}$ *M* (319 nm); 2, reagent $[6]_{CF}$, $[Ni^{2+}] + [6] = 2 \cdot 10^{-4}$ *M* (410 nm); 3, reagent $[13]_{aq.}$, $[Ni^{2+}] + [13] = 4 \cdot 10^{-3}$ *M* (510 nm); 4, reagent $[16]_{TBP}$, $[Ni^{2+}] + [16] = 1.67 \cdot 10^{-4}$ *M* (546 nm).

complex of [14] (9,10-phenanthrenequinonedioxime) was $2.49 \cdot 10^4$ at 456 nm. This value was the largest of all the nickel dioximates studied.

As mentioned above, [13] had the highest sensitivity for nickel, formed a water-soluble chelate compound and could be extracted into organic solvents as the ternary complex nickel–[13]–zephiramine. When the ternary complex was extracted into chloroform at pH 8, the excess of reagent formed an ion pair with the zephiramine, which was also extracted into chloroform with the nickel chelate. When a suitable amount of chloride ion was added to the aqueous solution, the nickel chelate was still extracted into the organic solvent but the excess of reagent was scarcely extracted. This means that the excess of reagent moves into aqueous solution by the exchange reaction as follows:

$$(NDS^- \cdot zeph^+) + Cl^- \rightleftharpoons NDS^- + (zeph^+ \cdot Cl^-)$$

When the ternary complex was extracted in the presence of a quaternary ammonium salt, this phenomenon was generally observed. As the excess of reagent was easily removed by this method, the absorbance of the reagent blank could be reduced.

Only reagents [13] and [16] showed synergic effects. On adding dioxane and zephiramine, the molar absorptivity of the nickel chelate of [13] increased, but from the mole ratio of nickel and [13] it is not supposed that this increase depended on the coordination of dioxane. The addition of dioxane causes an increase in the coordination number from 3 to 4, and zephiramine is useful for combination with the sulfonic group of reagent [13].

In conclusion, the dioxime compounds studied react readily with nickel and cobalt in general; Group II reagents (benzildioxime derivatives and furildioxime) are particularly useful as extraction–spectrometric reagents for nickel. The determination of nickel by extraction of the ternary complex (Ni^{2+}–[13]–zephiramine) has the highest sensitivity, this reagent—1,2-naphthoquinonedioxime-4-sulfonic acid—should prove useful.

SUMMARY

Sixteen dioxime compounds, including six new compounds, were synthesized and their reactions with nickel, cobalt, iron(II, III) and copper ions were examined. The nickel chelates of the glyoxime derivatives show hardly any absorption in the visible region, and are therefore unsuitable as color reagents. The nickel chelates of the benzildioxime derivatives can be extracted into organic solvents and provide a selective color reaction, so that useful extraction–spectrophotometric methods are possible. The metal complexes of quinonedioximes are extracted into some organic solvents, and the complexes have relatively large molar absorptivities in the visible region, but the reagents are not selective. However, the molar absorptivity of the ternary complex, Ni^{2+}–reagent–zephiramine, with 1,2-naphthoquinonedioxime-4-sulfonic acid was $2.03 \cdot 10^4$ at 480 nm, and that of the nickel complex of 9,10-phenanthrenequinonedioxime was $2.49 \cdot 10^4$ at 456 nm. The compositions of the nickel–dioxime complexes were examined spectrophotometrically.

REFERENCES

1 L. A. Tschugaeff, *Z. Anorg. Chem.*, 46 (1905) 144.
2 K. Yamasaki, *Nippon Kagaku Zasshi*, 80 (1959) 271.
3 C. V. Banks, *Inorg. Chem.*, 6 (1967) 1670.
4 S. Kuse, S. Motomizu and K. Tôei, *Nippon Kagaku Kaishi*, (1973) 1611.
5 N. Masuda and M. Kajiwara, *Jap. Anal.*, 17 (1968) 1352.
6 W. L. Semon and V. R. Damerell, *Org. Syn.*, Coll. Vol. II (1950) 204.
7 G. A. Pearse and R. T. Pflaum, *Anal. Chem.*, 32 (1960) 213.
8 C. C. Hach, C. V. Banks and H. Diehl, *Org. Syn.*, Coll. Vol. 4 (1963) 229.
9 K. Auwers and V. Meyer, *Ber.*, 21 (1888) 792.
10 A. J. Boulton, P. Hådjimihalkis, A. R. Katrizky and A. M. Hamid, *J. Chem. Soc. C*, (1969) 1901.
11 S. A. Reed, C. V. Banks and H. Diehl, *J. Org. Chem.*, 12 (1947) 792.
12 H. Goldschmidt and H. Schmidt, *Ber.*, 17 (1884) 2066.
13 J. Schmidt and J. Soll, *Ber.*, 17 (1907) 2454.
14 C. Graebe and E. Gfeller, *Ann.*, 276 (1893) 10.
15 M. A. Bambenek and R. T. Pflaum, *Inorg. Chem.*, 2 (1963) 289.
16 E. Booth and J. D. H. Strickland, *J. Amer. Chem. Soc.*, 75 (1953) 3017.

Analytica Chimica Acta, 70 (1974) 77–83

CATALYTIC DETERMINATION OF TRACE AMOUNTS OF VANADIUM BY MEANS OF THE CHROMOTROPIC ACID—BROMATE REACTION

TAKESHI YAMANE, TAKASHI SUZUKI and TOMOYUKI MUKOYAMA

Department of Applied Chemistry, Faculty of Engineering, Yamanashi University, Takeda, Kofu (Japan)

(Received 4th October 1973)

In recent years, catalytic methods of analysis have become an important means in trace analysis of obtaining high sensitivity combined with a relatively simple procedure. Many catalytic methods have been developed for the determination of traces of various elements[1,2]. Many of these are based on redox reactions involving oxidation-sensitive organic compounds such as phenylamines, phenols, etc.

Chromotropic acid (4,5-dihydroxynaphthalene-2,7-disulfonic acid) reacts with many metal ions and has found applications as a spectrophotometric reagent for many metals in analytical chemistry[3–5]. It is known that chromotropic acid is easily air-oxidized, particularly in the presence of heavy metals.

This paper describes an investigation of the vanadium-catalysed oxidation of chromotropic acid by bromate and a catalytic method for determining trace amounts of vanadium based on this catalytic reaction. The proposed method allows a simple determination of vanadium as low as 5 ng with good accuracy.

EXPERIMENTAL

Reagents and apparatus

Standard vanadium solution (500 μg ml^{-1}). Dissolve 0.574 g of ammonium metavanadate in water and dilute to 500 ml with water. Prepare more dilute solutions from this stock solution by dilution.

Chromotropic acid solution. Dissolve 0.50 g of chromotropic acid (disodium salt, Dotite Reagent) in water and dilute to 50 ml. Prepare freshly daily.

Potassium bromate solution. Dissolve 1.00 g of potassium bromate in water and dilute to 100 ml. This solution should be used within three days of preparation.

Acetic acid–sodium acetate buffer solution. Mix 10 *M* acetic acid and 2 *M* sodium acetate solution in a ratio of 1:1.6.

All reagents should be of the highest grade of purity obtainable.

A Hitachi Model EPU-2A spectrophotometer with 1 cm cells, a Hitachi–Horiba Model M-5 pH meter and a Sharp Model TE-14 thermoelectric thermobath were used for all experiments.

The temperature in the cell chamber was thermostated at 30±0.2°C by circulating water from an external thermostat-controlled water bath through the cell chamber fixed in the spectrophotometer.

Procedure

The rate of the oxidation of chromotropic acid by bromate was followed spectrophotometrically by measuring the rate of change in absorbance at 430 nm. All solutions were kept in a water bath at 30°C before use.

Place an aliquot of the sample or standard vanadium solution in a calibrated test tube (20 ml) with a ground-glass stopper. Add 1.3 ml of acetate buffer solution and 3 ml of chromotropic acid solution, and dilute with water to 19 ml. Then, warm the solution in the thermostated water bath at 30°C. After 10 min warming, add 1 ml of potassium bromate solution, simultaneously starting a stop-watch. Shake well, transfer a portion of this solution to the cell, and measure the absorbance at 430 nm at various reaction times.

The initial rate of the reaction was calculated graphically from absorbance *versus* time curves by extrapolation to zero time, and by determining the slope of the curve at this point. For convenience, the initial rate is expressed in this paper as A min^{-1}, where A represents absorbance.

RESULTS AND DISCUSSION

Absorption spectra

Figure 1 shows that the oxidation product of chromotropic acid has an absorption maximum at about 430 nm, at which the absorbance of the reactants, chromotropic acid and potassium bromate, is very small or negligible. Curve 2 was determined after cooling the reaction mixture to 10°C after several minutes of reaction.

Subsequent reaction rate studies were therefore made at 430 nm.

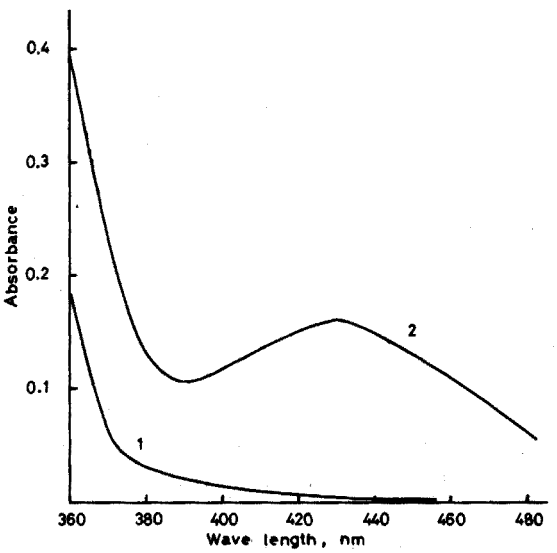

Fig. 1. Absorption spectra for: curve 1, reagent mixture of chromotropic acid and potassium bromate; curve 2, reagent mixture in the presence of vanadium after several minutes of reaction.

Effect of pH

The effect of pH on the rate of the oxidation of chromotropic acid by bromate was studied for a fixed amount of vanadium (30 ng). The pH was adjusted by the addition of acetic acid–sodium acetate buffer solution, in which the concentration of acetate was kept constant and that of acetic acid varied to avoid any salt effect on the reaction.

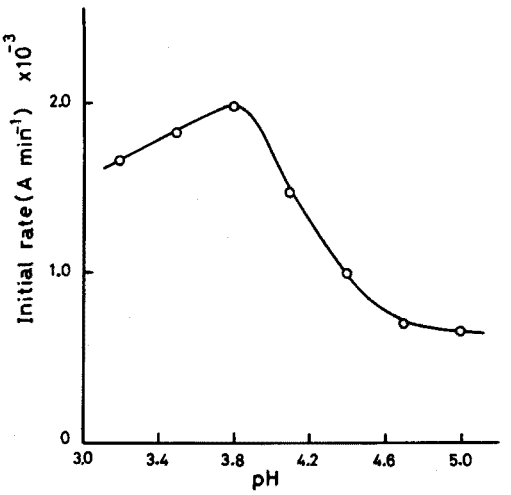

Fig. 2. Effect of pH on the reaction rate. Vanadium, 30 ng; chromotropic acid, $2.75 \cdot 10^{-3}$ *M*; bromate, $8.98 \cdot 10^{-3}$ *M*.

Figure 2 shows that there exists a maximal rate of the vanadium-catalysed reaction at about pH 3.8. The rate of the uncatalysed reaction was also studied and found to be almost negligible in the pH range examined. The pH value of 3.8 was chosen for the recommended procedure.

Reagent concentration

The rate of oxidation of chromotropic acid was measured for different concentrations of chromotropic acid and potassium bromate with a fixed amount of vanadium (30 ng). The rate of the vanadium-catalysed reaction increased when the concentrations of these reactants were increased (Table I).

A linear relationship was obtained between the initial concentration of chromotropic acid and the initial rate of the reaction, but a slight deviation was observed from this relationship as the concentration of chromotropic acid was further increased. No simple relationship was observed for the bromate dependence of the reaction rate. However, the uncatalysed reaction was found to be almost negligible in these concentration ranges.

Effect of temperature

The dependence of the rate of the catalysed reaction on temperature was studied in the presence of 30 ng of vanadium. The rate of the reaction increased by about 1.9 as the temperature was increased from 30 to 40°C. However,

TABLE I

RATE DEPENDENCE ON CHROMOTROPIC ACID AND BROMATE

(Vanadium taken, 30 ng; reaction temperature, 30°C)

Chromotropic acid ($\cdot 10^{-3}$ *M*)	*Bromate* ($\cdot 10^{-3}$ *M*)	*Initial rate* ($\cdot 10^{-4}$ *A min*$^{-1}$)
0.69	8.98	5.7
1.38	8.98	11.7
2.75	8.98	23.0
4.13	8.98	33.3
5.50	8.98	40.0
2.75	1.20	10.3
2.75	2.09	13.0
2.75	2.99	15.3
2.75	5.98	20.0
2.75	14.95	26.7

although higher sensitivity could be obtained at the higher reaction temperature, it was troublesome to control the temperature precisely at the elevated temperature. Constant temperature during the reaction is essential to obtain reproducible results, and therefore a reaction temperature of 30°C was chosen.

Calibration curves

The rate of the catalysed reaction as a function of vanadium concentration is shown in Fig. 3.

Two catalysed reactions were studied; for 0–50 ng of vanadium under the

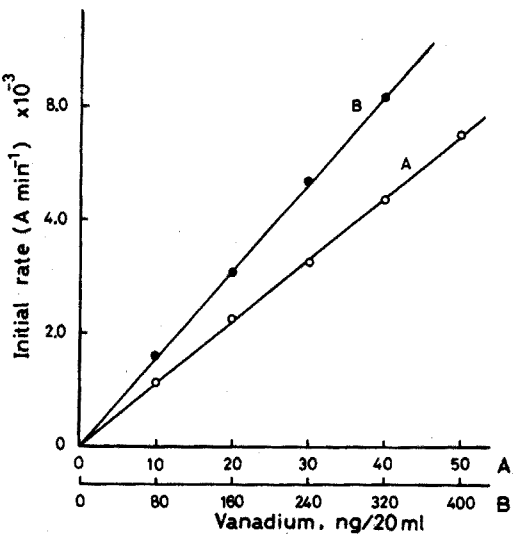

Fig. 3. Initial rate of the vanadium-catalysed oxidation as a function of initial concentration of vanadium. (A) Chromotropic acid, $4.13 \cdot 10^{-3}$ *M*; bromate, $8.98 \cdot 10^{-3}$ *M*. (B) chromotropic acid, $6.9 \cdot 10^{-4}$ *M*; bromate, $4.49 \cdot 10^{-3}$ *M*.

conditions of $4.13 \cdot 10^{-3}$ *M* chromotropic acid and $8.98 \cdot 10^{-3}$ *M* potassium bromate, and for 0–350 ng of vanadium under the conditions of $6.9 \cdot 10^{-4}$ *M* chromotropic acid and $4.49 \cdot 10^{-3}$ *M* potassium bromate; in both cases, the pH was 3.8 and the reaction temperature was 30°C. In both catalysed reactions, the rate was found to be first order with respect to vanadium concentration.

Under these conditions, the uncatalysed reaction was very slow and therefore the blank value was almost negligible; the stability of this reaction as background was sufficient for the determination of trace amounts of vanadium.

It is clear that vanadium down to 5 ng can be determined by measuring the initial rates of the reaction and constructing a calibration curve; the initial rate is directly proportional to the concentration of vanadium to be determined.

The relative standard deviations of the method at 20 ng of vanadium (10 determinations) and 160 ng of vanadium (7 determinations) were 2.5 and 2.0%, respectively.

It is important to note that there was some difference in the sensitivity of the method when different bottles of chromotropic acid were used, even from same manufacturer. This is probably due to the difficulty of purification of chromotropic acid. Therefore, the analysis should be made with the same lot of the reagent as used for the calibration curve.

Study of interferences

Interferences caused by foreign ions in the system were studied by taking solutions containing 20 ng of vanadium and the desired amounts of foreign ion.

The results are summarized in Table II. Several metal ions, such as copper, iron(III), molybdenum(VI) and silver, had a catalytic effect and thus showed positive interferences, while tungsten(VI) and iodide decreased the rate of the

TABLE II

EFFECT OF FOREIGN IONS

(Vanadium taken, 20 ng)

Foreign ion	*Added (μg)*	*Relative error (%)*	*Foreign ion*	*Added (μg)*	*Relative error (%)*
Mn(II)	100	3.5	Ag(I)	10	3.0
Zn(II)	100	− 1.5	Hg(II)	60	3.0
Pb(II)	100	− 6.0	Mo(VI)	10	4.5
	50	− 1.5	W(VI)	2	−24.2
Cr(III)	100	3.0		1	− 2.5
Cu(II)	2	24.6	Citric acid	500	−25.4
Co(II)	100	− 1.5	Oxalic acid	500	−85.1
Ni(II)	100	1.5	Tartaric acid	500	− 1.5
Ca(II)	200	0	Phosphate	500	0
Mg(II)	200	− 1.5	Bromide	100	0
As(III)	200	0		200	− 9.1
Se(IV)	200	3.0	Chloride	500	0
Al(III)	100	3.0	Fluoride	250	− 1.5
Fe(III)	2	16.6	Iodide	10	−16.7
Ag(I)	50	45.5		5	− 2.5

reaction and hence caused negative errors; particularly iron(III), copper and tungsten(VI) seriously interfered when present in concentrations 100 times that of the vanadium. Significant amounts of oxalic acid and citric acid also caused negative interferences. However, many of the ions examined were found to have no effect or only a slight effect on the determination of trace amounts of vanadium, even when present in 5000 times the amounts of this metal.

The effect of ionic strength was also studied with potassium chloride in the presence of 20 ng of vanadium. The rate of the catalysed reaction was decreased by about 6% when the concentration of potassium chloride was 0.05 *M*, but above this concentration (0.05–0.2 *M*) the rate was found to be almost constant.

Mechanism of the reaction

The vanadium ion demonstrated a profound catalytic effect on the oxidation of chromotropic acid by bromate. Under the conditions employed, the catalysed reaction was found to be first order with respect to vanadium and chromotropic acid, and the initial rate of the reaction is given by

$$v = k[\mathrm{V}][\mathrm{CA}]$$

where [V] and [CA] are the initial concentrations of vanadium and chromotropic acid, respectively, and k is the conditional rate constant.

It seems likely that an intermediate vanadium complex with chromotropic acid is involved in the course of the reaction;

$$\mathrm{CA} + \mathrm{V(V)} \rightarrow \mathrm{CA{:}V(V)}$$

Shnaiderman *et al.*[6] have studied the complex formation of vanadium with chromotropic acid and showed that the formation of the complex decreased with the addition of oxalate or citrate anion. In the present study, it was found that the rate of the vanadium-catalysed oxidation decreased with the addition of oxalic acid or citric acid as shown in the interference study. This suggests that the formation of vanadium complex must be considered in the course of the reaction.

However, further investigation, both experimental and theoretical, is necessary to elucidate the reaction mechanism. Details of the kinetic study will be described elsewhere.

CONCLUSIONS

It has been said that the reaction rate or tangent method in catalytic kinetic analyses is subject to a considerable operator error. However, in all experiments in this study, the absorbance *versus* rate curves are approximately linear within a 15-min reaction time, thus no special technique was required for the calculation of initial rate from the slope of the curves. Accordingly, the error arising from the graphical calculation seems to be very small.

The sensitivity of the catalysed reaction or the detection limit for the catalyst depends on the relative rates of the catalysed and uncatalysed reactions and the stability of this background uncatalysed reaction.

On the basis of the investigations described above, the vanadium-catalysed oxidation of chromotropic acid by bromate proved to be a simple, sensitive and

rapid means of determining trace amounts of vanadium.

Measurement times of about 20 min sufficed to determine vanadium at the stated levels.

SUMMARY

A catalytic reaction-rate method is described for the determination of trace amounts of vanadium; the method is based on the vanadium-catalysed oxidation of chromotropic acid by bromate. The reaction was followed spectrophotometrically by measuring the rate of change in absorbance of chromotropic acid at 430 nm. The method is sensitive, rapid and simple, and allows determination of as little as 5 ng of vanadium. Of the many ions examined, iron(III), copper and tungsten-(VI) interfered seriously at 100-fold concentrations. The relative standard deviation for 20 ng of vanadium (10 determinations) was 2.5%.

REFERENCES

1 K. B. Yatsimirskii, *Kinetic Methods of Analysis*, Pergamon, London, 1966, p. 64.
2 R. A. Greinke and H. B. Mark, Jr., *Anal. Chem.*, 44 (1972) 295R.
3 L. Sommer, *Acta Chim. Acad. Sci. Hung.*, 33 (1962) 23.
4 L. Sommer, *Z. Anal. Chem.*, 164 (1958) 299.
5 A. K. Mukherji and A. K. Dey, *J. Indian Chem. Soc.*, 35 (1958) 113.
6 S. Ya Shnaiderman, E. P. Klimenko and G. N. Prokofeva, *Izv. Vyssh. Ucheb. Zaved., Khim. Khim. Tekhnol.*, 12 (1969) 1637.

Analytica Chimica Acta, 70 (1974) 85–93

ENZYMATIC DETERMINATION OF ZINC BELOW ONE PART PER BILLION*

PAVEL LEHKY and ERIC A. STEIN
Department of Biochemistry, University of Geneva (Switzerland)
(Received 3rd October 1973)

Particulate aminopeptidase from pig kidney[1] (EC 3.4.1.2) is a metalloenzyme that contains 2 g-atoms of zinc per mole (m.w. 280,000)[2]. Although tightly bound, the metal can be removed from the enzyme and the resulting metal-free inactive apoenzyme can be prepared in gram amounts[3]. This apoenzyme has a high affinity for zinc and is readily reactivated by the latter metal, even after extended periods of storage, or upon exposure to heat and extreme pH. The assay of aminopeptidase activity is easy to perform, fast and sensitive, and does not require a more complex instrument than a recording photometer. As the recovery of activity is strictly proportional to the amount of zinc added to the apoenzyme (up to saturation), the aminopeptidase assay allows the quantitative determination of zinc(II). These features single out aminopeptidase as a reagent ideally suited for the assay of very low concentrations of zinc(II): a sample containing as little as 5 pg Zn ml^{-1} will cause a significant reactivation of aminopeptidase. The analytical procedure described here is not only highly sensitive, but also specific, since 0.1 ng Zn ml^{-1} can be assayed with 10% accuracy even in the presence of a ten- to hundred-fold excess of most other metals.

EXPERIMENTAL

Chemicals

"Specpure" divalent salts of Mg, Mn, Ca, Co, Ni, Cu, Zn, Cd, Hg (Johnson Matthey Chemicals, London), TES (N-tris[hydroxymethyl]methyl-2-aminoethane sulfonic acid; Sigma Chemical Company), Chelex X-100 chelating resin (Calbiochem), and Suprapure hydrochloric acid and EDTA (Merck) were used. All other chemicals were of analytical grade.

Demineralized water was double-distilled in an all-quartz apparatus. The still was rinsed daily to prevent accumulation of metal ions. Double-distilled water was stored in 30-l metal-free polyethylene bottles for no longer than one week. The zinc content of the water varied from 5 to 30 pg ml^{-1} as determined by the enzymatic procedure described below.

Containers and pipettes

Glassware was avoided in order to minimize contamination by traces of

* This paper is dedicated to Professor F. Leuthardt, Zurich, on the occasion of his 70th birthday.

metals. Only polyethylene or polypropylene vessels were used; they were filled with 1 *M* hydrochloric acid to remove metal contaminants. After 24 h, the containers were carefully emptied, rinsed with water, capped and stored in a dust-proof cabinet. Micropipettes ("BB" constriction type, Calbiochem, made of polymethylpentene) were cleaned with water, 50% HNO_3 (*pro analysi*), water, 1 *M* HCl (Suprapure) and again with water. In most cases, solutions were made or diluted by weighing.

Preparation of metal-free TES buffer

TES solutions, pH 7.0, were passed through a 1.2 × 17-cm polyethylene column filled with Chelex freshly rinsed with 250 ml of water and stored. Before use, the buffer was filtered once more through Chelex.

Preparation of apoaminopeptidase for zinc analysis

Aminopeptidase was isolated in pure form (specific activity 27–30 I.U.) from pig kidney* as described previously[2]. The apoenzyme was prepared by removal of zinc as follows: 10 ml of enzyme solution (5–10 mg ml^{-1} in 0.05 *M* TES, pH 7.0) was treated with a $\frac{1}{3}$ volume of wet Chelex; after 12 h at 4°, the resin was centrifuged off and washed with an equal volume of metal-free TES buffer. The combined washings and enzyme solution were treated twice more with Chelex. At this point the protein concentration was 2–3 mg ml^{-1}, as determined from the absorptivity[3] $E_{1\%}^{280} = 16.9$. Metal analysis by atomic absorption (Perkin-Elmer Model 303 spectrophotometer fitted with a recorder) indicated that the zinc content was below 0.02 p.p.m., the detection limit; the enzymatic activity was approximately 0.5% of that of untreated zinc-containing aminopeptidase. Such a solution of apoenzyme, stored frozen at −20° for 6 months, suffers no deterioration and regains full activity upon addition of zinc.

Principle of the enzymatic determination of zinc

When inactive apoaminopeptidase is added to the zinc-containing sample that is to be analyzed, a stoichiometric amount of enzyme reverts within a few seconds to its active form. To determine how much apoaminopeptidase has been reactivated, an aliquot is withdrawn from the reaction mixture and assayed for activity. The correlation between zinc content and enzyme activity yields a straight line between 0 and 2 g-atoms of zinc per mole of aminopeptidase (280,000), corresponding to 0 and 100% enzymatic activity, respectively[3]. The latter value is essentially constant for a given preparation of aminopeptidase, owing to the great stability of the enzyme. (A neutral aminopeptidase solution (0.5 mg ml^{-1}) stored for 2 years in a sealed tube, at room temperature, was shown to retain 95% of its original activity.) Moreover, excess of zinc has no effect on the enzymatic activity up to 200 g-atom mol^{-1}. Therefore, this assay yields all the information necessary to calculate the amount of zinc present in the sample, at least in the absence of interfering substances. When zinc has to be determined in the presence of other cations, or interfering substances of any kind, an internal standard should be used (see below).

* The same enzyme can now be obtained commercially from Sigma Chemical Co., St. Louis, Mo., USA.

After determination of the extent of reactivation by a sample of unknown chemical composition, one should check that nothing has interfered with the potential activity of apoaminopeptidase during interaction with the sample. To this effect, the apoenzyme is saturated with excess of zinc. If the reconstituted aminopeptidase shows a specific activity different from that of the native enzyme, inhibition or denaturation of aminopeptidase must be suspected and the zinc determination considered as invalid. However, this discrepancy seldom occurs (see Discussion).

Determination of aminopeptidase activity

The substrate used is 16.6 m*M* *L*-leucine-*p*-nitroanilide (first dissolved in 10% ethanol) made 0.5 *M* in TES and 0.1 m*M* in EDTA. The latter metal-binding agent is necessary to "neutralize" traces of metals that may contaminate the substrate[3]. The rate of liberation of *p*-nitroaniline is followed for 5–10 min at 405 nm with a recording photometer ($\varepsilon^{405} = 9620$ l mol^{-1} cm^{-1}). The assay is performed at 37° and pH 7.0 in a 1-ml glass cuvette with a 1-cm light path, by adding 0.5 ml of apoenzyme–sample mixture to 50 μl of EDTA-containing substrate. This order of addition is imperative to prevent adventitious enzyme activation by cuvette-derived metal ions.

Zinc determination

Depending upon whether the expected zinc concentration is in the 5–50 pg ml^{-1} or the 25–250 pg ml^{-1} range, one adds either 10 or 50 μl of apoaminopeptidase solution (0.1 mg ml^{-1}) to a sample diluted to 10 ml with metal-free buffer in a 10-ml polyethylene bottle. The latter is thermostatted at 37°, temperature equilibrium taking about 10 min. A 0.5-ml aliquot is added to 50 μl of substrate in the photometer cell and the aminopeptidase activity A_{Zn} is determined. After the increase in absorbance has been recorded for 1–5 min, 3 μl of 2 m*M* zinc sulfate (2 μM excess over EDTA) are added to the cuvette in which A_{Zn} has just been measured; this results in an immediate increase in activity (A_p). The latter measurement, made to ascertain that the apoenzyme has not been poisoned, can be omitted when one is working with a "clean" system, as A_p can be calculated from the amount of apoenzyme used for the assay.

The percentage reactivation P_r is given by the relation $P_r = (A_{Zn} - A_b) \cdot 100/A_p$, where A_b is the blank. The latter is determined as is done for A_{Zn}, but in the absence of sample.

To demonstrate that this analytical procedure applies to very low zinc concentrations, and that the relation between extent of reactivation and zinc concentration is linear, two calibration curves were established. The plots depicted in Fig. 1 and 2 were fitted by a computer program based on linear regression. The 95% confidence limits for each point are indicated by bars. The correlation coefficients calculated from the data of Fig. 1 and 2 were 0.991 and 0.995, respectively. For both sets of data, the slope of the curve was significantly different from zero. As the deviation from the origin was statistically not significant, there is no reason to suspect any systematic source of error in the measurements.

Determination of copper, cobalt and nickel

Most metals other than zinc are unable to confer activity to the apoenzyme.

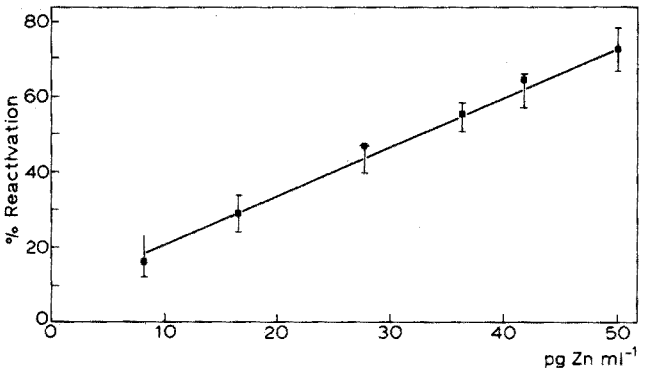

Fig. 1. Calibration curve for zinc at concentrations of 5–50 pg ml^{-1}.

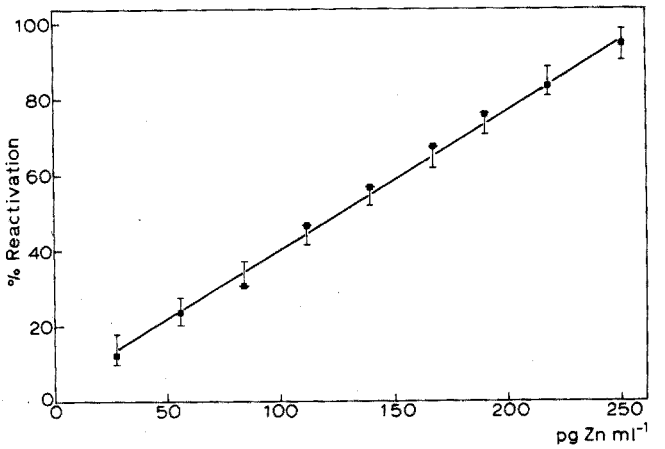

Fig. 2. Calibration curve for zinc at concentrations of 25–250 pg ml^{-1}.

The following cations, Be^{2+}, Mg^{2+}, Al^{3+}, Ca^{2+}, Sc^{3+}, Cr^{3+}, Mn^{2+}, Fe^{2+}, Fe^{3+}, Sr^{2+}, Pd^{2+}, Ag^{+}, Cd^{2+}, Sn^{2+}, Ba^{2+}, La^{3+}, Hg^{2+} and Pb^{2+}, were investigated, and failed to bring about any restoration of activity. In contrast, Cu^{2+}, Co^{2+} and Ni^{2+} could reactivate apoaminopeptidase[3] and therefore this enzyme could also be used to estimate the latter cations.

Because of the much lower affinity of the protein for Cu^{2+}, Co^{2+} and Ni^{2+} than for Zn^{2+}, the method in this case is less sensitive by two orders of magnitude. It is also less selective, as each of the three cations can be assayed only in the absence of the other two. In contrast to the reaction catalyzed by the zinc enzyme, which proceeds linearly with time, Fig. 3 shows that the rate of the reaction catalyzed by the Cu–, Co– and Ni–enzyme levels off within 10–30 min. Apparently, Cu^{2+}, Co^{2+} and Ni^{2+} are progressively removed from aminopeptidase during the assay, which is performed with EDTA-containing substrate[3]. Thus, EDTA, which does not affect the zinc enzyme under the conditions of the assay[3], provides a means of distinguishing Cu^{2+}, Co^{2+} and Ni^{2+} from Zn^{2+}, besides masking any metal contaminants in the substrate.

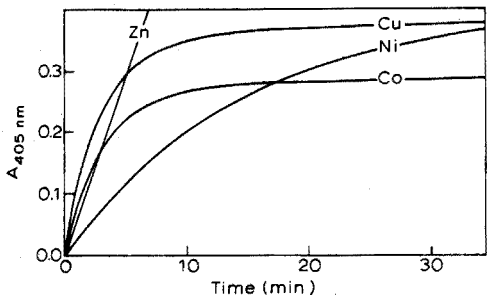

Fig. 3. Hydrolysis of leucine-*p*-nitroanilide by Zn–, Co–, Ni– and Cu–aminopeptidase in the presence of EDTA. The peptidases were prepared by reactivating the apoenzyme in the absence of EDTA with a two-fold excess of various metals. The reaction was started by the addition of the enzyme to the substrate. The final enzyme concentration was 0.75 μM.

The procedure for the determination of Cu^{2+}, Co^{2+} and Ni^{2+} is the same as for zinc, except that a higher concentration of apoenzyme (50 μg in 10 ml of buffered sample) must be used as the assay system contains much more metal than is the case for zinc. For determination of the aminopeptidase activity, the substrate is diluted 10 times with water; the assay is started by addition of 50 μl of apoenzyme–sample mixture to 0.5 ml of diluted substrate. Figure 3 shows clearly that it is imperative to measure the initial reaction rates. The calibration curves for Cu^{2+}, Co^{2+} and Ni^{2+} at concentrations ranging from 0.25–2.5 ng ml^{-1} are shown in Fig. 4.

Determination of zinc in the presence of other metals

To demonstrate that the enzymatic estimation of zinc is possible in the presence of a wide array of other cations, a typical sample for analysis was made up, containing 100 pg Zn ml^{-1} and a 10- to 100-fold molar amount of another cation, in TES buffer. After addition of 50 μl of a 0.1 mg ml^{-1} apoenzyme solution

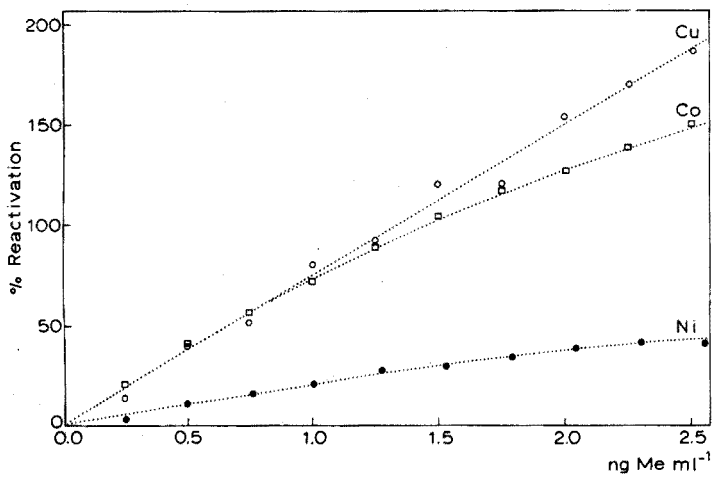

Fig. 4. Calibration curves for copper, cobalt and nickel.

to 10 ml of buffered sample, an aliquot of 0.5 ml was withdrawn and the extent of reactivation determined. In a second step, the zinc concentration of the remaining 9.5 ml of apoenzyme–sample mixture was increased by adding 111 pg Zn ml^{-1} as an internal standard, and the mixture reassayed. The resulting increase in activity was used to calculate the zinc concentration of the original sample (100 pg ml^{-1}). Table I presents the results of a series of such experiments performed in presence of a large variety of cations, and shows that zinc can be determined with a 10% error in the presence of a 100-fold molar amount of most metals, or of a 25-fold amount in the case of iron, cadmium, mercury or lead. The least favorable situation arises with cobalt, copper and nickel, where the 10% error level is already reached in presence of a 10-fold molar amount of the cation. As shown in Fig. 3, it is important in this case to let the reaction proceed for 10–30 min until the reaction rate becomes linear (as a consequence of the chelation of Cu^{2+}, Co^{2+} and Ni^{2+}) before A_{Zn} is determined.

TABLE I

DETERMINATION OF ZINC IN THE PRESENCE OF OTHER CATIONS

(The averages of three separate determinations of 100 pg Zn ml^{-1} as $ZnSO_4$ are presented with standard deviations; the experimental conditions are detailed in the text.)

Molar amount of metal ion		*Zn found (pg ml^{-1})*	*Molar amount of metal ion*		*Zn found (pg ml^{-1})*
NH_4^+	100×	100±4	Ni^{2+}	10×	128±5
Be^{2+}	100×	94±1	Cu^{2+}	10×	102±7
Mg^{2+}	100×	103±11	Sr^{2+}	100×	98±8
Al^{3+}	100×	101±8	Pd^{2+}	100×	109±3
Ca^{2+}	100×	95±5	Ag^+	100×	102±4
Sc^{3+}	100×	106±7	Cd^{2+}	25×	103±10
Cr^{3+}	100×	103±3	Ba^{2+}	100×	97±8
Mn^{2+}	100×	98±4	La^{3+}	100×	105±3
Fe^{2+}	25×	90±1	Hg^{2+}	25×	96±9
Co^{2+}	10×	101±8	Pb^{2+}	25×	93±5

Determination of zinc in physiological fluids

As an example, the enzymatic determination of zinc was carried out on 2 μl of bovine serum. The average of 6 measurements gave the value 1.06 μg Zn ml^{-1} with a standard deviation of ±0.03. Two determinations by atomic absorption spectrometry on a 300-fold larger sample gave 1.09 and 1.10 μg Zn ml^{-1}.

DISCUSSION

During the last decade, various enzymes have been proposed as highly sensitive reagents for the determination of trace metals. Guilbault[4] has provided an extensive review of the literature. However, enzymatic analysis has turned out to be generally disappointing because many metals proved to interfere with the assay, either by activating or by inhibiting the enzyme. Activation of an enzyme by an extrinsic metal activator is not selective enough to make such a system attractive

from an analytical point of view. The desirable selectivity may be achieved only in the instance of a genuine metalloenzyme, when a given metal is incorporated within the folds of the polypeptide backbone of the enzyme, in a unique structure that is so tight that the metal is considered to be part of the enzyme molecule[7]. The pioneering work of Townshend and Vaughan on the enzymatic determination of zinc[5,6] deserves mention with respect to such enzymes.

Pig kidney particulate aminopeptidase has been shown to be a suitable metalloenzyme containing 2 g-atom of zinc per mole. Although zinc is very firmly bound, a metal-free, inactive form of the enzyme (apoaminopeptidase) can be obtained[3]. In the presence of traces of free zinc ions, the apoaminopeptidase molecule reverts to a powerful catalyst able to hydrolyze 10^4 molecules of substrate per min. As the hydrolysis of 10^{-9} mole of substrate can be readily estimated, aminopeptidase (and consequently zinc) can be assayed with extreme sensitivity. Under ideal conditions, the procedure described above might allow the determination of zinc at concentrations lower than 1 pg ml^{-1}. In practice, however, the sensitivity of the test is limited by the presence of extraneous contaminants. These can be kept at an acceptable level if the precautions described in this work are scrupulously observed. The manipulation involved in the test are limited to: (1) the mixing of sample and reagent, (2) the pipetting of an aliquot, and (3) the mixing with the substrate in the photometer cell. As the latter operation is performed in the presence of EDTA, only the first two manipulations constitute a potential source of contamination. Because of the high stability of the zinc–apoenzyme complex, pH adjustment before the activity determination can often be avoided. In fact, mixing of sample and apoenzyme can be done at any pH between 4.5 and 9.0 for zinc concentrations above 10 ng ml^{-1}; for lower levels, one should not operate below neutrality.

The sensitivity of the present method compares very favorably with most other procedures so far described for zinc determinations, for instance, atomic absorption[8], neutron activation analysis[9], and even anodic pulse polarography[10] or atomic fluorescence flame spectrometry[11], which all require much more complex and expensive instrumentation.

The striking stability of apoaminopeptidase represents an important asset in its use as an analytical tool. Stored in solution at room temperature in the presence of toluol, the protein can retain 95% of its potential activity for two years. It is equally resistant to acidic and alkaline conditions, from pH 4 to 11, and is little affected by heavy metals such as Hg^{2+}, Cd^{2+}, Ag^{+}, etc. This behavior, unusual for an enzyme, is probably due to the absence of free sulfhydryl groups and to the presence of a large proportion of carbohydrates in the enzyme molecule (400 sugar residues, amounting to 20% of the molecular weight)[2].

A major advantage of the procedure proposed here is that interferences with the determination of zinc are easily evidenced. Non-linearity of the curve reveals the presence of Cu^{2+}, Co^{2+} or Ni^{2+}[3]. Failure fully to reactivate the reagent with an excess of zinc (A_p) indicates irreversible poisoning of the reagent. Reversible inhibition may also occur, for instance in the presence of Hg^{2+}, Cd^{2+}, Be^{2+} or Ni^{2+}. In this instance, one observes a progressive increase of A_p to its normal value, as zinc(II) in excess displaces extraneous cations[3]. In all cases the interferences are obvious and can usually be corrected by means of the "internal standard" method.

The affinity of apoaminopeptidase for Cu^{2+}, Co^{2+} and Ni^{2+} is considerably lower than that observed for zinc[3], which explains why these metals do not prevent the determination of zinc (at 0.1 ng ml^{-1}), even in ten-fold molar amounts. Zn^{2+} and either Cu^{2+} or Co^{2+} can be assayed simultaneously when they are present in similar concentrations. The initial reaction rate reflects the compounded effects of both zinc and copper (or cobalt), while the rate measured after a further 10 min is due to zinc(II) only. Simultaneous determination of Zn^{2+} and Ni^{2+} is less satisfactory, since Ni^{2+} is not as readily displaced from the reagent as Cu^{2+} or Co^{2+}

The distinction between free and bound trace elements is of major importance in the investigation of biological samples. By direct determination, classical methods such as atomic absorption allow only the determination of total zinc. In contrast, the enzymatic procedure detects available zinc, *i.e.* first free zinc, then loosely bound zinc and finally, after denaturation of the sample, firmly bound zinc. This constitutes another asset of aminopeptidase as an analytical reagent.

As the level of zinc in most mammalian tissues is significantly higher than that of the "sensitive" cations of nickel, cobalt and copper[1,2], the method described here is particularly well suited to the investigation of such biological samples, and has been tested successfully in the case of blood serum. Indeed, zinc is the most abundant intracellular trace element in the human body, and is instrumental in the functioning of many vital metalloenzymes, both intra- and extracellular. A general need for the clinical estimation of zinc levels, comparable to the present interest in iron deficiency, has been predicted[1,2].

This work was supported by grants 4740 and 3.652.71 from the Swiss National Science Foundation. We are grateful to Professor W. Haerdi, from the Department of Analytical Chemistry of this University, for valuable advice, and to M. M. Dumas for his skilful assistance during an undergraduate participation program.

SUMMARY

A stable and very sensitive reagent for the determination of zinc is obtained by removing zinc from pig kidney aminopeptidase, a commercially available metalloenzyme. Up to a given limit, the enzymatic activity of the reagent is strictly proportional to the concentration of zinc ions in the assay system. Aminopeptidase activity is determined by measuring the rate of release of *p*-nitroaniline from the chromogenic substrate *L*-leucine-*p*-nitroanilide. Thus, with a simple recording photometer, rapid and accurate determinations of free zinc ions in concentrations ranging from 5 pg–10 μg ml^{-1} can be achieved. The selectivity of the method is such that 0.1 ng Zn ml^{-1} can be assayed in the presence of a 10–100-fold molar amounts of a wide array of other cations with a relative error below 10%. The analytical procedure has been extended to the assay of Cu^{2+}, Co^{2+} and Ni^{2+} in the ng ml^{-1} range.

REFERENCES

1 E. D. Wachsmuth, I. Fritze and G. Pfleiderer, *Biochemistry*, 5 (1966) 169.
2 H. Wacker, P. Lehky, E. H. Fischer and E. A. Stein, *Helv. Chim. Acta*, 54 (1971) 473.

3 P. Lehky, J. Lisowski, D. Wolf, H. Wacker and E. A. Stein, *Biochim. Biophys. Acta*, 321 (1973) 274.
4 G. G. Guilbault, *Enzymatic Methods of Analysis*, Pergamon Press, Oxford, 1970, pp. 176–196.
5 A. Townshend and A. Vaughan, *Anal. Chim. Acta*, 49 (1970) 366.
6 A. Townshend and A. Vaughan, *Talanta*, 17 (1970) 289.
7 B. L. Vallee and W. E. C. Wacker, in H. Neurath (Ed.), *The Proteins*, Vol. 5, Academic Press, New York, 2nd edn., 1970, pp. 61–93.
8 *Standard conditions for zinc*, in Perkin-Elmer's *Analytical Methods for Atomic Absorption Spectrophotometry*, Norwalk Connecticut, U.S.A., 1971.
9 G. Roncari, H. Zuber and A. Wyttenbach, *Int. J. Peptide Protein Res.*, 4 (1972) 267.
10 A. M. Bond and D. R. Canterford, *Anal. Chem.*, 44 (1972) 721.
11 K. E. Zacha, M. P. Bratzel, Jr., J. D. Winefordner and J. M. Mansfield, Jr., *Anal. Chem.*, 40 (1968) 1733.
12 H. A. Schroeder and A. P. Nason, *Clin. Chem.*, 17 (1971) 461.

Analytica Chimica Acta, 70 (1974) 95–106

SPECTROPHOTOMETRIC STUDIES OF REDUCED MOLYBDOANTIMONYLPHOSPHORIC ACID

J. E. GOING and S. J. EISENREICH

Department of Chemistry, University of Wisconsin–Milwaukee, Milwaukee, Wis. 53201 (U.S.A.)

(Received 8th October 1973)

The photometric determination of phosphate at the trace level has been commonly based upon the formation of 12-molybdophosphoric acid, in a reduced or oxidized state or on the formation of a mixed heteropoly acid such as molybdovanadophosphoric acid[1]. At very low concentrations, the more sensitive reduced 12-molybdophosphoric acid form is preferred. Ascorbic acid has been widely acclaimed as the most suitable reductant even though the reduction rate is slow at room temperature. In 1962, Murphy and Riley[2] introduced the use of antimony(III) as potassium antimony tartrate as a means of increasing the reduction rate. Subsequently, the Murphy and Riley technique has become one of the most frequently used procedures, achieving tentative status in *Standard Methods for the Examination of Water and Wastewater*[1] and inclusion in the Environmental Protection Agency's *Methods for Chemical Analysis of Water and Wastes*[3]. The formation conditions for the Murphy and Riley procedure have largely been developed empirically although they are generally recognized to be a function of solution acidity and molybdate concentration. A study of the published procedures utilizing the combination of ascorbic acid and potassium antimony tartrate shows the variability in formation conditions[1–6]. The recommended acidity ranges from 0.11 to 0.99 *N* while the molybdate concentration ranges from 15 to 105 mg Mo/100 ml. No definite relationship has been reported between the solution acidity and the molybdate concentration. Such methodology makes it difficult to modify or vary the procedure should conditions require doing so.

Furthermore, no attempt has been made to explain the function and stoichiometry of antimony in the formation and reduction process although direct reduction of 12-molybdophosphoric acid by antimony(III) (ref. 7) has been reported. In a similar system, zirconium and titanium were reported to catalyze the reduction of 12-molybdophosphoric acid and recently zirconium, titanium, and thorium[9] as well as cerium[10] have been reported to form discrete mixed heteropolys with molybdophosphoric acid. Goldman and Hargis[11] have reported that bismuth forms an 18-molybdobismuthophosphoric acid which is reduced by ascorbic acid.

The present study was undertaken to establish the formation conditions of the ascorbic acid-reduced molybdophosphoric acid with and without antimony(III) present, with emphasis on the acidity–molybdate relationship, and to study the role of antimony in the formation and reduction process.

EXPERIMENTAL

Spectrophotometric measurements

Absorbance measurements were made on either a Beckman DU or a Heath–Schlumberger Model 721 spectrophotometer equipped with a red-sensitive photomultiplier tube. Some spectral measurements were obtained on a Cary 14 spectrophotometer. Ultraviolet spectra were obtained for solutions containing various combinations of 40.0 μM phosphate, 1.99 mM molybdate, 80.0 μM antimony, and 0.103 M sulfuric acid.

Spectrophotometric formation studies of reduced phosphomolybdic acid were carried out with the inclusion of a heating step in the procedure. Before final dilution, the solutions were heated to the first sign of boiling, cooled, and diluted. Formation studies made in the presence of antimony did not require heating. The absorbance was measured at 840 nm without antimony present and at 880 nm when it was present.

The composition of the reduced antimony heteropoly acid was determined by measuring the absorbances of solution of varying Sb/P ratios at 710, 840, and 880 nm. All solutions were heated before final dilution. Spectra of the solutions were also obtained.

The same experiment was repeated without heating the solutions. The absorbance of each solution was monitored at 880 nm for 30 min after the addition of ascorbic acid.

A solvent extraction study of the Sb/P ratio was performed by preparing the mole ratio solutions at pH 1.59. The solutions were extracted with n-butyl acetate for 15 min and centrifuged, and the absorbance of the organic phase was measured at 721 nm.

A mole ratio study of the Mo/P ratio was conducted by varying the Mo/P ratio from 3 to 50 while maintaining an acid/molybdate ratio of 75. The Sb/P ratio was maintained at 2.0. Absorbances were measured after 30 min. The same experiment run without antimony required the heating step previously described.

The Mo/P ratio was also studied by the continuous variations method. When antimony was present, the Sb/P ratio was maintained at 2:1. The acid was varied to maintain an acid/molybdate ratio of 75. The critical solutions were dispensed by a Pipetman adjustable digital microliter pipette (Rainin Instrument Co.). The solutions which did not contain antimony were heated as before.

The amount of ascorbic acid required for complete reduction was studied by a mole ratio experiment.

A sample of the solid molybdoantimonylphosphoric acid was prepared by reacting KH_2PO_4, $K(SbO)C_4H_4O_6 \cdot 1/2\ H_2O$, and $(NH_4)_6Mo_7O_{24} \cdot 4H_2O$ in molar ratios of 1:2:10 at a pH of 1.00 with an excess of ascorbic acid present. The solution was heated to boiling and cooled, and the solid precipitate was collected, washed, and dried at 80°C. Weighed samples were decomposed by boiling in aqua regia for 1 h. Phosphate was determined as reduced molybdoantimonylphosphoric acid[1]. Antimony was determined colorimetrically as the iodo complex[12] and by iodimetric titration[13]. Molybdenum was determined by back-titration based on EDTA[14].

Acidity measurements

Hydrogen ion concentrations were calculated from known additions of standard sulfuric acid. Acid/molybdate ratios were calculated from this hydrogen ion concentration.

Reagents

Stock solutions of molybdenum(VI) were prepared from reagent-grade $(NH_4)_6Mo_7O_{24}\cdot 4H_2O$ or $Na_2MoO_4\cdot 2H_2O$. The solutions were aged for 48 h before use[15]. Stock phosphate solutions were prepared from KH_2PO_4. Antimony(III) solutions were prepared from $K(SbO)C_4H_4O_6\cdot 1/2H_2O$. All solutions were prepared with doubly distilled water and stored in glass or polyethylene bottles. All glassware was carefully washed with 6 *M* hydrochloric acid and rinsed with doubly distilled water before use.

RESULTS AND DISCUSSION

Formation conditions

When a solution of phosphate and molybdate is acidified with sulfuric acid, 12-molybdophosphoric acid is formed. In the presence of a reducing agent such as ascorbic acid, the heteropoly acid is reduced to the blue form. The rate of reduction is quite slow at room temperature requiring at least one day to reach completion but can be increased considerably in practice by heating the solution. The reduced 12-molybdophosphoric acid is characterized by an absorption maximum at 840 nm with $\varepsilon = 26{,}400$. If antimony(III) is added as the tartrate as in the Murphy and Riley procedure[2], the reduction is complete in less than 10 min at room temperature and the resulting complex has absorption maxima at 880 and 710 nm with molar absorptivities of 22,400 and 17,000, respectively. The formation of both reduced heteropoly acids was studied extensively as a function of the solution acidity and molybdate molarity. The results are graphed in Figs. 1 and 2 as observed absorbance *versus* the acid/molybdate, $[H^+]/[MoO_4^{2-}]$, ratio. The most striking feature of the figures is the appearance of plateaux on the formation curves which correspond solely to the formation of reduced heteropoly acid. A plateau is seen to exist at each molybdate concentration from 0.0008 to 0.01 *M*, *i.e.* generally within the $[H^+]/[MoO_4^{2-}]$ range of 50–80 with 70 being central. Thus, the plateau or region of optimal formation occurs at the same $[H^+]/[MoO_4^{2-}]$ ratio, irrespective of the molybdate concentration. At the lower end of the ratio, reduction of excess of molybdate occurs, forming molybdenum blue and masking the reduced heteropoly acid. At the high end of the ratio, formation is inhibited resulting in decreased absorbance. Table I lists the various molybdate concentrations studied, the range in acidity corresponding to the plateau region and the corresponding calculated $[H^+]/[MoO_4^{2-}]$ ratios. Experimentally, the optimal conditions are very simply met by maintaining an $[H^+]/[MoO_4^{2-}]$ ratio of 70 ± 10. This is conveniently done in the preparation of the reagent solutions. It is interesting to note that the published procedures[1–6] based upon the Murphy and Riley technique all result in a final $[H^+]/[MoO_4^{2-}]$ value of 70 ± 4.

The present results parallel the conclusion of Strickland who suggests an $[H^+]/[MoO_4^{2-}]$ ratio of 3–5 for the reduction of 12-molybdosilicic acid with tin(II)

TABLE I

OPTIMAL FORMATION CONDITIONS AS $[H^+]/[MoO_4^{2-}]$ RATIOS

$[MoO_4^{2-}]$ (M)	Range of $[H_2SO_4]$ (M)	Range of $[H^+]/[MoO_4^{2-}]$
Reduced 12-MPA		
$2.80 \cdot 10^{-4}$	0.001–0.004	12–30
$1.40 \cdot 10^{-3}$	0.021–0.112	30–160
$4.20 \cdot 10^{-3}$	0.084–0.210	40–100
$8.40 \cdot 10^{-3}$	0.168–0.357	40–85
$1.21 \cdot 10^{-2}$	0.272–0.484	40–80
Reduced 12-MSbPA		
$8.40 \cdot 10^{-4}$	0.016–0.055	40–130
$1.40 \cdot 10^{-3}$	0.042–0.091	60–130
$1.60 \cdot 10^{-3}$	0.074–0.182	50–130
$8.40 \cdot 10^{-3}$	0.210–0.294	50–70
$1.68 \cdot 10^{-2}$	0.303–0.420	36–50

(ref. 16). The difference in values is due to the difference in phosphorus and silicon heteropoly acid behavior and in the choice of reductant. Also, Strickland did not study widely varying molybdate concentrations as was done in this work. His choice of an upper level of 5 was apparently due to the fact that the reduction reaction became very slow at higher acidities.

It should be noted that the formation curves for the reduction of 12-molybdophosphoric acid with and without antimony are essentially identical. Preliminary studies of the reduction of 12-molybdoarsenic acid with and without antimony show the same general behavior. Consequently, the criteria of the $[H^+]/[MoO_4^{2-}]$ ratio seems to be general for heteropoly acid reduction and may reflect more the behavior of molybdenum in acidic solution than the identity of the heteropoly acid.

In practice, use of the $[H^+]/[MoO_4^{2-}]$ criteria allows the experimenter to exercise control over the final solution acidity. This can be of importance, for example, in obtaining the optimal acidity for extraction of the reduced heteropoly without the need for any adjustments after formation is complete. In situations where a highly acidic solution may hydrolyze organophosphates or polyphosphates, it would be desirable to work at the lowest acidity possible.

The effect of ascorbic acid concentration on the extent of reduction was studied by a mole ratio procedure. Reduction of 12-molybdophosphoric acid, with or without antimony, required a 20-fold molar amount of ascorbic acid. No difference was observed up to a 200-fold molar amount. The higher concentration is used to minimize the time required for complete reduction.

Composition of the reduced heteropoly acid

Preliminary evidence that antimony(III) was incorporated into the heteropoly acid was obtained from the u.v. spectra of the oxidized complex. Addition of antimony(III) to a solution of 12-molybdophosphoric acid produced a bathochromic

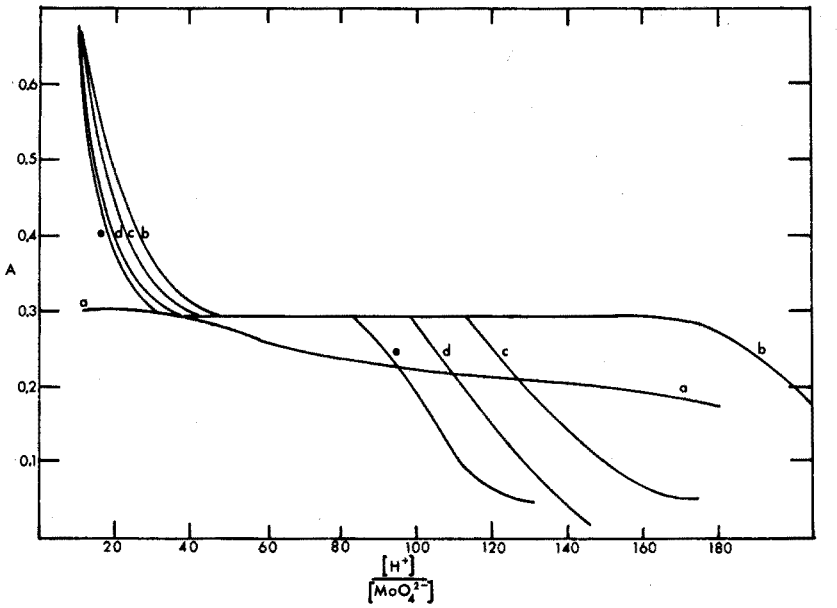

Fig. 1. Formation of reduced molybdophosphoric acid. [P], 10.5 μM, [Mo]: (a) $2.80 \cdot 10^{-4}$ M; (b) $1.40 \cdot 10^{-3}$ M; (c) $4.20 \cdot 10^{-3}$ M; (d) $8.40 \cdot 10^{-3}$ M; (e) $1.21 \cdot 10^{-2}$ M.

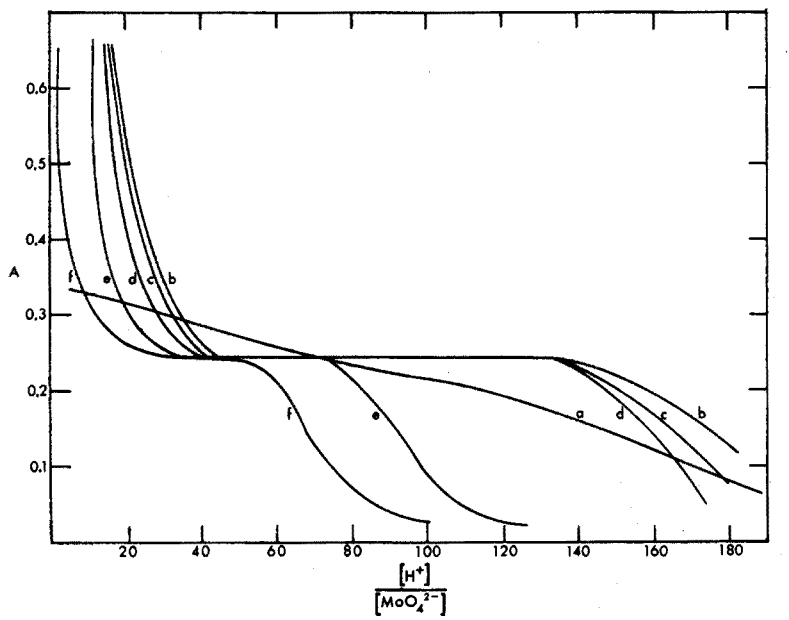

Fig. 2. Formation of reduced molybdoantimonylphosphoric acid. [P], 10.5 μM; [Sb], 21.0 μM; [Mo]: (a) $2.80 \cdot 10^{-4}$ M; (b) $8.40 \cdot 10^{-4}$ M; (c) $1.40 \cdot 10^{-3}$ M; (d) $2.80 \cdot 10^{-3}$ M; (e) $8.40 \cdot 10^{-3}$ M; (f) $1.60 \cdot 10^{-2}$ M.

shift in the u.v. spectra similar to the observations on the effects of bismuth[11], thorium[9], zirconium[9], titanium[9], and cerium[10]. Addition of antimony(III) to acidified molybdate did not result in any changes in the u.v. spectra, suggesting that antimony(III) reacts only with the heteropolymolybdates and not the isopolymolybdates. The addition of antimony(III) to a solution of reduced 12-molybdophosphoric acid produced no change in the near i.r. spectrum.

The marked change in the near i.r. spectra when 12-molybdophosphoric acid was reduced by ascorbic acid in the presence of antimony(III) indicated that antimony(III) was also involved in the formation of the reduced heteropoly acid.

Several similar ternary heteropoly acids have been reported as having a variety of phosphorus : metal : molybdenum molar ratios. Some are listed in Table II. All the studies were of oxidized heteropolys except those of molybdobismuthophosphoric acid and molybdoniobophosphoric acid.

TABLE II

STOICHIOMETRIES OF MIXED HETEROPOLY ACIDS

Heteropoly acid	*Reference*	*Ratio P:X:Mo*
Molybdovanadophosphate	18	1:1:11
		1:2:10
		1:3:9
Molybdotitanophosphate	9	1:1:12
Molybdothorophosphate	9	1:1:12
Molybdozirconophosphate	9,19	1:1:12
Molybdoniobophosphate	20	1:1:10
Molybdoniobophosphate	21	1:2:10
Molybdobismuthophosphate	11	1:1:18
Molybdocerophosphate	10	1:2:?
Tungstovanadoselenite	22	[a]
Molybdostannosilicate	23	[b]

[a] Se:V:W ratio of 1:2:10.
[b] Si:Sn:Mo ratio of 1:2:10.

Mole ratio studies of the Sb:P ratio were initially conducted with a heating step included in the procedure. Consequently, any phosphate not incorporated into the reduced molybdoantimonylphosphoric acid would form reduced 12-molybdophosphoric acid. The spectra for the mole ratio experiment are shown in Fig. 3 and illustrate the transformation from reduced 12-molybdophosphoric acid to reduced molybdoantimonylphosphoric acid (MSbPA). Mole ratio plots of the respective absorption maxima are shown as curve A of Fig. 4. The plots all bend at an Sb/P ratio of 2, indicating that two antimony atoms are being incorporated into the ternary complex. Murphy and Riley[2] reported a ratio of 1:1, however, their reported spectrum corresponds to that obtained in this study at Sb/P ratios of 2 or greater. A second mole ratio experiment was performed to verify the results. All the solutions were prepared as before at a pH of 1.59 and were extracted with butyl acetate. At this pH, butyl acetate extracts reduced MSbPA but not reduced 12-molybdophosphoric acid[17]. The absorbance of the organic phase at 721 nm

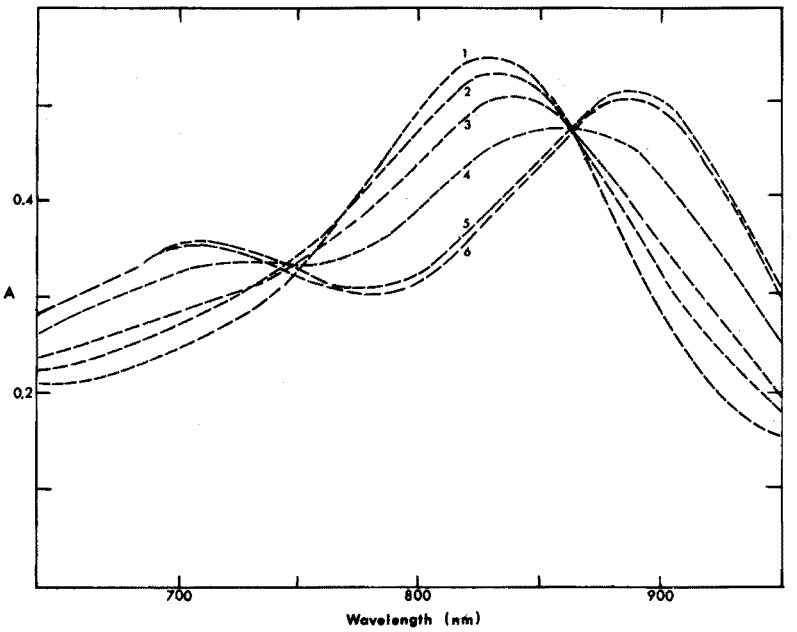

Fig. 3. Effect on spectra of increasing antimony concentration. [KH_2PO_4], 21.2 μM; [Na_2MoO_4], 0.70 mM; [H_2SO_4], 0.030 M; [ascorbic acid], 1.13 mM; [Sb]/[P]: (1) 0.47; (2) 0.71; (3) 0.95; (4) 1.42; (5) 1.89; (6) 2.37–4.74.

plotted *versus* the Sb/P ratio as curve B, Fig. 4, again indicates a 2:1 ratio. An additional experiment was conducted in which the solutions were not heated. Consequently, only reduced MSbPA was formed in the first 15 min. These results are shown as curve C, Fig. 4, and again confirm a 2:1 ratio for Sb:P.

The stoichiometry of heteropoly acids with respect to molybdenum has long been difficult to determine with great certainty. Initially a mole ratio experiment was conducted in which the molybdate was varied and all other reagents were kept constant. This approach was discarded when molybdenum blue formation interfered. Consequently, the acidity was adjusted in each solution to maintain a $[H^+]/[MoO_4^{2-}]$ ratio of 76. The results for the formation of reduced 12-molybdophosphoric acid and MSbPA are shown in Fig. 5. The extrapolated lines intersect at a Mo/P ratio of 24–26 for both heteropolys. Since 12-molybdophosphoric acid is known to contain only 12 molybdenum atoms per phosphorus, the results only indicate that a 26-molar excess of molybdenum is necessary to drive either reaction to completion.

Continuous variations studies of the Mo:P ratio in heteropoly acids have been used with limited success. Shkaravskii[19] reported a 12:1 ratio for the reduced molybdoniobophosphoric acid and Murata *et al.*[9] reported 12:1 ratios for the titanium, zirconium and thorium mixed molybdophosphates. Results of the continuous variations study of reduced 12-molybdophosphoric acid and MSbPA are shown in Fig. 6. The experiments were run in parallel with the same adjustable micrometer pipet to dispense the solutions. The $[H^+]/[MoO_4^{2-}]$ ratio was kept constant. The results tend to indicate a Mo:P ratio of 12:1 for reduced 12-molybdo-

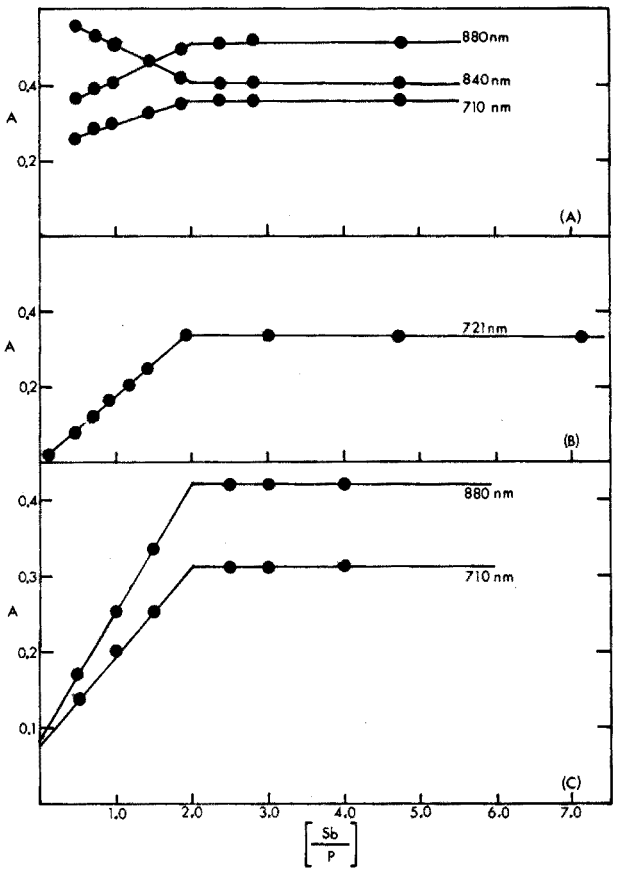

Fig. 4. Determination of Sb:P by mole ratio method. (A) Molybdoantimonylphosphoric acid, aqueous, heated; (B) Molybdoantimonylphosphoric acid, butyl acetate extract, heated; (C) molybdoantimonylphosphoric acid, aqueous, unheated.

phosphoric acid and 10:1 for reduced MSbPA. While the inherent uncertainty of the experiment prevents stating the ratios as unequivocal, it is apparent that they differ by about two. Consequently, the Mo:P ratio for reduced MSbPA was concluded to be 10:1.

Elemental analysis of solid reduced MSbPA was conducted for phosphorus, antimony and molybdenum. The Sb:P ratio for duplicate analyses of duplicate preparations was invariably 2.0:1.0. The Mo/P ratio was variable and averaged at 11.4. This ratio can be expected to be high if co-precipitation of molybdenum blue occurs. This would have no effect on the Sb:P ratio, however.

From the present results and from earlier information on the molybdovanadophosphate[18], molybdoniobophosphate[20], molybdovanado selenite[22] and the molybdostannosilicate[23], it was concluded that the stoichiometry of the reduced MSbPA is $PSb_2Mo_{10}O_{40}$. Changes in the u.v. spectra indicate that antimony(III) reacts with 12-molybdophosphoric acid presumably by replacing two molybdenum atoms by two antimony atoms. This new mixed heteropoly is reduced by ascorbic

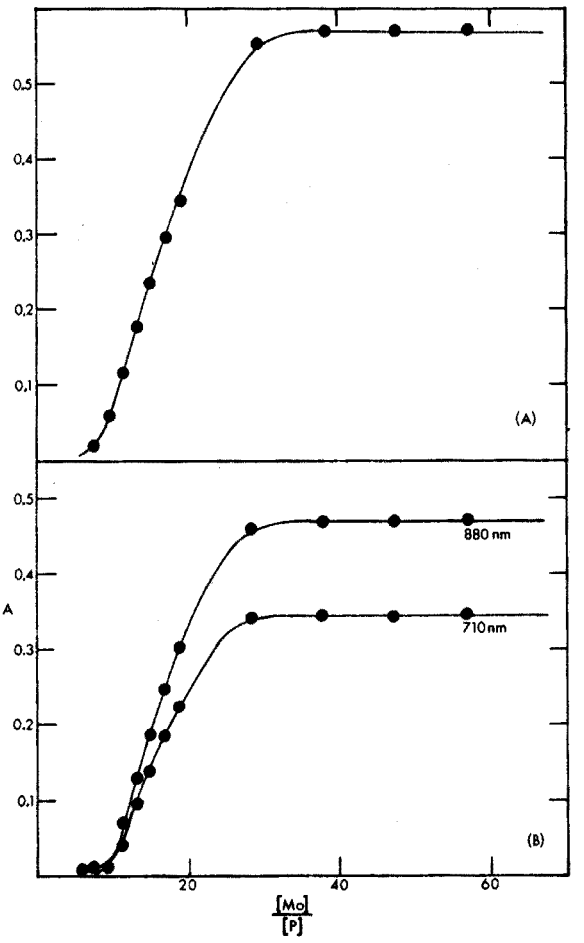

Fig. 5. Study of Mo:P by mole ratio method. (A) Molybdophosphoric acid; (B) molybdoantimonylphosphoric acid; [P], 21.2 μM; [Sb], 41.4 μM; $[H^+]/[MoO_4^{2-}]$, 75.

acid at a much higher rate than 12-molybdophosphoric acid. Antimony probably either alters the structure of the heteropoly so that the reduction rate is increased, or facilitates the transfer of electrons from the ascorbic acid reductant to the molybdenum cage. In the second case, antimony(III) may be functioning as a reducing agent itself and the resulting antimony(V) is subsequently reduced to antimony(III) by the ascorbic acid. This is not altogether unreasonable since antimony(III) has been reported to reduce 12-molybdophosphoric acid by itself although at a higher acidity and at 100°C (ref. 7). The actual mechanism of formation and reduction deserves further study.

Significance

The consistency of the $[H^+]/[MoO_4^{2-}]$ ratio in the formation of both reduced heteropolys can be cautiously interpreted in terms of molybdate polymerization. Previous studies of the formation of reduced 12-molybdophosphoric acid

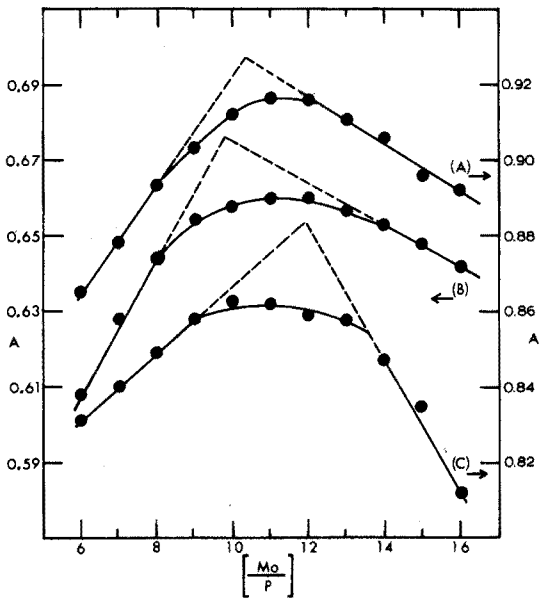

Fig. 6. Determination of Mo:P by continuous variations method. (A) Molybdoantimonylphosphoric acid, 880 nm; (B) molybdoantimonylphosphoric acid, 710 nm; (C) molybdophosphoric acid, 840 nm; [P]+[Mo], $4.00 \cdot 10^{-4}$ *M*; [Sb]=2[P]; $[H^+]/[MoO_4^{2-}]$, 70.

and reduced MBiPA have suggested that molybdate is present and reacting as a dimer[11,15]. Studies of the reduced 12-molybdophosphoric acid have been made at $[H^+]/[MoO_4^{2-}]$ ratios of 75 (ref. 15) and 82 (ref. 24) with sulfuric acid, and at a ratio of 100 with nitric acid[11]. Ascorbic acid was used as the reducing agent. Since the existence of dimerized molybdenum was observed at a $[H^+]/[MoO_4^{2-}]$ ratio that coincides with the center of the formation plateau, it would seem that the plateaux correspond to the regions of existence of molybdenum dimers. It should be pointed out that there is no direct evidence that all of the molybdenum is dimerized.

At the lower ratios, or when the acidity is decreased, polymerization of molybdenum is favored and molybdenum blue formation becomes dominant. This is evidenced by the sharply rising absorbances in those regions in Figs. 1 and 2. At high ratios, or high acidity, the formation of reduced heteropoly is diminished, presumably as a result of formation of molybdenyl cationic species which are unreactive with phosphate. The plateau region is where the molybdenum has been sufficiently depolymerized to prevent molybdenum blue formation and where the phosphate-reactive form of molybdenum, presumably the dimer, predominates.

As the molybdate concentration is increased, a higher acidity is required to prevent molybdate polymerization and the subsequent molybdenum blue formation. Conversely, at lower molybdenum concentrations, a less acidic solution suffices. This is in agreement with the trends shown in Figs. 1 and 2. Strickland has reported a similar trend in hydrochloric and sulfuric acid media with tin(II) as reductant[16].

GENERAL PROCEDURES

The proper conditions can now be set forth for the optimal formation of

reduced MSbPA. The ratio of $[H^+]/[MoO_4^{2-}]$, for sulfuric acid, should be 70 ± 10 for molybdate concentrations ranging from 0.0008 to 0.01 *M*. Molybdate should be present in excess over phosphate by at least a 25:1 ratio, 40:1 being preferable. The antimony concentration must be at least twice the maximum phosphate level, but should not exceed about 0.0001 *M* owing to solubility problems[2]. Ascorbic acid must be at least 20 times the maximum phosphate level although in practice a very large excess is used.

The mixed reagent solutions described below are prepared so that they can be diluted by as much as 1–50 ml for phosphate levels no greater than $2.5 \cdot 10^{-5}$ *M* (2.4 p.p.m. PO_4^{3-}) or by as little as 1–5 ml for higher phosphate concentrations or if a higher acidity is required. Two procedures are given, the first allows the experimenter to choose the acid–molybdate concentration; the second is designed for analysis of a fixed volume of sample.

Procedure 1

Mixed reagent. Dissolve 2.12 g of $Na_2MoO_4 \cdot 2H_2O$ in 150 ml of distilled water. Add 20.8 ml of concentrated sulfuric acid slowly with stirring. Cool to room temperature, add 0.668 g of potassium antimony tartrate, and dilute to 250 ml. The reagent is stable for several weeks at room temperature.

Ascorbic acid. Prepare a 1% solution daily.

Pipet an appropriate volume of the unknown sample into a 50-ml volumetric flask. Add 1 drop of phenolphthalein to the solution. If a red color develops, add 0.5 *M* sulfuric acid to discharge the color; 1.0–10.0 ml of mixed reagent may be added. For most work, add 5 ml of mixed reagent and 2 ml of ascorbic acid and dilute to volume. Measure the absorbance at 880 nm after 10 min but no later than 30 min *versus* a reagent blank.

Procedure 2

Mixed reagent. Prepare the mixed reagent as before with the addition of 2.0 g of ascorbic acid after addition of the antimony. The solution is stable for one week at 4°C.

Add 1 drop of phenolphthalein to 50.0 ml of sample. If a red color develops, add 3 *M* sulfuric acid dropwise to discharge the color. Add 5.0 ml of mixed reagent containing ascorbic acid and mix. Measure the absorbance at 880 nm after 10 min but no later than 30 min *versus* a reagent blank.

The use of a Cary 14 at Marquette University, Milwaukee, Wisconsin, and the assistance of Mark Marcus in obtaining near-i.r. spectra, are gratefully acknowledged. Support for S.J.E. was provided by the Graduate School, University of Wisconsin–Milwaukee, for 1970–71.

SUMMARY

Spectrophotometric studies have been used to determine the optimal formation conditions and stoichiometry of the reduced molybdoantimonylphosphoric acid. It was found that a $[H^+]/[MoO_4^{2-}]$ ratio of 70 ± 10 was optimal for formation between 0.0008 and 0.01 *M* molybdenum. This corresponds to solution conditions

that favor the existence of the dimeric form of molybdenum. The $[H^+]/[MoO_4^{2-}]$ criteria allows simple variation of experimental conditions. The stoichiometry of the reduced heteropoly acid was surmised to be $PSb_2Mo_{10}O_{40}$ from spectral studies and elemental analysis.

REFERENCES

1 *Standard Methods for the Examination of Water and Wastewater*, 13th edn., American Public Health Assoc., 1971, p. 532.
2 J. Murphy and J. P. Riley, *Anal. Chim. Acta*, 27 (1962) 31.
3 *Methods for Chemical Analysis of Water and Wastes*, Environmental Protection Agency, 1971, p. 235.
4 K. Stephens, *Limnol. Oceanogr.*, 8 (1963) 361.
5 G. P. Edwards, A. H. Molof and R. W. Schneeman, *J. Amer. Water Works Ass.*, 57 (1965) 917.
6 P. Vogler, *Int. Rev. Gesamten Hydrobiol.*, 50 (1965) 33.
7 A. I. Kokorin, *Zavod. Lab.*, 12 (1946) 64.
8 M. Jean, *Anal. Chim. Acta*, 14 (1956) 348.
9 K. Murata, Y. Yokoyama and S. Ikeda, *Anal. Chim. Acta*, 48 (1969) 349.
10 H. N. Johnson, G. F. Kirkbright and R. J. Whitehouse, *Anal. Chem.*, 45 (1973) 1603.
11 H. D. Goldman and L. G. Hargis, *Anal. Chem.*, 41 (1969) 490.
12 A. Elkind, K. H. Gayer and D. F. Boltz, *Anal. Chem.*, 25 (1953) 1744.
13 in N. H. Furman (Ed.), *Standard Methods of Chemical Analysis*, Vol. 1, Van Nostrand, Princeton, 6th edn., 1962, p. 97.
14 E. Lassmer and R. Scharf, *Z. Anal. Chem.*, 168 (1959) 429.
15 S. R. Crouch and H. V. Malmstadt, *Anal. Chem.*, 39 (1967) 1084.
16 J. D. H. Strickland, *J. Amer. Chem. Soc.*, 74 (1952) 872.
17 J. E. Going and S. J. Eisenreich, *Extraction of Reduced Heteropoly Acids*, Pittsburg Anal. Conf. Proc., April 1972.
18 G. A. Tsigdinos and C. J. Hallada, *Inorg. Chem.*, 7 (1968) 437.
19 Y. F. Shkaravskii, *Russ. J. Inorg. Chem.*, 11 (1966) 64.
20 V. F. Barkovskii and M. I. Zaboeva, *Russ. J. Inorg. Chem.*, 10 (1965) 487.
21 G. A. Tsigdinos, *Climax Monograph; Heteropoly Compounds of Molybdenum and Tungsten*, Bull. Cdb-12a (revised), Nov. 1969.
22 N. A. Polotebnova, *Russ. J. Inorg. Chem.*, 10 (1965) 815.
23 M. Fournier, R. Massert and P. Souchay, *C.R. Acad. Sci., Sec. C*, 272 451 (1971).
24 S. R. Crouch and H. V. Malmstadt, *Anal. Chem.*, 39 (1967) 1090.

Analytica Chimica Acta, 70 (1974) 107–111

THIOBARBITURIC ACID-REACTING SUBSTANCES DERIVED FROM AUTOXIDIZING LINOLEIC AND LINOLENIC ACIDS

J. M. C. GUTTERIDGE, J. STOCKS and T. L. DORMANDY
Department of Chemical Pathology, Whittington Hospital, London, N.19 (England)
(Received 6th October 1973)

The coloured complex formed between thiobarbituric acid (TBA) and aerobically incubated tissue has gained wide acceptance as a measure of lipid autoxidation both in the food industry and in biological research[1–3]. The TBA-reactive substance is generally referred to as malonyldialdehyde (MDA); but its exact relation to various polyunsaturated lipids and their peroxides is still uncertain. In particular, developments in chromatographic techniques have revealed a number of TBA-reactive autoxidation fragments[4–7]; and it has been suggested that MDA may not be among them[6]. These questions have acquired added practical importance in the light of recent clinical observations. The susceptibility of various human tissues to autoxidation as measured by the TBA/MDA reaction has now been shown to be related to degenerative disease[8], and some autoxidation products have been found to be potent anti-tumour[9] and antibacterial agents[10]. It was therefore decided to explore more fully the significance and specificity of the TBA reaction. Previous studies on the aldehydic products of lipid peroxidation were extended by using a combination of chromatographic procedures, and the results are of interest in relation to the role of lipid peroxidation in various examples of cellular injury.

EXPERIMENTAL

Chemicals

Linoleic (18:2) and linolenic (18:3) acids (99% pure; Koch Light Ltd.) were used as the fatty acids.

Phosphate–saline buffer, pH 7.4. 17.6 ml of 0.5 *M* potassium dihydrogenphosphate and 60.3 ml of 0.5 *M* potassium hydrogenphosphate were diluted to 1 l with 0.15 *M* sodium chloride.

Thiobarbituric acid reagent (TBA). Add 1 g of TBA (B.D.H.) to 10 ml of 0.1 *M* sodium hydroxide, add 50 ml of water, heat to dissolve, cool and dilute to 100 ml. Chloroform, diethyl ether and trichloroacetic acid were of AnalaR grade (B.D.H.); hexane (pure; Koch Light Ltd.) and Schiff's reagent (B.D.H.) were also used.

Thin-layer plates. (1) ITLC–SAF fibreglass sheets (Gelman Instrument Co., Michigan; Anachem Ltd.); (2) Silica gel–glass plates (Merck, Darmstadt; Anderman & Co. Ltd.).

Procedure

Pure fatty acid (2 g) was added to 150 ml of phosphate–saline buffer, pH 7.4, which was then shaken vigorously to form a suspension. This was then dispensed into glass dishes and left open with a large surface area exposed in daylight to the air and mixed with the aid of a magnetic stirring bar for the required length of time.

After autoxidation, the yellowish-brown lipid remaining on the surface was removed by filtering through a double thickness of Whatman No. 1 filter paper previously wetted with phosphate buffer. The clear neutral filtrate was then extracted with chloroform and ether.

The clear aqueous phases were extracted twice in a separating funnel with 200 ml of chloroform and once with 200 ml of ether. The combined solvent phases were pooled for evaporation at 40°C in a rotary vacuum evaporator. The residue was dissolved in 0.5 ml of chloroform for thin-layer chromatography.

The entire solvent extract (0.5 ml) was applied to a 20 × 20 cm ITLC–SAF fibreglass sheet as a band covering the entire width except for a 1-cm margin at each side. The sheet was developed in the solvent system hexane/ether/butanol ethanol (60:40:1:1). Strips, 2 cm wide, were cut from each edge of the sheet for locating the fractions. These were stained with Schiff's reagent, resulting in a colour range from red through deep purple to dark brown. Bands were marked as soon as possible, because the background rapidly darkened to a deep red. When dry, the two margin strips were placed back alongside the main sheet and the various bands were marked and numbered for elution.

The marked bands were cut out with a pair of scissors and chopped into small strips in a test tube. Each fraction was eluted three times with 10 ml of solvent. Three solvents, ether, chloroform and ethanol, were used for each sequential extraction. The pooled solvent phases were evaporated to dryness at 40°C in a rotary vacuum evaporator. The residue from each fraction was then dissolved in 0.5 ml of ethanol for biological testing and TBA reactivity.

A portion (0.1 ml) of ethanolic extract from each fraction was placed in a test tube fitted with a 20-cm air condenser, and 4 ml of 28% trichloracetic acid and 1 ml of TBA reagent, were added; the tubes were then heated for 15 min at 100°C. The tubes were cooled and the solutions scanned from 700 to 400 nm with a Pye-Unicam SP800 spectrophotometer.

Aliquots (50 μl) of the initial chloroform/ether extract of water-soluble autoxidation products were run on silica gel glass plates in the previously described solvent and stained by spraying the TBA/trichloroacetic acid reagents in a reversed volume ratio to that used for colour development in aqueous solutions (*i.e.* 4 ml TBA plus 1 ml of trichloroacetic acid). The plates were then heated for 2 min at 100°C.

The TBA-stained glass plates were scanned under reflected light in a Joyce Loebl "Chromoscan" with a 530 nm green filter.

RESULTS

Linoleic acid (18:2) after autoxidation for 96 h showed 15 distinct t.l.c. bands after location with Schiff's reagent (Fig. 1). These were eluted as 10 zones and scanned from 700 to 400 nm after reaction with TBA and trichloroacetic acid reagents. Seven of these had peak absorbance maxima at 532 nm, many showing additional peaks at 500, 455 and 452 nm.

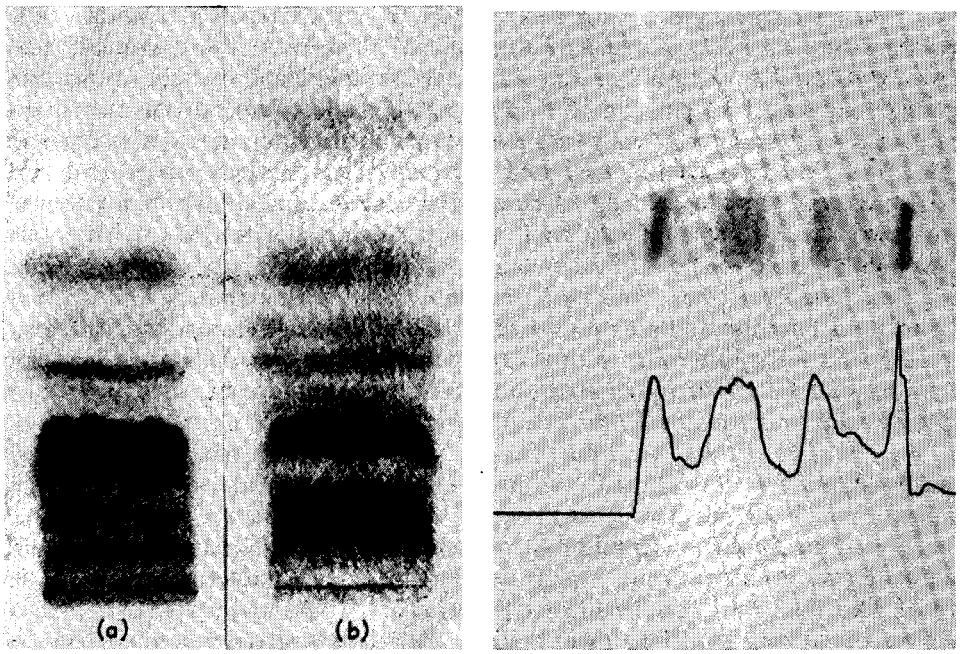

Fig. 1. Schiff-reacting autoxidation fractions. Water-soluble autoxidation compounds separated on silica gel fibreglass sheets and located with Schiff's reagent. (a) Linoleic acid (18:2) autoxidized for 96 h; (b) linolenic acid (18:3) autoxidized for 46 h.

Fig. 2. Thiobarbituric acid-reacting compounds from autoxidized linoleic acid. Thin-layer chromatogram of water-soluble autoxidation compounds separated on silica gel glass plates and located with thiobarbituric acid reagent.

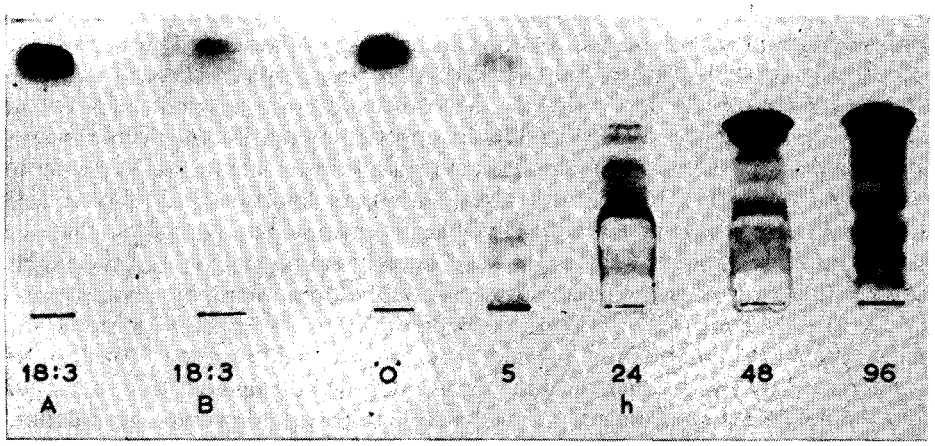

Fig. 3. Autoxidation of linolenic acid at time intervals during 0–96 h. Water-soluble extracts after autoxidation for a given time. The bands A and B are samples of pure linolenic acid applied to the silica gel glass plate. Band A was located by spraying (1 + 1) sulphuric acid and heating. All other compounds on the chromatogram were located with TBA.

Linolenic acid (18:3) after autoxidation for 46 h showed 15 distinct Schiff-reacting bands (Fig. 1) of which 12 were eluted. Of these 9 absorbed at 532 nm; other minor peaks occurred at 455, 472 and 506 nm. Thin-layer chromatograms stained with the TBA reagents showed that 8–12 bands were present after direct application of the solvent extract from the aqueous phase of autoxidation for both 18:2 and 18:3 fatty acids. These ranged from yellow through orange to bright red in colour when located on silica gel plates (Fig. 2). The chromatograms of extracted water-soluble autoxidation products located with TBA which were prepared at timed intervals after linolenic acid had been left exposed to air in the phosphate buffer, is shown in Fig. 3; this shows that the number of TBA-reacting compounds increase as time progresses. A large TBA-reactive zone could be seen at zero time when linolenic acid was extracted after filtration. This was isographic with the pure fatty acid and disappeared from the chromatograms after progressive autoxidation.

DISCUSSION

The preliminary identification of Schiff-reacting compounds among lipid autoxidation products permits a more accurate and discriminating study of MDA or MDA-like substances than the direct application of the TBA reagent to the thin-layer chromatographic plate. The present findings, with this two-stage procedure, confirm previous reports about the need for caution in using the TBA reaction as a measure of lipid peroxidation, but point to a number of conclusions and raise several questions.

Among the water-soluble secondary breakdown products of autoxidized linolenic acid, at least 9 give a TBA reaction which is spectrophotometrically indistinguishable from the MDA/TBA complex originally described by Kohn and Liversedge[1]. It is, therefore, highly unlikely that the MDA assay, now widely used as a measure of lipid autoxidation in biological material, measures the formation of a single substance. More probably, a number of more-or-less close precursors of MDA are first converted to MDA when the mixture is boiled in trichloroacetic acid, and then react with TBA to give the same coloured complex.

In the present context, the term MDA implies a substance which gives a characteristic colour reaction with TBA. That this substance may not be MDA as defined by the formula $CHO–CH_2–CHO$ is suggested by our findings with linoleic-acid autoxidation. Theoretically, linoleic acid should not generate MDA owing to its structural formula[11]. In fact, at a slower rate than linolenic acid, linoleic acid autoxidation also yields at least 7 MDA-like fragments. The possibility that the present samples of linoleic acid might have been contaminated with more highly unsaturated fatty acids was excluded by gas–liquid chromatographic analysis[12].

Even less consistent with the concept of MDA as an homogeneous and specific secondary autoxidation product was the invariable presence of a single characteristic MDA spot, when the aqueous filtrates of linolenic-acid (and to a lesser extent, linoleic-acid) emulsions were chromatographed at zero-time autoxidation. The possibility that water-soluble autoxidation products might have been present in the parent material could be excluded by the chromatographic appearance which showed a single band, and not a number of bands. Similarly, the possibility that MDA precursors in the filtrate might have autoxidized during the chromatographic

run was remote, for there was no hint of "tailing". To explain the findings, one must first assume that when fresh linoleic-acid and linolenic-acid emulsions are filtered at the start of autoxidation experiments, traces of the lipid escape into the aqueous phase. Secondly. when boiled with TBA in trichloroacetic acid, the fatty acids themselves may undergo partial oxidation to yield MDA. If the first assumption is accepted, an alternative mechanism can be envisaged. Although the MDA/TBA complex is generally accepted as a measure of the formation of water-soluble autoxidation products, the possibility exists that some TBA–reactive substances (or chemical groups) are lipophilic and remain bound to the lipid phase.

Three practical implications may be mentioned. First, although all the available evidence suggests that the MDA/TBA reaction of Kohn and Liversedge[1] does reflect lipid autoxidation, since "MDA" represents a number of autoxidation products generated at different rates from different polyunsaturated fatty acids, it is not necessarily an accurate mole-for-mole measure of autoxidation when applied to an heterogeneous biological preparation. Secondly, linoleic acid cannot be excluded as a possible source of MDA. Thirdly, since apparently non-autoxidized fatty acids themselves can yield MDA, it is essential that the trichloroacetic-acid precipitate of biological material should be carefully separated before the supernate is allowed to interact with TBA.

We are grateful to Mr. G. Rance for advice and assistance with illustrations.

SUMMARY

Thin-layer chromotographic techniques are described for the preparation and separation of water-soluble compounds formed by the autoxidation of pure linoleic and linolenic acids. Location of 15 main fractions with Schiff's reagent on fibreglass sheets was possible. These could be eluted for biological testing and chromogenic behaviour with thiobarbituric acid reagent. At least 7 bands from autoxidized linoleic acid and 9 from autoxidized linolenic acid had peak absorbance maxima at 532 nm identical to that characteristically given by malonyldialdehyde (MDA). Possible reactions and interpretations for the MDA test are discussed.

REFERENCES

1 H. I. Kohn and M. Liversedge, *J. Pharmacol.*, 82 (1944) 292.
2 F. Bernheim, M. L. C. Bernheim and K. M. Wilbur, *J. Biol. Chem.*, 174 (1948) 257.
3 S. Patton and W. Hofeditz, *J. Dairy Sci.*, 34 (1951) 669.
4 B. C. Tarladgis, A. M. Pearson and L. R. Dugan, *J. Amer. Oil Chem. Soc.*, 39 (1962) 34.
5 L. D. Saslow, L. M. Corwin and V. S. Waravdekar, *Arch. Biochem. Biophys.*, 114 (1966) 61.
6 L. D. Saslow, H. J. Anderson and V. S. Waravdekar, *Nature (London)*, 200 (1963) 1908.
7 J. Franz and B. T. Cole, *Arch. Biochem. Biophys.*, 96 (1962) 382.
8 J. A. Dormandy, E. Hoare, J. Colley, D. E. Arrowsmith and T. L. Dormandy, *Brit. Med. J.*, 4 (1973) 576.
9 E. Schauenstein, *J. Lipid Res.*, 8 (1967) 417.
10 J. M. C. Gutteridge, P. Lamport and T. L. Dormandy, *J. Med. Microbiol.*, in press.
11 L. K. Dahle, E. G. Hill and R. T. Holman, *Arch. Biochem. Biophys.*, 98 (1962) 253.
12 J. M. C. Gutteridge, J. Stocks and T. L. Dormandy, *Clin. Chim. Acta*, 48 (1973) 317.

Analytica Chimica Acta, 70 (1974) 113–120

ANALYTICAL USES OF SOME N-NITROSO-N-ALKYL (OR -N-CYCLOALKYL)HYDROXYLAMINES

PART II. SOLVENT EXTRACTION OF METAL HEXAHYDROCUPFERRATES

F. BUSCARONS and J. CANELA

Department of Analytical Chemistry, Faculty of Sciences, University of Barcelona, Barcelona (Spain)

(Received 26th September 1973)

In a recent paper[1], the reactions and properties of a new reagent "hexahydrocupferron" (the sodium salt of N-nitroso-N-cyclohexylhydroxylamine) were reported and its advantages of stability compared with cupferron were discussed. Most of the precipitates formed between hexahydrocupferron and metals were soluble in organic solvents, and this could be utilized to increase the selectivity and sensitivity of the reactions.

In the present paper, a systematic study at different pH values of the extraction with chloroform of 17 metals as hexahydrocupferrates is described; the extraction constants were calculated from these results[2], and some possible applications in analysis are suggested.

The extraction equilibrium can be described by

$$M^{n+} + n(HA)_{org} = (MA_n)_{org} + n\,H^+$$

where the subscript "org" denotes the organic phase, M^{n+} any metal ion, HA the reagent, and MA_n the formed complex. The logarithm of the equilibrium constant (K_0) can be expressed as

$$\log K_0 = \log R - n\,pH - n \log [AH]_{org} \qquad (1)$$

where R is the ratio of the metal in the two layers. If the equation is applied at a pH value ($pH_{\frac{1}{2}}$) for which the extraction yield is 50% ($R=1$), and if the overall reagent concentration is much greater than the metal complex concentration ($[HA]_{org}$ = [overall reagent]), eqn. (1) can be simplified to:

$$\log K_0 = -n\,pH_{\frac{1}{2}} - n \log [\text{overall reagent}] \qquad (2)$$

In general, the extraction constants with hexahydrocupferron were found to be smaller than those with cupferron, but this hardly affected its analytical uses (Table I).

Some metals (Sb(III), Ti, Fe(III), Mo, Bi and V) were quantitatively extracted even from relatively highly acidic medium; hence it was impossible to determine their extraction constants. The extractability of the other metals examined decreased in the following order: Cu, Pb, Al and Mn, which is the same order as that described by Starý and Smižanská[3] for the cupferron complexes. The

TABLE I

EXTRACTION DATA FOR METAL HEXAHYDROCUPFERRATES AND CUPFERRATES

Metal ion	*pH range of zero extraction*	*pH range of maximal extraction*	$pH_{\frac{1}{2}}$[a]	*log* K_0[a]	$pH_{\frac{1}{2}}$[b]	*log* K_0[b]
Cu^{2+}		1.70–11.0[c]	0.50	−0.30	0.03	2.66
Pb^{2+}	0–2.10	3.70–11.0[c]	2.72	−2.84	2.06	−1.53
Bi^{3+}		1.20–9.30[c]	0		−0.4	5.08
Sb^{3+}		0–11.0[c]	0		0	
Al^{3+}	0–0.90	2.85–9.40[c]	1.48	−8.37	3.51	−3.5
Ti^{4+}		0–11[c]	0		0	
Fe^{3+}		0–10.4[c]	0		0	
Co^{2+}	0–2.25	2.25–6.65			3.18	−3.56
	6.6–11.0	(15.4%)				
Ni^{2+}	0–3.80	5.10–5.70				
	10–11	(5.3%)				
Mn^{2+}	0–5.08	7.10–9.65	7.0			
		(53.4%)				
W^{6+}	4.6–11	0–1.53				
		(42.3%)				
Mo^{6+}	7.1–11	0–2.80[c]	0		0	
V^{5+}	8.2–11	0–3.85[c]	0		0	

[a] Hexahydrocupferron values.
[b] Cupferron values by Starý and Smižanská (ref. 3).
[c] Quantitative extraction.

hexahydrocupferrates of tungsten, cobalt and nickel were extracted only to a small extent, whereas alkaline earths and magnesium were not extracted at all.

The low extraction yields for nickel and cobalt could not be explained by a slow kinetic process, as in the case of the nickel–cupferron complex[3], because these metals were not extracted to a greater extent even on prolonged shaking.

The variation in the extraction of manganese(II) with shaking time, its behaviour in the presence of reductants and oxidants, and its colour change (colorless in the aqueous and green in the organic phase) seemed to be due to an oxidation process of manganese(II) followed by extraction of a new complex, rather than to slow kinetics[3].

The extraction behaviour at different pH values suggests many separations (see below). As examples of analytical application, it was found possible to extract trace amounts of bismuth or antimony(III) in the presence of lead, and aluminium in cobalt with satisfactory results.

Extractive separations of major components are often more complete than those based on precipitation. Accordingly as other examples of application, the extraction of some metals (Fe(III), Zr(IV) and Th(IV)) that react with eriochrome black T[4] and interfere seriously in the complexiметric titration of divalent metals (Mn, Zn, Cd, Mg, Pb and Co), was studied; the results showed that a single extraction at pH 0.3–1.0 sufficed to permit the titration with an accuracy better than 1%, even when the concentration of interfering metal was 10-fold that of the element to be titrated.

EXPERIMENTAL

Reagents

All reagents used were of A.R. quality. Chloroform was purified by shaking with concentrated sulfuric acid followed by distillation. Hexahydrocupferron was recrystallized from water.

Instruments

The pH measurements were done with a Radiometer pHM4e (Copenhagen) with a glass electrode and a saturated calomel reference electrode. Spectrophotometric measurements were made on a Perkin Elmer M124 instrument.

Distribution measurements

Chloroform (20 ml) was shaken on a mechanical shaker with an equal volume of aqueous phase which was 0.05 *M* in hexahydrocupferron and $2 \cdot 10^{-3}$–$5 \cdot 10^{-4}$ *M* in metal ion. The pH was adjusted by addition of sodium hydroxide or perchloric acid, and the ionic strength was made constant by addition of sodium perchlorate to give a 0.1 *M* solution (except, of course, for experiments below pH 1.2).

As hexahydrocupferron does not decompose so quickly in acidic solutions as cupferron, a shaking time of 15 min was used in all cases except for Ni, Co and Mn. This was found to be quite sufficient for attainment of equilibrium in all the systems investigated (except Mn).

TABLE II

ANALYTICAL METHODS FOR DETERMINATION OF DISTRIBUTION RATIOS AND COMPLEXIMETRIC TITRATIONS

Metal	*Method*
Pb	Spectrophotometric with HCl (1+1) at 271 nm, and complexiметric in the presence of tartrates
Cu	Colorimetric as oxinate extracted with chloroform (500 nm)
Cd	Complexiметric, in the presence of Zn^{2+}-complexonate
Bi	Spectrophotometric with EDTA at 263 nm
Sb	Colorimetric with KI at 425 nm
Fe	Colorimetric with thiocyanate and acetone at 480 nm
Al	Turbidimetric as hexahydrocupferrate at 420 nm (ref. 1)
Co	Colorimetric with thiocyanate and acetone at 625 nm, and complexiметric by back-titration with zinc solution
Ni	Colorimetric as dimethylglyoximate at 530 nm
Mn	Complexiметric in the presence of ascorbic acid
Zn	Complexiметric
Ti	Colorimetric with hydrogen peroxide at 436 nm
W	Spectrophotometric as tungstovanadophosphoric acid at 380 nm
V	Spectrophotometric with hydrogen peroxide at 290 nm
Mo	Colorimetric with thiocyanate at 465 nm
Ca, Mg	Complexiметric
Sr, Ba	Complexiметric by back-titration with zinc solution

After the two phases had been separated, the equilibrium concentration of metal in the organic and/or the aqueous phase was determined by the methods summarized in Table II. At very high pH values, distribution measurements were impossible, for the reagent behaved as a surface-active agent and emulsified the phases.

All experiments were carried out at 20°.

RESULTS

Magnesium, calcium, strontium and barium

These elements were not extracted with chloroform throughout the pH region investigated.

Copper, lead and bismuth

The extraction curves for these elements are shown in Fig. 1. Bismuth(III) was quantitatively extracted in the pH region 1.2–9.3, and copper(II) between 1.7 and 11.0 ($pH_{\frac{1}{2}}=0.50$). Lead(II) was extracted only at pH values higher than 2.1, extraction being quantitative between pH 3.7 and 11.0 ($pH_{\frac{1}{2}}=2.72$).

Antimony, aluminium, titanium and iron

Antimony(III) and titanium(IV) were quantitatively extracted over the whole pH region investigated. Iron(III) was quantitatively extracted in the pH range 0.5–10.5; at higher pH values the extraction yield of iron decreased, probably because of hydrolysis. The extraction of aluminium(III) began at pH 0.9 and became quantitative between pH 2.8 and 9.4 ($pH_{\frac{1}{2}}=1.48$) (Figs. 2 and 3).

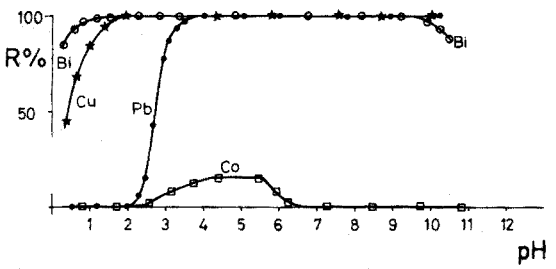

Fig. 1. Extraction ratios of Bi(III), Cu(II), Pb(II) and Co(II) with chloroform in presence of 0.05 *M* hexahydrocupferron versus the pH values of the aqueous phase.

Cobalt and nickel

The cobalt(II) extraction reached a maximum (15.4%) in the pH region 4.5–5.5 (Fig. 1), whereas nickel(II) was extracted in the pH region 3.8–7.5 to an extent of 5.3% (Fig. 3). The extraction remained the same whether the shaking time was 30 or 45 min, even when the solution was 0.5 *M* in reagent.

Manganese

Under the same conditions as for the other elements (0.05 *M* reagent and shaking for 15 min), manganese(II) was extracted at pH values higher than 5.0, extraction reaching a maximum (53.4%) between 7.5 and 9.6 (Fig. 3). If solutions

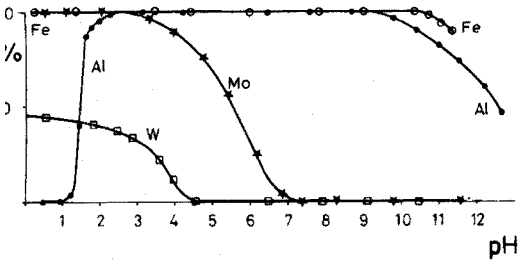

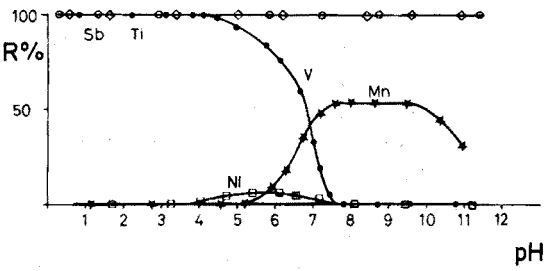

Fig. 2. Extraction ratios of Fe(III), Al(III), Mo(VI) and W(VI) with chloroform in the presence of 0.05 *M* hexahydrocupferron versus the pH values of the aqueous phase.

Fig. 3. Extraction rates of Sb(III), Ti(IV), V(V), Ni(II) and Mn(II) with chloroform in the presence of 0.05 *M* hexahydrocupferron versus the pH values of the aqueous phase.

were shaken for 30 or 60 min, the amounts of ion extracted increased to 72.9 and 86.4%, respectively, without changing the mentioned pH values. In the presence of ascorbic acid, there was no extraction below pH 7.5; in the presence of ammonium persulfate the amount of metal extracted at pH 7.5 reached 75.3% after shaking for only 15 min.

Tungsten, molybdenum and vanadium

Molybdenum(VI) was extracted quantitatively in the pH region 0–2.8; above

TABLE III

EXTRACTION OF TRACE ELEMENTS FROM MIXTURES WITH LEAD OR COBALT SALTS

Extraction of 60.75 μg Sb(III) from Pb(II)

Pb (μg)	*Pb:Sb ratio*	*Sb found (μg)*	*Relative error (%)*
607.6	10	62.14	+2.7
3,036.0	50	61.84	+1.8
6,076.0	100	59.53	−2.1
30,380.0	500	57.60	−5.2

Extraction of 209 μg Bi(III) from Pb(II)

Pb (μg)	*Pb:Bi ratio*	*Bi found (μg)*	*Relative error (%)*
209	10	203.6	−2.6
1,045	50	212.7	+1.8
2,090	100	203.4	−2.7
10,450	500	215.6	+3.2

Extraction of 270 μg Al(III) from Co(II)

Co (μg)	*Co:Al ratio*	*Al found (μg)*	*Relative error (%)*
270	10	265.7	−1.6
1,350	50	266.8	−1.2
2,700	100	275.4	+2.0
13,500	500	276.5	+2.4

pH 7.1 it was not extracted at all (Fig. 2). Vanadium(V) behaved similarly; it was quantitatively extracted at pH between 0 and 3.85 and not at all above 7.8 (Fig. 3). The extraction of tungsten(VI) reached a maximum (42.3%) in the pH region 0–1.5; at higher pH values extraction decreased and became zero above pH 4.6 (Fig. 2). The decreasing extraction ratios of these elements at high pH values is surely due to the formation of non-extractable anions.

Extraction of trace elements from binary mixtures

In a 100-ml separatory funnel, a constant amount of the trace element was shaken with chloroform in the presence of different amounts of a non-extractable

TABLE IV

TITRATION OF DIVALENT METALS AFTER HEXAHYDROCUPFERRON EXTRACTION OF INTERFERING METAL

Metal extracted[a]	*Metal determined*	*Ml 0.05 M EDTA*		
		Theory	*Actual*	*Diff.*
Fe([Fe] = [M])	Mg	4.27	4.19	−0.08
	Zn	4.60	4.57	−0.03
	Cd	4.08	4.08	0.00
	Mn	4.77	4.78	0.01
	Pb	4.63	4.61	−0.02
	Co	3.95	3.99	0.04
Fe ([Fe] = 10[M])	Mg	4.27	4.25	−0.02
	Zn	4.60	4.59	−0.01
	Mn	4.77	4.80	0.03
	Pb	4.63	4.62	−0.01
Zr ([Zr] = [M])	Mg	4.27	4.27	0.00
	Zn	4.60	4.58	−0.02
	Cd	4.08	4.13	0.05
	Mn	4.77	4.77	0.00
	Pb	4.63	4.60	−0.03
Zr ([Zr] = 10[M])	Mg	4.27	4.36	0.09
	Zn	4.60	4.53	−0.07
	Mn	4.77	4.78	0.01
	Pb	4.63	4.69	0.06
Th ([Th] = [M])	Mg	4.27	4.27	0.00
	Zn	4.60	4.58	−0.02
	Mn	4.77	4.72	−0.05
	Pb	4.63	4.64	0.01
Th ([Th] = 10[M])	Mg	4.27	4.26	−0.01
	Zn	4.60	4.63	0.03
	Mn	4.77	4.72	−0.05
	Pb	4.63	4.62	−0.01
Fe + Zr + Th	Mg	4.27	4.38	0.11
([Fe + Zr + Th] = 3[M])	Mn	4.77	4.69	−0.08

[a] M denotes any divalent metal to be titrated.

element and 20 ml of a 0.5 *M* hexahydrocupferron solution. The pH values were fixed by adding perchloric acid to make the aqueous phases 0.1 *M* in the cases of bismuth and antimony, or by adding phthalate buffer (pH 2.85) in the case of aluminium; mixtures were extracted twice with, respectively, 20 and 5 ml of chloroform.

The organic layers were collected, evaporated to dryness, and mineralized in nitric or perchloric acid, and the amount of metal ion was determined by the analytical methods summarized in Table II.

The results are shown in Table III.

Complexiметric titrations after hexahydrocupferron removal of interferences

About 0.22 mmol of a titratable divalent metal, and equal or 10-fold molar quantities of the element to be extracted, were pipetted into a separatory funnel, and 25 ml of chloroform and 5 ml of 0.3 *M* hexahydrocupferron reagent for each 0.25 mmol of extractable metal were added. The pH was adjusted by making the solutions 0.2 *M* in hydrochloric acid and the mixtures were shaken for 10 min. The aqueous layers were then titrated with 0.05 *M* EDTA by the methods given in Table II. Data obtained from these determinations are given in Table IV.

SUMMARY

The extraction of the hexahydrocupferrates of 17 metals (Cu, Pb, Bi, Sb, Al, Ti, Fe, Co, Ni, Mn, W, Mo, V, Ca, Sr, Ba and Mg) with chloroform is studied in relation to pH values. The extraction constants are calculated and compared with those of cupferron; these can be used to determine the optimal conditions for the separation of many metals. As examples of analytical applications, extractive separations of trace amounts of Sb(III), Bi and Al from, respectively, Pb, Pb and Co were checked. A single extraction allows the removal of major amounts of some metals (Fe, Th and Zr) which interfere in the complexiметric titration of divalent metals (Mn, Zn, Mg, Cd, Pb and Co).

REFERENCES

1 F. Buscarons and J. Canela, *Anal. Chim. Acta*, 67 (1973) 349.
2 Yu. A. Zolotov, *Extraction of Chelate Compounds*, Ann Arbor-Humphrey, 1970, Ch. VI, p. 220.
3 J. Starý and J. Smižanská, *Anal. Chim. Acta*, 29 (1963) 545.
4 G. Schwarzenbach, *Die Komplexometrische Titration*, Enke, Stuttgart, 1955, p. 33.

Analytica Chimica Acta, 70 (1974) 121–126

EFFECTS OF QUATERNARY AMMONIUM BASES ON VALENCE-SATURATED BUT COORDINATION-UNSATURATED CHELATES

PART I. EXTRACTION OF CHELATES OF GLYOXAL BIS-(2-HYDROXYANIL) AND *o*-(SALICYLIDENEAMINO)PHENOL

MASAKICHI NISHIMURA, SHINICHIRO NORIKI and SEIJI MURAMOTO

Analytical Chemistry Division, Department of Chemistry, Faculty of Fisheries, Hokkaido University, Hakodate 040 (Japan)

(Received 1st October 1973)

A metal ion reacting with a chelating agent can give (a) a positively or negatively charged metal chelate, (b) a valence-saturated (for the central metal atom) but coordination-unsaturated chelate, and (c) a valence- and coordination-saturated chelate.

The valence- and coordination-saturated chelates (c), *e.g.* cobalt oxinate[1] or nickel dimethylglyoximate[2], are easily extracted into organic solvents. The charged metal chelates (a), *e.g.* tin(IV) oxinate or magnesium–eriochrome black T, are extracted by ion-association or coupling with an ion having opposite charge, such as chloride ion[3] or a cationic surface-active agent[4].

The valence-saturated, but coordination-unsaturated chelates (b) are poorly extracted into inactive solvents, *e.g.* benzene and 1,2-dichloroethane. If the coordinated water molecule (or molecules) in the chelate (b) is expelled by another organic molecule (or molecules), *i.e.* if the coordination is saturated, the chelate can be extracted into inactive solvents.

Nowadays, quaternary ammonium bases are extensively used for extraction of anionic complexes by coupling, but there has been no report for neutral complexes. The authors' interest is in the peculiar effects of quaternary ammonium bases on a neutral but coordination-unsaturated chelate, and it has been found that some coordination-unsaturated chelates change to coordination-saturated chelates in the presence of a quaternary ammonium base. As a representative of quaternary ammonium bases, tetradecyldimethylbenzylammonium chloride(I), the so-called zephiramine, was chosen.

Glyoxal bis-(2-hydroxyanil) (GHA; II), a quadridentate ligand, has been used for the spectrophotometric determination of calcium[5,6] because of its superior selectivity. The 1:1 chelate, however, is unstable and not extractable into inactive solvents; but extraction of the calcium–GHA chelate into 1,2-dichloroethane in the presence of zephiramine has been reported[7], and the colour of the extract was very stable.

o-(Salicylidene-amino)phenol (SAPH; III), a tridentate ligand, gives 1:1

chelates with divalent cations such as cobalt, manganese, nickel and zinc[8]. These chelates are hardly extracted into inactive solvents.

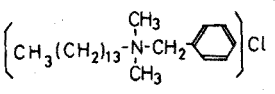

I

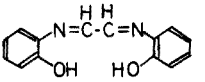

II

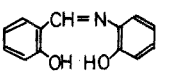

III

EXPERIMENTAL

Reagents

GHA solution, $1.5 \cdot 10^{-2}$ M. Dissolve 0.360 g of glyoxal bis-(2-hydroxyanil) in 100 ml of ethanol.

SAPH solution, $5 \cdot 10^{-3}$ M. Dissolve 0.268 g of *o*-(salicylideneamino)phenol in 250 ml of ethanol.

Zephiramine solution, $5 \cdot 10^{-3}$ M. Dissolve 0.920 g of tetradecyldimethylbenzylammonium chloride in 500 ml of water.

Buffer solution, pH 9–13. Mixtures of 0.1 *M* sodium hydroxide and 0.05 *M* sodium borate solution are used.

Metal solutions. Prepare a $5 \cdot 10^{-3}$ *M* solution of calcium, nickel or zinc, and a $1 \cdot 10^{-2}$ *M* solution of cadmium, by dissolving calcium carbonate and the other metal sulfates. Standardize the metal solution against a standard solution of EDTA, if necessary.

1,2-Dichloroethane was used without further purification.

Procedure for determinations of calcium and cadmium with GHA

Into a separatory funnel, transfer the metal solution, 2 ml of buffer pH 12.8 for calcium or buffer pH 13.0 for cadmium, 2 ml of ethanol and 1 ml of the GHA solution. Adjust the volume to 20 ml with water. After 1 min, add 1 ml of the zephiramine solution and 20 ml of 1,2-dichloroethane and shake the funnel for 1 min. Separate the organic phase and dry with anhydrous sodium sulfate. Measure the absorbance at the wavelength of the absorption maximum, 530 nm for the calcium–GHA or 560 nm for the cadmium–GHA chelate.

A constant absorbance was obtained in the pH ranges of 12.7–13.0 for calcium and 12.5–13.3 for cadmium, with a concentration of GHA more than 8 times that of each metal, on shaking for 1–4 min.

Procedure for determinations of nickel and zinc with SAPH

Transfer the metal solution, buffer pH 11 for nickel and zinc, 0.5 ml of the SAPH solution, and 1 ml of the zephiramine solution to a separatory funnel, and dilute to 20 ml with water. Add 20 ml of 1,2-dichloroethane and shake the funnel for 1 min. Separate the organic phase, dry with anhydrous sodium sulfate, and measure the absorbance at the wavelength of the absorption maximum, 440 nm for nickel or 425 nm for zinc.

A constant absorbance was measured in the pH ranges of 10.0–11.5 for

nickel and 9.5–11.3 for zinc, with a concentration of SAPH more than 4 times that of each metal. The absorbance decreased slightly for a few minutes immediately after shaking, and then the colour was stable for at least 1 h.

COMPOSITION OF THE CHELATES EXTRACTED IN THE PRESENCE OF ZEPHIRAMINE

GHA chelates

In the absence of zephiramine, it has been reported that GHA (expressed as H_2A) forms an uncharged and non-extractable 1:1 chelate with a divalent metal ion, namely the M(A) chelate, in a strongly alkaline medium[9] (*ca.* pH 12). Under the same conditions except for the presence of zephiramine, an extractable calcium or cadmium chelate was formed, and the calcium–GHA or cadmium–GHA molar ratio in the extract was determined to be 1:2 by the continuous variations method (see *e.g.* Fig. 1 for calcium).

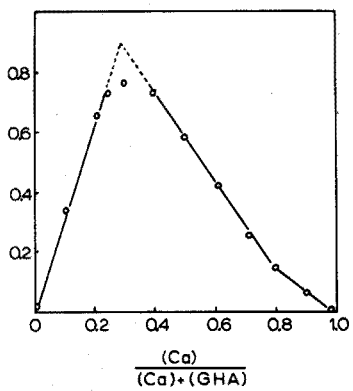

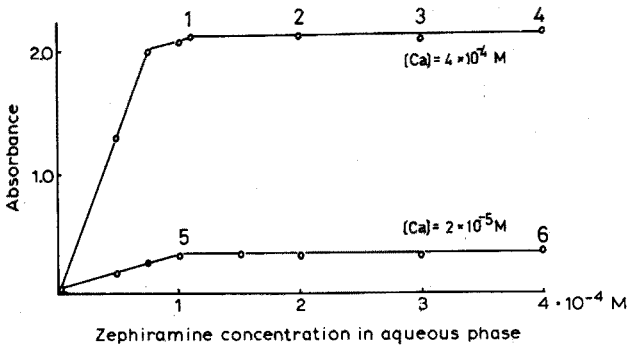

Fig. 1. Calcium–GHA ratio in the presence of zephiramine. $[Ca]+[GHA]=2\cdot10^{-4}$ *M*; $[zeph]=2\cdot10^{-4}$ *M*.

Fig. 2. Absorbance of the Ca–GHA chelate at a constant concentration of calcium. The numbers on the lines show the [zeph]/[Ca] ratio: (1) 0.25, (2) 0.5, (3) 0.75, (4) 2.0, (5) 5.0 and (6) 20. $[GHA]=7.5\cdot10^{-3}$ *M*; $V_{org}=20$ and 50 ml.

In order to examine the stoichiometry between the metal and the zephiramine, two experiments were made, by varying the concentration of either calcium or zephiramine. Figure 2 shows that the extraction was complete when the zephiramine concentration was more than $1\cdot10^{-4}$ *M* regardless of the concentration of calcium, and a constant absorbance was obtained even when the zephiramine–calcium molar ratio was 0.25–20. Moreover, at a constant concentration of zephiramine, the relationship between the calcium concentration and the absorbance showed a single straight line, regardless of the molar ratios of zephiramine to calcium (1, 0.5 and 0.3) as shown in Fig. 3. These experiments indicate that the presence of a certain amount of zephiramine is necessary for the formation of the 1:2 Ca–GHA chelate, but there is no stoichiometric relationship between the amounts of zephiramine and calcium as to the formation of the extractable chelate. Probably the extracted chelate has no zephiramine in its composition. The same fact was observed in the relation between zephiramine and cadmium (Fig. 4).

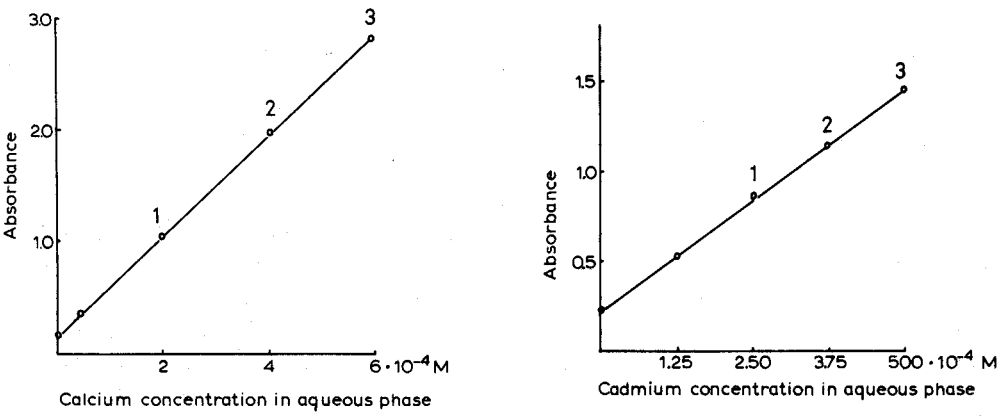

Fig. 3. Absorbance of the Ca–GHA chelate at a constant concentration of zephiramine. The numbers on the line show the [zeph]/[Ca] ratio: (1) 1.0, (2) 0.5, and (3) 0.3. [GHA] = $5 \cdot 10^{-3}$ M; [zeph] = $2 \cdot 10^{-4}$ M; V_{org} = 50 ml.

Fig. 4. Absorbance of the Cd–GHA chelate at a constant concentration of zephiramine. The numbers on the line show the [zeph]/[Cd] ratio: (1) 1.0, (2) 0.7, and (3) 0.5. [GHA] = $4 \cdot 10^{-3}$ M; [zeph] = $2.5 \cdot 10^{-4}$ M; V_{org} = 50 ml.

For these reasons, the chelates extracted in the presence of zephiramine are assumed to have composition ratios Ca:GHA and Cd:GHA of 1:2, with no zephiramine in the molecules.

SAPH chelates

SAPH (expressed as H_2L), which has a similar structure to GHA, forms a non-extractable M(L) chelate in the absence of zephiramine[8,10]. In the presence of zephiramine, however, the M(L) chelate changes to an extractable chelate, whose composition was investigated by the continuous variations method. As shown in Figs. 5 and 6, the zinc–SAPH ratio in the extract was found to be 1:2, and the

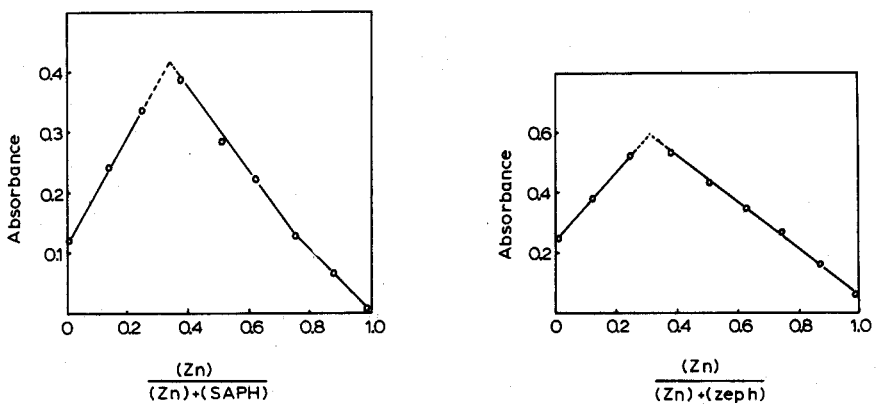

Fig. 5. Zinc–SAPH ratio in the presence of zephiramine. [Zn] + [SAPH] = $1.0 \cdot 10^{-4}$ M; [zeph] = $2.5 \cdot 10^{-4}$ M.

Fig. 6. Zinc–zephiramine ratio in the Zn–SAPH chelate. [Zn] + [zeph] = $1.0 \cdot 10^{-4}$ M; [SAPH] = $4.0 \cdot 10^{-4}$ M.

metal–zephiramine ratio was also 1:2. The same observations were made for the nickel–SAPH chelate.

Thus, the chelates extracted in the presence of zephiramine must have composition ratios, Zn or Ni:SAPH:zeph, of 1:2:2.

CONCLUSIONS

The results of this study are summarized in Table I. An interesting fact is that a certain amount of zephiramine is necessary for extraction of the calcium– or cadmium–GHA chelate, but the extracted chelate itself contains no zephiramine. With regard to the calcium– and cadmium–GHA chelates, it may be assumed that the water or alcohol molecules involved in the ordinary non-extractable 1:1 chelate are replaced by a GHA molecule (H_2A) by the action of zephiramine. Judging from the compositions and the fact that a chelate extractable into inactive solvents has no charge, it is likely that $Ca(A)(H_2A)$ and $Cd(A)(H_2A)$ are formed and extracted into 1,2-dichloroethane in the presence of zephiramine. This phenomenon is a kind of synergism, and may be called "self-synergism" induced by the presence of zephiramine.

TABLE I

GHA AND SAPH CHELATES

Ligand	*Metal*	*pH*	*Absence of zeph* *M:L*	*Presence of zeph* *M:L:Z*	*ε* *of the extract*
GHA	Ca	12.8	1:1[a]	1:2:0	$1.3 \cdot 10^4$
	Cd	13.0	1:1[a]	1:2:0	$5.2 \cdot 10^3$
SAPH	Ni	11.0	1:1	1:2:2	$2.4 \cdot 10^4$
	Zn	11.0	1:1	1:2:2	$8.0 \cdot 10^3$
	Cu	9.2	1:1[b]	1:1:0	$1.6 \cdot 10^4$

[a] Value taken from ref. 9.
[b] Value taken from ref. 10.

SAPH usually gives a 1:1 chelate with a divalent cation[8], and the nickel and zinc chelates also change to a 1:2 chelate in the presence of zephiramine. In contrast to the uncharged 1:2 calcium–GHA chelate, it is assumed that the 1:2 zinc–SAPH chelate has two negative charges as a result of higher chelation; the charged chelate then couples with two molecules of zephiramine, the product being extracted into 1,2-dichloroethane as $Zn(L)_2(zeph)_2$. The same phenomenon was observed in case of nickel–SAPH chelate.

Although ethanol was used for dissolution of GHA or SAPH in the reagent solution, a certain concentration of ethanol also seems to be necessary to complete the extractions of the GHA and SAPH chelates.

It can be seen that zephiramine has an effect of changing a coordination-unsaturated chelate to a coordination-saturated chelate by replacing water or alcohol molecules with the same reagent as the ligand. If the resulting chelate has no charge, the chelate is directly extracted into an inactive solvent, as shown

for the calcium–GHA chelate; and if the chelate is negatively charged as a result of higher coordination, it is extracted by coupling with zephiramine added already in the solution, as shown for the zinc–SAPH chelate.

In the absence of zephiramine, copper forms a water-insoluble 1:1 chelate with SAPH, and the chelate itself is extractable into an inactive solvent[10]. For the 1:1 copper–SAPH chelate, the addition of zephiramine has no effect.

Although the mechanism of the effect of zephiramine on chelate formation is not completely understood, the use of a quaternary ammonium base affords a new field of study in the solvent extraction of metals. The formation of a highly coordinated chelate by the action of zephiramine has importance not only in chelate chemistry but also in practical analytical chemistry, because the colour of such a chelate is much stronger and more stable than that of the ordinary chelate[7].

SUMMARY

The effects of tetradecyldimethylbenzylammonium chloride (zephiramine), a quaternary ammonium base, on chelate formation and extraction of metals were studied. By the action of zephiramine, the non-extractable 1:1 calcium– or cadmium–glyoxal bis-(2-hydroxyanil) chelate changes to an extractable uncharged chelate, $Ca(A)(H_2A)$ or $Cd(A)(H_2A)$, by replacing water molecules with GHA molecules (H_2A). This is a new type of synergism. In the presence of zephiramine, the non-extractable 1:1 zinc– or nickel–*o*-(salicylideneamino) phenol chelate also changes to a negatively charged $Zn(L)_2^{2-}$ or $Ni(L)_2^{2-}$ chelate which can be extracted by coupling with two molecules of zephiramine.

REFERENCES

1 J. Starý, *Anal. Chim. Acta*, 28 (1963) 132.
2 E. B. Sandell, *Colorimetric Determination of Traces of Metals*, New York, 1959, p. 665.
3 A. R. Eberle and M. W. Lerner, *Anal. Chem.*, 34 (1962) 627.
4 K. Fukamachi, H. Kohara and N. Ishibashi, *Bunseki Kagaku*, 19 (1970) 1529.
5 F. Umland and K.-U. Meckenstock, *Z. Anal. Chem.*, 176 (1960) 96.
6 J. R. W. Kerr, *Analyst*, 85 (1960) 867.
7 M. Nishimura and S. Noriki, *Bunseki Kagaku*, 21 (1972) 640.
8 K. Isagai, *Nippon Kagaku Zasshi*, 82 (1961) 1172.
9 E. Bayer, *Ber.*, 90 (1957) 2325.
10 H. Ishii and H. Einaga, *Bunseki Kagaku*, 18 (1969) 230.

Analytica Chimica Acta, 70 (1974) 127–132

PHOTOMETRIC AND POTENTIOMETRIC STUDY OF METAL COMPLEXES OF 2-(3′-SULFOBENZOYL)PYRIDINE-2-PYRIDYLHYDRAZONE

J. E. GOING and C. SYKORA*

Department of Chemistry, University of Wisconsin–Milwaukee, Milwaukee, Wis. 53201 (U.S.A.)

(Received 8th October 1973)

Various tridentate substituted hydrazone ligands have recently been suggested as highly sensitive colorimetric[1–4] or fluorimetric[5,6] reagents for heavy metal ions. These ligands are unique in having an ionizable imino proton on a nitrogen that is not directly involved in complexation. Initially, cationic bis complexes, $M(HL)_2^{2+}$, are formed with divalent metals. The complexation enhances the acidity of the imino protons which then can be removed by raising the pH, resulting in the formation of uncharged water insoluble complexes, ML_2^0. Several studies have been reported on the solvent extraction of the neutral complexes[7,8]

In a study of the solvent extraction of heavy metal complexes of 2-benzoylpyridine-2-pyridylhydrazone (BPPH), it became necessary to know the formation constants of the bis cationic complexes and the acid dissociation constants of the imino protons of the cationic complexes. These constants have been difficult to obtain owing to the insolubility of the ligand in water and the even greater insolubility of the neutral complexes.

Consequently, we have synthesized a sulfonated form of BPPH, 2-(3′-sulfobenzoyl)pyridine-2-pyridylhydrazone (HL-S), to circumvent the solubility problems. This paper describes the study of the formation constants and acid dissociation constants of the zinc, cadmium, mercury and cobalt complexes. The analytical applicability is discussed and the isolation of the anionic deprotonated complexes on an anion exchange resin is reported.

EXPERIMENTAL

Reagent

2-Benzoylpyridine was sulfonated by the procedure of Bradsher *et al.*[9]. An 80% yield of 2-(3′-benzoyl)pyridine was obtained. Equimolar (0.06 mol) quantities of

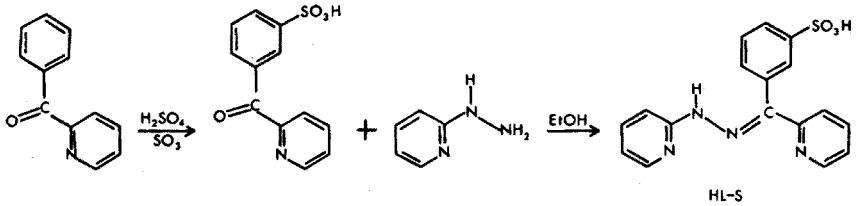

* National Science Foundation, undergraduate research participant, Summer 1973.

2-(3'-benzoyl)pyridine and 2-pyridylhydrazine (Aldrich) were mixed in 200 ml of ethanol and heated to reflux temperature for 1 h. Within 30 min, yellow crystals had appeared. The precipitate was suction-filtered, washed with water and recrystallized from ethanol–water. The recrystallized product was obtained in 66% yield. The reaction scheme is shown above. The u.v. absorption spectrum was essentially identical to that of the unsulfonated ligand[1], BPPH.

The ligand was soluble to about $5 \cdot 10^{-3}$ *M* in basic solutions, and more soluble in acids because of protonation of the pyridine rings. Stock solutions of concentration $2 \cdot 10^{-3}$ *M* were prepared at pH 2.0 using heat to hasten the dissolution.

Qualitative tests showed that the ligand formed intensely colored yellow complexes in basic solution with zinc, cadmium and mercury; the absorption maxima occurred at 440 nm, 444 nm, and 444 nm, respectively. An orange complex formed with cobalt and showed an absorption maximum at 480 nm. The ligand itself showed negligible absorption at these wavelengths. The complexes were all water-soluble.

Potentiometric titrations of the ligand and its complexes were done with a Corning Model 12 expanded scale pH meter at 25 ± 1°C.

Spectrophotometric studies

A Heath–Schlumberger Model 721 spectrophotometer was used for all spectral and absorption measurements.

The effect of pH on color formation was determined by adding sodium hydroxide to a solution of the metal ion with a 50-fold molar excess of ligand. Ionic strength was maintained at 0.10 *M* with sodium perchlorate. Zinc, cadmium and mercury required a pH between 11 and 13 for complete color formation. For subsequent studies, base was added until color formation was observed and then the solution was buffered with 0.01 *M* disodium hydrogenphosphate, pH 12.5. Color formation of the cobalt complex was complete between pH 4 and 10 in agreement with previous studies[1]. For the subsequent studies, a 0.01 *M* acetate buffer at pH 5.0 was used for pH control.

Mole ratio and continuous variations studies were employed to determine the compositions of the complexes. All the metals studied formed 2:1 complexes. A 5-fold molar amount was sufficient for complete formation of the zinc, cadmium and cobalt complexes. Mercury required a 50-fold amount of ligand.

As shown in Table I, all of the complexes have extremely large molar

TABLE I

SPECTRAL DATA OF METAL COMPLEXES

Metal	λ_{max} *(nm)*	*L/M*	*ε*	*pH*
Zn	440	2	49,000	12–13
Cd	444	2	48,000	12–13
Hg	444	2	38,000	11–13
Co	480	2	31,000	4–10

absorptivities, indicating their usefulness for colorimetric analysis. The sensitivity of the reagent approaches that of reagents such as dithizone, PAN or PAR. Furthermore, the ligand spectrum does not overlap the complex spectra and no extractions are required due to insolubilities.

Potentiometric titrations

The spectrophotometric studies demonstrated the solubility of the ligand and the complexes at low concentrations of *ca.* 10^{-5} *M*. Preliminary studies showed solubility at higher concentrations of *ca.* 10^{-3} *M*. Consequently, as had been hoped, potentiometric titrations were feasible at reasonable concentrations, and it was not necessary to resort to mixed solvents[2], extraction titrations[10] or titration at very low concentration.

The acid dissociation constants of HL-S were determined by repeated titration of the ligand in a known excess of perchloric acid with standard sodium hydroxide. The titration is shown as curve 1, Fig. 1. The ionic strength was maintained at 0.10 *M* $NaClO_4$ for all the titrations. The acid dissociation constants are defined by the equations

$$K_1 = \frac{[H_2L-S^0][H^+]}{[H_3L-S^+]}, \qquad K_2 = \frac{[HL-S^-][H^+]}{[H_2L-S^0]}$$

where $H_3L\text{-}S^+$ corresponds to the ligand protonated on both pyridine rings, $H_2L\text{-}S^0$ to the ligand protonated on one pyridine ring, and $HL\text{-}S^-$ to the unprotonated ligand. The net charge was evaluated on the assumption that the sulfonic acid group was completely ionized in aqueous solution. The liberated sulfonic acid proton is titrated with excess of perchloric acid. From the volume of standard base required to neutralize the sulfonic acid, the purity of the reagent was calculated to be $100.0 \pm 0.1\%$. The pK_1 and pK_2 values were found to be 3.62 and 6.01, respectively. Green *et al.*[10] reported values of 2.87 and 5.71 for 2-pyridinealdehyde-2-pyridylhydrazone (PAPHY) and Heit and Ryan[2] reported a pK_2 value of 5.26 for 2-pyridinealdehyde-2-quinolylhydrazone in 1:1 dioxane–water.

Titration of the ligand in the presence of heavy metal ions indicated strong complexation as shown by the titration curves 2–5 of Fig. 1. The formation constants for the protonated form of the complexes are defined[10] as:

$$\beta_1 = \frac{[MHL-S]}{[M][HL-S]}, \qquad \beta_2 = \frac{[M(HL-S)_2]}{[M][HL-S]^2}$$

The term "protonated" refers to the fact that the imino protons are still present on the complexes. Complexes in which these protons have been removed are termed "deprotonated". The formation constants were determined for the zinc, cadmium and mercury protonated complexes by application of the linear plot technique[11] to the equation

$$\bar{n} = \frac{\beta_1[HL-S] + 2\beta_2[HL-S]^2}{1 + \beta_1[HL-S] + \beta_2[HL-S]^2}$$

Values of [HL-S] were calculated from the pK_1 and pK_2 values previously determined. Plots of $\{((2-\bar{n})[HL\text{-}S])/(\bar{n}-1)\}$ against $\{\bar{n}/((\bar{n}-1)[HL\text{-}S])\}$ were linear. The

TABLE II

EQUILIBRIUM CONSTANTS OF METAL COMPLEXES

(Acid dissociation constants of sulfonated BPPH: $pK_1 = 3.62$, $pK_2 = 6.01$)

	Zn	*Cd*	*Hg*
$\log \beta_1$	6.6	5.6	8.1
$\log \beta_2$	12.8	11.0	15.0
pK_3	7.69	8.09	6.99
pK_4	8.96	9.81	8.88

slope and intercept were $1/\beta_2$ and β_1/β_2, respectively, and were found by a linear regression analysis of the data. The results are listed in Table II.

The titration curves of zinc, cadmium and mercury show a single titration break corresponding to the neutralization of the perchloric acid and the sulfonic acid and indicate only bis complex formation. This parallels the observations of Green *et al.*[10] for the reaction of PAPHY with zinc and cadmium. The log β_2 values for sulfonated BPPH are slightly larger than those for PAPHY, 12.8 *versus* 11.2 for zinc, and 10.9 *versus* 10.1 for cadmium. No formation constants have been previously reported for mercury.

Formation constants for cobalt could not be calculated from the titration data. As shown in curve 5, Fig. 1, titration of the cobalt complex required one additional OH^- per cobalt atom. It has been shown that complexed cobalt(II) is oxidized

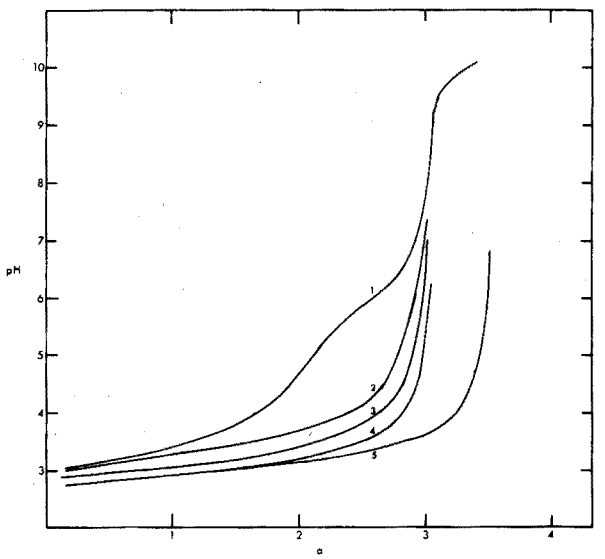

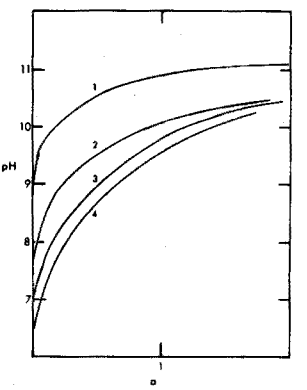

Fig. 1. pH titration of ligand (10^{-3} *M*) in $3 \cdot 10^{-3}$ *M* perchloric acid: (1) alone; (2)–(5), with $0.5 \cdot 10^{-4}$ *M* Cd, Zn, Hg, Co, respectively; *a*, moles of NaOH per mole of ligand.

Fig. 2. pH titration of $1.0 \cdot 10^{-3}$ *M* protonated bis complexes: (1) ligand alone; (2)–(4), with Cd, Zn, Hg, respectively; *a*, moles of NaOH per mole of ligand.

to cobalt(III) by dissolved oxygen[1], resulting in the consumption of one imino proton and an increase in the acidity of the second imino proton. Thus the titration break does not occur until the one remaining imino proton has been neutralized. Consequently, the protonated form of the complex does not exist. Formation constants calculated from the mole ratio and continuous variations curves indicate log β_2 to be about 11.6.

Further titration of the zinc, cadmium and mercury complexes results in deprotonation of the complex. The resulting species has a net charge of 2− as a result of the sulfonate groups and can be termed the anionic deprotonated form. Titration curves are shown in Fig. 2 for $1.00 \cdot 10^{-3}$ *M* complexes. The complex acid dissociation constants are defined as

$$K_3 = \frac{[M(HL-S)(L-S)^-][H^+]}{[M(HL-S)_2^0]}, \qquad K_4 = \frac{[M(L-S)_2^{2-}][H^+]}{[M(HL-S)(L-S)^-]}$$

In fact, the titration curves of Figs. 1 and 2 were obtained as a single titration and are separated solely for illustration.

The titration curves were interpreted as simply a dibasic acid titration and the K_3 and K_4 values were derived conventionally. The p*K* values are listed in Table II and are in agreement with the values for the zinc and cadmium complexes of PAPHY[10]. No values could be determined for cobalt for the reason previously cited. No values for mercury complexes have previously been reported.

Isolation on anion-exchange resin

At pH 12, the zinc, cadmium and mercury complexes have a net charge of 2− as a consequence of the two anionic sulfonate groups. The complex could be expected to have a high affinity for an anion-exchange resin as a result of these groups[11]. Since the complexes are fairly large, a low cross-linked resin was used to minimiz exclusion by sieve action[12]. Solutions of 250 and 1000 ml containing 0.5 μmol of zinc cadmium or mercury and 12.5 μmol of ligand were made basic to pH 12.5 and passed through a 1 × 2 cm column of Bio-Rad AG 1-X2, 50–100 mesh at a flow rate of 4 ml min^{-1}. The metal complex and excess of ligand were completely removed and could easily be seen at the top of the column. Elution with 1 *M* hydrochloric acid was unsatisfactory, owing to retention of the metal chloro complexes. Elution with 0.5 *M* sulfuric acid gave 100% recovery of the metal ions and excess of ligand in the first 20 ml of acid. It should be possible to extend the system to much smaller quantities of metal ions and/or larger volumes of solution. Isolation of trace metal ions from natural and sea water should be easily accomplished by this technique and could readily be done at the sampling site. The small column of resin could be returned to the laboratory for the final analysis. Mixtures of metal ions would best be determined by atomic absorption. Studies are underway in this area.

CONCLUSIONS

The sulfonated form of 2-benzoylpyridine-2-pyridylhydrazone forms both protonated and deprotonated bis complexes with zinc, cadmium and mercury. The overall charges of the two types of complexes are 0 and 2−, respectively. Cobalt is

oxidized upon complexation to the 3+ state and only the bis deprotonated complex with a net charge of 1− is formed.

The protonated form of the zinc, cadmium and mercury complexes exists in acidic and neutral solution. The imino proton acid dissociation constants of the complexes are 7–8 for pK_1 and 9–10 for pK_2. The deprotonated forms of the complexes only exist at pH 11 or greater. The additional positive charge of the cobalt(III) complex causes the imino proton to be more acidic than when the metal ion has a 2+ valency. Although the dissociation constant could not be determined, the complex is completely formed by pH 4.

The deprotonated complexes are suitable for trace colorimetric analysis as the data in Table I indicate. With the exception of the cobalt complex, however, the absorption maxima are all too similar to allow identification. The protonated complexes are essentially colorless.

The deprotonated zinc, cadmium and mercury complexes have peripheral anionic sites owing to the sulfonate group and a net charge of 2−. The complexes are effectively retained by anion exchange resins. It is expected that this procedure will be useful for the isolation of trace quantities of metal ions from large volumes of solution.

SUMMARY

The composition, formation conditions and stability constants of metal complexes of 2-(3′-sulfobenzoyl)pyridine-2-pyridylhydrazone are reported. Two types of complexes are formed having net charges of 0 and 2− with divalent cations. The anionic form of the complex is quantitatively retained by anion-exchange resins and can be recovered by acid solution.

REFERENCES

1 J. E. Going and R. T. Pflaum, *Anal. Chem.*, 42 (1970) 1098.
2 M. L. Heit and D. E. Ryan, *Anal. Chim. Acta*, 32 (1965) 448.
3 G. G. Sims and D. E. Ryan, *Anal. Chim. Acta*, 44 (1969) 139.
4 J. Abraham, M. Winpe and D. E. Ryan, *Anal. Chim. Acta*, 46 (1969) 431.
5 R. E. Jensen and R. T. Pflaum, *Anal. Chem.*, 38 (1966) 1269.
6 D. E. Ryan, F. Snape and M. Winpe, *Anal. Chim. Acta*, 58 (1972) 101.
7 R. W. Frei, G. H. Jamro and O. Navratil, *Anal. Chim. Acta*, 55 (1971) 125.
8 M. A. Quddus and C. F. Bell, *Anal. Chim. Acta*, 42 (1968) 503.
9 C. K. Bradsher, J. C. Parham and J. D. Turner, *J. Heterocycl. Chem.*, 2 (1965) 228.
10 R. W. Green, P. S. Hallman and F. Lions, *Inorg. Chem.*, 3 (1964) 376.
11 F. J. C. Rossotti and H. Rossotti, *The Determination of Stability Constants*, McGraw-Hill, New York, 1961, Chap. 5.
12 F. Helfferich, *Ion Exchange*, McGraw-Hill, New York, 1962, Chap. 5.

Analytica Chimica Acta, 70 (1974) 133–139

FLUORIMETRIC DETERMINATION OF REDUCING SUGARS WITH ETHYLENEDIAMINE SULFATE

S. HONDA, K. KAKIMOTO, K. SUDO, K. KAKEHI and K. TAKIURA

Faculty of Pharmaceutical Sciences, Osaka University, Toneyama, Toyonaka, Osaka-fu (Japan)

(Received 20th September 1973)

In a previous paper[1], a sensitive chromatographic detection of carbohydrates by fluorescence reactions with ethylenediamine sulfate was reported. Further investigation of these reactions has made it possible to determine microgram quantities of various reducing sugars. Since the reaction conditions used in this determination were neutral or weakly alkaline, reducing sugars could be determined accurately without interference from cleavage of glycosidic linkages in concomitant glycosides, in contrast to a number of reported fluorimetric methods[2–6], which require acidic conditions. Accordingly, this method is appropriate for the micro determination of free sugars in the presence of glycosides as well as neutral polysaccharides.

pH dependence of fluorescence formation

Among a variety of buffers examined, phosphate buffer was found to give the most intense fluorescence. Figure 1 shows the pH dependence of fluorescence

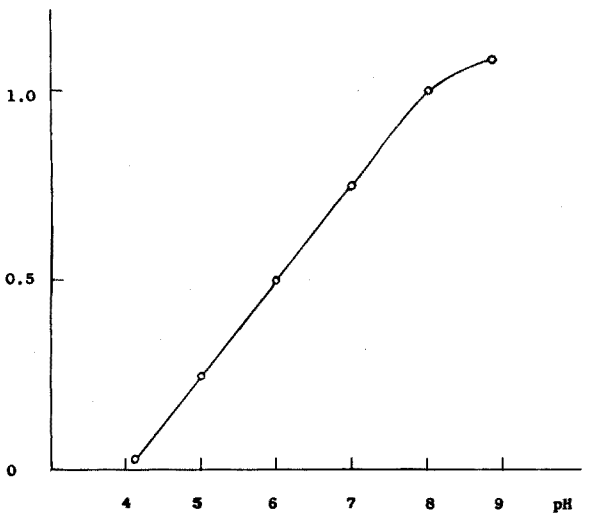

Fig. 1. pH dependence of fluorescence formation in 0.6 M phosphate buffer. D-glucose, $2.00 \cdot 10^{-4}$ M; ethylenediamine sulfate, $2.00 \cdot 10^{-2}$ M; reaction time, 3 h.

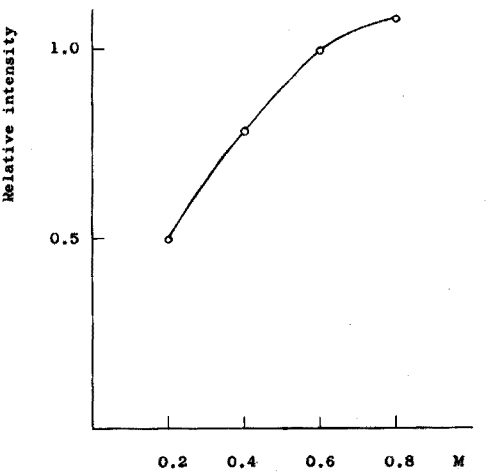

Fig. 2. Effect of buffer concentration. D-glucose, $2.00 \cdot 10^{-4}$ M; ethylenediamine sulfate, $2.00 \cdot 10^{-2}$ M; phosphate buffer, pH 8.00; reaction time, 3 h.

formation from D-glucose in 0.6 *M* phosphate buffer. The data indicate that fluorescence formation increased with increasing pH. However, since high pH values diminish the buffer effect, a pH around 8 was considered to be appropriate.

Buffer concentration also affected the fluorescence formation, as shown in Fig. 2. At high concentrations, a more intense fluorescence was observed, but a very high concentration was unprofitable, because at low room temperatures measurement could be prevented by the precipitation of a crystalline phosphate salt. The upper limit was shown to be 0.6 *M*.

Effect of reagent amount

For complete development of fluorescence, it was necessary to use an amount of the reagent more than 10-fold molar relative to the carbohydrates (Fig. 3). However, taking the buffer effect into account, the concentration was kept below $2 \cdot 10^{-2}$ *M*.

Course of fluorescence reactions

The fluorescence formation increased linearly for 3 h. Thereafter the reaction rate slowed down gradually to reach a plateau after *ca.* 10 h. Although the reaction was still in progress after 3 h, this reaction time was considered to be appropriate for the rapidity of determination.

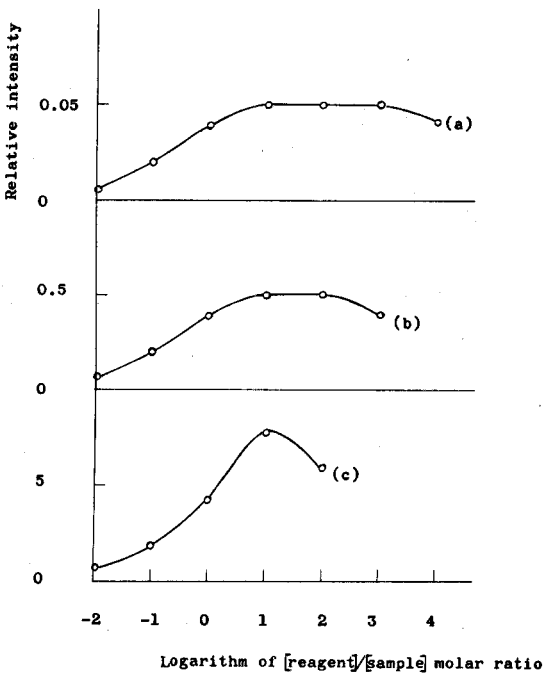

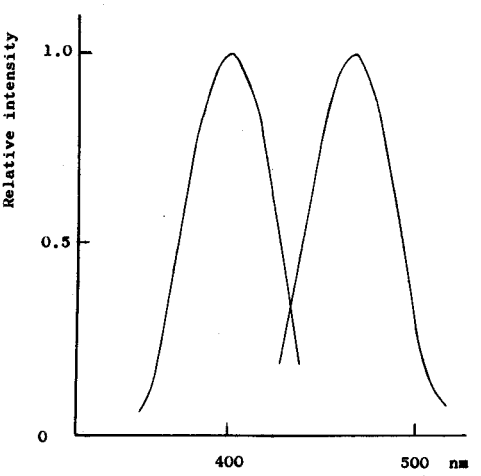

Fig. 3. Effect of reagent amount. D-glucose: (a) $1.00 \cdot 10^{-5}$ *M*; (b) $1.00 \cdot 10^{-4}$ *M*; (c) $1.00 \cdot 10^{-3}$ *M*. 0.6 *M* phosphate buffer, pH 8.00; reaction time, 3 h.

Fig. 4. Fluorescence spectrum. D-glucose, $2.00 \cdot 10^{-4}$ *M*; ethylenediamine sulfate, $2.00 \cdot 10^{-2}$ *M*; 0.6 *M* phosphate buffer, pH 8.00; reaction time, 3 h.

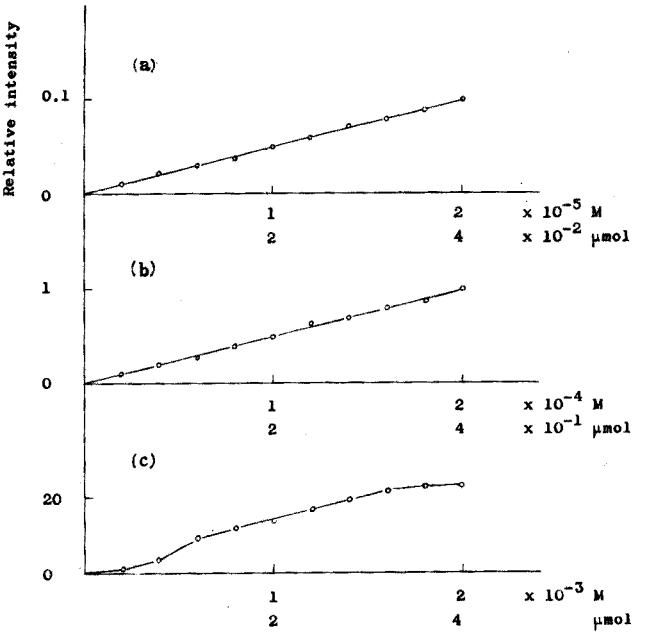

Fig. 5. Calibration curve of D-glucose. Ethylenediamine sulfate, $2.00 \cdot 10^{-2}$ *M*; 0.6 *M* phosphate buffer, pH 8.00; reaction time, 3 h.

Fluorescence spectra and calibration

The reaction mixture obtained from D-glucose at pH 8.00 gave excitation and emission maxima at 400 and 465 nm, respectively (Fig. 4). Other reducing sugars, except oligosaccharides, gave similar spectra.

As depicted in Fig. 5, D-glucose gave a sigmoid curve which showed linearity for sample concentrations of $2 \cdot 10^{-6}$–$2 \cdot 10^{-4}$ *M*. These concentrations corresponded to sample amounts of $4 \cdot 10^{-3}$–$4 \cdot 10^{-1}$ µmol. D-Galactose and D-mannose gave calibration curves exactly the same as Figs. 5(a) and (b) for these concentration ranges; the curves obtained for D-fructose were also linear but showed slightly greater sensitivity, being similar to the curves for D-arabinose, a pentose (Fig. 6). The calibration curves for three pentoses are shown in Fig. 6.

Replicate determinations of various amounts of D-glucose are given in Table I. These data show that this method is accurate and reproducible.

TABLE I

REPRODUCIBILITY OF DETERMINATION

(10 determinations were done at each level.)

D-glucose added (µmol)	*Ave. D-glucose found (µmol)*	*Standard deviation*
$4.00 \cdot 10^{-3}$	$3.95 \cdot 10^{-3}$	$0.088 \cdot 10^{-3}$
$4.00 \cdot 10^{-2}$	$4.03 \cdot 10^{-2}$	$0.070 \cdot 10^{-2}$
$4.00 \cdot 10^{-1}$	$3.98 \cdot 10^{-1}$	$0.066 \cdot 10^{-1}$

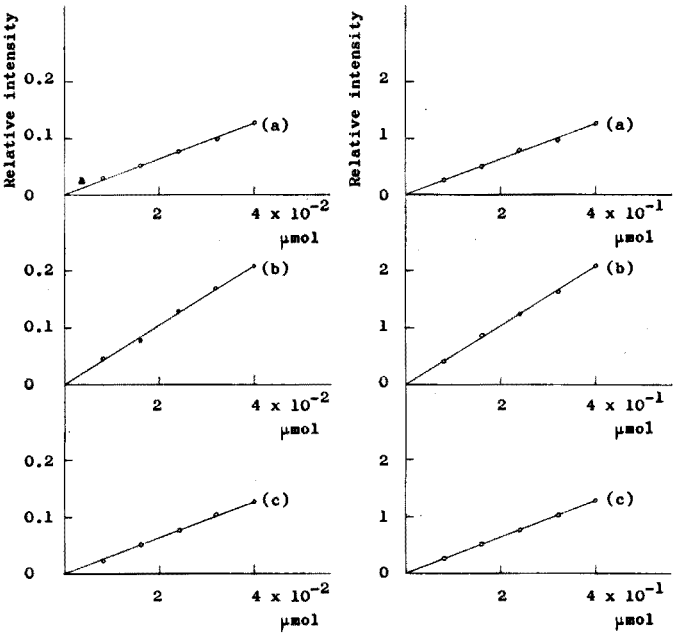

Fig. 6. Calibration curves of pentoses: (a) D-arabinose; (b) D-ribose; (c) D-xylose. The reaction conditions were identical with those for the calibration of D-glucose (Fig. 5).

EXPERIMENTAL

Reagents

Ethylenediamine sulfate was commercially available (Tokyo Kasei Co. Ltd., guaranteed grade). All carbohydrate samples were from commercial sources.

General procedure

In each measurement, in a search for appropriate reaction conditions, an aqueous solution of ethylenediamine sulfate (1.00 ml), a buffer solution (2.00 ml) and an aqueous solution of a carbohydrate sample (2.00 ml) were mixed in a Pyrex tube (1.8 cm i.d. × 20 cm) with a glass stopper, and heated on a boiling water bath. The fluorescence formed was measured with a Hitachi MPF-2A spectrophotofluorimeter.

Recommended procedure for the determination of reducing sugars

To a buffered reagent solution (3.00 ml), prepared by mixing $2 \cdot 10^{-2}$ *M* ethylenediamine sulfate (1 volume) and 0.6 *M* phosphate buffer (pH 8.00, 2 volumes), add the sample solution (2.00 ml) containing $4 \cdot 10^{-3}$–$4 \cdot 10^{-1}$ μmol of a reducing sugar. Heat the mixture for 3 h on a boiling water bath. Read the fluorescence intensity at 400 nm (excitation) and 465 nm (emission) within 24 h. A standard, a reagent blank and an unknown should be run in triplicate. Calculation is made on the basis that the fluorescence intensity is directly proportional to the amounts of reducing sugars.

The buffered reagent solution used was stable for at least 1 month. Thereafter the reagent blank increased gradually.

RESULTS AND DISCUSSION

Relative intensities of fluorescence formed from various carbohydrates

The fluorescence intensities from various carbohydrates ($4 \cdot 10^{-3}$ μmol) were compared, and the results are summarized in Table II. Table II also lists the unreactive compounds: non-reducing monosaccharides including alditols, aldonic acids and glycosides gave no fluorescence with ethylenediamine sulfate, nor did neutral polysaccharides. All of the reducing sugars, including aldoses, ketoses, deoxy sugars, amino sugars and uronic acids, formed fluorescence with excitation and emission maxima at around 400 and 465 nm, respectively. In the aldose family, all of the relative fluorescence intensities of hexoses, referred to D-glucose, were approximately unity. Of pentoses, D-arabinose and D-xylose gave the same relative intensity (1.25), which was somewhat higher than those of hexoses, whereas D-ribose gave an extraordinarily high value (2.09) for unknown reasons; the commercial sample may have been contaminated with some impurities. The overproduction

TABLE II

COMPARISON OF THE FLUORESCENCE INTENSITIES FORMED FROM VARIOUS CARBOHYDRATES[a]

Carbohydrate	λ_{max} *(Ex) (nm)*	λ_{max} *(Em) (nm)*	*Relative intensity*[b]		*No fluorescence obtained for*
			at λ_{max}	*at 400 nm (Ex) /465 nm (Em)*	
DL-Glyceraldehyde	400	465	1.53	1.53	Glycerol
D-Arabinose	400	465	1.25	1.25	Erythritol
D-Ribose	400	465	2.09	2.09	D-Dulcitol
D-Xylose	400	465	1.25	1.25	D-Mannitol
D-Galactose	400	465	0.98	0.98	D-Sorbitol
D-Glucose	400	465	1	1	D-Arabonic acid
D-Mannose	400	465	1.01	1.01	D-Gluconic acid
D-Fructose	400	465	1.12	1.12	Methyl α-D-glucopyranoside
L-Sorbose	400	465	1.16	1.16	Methyl β-D-glucopyranoside
2-Deoxy-D-ribose	400	490	0.36	0.31	Phenyl α-D-glucopyranoside
2-Deoxy-D-glucose	400	460	0.12	0.11	Phenyl β-D-glucopyranoside
L-Rhamnose	400	465	1.47	1.47	Adenosine
D-Galactosamine HCl	400	465	1.61	1.61	2'-Deoxyadenosine
D-Glucosamine HCl	400	465	1.66	1.66	Sucrose
N-Acetyl-D-galactosamine	390	465	1.55	1.41	Raffinose
N-Acetyl-D-glucosamine	375	465	2.04	1.53	Amylose
D-Galacturonic acid	400	465	1.67	1.67	Glycogen
D-Glucuronic acid	400	465	1.83	1.83	Dextran
Maltose	375	463	1.37	1.00	
Cellobiose	375	463	1.30	1.06	
Lactose	375	463	1.30	1.00	

[a] A sample amount of $4.00 \cdot 10^{-1}$ μmol was used for each carbohydrate.

[b] Average values of 5 measurements.

of fluorescence was much more prominent in the case of D-erythrose, one of the tetroses (4.16); in this case the purest sample commercially available was still syrupy, and the purity of the sample was suspect. With these two aldoses, further purification of samples would be necessary before their fluorescence intensities are discussed in relation to their structures. DL-Glyceraldehyde, the lowest member of this family, gave the highest intensity (1.53) except for the above two aldoses. On the other hand, the fluorescence formed from ketohexoses was *ca.* 15% higher than that from aldohexoses. The low yield of fluorescence from 2-deoxysugars was notable, and suggested the participation of the C-2 hydroxyl group in these fluorescence reactions. L-Rhamnose, a 6-deoxyaldose, resembled aldopentoses in fluorescence formation. Amino sugars and uronic acids were classes of sensitive compounds, giving relative intensities ranging from 1.5 to 2.0. Although non-reducing oligosaccharides gave no fluorescence, all of reducing oligosaccharides inspected gave characteristic excitation curves which had maxima at 375 nm, along with shoulders at 400 nm. Their emission maxima were observed at 463 nm, slightly shifted from those of reducing monosaccharides. Apparently, at least two fluorescent materials must be formed from these oligosaccharides. However, their relative intensities measured at 400 (excitation) and 465 nm (emission), *i.e.* at the same wavelength used for reducing monosaccharides, were approximately unity. In some cases (DL-glyceraldehyde, amino sugars and uronic acids), the relative fluorescence intensities thus obtained did not accord with the data reported in the chromatographic detection of these carbohydrates[1]. However, it must be considered that the reaction conditions, especially pH and temperature, used in the two analyses, were not identical.

Determination of D-glucose in the presence of large amounts of methyl α-D-glucopyranoside

Since the ethylenediamine sulfate method is specific for reducing sugars, the determination of reducing sugars in the presence of large excesses of glycosides is possible. Table III shows the results obtained for D-glucose in the presence of methyl α-D-glucopyranoside; it is obvious that D-glucose can be determined in the presence of at least 100-fold amounts of methyl α-D-glucopyranoside.

Determination of D-glucose in the presence of large amounts of amylose

Similarly D-glucose ($4 \cdot 10^{-3}$ μmol) could be determined without interference from 100-fold amounts of amylose.

TABLE III

DETERMINATION OF D-GLUCOSE IN THE PRESENCE OF METHYL α-D-GLUCOPYRANOSIDE

(In each case $4.00 \cdot 10^{-1}$ μmol of D-glucose was used.)

Methyl α-D-glucopyranoside added (μmol)	0	2.0	4.0	8.0	16.0	24.0	32.0	40.0
D-Glucose found $\cdot 10^{-1}$ (μmol)	3.92	3.89	3.92	4.16	4.08	3.89	4.00	4.12

SUMMARY

A new simple method of fluorimetric determination of reducing sugars is proposed. In phosphate buffer (pH 8.00) containing more than a 10-fold molar amount of ethylenediamine sulfate, reducing sugars ($4 \cdot 10^{-3}$–$4 \cdot 10^{-1}$ μmol) may be determined without interference from glycosides or neutral polysaccharides.

REFERENCES

1 S. Honda, K. Kakimoto, K. Kakehi and K. Takiura, *Anal. Chim. Acta*, 64 (1973) 310.
2 T. Momose and Y. Okura, *Chem. Pharm. Bull. (Tokyo)*, 7 (1959) 31.
3 L. Coassino-Lokar, *Univ. Studi Trieste, Fac. Econ. Commer., 1st Merceol., Publ.*, 27 (1966) 19.
4 C. G. Rodgers, C. W. Chambers and N. A. Clarke, *Anal. Chem.*, 38 (1966) 1851.
5 H. Hirayama, K. Hiraki and Y. Nishikawa, *Bunseki Kagaku*, 20 (1971) 1435.
6 S. Nakano, H. Taniguchi, T. Furuhashi and K. Mikoshiba, *Yakugaku Zasshi*, 93 (1973) 350.

Analytica Chimica Acta, 70 (1974) 141–148

FLUORIMETRIC DETERMINATION OF CARBOHYDRATES IN SEA WATER

HIROSHI HIRAYAMA

Department of Fundamental Education, Faculty of Science and Technology, Kinki University, Kowakae, Higashi-Osaka (Japan)

(Received 7th September 1973)

Various methods have been proposed for the determination of carbohydrates in sea water, lake water or river water, most of which are based on spectrophotometry after reaction with anthrone or phenol–sulfuric acid[1–3]. Strictly controlled conditions are required for separate determinations of pentose and hexose by these methods.

A fluorimetric determination of pentose with anthrone, which is relatively selective for pentose in presence of hexose has already been reported[4]. Momose and Ohkura[5] proposed a fluorimetric determination of hexose with 5-hydroxy-1-tetralone, which does not form a fluorescent complex with pentose[6]. It should, therefore, be possible to determine pentose and hexose separately.

In the work reported here, the fluorimetric determination of pentose and hexose in sea water was studied. Since the concentration of carbohydrates in sea water is very low, a prior separation is essential. For this purpose, adsorption of carbohydrates onto activated carbon, and desalination by electrodialysis with an ion-exchange membrane were examined. Finally, a relatively simple method for the fluorimetric determination of pentose and hexose in sea water was established.

EXPERIMENTAL

Reagents

Anthrone solution, 0.01%. 10 mg of anthrone (special grade, Nakarai Chemicals Co.,) was dissolved in 100 ml of 65% sulfuric acid solution. The solution was prepared just before use.

5-Hydroxy-1-tetralone solution, 0.03%. 30 mg of the reagent (Ishizu Pharmaceutical Co.,) was dissolved in 100 ml of concentrated sulfuric acid.

Carbohydrate solutions, 10 μg ml^{-1}. D-Xylose, D-ribose, L-arabinose, D-glucose, D-galactose, D-mannose, D-fructose, and L-sorbose were employed. Special-grade materials were purified by recrystallization, and dissolved in water.

Copper solution, 100 μg Cu ml^{-1}. 40 mg of copper(II) sulfate pentahydrate, recrystallized, was dissolved in 100 ml of water.

Uranine solution (0.15 μg ml^{-1}) was used as the reference standard for the fluorimeter settings. Artificial sea water was prepared as recommended by Lyman and Fleming[7]. Activated charcoal for chromatography (100–200 mesh) was used. Other materials were of reagent grade.

Apparatus

Hitachi fluorescence spectrophotometers, model MPF-2A and model 203, were used. A Sartorius Electro-Dialyzer SM 16531 with a model 50 T power supply (controlled voltage and current: d.c., 1000 V; 1–500 mA; M. and S. Instruments Trading Inc.) was used for the electrodialysis. As dialysis membrane, Selemion CMV (Asahi Glass Co.; styrene–butadiene copolymer, strong acid cation-exchanger, Na^+-type, 0.22–0.25 mm thick) and AMV (Asahi Glass Co., styrene–butadiene copolymer, strong base anion-exchanger, Cl^--type, 0.18–0.20 mm thick) were employed.

Fluorimetric determination of pentose with anthrone

The fluorimetric determination of pentose with anthrone has already been reported in detail[4]. The general procedure was as follows. To 1 ml of sample solution containing 1–15 μg of pentose, placed in a stoppered test tube and cooled in an ice bath, slowly add 10 ml of anthrone solution. Mix carefully, heat in a boiling water bath for 15 min, cool in the ice bath for 10 min or more, and then warm to room temperature in running water. Measure the fluorescence at 505 nm with excitation at 465 nm.

The uranine solution, or a standard solution containing 10 μg of xylose and similarly treated, was used as the reference. The relative error of the procedure was 2%.

Sea water contains large amounts of electrolytic salts, and so the effect of salts on the fluorimetry of pentose was studied. Sodium chloride had no effect on the fluorescence of xylose (8 μg) up to a concentration of *ca.* 0.01 mg ml^{-1}, but the fluorescence intensity then decreased gradually as the amount of sodium chloride increased up to *ca.* 0.5 mg ml^{-1}, whereafter it decreased more rapidly. This interference necessitated a preliminary separation.

Fluorimetric determination of hexose

The general procedure was as follows. To 1 ml of sample solution containing 1–10 μg of hexose, placed in a stoppered test tube and cooled in an ice bath, add 0.2 ml of copper solution, 0.3 ml of water, 2.5 ml of 5-hydroxy-1-tetralone solution, and 1 ml of concentrated sulfuric acid, mixing and cooling thoroughly during each addition. Then heat in boiling water for 30 min, add 5 ml of water, and cool in the ice bath for 5 min. Warm to room temperature (15–20°C), and measure the fluorescence at 525 nm with excitation at 494 nm.

Uranine solution or a solution containing 8 μg of glucose was used as the reference standard. The relative error of the method was 2%.

The influence of foreign salts has been investigated by Ohkura *et al.*[8]: more than 100 μg of sodium chloride, aluminium, potassium, and calcium ions interfered with the determination of hexose.

Separation and concentration of carbohydrates

Adsorption onto active carbon and electrodialysis with an ion-exchange membrane were examined as separation techniques; evaporation under reduced pressure was adopted as the concentrating procedure.

Adsorption of carbohydrates on activated carbon. Carbohydrates can be

adsorbed onto activated carbon and then desorbed into ethanolic solution[9,10], which seemed promising for a separation from inorganic salts. The adsorption and desorption behavior of carbohydrates was studied as follows. Activated carbon powder was packed in a column, 30 mm in diameter and 20 or 60 mm high, and washed well with water. Artificial sea water (50 ml) containing 180 μg of carbohydrate (glucose) was passed down the column at a flow rate of 2 ml min^{-1}, and the glucose adsorbed was then eluted with aqueous 5% ethanol at a flow rate of 1 ml min^{-1}. The eluate was collected in 5-ml portions and the fractions were separately evaporated under reduced pressure*. The residues were diluted with water in 10-ml volumetric flasks, and 1 ml of each of the solutions was employed for the fluorimetric determination. Typical elution curves for glucose are shown in Fig. 1.

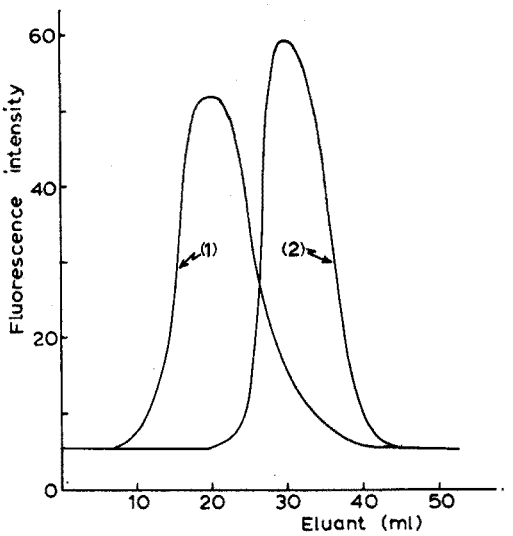

Fig. 1. Elution curves of glucose from activated carbon columns. (1) Height of column, 20 mm. (2) Height of column, 60 mm. Eluant, 5% ethanol. Glucose 180 μg.

The recovery of glucose decreased somewhat as the column became higher. About 95% of the glucose was removed with a 20-mm column, and about 90% with a 60-mm column. Xylose—a pentose—was similarly adsorbed, but not completely desorbed, the recovery being about 40% or less.

Because the column technique was time-consuming for the treatment of large volumes of sample solution, the batch technique was also examined. The results are presented in Table I and Fig. 2, which summarize the adsorption and desorption behavior of xylose. When 7.5 g of active carbon was used, more than 95% of glucose was adsorbed from 500 ml of artificial sea water sample and 93% (98% of adsorbed fraction) could be recovered by leaching with aqueous

* Alcohol increases the fluorescence of the glucose–5-hydroxy-1-tetralone complex, equimolar amounts causing an error of about +5%, and 40-fold amounts an error of +15–16%. Therefore, alcohol must be removed before the determination. The determination of pentose with anthrone is not affected by alcohol.

TABLE I

ADSORPTION AND DESORPTION OF PENTOSE AND HEXOSE ON ACTIVATED CARBON

Sample (μl/ml)	*Active carbon (g)*	*C_2H_5OH (%-ml)*	*Stirring time (min)*	*Adsorption (%)*	*Desorption (%)*	*Recovery (%)*
Xylose 750/50	5[a]	5–40	60	93.8	17	16
Xylose 750/50	5[b]	5–40	60	68.5	15	10.3
Xylose 750/50	5[a]	30–40	120	95.4	38	36.3
Xylose 750/50	5[b]	30–40	120	80.2	18	14.3
Glucose 180/50	1.25[a]	5–40	30	100	99.4	99.3
Glucose 360/500	5[a]	5–40	20	60	98.1	59
Glucose 360/500	7.5[a]	5–40	20	98	95	93

[a] Nakarai Chemicals Ltd.
[b] Wako Pure Chemical Ind. Ltd.

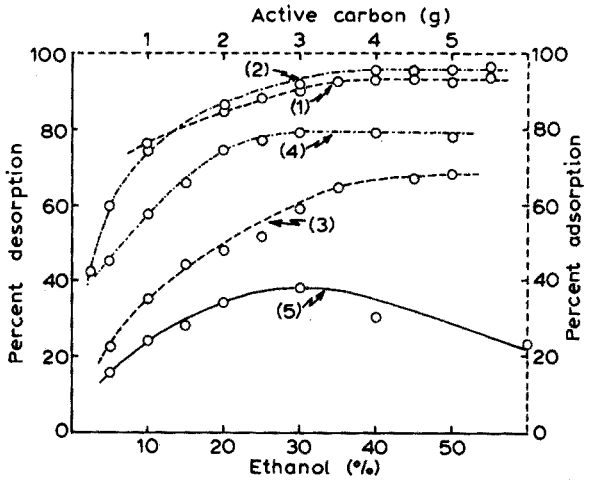

Fig. 2. Adsorption and desorption of pentose on activated carbon by the batch method. (1) Adsorption curve, stirring for 60 min (Nakarai Chem. Co.,); (2) adsorption curve, stirring for 120 min (Nakarai Chem. Co.,); (3) adsorption curve, stirring for 60 min (Wako Pure Chem. Ind. Ltd.); (4) adsorption curve, stirring for 120 min (Wako Pure Chem. Ind. Ltd.); (5) desorption curve.

5% ethanol. However, the recovery of xylose was too low, especially in the desorption process, for this procedure to be applied to the separation of pentose.

Removal of salts by ion-exchange membrane electrodialysis. Since the adsorption technique was unsuccessful for pentoses, electrodialysis[11] with an ion-exchange membrane was examined.

The electrodialyzer was arranged as shown in Fig. 3. The cells were tightly fixed together with silicone packings by means of screw B.

The sea-water sample (100 ml) was placed in the center cell of the dialyzer and stirred at 1600 rev min^{-1}. A current of 250–350 mA (d.c.) at a potential of 90–100 V was applied, and during the electrodialysis, water was circulated through the outer cells by a small pump P. (If the ion concentration became excessive, fresh water was added to the water pool W.)

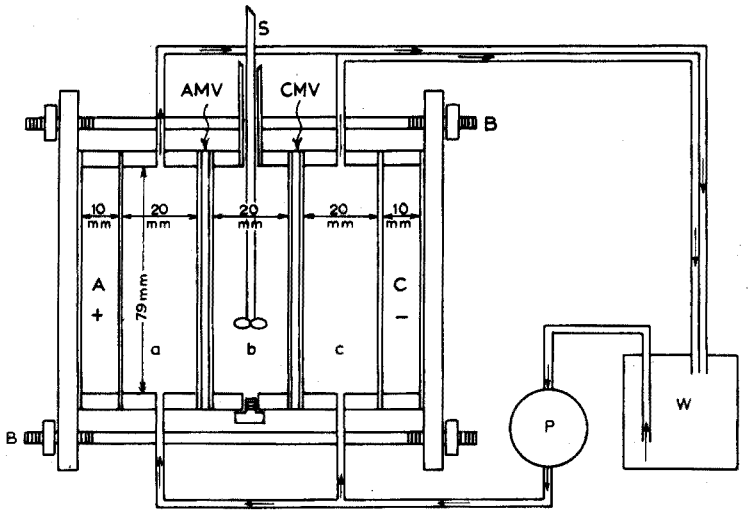

Fig. 3. Schematic diagram of electrodialyzer. A, carbon electrode (+); B, bolt; C, carbon electrode (−); a, anode cell; b, center cell (sample cell with a capacity of 100 ml); c, cathode cell; S, stirrer; P, pump; W, water pool; AMV, anion-exchange membrane (Selemion AMV); CMV, cation-exchange membrane (Selemion CMV).

Under the conditions used, complete desalination of 100 ml of sea water with a chlorinity of 19‰ required dialysis for about 5.5 h. At the end of the dialysis, the current was stopped, water in the outer cell was removed, and the purified sample was transferred to a Claissen flask. The center cell was then washed with water, which was combined with the sample, and the resulting solution was evaporated at 40°C under 15-mm Hg pressure. The residue was diluted with water in a 25-ml volumetric flask, and 1 ml of the solution was used for the determination of carbohydrates.

Figure 4 shows the behavior of chloride ion and calcium + magnesium ions, all of which can be completely removed by dialysis for 5.5 h. Table II summarizes the recovery of carbohydrates; for these results, 100-ml samples of artificial sea water containing a definite amount of xylose and glucose were used.

TABLE II

RECOVERY OF CARBOHYDRATES AFTER ELECTRODIALYSIS

Sample	*Electrodialysis time (h)*	*Added (mg)*	*Found (mg)*	*Recovery (%)*
Xylose	5.5	1.00	0.99	99.0
Xylose	5.5	1.00	0.99_3	99.3
Xylose	5.5	0.10	0.10	100.0
Glucose	5.5	1.00	0.97_4	97.4
Glucose	5.5	1.00	1.00	100.0
Glucose	5.5	0.10	0.09_8	98.0

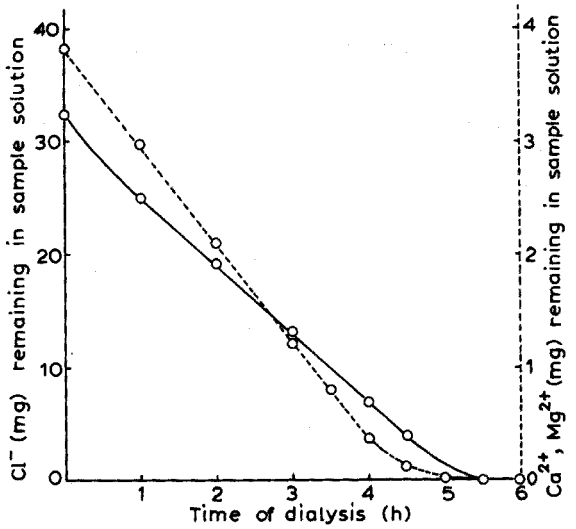

Fig. 4. Electrodialysis behavior of chloride, magnesium and calcium ions. 90 V/250 mA. Chloride (—) was determined by titration with silver(I) solution, and the metal ions (----) with EDTA.

The loss of carbohydrates was less than 3%; it was observed that the loss occurred mainly during evaporation.

Determination of carbohydrates in sea water

Sea-water samples were treated by the following procedure. Immediately after the sampling, 1–2 ml of saturated mercury(II) chloride solution was added for each liter of sea water, to prevent the consumption of carbohydrates by micro-organisms. The water was then filtered through a membrane filter (3-μm pore size), and 100 ml of the filtered water was employed for electrodialysis, evaporation and the fluorimetric determination of pentose and hexose, as described above.

The results obtained with several sea-water samples are presented in Table III. Samples collected in the bay of Kojima, Osaka prefecture, contained 240 μg of pentose (calculated as furfural) and 260 μg of hexose (as glucose) per liter. The values agree well with those reported for coastal sea water by Vaccaro *et al.*[12] The samples collected just offshore of Misaki Town, Osaka prefecture, contained a much larger amount of hexose (800–1600 $\mu g\ l^{-1}$), and the suspended matter also included a comparatively large amount of hexose (222 $\mu g\ l^{-1}$). These phenomena may result from the fact that the sea water in Osaka bay contains much organic matter owing to contamination by sewage. The pentose and hexose contents of lake water, sampled near Ukimido in Lake Biwa, are also presented in Table III.

The author wishes to express his sincere thanks to Professor Yasuharu Nishikawa, assistant Professor Keizo Hiraki, Faculty of Science and Technology, Kinki University, and Professor Masayuki Tabushi, Tohoku Women's college, for their kind advice.

TABLE III

CARBOHYDRATES IN SEA WATER

(All sea-water samples were taken in the stated positions in Osaka Prefecture.)

No.	*Sample*	*$HgCl_2$ added (ml l^{-1} of sea water)*	*Pentose in sea water as furfural ($\mu g\ l^{-1}$)*[a]	*Hexose in sea water as glucose ($\mu g\ l^{-1}$)*[a]
1	Offshore, Misaki-cho, (June 12, 1972)	0.6	225.0	758.0
		1.0	231.0	780.0
		1.6	227.5	757.5
		2	240.0	812.0
			Average: 230.9	776.9
2	Offshore, Kojima, (May 29, 1972)	1	205.0	275.0
		1.6	225.0	276.0
			Average: 215.0	275.5
3	Offshore, Kojima, (June 20, 1972)	1	245.0	250.0
		1	245.2	278.0
			Average: 245.1	264.0
4	Offshore, Misaki-cho, (July 21, 1972)	2	287.5	843.8
5	Seashore, Misaki-cho, (July 21, 1972)	2	225.0[b]	1672.8[b]
			12.5[c]	222.0[c]
6	Lake of Biwa, Shiga pref., (June 10, 1972)	2	225.0	406.3

[a] Average errors in each sample were within $\pm 6\%$.

[b] Sample water was filtered through a membrane filter (pore size 3 μm) and the filter was leached with 10% ethanolic solution; the ethanol was evaporated, and the carbohydrates were determined. The values given correspond to soluble carbohydrates in the filtrate.

[c] These values correspond to the carbohydrates in the suspended matter removed on the above membrane filter.

SUMMARY

Fluorimetric determinations of pentose with anthrone, and of hexose with 5-hydroxy-1-tetralone, are applied to the analysis of sea water. Adsorption on activated carbon and ion-exchange membrane electrodialysis were studied for preliminary separations. Activated carbon was suitable for the separation and concentration of hexose, but not pentose. Electrodialysis allowed complete desalination without loss of carbohydrates; pentose and hexose in sea water could be determined after evaporation under reduced pressure. Several sea-water samples were analysed, and the pentose content was estimated to be 225–288 $\mu g\ l^{-1}$ (as furfural), but the hexose content varied from 250 to 1670 $\mu g\ l^{-1}$ (as glucose) owing to contamination by sewage.

REFERENCES

1 R. Dreywood, *Ind. Eng. Chem., Anal. Ed.*, 18 (1946) 499.
2 R. Sawamura and T. Koyama, *Chem. Pharm. Bull. (Tokyo)*, 11 (1963) 274.
3 M. Dubois, K. A. Gilles, J. K. Hamilton, P. A. Rebers and F. Smith, *Anal. Chem.*, 23 (1956) 350; *Nature*, 168 (1951) 167.
4 H. Hirayama, K. Hiraki and Y. Nishikawa, *Japan Analyst*, 20 (1971) 1345.
5 T. Momose and Y. Ohkura, *Chem. Pharm. Bull. (Tokyo)*, 7 (1959) 31.
6 H. Hirayama, K. Hiraki and M. Saitoh, *J. F. S. T. Kinki Univ.*, 8 (1973) 303.
7 J. P. Riley and G. Skirrow, *Chemical Oceanography 1*, Academic Press, London and New York, 1965, p. 648 ff.
8 Y. Ohkura, Y. Watanabe and T. Momose, Nihon Yakugakukai, Symposium, Absorption analysis and Fluorescence analysis, Lecture purport, (1970) 67.
9 F. M. Middleton, *Ind. Eng. Chem.*, 52 (1960) 73A.
10 J. Kaneko, Kagakutokogyo, 16 (1963) 124.
11 B. O. Josefsson, *Anal. Chim. Acta*, 52 (1970) 65.
12 R. F. Vaccaro, S. E. Hicks and H. W. Jannasch, *Limnol. Oceanogr.*, 13 (1968) 356.

Analytica Chimica Acta, 70 (1974) 149–156

CAUSES D'ERREURS ET PRÉCAUTIONS À PRENDRE LORS DU TITRAGE DES THIOLS ET DU SULFURE D'HYDROGÈNE PAR L'ARGENT ET POTENTIOMÉTRIE AU MOYEN D'UNE ÉLECTRODE À MONOCRISTAL DE SULFURE D'ARGENT

FRANCIS PETER et ROBERT ROSSET

Laboratoire de Chimie Analytique, Ecole Supérieure de Physique et de Chimie de Paris, 10, rue Vauquelin 75231-Paris (France)

(Reçu le 26 Octobre 1973)

Dans un précédent mémoire[1] nous avons montré que le dosage des sulfures et des thiols (mercaptans) par précipitation par les ions argent pouvait être commodément suivi par potentiométrie à courant nul au moyen d'une électrode à monocristal de sulfure d'argent (électrode dite "spécifique" des ions sulfure). Toutefois, en effectuant de nombreux dosages, nous avons constaté que la méthode présentait plusieurs causes d'erreurs. Déjà dans le précédent mémoire[1] nous avions signalé que dans le cas du sulfure d'hydrogène et de l'éthanethiol le sens du titrage (dosage du thiol par l'argent ou de l'argent par le thiol) avait une influence sur le résultat de l'analyse. Ce sont ces différentes causes d'erreur, liées à la réaction de titrage utilisée et non au fonctionnement de l'électrode indicatrice, que nous discuterons dans les lignes qui suivent. Il s'agit, successivement, de la volatilité des produits au cours du dosage et de l'influence du pH sur cette volatilité, des réactions chimiques secondaires et des réactions d'adsorption.

PARTIE EXPÉRIMENTALE

On se reportera[1] pour tout ce qui concerne les produits chimiques, la préparation des solutions, les électrodes, appareils de mesure et la cellule. Précisons seulement que la microburette à piston étanche était de marque Gilmont.

Le sulfure d'argent stoechiométrique a été préparé en versant la quantité théorique nécessaire de nitrate d'argent pour précipiter du sulfure de sodium en solution aqueuse. On vérifie l'équivalence des quantités d'argent et de sulfure en mesurant le potentiel d'une électrode à monocristal de sulfure d'argent ($-0{,}1$ V *vs.* ECS environ). Le sulfure est alors filtré, lavé à l'eau et séché à l'étuve à 100° pendant 24 h.

Lors de l'étude de l'adsorption des ions Ag^+ par passage d'une solution d'argent(I) sur une colonne de sulfure d'argent, on a utilisé une colonne en verre cylindrique de 1 cm de diamètre intérieur et 10 cm de longueur. Le débit était de 45 ml h^{-1}. Le volume interstitiel (V_i) de la colonne a été mesuré par passage sur le sulfure d'argent d'une solution 0,01 *M* de nitrate de sodium. La solution effluente est fractionnée en échantillons de 1 ml dans lesquels on dose Na^+ par spectrophotométrie de flamme. On a trouvé $V_i = 8$ ml.

RÉSULTATS

Volatilité des produits

Le sulfure d'hydrogène et les deux premiers termes des thiols (méthane et éthanethiol) ont une volatilité telle que leur dosage peut être entaché d'erreurs importantes en l'absence de précautions particulières.

Le phénomène peut être facilement mis en évidence en effectuant le titrage dans le sens classique (solution de sulfure d'hydrogène ou de thiol dans la cellule en milieu éthanol–benzène à pH 10,8 et solution de nitrate d'argent dans l'isopropanol dans la burette) et en étudiant l'influence de la durée du titrage sur le résultat du dosage. Le tableau I rassemble ces résultats dans le cas de solutions de sulfure d'hydrogène ou d'éthanethiol. On constate que dès que la durée du titrage dépasse environ 3 min on obtient un titre par défaut; l'écart peut être considérable en dépit de la valeur assez élevée du pH. Il est lié à la volatilité des produits car on ne l'observe pas lorsque l'on effectue le titrage en sens inverse du sens classique, la solution d'H_2S ou de thiol étant, cette fois, contenue dans une microburette à piston étanche. (La cellule contient alors du nitrate d'argent en milieu éthanol–benzène à pH 10,8 et la solution titrante d'H_2S ou d'éthanethiol est préparée dans le l'isooctane.) On ne l'observe pas non plus dans le cas des thiols plus lourds que l'éthanethiol.

TABLEAU I

L'INFLUENCE DE LA DURÉE DU TITRAGE

Substance titrée	*Durée du titrage en min*[a]	*Écart relatif par rapport au point équivalent (%)*
H_2S	2	0
	3	0
	4	− 1
	5	− 3,5
	7	−18
	9	−14
	10	−18
	11	−25
C_2H_5SH	3	0
	9	− 4

[a] Mesurée au point équivalent.

Bien entendu, le pH a une influence considérable sur la volatilité des produits. Nous avons fait varier le pH entre 12 et 6,7 dans le cas de solutions aqueuses de sulfure de sodium et de titrages effectués dans le sens classique. Le tableau II donne les écarts obtenus pour une durée du titrage de 5 min. A pH 6,7 voisin du premier pK_A du sulfure d'hydrogène (H_2S/HS^-: 7,0) la volatilité de H_2S est très importante d'où les pertes qui atteignent près de 20%. A pH 9,3 où il y a pourtant moins de 1% de H_2S les pertes ne sont pas négligeables. Enfin à pH 12 on obtient un titre par excès, des ions argent étant consommés par précipitation à l'état d'hydroxyde.

TABLEAU II

L'INFLUENCE DU pH SUR LE TITRAGE DU SULFURE DE SODIUM

Solution-tampon utilisée	*pH*	*Écart relatif par rapport au point équivalent (%)*
Soude 10^{-2} *M*	12	+ 2
Borate	9,3	− 3,5
Phosphate	6,7	− 19

Il résulte de ce qui précède que dans le cas du sulfure d'hydrogène et des deux premiers thiols, si l'on veut éviter toute erreur systématique par volatilité des produits, il faut opérer soit avec une cellule strictement étanche ce qui est très délicat à réaliser soit de préférence par titrage en sens inverse du sens classique, la solution de nitrate d'argent dans le solvant mercaptan étant dans la cellule et la solution d'H_2S ou de thiol à titrer étant prélevée dans une microburette à piston étanche.

Dans le précédent mémoire[1] nous avions signalé que lors du titrage de l'argent par H_2S ou par l'éthanethiol on observait un écart au point équivalent par rapport à celui obtenu dans le sens de titrage classique. Cet écart provenait de la volatilité des produits lors de l'étalonnage. En effet celui-ci étant effectué par addition d'argent à la solution d'H_2S ou de thiol il y avait une perte du composé sulfuré d'où un titre par défaut. En opérant en sens inverse et en prélevant cette fois la solution d'H_2S ou de thiol dans une microburette étanche, on obtenait un titre apparemment par excès (point équivalent atteint pour un volume moindre que celui escompté).

Réactions chimiques secondaires

Si l'on effectue les titrages en sens inverse du sens classique comme cela vient d'être recommandé, il y a alors des ions Ag^+ libres dans la cellule de titrage jusqu'au point équivalent. Or, une solution aqueuse d'ions sulfure contient des ions OH^-, S^{2-} étant une base assez forte (HS^-/S^{2-}, $pK_A = 13{,}5$). Il nous faut donc examiner le rôle d'une précipitation éventuelle d'hydroxyde d'argent au cours du titrage des sulfures en milieu aqueux. L'hydroxyde d'argent AgOH est beaucoup moins insoluble que le sulfure Ag_2S (AgOH↓, ps = 8; Ag_2S↓, ps = 49,2) de sorte qu'en principe si AgOH précipite pendant le titrage il doit être immédiatement transformé en sulfure selon:

$$2\ AgOH\downarrow + S^{2-} \rightarrow Ag_2S\downarrow + 2\ OH^-$$

la constante d'équilibre de cette réaction étant très grande:

$$|OH^-|^2/|S^{2-}| = 10^{-16}/10^{-49,2} = 10^{33,2}$$

Mais on sait que l'hydroxyde d'argent se déshydrate rapidement en oxyde d'argent selon la réaction:

$$2\ AgOH\downarrow \rightarrow Ag_2O\downarrow + H_2O$$

et il est possible que la réaction des ions sulfure sur l'oxyde d'argent soit beaucoup plus lente qu'avec l'hydroxyde.

TABLEAU III

L'INFLUENCE DU pH SUR LE TITRAGE D'IONS ARGENT(I)

Solution - tampon utilisée	*pH*	*Écart relatif par rapport au point équivalent (%)*[a]
NaOH 10^{-2} *M*	12,0	−8
Ammoniaque 0,1 *M* (+$NaNO_3$ 1 *M*)	9,1	−4,5
Phosphate 0,1 *M*	6,8	−2,5
Hexaméthylènetétramine	5,2	−1,5
Acide trichloracétique, acide nitrique ou acide perchlorique (+$NaNO_3$ 1 *M*)	1,1 à 2,5	0

[a] Écart = 100 × (volume de solution de sulfure au point équivalent expérimental−volume au point équivalent théorique)/volume au point équivalent expérimental.

Pour en décider nous avons effectué divers titrages d'ions Ag^+ par des solutions de sulfure, en solution aqueuse à des pH compris entre 1 et 12. Les résultats obtenus sont rassemblés dans le tableau III.

On constate que l'écart par rapport au point équivalent diminue régulièrement lorsque l'acidité du milieu augmente pour s'annuler quand le milieu est suffisamment acide pour empêcher toute précipitation d'hydroxyde d'argent (en milieu Ag^+ 10^{-2} *M*, AgOH ne précipite qu'au-dessus de pH 8; toutefois si la solution d'argent n'est pas suffisamment acide, le pH de la solution peut devenir localement supérieur à 8 à l'endroit où tombent les gouttes de la solution de sulfure d'où précipitation d'AgOH et deshydratation rapide en Ag_2O).

La précipitation d'hydroxyde d'argent en solution aqueuse et dans le sens titrage de l'argent par les ions sulfure a donc une grande importance. Dans ce cas il est essentiel, pour avoir des résultats exacts, d'opérer en milieu suffisamment acide (pH compris entre 1 et 2). Si l'on opère en milieu neutre ou alcalin on obtient les titres des solutions de sulfure par excès. C'est ce que nous avons constaté lorsque l'on opère en milieu neutre non tamponné par exemple $NaNO_3$ ou $NaClO_4$ 1 *M*; les écarts varient entre 5 et 8% selon les essais pour des concentrations initiales en Ag^+ comprises entre $5 \cdot 10^{-2}$ et $5 \cdot 10^{-4}$ *M*. Des écarts du même ordre avaient été observés lors du titrage en sens inverse du sens classique par Hseu et Rechnitz[2].

Remarques. (1) Lors des titrages effectués en milieu organique à pH 10,8 (en prenant comme origine pH 1 pour une solution d'acide perchlorique 0,1 *M* dans le solvant considéré) le phénomène précédent n'a pas à être pris en considération car AgOH ne précipite pas en milieu organique à ce pH.

(2) Les solutions de sulfure vieilles de quelques jours contiennent des quantités appréciables de sulfite et de thiosulfate. Les méthodes classiques de dosage[3] donnent les résultats suivants pour une solution de sulfure initialement 0,1015 *M* au bout de huit jours: sulfure, 0,0968 *M*; thiosulfate, 0,0036 *M*; sulfite, 10^{-4} *M*. Les polysulfures n'apparaissent qu'au bout de plusieurs semaines. Le sulfite d'argent est beaucoup moins insoluble que le sulfure (ps = 13,8) mais il est titré en même

temps par la réaction considérée; le thiosulfate d'argent, lui, est soluble. Dans le cas d'une solution vieille de sulfure on titrera donc en fait la somme sulfure + sulfite et les thiosulfate échapperont au dosage.

Les réactions d'adsorption

L'adsorption des ions Ag^+ sur le sulfure d'argent est connue depuis longtemps en photographie[4]. On sait[5,6] que cette adsorption ne devient appréciable que pour $Ag^+ > 10^{-5}$ *M*: le sulfure d'argent est alors chargé positivement en présence de nitrate d'argent.

Nous nous sommes proposés de déterminer l'importance sur la précision du dosage d'une adsorption éventuelle des ions Ag^+ sur le précipité de sulfure d'argent lorsque l'on effectue le titrage dans le sens inverse du sens classique où, précisément, le précipité de sulfure d'argent est, jusqu'au point équivalent, en présence d'ions Ag^+.

Pour évaluer l'importance de l'adsorption nous avons mis en oeuvre deux techniques: le passage d'une solution d'argent sur une colonne de sulfure d'argent stoechiométrique, et la mesure directe de l'adsorption des ions argent par potentiométrie au moyen d'une électrode à monocristal de sulfure d'argent.

Passage d'une solution d'argent(I) sur une colonne de sulfure d'argent. Sur une colonne de 1 cm de diamètre intérieur et de 10 cm de hauteur, remplie de 19,68 g d'Ag_2S stoechiométrique (voir Partie Expérimentale) on fait passer 200 ml d'une solution 10^{-2} *M* de nitrate d'argent, puis on lave la colonne à l'eau désionisée. La variation de la concentration des ions Ag^+ dans l'effluent est représentée Fig. 1. Les ions Ag^+ apparaissent dans l'effluent avec un retard par rapport au volume interstitiel de la colonne (16 à 17 ml au milieu du front au lieu de 8 ml). Par ailleurs en dosant Ag^+ dans l'effluent et les eaux de lavage on constate que la colonne a retenu 12 mg d'argent soit $6 \cdot 10^{-4}$ g d'argent par g de sulfure d'argent.

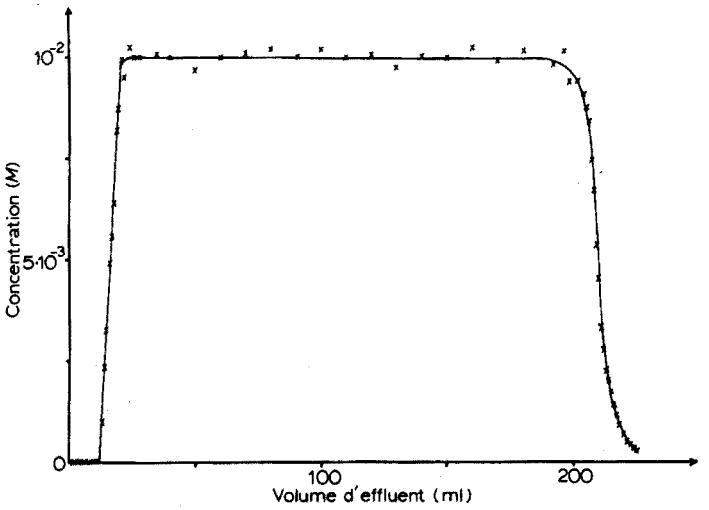

Fig. 1. Passage d'une solution de nitrate d'argent 10^{-2} *M* sur une colonne de sulfure d'argent Ag_2S (explications dans le texte).

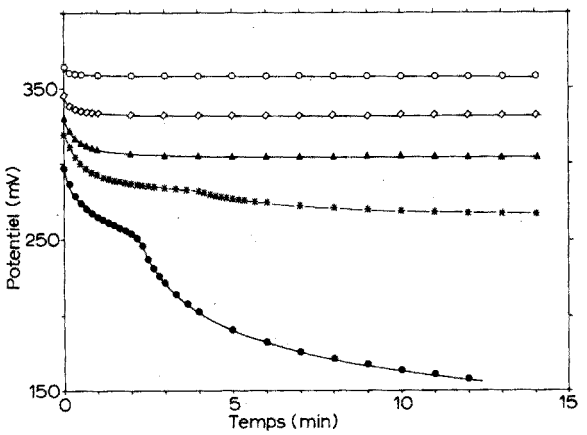

Fig. 2. Variation du potentiel d'une électrode indicatrice des ions Ag^+ en fonction du temps mettant en évidence l'adsorption des ions Ag^+ par Ag_2S. Concentration initiale de la solution en $Ag^+(M)$: (○) 10^{-3}; (◇) $5 \cdot 10^{-4}$; (△) $3 \cdot 10^{-4}$; (*) $2 \cdot 10^{-4}$; (●) 10^{-4}.

Mesure de l'adsorption par potentiométrie directe sur une électrode à monocristal de sulfure d'argent. Dans 50 ml de solutions de nitrate d'argent de concentrations comprises entre 10^{-3} et 10^{-4} M on disperse 1 g de sulfure d'argent et suit la variation du potentiel d'une électrode à monocristal de sulfure d'argent en fonction du temps. Le faisceau de courbes obtenues est représenté Fig. 2. Connaissant la courbe de réponse de l'électrode $E = f(pAg)$, on peut calculer les quantités d'ions Ag^+ fixé par le sulfure d'argent. Le tableau IV rassemble les résultats obtenus.

TABLEAU IV

L'ADSORPTION DES IONS ARGENT SUR LE SULFURE D'ARGENT

Concentration initiale de la solution en Ag^+ (M)	*Masse d'argent adsorbée (g) par g de Ag_2S*
10^{-4}	$5{,}4 \cdot 10^{-4}$
$2 \cdot 10^{-4}$	$9{,}2 \cdot 10^{-4}$
$3 \cdot 10^{-4}$	10^{-3}
$5 \cdot 10^{-4}$	10^{-3}
10^{-3}	10^{-3}

Ils sont en accord avec les précédents à savoir sensiblement 10^{-3} g d'argent par g d'Ag_2S. Or pour avoir les écarts de l'ordre de 5 à 8% observés lors du titrage de Ag^+ par une solution de sulfure il faudrait que les quantités d'argent adsorbé soit d'environ $5 \cdot 10^{-2}$ g par g d'Ag_2S soit 50 fois plus grande que ce qu'elles sont en réalité.

L'importance des phénomènes d'adsorption des ions Ag^+ sur le sulfure d'argent est donc négligeable. C'est bien la précipitation de l'hydroxyde d'argent

qui est responsable des écarts observés dans le sens inverse du sens classique de titrage en milieu aqueux neutre ou alcalin.

Influence de la gélatine

Nous avons vu qu'en milieu neutre la précipitation d'hydroxyde d'argent et sa déshydratation en Ag_2O provoquait des erreurs par défaut lors du titrage de Ag^+ par une solution de sulfure. Or (Fig. 3), l'addition de gélatine à des teneurs comprises entre 0,03 et 2,5% permet de supprimer tout écart au point équivalent théorique. On sait depuis longtemps que la gélatine empêche la coagulation du sulfure d'argent[7] et, en effet, en solution aqueuse la présence de gélatine en concentration supérieure à 0,03% empêche la formation d'agglomérats de sulfure d'argent. Celui-ci reste colloïdal. On peut penser que, de même, la présence de gélatine soit empêche la déshydratation de AgOH en Ag_2O soit, en maintenant Ag_2S à l'état colloïdal assure une vitesse de réaction suffisante entre Ag_2S et AgOH (ou Ag_2O) pour empêcher tout écart au point équivalent.

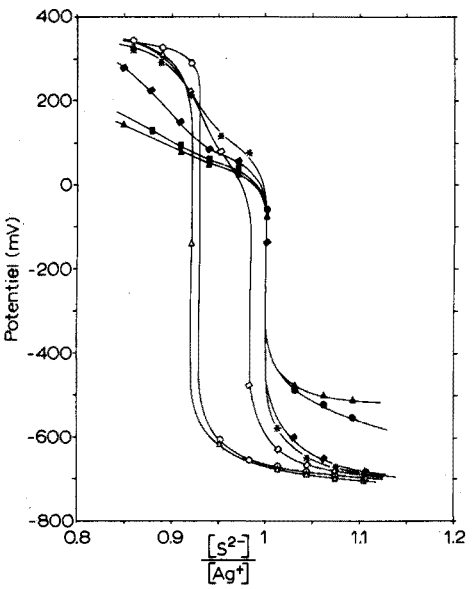

Fig. 3. Influence de la gélatine sur le titrage des ions Ag^+ par une solution de sulfure en solution aqueuse en milieu neutre ($NaNO_3$ ou $NaClO_4$ *M*). L'écart au point équivalent s'annule pour une concentration en gélatine comprise entre 0,03 et 2,5%. (○) 0%; (△) 0,01%; (◇) 0,02%; (*) 0,03%; (◆) 0,1%; (●) 0,5%; (▲) 2,5%.

L'addition d'une faible quantité de gélatine est donc un moyen commode de rendre exact le titrage de l'argent par une solution de sulfure en solution aqueuse.

CONCLUSIONS

En raison de la volatilité du sulfure d'hydrogène et des deux premiers termes

des thiols (méthane et éthanethiol) il est recommandé pour éviter toute perte des produits d'opérer en sens inverse du sens classique, la solution organique de nitrate d'argent étant dans la cellule et la solution titrante d'H_2S ou de thiols étant contenue dans une microburette à piston étanche.

Si ce titrage en sens inverse du sens classique est effectué en solution aqueuse il faut éviter toute précipitation d'hydroxyde d'argent ce qui peut être obtenu de deux manières: (1) soit en opérant en milieu acide à un pH compris entre 1 et 2, (2) soit en ajoutant préalablement à la solution d'argent à titrer de la gélatine à une concentration de 0,1% environ (en fait elle peut être comprise entre 0,03 et 2,5% la déformation des courbes devenant plus importante lorsque la teneur en gélatine augmente).

En revanche il n'y a pas de précipitation de AgOH en milieu éthanol–benzène à pH 10,8.

RÉSUMÉ

Diverses causes d'erreurs peuvent affecter la précision du dosage du sulfure d'hydrogène et des thiols par précipitation par l'argent(I). Le sulfure d'hydrogène, le méthane et l'éthanethiol ont une volatilité telle qu'il est recommandé d'opérer en sens inverse du sens classique, la solution d'argent étant dans la cellule de titrage et la solution titrante des composés soufrés à doser étant contenue dans une microburette à piston étanche. Si ce titrage est effectué en solution aqueuse, il faut éviter toute précipitation d'hydroxyde d'argent ce qui peut être obtenu soit en opérant en milieu suffisamment acide (pH compris entre 1 et 2), soit en ajoutant préalablement à la solution à titrer de la gélatine à une concentration de l'ordre de 1%.

SUMMARY

Various causes of errors can affect the accuracy of the titration of hydrogen sulfide and thiols by precipitation with silver(I). Hydrogen sulfide, methanethiol and ethanethiol are so volatile that titrations should be done in the opposite direction to the classical method; the sulfur compounds to be determined should be contained in a micrometer buret with a tight teflon plunger and used as the titrant. If the titration is carried out in aqueous solution, silver hydroxide precipitation must be avoided; this can be done by operating in a sufficiently acidic medium (pH range 1–2), or by adding a gelatin solution to the solution to be titrated, as a concentration of about 1%.

REFERENCES

1 F. Peter et R. Rosset, *Anal. Chim. Acta*, 64 (1973) 397.
2 T. M. Hseu et G. A. Rechnitz, *Anal. Chem.*, 40 (1968) 1054.
3 G. Charlot, *Bull. Soc. Chim.*, 6 (1939) 1447; *Analyse Quantitative Minérale*, Masson, Paris, 1966, p. 918.
4 T. H. James, *J. Amer. Chem. Soc.*, 61 (1939) 648.
5 J. Barr et H. O. Dickinson, *J. Phot. Sci.*, 9 (1961) 222.
6 M. Tamura, H. Hada et S. Kawai, *Nippon Shashin Gakkai Kaishi*, 26 (1963) 167; *Chem. Abstr.*, 61 (1964) 6565 h.
7 A. A. Titov, *Kino, Foto. Khim. Prom*, 9 (1938) 44; *Kim. Referat. Zhur.*, 2 (1939) 129; *Chem. Abstr.*, 34 (1940) 9291.

Analytica Chimica Acta, 70 (1974) 157–167

THE DETERMINATION OF AMMONIUM ION IN AIRBORNE PARTICULATES WITH SELECTIVE ELECTRODES

M. L. EAGAN and L. DUBOIS

Chemistry Division, Technology Development Branch, Air Pollution Control Directorate, Environmental Protection Services, Ottawa, Ontario (Canada)

(Received 17th July 1973)

A simple and accurate method for the determination of ammonium in airborne particulates is of interest, because of the possibility that the main oxidation product of sulfur dioxide may be ammonium sulfate rather than sulfuric acid[1]. Several mechanisms have been proposed for this oxidation[2]. Since sulfur dioxide is one of the principal air pollutants, it is of interest to determine its reactions in the atmosphere. The significance of ammonium sulfate in the atmosphere is related to health, corrosion[3] and visibility[4].

The principal source of ammonia gas appears to be the ammonia released from animal urine, by the action of the ubiquitous enzyme urease. Less significant sources are rotting organic matter, combustion of fuel, losses from fertilizer, sewage and losses from chemical processing.

Nesslerization has been widely employed for the determination of trace concentrations of atmospheric gaseous ammonia[5]. Okita and Kanamori[6] suggested that results obtained from this method are too high owing to interference by other atmospheric impurities. Presumably these interferences could be avoided by distilling the sample into a boric acid solution. They also suggested that the sampling of total ammonia content in air, *i.e.*, both gaseous and particulate components, by scrubbing was inefficient and that the use of sulfuric acid-impregnated glass-fibre filters was more effective.

The method discussed below is sufficiently sensitive and is much less complicated than most of the chemical methods in use.

Basis of the method

The Orion ammonia electrode responds in a Nernstian manner to changes in hydroxide ion concentration. When the electrode is in equilibrium, the ammonia diffusing through the membrane can be directly related to $[OH^-]$, and the Nernst equation can be written:

$$E = E_0 - 2.303(RT/F)[NH_3]$$

The partial pressure of ammonia and the concentration are related by $P_{NH_3} = k[NH_3]$, where the proportionality constant k varies with dissolved species. Therefore the ionic strength of the samples and standards must be constant.

The Nernst equation applies to the manner in which the organic sensor

material in the Beckman electrode responds to ammonium activity[7]:

$$E = E_0 - 2.303(RT/F)\gamma_{NH_4^+}[NH_4^+]$$

In order to keep $\gamma_{NH_4^+}$, the activity, constant, the ionic strength of the sample must be kept constant.

EXPERIMENTAL

Apparatus

One of the electrodes was an ammonia-selective Orion electrode, Model 95-10. The electrode was assembled and pre-soaked in 0.1 *M* ammonium chloride solution for 30 min before use. Between analyses the electrode was immersed in this solution. The other electrode, an ammonium-selective electrode, was a Beckman SelectIon 39626. The electrode was pre-soaked in 10^{-3} *M* ammonium chloride solution before use. The electrode was stored dry in a storage chamber.

The Orion electrode had an internal reference electrode while the Beckman required a calomel reference electrode (Fisher Calomel Reference, Porous Plug type), which was immersed in a salt bridge solution to prevent interference by KCl leakage.

An Orion 801 digital pH meter was used with the electrodes.

Reagents

Water of a very low ammonia content was obtained from a Super-Q System (Millipore Corporation). The ammonia content of this deionized water was found to be negligible when the Tetlow and Wilson[8] method was used.

Sodium hydroxide solutions (1 *M*) were freshly prepared as they appeared to absorb ammonia from the air.

Ammonium chloride standard solution (0.1 *M*; Orion) was diluted to the following ammonium concentrations: 10, 5, 1, 0.5 and 0.1 p.p.m. These standard dilutions were prepared daily.

Samples were stored in polyethylene bottles with leak-proof screw caps.

Sample preparation

The actual air sampling and aqueous extraction of the glass-fibre filters have already been described[9]. The method briefly was as follows: water-soluble impurities were leached out of the filters with hot distilled water before use. Sampling was done with a conventional high-volume sampler which drew about 2000 m^3 air in a 24-h period. An area aliquot, usually a 47-mm diameter circle was cut from the exposed area of the filter and extracted with deionized water. The disc was immersed in about 5 ml of water and heated just to boiling. This operation was repeated five times and the combined extracts, after filtration through 0.2 μm Millipore membrane filters, were diluted to 25 ml with deionized water.

Calibration curve

The series of dilutions, 0.1, 0.5, 1.0, 5 and 10 p.p.m. of ammonium ion, were made up in volumetric flasks. While the solution was stirred gently, the Beckman electrode was immersed in 10 ml of the 0.1-p.p.m. solution. When the

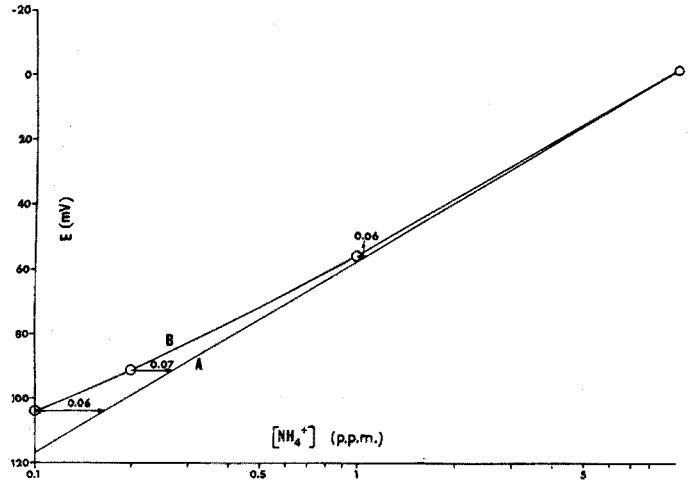

Fig. 1. Comparison of calibration curves for standards in water (A) and filter blank (B) using Orion electrode.

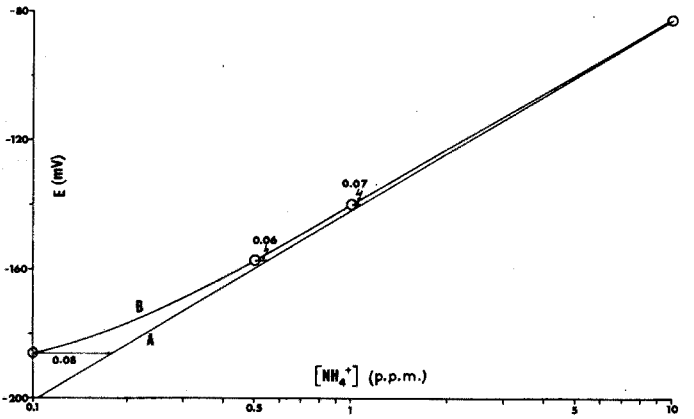

Fig. 2. Comparison of calibration curves for standards in water (A) and filter blank (B) using Beckman electrode.

electrode reached equilibrium, the potential in mV was read. The electrode was removed, washed with deionized water and dried with a soft tissue. Sodium hydroxide (0.2 ml of 1 *M*) was added to the 10-ml standard sample and the Orion electrode was immersed in it. The reading (*E* mV) was taken when the electrode reached equilibrium. The above procedure was repeated for the more concentrated standard solutions. Calibration curves of *E vs.* concentration were constructed for both electrodes.

Figures 1A and 2A are typical calibration curves for the Orion and Beckman electrodes, respectively.

Measurement

The samples were handled in a similar manner to the standard solutions.

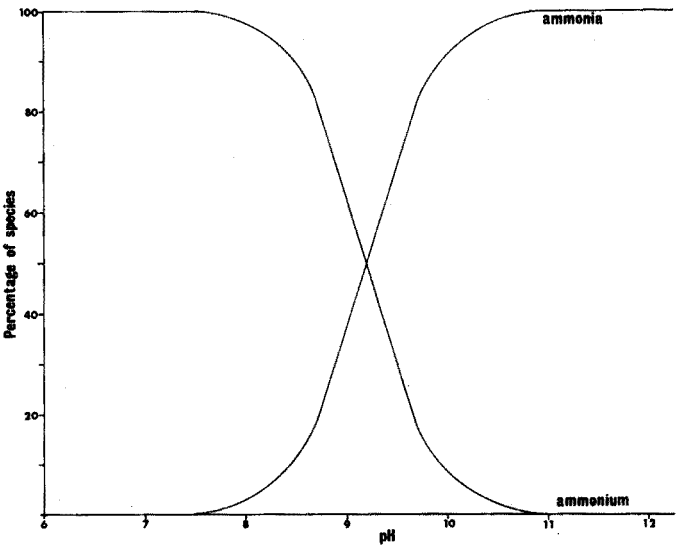

Fig. 3. Fraction of ammonia and ammonium as a function of pH.

The concentration of the samples was calculated from the calibration curve by using the E(mV) obtained at equilibrium. The pH of the samples was determined before each reading to ensure that it was properly adjusted.

Ammonia gas is readily soluble in water, becoming partially ionized to the ammonium ion. The extent of ionization can be varied by adjustment of pH. The pK value for ammonium ion is 9.27, therefore at pH 9.27 there will be equal amounts of ammonium ion and ammonia. Figure 3 shows the fraction of ammonia and ammonium ion as a function of pH. Since the Beckman electrode is sensitive to the ammonium ion, the sample must be at a pH less than 7.5. The water extracts were found to satisfy this condition in their natural state. The Orion electrode is sensitive only to ammonia gas, therefore the pH must be greater than 11.0 (Fig. 3). A pH between 11.0 and 12.0 was achieved by adding 0.2 ml of 1 M sodium hydroxide to a 10-ml water extract sample. The amount of sodium hydroxide was kept to a minimum since larger amounts created interferences in the lower concentration range, possibly by contamination in the reagent.

In order to minimize changes in the slope of the calibration curve, the room was kept at a constant temperature between 19 and 22°C during a series of analyses and a sheet of insulation was used between the sample and the magnetic stirrer.

RESULTS

Blank determination

With each series of samples analyzed, a filter blank concentration was determined. The filter blank solution was prepared by extracting an unexposed 47-mm disc as described in sample preparation. An average filter blank concentration of 0.06 was measured by calculation from calibration curves. This amount also represents minimum detectability.

Figures 1B and 2B show a comparison of calibration curves obtained by standards prepared in deionized water and filter blank solution for the Orion and Beckman electrodes, respectively. The deviation between the calibration curves agrees with the blank determination of 0.06. These results indicate there is an ammonium reading in the blank, but there is no effect of the background on the added ammonium.

It was known from previous analyses that Ca, Mg, Ba, K and Zn ions were present in appreciable concentrations in the blank filter. The interference caused by these ions for the Beckman electrode can be calculated by Nicolsky's equation:

$$E = E_0 - (RT/F) \ln[a_{NH_4^+} + K(a_{i^{z+}})^{1/z^+}]$$

where $a_{i^{z+}}$ is the ionic activity of the ith species, $z+$ the charge of the interfering ion, and K the selectivity coefficient for ammonium ion with respect to the interfering ion i^{z+}. The total interference of the ions was calculated to be 0.053 p.p.m. of ammonium ion using predetermined selectivity coefficients[7] of the ions and their approximate concentrations in the blank. This value is comparable to the measured blank and would suggest the blank reading from the Beckman electrode arises primarily from the effect of interfering ions.

Interferences

As previously discussed, the ionic strength must either be constant or very small if a calibration curve is to be used to determine concentration. The average ionic strength of a water extract was estimated to be $2 \cdot 10^{-2}$.

The standard addition procedure involves the addition of an aliquot of the species of interest to the unknown sample solution, without significantly changing the ionic strength of the system. The activity coefficient can be assumed to remain

TABLE I

COMPARISON OF STANDARD ADDITION DETERMINATIONS TO CALIBRATION CURVE DETERMINATIONS

Sample	*Concn. by calib. curve* ($\mu g\ ml^{-1}$)	*Concn. by standard addition* ($\mu g\ ml^{-1}$)	*% Difference*
Orion electrode			
1	1.6	1.6	0
2	1.5	1.5	0
3	5.5	5.7	3.5
Beckman electrode			
4	7.0	7.1	1.4
5	6.4	6.6	3.1
6	1.1	1.2	8.3
7	3.9	3.8	2.6
8	5.2	5.1	1.9
9	5.2	5.6	7.4
10	7.3	6.7	8.6

constant and the observed e.m.f. change can be related to the original unknown concentration rather than activity. Table I shows a comparison of ammonium ion determinations by the standard addition and calibration curve methods for ten varied samples. The values compare favorably, indicating that little error arises from the ionic strength of such sample solutions with concentrations of ammonium of this magnitude.

Figures 4 and 5 further illustrate that the ionic strengths of the samples and the calibration solutions are constant or insignificant. A series of known concentrations of ammonium chloride was absorbed on 47-mm discs of particulate samples. The resulting curve is compared to a normal calibration curve. Both the curves determined with the Orion electrode and the Beckman electrode show the

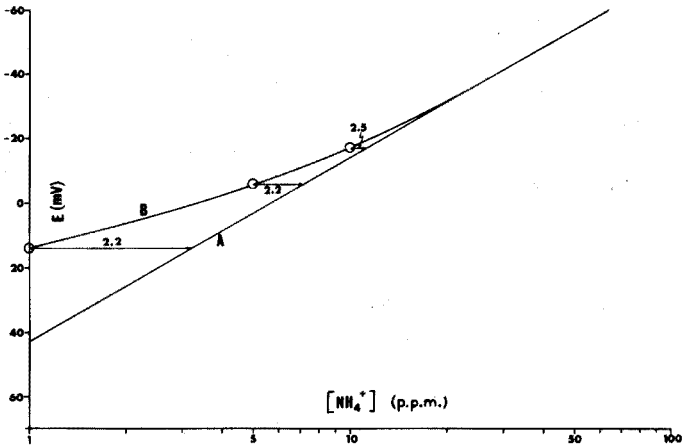

Fig. 4. Comparison of calibration curves (Orion electrode) for standards in water (A) and absorbed on particulate sample of 2.2 μg ml^{-1}, then extracted (B).

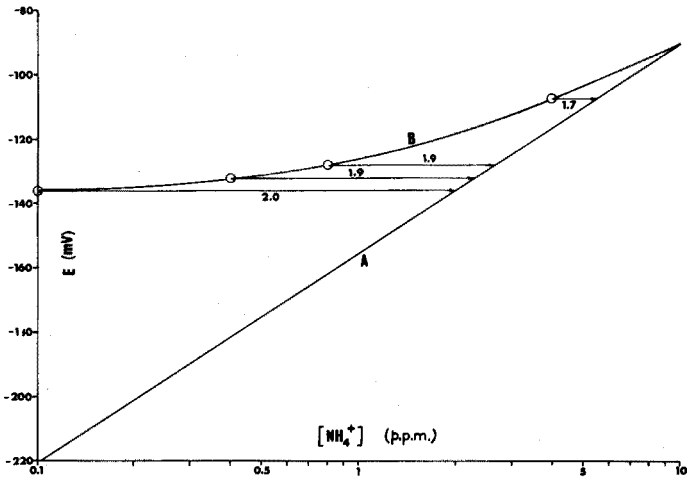

Fig. 5. Comparison of calibration curves (Beckman electrode) for standards in water (A) and absorbed on particulate sample of 1.9 μg ml^{-1}, then extracted (B).

appropriate divergence from linearity for samples containing 2.1 p.p.m. and 1.9 p.p.m. NH_4^+, respectively, which are the concentrations previously arrived at by direct calculation from a calibration curve. It can be concluded that the presence of particulate matter does not affect the determination.

Consistently higher results were observed when the Beckman electrode was used. Lack of selectivity is the most probable explanation. When average concentrations of the interfering ions in aqueous extracts for the year of 1972 were used in calculating from Nicolsky's equation, an interference of 0.20 p.p.m. of NH_4^+ was estimated. Results recalculated considering this factor were in much better agreement with results from the Orion electrode.

Precision

To evaluate reproducibility, the calibration procedure was repeated four times for each electrode, over a six month period during which the membrane in the Orion electrode and the sensor unit in the Beckman electrode were changed. The mean slope for the curves determined with the Beckman electrode was 58.24 ± 2.52 which approaches the ideal slope of 59 more accurately than the mean slope 56.30 ± 1.96 determined with the Orion electrode. This observation can be explained by the better linear response of the Beckman electrode in the low concentration range. The variability found proves that it is necessary to prepare a calibration curve for every series of analysis.

To estimate the repeatability of sample analysis, a number of duplicate determinations were carried out. In each case, a new area aliquot was taken from the filter sample and put through the extraction procedure. Table II includes the

TABLE II

STATISTICAL ANALYSIS

Comparison of methods	*N*	*Mean difference*	*s of diff.*	t_{calc}	*t.95*
Duplicate extracts measured with Beckman	24	0.28	0.44	0.12	2.20
Duplicate extracts measured with Orion	24	0.19	0.24	0.32	2.20
Analysis by absorp. method and Beckman	29	0.22	0.21	1.51	2.46
Analysis by absorp. method and Orion	31	0.14	0.20	2.41	2.46
Analysis by Orion and Beckman	76	0.31	0.41	0.74	1.96

	Linear regression analysis		
	Correlation coefficient	*Slope*	*Intercept*
Orion/Beckman	0.97	1.03	−0.09
Absorp. method/Beckman	0.99	0.90	−0.008
Absorp. method/Orion	0.98	0.93	0.12

statistical results from this operation. The mean concentration for the Orion series of analysis was 1.70 p.p.m. with a mean deviation of 0.19. The mean concentration for the Beckman electrode series was 1.58 with a mean deviation of 0.28. This deviation includes errors introduced by the sampling technique as well as electrode measurements. The significance of the differences in the means of the concentrations for the duplicate extracts series was tested by a two tailed "Student's" t test. Essentially no difference was found between the groups at a 95% confidence level. These results support the assumption that ammonium is uniformly distributed on the filter, and prove area aliquots as a valid means of sampling.

Accuracy

In order to test the accuracy of the aqueous extraction technique, a series of calibration curves, each with a different variable being tested, (Fig. 6) was prepared. Series of known concentrations of ammonium chloride were absorbed on unexposed filter discs and extracted by three different methods: with hot water as described under *Procedure* (curve A); with cold water (B); and with ultrasonic disintegration (C). An additional calibration curve (D) was constructed for the same ammonium concentrations without absorbing the solutions on filter discs but imitating the extraction with hot water. The comparison of these curves with a normal calibration curve showed that all the ammonium ion was not being recovered by all four methods. An average of 4% $[NH_4^+]$ was lost without filters, which could be due to evaporation and experimental error. With cold water there was a 15% loss indicating that ammonium ion was being incorporated into the filter. The 21% $[NH_4^+]$ not recovered with hot water extraction appears to be a combination of the above effects. For the ultrasonic disintegrator there was a loss of 26% which could be enhanced evaporation and non-recovery from the filter. An experiment was carried out to support the idea that ammonium ion reacts with the filter. A calibration

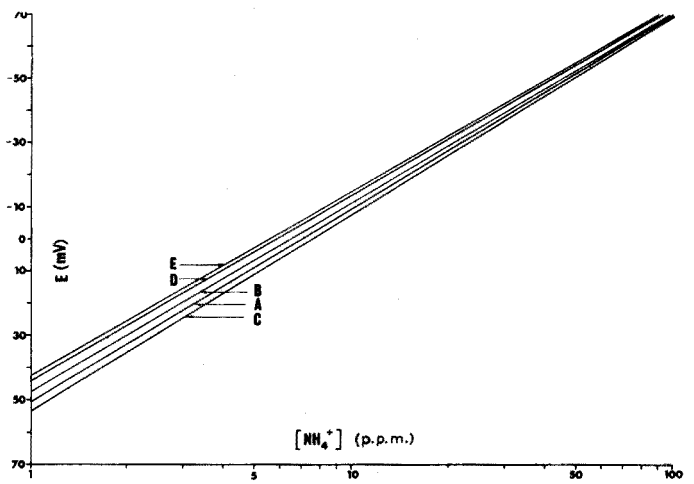

Fig. 6. A comparison of five calibration curves. Standards in water (E); standards heated in water then diluted (D); standards absorbed on blank filters then extracted by cold water (B); hot water (A); disintegrator (C).

curve was constructed with normal calibration solutions, then unexposed filters were immersed in the solutions and the readings were again taken. The resulting curve was identical to that determined with cold water extraction. Therefore it can be concluded that the largest loss arises from ammonium ion remaining in the filter and that cold water extraction is the most efficient method. The convenience of being able to use hot water extracts for other dissolved ions, such as sulfates, led us to choose hot water extraction for the method. The effect of reaction with the filter may be avoided in a particulate sample, as the ammonium ion would not be absorbed on the filter but would remain in or on the particles. The complete recovery of known concentrations added to a particulate sample in Figs. 4 and 5 indicates no loss to the filter.

TABLE III

A COMPARISON OF DIFFERENT AQUEOUS EXTRACTION TECHNIQUES

Sample	*Cold water extract* ($\mu g\ ml^{-1}$)	*Hot water extract* ($\mu g\ ml^{-1}$)	*Disintegrator extract* ($\mu g\ ml^{-1}$)	*Mean difference*
1	6.4	6.2	5.7	0.3
2	2.1	2.1	2.1	0
3	0.41	0.34	0.32	0.04
4	1.3	1.1	1.2	0.1
5	2.4	2.2	2.1	0.1
6	1.7	1.5	1.4	0.1
7	1.6	1.3	1.5	0.1

Table III summarizes the results of seven samples analyzed in parallel by the three different extraction methods. The comparison is acceptable with an average difference of 0.11 p.p.m.

The accuracy of the measurement step was investigated by comparing results obtained from the Orion and the Beckman electrodes on the same extracts and then comparing these results with measurements done by the absorptiometric indophenol blue method. The statistical analysis is given in Table II. A two-tailed "Student's" t test showed the Orion and Beckman electrode analyses to be not significantly different. Linear regression analysis gave a slope of 1.03 and an intercept of -0.09, both indicating that the Beckman electrode gave slightly higher results. This is as expected since interfering ions, particularly alkali metals, can effect the Beckman electrode while the Orion electrode is more selective.

It appears that the ammonium-sensitive Beckman electrode is more accurate at low concentrations, owing to better Nernstian response, whereas the ammonia-sensitive Orion electrode is better at higher concentrations where the concentration of interfering ions is also high. These facts are illustrated when linear regression analysis is used to compare the two methods with the indophenol blue method. Above 1.5 p.p.m., the results from the Orion electrode show better agreement while below 1.5 p.p.m. the results from the Beckman electrode have superior agreement. According to the t-test the results with both electrodes are not significantly different from those determined by the absorptiometric method.

DISCUSSION

The selective electrode technique for measuring particulate ammonium ion is acceptably accurate in the range of 0.03–30 $\mu g\ m^{-3}$ (0.1–10 $\mu g\ NH_4^+\ ml^{-1}$ of prepared solution). The average difference between duplicate measurement was 0.3 $\mu g\ ml^{-1}$. Since there is a logarithmic relationship between concentration and potential, the measurement error will vary as a percentage of the sample concentration and the results can be expressed only to two significant figures. The sources of error include the analytical error, the error in measuring the air volume, and the efficiency of collecting ammonium compounds on a glass fibre filter. Further work on testing the efficiency of this sampling method is being carried on.

The two electrodes tested have individual advantages and their combined use would cover almost all concentrations of air particulate samples likely to be encountered.

The levels of ammonia being measured in the aqueous extracts are in the lower range of detection for the electrodes. Great care must be exercised in obtaining potential readings at equilibrium, and the sample solution must be guarded against loss or gain of ammonia from the atmosphere by avoiding long periods of storage and by allowing minimal exposure to air during measurement. Some improvements in sensitivity may be obtained by sampling a larger volume of air and by treating more of the filter.

Junge[10] reported measurements on the chemical composition of particulate samples for a number of stations; he found that ammonium and sulphate ions were the largest fraction of the soluble ions analyzed. His results together with American Air Quality Data[11] and some results of the present work are shown in Table IV. Junge has postulated that the bulk of the sulfate in air is in the form of ammonium sulfate. Only four of his results support this statement and this is

TABLE IV

AVERAGE CONCENTRATIONS OF PARTICULATE AMMONIUM AND SULPHATE ION IN THE ATMOSPHERE

Location	*Ammonium ion* ($\mu g\ m^{-3}$)	*Sulphate ion* ($\mu g\ m^{-3}$)	*Calculated* $\%[SO_4^{2-}]$ *as* $(NH_4)_2SO_4$	*Source*
Frankfurt (winter)	6.2	23	71.7	Junge (1963)
Frankfurt (summer)	1.9	5.8	87.1	Junge (1963)
Round Hill (summer)	1.0	5.9	45.1	Junge (1963)
Florida	0.12	0.6	53.3	Junge (1963)
Hawaii	0.05	1.1	11.8	Junge (1963)
U.S.A. 1964–65	0.57	10.51	14.5	Air Quality Data (64–65)
1966	0.78	8.56	24.9	Air Quality Data (1966)
1967	1.04	8.43	32.9	Air Quality Data (1967)
Montreal 1969–70	1.68	18.40	24.3	This work
Ottawa (Sept. 72–Feb. 73)	0.33	8.1	10.6	This work

with the assumption that all of the ammonium reacts with sulfate ions. The present results and the Air Quality Data as well as Junge's figures from Hawaii show that only a small amount of the sulfate can be present as ammonium sulfate. It may be suggested that there are additional products of sulfur dioxide such as calcium sulfate[1,2].

SUMMARY

The accurate and rapid measurement of ammonium ion in airborne particulates is described, with particular reference to so-called high-volume air samples collected on glass-fibre filters. The method involves aqueous extraction of a part of the filter followed by analysis with a selective electrode; an Orion ammonia electrode and a Beckman ammonium electrode were compared. Varying ionic strength of the sample extracts had no effect and small interferences by other elements with the Beckman electrode could be taken into account. For a typical air sample of 2000 m^3, the ammonium content could be determined accurately down to 0.03 $\mu g\ m^{-3}$. The accuracy was established by comparison with an absorptiometric method. Recovery of standard added ammonium was quantitative. Three different methods of extraction were compared.

REFERENCES

1 H. A. C. McKay, *Chem. Ind. (London)*, (1969) 1162.
2 C. E. Junge and T. S. Ryan, *Quart. J. Roy. Meteorol. Soc.*, 84 (1958) 46.
3 S. Mimer, *Air pollution aspects of ammonia.* National Air Pollution Control Admin., Consumer Protection & Environmental Health Services, Department of Health, Education & Welfare, U.S.A., 1969.
4 A. E. Eggleton, *Atmos. Environ.*, 3 (1969) 355.
5 A. C. Stern, *Air Pollution*, Vol. II, *Analysis, monitoring and surveying*, Academic Press, New York, 1968.
6 T. Okita and S. Kanamori, *Atmos. Environ.*, 5 (1971) 621.
7 R. E. Cosgrove, C. A. Mask and I. H. Krull, *Anal. Lett.*, 3 (1970) 457.
8 J. A. Tetlow and A. L. Wilson, *Analyst (London)*, 89 (1964) 453.
9 L. Dubois, A. Zdrojewski, T. Teichman and J. L. Monkman, *J. Environ. Anal. Chem.*, March 1971.
10 C. E. Junge, *Air Chemistry and radioactivity*, Academic Press, New York, 1963.
11 Quality Data from the NASN, 1964–65, 1966, 1967. U. S. Dept. of Health Education and Welfare, Public Health Service.
12 L. Sumi, A. Cookery and J. L. Monkman, *Calcium Sulfate Content of Urban Air*, Monograph No. 3, American Geophysical Union, 1959.

Analytica Chimica Acta, 70 (1974) 169–176
Elsevier Scientific Publishing Company, Amsterdam – Printed in The Netherlands

A POTENTIOMETRIC STUDY OF THE OXIDATION OF COBALT(II) WITH GOLD(III) CHLORIDE IN PRESENCE OF 1,10 PHENANTHROLINE OR 2,2′-BIPYRIDINE

A NEW TITRATION OF COBALT(II) AND ITS APPLICATION TO NICKEL-BASE ALLOYS

B. V. RAO, S. V. ATHAVALE, T. H. RAO, S. L. N. ACHARYULU and R. V. TAMHANKAR
Defence Metallurgical Research Laboratory, Hyderabad (India)
(Received 9th October 1973)

It has been shown by Rao *et al.*[1] that gold(III) can be reduced to the metal quantitatively with cobalt(II) nitrate in a weakly acidic medium in the presence of 1,10-phenanthroline or 2,2′-bipyridine. The cobalt(II) is oxidized by gold(III) in 1,10-phenanthroline and 2,2′-bipyridine medium according to the reactions:

$$+3[Co(1,10\text{-phen})_3]^{2+} \rightarrow Au^0 + 3[Co(1,10\text{-phen})_3]^{3+} \quad (1)$$

$$Au^{3+} + 3[Co(2,2'\text{-bipy})_3]^{2+} \rightarrow Au^0 + 3[Co(2,2'\text{-bipy})_3]^{3+} \quad (2)$$

The redox nature of these reactions was established both by the gravimetric evaluation of the gold metal and by the indirect titration of ferroin or the iron(II)–2,2′-bipyridine complex formed by addition of excess of iron(III) to the unconsumed cobalt(II) in the filtrate[1], followed by titration with cerium(IV) solution.

In the present investigation, the oxidation of cobalt(II) with gold(III) in a medium containing 1,10-phenanthroline or 2,2′-bipyridine was studied in detail by direct potentiometric titrations; the redox character of the above-mentioned reactions was verified, and a new method for the potentiometric titration of cobalt(II) with gold(III) was developed. This appears to be the first time that gold(III) chloride has been used as an oxidimetric titrant.

Methods for the accurate determination of cobalt are increasing in importance, since cobalt forms an important constituent of modern metallurgical products. Several types of potentiometric titration[2–8] have been employed. Vydra and Pribil[9] have described potentiometric titrations of cobalt(II) with iron(III) chloride, in weakly acidic medium, in the presence of 1,10-phenanthroline[9] and 2,2′-bipyridine[10]. The same authors[11] have also reported an indirect method based on adding an excess of iron(III) to the cobalt(II) in 1,10 phenanthroline solutions and titrating the ferroin formed. Cobalt has also been determined potentiometrically by oxidation of the bivalent ion with potassium molybdicyanide in ammoniacal medium[12].

EXPERIMENTAL

Apparatus

A universal potentiometer (Type K-3, Leeds–Northrup Co., Philadelphia)

with a platinum–SCE electrode pair was used for the titrations. A Metrohm pH-meter(Herisau) with a combined glass electrode was used for the pH measurements.

Reagents

Gold(III) chloride solution(0.05 M). 4.925 g of spectrographically pure gold was dissolved in aqua regia. After slow evaporation nearly to dryness, the solution was acidified with hydrochloric acid and diluted to 500 ml.

Cobalt(II) nitrate solution (0.05 M). 2.947 g of high-purity cobalt (Johnson Matthey) was dissolved in nitric acid and the solution was diluted to 1 l. The test solutions and standard titrant solutions were prepared from the respective 0.05 *M* solution by accurate dilution.

1,10-Phenanthroline solution (0.1 M). 19.823 g of 1,10 phenanthroline (E. Merck) was dissolved in water weakly acidified with hydrochloric acid and the solution was made up to 1 l.

2,2′-Bipyridine solution (0.1 M). 15.62 g of 2,2′-bipyridine (E. Merck) was dissolved in the minimal quantity of hydrochloric acid, and the solution was diluted to 1 l. More dilute solutions (0.02 *M*) were prepared by suitable dilution.

Buffer solutions of pH 3–6 were prepared by mixing calculated molar quantities of sodium acetate and acetic acid; the pH was checked with the combined glass electrode.

Solutions of various ions at concentrations of 5 mg ml^{-1} were prepared from analytical-grade reagents for Ag(I), Cu(II), Zn(II), Fe(II), Ni(II), Cd(II), Mn(II), Pb(II), Pd(II), Hg(II), Al(III), Cr(III), Se(IV), Th(IV), U(VI), SO_4^{2-}, Cl^- and PO_4^{3-}. Other solutions were prepared from reagent grade chemicals.

Preliminary studies

For series of potentiometric titrations of cobalt(II) with gold(III) chloride according to reactions 1 and 2, the influence of the concentration of 1,10-phenanthroline or 2,2′-bipyridine, pH and temperature was studied. These titrations were carried out in the following way.

To 3 ml of 0.02 *M* cobalt(II) nitrate solution were added 10 ml of a suitable sodium acetate–acetic acid buffer and an appropriate amount of 0.02 *M* 1,10-phenanthroline or 0.02 *M* 2,2′-bipyridine solution. The solution was then diluted to 50 ml and titrated with 0.01 *M* gold(III) chloride solution potentiometrically.

Effect of phenanthroline and bipyridine. Several potentiometric determinations of a constant amount of cobalt(II) were carried out with 0.01 *M* gold(III) chloride at pH 4 in the presence of various quantities of 1,10-phenanthroline and 2,2′-bipyridine. The results showed that for 1:1 or 1:2 ratios of cobalt: phenanthroline or cobalt:bipyridine, the reaction did not proceed quantitatively, whereas it did so when the ratio was 1:3. Higher concentrations of 1,10-phenanthroline and 2,2′-bipyridine do not influence the size of the potential jump. It is, therefore, evident that the minimal concentration of phenanthroline or bipyridine, expressed in molarity, must be 3–4 times higher than the concentration of cobalt.

Effect of pH. The effect of pH on the course of the reactions was also studied. Figures 1 and 2 show the curves for the titration of cobalt(II) in the presence of a constant molar excess (1:5) of 1,10-phenanthroline or 2,2′-bipyridine,

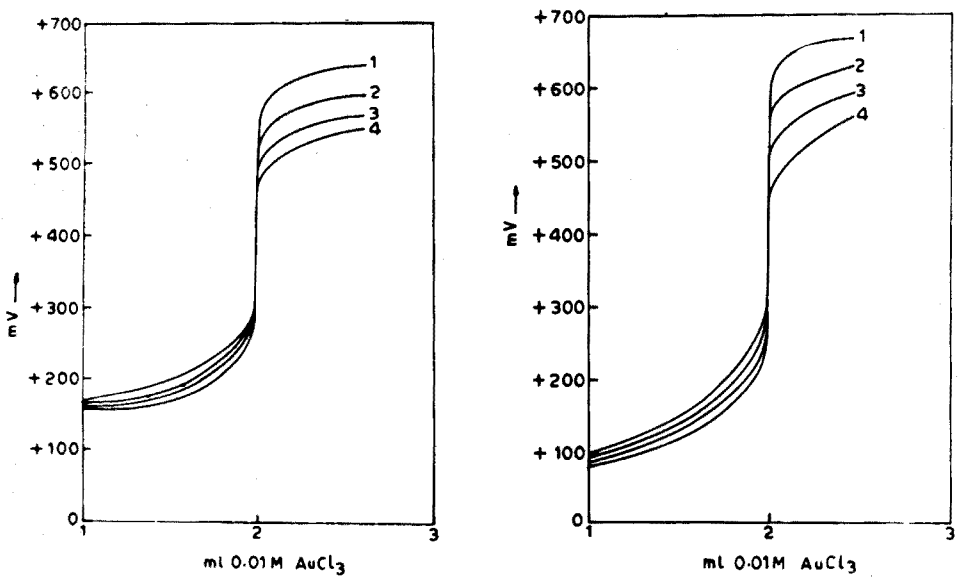

Fig. 1. Effect of pH on the oxidation of cobalt(II) with gold(III) chloride solution. 3 ml of 0.02 *M* cobalt(II) nitrate, 20 ml of 1 *M* buffer solution(sodium acetate–acetic acid) and 15 ml of 0.02 *M* 1,10 phenanthroline (total volume, 50 ml) titrated with 0.01 *M* gold(III) chloride. 1, pH 3; 2, pH 4; 3, pH 4.5; 4, pH 5.

Fig. 2. Effect of pH on the oxidation of cobalt(II) with gold(III) chloride solution. Conditions as for Fig. 1 except that 2,2′-bipyridine was used instead of 1,10-phenanthroline. 1–4, as in Fig. 1.

at different pH levels. It can be seen that as the pH decreases in the range 5–3, the potential jump at the equivalence point increases. Titrations carried out in an unbuffered medium at pH 3 showed almost the same potential increase at the equivalence point as in a buffered medium at the same pH. At pH values between 1.5 and 3.0, the reactions were also quantitative but above pH 6.0, the potential increase at the equivalence point was much smaller. Thus the pH of the titrated solution was not critical within the range 1.5–5.5.

Effect of temperature. At temperatures between 40 and 50°C, the equilibrium was established and the potential stabilized more quickly than at room temperature.

Recommended procedure

To the titration vessel transfer a solution containing 0.2–40 mg of cobalt(II), and add a suitable volume of 1,10-phenanthroline or 2,2′-bipyridine solution such that its concentration will be at least four times higher than that of cobalt(II). Adjust the pH to 3–5 by the addition of a suitable sodium acetate–acetic acid buffer. Heat to about 50°C. Titrate with 0.05–0.001 *M* standard gold(III) chloride solution, with stirring, to a potentiometric end-point. The potential increase at the equivalence point amounts to 180–300 mV for 0.04 ml of the standard solution. The time required is about 25 min.

RESULTS

Various potentiometric determinations of amounts of cobalt(II), between 0.21 mg and 41.44 mg, were carried out as described above, and some typical results are given in Table 1. Two representative titration curves are shown in Figs. 3 and 4.

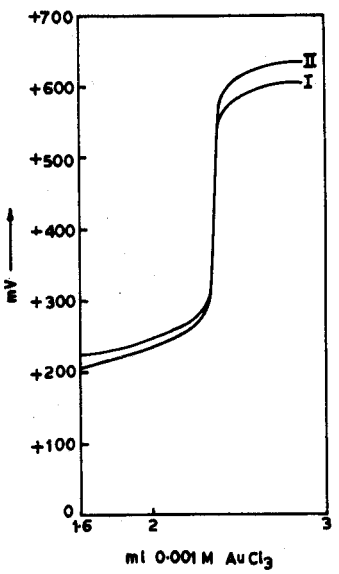

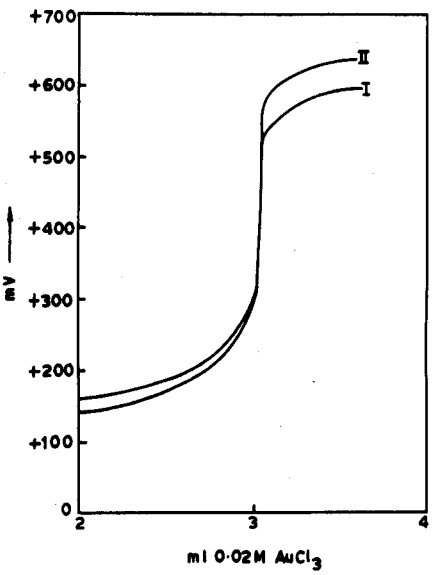

Fig. 3. Potentiometric titration of 0.424 mg of cobalt(II) with 0.001 *M* gold(III) chloride at 40°C in presence of 1,10-phenanthroline(I) and 2,2'-bipyridine(II).

Fig. 4. Potentiometric titration of 10.61 mg of cobalt(II) with 0.02 *M* gold(III) chloride at 40°C in presence of 1,10-phenanthroline(I) and 2,2'-bipyridine(II).

Effect of diverse ions

Various ions were added to the solutions to ascertain their effect on the determination of cobalt. To a solution containing 1.7682 mg or 5.3046 mg of cobalt(II) were added standard solutions containing different amounts of foreign ions. A suitable amount of 0.02–0.1 *M* phenanthroline or bipyridine was added. the solution was adjusted to pH 4.0 with dilute sodium hydroxide solution and 25 ml of sodium acetate–acetic acid buffer(pH 4.0) were added. The solution was then diluted to 100 ml and titrated as described above. The results (Table II) indicate that there is no interference from most common ions.

Even small quantities of iron(III) caused significant interference since cobalt(II) reduces iron(III) to iron(II) under the conditions used. Iron(III) can, however, be removed as hydroxide and the cobalt determination then carried out in the usual way, in weakly acidic medium. Silver(I), palladium(II) or mercury(II) make the determination impossible even when present in low concentration, be-

TABLE I

TITRATION OF COBALT(II) WITH GOLD(III) CHLORIDE

Co present (mg)	*Co found (mg) in presence of*		*Co present (mg)*	*Co found (mg) in presence of*	
	Phenanthroline	*Bipyridine*		*Phenanthroline*	*Bipyridine*
0.212	0.205	0.216	3.536	3.572	3.501
	0.219	0.209		3.501	3.483
0.424	0.417	0.432	5.305	5.269	5.340
	0.439	0.417		5.269	5.269
0.637	0.630	0.644	10.61	10.68	10.61
	0.622	0.622		10.54	10.54
0.849	0.838	0.838	21.22	21.11	21.69
	0.863	0.863		21.16	21.16
1.061	1.079	1.043	31.83	32.04	31.73
	1.039	1.079		31.93	31.73
1.768	1.768	1.786	42.44	42.53	42.35
	1.751	1.733		42.35	42.35

TABLE II

DETERMINATION OF COBALT(II) IN THE PRESENCE OF VARIOUS IONS

(Cobalt present 1.768 mg or 5.3050 mg)

Foreign ion added	*Amount taken (mg)*	*Cobalt found (mg) in presence of*		*Foreign ion added*	*Amount taken (mg)*	*Cobalt found (mg) in presence of*	
		Phenanthroline	*Bipyridine*			*Phenanthroline*	*Bipyridine*
Ni(II)[a]	20	1.786	1.751	Cr(III)	20	1.751	1.751
	20	5.269	5.340		20	5.305	5.269
Zn(II)[a]	25	1.768	1.786	Ti(IV)	10.5	1.751	1.786
	50	5.340	5.340		21.0	5.340	5.269
Cd(II)[a]	10	1.786	1.786	Se(IV)	50	1.786	1.751
	20	5.269	5.340		50	5.269	5.269
Pb(II)	50	1.768	1.751	Th(IV)	40	1.751	1.786
	50	5.269	5.340		90	5.269	5.269
Mn(II)	30	1.786	1.751	U(VI)	20	1.751	1.751
	40	5.340	5.269		50	5.340	5.269
Fe(II)	0.4	1.786	1.751	Mo(VI)	12.5	1.751	1.751
	1.1	5.340	5.340		12.5	5.269	5.340
Al(III)	20	1.751	1.786	PO_4^{3-}	30	1.751	1.786
	20	5.269	5.269		90	5.269	5.269

[a] Additional complexing agent added.

cause of the formation of insoluble precipitates. Palladium(II) can be eliminated by removing the quantitatively precipitated palladium(II)–phenanthroline complex in 1–5% hydrochloric acid medium; silver(I) can be removed by separating the insoluble silver chloride with a solution of sodium chloride.

Metal ions that do not react with 1,10-phenanthroline or 2,2′-bipyridine, *e.g.* Ca(II), Ba(II), Mg(II), Pb(II), Mn(II), Al(III), Cr(III), Se(IV), Th(IV) and

U(VI), do not interfere. The presence of anions such as Cl^-, NO_3^-, SO_4^{2-} and PO_4^{3-} had no unfavourable effect. Some bivalent cations, *viz.* Ni(II), Cd(II) and Zn(II), interfered because they form stable complexes with 1,10 phenanthroline and 2,2′-bipyridine and so suppress the formation of the cobalt complexes; this effect could be avoided by the addition of excess of reagent.

Low values to the extent of 10% were obtained when copper(II) was present in a 5:1 ratio relative to cobalt. With regard to molybdenum(VI), the effect of pH was critical; at pH 4.0 and above, titrations were feasible, but below pH 3.5, molybdenum(VI) seemed to be reduced by cobalt(II) to a blue molybdenum complex in the presence of phenanthroline or bipyridine and titration with gold(III) was not possible. Further investigations regarding reduction of molybdenum(VI) with cobalt(II) are in progress.

Application of the method to special alloys

The proposed method is applicable for the determination of cobalt in metallurgical materials which contain either no iron at all or in very small quantities. Metallic mercury can be used to reduce iron(III) quickly and quantitatively in 2 *M* hydrochloric acid medium[13]. Most nominally iron-free alloys and other materials contain at least small quantities of iron, and any iron present must be reduced completely to its divalent state. The mercury(I) chloride formed during the reduction is filtered off along with the remaining mer-

TABLE III

DETERMINATION OF COBALT IN NICKEL-BASE HIGH-TEMPERATURE ALLOYS

Type of alloy		*Cobalt found (%) in presence of*	
	Cobalt present (%)	*Phenanthroline*	*Bipyridine*
Nimonic–90	17.0[b]	16.89	17.15
B.C.S. No. 310/1[a]		17.06	17.06
Waspaloy	13.95[b]	14.06	13.97
N.B.S. No. 349[c]		13.88	13.88
Nimonic–105[d]	19.0[e]	19.10	18.92
		18.92	18.92
Nimocast–258[f]	20.33[e]	20.42	20.42
		20.51	20.42

[a] 19.45% Cr, 2.43% Ti, 1.06% Al, 0.068% C, 0.35% Mn, 0.46% Si, 0.25% Fe, 58.6% Ni and 17.0% Co.

[b] Standard values.

[c] 19.45% Cr, 4.03% Mo, 3.11% Ti, 1.25% Al, 0.3% Si, 0.42% Mn, 0.006% Cu, 0.077% Zr, 0.0043% B, 0.074% C, 0.142% Fe, 57.14% Ni, and 13.95% Co.

[d] 14.7% Cr, 1.7% Ti, 4.3% Al, 4.2% Mo, 0.25% Mn, 19.0% Co, 0.1% Si, 0.12% Fe and the rest Ni.

[e] Values obtained by the redox method of Vydra and Pribil (ref. 9).

[f] 9.4% Cr, 3.6% Ti, 4.0% Al, 3.4% Mo, 0.1% Mn, 20.33% Co, 0.16% Fe and the rest Ni.

cury. The practical application of the proposed method is illustrated for high cobalt concentrations in special alloys.

Procedure. Dissolve 0.5 g of alloy in an acid mixture (HNO_3:HCl = 1:3) and evaporate the solution nearly to dryness. Add 5 ml of concentrated hydrochloric acid and evaporate to a small volume. Dilute with water, filter off the undissolved residue and dilute the solution to 250 ml. Take an aliquot of 25 ml (or 50 ml), and add hydrochloric acid to give a final acid concentration of 2 *M*. Shake strongly with 2 g of mercury for about 10 min, separate the mercury and dilute and filter the solution. Neutralize the filtrate with 20% sodium hydroxide to *ca.* pH 4. Add 10–20 ml of sodium acetate–acetic acid buffer, pH 4, and 20 ml of either 0.1 *M* phenanthroline or bipyridine solution. Dilute to 100–150 ml, and titrate with 0.005–0.02 *M* gold(III) chloride solution. In the vicinity of the end-point, particularly in titrations with dilute solutions of the titrant, it is necessary to wait for 3–4 min between additions.

The results (Table III) were accurate and reproducible, and compared well with standard values or those obtained by the well-known redox method of Vydra and Pribil[9].

DISCUSSION

Cobalt(II) cannot be determined oxidimetrically since the redox potential of the Co(II)/Co(III) system is too low (−1.79 V). The formation of complexes with 1,10-phenanthroline or 2,2′-bipyridine alters the oxidation potential of the couple to values of 0.37 V or 0.31 V, respectively. Under appropriate conditions, the cobalt(II) complex can then be titrated with gold(III) chloride.

For these redox reactions to proceed quantitatively, it is necessary to use a 3–4-fold excess of 1,10 phenanthroline or 2,2′-bipyridine. The mechanisms and the optimal experimental conditions for the two reactions are practically identical. No significant difference was observed in the study of these reactions, except that the potential increase at the equivalence point was greater in the presence of 2,2′-bipyridine.

The pH is important but not critical within the range of 1.5–5.5. At temperatures of 40–50°C, the rate of reaction increases and the stabilization of the potential is faster.

The titration is readily applied to high-temperature nickel alloys.

SUMMARY

The redox reaction between cobalt(II) and gold(III) chloride in the presence of 1,10-phenanthroline or 2,2′-bipyridine was studied, and a titration of the cobalt(II) complex with a gold(III) chloride solution was developed. A 4-fold amount of 1,10-phenanthroline or 2,2′-bipyridine was necessary for rapid quantitative reaction; the permissible pH range was 1.5–5. The oxidation of the cobalt(II) complex proceeds rapidly at 40–50°C, and a direct potentiometric titration was possible. The following maximum errors were obtained: 3.3% for 0.2–1.0 mg Co, 2.0% for 1–5 mg Co, and 0.70% for 10–40 mg Co. The following ions did not interfere: Ni(II), Zn(II), Pb(II), Cd(II), Mn(II), Fe(II), Cr(III), Al(III), Th(IV), Se(IV), Ti(IV), U(VI),

Mo(VI), SO_4^{2-} and PO_4^{3-}. Even small quantities of silver(I), copper(II), palladium-(II), mercury(II) and iron(III) interfered. The method was applied to the determination of high cobalt contents in high-temperature nickel–base alloys.

REFERENCES

1 B. V. Rao, S. V. Athavale and S. L. N. Acharyulu, *Chim. Anal. (Paris)*, 53 (1971) 323.
2 E. Muller and H. Lauterbach, *Z. Anal. Chem.*, 61 (1922) 457; 62 (1923) 23.
3 O. Tomicek and F. Freiberger, *J. Amer. Chem. Soc.*, 57 (1935) 801.
4 P. Dickens and G. Maasen, *Arch. Eisenhattenw.*, 9 (1935) 487.
5 B. Bagshawe and J. D. Hobson, *Analyst (London)*, 73 (1948) 152.
6 R. Pribil and V. Malicky, *Collect. Czech. Chem. Commun.*, 14 (1949) 413.
7 R. Pribil and L. Svestka, *Collect Czech. Chem. Commun.*, 15 (1950) 31.
8 J. J. Lingane, *Anal. Chim. Acta*, 30 (1964) 319.
9 F. Vydra and R. Pribil, *Talanta*, 5 (1960) 44; *Collect. Czech. Chem. Commun.*, 26 (1961) 2169.
10 F. Vydra and R. Pribil, *Talanta*, 8 (1961) 824.
11 F. Vydra and R. Pribil, *Talanta*, 5 (1960) 92.
12 B. Kratochvil and H. Diehl, *Talanta*, 3 (1960) 346.
13 T. Yoshimura, *J. Chem. Soc. Jap., Pure Chem. Sect.*, 73 (1952) 122; *Anal. Abstr.*, 46 (1952) 6989.

Analytica Chimica Acta, 70 (1974) 177–187

A SIMPLE APPROXIMATE CALCULATION METHOD FOR ASSESSING THE USEFULNESS OF X–Y RECORDERS IN RAPID-SCAN VOLTAMMETRIC TECHNIQUES

A. M. BOND

Department of Inorganic Chemistry, University of Melbourne, Parkville, Victoria 3052 (Australia)

J. H. CANTERFORD

Division of Mineral Chemistry, C.S.I.R.O., P.O. Box 124, Port Melbourne, Victoria 3207 (Australia)

(Received 15th August 1973)

Many of the modern techniques of both polarography at dropping electrodes and voltammetry at stationary electrodes are designed to permit fast scan rates of potential, and in fact their electroanalytical advantages stem from this feature. For example, short drop-time techniques in polarography enable scan rates far in excess of those normally associated with polarography to be used, providing substantial time-saving in analytical applications and advantages in kinetic and related investigations[1]. The use of fast scan rates in linear sweep voltammetry at both stationary and dropping mercury electrodes (DME) is now well established[2,3]

With the development of fast scanning techniques, the recording of the current–voltage (i–V) curves needs to be considered carefully. Two common ways of recording are the oscilloscope and the X–Y recorder. The use of an X–Y recorder has several inherent advantages over an oscilloscope. However, because there is the possibility of recorder distortion resulting from the use of fast scan rates, there is a need for assessment of the capability of a normal X–Y recorder to provide distortion-free i–V curves at considerably higher scan rates than those associated with standard techniques.

Recorder distortion introduced by the application of damping has been considered in some detail with respect to a wide variety of techniques[4–8]. However, distortion induced by the use of fast scan rates has yet to receive much consideration. The present paper reports a theoretical and experimental study of the effects of variations in scan rate, and the results should facilitate the choice of a suitable X–Y recorder for fast scanning techniques. It should be recognized that a rigorous theoretical treatment presents many problems because of the large number of variables, *e.g.*, recorder characteristics and associated electronic circuitry. The present work is designed to be generally useful to analytical chemists. Since scan rate and response time are the two readily measured and controlled parameters, discussion is restricted to the relationships derived from these. Accordingly, a simple and general, but necessarily approximate, treatment is evolved. Applications to rapid d.c., a.c. (fundamental and second harmonic) and linear-sweep a.c. techniques are presented.

EXPERIMENTAL

Reagents

All chemicals used were of reagent grade quality.

Instrumentation.

The DME used had a natural drop time of 2.3 s (in distilled water at zero applied potential and a pressure of about 70 cm Hg). Short controlled drop times of 0.16 s were obtained with a Metrohm Polarographie Stand E354. Shorter drop times than this (down to 50 ms) were achieved by modifications of the Princeton Applied Research drop timer, model PAR-172, and associated circuitry. Metrohm hanging drop assembly BM503 was used to provide a stationary mercury electrode. All potentials were measured relative to a Ag/AgCl (5 *M* NaCl) reference electrode. All solutions were degassed with argon and thermostatted at $(25.0 \pm 0.1)°$.

Two polarographic systems with completely different types of X–Y recorder were used to evaluate the theory.

Type A: Metrohm Polarecord E261. D.c. techniques were used in the normal fashion. A.c. polarography was carried out with this Polarecord in conjunction with the Metrohm a.c. Modulator E393. An a.c. voltage of 10 mV r.m.s. at 50 Hz was used. To minimize cell impedance, the modulated a.c. voltage was applied through an auxiliary tungsten electrode. With zero damping, the recorder had a Y (or current)-axis full-scale deflection time of 1.0 s. The chart paper had two speeds in the X-direction, namely 250 cm/6 min and 250 cm min^{-1}. This instrument uses a Y-*t* recorder with a chart speed synchronized with the potential scan rate. The voltage per cm of chart paper could be adjusted in the range -0.5, -1.0, -2.0 and -3.0 V/250 cm. Various combinations of the appropriate variables were used, as noted in the text, to vary the scan rate.

Type B: Princeton Applied Research Electrochemistry System Model 170. A three-electrode system was used with tungsten as the third, or counter, electrode. The recorder used with this instrument had a response time for full-scale deflection in the Y (or current)-axis direction of 0.5 s. Selected scan rates of potential, such as 1, 2, 5, 10, 20, 50, 100 and 200 mV s^{-1} could be chosen. Chart paper remained stationary on the recorder. An applied potential of 10 mV p-p was used in the a.c. work at frequencies noted in the text and tables. Phase-sensitive detection was used with this instrument, with the circuitry recommended by the instrument manufacturer. Second harmonic a.c. polarography and voltammetry were achieved with circuitry recently designed in these laboratories.

THEORY

For any recorder, the characteristic either well known or easily measured is the response time, measured as units of distance (Y) per unit time (t'). Whether the response time is sufficient to record accurately an i–V curve, will depend on the relationship between the actual shape of the i–V curve and the scan rate used. In polarography, the shapes of the i–V curves are well known, particularly for reversible electrode processes.

The full theoretical description of the relationship between response time,

the shape of the curve and the scan rate of potential is given below for d.c. polarography. The model assumes that there is no distortion caused by recorder characteristics other than an insufficient response time; damping is assumed to be completely absent and in a.c. polarography, for example, lock-in amplifiers etc. have sufficiently short time constants to cause no distortion in their own right in the presence of fast scan rates.

D.c. polarography

In d.c. polarography the maximum scan rate allowable is limited by the drop time. Thus the scan rate must not exceed the time scale of the drop time, to avoid departure from potential–current relationships, essential to polarographic theory. If the scan rate becomes too fast, then one is dealing with another voltammetric technique. In the extreme case, where the scan rate is so fast that the complete polarogram is recorded in one drop the technique is called linear-sweep voltammetry, for which the theory has been well established[3]. Discussion of this limiting case will be given later.

The equation for a reversible d.c. wave is

$$E = E_{\frac{1}{2}}^{r} + \frac{RT}{nF} \ln \left\{ \frac{i_d - i}{i} \right\} \tag{1}$$

where E is the d.c. potential, $E_{\frac{1}{2}}^{r}$ the reversible half-wave potential, i_d the diffusion current, and i the current at E; R, T, n, F have the usual electrochemical meanings.

Consideration of recording procedures indicates that distortion will be related to the point where the rate of change of current as a function of potential exceeds the capability of the recorder. It should be possible to relate this rate of change, and so the recorder distortion, to the response time of the recorder. Thus the calculations below are carried out in order to obtain the rate of change, and in particular, its maximum allowable value.

Rearrangement of eqn. (1) gives:

$$i = i_d/(1+e^x) \tag{2}$$

where $x = (nF/RT)(E - E_{\frac{1}{2}}^{r})$

Differentiation of eqn. (2) leads to:

$$\frac{di}{dE} = -i_d e^x (1+e^x)^{-2} (nF/RT) \tag{3}$$

which has the derivative:

$$\frac{d^2 i}{dE^2} = i_d \left(\frac{nF}{RT}\right)^2 \left[\frac{e^x(e^x-1)}{(1+e^x)^3}\right] \tag{4}$$

The right hand side of eqn. (4) is zero when $e^x = 1$, or when $E = E_{\frac{1}{2}}^{r}$. Thus the maximum value of di/dE is given by

$$\left(\frac{di}{dE}\right)_{max} = \frac{-i_d}{4}\left(\frac{nF}{RT}\right) \tag{5}$$

The response "time" has the dimensions of distance (Y) per unit time, *i.e.*,

for d.c. polarography, current per unit time. Thus eqn. (5) has to be extended to the same dimensions. This is simply done by incorporating the scan rate of the potential term in eqn. (5).

Since

$$\frac{di}{dt} = \frac{di}{dE} \cdot \frac{dE}{dt}$$

where t is the travel time in the X-direction of the recorder, E is the applied d.c. potential, and dE/dt is the scan rate of d.c. potential in the X direction of the recorder (this is a constant which can be set at different values on the recorder) then

$$\left(\frac{di}{dt}\right)_{max} = \left(\frac{di}{dE}\right)_{max} \frac{dE}{dt} \tag{6}$$

Hence from eqns. (5) and (6)

$$\left(\frac{di}{dt}\right)_{max} = \frac{-i_d}{4} \frac{nF}{RT} \cdot \frac{dE}{dt} \tag{7}$$

Now

$$\left(\frac{di}{dt}\right)_{max} = \left[\left(\frac{\Delta i}{\Delta t}\right)_{max}\right]_{\Delta t \to 0} = \frac{-i_d}{4} \left(\frac{nF}{RT}\right) \frac{dE}{dt} \tag{8}$$

If $\Delta i/\Delta t$ were to exceed the response time of the recorder, when $\Delta t \leqslant t'$, then wave distortion would necessarily occur. Thus the condition necessary for the recorder to produce a wave without distortion is

$$(\Delta i/\Delta t)_{\Delta t \leqslant t'} < \text{response time of recorder} \tag{9}$$

Equation (8) is an excellent approximation to the LHS of eqn. (9) and thus recorder distortion for the purposes of this paper will be assumed to occur when

$$(\Delta i/\Delta t)_{\Delta t \to 0} > \text{response time of recorder}$$

In recording a d.c. polarogram with an X–Y recorder, the wave should normally incorporate as much of the Y-axis as possible. If the wave occupies the entire Y-axis, then i equals i_d, which is the full-scale deflection of the recorder and the response time is equivalent to i_d/t', *i.e.* a response time of 0.5 s can be considered to be equivalent to $2 \times i_d$ A s^{-1}. Recorder distortion will therefore occur in the first instance when

$$\left[\left(\frac{\Delta i}{\Delta t}\right)_{max}\right]_{\Delta t \to 0} \geqslant \frac{i_d}{t'}$$

or when

$$\frac{-i_d}{4} \cdot \frac{nF}{RT} \cdot \frac{dE}{dt} \geqslant \frac{i_d}{t'}$$

At 25°, distortion occurs in d.c. polarography when

$$\frac{-i_d n}{0.104} \cdot \frac{dE}{dt} \geqslant \text{response time of recorder}$$

or

$$\frac{dE}{dt} \geqslant -\frac{0.104}{nt'} \text{ V s}^{-1} \tag{10}$$

With the Metrohm system, where the response time is 1 s for full-scale deflection, the maximal value of the scan rate for distortion-free polarograms is $104/n$ mV s^{-1}. For the PAR system, which has a response time of 0.5 s, distortion occurs when the scan rate is greater than $208/n$ mV s^{-1}. These figures apply, of course, to the case where the i–V curve occupies the full scale (Y-axis) of the recorder. In practice, this ideal situation is rarely attained and, for example, if only half the Y-axis is occupied, then the theory predicts that double the scan rate can be used.

Fundamental harmonic rapid a.c. polarography

In a.c. polarography, short drop times can be used to achieve fast scan rates of potential[1]. Theoretically[9], the shape of a reversible a.c. wave is given by the expression

$$E = E_{\frac{1}{4}}^{r} + \frac{2RT}{nF} \ln \left[\left(\frac{I_p}{I} \right)^{\frac{1}{4}} \pm \left(\frac{I_p - I}{I} \right)^{\frac{1}{4}} \right] \tag{11}$$

provided $\Delta E \leqslant 8/n$ mV, where E = d.c. component of potential, $E_{\frac{1}{4}}^{r}$ = reversible half-wave potential = E_p, E_p = a.c. summit or peak potential, I_p = alternating current at peak potential, I = alternating current at potential E, ΔE = amplitude of applied alternating potential, and n, R, T and F have their usual electrochemical meanings.

Re-arrangement of eqn. (11) gives

$$I = 4I_p \left[\frac{e^x}{(1+e^x)^2} \right] \tag{12}$$

The value of x is as noted for eqn. (2).

The normal rules of differentiation give

$$\frac{dI}{dE} = -4I_p \left[\frac{e^x(e^x-1)}{(1+e^x)^3} \right] \frac{nF}{RT} \tag{13}$$

The maximum value of eqn. (13) occurs when $d^2I/dE^2 = 0$, *i.e.* when

$$4I_p \left(\frac{RT}{nF} \right)^2 \cdot \left[\frac{e^{2x} - 4e^x + 1}{(1+e^x)^4} \right] e^x = 0 \tag{14}$$

This occurs when $e^x = 0$ (minimal value and thus rejected) or when $e^{2x} - 4e^x + 1 = 0$, *i.e.* when $e^x = 2 \pm \sqrt{3}$. This gives

$$\left(\frac{dI}{dE} \right)_{max} = \pm \frac{\sqrt{3}}{18} \cdot 4I_p \frac{nF}{RT} = \pm \frac{2\sqrt{3}}{9} \cdot I_p \cdot \frac{nF}{RT} \tag{15}$$

Thus recorder distortion occurs when

$$\frac{2\sqrt{3}}{9} \cdot I_p \frac{nF}{RT} \cdot \frac{dE}{dt} \geqslant \text{response time of the recorder .}$$

With I_p equal to the full-scale deflection on the Y-axis:

$$\frac{dE}{dt} \leqslant \frac{3\sqrt{3}}{2} \cdot \frac{nF}{RT} \cdot \frac{1}{t'} \tag{16}$$

At 25°, the maximum allowable scan rate for distortion-free i–V curves is thus:

$$(dE/dt)_{max} = 66.7/nt' \text{ mV s}^{-1} \tag{17}$$

Second harmonic rapid a.c. polarography

Calculations based on the above procedure give a maximum allowable scan rate of potential for distortion-free i–V curves of $59.2/nt'$ mV s^{-1} at 25°.

A.c. voltammetry at stationary electrodes

Linear-sweep voltammetric techniques are invariably used with rapid scan rates of potential. In the a.c. method, Underkofler and Shain[10] have shown that the wave shape and height are independent of scan rate and identical to those for polarographic conditions provided that the frequency time scale is considerably greater than the d.c. scan rate. Similar considerations would be expected for second harmonic a.c. voltammetry at stationary electrodes, so that the equations derived for polarography are directly applicable to a.c. voltammetry.

D.c. voltammetry at stationary electrodes

In d.c. voltammetry, simple analytical solutions describing the shape of the i–V curve are not available, so that this technique is not considered. The shape is however somewhat akin to a d.c. polarogram and similar results should be expected.

Results of the above theoretical considerations are summarized in Table 1.

TABLE 1

MAXIMUM ALLOWABLE SCAN RATES (mV s^{-1})

Technique	*General*[a]	25°
D.c. polarography	$\frac{4RT}{nFt'}$	$\frac{104}{nt'}$
Fundamental a.c. polarography and voltammetry	$\left(\frac{3\sqrt{3}}{2}\right)\frac{RT}{nFt'}$	$66.7/nt'$
Second harmonic a.c. polarography and voltammetry	$\left(\frac{4\sqrt{3}}{3}\right)\frac{RT}{nFt'}$	$59/nt'$

[a] t' = response time of the recorder.

RESULTS AND DISCUSSION

From the theoretical discussion, the influence of scan rate is directly proportional to the value of n and t', the response time. To obtain variation

in n, the systems chosen were thallium(I), cadmium(II), lead(II) and indium(III) (all in 1 M sodium chloride) at *ca.* $4 \cdot 10^{-4}$ M. These four systems closely obey the equation for reversible reduction to the respective amalgams and provide examples where n equals 1, 2 and 3. To verify the effects of response time, two different recorders were used (see Experimental). Obviously, the correct approach to assessing the presence of distortion is to record the measured current at the potential where (di/dE) reaches a maximum. However, where distortion is introduced at a given potential, it will induce a phase lag in recording part of the remainder of the polarogram, and distortion was measured in terms of apparent changes in shape, height or peak position.

D.c. polarography

The Metrohm instrumentation has a maximum scan rate of 50 mV s^{-1} and a response time of 1 s. Thus only with $n=3$ would any distortion be expected. Unfortunately, this maximal scan rate could not be used with high precision, particularly with $n=3$. However, no measurable distortion was observed with the scan rate of 50 mV s^{-1} when $n=1$ or $n=2$ (drop time=0.16 s). With the PAR equipment, high scan rates can be used with high precision. For $n=1$, a scan rate of up to 100 mV s^{-1} was found to provide distortion-free recording. At higher scan rates of 200 mV s^{-1}, where distortion would be expected, the potential covered per unit drop was too large to provide unambiguous data. For $n=2$, no distortion was encountered at 100 mV s^{-1}, but with $n=3$ an apparent negative shift in $E_{\frac{1}{4}}$ was observed, and this is attributed to recorder distortion as predicted by theory. A.c. techniques undoubtedly provide a better test.

Fundamental harmonic rapid a.c. polarography

For thallium(I) it was confirmed that wave shape, I_p and E_p are independent of scan rate up to 50 and 100 mV s^{-1} with the Metrohm and PAR instruments, respectively. Figure 1 shows the results obtained for thallium(I) with Metrohm instrumentation. For indium(III) a slight decrease was observed in I_p values for the two highest scan rates with Metrohm instrumentation (Fig. 2). At the highest

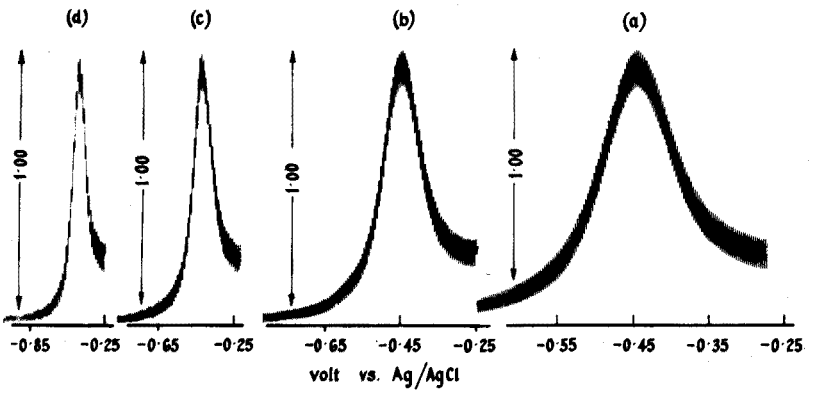

Fig. 1. Rapid a.c. polarograms of thallium(I) in 1 M sodium chloride, with scan rates of (a) 8.33, (b) 16.67, (c) 33.3 and (d) 50.0 mV s^{-1} (Metrohm Instrument). Peak currents are given as values relative to slowest scan rate.

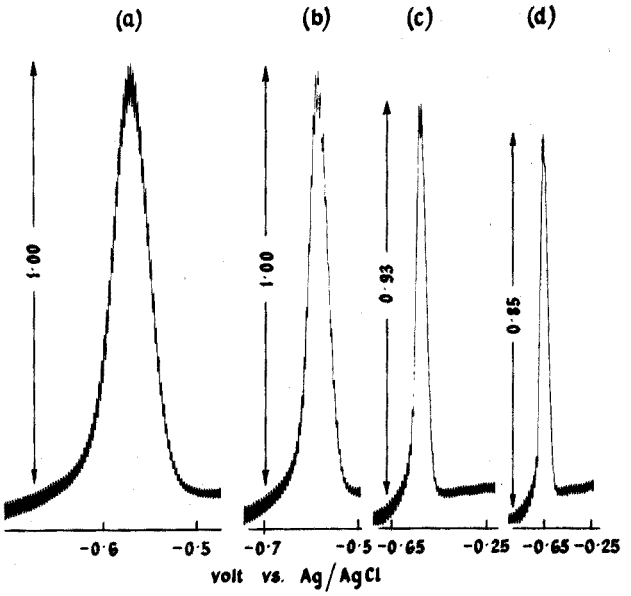

Fig. 2. Rapid a.c. polarograms of indium(III) in 1 *M* sodium chloride, with scan rates of (a) 8.33, (b) 16.67, (c) 33.3 and (d) 50.0 mV s^{-1} (Metrohm Instrument). Peak currents are given as values relative to slowest scan rate.

TABLE II

APPARENT VARIATION OF PARAMETERS FOR THE RAPID A.C. POLAROGRAM OF INDIUM(III) IN 0.1 *M* KCl AS A FUNCTION OF SCAN RATE
(PAR equipment at 80 Hz)

Scan rate ($mV\ s^{-1}$)	$-E_p$ (*V vs. Ag/AgCl*)	*Relative* I_p
1.0	0.563	1.00
2.0	0.563	1.00
5.0	0.564	1.00
10.0	0.562	1.00
20.0	0.563	1.00
50.0	0.565	0.90
100.0	0.570	0.70

scan rate, the observed I_p value was 85% of that recorded at the slowest scan rate. With PAR instrumentation (see Table II) distortion was observed with scan rates of 50 mV s^{-1} or greater, as is expected from the theoretical considerations. Results for cadmium(II) with PAR equipment are given in Fig. 3. In complete accordance with theory, no distortion is found until the scan rate is 100 mV s^{-1} or greater (see Fig. 3, e and f).

Stationary electrode a.c. voltammetry at a hanging drop mercury electrode

The predicted independence of peak height on scan rate has been proved

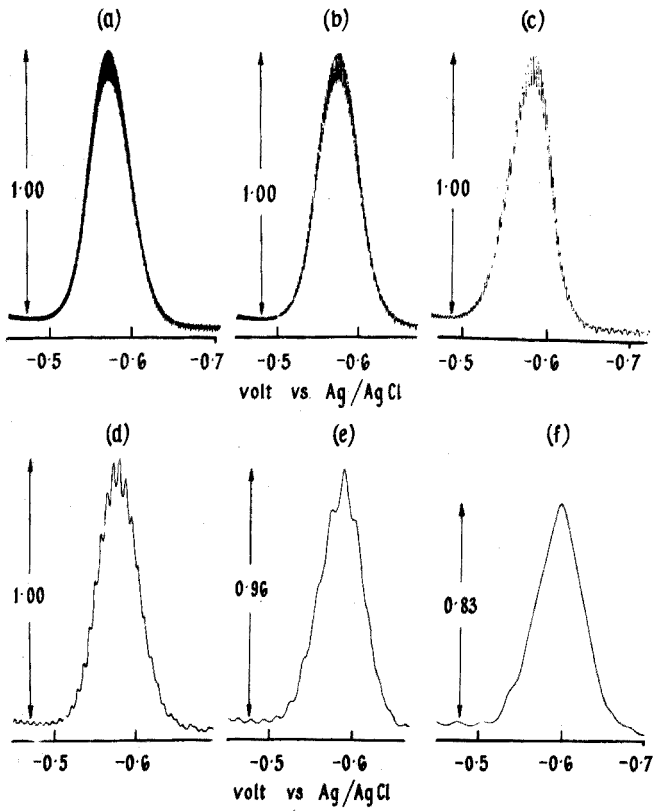

Fig. 3. Rapid a.c. polarograms of cadmium(II) in 0.1 *M* potassium chloride at 400 Hz and scan rates of (a) 5, (b) 10, (c) 20, (d) 50, (e) 100 and (f) 200 mV s^{-1} (PAR Instrument). Peak currents are given as values relative to slowest scan rate.

experimentally by means of a cathode ray oscilloscope recorder[10]. From previous considerations, it would be expected therefore that the peak height of an a.c. voltammogram at a hanging drop mercury electrode would be independent of scan rate as measured on an X–Y recorder, provided that no distortion due to the recorder itself is incurred. Furthermore, since a stationary electrode is used, any effects of the recorder should be the same as those observed with rapid a.c. polarography, if the previous conclusions are correct.

For indium(III) in sodium chloride and with a hanging drop mercury electrode, as with a.c. polarography, peak heights were independent of scan rate except for the two highest rates when recorded with Metrohm equipment. For the highest scan rate of 50 mV s^{-1}, I_p was again *ca.* 85% of the value for the slowest scan rate. A typical set of a.c. voltammograms obtained with the hanging drop electrode is shown in Fig. 4. The results with the stationary mercury electrode are again in excellent agreement with theoretical considerations.

With a large mercury pool electrode, it was observed that the a.c. peak height for the reversible reduction of thallium(I) in 50% hydrofluoric acid was independent of scan rate for those rates possible with the Metrohm apparatus used in this work[11].

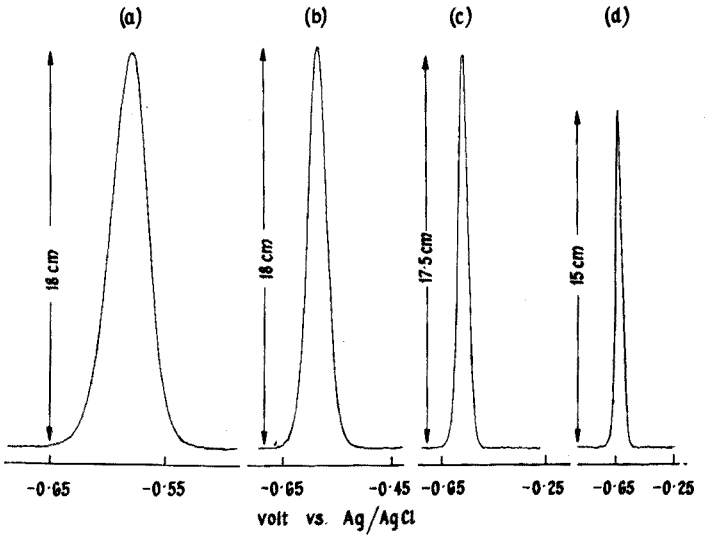

Fig. 4. Linear-sweep a.c. voltammograms of indium(III) in 1 *M* sodium chloride obtained with the hanging drop mercury electrode. Scan rates of (a) 8.33, (b) 16.67, (c) 33.3 and (d) 50.0 mV s^{-1} (Metrohm Instrument). Peak currents are given in cm, where 25 cm is the full scale of the Y or current axis.

Second harmonic a.c. measurements

These provided essentially identical agreement to the results found with the fundamental harmonic at both the DME and stationary electrodes.

CONCLUSION

The theoretical results presented in this paper permit the calculation of the maximal scan rates that can be employed with X–Y recorders of known response times provided that no damping is applied. In particular, it has been demonstrated that, with normal X–Y recorders having response times in the range 0.5–1.0 s, scan rates of up to $(50/nt')$ mV s^{-1} can be used reliably in a.c. techniques without incurring significant distortion, and rates up to $(100/nt')$ mV s^{-1} in d.c. polarography.

SUMMARY

A simple approximate calculation method is given which permits determination of the maximal scan rates of potential allowable for distortion-free recording of current–voltage curves with X–Y recorders. For the calculations only the response time of the recorder, the wave shape and the scan rate of potential need be known. Stationary mercury electrodes and rapid polarography with a dropping mercury electrode at controlled drop times were examined. Electroanalytical implications are discussed, with particular emphasis on the rapid a.c. polarographic method with short controlled drop times and on stationary-electrode fundamental and second harmonic a.c. voltammetry. Theoretically and experimentally it has been

shown that an X–Y recorder with 0.5–1.0-s response time can be used for scan rates up to about $(50/nt')$ mV s^{-1} with a.c. techniques and about $(100/nt')$ mV s^{-1} with d.c. polarography (t' = response time of recorder, n = number of electrons).

REFERENCES

1 A. M. Bond. *J. Electrochem. Soc.*. 115 (1971) 1588.
2 R. N. Adams, *Electrochemistry at Solid Electrodes*, Dekker, New York, 1969.
3 H. Schmidt and M. von Stackelberg, *Modern Polarographic Methods*, Academic Press, New York-London. 1963.
4 *G. E. Philbrook and M. H. Grubb, Anal. Chem., 19 (1947) 7.*
5 I. M. Kolthoff and J. J. Lingane, *Polarography*, Interscience, New York-London, *2nd Ed., 1952*, Vol. 1, pp. 297–371.
6 H. Strehlow, *Z. Elektrochem.*, 55 (1957) 420.
7 W. E. Thomas and W. B. Schaap, *Anal. Chem.*, 41 (1969) 137.
8 I. G. McWilliam and H. C. Bolton, *Anal. Chem.*, 41 (1969) 1762 and references therein.
9 D. E. Smith in A. J. Bard (Ed.), *Electroanalytical Chemistry*, Marcel Dekker, New York, 1967, Vol. 1, Ch. 1, p. 33.
10 W. L. Underkofler and I. Shain, *Anal. Chem.*, 37 (1965) 218.
11 A. M. Bond, T. A. O'Donnell and R. J. Taylor, *Anal. Chem.*, 44 (1972) 434.

Analytica Chimica Acta, 70 (1974) 189–198

CHELATING RESINS FROM 8-HYDROXYQUINOLINE

J. R. PARRISH and R. STEVENSON
Department of Chemistry, Rhodes University, Grahamstown (South Africa)
(Received 5th July 1973)

The recent paper by Vernon and Eccles[1] on ion-exchange resins incorporating 8-hydroxyquinoline (oxine) as the functional group, prompts us to publish results which lead to a different conclusion.

The first resins made from oxine, resorcinol and formaldehyde had very low capacities owing to insufficient swelling[2], but Pennington and Williams[3] prepared a resin of this type which had a water regain of 3.72 g g^{-1} and a high capacity for copper (6.5 meq g^{-1} at pH 5.5). Although no kinetic experiments were reported, the exchange rate of this resin cannot have been satisfactory because "the 24-hour absorption period did not achieve complete equilibrium", and an attempted separation of copper from nickel on a 30-cm column of the resin failed. In an attempt to repeat the work of Pennington and Williams, Vernon and Eccles[1] obtained a resin with a water regain of 0.29 g g^{-1} and a copper capacity of only 0.1 meq g^{-1} at pH 5.5. They concluded that oxine-containing resins produced by polycondensation had inferior properties to those of a resin derived from macroporous polystyrene.

However, if the general method of Pennington and Williams, which was not described in full detail in their paper, is followed, it is possible to prepare condensation resins of high water regain and capacity. In the work discussed here, a study of the rate-controlling factors has led to the synthesis of modified resins with high exchange rates, suitable for rapid separations on columns. Some of the results reported here are taken from a thesis by Stevenson[4].

EXPERIMENTAL

Preparation of resins

Oxine, formaldehyde and resorcinol were condensed in 1.5 *M* sodium hydroxide solution according to the procedure of Pennington and Williams[3], but the proportion of resorcinol and the degree of dilution were varied. The effects of these variables and of the conditions of curing on the water regains of the resins were investigated. Reproducible water regains were obtained only when the resins were cured in tightly sealed jars which prevented the escape of water vapour, or when all the water was driven off. A resin of high capacity and water regain was made as follows.

Resin 1. Oxine (0.1 mol) was mixed with 1.5 *M* sodium hydroxide solution (63 ml) and 37% formaldehyde solution (15 ml). Gentle warming was necessary for complete dissolution. A solution of resorcinol (0.067 mol) in 1.5 *M* sodium

hydroxide (13 ml) was then added with stirring. Finally more 37% formaldehyde (15 ml) was added, and the whole mixture was poured quickly into liquid paraffin (500 ml) previously heated to 80°C. The suspension was stirred mechanically for 30 min at a rate necessary to obtain beads of the required size, and then transferred to a preserving jar. This was tightly sealed, and heated in an oven at 95°C for 16 h. The beads were filtered off, washed rapidly with chloroform and then alcohol, and stored under water.

In some resins, acidic or basic groups were incorporated by the addition of potassium phenol sulphonate or a guanidinium salt to the initial mixture. The resin used for column separations was made as follows.

Resin 2. Oxine (0.06 mol) and potassium phenol sulphonate (0.02 mol) were treated with 1.5 *M* sodium hydroxide (42 ml) and 37% formaldehyde (12 ml), but the addition of water (8 ml) was necessary as well as heating to obtain a solution. A solution of resorcinol (0.054 mol) in 1.5 *M* sodium hydroxide (15 ml) and 37% formaldehyde (6 ml) were then added. A precipitate formed which dissolved when the mixture was stirred and heated. As soon as the mixture thickened it was poured into liquid paraffin at 80°C, and treated as described for resin 1.

Conditioning of resins

The resins were ground (if they had not been prepared in bead form) and sieved wet to obtain the desired particle size. The particles were transferred to wide columns and were washed with 0.1 *M* sodium hydroxide until the effluent was colourless. They were then washed successively with water, 1 *M* hydrochloric acid, water, buffer of pH 5.5, and water.

Characterization of resins

All measurements were made at 20°C.

Water regain. The method of centrifuging[5] was used.

Capacity. Samples of wet resin (1 g) were shaken mechanically with 0.025 *M* solutions (100 ml) of the metal cation with the addition of the appropriate buffer (20 ml) until equilibrium had been attained. The final pH was measured before the resin was filtered off and washed with water. The absorbed metal was eluted with 1.5 *M* nitric acid (100 ml), and determined by titration with EDTA. Another sample of wet resin was dried at 110°C for 16 h to determine the water content. Capacities were expressed as milligram-equivalents per g of dry resin. For the initial comparison of different resins, the capacity for copper at pH 5.5 was chosen as a measure of the chelating capacity.

Exchange rates. A comparison of the rates of exchange of different resins under practical conditions was obtained by determination of the amount of copper absorbed at pH 5.5 after given periods of mechanical shaking. From a plot of copper absorbed against the time allowed for absorption, the time for half the maximal absorption ($t_{\frac{1}{2}}$) was found. The $t_{\frac{1}{2}}$ values were used to compare the resins with commercial resins such as Amberlite IR120, which is known to have a satisfactory rate of exchange.

Since the $t_{\frac{1}{2}}$ values varied with the particle size of the resins, a narrow range (30–40 mesh) of particle size was selected for the determination of exchange

rates. The concentration of the solution and the proportion of resin were the same as those used for the determination of capacity. In a separate series of experiments with a single resin, the $t_{\frac{1}{2}}$ value was found to decrease with increasing concentration of copper until the latter reached a value of 0.15 *M*, after which the value became independent of concentration. This value presumably depended on the particular resin and the degree of agitation, but it indicated that at the much lower concentration of copper used in measuring the $t_{\frac{1}{2}}$ values of different resins, the exchange rate was not controlled by particle diffusion alone.

Preparation of buffers

Buffer solutions with pH values between 0.5 and 6.0 were made by mixing 1 *M* sodium acetate solution with 1 *M* hydrochloric acid in the required proportions. For the absorption of calcium and magnesium ions only, buffer solutions of pH 8.5–9.5 were made by mixing 1 *M* ammonium chloride with the appropriate volume of 2% ammonia solution.

Column separations

Resin 2 (44–72 mesh) was packed to a height of 9 cm in a column of internal diameter 1 cm. The resin was rinsed with buffer solution, and then a mixture (100 ml) of 0.01 *M* solutions of the metals to be separated was passed through the column. The ions not absorbed were eluted with the same buffer solution (25 ml). The absorbed metal was then eluted with 1 *M* nitric acid. The flow rate for absorption, rinsing and elution was 3 ml min^{-1}.

For faster separations, the solutions were pumped through a 25 cm by 8 mm bed of 52–200 mesh resin at rates of up to 20 ml min^{-1} by a Watson–Marlow MHRE Flow Inducer.

RESULTS AND DISCUSSION

The ability of a resin to exchange ions rapidly from an aqueous solution requires sufficient water in the resin phase to permit rapid diffusion of the exchanging ions. The water content of a resin is conveniently expressed as the water regain[5] of a standard form of the resin, invariably the hydrogen form of cation-exchange resins, and usually the chloride form of anion-exchange resins. The average water regain of commercial ion-exchange resins is about 1 g g^{-1}. Thus a value of 1.0 g g^{-1} was measured for random samples of Amberlite IR120 and also for the commercial chelating resin Dowex A1 in the hydrogen form. The latter resin is much more swollen in the sodium form, for which a value of 2.7 g g^{-1} was found. The published[6] moisture content of 76.2% corresponds to a water regain of 3.2 g g^{-1} for the sodium form. These figures indicate that the water regain of a chelating resin should fall in the range 1–3 g g^{-1}, and they illustrate the importance of defining the ionic form of the resins when one compares water regains.

Since resins made from oxine and resorcinol contain both weakly acidic and weakly basic groups, salts are formed when the resins are treated with either alkalis or acids. The salt form hydrolyses when the resin is washed with water, but large volumes of water are required for complete hydrolysis. Thus after

treatment with hydrochloric acid, resin 1 required 400 bed-volumes of water to remove chloride ion and to raise the pH of the effluent to 4.2. Resins were prepared for analysis in this way, but for the determination of water regains the resins were washed with 1 *M* hydrochloric acid, water, sodium acetate buffer of pH 5.5 and finally with water. This procedure gave the non-ionized form of the resin, which is the form with the minimal water regain. An unexpected result was obtained when the resins were treated with 0.1 *M* sodium hydroxide before being washed with pH 5.5 buffer and water. The bed volume of a resin treated in this way was 50% greater than that of the same resin which had been treated initially with hydrochloric acid instead of sodium hydroxide. At first, it was thought that the swollen sodium form had not hydrolysed completely, but analysis showed no sodium in the resin (except for a resin which contained sulphonate groups as well as oxine) and the total ash was only 0.04% of the dry resin. The only explanation for the increased swelling and higher water regain (3.5 as opposed to the "normal" value of 1.8 g g^{-1}) seems to be that the resin exists at least partially in zwitterionic form. On treatment with acid and then water, the resin reverts to its normal volume.

Control of swelling

Pennington and Williams[3] obtained resins of high moisture content by preparing the resins in dilute solution, and by the use of very mild curing conditions. They suggested that many methylol groups remained unreacted in the final resins, but they did not stress that the resins must never be dried. Even partial loss of water results in further crosslinking which lowers the water regain. In our work, a resin with an original water regain 1.86 g g^{-1} was allowed to dry at room temperature, and a second determination of the water regain after re-soaking the resin, gave a value of 1.06 g g^{-1}. Irreversible changes caused by the drying of condensation resins were reported by Holdoway *et al.*[7], and also by Jakubovic[8] who mentioned the condensation of methylol groups to methylene or ether bridges as a possible explanation.

When the resins were heated in open vessels at temperatures above 100°C for 1 day or longer, they became fully cured. The highest water regains obtained with fully cured resins were in the range 0.50–0.55 g g^{-1}, which is too low to allow a reasonable reaction rate. Satisfactory water regains were obtained when sufficient water was present during the curing process, but sealed containers were essential for reproducible results. The values in Table I were obtained in this way and refer to a curing period of 4 days. Higher water regains can be obtained by curtailing the period of curing, but resins prepared in this way may be less stable towards change in water regain during use. A sample of resin 2 which had been heated at 80°C for 30 min only, had a water regain of 2.55 g g^{-1} as compared to 1.89 g g^{-1} for a sample which had been cured at 95°C for 16 h.

Comparison of the water regains in Table I shows the relatively small effect of the curing temperature compared to that of the proportion of water used. When the proportion of resorcinol was decreased, while the total amount of formaldehyde and sodium hydroxide solution remained constant, the water regain increased. When the resorcinol, formaldehyde and sodium hydroxide were decreased in proportion, so that the molar ratio of formaldehyde to resorcinol

TABLE I

EFFECT OF EXPERIMENTAL CONDITIONS ON THE WATER REGAIN

(In all cases 1.85 mol of formaldehyde was taken per mol of oxine initially, and then resorcinol and formaldehyde were added in the ratios shown. The solid constituents were dissolved in 1.5 *M* sodium hydroxide, and the formaldehyde was added as a 37% solution in water. The curing time was 4 days.)

Percentage of water in original mixture	*Resorcinol: oxine molar ratio*	*Formaldehyde: resorcinol molar ratio*	*Curing temperature °C*	*Water regain*
59	0.68	1.36	102	0.68
73	0.68	1.36	102	1.91
73	0.68	1.36	142	1.75
70	1.36	1.36	98	1.13
73	1.02	1.81	98	1.57
74	0.68	2.72	98	2.25
76	0.45	4.07	98	2.98
71	1.02	1.36	98	1.25
73	0.68	1.36	98	1.93
75	0.45	1.36	98	1.97

remained constant, the water regain increased, but less steeply than before. Thus resins can be prepared with water regains in the range 1–3 g g^{-1}, but the choice of experimental variables is limited by practical difficulties. If the original solution is too dilute, or if the proportion of resorcinol is too low, precipitation instead of gelation may occur. Resins with water regains greater than about 2.5 g g^{-1} were very soft and gave coloured effluents on treatment with alkalis.

Bernhard and Grass[9] reported excessive swelling in alkalis by resins prepared from oxine, resorcinol and formaldehyde, and they stated that the difference in volume between the hydrogen and the sodium forms made the resins practically unusable in columns. The actual water regains of such resins were not recorded, but the authors described a resin designed to overcome this difficulty, and made by the substitution of furfural for the formaldehyde. After equilibration with a sodium acetate buffer of pH 4, this resin had a water content of 72.0%, corresponding to a water regain of 2.57 g g^{-1}. Resins with this or a lower water regain can be made from formaldehyde. The increased swelling in sodium hydroxide solutions is not relevant when use of the resin in columns is limited to the pH range 0–5, as in the present work. Over this range the change in bed volume was not more than 15% for resins of water regain below 2.0 g g^{-1}. The use of furfural resulted in a resin which contained carboxyl groups as well as the oxine groups[9], and the capacity and exchange rate of the resin were lower than those of the best resins described here.

Exchange rates

The times for half the maximal absorption ($t_{\frac{1}{2}}$) of copper(II) ions, measured under arbitrary conditions, are plotted against the water regains of the resins in Fig. 1. Curve B represents resins which contain phenol sulphonic acid groups as well as oxine groups. The presence of these ionized groups increases the

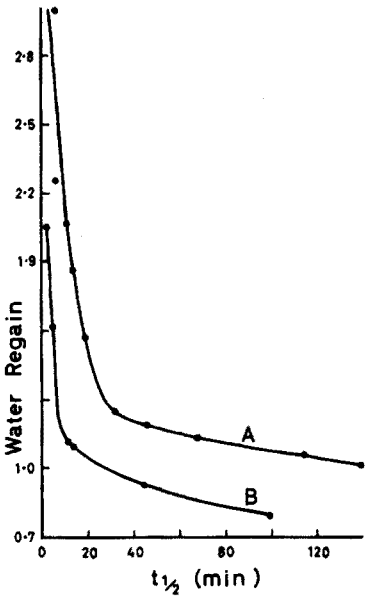

Fig. 1. The relation between $t_{\frac{1}{2}}$ values and water regain of oxine-containing condensation resins. Curve A represents resins with no strongly ionized groups, curve B resins which contain sulphonate groups.

exchange rate at the same water regain, presumably by increasing the diffusion rate of cations within the resin. However, for both types of resin, the $t_{\frac{1}{2}}$ value increases rapidly when the water regain falls below a critical value. If it is assumed that a satisfactory chelating resin must exchange ions at least as rapidly as the carboxylic acid resin, Amberlite IRC50, ($t_{\frac{1}{2}}=20$ min), the water regain of an oxine resin must be greater than 1.5 g g^{-1} (or 1.0 if sufficient sulphonic acid groups are introduced). The optimal water regain is about 2.0 g g^{-1}; increases beyond 2.5 g g^{-1} had no appreciable effect on the $t_{\frac{1}{2}}$ values, and the physical properties of the resins deteriorated.

Resin 1 is an example of one of the best resins that could be made without sulphonic acid groups. A $t_{\frac{1}{2}}$ value of 6.5 min was shown by a batch of this resin. However, a $t_{\frac{1}{2}}$ value of only 2 min was found for the chelating resin, Dowex A1, and for the sulphonic acid resin, Amberlite IR120. (The $t_{\frac{1}{2}}$ value of the latter resin was measured in the absence of a sodium acetate buffer.) To make an oxine resin of comparable $t_{\frac{1}{2}}$ value, sulphonic acid groups had to be introduced. Resin 2 is an example; its $t_{\frac{1}{2}}$ value was 2.5 min.

Capacity of the resins

The exact structure of the resins depends not only on the proportions of oxine and resorcinol used, but also on the extent of the reaction with formaldehyde. It is therefore not possible to calculate an exact theoretical capacity for one of these resins. An expected capacity can be calculated from the percentage of nitrogen found by analysis. Thus a typical resin contained 4.97% N, and if the oxine groups form a 1:1 complex with copper(II) ions, the expected capacity would be 7.1 meq g^{-1}. In practice, the capacity for copper at pH 5–5.5 was

about 7.0 meq g^{-1} for all the resins made with a 0.68 molar ratio of resorcinol to oxine, provided that their water regains were greater than 0.9 g g^{-1}. A resin with water regain of 0.62 g g^{-1} had an experimental capacity of only 4 meq g^{-1}. Presumably some of the chelating groups become inaccessible when the swelling is low. Inadequate swelling is undoubtedly the reason for the low capacity reported by Vernon and Eccles for a resin of this type, as they themselves suggested[1].

At high pH the phenolic groups in these condensation resins ionize, and higher, but less selective, capacities are observed. At pH 5 it may be assumed that copper is held only as a complex with the oxine groups, although Pennington and Williams suggested that copper could be chelated at this pH value by phenolic alcohol groups[3]. They reported a copper capacity of 2 meq g^{-1} for a resorcinol–formaldehyde resin containing no oxine. It seems more probable that the copper was held by carboxyl groups resulting from oxidation of the methylol groups. The infrared spectra of the present oxine resins showed no appreciable absorption band that could be attributed to carboxyl groups.

Bands at 1218, 1163 and 1038 cm^{-1} in the infrared spectrum[10] confirmed the presence of sulphonic acid groups in oxine resins when phenol sulphonic acid had been used in their synthesis. Elementary analysis of one of the resins for sulphur and nitrogen showed that the molar ratio of sulphonic acid groups to oxine groups was 0.39 in the final resin, when the ratio in the original mixture was 0.33. A resin of this type would be expected to show a reduced capacity for copper, on account of the presence of phenol sulphonic acid residues, which would take up very little copper from sodium acetate buffers. On the assumption that all the formaldehyde used had reacted, but only the minimal number of methylol groups had condensed to form methylene bridges, a copper capacity of 5.3 meq g^{-1} was calculated. Experimental values were 5.0 and 5.4 meq g^{-1} for resins of water regain 1.89 and 1.66 g g^{-1}, respectively.

Selectivity

The selectivity of the oxine–resorcinol–formaldehyde resins is illustrated in Fig. 2, in which the capacity of a typical resin for six chosen metal ions is

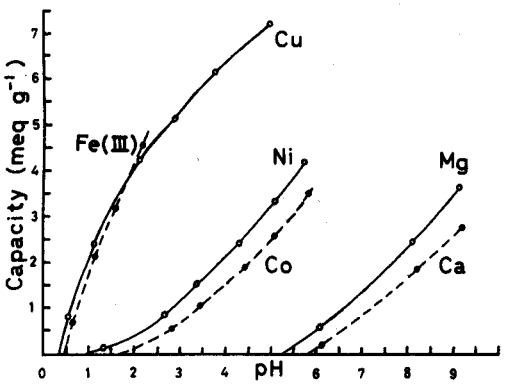

Fig. 2. The capacity of an oxine–resorcinol–formaldehyde resin for six metal ions as a function of pH.

plotted against the final pH of the solution after equilibration. The curves were continued to low pH values at which zero absorption occurs, since this is the region of interest for rapid separations by selective absorption. Figure 2 can be compared with similar plots by other authors showing the absorption of metals by oxine resins. It is similar to the incorrectly labelled[11] diagram of Pennington and Williams, except that their curve for magnesium showed appreciable absorption even at pH 2, whereas no absorption was found here below pH 5. As expected from the Irving–Williams series[12], and from the known values[13] of the stability constants of the complexes of nickel and cobalt with oxine, the resin showed slightly greater absorption of nickel than of cobalt. In contrast, the diagram of Vernon and Eccles[1] shows the opposite order.

Similar behaviour to that shown in Fig. 2 was exhibited by a resin which contained phenol sulphonic acid groups as well as oxine. The difference was that the capacity for all the ions was lower, and this resin did absorb some calcium and magnesium ions below pH 5. This is ascribed to inselective absorption by the sulphonic acid groups. It is a disadvantage, but it can be reduced by increasing the concentration of sodium ion in the buffer, and it does not prevent quantitative separations on columns. Resins made from the condensation of a guanidinium salt with oxine, resorcinol and formaldehyde did not show this inselective absorption of cations, and the exchange rates were higher than those of resins of the same water regain but without the guanidinium groups. However, the actual water regains were all below 1.0 g g^{-1}, and the $t_{\frac{1}{2}}$ values were greater than 30 min, so that these resins were not considered suitable for column separations.

Separations

Copper was separated from nickel at pH 2 on a column of resin 2 as described under Experimental. At this pH the nickel was eluted quantitatively by 25 ml of buffer solution, as shown by precipitation with dimethylglyoxime. The copper was retained, but it could be recovered quantitatively by elution with 1 *M* nitric acid.

Nickel and magnesium were separated at pH 4.5, the nickel being retained and the magnesium eluted. Since the resin is itself a buffer, it is not suitable for separations by chromatographic elution with dilute buffers. Selective absorption is a faster technique than chromatographic elution, and although gravity flow was used for the above separations, pumping can be used to reduce the time required. Thus, in a preliminary experiment 25 ml of 0.025 *M* copper solution was buffered to pH 5.5 and passed through a column of resin at 20 ml min^{-1}. The copper was quantitatively retained, and the time required for absorption and washing the resin was about 5 min. This technique should be useful for the rapid removal of an interfering cation or for the rapid isolation of a desired cation before determination by complexiметric titration or absorption spectrophotometry.

Resins from polystyrene

Resins based on cross-linked polystyrene have the advantage of greater physical and chemical stability than is shown by condensation resins. Oxine has been coupled to cross-linked, diazotized poly(aminostyrene), but even at 2% cross-

linking the resin had a very slow exchange rate[14]. Attempts were made to improve this resin by using 1% cross-linked polystyrene and by adjusting the reaction conditions of Davies *et al.*[15] to obtain the highest possible conversions in the nitration, reduction, diazotization and coupling steps. The reduction was carried out in the absence of alcohol at 107°C for 16 h, and a five-fold excess of oxine was used for coupling. The resulting resin (Resin 3, Table II) had 75% of the theoretical capacity for copper.

TABLE II

PROPERTIES OF OXINE-CONTAINING POLYSTYRENE RESINS

Resin	*Copper capacity (meq g^{-1} at pH 5)*	*Water regain*	*$t_{\frac{1}{2}}$ value (min)*
3	5.48	1.42	104
4	5.17	2.23	43
5	3.54	0.91	140
6	2.84	1.14	100

Three other resins were made with a proportion of strongly basic or strongly acidic groups in addition to the oxine groups. Resin 4 was made by partial chloromethylation and quaternization of 1% cross-linked polystyrene to give a strongly basic resin of capacity 1.5 meq g^{-1}. This was converted to the nitrate form before the introduction of the oxine groups by the method used for resin 3. Resin 5 was made by partial (20%) sulphonation of 1% cross-linked poly(aminostyrene) with cold 60% oleum before diazotization and coupling to oxine. Resin 6 was similar to resin 4, but 8-hydroxyquinoline-5-sulphonic acid was used instead of oxine in the coupling step, so as to introduce both strongly acidic and strongly basic groups into the same resin.

The properties of the resins are shown in Table II. Only resin 4 had a high water regain, and its $t_{\frac{1}{2}}$ value was four times greater than would be expected for a condensation resin of the same water regain (Fig. 1). Possible explanations for these disappointing results are that further cross-linking occurred during the coupling reaction, limiting the swelling, and that at a given water regain the hydrophobic polystyrene matrix offers more resistance to the diffusion of ions than the hydrophilic matrix of the condensation resins. In other words, the internal water is less evenly distributed in the polystyrene resins.

Hirsch *et al.*[16] described two chelating resins made from a macroporous styrene–divinylbenzene copolymer (Amberlite XAD-1). These resins showed little or no volume change on conversion from one ionic form to another, and they were used for column separations. No water regains or exchange rates were reported, and the resins were not compared directly with similar gel-type resins. A different macroporous copolymer (Amberlite XAD-2) was used by Vernon and Eccles[1] for their oxine-containing chelating resin, and although the water regain was only 0.68 they showed that the resin could be used for column separations. The reported $t_{\frac{1}{2}}$ values cannot be compared with the present figures, which were obtained under a different set of arbitrary conditions.

Macroporous polystyrene-based chelating resins appear to have promise, but they have not been shown to be better than condensation resins of suitable water regain. The macropore volume, the average pore diameter, the divinylbenzene content and the overall water regain of macroporous resins are variables which need to be studied before the optimal results can be obtained. It is not clear whether the incorporation of strongly ionized groups would improve the exchange rate in macroporous chelating resins, or whether fine particles of gel-type resins with superficial chelating groups as suggested earlier[17], would prove as advantageous as macroporous resins for column separations.

SUMMARY

The preparation and properties of chelating resins containing the oxine group have been studied. Condensation resins with the optimal swelling properties were made by control of the water content during curing. The resins have high capacity and selectivity, and a fast exchange rate resulted from the incorporation of a proportion of sulphonic acid groups. A resin of this type was used for rapid column separations. Polystyrene-based resins of the gel-type were less satisfactory.

REFERENCES

1 F. Vernon and H. Eccles, *Anal. Chim. Acta*, 63 (1973) 403.
2 J. R. Parrish, *Chem. Ind. (London)*, (1955) 386.
3 L. D. Pennington and M. B. Williams, *Ind. Eng. Chem.*, 51 (1959) 759.
4 R. Stevenson, M.Sc. Thesis, University of South Africa, Pretoria, 1962.
5 J. R. Parrish, *J. Appl. Chem.*, 15 (1965) 280.
6 *Dowex Chelating Resin A1*, The Dow Chemical Company, Michigan, 1959.
7 M. J. Holdoway, E. S. Lane and J. L. Willans, *Chem. Ind. (London)*, (1959) 483.
8 A. O. Jakubovic, *J. Chem. Soc.*, (1960) 4820.
9 H. Bernhard and F. Grass, *Monatsh. Chem.*, 98 (1967) 1050; *Mikrochim. Acta*, (1966) 426.
10 D. Whittington and J. R. Millar, *J. Appl. Chem.*, 18 (1968) 122.
11 Corrections, *Ind. Eng. Chem.*, 51 (1959) 1044.
12 H. Irving and R. J. P. Williams, *J. Chem. Soc.*, (1953) 3192.
13 L. G. Sillen and A. E. Martell, *Stability Constants of Metal-Ion Complexes*, The Chemical Society, London, 1964.
14 J. R. Parrish, *Chem. Ind. (London)*, (1956) 137.
15 R. V. Davies, J. Kennedy, E. S. Lane and J. L. Willans, *J. Appl. Chem.*; 9 (1959) 368.
16 R. F. Hirsch, E. Gancher and F. R. Russo, *Talanta*, 17 (1970) 483.
17 J. R. Parrish, *Nature*, 207 (1965) 402.

Analytica Chimica Acta, 70 (1974) 199–202

SHORT COMMUNICATION

Activation analysis for trace tellurium in rocks by extraction of the daughter nuclide

N. LAVI

Isotope Application Dept., Soreq Nuclear Research Centre, Yavne (Israel)

(Received 20th July 1973)

The determination by activation analysis of trace amounts of tellurium as found in rocks requires chemical processing of the irradiated samples because of the many interferences. Two products ^{131m}Te ($t_{\frac{1}{2}}$=30 h [1]) and ^{131}Te ($t^{\frac{1}{2}}$=25 min [1]) are obtained by thermal neutron activation of ^{130}Te. The ^{131}Te decays in two ways: 18% goes through isomeric transition to the ground state of ^{131}Te and 82% decays[2] by β-emission to excited levels of ^{131}I ($t_{\frac{1}{2}}$=8.05 d [1]). Since the half-life of the mother ^{131}Te is very short compared to that of the ^{131}I daughter, if the sample is left to decay for 6–8 h after the end of irradiation, the activity of ^{131}Te is negligible and the system behaves with a half-life of 8.05 d [1].

The contribution of the ^{131m}Te to the activity of ^{131}I behaves with a half-life of 30 h but since since the cross-section of the ^{130}Te (n, γ) reaction is 0.04 barns for ^{131m}Te formation against 0.22 barns for the 25-min ^{131}Te [3], this component is small (*ca.* 14 %) compared to the 25-min component. This contribution can be reduced to a negligible amount by allowing a delay of a few days after irradiation. Therefore the iodine activity extracted from the sample is proportional to the amount of tellurium which was irradiated.

A procedure has been developed for the separation of ^{131}I activities from the other isotopes produced from the irradiated sample; this has been applied to determine iodine in fission products[4]. Iodide is first oxidized to iodate with permanganate acidic solution, and iodine is formed by treatment with hydroxyammonium chloride and extracted with carbon tetrachloride. Back-extraction with water containing sodium pyrosulfite and ammonia (to prevent precipitation of Ag_2SO_3) produces iodide, which is precipitated as silver iodide and counted with a Ge(Li) detector, in order to ascertain the purity of the separated ^{131}I. The purity was found to be satisfactory, so that the less expensive and more efficient NaI (Tl) detectors can be used. This procedure was applied to determine tellurium in rocks by activation analysis, by means of extraction of the daughter nuclide.

Experimental

Irradiation and dissolution of samples. Wrap the rock samples (50–250 mg) in

aluminium foil. Add tellurium nitrate standards (0.01–1 μg Te) to other rock samples (see Table II) and wrap these similarly. Place the rock samples, samples treated with standards, and aluminium foil blanks into quartz ampoules, and irradiate for 4 days at a thermal neutron flux of $7 \cdot 10^{12}$ n cm^{-2} s^{-1} (IRR-1 reactor). After 7 days, transfer the samples to platinum crucibles containing potassium iodide carrier (20 mg I^-) and dissolve by heating with 10 ml of sulfuric acid. Dissolve the residue in 8 *M* sodium hydroxide and acidify with 6 *M* hydrochloric acid.

Transfer the standard and sample solutions to separatory funnels, using 25 ml of water for each. Add 2 ml of concentrated nitric acid and 1 ml of 2 *N* potassium permanganate to produce iodate. Add 10 ml of 2 *M* hydroxyammonium chloride solution and extract the iodine by shaking with three 25-ml portions of carbon tetrachloride. Wash the separated organic layer with 15 ml of water containing 6–7 drops of reducing solution (1 g of sodium pyrosulfite and 5 ml of ammonia liquor in 25 ml of water), shaking until both phases are colorless: discard the organic layer. Transfer the aqueous layer to a 100-ml beaker, add 3 ml of 6 *M* nitric acid and boil for some minutes to expel sulfur dioxide which interferes with precipitation of silver iodide. Add 2 ml of 0.1 *M* silver nitrate solution to precipitate silver iodide.

Filter the solution with suction through a Whatman 41 paper supported on sintered glass and wash with 20 ml of water and 10 ml of ethanol. Dry the precipitate, mounted on an aluminium disc and covered with a thin mylar sheet, at 100° under an infrared lamp.

The chemical yield is *ca.* 80%.

Counting. Measure the activity ^{131}I with a 60-cm^3 Ge(Li) detector, counting for 40 min. A true coaxial detector was used. The output signal was passed through a 101 preamplifier (Seforad Ltd., Emek Hayarden, Israel) and a linear amplifier (Tennelec TCL03 BLR, U.S.A.), for analysis by a 4096-channel analyzer (Packard).

The energy resolution (f.w.h.m.) of the system was 1.6 keV for 122-keV ^{57}Co γ-rays and 2.6 keV for 1332-keV ^{60}Co γ-rays. The absolute photopeak efficiency curve of the Ge(Li) detector was obtained by counting absolutely calibrated sources (I.A.E.A., Vienna). The 364.5-keV peak of ^{131}I (branching ratio 82% [1]) was chosen.

Calculate the tellurium concentration in p.p.m. from:

$$\text{Te (p.p.m.)} = xA/(Ay-A)w \qquad (1)$$

where A is the peak area of the ^{131}I–364.5-keV γ-ray of the treated sample; Ay is the corresponding peak area of the treated sample + standard, measured under the same geometrical conditions and corrected to the time of measuring A, w is the weight of sample taken (in g), and x is the tellurium weight in standard added (in μg).

Results and discussion

The method used for the separation of the daughter nuclide is highly efficient, so that tellurium can be accurately determined in rocks by separating iodine from the bulk of the other isotopes obtained by irradiation. The use of internal tellurium standards with the samples corrects for the contribution of

^{131m}Te to ^{131}I, because all samples and standards are irradiated for the same time and eventually separated simultaneously. The activity of ^{131}I is thus proportional to the amount of tellurium which was irradiated. The γ-ray spectra of ^{131}I extracted from a 1-μg tellurium standard and a rock sample are given in Fig. 1.

The reproducibility of the separation described was studied by adding different amounts of irradiated tellurium tracer to the nonirradiated rock solution. Table I shows the results obtained.

The results for the determination of tellurium in rock samples by the developed procedure are given in Table II. The results are in good agreement with those obtained by spectrographic analysis[5].

TABLE I

REPRODUCIBILITY OF ^{131}I SEPARATION

Weight of Te standard added (μg)	*Peak area (counts in 40 min)*	*Counts/μg Te*	*Weight of Te standard added (μg)*	*Peak area (counts in 40 min)*	*Counts/μg Te*
0.01	619	61900	0.2	12170	60850
0.01	595	59500	0.2	11850	59250
0.02	1196	59800	0.5	30890	61780
0.02	1190	59500	0.5	31400	62800
0.05	3090	61800	1.0	62150	62150
0.05	3120	62400	1.0	61880	61880
0.1	6120	61200		Average counts	61134 ± 1185
0.1	6107	61070			(1.94%)

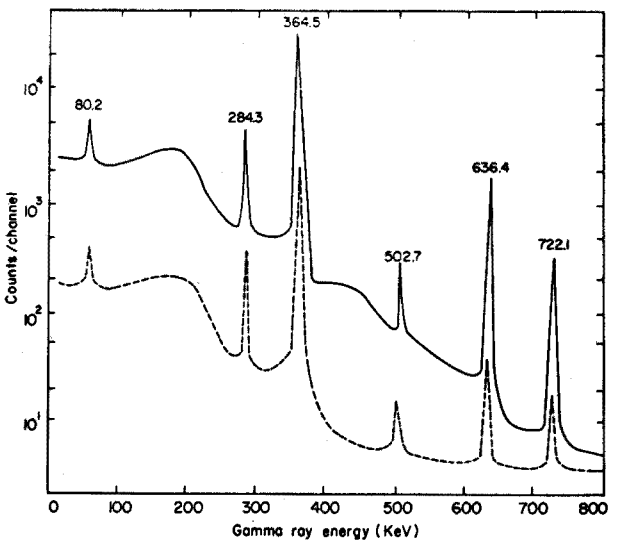

Fig. 1. A comparison of γ-ray spectra of ^{131}I obtained from a 1-μg Te standard (——) and a 102.5-mg rock sample (---). 60 cm^3 Ge(Li) detector, 4 days irradiation, 40 min counting time, 7 days after end of irradiation.

TABLE II

TELLURIUM CONTENT OF ROCK SAMPLES

Weight in aliquot taken (mg)	*Weight of Te standard in aliquot added (μg)*	*A*[a]	*Ay*[a]	*Ay-A*	*Te (p.p.m.) in sample*	
					Present method	*Spectrographic method (ref. 5)*
Syenite Rock-1 (Canadian Association for Applied Spectroscopy Standards)						
53	—	2206				
53	0.1		8106	5900	0.705	0.8
102.5	—	4611				
102.5	0.1		10620	6009	0.748	
155	—	6786				
155	0.1		12786	6000	0.730	
205	—	8865				
205	0.1		14915	6050	0.715	
260	—	11500				
260	0.1		17350	5850	0.755	
					0.730 ± 0.021 (2.88%)	
B.C.R.I.St. (U.S. Geological Survey)						
105	—	320				
105	0.01		906	586	0.052	0.05
205	—	680				
205	0.01		1300	620	0.055	
240	—	830				
240	0.01		1445	615	0.056	
					0.054 ± 0.0023 (4.25%)	

[a] See eqn. (1).

REFERENCES

1 M. A. Wakat, *Nuclear Data Tables*, 8, 1971, p. 467.
2 C. M. Lederer, J. M. Hollander and I. Perlman, *Table of Isotopes*, 6th Ed., Wiley, New York, 1967, p. 68.
3 *Chart of the Nuclides*, 3rd Ed., Bundesminister für Wissenchaftlich Forschung, Bonn, 1968.
4 N. Lavi, *J. Radioanal. Chem.*, in press.
5 I. Shoenfeld, to be published.

Analytica Chimica Acta, 70 (1974) 203

SHORT COMMUNICATION

Errors in the ASTM X-ray Powder Diffraction File for gamma hexachlorocyclohexane (gammexane, benzene hexachloride), and 1,2,3,4,5,6-hexachlorocyclohexane (lindane).

G. SMITH and C. H. L. KENNARD

Department of Chemistry, University of Queensland, Brisbane, Qld., 4067 (Australia)

(Received 11th September 1973)

Although the ASTM 1970 Organic Index to the X-ray Powder Diffraction File has two entries: 5-0449 Gamma hexachlorocyclohexane (Gammexane, benzene hexachloride) and 8-686, 1,2,3,4,5,6-Hexachlorocyclohexane (Lindane), these compounds are identical[1,2]. The cell dimensions[3] should be $a=8.52$, $b=10.27$, $c=13.94$ Å, $\beta=121°\ 16'$, $P2_1/c$, $Z=4$. The powder pattern for the γ (aaaeee) isomer of 1,2,3,4,5,6-hexachlorocyclohexane is that listed for 5-0449. The reference given for 8-686 refers to the β-isomer[4] although there is an ASTM entry 8-811 for this compound.

REFERENCES

1 E. E. Toops and J. A. Riddick, *Anal. Chem.*, 23 (1951) 1106.
2 E. Y. Spencer, *Guide to the Chemicals used in Crop Protection*, Canadian Department of Agriculture, 5th Edn., 1968, p. 3–4.
3 G. W. Van Vloten, Ch. A. Kruissink, B. Strijk and J. M. Bijvoet, *Acta Crystallogr.*, 3 (1950) 139.
4 R. G. Dickinson and C. Bilicke, *J. Amer. Chem. Soc.*, 50 (1928) 764.

Analytica Chimica Acta, 70 (1974) 204–206

SHORT COMMUNICATION

The determination of manganese in lubricating oils by carbon filament atomic absorption spectrometry

G. L. EVERETT and T. S. WEST
Department of Chemistry, Imperial College of Science and Technology, London SW7 2AY (England)
R. W. WILLIAMS
B.P. Research Centre, Sunbury-on-Thames, Middlesex (England)
(Received 10th October 1973)

The use of the carbon filament atom reservoir for the determination of several trace elements in lubricating oils has been described in previous communications from this laboratory[1–3]. The extension of the technique to include manganese is described here.

Manganese compounds are used as additives in the petroleum industry although they are not as frequently found or as important as other trace elements, *e.g.* vanadium. For example, methylcyclopentadienylmanganese tricarbonyl (AK-33X) is used in aircraft fuel as an anti-knock agent and also as an additive to heating oils to reduce flue gas smoke. However, the importance of controlling manganese levels in fuel oils, etc., cannot be overstressed because concentrations of 0.005 p.p.m. (w/v) and above in the atmosphere may lead to a danger of contraction of pneumonia and manganism[4].

Instrumental arrangement

This was basically the same as described previously[3] except that there was no need for a damping condenser across the input terminals of the oscilloscope, owing to the difference in thermal and spectral characteristics of manganese.

The experimental parameters used were: monochromator slit-width, 0.03 mm; lamp-current, 10 mA; nitrogen flow rate, 2.5 l min^{-1}; E.H.T., −1100 V; collimator slit size, 0.5 × 3 mm. Manganese atomic lines at 279.48 nm and 403.1 nm were used. The less sensitive line at 403.1 nm permits high concentration ranges to be used so that the analytical method described here extends over a 3.5 decade sequence, *i.e.* from $5 \cdot 10^{-3}$–10 p.p.m.

Calibration solutions

Manganese naphthenate was dissolved in redistilled 100°–120° boiling range petroleum ether to give a stock solution of 314 p.p.m. Mn. All solutions were freshly made up by dilution of this stock. The solvent, petroleum ether, gave no blank reading when subjected to atomic absorption measurements as proposed.

Sample addition and pretreatment

Samples of standards or specimen samples were introduced onto the filament by means of 1-μl disposable Drummond glass micropipettes (Shandon Scientific Ltd.). Samples were dried at 1.2 V (100°) for 10 s, ashed at 3.6 V (580°) for 15 s and then atomized at 11.4 V (*ca.* 2800°). This sequence may be repeated with fresh samples every 90 s. The reproducibility of this procedure calculated from 15 replicates at the 0.1-ng level of manganese was $\pm 3\%$.

TABLE I

ATOMIC ABSORPTION SENSITIVITY AND DETECTION LIMIT DATA FOR MANGANESE NAPHTHENATE SOLUTIONS ON THE CARBON FILAMENT

Wavelength (nm)	*Sensitivity for 1% absorption (g)*	*Detection limit (S:N = 2) (g)*
279.48	$2.5 \cdot 10^{-12}$	$3.3 \cdot 10^{-12}$
403.1	$2.5 \cdot 10^{-11}$	$5.0 \cdot 10^{-11}$

TABLE II

ANALYSIS OF MANGANESE IN LUBRICATING OILS AND AIRCRAFT FUEL BY ATOMIC ABSORPTION AT A CARBON FILAMENT

Sample	*Mn found % (w/w)*	*Mn given[a] % (w/w)*	*Sample*	*Mn found (p.p.m.)*	*Mn given[b] (p.p.m.)*
Lubricating oil			Aircraft turbine distillates		
1	1.10	1.07	Progil 1	0.050 ± 0.005	<0.1
2	0.60	0.58	2	0.051 ± 0.005	<0.1
3	0.30	0.30	Libyan 1	0.069 ± 0.007	<0.1
4	0.15	0.16	2	0.056 ± 0.005	<0.1
5	0.06	0.077	3	0.065 ± 0.006	<0.1

[a] Calculated values as supplied by BP Ltd.
[b] Flame A.A.S. data supplied by BP Ltd.

Results

The 1% absorption sensitivities and limits of detection are shown in Table I. These compare very well with the corresponding data for aqueous solutions of manganese on the carbon filament atom reservoir[5]. The calibration at 279.48 nm is linear from 0–0.1 ng and useable to 0.2 ng, but that for 403.1 nm is curved over the complete range, 0.2–10 ng. This is thought to be largely due to the fact that a triplet of lines (403.1, 403.3, 403.4 nm) of differing oscillator strengths are included in the band-pass of the monochromator used in these experiments.

Five synthetic SAE 10 lubricating oils were analysed at 403.1 nm and two aircraft turbine distillates at 279.48 nm. The results are shown in Table II.

Conclusion

Manganese in lubricating oils may be readily determined in the range

0.005–10 p.p.m. by choice of either of two resonance wavelengths at 279.48 and 403.1 nm. The reproducibility and accuracy of the method are good, and it is fast, simple and efficient.

We are grateful to the SRC for the award of a CAPS Studentship to G.L.E. and to BP Ltd. for the provision of standards and analytical samples.

REFERENCES

1 J. F. Alder and T. S. West, *Anal. Chim. Acta*, 58 (1972) 331.
2 J. F. Alder and T. S. West, *Anal. Chim. Acta*, 61 (1972) 135.
3 G. L. Everett, T. S. West and R. W. Williams, *Anal. Chim. Acta*, 66 (1973) 301.
4 J. W. Hwang, *Anal. Chem.*, 44 (1972) 20A.
5 L. C. Ebdon, G. F. Kirkbright and T. S. West, *Anal. Chim. Acta*, 58 (1972) 39.

Analytica Chimica Acta, 70 (1974) 207–212

SHORT COMMUNICATION

1-(2-Carboxy-5-sulfonatophenyl)-3-hydroxy-3-phenyltriazene, a reagent for spectrophotometric analysis

D. CHAKRABORTI

Department of Inorganic and Analytical Chemistry, Jadavpur University, Calcutta-32 (India)

(Received 11th July 1973)

A water-insoluble organic reagent used for colorimetric analysis can often be made water-soluble, without changes of other essential properties, by introducing a sulfonic acid group (sodium salt) in addition to the chelating group. Sometimes, however, the mere presence of the sulfonic acid group as a non-coordinating centre, as well as a shift in its position, may cause anomalous behaviour compared to the parent reagent, in terms of pH and temperature effects, reaction rates, etc.; such changes are thought to be due to resonance effects and steric interaction[1–3].

The present communication describes a study of 1-(2-carboxy-5-sulfonatophenyl)-3-hydroxy-3-phenyltriazene (reagent C), a 5-sulfonato (sodium salt) derivative of 1-(*o*-carboxyphenyl)-3-hydroxy-3-phenyltriazene (reagent B)[4], as a spectrophotometric reagent for various metal ions. Because the sulfonic acid group in the 5-position, reagent C differs in some respects from the parent reagent (reagent B), and also from reagent A, which is a 4-sulfonato (sodium salt) derivative of the same parent reagent[5–7]. The characteristic features of the three reagents are as follows: reagent A shows no color reaction with titanium(IV), but reagents C and B (ref. 8) both form colors. Reagent A (ref. 5) is highly sensitive for molybdenum(VI), whereas reagents B and C show poor spectrophotometric sensitivity for this metal. Reagent A is quite efficient as a metallochromic indicator and for indirect spectrophotometric determinations of fluoride and oxalate[7], whereas reagents B and C yield poor end-points and cannot be used for the anion determinations, because of the instability of the iron(III)–reagent complex.

Amongst several reported triazenes including reagents A and B, reagent C proves to be the most efficient spectrophotometric reagent for iron(III) and vanadium(V), hence these complexes with reagent C are described here in detail, whereas the complexes with Cu(II), Ni(II), Pd(II), Ti(IV) and Mo(VI) are simply summarized (Table I). Determinations of V(V), Fe(III), Cu(II), and Pd(II) in binary mixtures were carried out with the help of sodium thiosulfate as masking agent.

Preparation of 1-(2-carboxy-5-sulfonatophenyl)-3-hydroxy-3-phenyltriazene

4-Sulfoanthranilic acid was diazotized in the cold and coupled with freshly

TABLE I

1-(2-CARBOXY-5-SULFONATOPHENYL)-3-HYDROXY-3-PHENYLTRIAZENE AS A SPECTROPHOTOMETRIC REAGENT FOR Pd^{2+}, Mo^{6+} Ni^{2+}, Cu^{2+} AND Ti^{4+}

Ion	*Color*	*Absorbance (nm)*	*Reagent required*	*Beer's law (p.p.m.)*	*Optimal range (p.p.m.)*	*Sensitivity ($\mu g\ cm^{-2}$)*	*Molar absorptivity*	*Photometric error (%)*	*pH range*	*Composition*	*Dissn. const.*	*Stability of complex (h)*
Pd^{2+}	Yellow	410[a] 420[b]	5 ml 0.1% w/v	0.5– 7.0	1.0– 7.0	0.0072	15178	2.74	1.0– 5.7	1:2	$4.0 \cdot 10^{-11}$	36
Mo^{6+}	Light yellow	410–430				0.168						
Ni^{2+}	Yellow green	410[a] 410[b]	7 ml 0.025% w/v	0.125– 1.5	0.25– 1.5	0.0018	34375	2.82	9.8– 10.5	—	—	18
Cu^{2+}	Yellow green	400[a] 410[b]	3 ml 0.025% w/v	0.25– 4.0	0.5– 4.0	0.0042	15161	2.74	1.8– 9.7	1:2	$5.0 \cdot 10^{-11}$	48
Ti^{4+}	Golden yellow	420[a] 420[b]	8 ml 0.2% w/v	0.25– 5.0	0.5– 5.0	0.0067	7108	2.82	1.8– 3.5	—	—	10

[a] Maximum absorbance.
[b] Working absorbance.

prepared phenylhydroxylamine. The pH of the mixture was raised to 5.0–6.0 with saturated sodium acetate solution. The deep yellow precipitates were filtered and crystallized thrice from water, when yellow crystals (m.p. 180°, decomp.) were obtained (found: 11.7% N, 43.47% C, 2.81% H; required 11.7% N, 43.45% C, 2.8% H). The reagent is stable to heat, light and air and can be stored indefinitely. The analogous 4-sulfonatophenyl reagent was prepared similarly from 5-sulfoanthranilic acid as the starting material.

Apparatus and solutions

Apparatus and solutions of iron(III) chloride, ammonium vanadate, copper sulfate, palladium chloride, nickel chloride, ammonium molybdate, and titanium(IV) as sulfate were the same as reported previously[5–9].

The reagent was used as 0.2%, 0.1% and 0.025% (w/v) solutions in water.

Absorbance curves

Vanadium(V). Mix the solution containing 100 or 50 μg of vanadium(V) with the reagent solution (6 ml, 0.025% w/v) and 10 ml of distilled water. Adjust the pH to about 4.0, dilute to 25 ml in a volumetric flask and measure the absorbance against the reagent as blank. The absorbance spectra (curves A and B in Fig. 1) show maximal absorption at 400 nm.

Iron(III). To the iron solution (100 or 50 μg of iron) in a 50-ml beaker, add the reagent solution (5 ml, 0.1%) and adjust its pH to 4–6 with dilute hydrochloric acid; transfer the solution to a 25-ml volumetric flask, dilute to the mark with water, mix and measure the absorbance of the violet complex against a reagent blank. Curves C and D in Fig. 1 show that the absorbance of the iron(III) system is maximal at 400 nm.

Effect of variables

All measurements for iron(III) and vanadium(V) were made at 410 nm; at this wavelength, the absorption of the reagent itself was much less.

The color intensities remained unchanged in the pH ranges 2.1–5.9 for vanadium(V) and 3.3–10.2 for iron(III). The intensity decreased outside these pH limits.

For complete color development, 4 p.p.m. of vanadium(V) or iron(III) required 5 ml (0.025% w/v) or 4 ml (0.1% w/v) of reagent solutions, respectively. The color intensities remained constant for 36 h for vanadium(V) and 72 h for iron(III).

Beer's Law and molar absorptivity

Beer's law was obeyed over the range 0.25–5.0 p.p.m. for vanadium and 0.5–8.0 p.p.m. for iron. The optimal concentration ranges evaluated by Ringbom's method[10] were 0.50–5.0 and 1.0–8.0 p.p.m. for vanadium(V) and iron(III), respectively. The percentage relative errors per 1% absolute photometric error[11] for the systems were 2.81 for vanadium(V) and 2.75 for iron(III). The Sandell sensitivities ($\log I_0/I = 0.001$)[12] were 0.00548 μg cm^{-2} for vanadium(V) and 0.0071 μg cm^{-2} for iron(III), with molar absorptivities of 9180 and 7890, respectively.

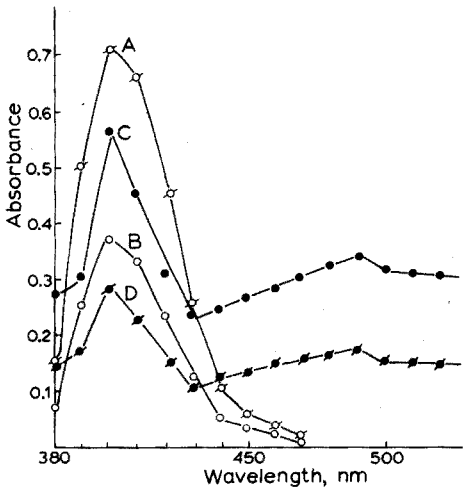

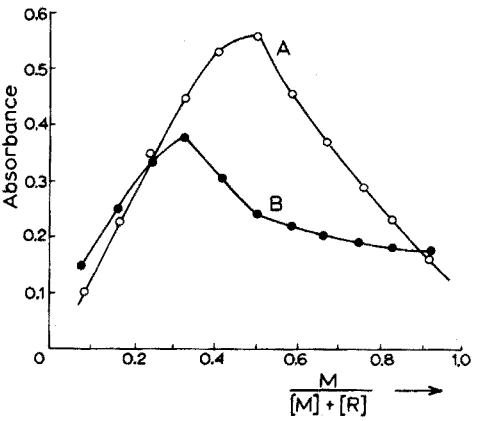

Fig. 1. Absorption spectra: (A) vanadium(V), 4 p.p.m.; (B) vanadium(V), 2 p.p.m.; (C) iron(III), 4 p.p.m.; (D) iron(III), 2 p.p.m.

Fig. 2. Job's method (equimolar): (A) [vanadium(V)] = [reagent] = $3.0 \cdot 10^{-4} M$; (B) [iron(III)] = [reagent] = $0.5 \cdot 10^{-3} M$.

Composition of the complexes

The compositions of the vanadium and iron complexes were determined by the modified Job's method of continuous variations[13] (Fig. 2). The curves indicate that vanadium combines with the reagent in the ratio of 1:1, but iron combines in the ratio 1:2. These results were confirmed by the mole ratio method[14].

The degree of dissociation, α, was calculated from Harvey and Manning's equation[15]. The instability constants evaluated from the equation $K = (m\,\alpha\,c)^m \cdot (n\,\alpha\,c)^n / c(1-\alpha)$ where $m = n = 1$ for vanadium(V) and $m = 1$, $n = 2$ for iron(III), are given in Table II. The stability constants of the complexes were also evaluated from a study of the absorbance of complementary mixtures of non-equimolar solutions of metal ions and reagent. The values calculated from the equation[16] are also reported in Table II.

Effect of diverse ions

The ions studied for interference in the vanadium(V) and iron(III) systems were those mentioned earlier[5]. Ions such as phosphate, oxalate, fluoride, tartrate, citrate which interfered[5] in the iron(III)–reagent A method could be tolerated to a much greater extent in the iron(III)–reagent C system.

In the iron(III) system, EDTA, Pd(II), Ti(IV), Cu(II), V(V) interfered. In the presence of sodium thiosulfate, 50 p.p.m. of Cu(II) and 8 p.p.m. of Pd(II) could be tolerated.

In the vanadate system, Cu(II), Ti(IV), Pd(II), Fe(III) and EDTA interfered. However, in the presence of thiosulfate, Cu(II) and Pd(II) up to 10 p.p.m. could be tolerated.

TABLE II

STABILITY CONSTANTS OF 1-(2-CARBOXY-5-SULFONATOPHENYL)-3-HYDROXY-3-PHENYLTRIAZENE COMPLEXES

Harvey–Manning method

Complex	E_m	E_s	c	α	K
V(V)	0.73	0.595	$4 \cdot 10^{-4}$	0.184	$1.6 \cdot 10^{-5}$
Fe(III)	0.49	0.38	$1 \cdot 10^{-3}$	0.22	$5.4 \cdot 10^{-8}$

Majumdar–Sen method

Metal concn. (c)	*Reagent concn. (M)*	m	n	p	x	K
V(V), $1.5 \cdot 10^{-4}$	$4.5 \cdot 10^{-4}$	1	1	3	0.33	$2.2 \cdot 10^{-5}$
Fe(III), $0.5 \cdot 10^{-3}$	$1.0 \cdot 10^{-3}$	1	2	2	0.58	$6.3 \cdot 10^{-8}$

Determination of metal ions in binary mixtures

For the determination of: (i) vanadium(V), copper(II); (ii) vanadium(V), palladium(II); (iii) iron(III), copper(II); (iv) iron(III), palladium(II) in the presence of each other, the procedure described above for the absorbance measurement was followed, with the addition of complexing agent. To the sample solution were added 5 ml of the reagent solution (0.1% w/v) and distilled water, to dilute eventually to 25 ml. After suitable adjustment of conditions (see below), the measurements were made at 410 nm.

(i) Vanadium and copper. First in an aliquot of the solution, the total absorbance (A) caused by the two metal ions was measured, the pH being maintained at 2.1–5.9. The absorbance (B) of vanadium(V) alone was then measured in a second aliquot treated with 5 ml of 1% sodium thiosulphate solution and adjusted to about pH 4.0. (A–B) gave the amount of copper(II) present (Table III).

TABLE III

DETERMINATION OF BINARY MIXTURES

Binary mixture	*Amount present (p.p.m.)*	*Amount found (p.p.m.)*	*Binary mixture*	*Amount present (p.p.m.)*	*Amount found (p.p.m.)*
V(V)	1.0	0.977	V(V)	3.0	2.97
Cu(II)	2.0	2.01	Pd(II)	1.0	1.01
V(V)	2.0	1.966	V(V)	2.0	1.954
Cu(II)	1.0	1.02	Pd(II)	2.0	2.03
Fe(III)	4.0	3.97	Fe(III)	4.0	3.94
Cu(II)	2.0	2.04	Pd(II)	2.0	2.04
Fe(III)	2.0	1.94	Fe(III)	3.0	2.96
Cu(II)	3.0	3.03	Pd(II)	2.0	2.07

(ii) Vanadium and palladium. These metals were determined in the same way as vanadium and copper, except that in the first step the pH was adjusted to 2.1–5.7. Results are given in Table III.

(iii) Iron and copper. The absorbance (A) of the two metal ions was measured in an aliquot at pH 3.3–9.7. Then, in another aliquot, the absorbance (B) for only iron(III) was measured; an interval of 15 min was allowed after the addition of 5 ml of sodium thiosulphate (1% w/v) at about pH 4.0. ($A-B$) gave the amount of copper(II) present (Table III).

(iv) Iron and palladium. At pH 3.3–5.7 the absorbance (A) for both iron(III) and palladium(II) was obtained. In another aliquot containing sodium thiosulphate (5 ml, 1%), at about pH 4.0, the absorbance (B) of only iron(III) was obtained. Palladium(II) was then found by difference (Table III).

The author acknowledges his indebtedness to Prof. A. K. Majumdar for encouragement and advice.

REFERENCES

1 E. L. Stelle and J. H. Yoe, *Anal. Chem.*, 29 (1957) 1622.
2 H. C. Wingfield and J. H. Yoe, *Anal. Chim. Acta*, 14 (1956) 446.
3 E. L. Stelle and J. H. Yoe, *Anal. Chim. Acta*, 20 (1959) 205.
4 A. K. Majumdar and S. C. Saha, *Anal. Chim. Acta*, 40 (1968) 299.
5 A. K. Majumdar and D. Chakraborti, *Anal. Chim. Acta*, 53 (1971) 127.
6 A. K. Majumdar and D. Chakraborti, *Anal. Chim. Acta*, 53 (1971) 393.
7 A. K. Majumdar and D. Chakraborti, *Anal. Chim. Acta*, 55 (1971) 450.
8 A. K. Majumdar and S. C. Saha, *Anal. Chim. Acta*, 44 (1969) 85.
9 A. K. Majumdar and D. Chakraborti, *Z. Anal. Chem.*, 257 (1971) 33.
10 A. Ringbom, *Z. Anal. Chem.*, 115 (1938) 332.
11 G. H. Ayres, *Anal. Chem.*, 21 (1949) 652.
12 E. B. Sandell, *Colorometric Determination of Traces of Metals*, Interscience, New York, 3rd Edn., 1959.
13 P. Job, *Compt. Rend.*, 180 (1925) 928; *Ann. Chim. (Paris)*, 9 (1928) 113.
14 J. H. Yoe and A. K. Jones, *Ind. Eng. Chem., Anal. Ed.*, 16 (1944) 111.
15 A. E. Harvey Jr. and D. L. Manning, *J. Amer. Chem. Soc.*, 72 (1950) 4488.
16 A. K. Majumdar and B. Sen, *Anal. Chim. Acta*, 8 (1953) 369.

Analytica Chimica Acta, 70 (1974) 213–216

SHORT COMMUNICATION

2,2,5,5-Tetrakis(carboxymethylthio)-*p*-dithian, ein neues Nachweisreagens für Kohlenhydrate und aromatische Aldehyde

G. KUNOVITS

Abteilung für Vitamin- und Ernährungsforschung, F. Hoffmann-La Roche & Co. A.G., Basel (Schweiz)

(Eingegangen den 28. September 1973)

In einer früheren Publikation[1] wurde die Reaktion der Kohlenhydrate und aromatischer Aldehyde mit Cystein und Thioglykolsäure beschrieben. Wir stellten dabei fest, dass Furfurol und Dihydroxyäthylfurfurol (Abbauprodukte der Pentosen und Heptosen) mit Cystein nach Ringöffnung Thiomethinfarbstoffe der folgenden allgemeinen Formel bilden (Dische-Reaktion):

$$[R\text{–}S\text{=}CH\text{–}CH\text{=}CH\text{–}\underset{\displaystyle OH}{\underset{|}{C}}\text{=}CH\text{–}S\text{–}R]^{\oplus}\cdot X^{\ominus}$$

wo

$X = HSO_4, ClO_4$; R = aliphatischer Rest.

Auffallend bei dieser Reaktion ist die Tatsache, dass der Ring des Hydroxymethylfurfurol (Abbauprodukt der Hexosen, im weiteren HMF) infolge Resonanzstabilisierung durch Cystein nicht aufgespalten wird und die Bildung der Thiomethinfarbstoffe ausbleibt. Mit Thioglykolsäure konnten wir dagegen unter bestimmten Reaktionsbedingungen zum rotvioletten Thiomethinkation gelangen. Inzwischen isolierten wir das nachstehend beschriebene Thioglykolid, das mit Kohlenhydraten und aromatischen Aldehyden in H_2SO_4 (70 vol%) analog der Thioglykolsäure in H_2SO_4 (90 vol%) reagiert.

2,2,5,5-Tetrakis (carboxymethylthio)-p-dithian (TCD)

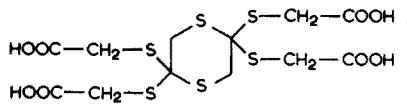

Die Verbindung haben wir nach den Angaben von Schöberl und Wiehler[2] aus einem Gemisch von Thioglykolsäure und konzentrierter Salzsäure nach Lagerung unter Stickstoff isoliert.

Diese Tetracarbonsäure ist schwer löslich in kaltem Wasser, Benzol, Äther, chlorierten Kohlenwasserstoffen, wenig löslich in Aceton, Äthanol, Eisessig und heissem Wasser, leicht löslich in Dimethylformamid und Dimethylacetamid. Mit konzentrierter H_2SO_4 und $HClO_4$ (70%) entsteht eine orangerote Halochromie,

die innerhalb einiger Min zu Zitronengelb verblasst. Diese Farbe verschwindet aber nach Verdünnung mit Wasser sofort.

Nachweis von Kohlenhydraten

Lösung. 30 mg TCD ad 10 ml Dimethylformamid (TCD-Reagens). Die TCD ist bei der Fluka A.G. (Buchs, Schweiz) erhältlich.

Ausführung. In einem starkwandigen Reagensglas mit Schliff von 5–10 ml Inhalt werden 2.5 ml H_2SO_4 (70 vol%), 0.1 ml Kohlenhydratlösung (0.1 mg ml^{-1}) in Wasser und 0.1 ml Reagens vorgelegt und gut gemischt. Die Mischung wird während 15 Min im siedenden Wasserbad erhitzt und sofort auf Zimmertemperatur abgekühlt. Anschliessend misst man die Extinktion der Probe bei 550 nm gegen eine Blindprobe. Die Extinktion ist proportional der Konzentration des betreffenden Kohlenhydrats (Konzentrationsbereich 10^{-4}–10^{-5} *M*).

Für die Prüfung der Nachweisreaktion haben wir die molaren Extinktionskoeffizienten einiger reiner Zucker und verwandter Stoffe ermittelt. Aus Tabelle I ist ersichtlich, dass die wichtigsten Zucker etwa den gleichen molaren Extinktionskoeffizienten besitzen. Die hohen Koeffizienten für Maltose und Saccharose (etwa doppelt so hoch wie bei Glucose) ergeben sich aus der Struktur (Disaccharide).

TABELLE I

REAKTION DER KOHLENHYDRATE MIT TCD

Kohlenhydrat	λ_{max}	*Farbe*	*log* ε^a
Xylose	525	orangerot	4.30
Fructose	550	rot	4.48
Galaktose	550	rot	4.21
Glucose	550	rot	4.43
Maltose	550	rot	4.70
Saccharose	550	rot	4.72
Sedoheptulose	520	orangerot	4.16
Ascorbinsäure	520	orange	3.52
Glucuronsäure	520	orange	3.93

[a] Molarer Extinktionskoeffizient.

Nachweis von Blutzucker

Lösungen. Siehe oben, anstelle von Kohlenhydrat enteiweisstes Filtrat (0.1 ml Vollblut + 1.0 ml Trichloressigsäure 15%).

Ausführung. Siehe oben, anstelle von 0.1 ml Kohlenhydratlösung 0.05 ml enteiweisstes Filtrat.

Der Vergleich dieser Methode mit der bekannten *o*-Toluidin-Methode ergab, dass das TCD-Reagens etwa achtmal empfindlicher ist als *o*-Toluidin.

Nachweis von Ketohexosen neben Aldohexosen

Während für den Abbau von Aldohexosen zu HMF durch Säuren Hitzeeinwirkung notwendig ist, werden Ketohexosen von der H_2SO_4 in der Kälte vollständig zu HMF umgewandelt. Das TCD-Reagens reagiert spontan bei Zimmertemperatur mit HMF. Aldohexosen stören nicht. Die Geschwindigkeit der Wasser-

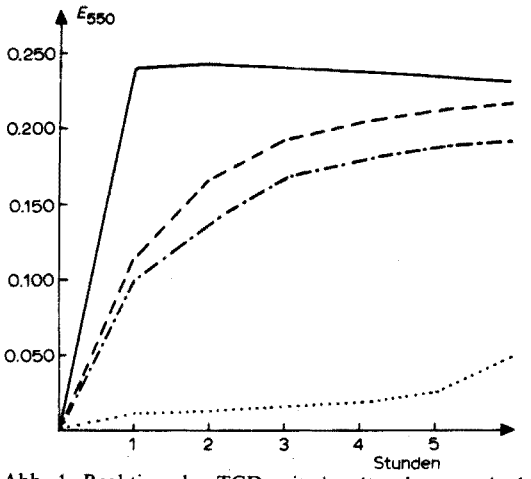

Abb. 1. Reaktion des TCD mit den Ketohexosen in kalter H_2SO_4 in Abhängigkeit von der Zeit: (—) D-Tagatose; (——) D-Fructose; (—·—) L-Sorbose; (· · · ·) D-Glucose.

abspaltung bei den einzelnen Ketohexosen ist jedoch unterschiedlich (Abb. 1). Bei der Messung der Extinktion muss diese Tatsache berücksichtigt werden.

Ausführung. 2.5 ml H_2SO_4 (70 vol%), 0.1 ml Kohlenhydratlösung (0.1 mg ml^{-1}) und 0.1 ml TCD-Reagens werden zusammengemischt und bei Zimmertemperatur stehen gelassen.

TABELLE II

REAKTION DES TCD MIT AROMATISCHEN ALDEHYDEN

Aldehyd	λ_{max}	*log* ε^a	*Farbe*
Benzaldehyd	480	4.52	orange
2-Hydroxybenzaldehyd	530	4.50	orangerot
3-Hydroxybenzaldehyd	480	4.31	orange
4-Hydroxybenzaldehyd	540	4.41	rot
2-Methoxybenzaldehyd	540	4.36	rot
3-Methoxybenzaldehyd	480	4.38	orange
4-Methoxybenzaldehyd	550	4.64	rot
2,4-Dihydroxybenzaldehyd	560	3.58	rosa
3,4-Dihydroxybenzaldehyd	560	4.44	rotviolett
2,3-Dimethoxybenzaldehyd	480	4.27	orange
2,4-Dimethoxybenzaldehyd	572	3.09	olivgrün
2,5-Dimethoxybenzaldehyd	574	4.08	dunkelgrün
2-Nitrobenzaldehyd	keine Reaktion		
3-Nitrobenzaldehyd	keine Reaktion		
4-Nitrobenzaldehyd	keine Reaktion		
Veratrumaldehyd	562	4.54	rotbraun
Vanillin	562	4.37	rotviolett
Syringaaldehyd	582	4.42	grün
Piperonal	572	4.30	olivgrün
Zimtaldehyd	550	4.45	rot
2-Hydroxynaphtaldehyd	keine Reaktion		

[a] Molarer Extinktionskoeffizient.

Nachweis von aromatischen Aldehyden

Wenn man das TCD-Reagens mit Hydroxy- oder Methoxy-substituierten Benzaldehyden bei Zimmertemperatur in H_2SO_4 (70 vol%) stehen lässt, werden die Mischungen in 1–2 Stunden unterschiedlich je nach Aldehyd von orange bis dunkelgrün gefärbt. Wir haben 21 Aldehyde untersucht (Tabelle II).

Ausführung. Siehe oben für Ketohexosen.

LITERATUR

1 G. Kunovits, *Anal. Chim. Acta*, 55 (1971) 221.
2 A. Schöberl und G. Wiehler, *Ann. Chem.*, 595 (1955) 101.

Analytica Chimica Acta, 70 (1974) 217–221

SHORT COMMUNICATION

Dosage spectrophotométrique de traces de fluorure après extraction par solvant

H. CHERMETTE

Institut de Physique Nucléaire, Université Claude Bernard, Lyon-1; Institut National de Physique Nucléaire et Physique des Particules, 43, Bd du 11 Novembre 1918, 69621-Villeurbanne (France)

M. PERROUSSET et J. RATELADE

Institut de Chimie et de Physique Industrielle, 25, rue du Plat, 69288-Lyon Cedex 1 (France)

(Reçu le 10 octobre 1973)

Le dosage précis du fluorure dans les solutions aqueuses est un problème important en chimie analytique à cause entre autres du danger que pourrait représenter une trop forte concentration de cet élément (pollution). A l'heure actuelle, deux méthodes commodes sont largement utilisées: la spectrophotométrie et la potentiométrie à l'aide de l'électrode spécifique au fluorure. Cette dernière, la plus récente, permet souvent un dosage direct dans le milieu, mais une séparation préalable est cependant nécessaire en cas d'interférences ou de faibles teneurs en fluorure[1]. Par contre, les méthodes colorimétriques présentent en général des interférences provoquées par des ions usuels, aussi il est difficilement envisageable d'apporter, comme l'ont cependant proposé quelques auteurs[2,3], des corrections dépendant des teneurs en ions interférants, ne serait-ce qu'à cause de l'ignorance de ces concentrations. La séparation préalable semble donc nécessaire et nous montrons ici que l'extraction par solvant à l'aide du dichlorure de triphénylantimoine, proposée récemment pour la séparation sélective du fluorure[4] permet le dosage systématique du fluorure par spectrophotométrie dans d'aussi bonnes conditions que par potentiométrie.

A l'heure actuelle, le dosage colorimétrique du fluorure le plus utilisé est celui obtenu par décoloration du complexe zirconium eriochrome cyanine R (ECR), proposé pour la première fois par Mégregian[2], puis Thatcher[5], Kletch et Richards[6]. C'est ce composé que nous avons utilisé.

Techniques expérimentales

Réactifs. Dichlorure de triphénylantimoine (TPA; Alpha Inorganics), solution 10^{-2} *M* dans le tétrachlorure de carbone; acide cyclohexanediaminetétraacétique (CDTA; Prolabo), solution 10^{-1} *M* dans l'eau distillée du sel de sodium; tampon phosphate, pH 5.8 : 90% de NaH_2PO_4 (Merck pour analyse) 0.05 *M*, et 10% de Na_2HPO_4 (Prolabo) 0.05 *M* (% en volumes); eriochrome cyanine R (ou solochrome cyanine R) (ECR; Kuhlmann), solution $3.35 \cdot 10^{-3}$ *M* dans l'eau bidistillée; nitrate de zirconyle (Prolabo): solution $0.834 \cdot 10^{-3}$ *M* dans l'eau bidistillée.

Les réactifs usuels étaient des produits Normapur—Prolabo de pureté analytique.

Appareillage. Les dosages ont été effectués sur un spectrophotomètre Jean et Constant Prolabo No. 1046 avec des cuves de largeur 20 mm. Les extractions par solvant ont été réalisées dans des ampoules en polypropylène munies de robinets de téflon, agitées à l'aide d'un agitateur mécanique.

Séparation du fluorure. Pour un volume V_0 compris entre 1 et 200 ml de solution contenant le fluorure (10^{-3}–10^{-7} $M=c$) à doser, est ajouté 1 ml de CDTA, 5 ml de tampon phosphate et 20 ml (V_1) de TPA, Après 10 min d'agitation et décantation, V_2 ml de phase organique sont mis à agiter 10 min avec 10 ml (V_3) de soude 10^{-1} M. Une fraction de la phase aqueuse est alors agitée 10 min avec 20 ml de tétrachlorure de carbone. La phase aqueuse contient alors le fluorure à doser à la teneur $c(V_0/V_1)\cdot(V_2/V_3)$ (Solution A).

Dosage colorimétrique. A 40 ml de solution A sont ajoutés 5 ml de ECR et 5 ml de nitrate de zirconyle. L'absorbance du mélange est mesurée dans les 15 min suivantes, par suite de la faible stabilité des solutions. Le blanc est une solution de référence contenant 10 ml de ECR et 7 ml d'HCl dans 100 ml de solution.

Dosage colorimétrique avec l'eriochrome cyanine R

Interférences et conditions expérimentales. Une étude détaillée du dosage du fluorure par décoloration de ce composé a été effectuée récemment par Dixon[3]. Les principales interférences ont été notées parmi lesquelles, on remarque surtout celles d'ions minéraux tels que sulfate, phosphate, aluminium ou fer(III), souvent à de très faibles teneurs (inférieures à celle du fluorure).

Nous avons effectué nos mesures à la longueur d'onde de 525 nm, pour laquelle l'absorption du complexe a été trouvée maximale; (Megrégian: 527 nm[2], Dixon: 540 nm[3]) alors que l'ECR seul a son maximum d'absorption situé vers 465 nm.

Une étude de l'influence de l'acidité montre que la valeur de pH optimale pour effectuer les mesures doit être voisine de 1.4; ce résultat est en accord avec la valeur obtenue par Dixon[3] avec l'acide chlorhydrique et ne semble pas provenir de la nature de l'acide puisque nous avons obtenu les mêmes résultats avec les acides chlorhydrique, sulfurique et nitrique (Figs. 1 et 2).

Formule du complexe. Dans les conditions définies ci-dessus et à partir d'un milieu exempt d'ions interférants, il est possible de déterminer la formule du complexe en utilisant la méthode des rapports molaires[7]. Par suite de l'absorption encore importante du colorant seul, à la longueur d'onde d'absorption maximale du complexe, nous avons mesuré l'affaiblissement de l'absorption à concentration constante en ECR, et pour des concentrations variables de nitrate de zirconyle, le blanc du spectrophotomètre étant la solution de référence d'ECR. De la courbe obtenue (Fig. 3) on déduit que le complexe zirconium–eriochrome cyanine comporte 2 ECR pour un Zr.

Dosage du fluorure. Le fluorure est séparé par extraction par solvant, après fixation du pH à une valeur comprise entre 3 et 6 et masquage éventuel de cations par le CDTA, à l'aide de dichlorure de TPA en solution dans le tétrachlorure de carbone. De la phase organique, le fluorure est alors réextrait à l'aide d'une phase aqueuse alcaline qui est en suite lavée par le tétrachlorure de carbone

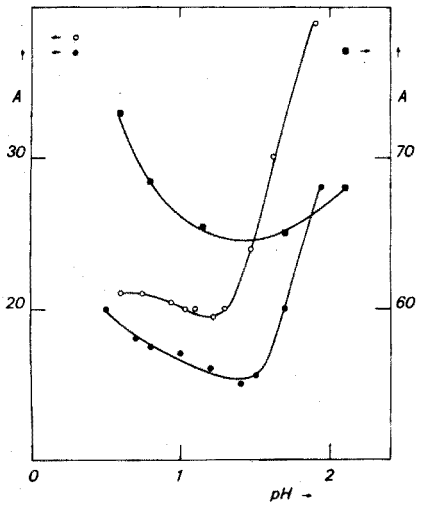

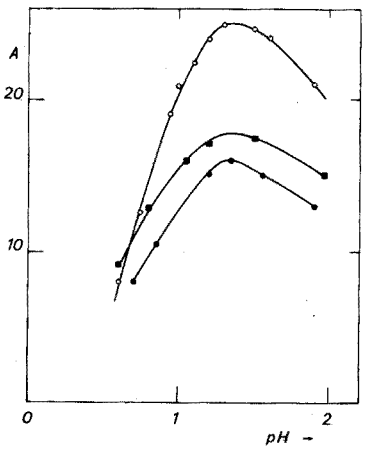

Fig. 1. Variation de l'absorbance de l'ECR (10^{-3} *M*) avec l'acidité: (■) acide nitrique, (○) acide chlorhydrique, (●) acide sulfurique.

Fig. 2. Variation de l'absorbance du complexe Zr–ECR (10^{-3} *M*) avec l'acidité: (■) acide nitrique, (○) acide chlorhydrique, (●) acide sulfurique.

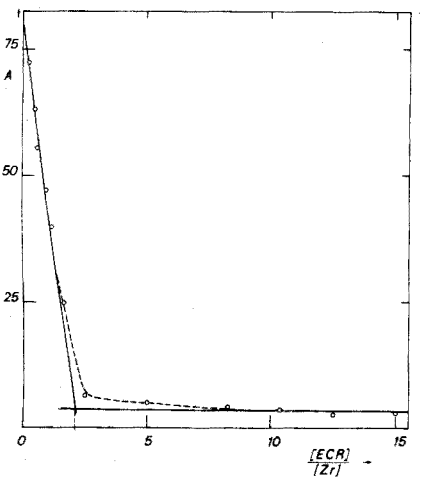

Fig. 3. Détermination de la formule du complexe $Zr(ECR)_2$.

pour éliminer les traces de TPA restant dans la solution[4]. L'acide chlorhydrique est alors ajouté à la phase aqueuse afin de fixer le pH à la valeur de 1.4 pour le dosage colorimétrique.

La limite de sensibilité, classiquement de $5 \cdot 10^{-7}$ M^3 peut être améliorée d'un facteur 100 si l'extraction est utilisée pour concentrer dans ce rapport le fluorure ainsi séparé[4].

Tentative de dosage en phase organique

Afin d'éviter les deux étapes constituées par la réextraction du fluorure en

phase aqueuse et du lavage de celle-ci (pour éliminer les traces de triphénylantimoine), et donc de rendre plus rapide la séparation nécessaire au dosage, nous avons envisagé un dosage colorimétrique direct en phase organique.

Pour cela, le solvant permettant le dosage doit répondre à plusieurs conditions: solubiliser l'halogénure de triphénylantimoine, solubiliser le complexe zirconium–ECR, ne pas absorber aux mêmes longeurs d'onde que le complexe et être non miscible à l'eau et décanter assez facilement.

Parmi les solvants envisageables (hydrocarbures aliphatiques et aromatiques, tétrachlorure de carbone, éther éthylique, alcools), seuls les alcools à longues chaînes semblent répondre à ces conditions et en particulier l'octanol-1. Avec ce dernier nous avons voulu vérifier que la valeur du coefficient de partage de l'hydroxyfluorure de triphénylantimoine était suffisamment élevée pour que l'extraction du fluorure puisse être considérée comme totale; pour cela le fluorure a été réextrait en phase aqueuse, puis dosé potentiométriquement[4].

En fait la réextraction n'est pas quantitative (environ 60% pour des concentrations de l'ordre de 10^{-4} M), ce qui proviendrait de la formation d'un louche dans la phase aqueuse alcaline, lequel ne disparait pas par lavage avec un solvant organique.

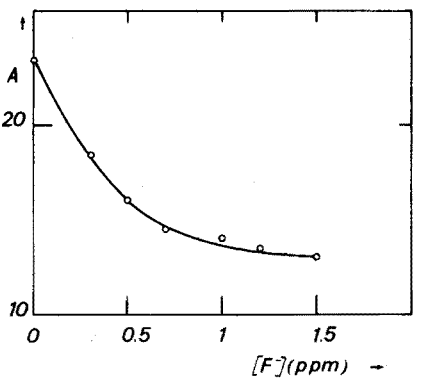

Fig. 4. Étalonnage (loi de Beer) dans le n-octanol à 470 nm.

Le dosage colorimétrique n'est possible dans ce solvant qui si la loi de Beer est vérifiée. La Fig. 4 montre clairement que le dosage est difficile, par suite de la compétition pour le fluorure entre le TPA et le $Zr(ECR)_2$. La concentration de ces deux espèces en présence doit être rigoureusement la même pour toutes les mesures et de plus, la courbe d'étalonnage non linéaire, montre une sensibilité faible. En outre, le dosage colorimétrique dans l'octanol ne doit pas être effectué en présence d'une phase aqueuse, par suite du partage du complexe $Zr(ECR)_2$. Le coefficient de partage de ce composé, mesuré spectrophotométriquement (affaiblissement de l'absorbance au cours de deux extractions successives) est trouvé égal à 1.4.

Conclusion

L'extraction préalable de traces de fluorure au moyen de triphénylantimoine permet le dosage potentiométrique ou colorimétrique à des teneurs aussi faibles

que 10^{-8} *M*. Mais dans les deux cas, il est nécessaire d'obtenir le fluorure en phase aqueuse pour avoir une bonne sensibilité.

Nous remercions Mmes M. Gelin, D. Sandino, MM. M. Benmalek, C. Martelet, et J. Tousset pour les discussions fructueuses que nous avons eues avec eux.

BIBLIOGRAPHIE

1 J. E. Harwood, *Water Res.*, 3 (1969) 273.
2 S. Megregian, *Anal. Chem.*, 25 (1954) 1161.
3 E. S. Dixon, *Analyst (London)*, 95 (1970) 272
4 H. Chermette, C. Martelet, D. Sandino, M. Benmalek and J. Tousset, *Anal. Chim. Acta*, 59 (1972) 373.
5 L. L. Thatcher, *Anal. Chem.*, 29 (1957) 1709.
6 R. A. Kletch and F. A. Richards, *Anal. Chem.*, 42 (1970) 1435.
7 G. Charlot, *Les Méthodes de Chimie Analytique. Analyse Quantitative Minérale*, Masson, Paris, 1961, p. 426.

Analytica Chimica Acta, 70 (1974) 222–226

SHORT COMMUNICATION

Extraction and atomic-absorption spectrometric determination of trace copper with zinc dibenzyldithiocarbamate*

N. ICHINOSE

Department of Chemistry, Faculty of Liberal Arts, Yamaguchi University, Yamaguchi-City (Japan)

(Received 26th July 1973)

In order to increase the sensitivity of analysis, the atomic absorption spectrometric determination of copper has been made by extracting copper as a pyrollidinedithiocarbamate (APDC) complex[1–4] or diethyldithiocarbamate (DDC) complex[5] from an aqueous solution into methyl isobutyl ketone (MIBK) and by spraying the MIBK extract into the flame. However, these analytical procedures are complicated and their application to practical samples is restricted, because the reagents (APDC and NaDDC) are too unstable to be used with acid solutions so that the pH before extraction must be controlled in a suitable range.

In the present work, micro amounts of copper were determined by extraction as a copper dibenzyldithiocarbamate (CuDBC) chelate[6–9] from various acidic media into MIBK, followed by introduction of the extract into an air–acetylene flame. The method established is relatively simple and has the advantage of using a fairly wide range of acidities compared to the APDC or DDC method.

Experimental

Apparatus. The atomic absorption measurements were made with a Hitachi Model 207 atomic absorption spectrophotometer equipped with a copper hollow-cathode lamp (324.8 nm). An air–acetylene flame was used with a water-cooled 10-cm slot burner.

Reagents. A stock copper solution was prepared by dissolving 1.000 g of electrolytic copper in 50 ml of 6 *M* nitric acid, and diluting the resulting solution with water to 1 l in a volumetric flask. Working standards ($\geqslant$0.1 p.p.m.) were prepared by suitably diluting an aliquot of the stock solution with dilute nitric acid. For standard solutions in other acids, an aliquot of the stock solution was evaporated to dryness, the residue was dissolved in the desired acid, and the solution was again evaporated to dryness. This treatment was repeated until the residue was free of nitrate. The final residue was dissolved in the desired acid and diluted to a known volume.

ZnDBC–MIBK solution ($\leqslant$0.07%) was prepared by dissolving ZnDBC (laboratory reagent; B.D.H.) in MIBK by shaking for about 20 min. The solution was stored in an amber glass-stoppered bottle in a refrigerator.

* Paper read at the Meeting of the Chemical Society of Japan, Hiroshima, October, 1970.

Other reagents were of analytical-reagent grade.

General procedure. Shake 25 ml of an acidic solution containing less than 5 μg of copper(II) for a certain time (240 shakes/min) with 5 ml of ZnDBC–MIBK solution in a 50-ml separatory funnel. Separate the phases and centrifuge the extract for 2 min at 3000 rev min^{-1}. Measure the absorbance of copper in the extract against a reagent blank. The ambient temperature was fairly constant at $20\pm2°C$.

Results and discussion

Atomic absorption of copper. Initially, the effects of variation in the air–acetylene flow ratio and the hollow-cathode lamp current on the absorbance of copper were examined at the burner height adjusted for maximal absorption. On the basis of these tests, the optimal air flow rate was 11 l min^{-1} and the acetylene flow rate 1.75 l min^{-1}; the dependence of the absorbance on the air–fuel ratio was smallest under these conditions, changes in the acetylene flow from 1.5 to 2.25 l min^{-1} being without effect.

When the lamp current was increased in the range 3–8 mA, the absorbance decreased gradually, but remained essentially constant in the range 10–15 mA. All subsequent measurements were made at 11 mA.

Effect of shaking time on the extraction. The effect of the shaking time on the extractions of the CuDBC complex from various acidic solutions into MIBK was studied. No perceptible change in the absorbance of copper occurred at shaking times from 1 to 7 min in extractions from 0.2 *M* perchloric acid solution. In contrast, the absorbance for extraction from 0.2 *M* hydrochloric or nitric acid solution increased up to shaking times of 4 min; extraction from 0.75 *M* sulfuric acid increased steeply with shaking time up to 3 min. Therefore, a shaking time of 5 min was used in all further extractions.

Effect of acidity and reagent concentration on the extraction of copper. Tests were made to determine the conditions that would allow quantitative extraction of copper into MIBK. Figure 1 shows plots of absorbance *vs.* acidity for copper extractions from nitric, hydrochloric, sulfuric or perchloric acid with 0.05% ZnDBC–MIBK solution.

In further tests, the initial acidity of the aqueous phase was adjusted to be about 0.2 *M* in nitric, hydrochloric or perchloric acid or about 0.75 *M* in sulfuric acid; constant absorbance with excellent sensitivity was obtained in the ranges 0.1–0.3 *M* for nitric and perchloric acids, 0.1–0.9 *M* for hydrochloric acid, and

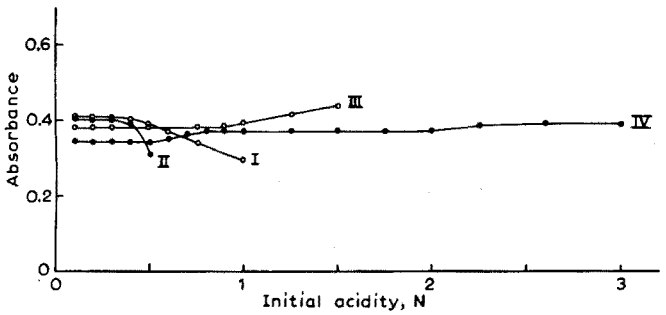

Fig. 1. Effect of acid concentration on absorbance of copper. Cu^{2+}, 0.12 p.p.m.; ZnDBC–MIBK, 0.05%. I, $HClO_4$; II, HNO_3; III, HCl; IV, H_2SO_4.

0.05–0.25 *M* or 0.4–1 *M* for sulfuric acid. Deviations in the absorbance were large in the range above 1 *M* for sulfuric acid. The reason why the absorbance of copper decreased drastically in the acidity region above 0.4 *M* of nitric or perchloric acid may be that the CuDBC complex produced was decomposed by the oxidizing action of the acid.

Tests of the variation of copper absorbance with increasing concentrations of ZnDBC in MIBK in the different acid solutions showed that the optimal concentration of the reagent was in the range 0.04%–0.07%, within which range the copper absorbance remained constant for a particular acid. In all further work, 5 ml of a 0.05% ZnDBC–MIBK solution was chosen as the optimum for all the acids used.

Stability of the CuDBC complex. To check the stability, several solutions were extracted as described under the recommended procedure, and the separatory funnels were stood under diffuse daylight. The absorbances of the organic phase were measured by atomic-absorption spectrometry at different times after extraction. The absorbance of copper in extractions from hydrochloric or sulfuric acid solution was constant for at least 1 h. The absorbance increased slightly for standing times above 45 min in the case of nitric acid, and above 35 min in the case of perchloric acid.

The ZnDBC–MIBK solution, which was kept in a dark refrigerator, was stable for at least 3 months.

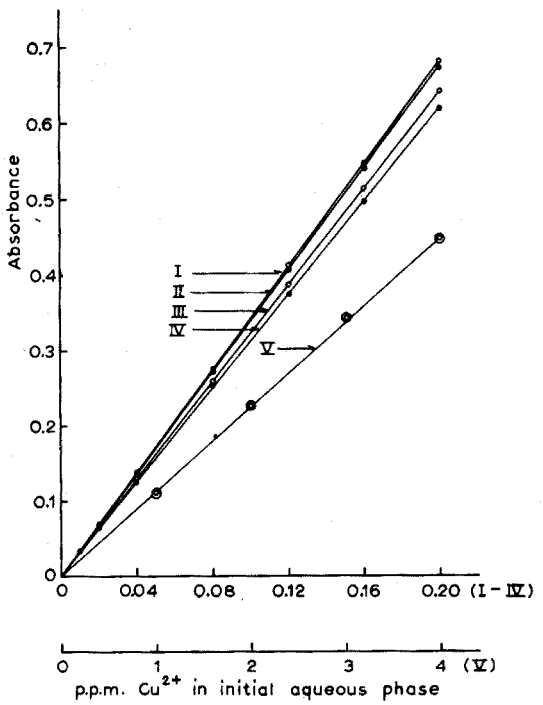

Fig. 2. Calibration curves. I–IV: ZnDBC–MIBK extraction (I, 0.2 *M* $HClO_4$; II, 0.2 *M* HNO_3; III, 0.2 *M* HCl; IV, 0.75 *M* H_2SO_4). V: Without extraction (0.75 *M* H_2SO_4 aqueous solution).

Preparation of calibration curves. Calibration curves were prepared by extracting varying amounts of copper from nitric, hydrochloric, sulfuric or perchloric acid solutions by the recommended procedure. As Fig. 2 shows, each calibration curve(I–IV) obtained was linear for the concentration range 0–0.2 p.p.m. of copper in the initial aqueous solution. The ratio of the sensitivity for copper between the extraction method (IV) and the aqueous method (V) was about 27.6.

The precision of the measurements was tested by repeatedly measuring the absorbance of 10 identical sample solutions. The results (Table I) show that the extraction method provides greater precision than the aqueous method.

TABLE I

PRECISION DATA

Number of determinations in each set: 10)

	Extraction method				*Aqueous method*
	$HClO_4$ (0.2 M)	*HNO_3 (0.2 M)*	*HCl (0.2 M)*	*H_2SO_4 (0.75 M)*	*H_2SO_4 (0.75 M)*
Cu^{2+} (p.p.m. in initial aq. soln.)	0.12	0.12	0.12	0.12	3.00
Mean absorbance	0.409	0.406	0.385	0.375	0.370
Coefficient of variation (%)	1.0	1.2	1.1	0.8	1.4

TABLE II

EFFECT OF DIVERSE IONS ON THE DETERMINATION OF COPPER

Ion	*Amount (μg)*	*Recovery (%)*[a]			
		$HClO_4$ (0.2 M)	*HNO_3 (0.2 M)*	*HCl (0.2 M)*	*H_2SO_4 (0.75 M)*
Ag^+	100	99.6	100	101	100
	200	100	100	102	101
Bi^{3+}	10	100	100	101	101
	25	101	100	102	93.6
	50	102	102	102	92.1
	100	102	101	101	90.0
Ca^{2+}	100	100	100	100	99.0
	1000	100	102	100	98.7
Co^{2+}	100	102	100	100	100
	1000	100	101	101	100
Fe^{3+}	100	98.9	98.0	99.9	101
	1000	99.0	101	99.9	100
Hg^{2+}	100	98.4	98.4	98.7	100
	200	98.0	98.4	100	96
Mo^{6+}	100	98.4	100	101	100
	1000	101	101	101	97.3
Ni^{2+}	100	100	100	100	99.7
	1000	99.6	101	99.8	99.0
W^{6+}	100	100	99.6	98.9	101
	1000	100	99.6	99.6	101

[a] Each aqueous solution contained 0.12 p.p.m. of copper(II).

Interferences. The effects of the main interfering elements, listed by Martens *et al.*[6] and Wilson[8], on the extraction method were tested for different acid media. The results are summarized in Table II. Bismuth(III) in sulfuric acid medium interfered seriously with the determination of copper, but there were no other significant interferences.

Recommended procedure

Shake 25 ml of an acidic solution (0.2 *M* in the case of nitric, hydrochloric or perchloric acid, or 0.75 *M* in the case of sulfuric acid) containing not less than 5 μg of copper for about 5 min (240 shakes/min) with 5 ml of 0.05% ZnDBC–MIBK solution in a 50-ml separatory funnel. Separate the phases and centrifuge the extract for 2 min at 3000 rev min^{-1}. Measure the absorbance of copper in the supernatant extract against a reagent blank.

The operating conditions of the instrument are as follows: wavelength, 324.8 nm; lamp current, 11 mA; slit width, 0.18 nm; burner height adjusted for maximal absorption; pressure and flow rate of air, 1.8 kg cm^{-2}, 11 l min^{-1}; pressure and flow rate of acetylene, 0.5 kg cm^{-2}, 1.75 l min^{-1}.

The author expresses his deep gratitude to Dr. Hidehiro Gotô of the President of Toyama University, Prof. Dr. Taitiro Fujinaga of Kyoto University, Prof. Dr. Shigerō Ikeda of Ōsaka University and Prof. Dr. Kenjiro Hayashi of Yamaguchi University, for their kind guidance.

REFERENCES

1 J. E. Allan, *Spectrochim. Acta*, 17 (1961) 459.
2 D. J. Trent and W. Slavin, *At. Absorption Newslett.*, 3 (1964) 118.
3 M. Nagura and Iida, *Bunseki Kagaku*, 17 (1968) 1513.
4 Y. Yamamoto, T. Kumamaru, Y. Hayashi and M. Kanke, *Bunseki Kagaku*, 20 (1971) 347.
5 I. Atsuya, *Bunseki Kagaku*, 15 (1966) 247.
6 R. I. Martens and R. E. Githens, Sr., *Anal. Chem.*, 24 (1952) 991.
7 D. C. Abbott and J. R. Harris, *Analyst (London)*, 87 (1962) 487.
8 A. L. Wilson, *Analyst (London)*, 87 (1962) 884.
9 O. P. Bhargava, *Talanta*, 16 (1969) 743.

Analytica Chimica Acta, 70 (1974) 227–228

SHORT COMMUNICATION

A modification of the determination of cysteine with *o*-iodosobenzoic acid

KRISHNA K. VERMA and SAMEER BOSE
Department of Chemistry, University of Jabalpur, Jabalpur, M.P. (India)
(Received 4th June 1973)

o-Iodosobenzoic acid has been used quite extensively as a relatively selective reagent for the determination of thiol groups[1–3]; the oxidation of either cysteine or glutathione by this reagent goes to completion at neutral pH and a stoichiometric relationship between oxidant and reductant is maintained.

$$2RSH + OI \cdot C_6H_4 \cdot CO_2K \rightarrow RSSR + I \cdot C_6H_4 \cdot CO_2K + H_2O$$

In most procedures based on this reaction, an excess of the reagent is added and the residual amount is determined by adding acidified potassium iodide; the liberated iodine is then immediately titrated with standard thiosulphate solution. The excess must be kept as small as is compatible with analytical accuracy if not precision; large excesses of *o*-iodosobenzoate in the determination of cysteine or glutathione leads to high results, so that preliminary experimentation to establish a suitable excess is necessary.

The present study involves the oxidation of cysteine by an excess of *o*-iodosobenzoate, which is then determined by adding a measured amount of ascorbic acid (which reacts with iodosobenzoate in a molar ratio of 1:1), followed by a back-titration with iodine. The actions of the various ingredients on the determination of cysteine by this method were examined and the following facts were noted. First, when cysteine and about a 100% excess of *o*-iodosobenzoate were allowed to react at pH 7, no over-oxidation was observed even after 60 min. Secondly, when the excess of *o*-iodosobenzoate was determined by adding an acidified solution of potassium iodide, a delay of 1 min in the titration of liberated iodine led to high results, compared to those obtained with immediate titration. With a 100% excess of reagent, the results were about 4% high. Thirdly, the results were increasingly high when cysteine was estimated with a 1–4-fold excess of the reagent, which was back-titrated after addition of acidified potassium iodide. However, under identical conditions, when the excess was determined by adding ascorbic acid and titrating with iodine, the results were practically unaffected.

Clearly, it is the liberated iodine and not the oxidant itself (as originally thought[1]), which causes over-oxidation, the extent of which increases with increasing amounts of liberated iodine. The back-titration procedure is the key to the discrepancy. Shinohara[4] has shown that cysteine is oxidized to cysteic acid by a

large excess of iodine. Danehy and Oester[5] observed that the over-oxidation of cysteine by iodine increases with increasing dilution of the cysteine solution. Under the conditions of direct titration with iodine, 2 atoms of iodine per mol of cysteine are consumed; more iodine is bleached when it is titrated with cysteine. The following modified method is proposed.

Experimental

Reagents. A stock solution (*ca.* 0.02 *M*) of *o*-iodosobenzoate was prepared by adding to the acid reagent a slight excess of *M* potassium hydroxide solution and diluting suitably. The solution was standardized by addition of ascorbic acid and titration with iodine solution, as described below. The strength, thus determined, was in agreement with the value obtained iodimetrically[1].

Cysteine hydrochloride, which was shown to be 99.4% pure by total sulphur analysis and 99.6% pure by total acid analysis, was used.

Phosphate buffer[1], pH 7, was prepared by dissolving 117.7 g of dipotassium hydrogenphosphate and 44.1 g of potassium dihydrogenphosphate in 1 l of water.

All other chemicals were reagent grade.

Procedure. The sequence of additions, both in the blank determination of *o*-iodosobenzoate and in the determination of residual reagent after reaction with cysteine, was reversed compared to that followed in the original procedure[1]; the accuracy was found to be unimpaired.

To 10 ml of sample solution containing 0.1–2.0 mmol of cysteine, add 5 ml of phosphate buffer, after which add 10 ml of a suitably diluted solution of *o*-iodosobenzoate, so that it will be about 50% in excess. Swirl the contents for about 30 s, and add a measured excess of 0.05 *M* ascorbic acid and 5 ml of *M* hydrochloric acid solution; back-titrate with 0.05 *M* iodine in the usual manner. Run a blank determination also.

Results

When the above procedure was used, a series of six determinations of cysteine in the range 0.1–1 mmol gave an average recovery of 99.7% with a standard deviation of 0.2%. The only critical point appears to be the adjustment to pH 7. The modified procedure is, therefore, reliable.

REFERENCES

1 L. Hellerman, F. P. Chinard and P. A. Ramsdell, *J. Amer. Chem. Soc.*, 63 (1941) 2551.
2 H. Stern, in K. Paech and M. V. Tracey (Eds.), *Modern Methods of Plant Analysis*, Vol. VI, Springer-Verlag, Berlin, 1963, p. 39.
3 F. P. Chinard and L. Hellerman, in D. Glick (Ed.), *Methods of Bio-chemical Analysis*, Vol. I, Interscience, New York, 1961, p. 9.
4 K. Shinohara, *J. Biol. Chem.*, 96 (1932) 285.
5 J. P. Danehy and M. Y. Oester, *J. Org. Chem.*, 32 (1967) 1491.

Analytica Chimica Acta, 70 (1974) 229–232

SHORT COMMUNICATION

A modified fluorimetric determination of chloroquine in biological samples

STEPHEN G. SCHULMAN
College of Pharmacy, University of Florida, Gainesville, Florida 32610 (U.S.A.)
JOHN F. YOUNG
National Center for Toxicological Research, Jefferson, Arkansas 72079 (U.S.A.)
(Received 15th August 1973)

The antimalarial chloroquine has enjoyed recent popularity as an agent in the treatment of rheumatoid arthritis. However, in the large doses employed in the treatment of arthritis, toxic side effects have been noted[1], notably deformation of the lens of the eye. Consequently, the determination of chloroquine in biological samples is of current interest.

A fluorimetric procedure for the determination of chloroquine in biological fluids has been reported by Rubin *et al.*[1]. In this procedure, the sample was diluted tenfold with ethanol, centrifuged, adjusted to pH 9.5 with borate buffer, and extracted with methylene chloride; the methylene chloride extract was then shaken with pH 7.85 phosphate–borate buffer. The aqueous phosphate–borate buffer extract was diluted with an equal volume of 0.1 *M* sodium hydroxide in 50% ethanol, and the fluorescence of this solution was measured to determine the metabolites of chloroquine. The unmetabolized chloroquine was then determined by extracting a portion of the methylene chloride extract with 0.1 *M* hydrochloric acid, adjusting the extract to pH 13 with 0.2 *M* sodium hydroxide in 50% ethanol, and comparing fluorimetrically with an appropriate standard.

In the present study, the variations of the absorption and fluorescence spectra of chloroquine were investigated throughout the pH range and in concentrated sulfuric acid media; it was found that while the pH conditions specified by Rubin *et al.*[1] are probably ideal for the separation of chloroquine from its metabolites, these pH conditions do not provide maximal sensitivity in the fluorimetric analysis.

Experimental

A pure sample of chloroquine phosphate was donated by Dr. S. Archer of the Sterling-Winthrop Institute, Rensselaer, N.Y. Analytical reagent-grade sulfuric acid and sodium hydroxide (Mallinckrodt Chemical Works, St. Louis, Mo.) were used. Sulfuric acid solutions were prepared by dilution with distilled deionized water; the corrected Hammett acidity scale of Jorgenson and Hartter[2] was employed to calibrate the sulfuric acid solutions. Solutions in the pH region 1–3 were prepared by dilution of sulfuric acid. Acetate, phosphate and borate buffers

were employed to prepare solutions in the pH region 4–10. Dilute sodium hydroxide solutions were employed for solutions of pH 11–14. A 100-μl aliquot of a $1 \cdot 10^{-4}$ *M* stock solution of chloroquine phosphate in ethanol was delivered to a 10.00-ml volumetric flask filled with buffer or acid solution, and mixed by inversion, to prepare each solution for spectrometric measurement. Each solution was prepared immediately before spectra were taken, in order to minimize decomposition errors.

Fluorescence spectra were taken on a Perkin-Elmer MPF-2A fluorescence spectrophotometer, the monochromators of which were calibrated against the xenon line emission spectrum; output was corrected for wavelength variable response of lamp, monochromators and phototube by means of a rhodamine B quantum counter. Absorption spectra were taken on a Beckman DB-GT spectrophotometer. pH measurements were made on an Orion model 801 digital pH meter with a Corning combination pH electrode.

Results and discussion

Chloroquine has three basic nitrogen atoms and is therefore capable of demonstrating three protolytic equilibria involving four distinct species. These species along with their long wavelength absorption (λ_a) and fluorescence (λ_f) maxima and the pK_a values corresponding to their interconversions are depicted in scheme 1.

Scheme 1

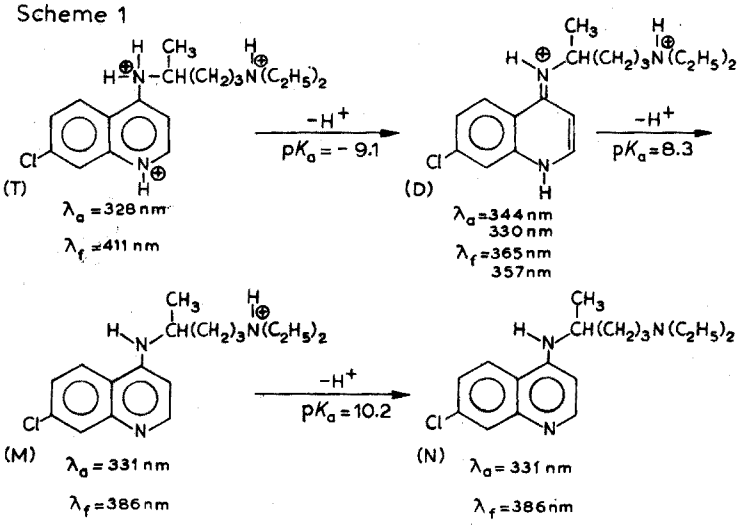

The triply charged cation (T), singly charged cation (M) and neutral molecule (N) all demonstrate structureless fluorescence bands and long wavelength absorption bands with blurred vibrational structure. The spectral features of these species given in scheme 1 correspond to the band maxima. The doubly charged cation (D), however, exhibits well defined vibrational fine structure in absorption and fluorescence, and in this case the two most distinct and intense vibrational features of the absorption and fluorescence bands are presented. The doubly charged cation (D) is represented as a protonated cyclic vinyl-type amidine rather than as a

protonated aminoquinoline. The basis for this structural assignment has been well established for 4-aminoquinoline[3] and is apparently applicable here as well.

The conversion from (T) to (D) produces substantial changes in the absorption and fluorescence spectra, the variations of both types of spectra yielding $pK_a = -9.1$. This is in contrast to 4-aminoquinoline, in which the corresponding pK_a value obtained by fluorimetry is some two orders of magnitude more basic than that determined by absorptiometry, a result attributed to ionization of the latter compound in the excited state from which fluorescence arises. That the same phenomenon is not observed in chloroquine indicates that the life-times of the excited states of the tri-cation and di-cation derived from chloroquine are too short for excited-state dissociation to compete with fluorescence[4]. The conversion from (D) to (M) in chloroquine also yields the same pK_a value whether determined absorptiometrically or fluorimetrically. This is analogous to the behavior of 4-aminoquinoline with respect to dissociation from the heterocyclic ring nitrogen atom[3].

Whereas the dissociations of (T) to (D) and that of (D) to (M) both involve dissociation from a site intimately coupled to the aromatic system, and therefore perturb the absorption and fluorescence spectra with respect to both wavelength and intensity, the dissociation of (M) to (N) arises from a site far removed from the aromatic part of chloroquine. Consequently, the dissociation of (M) to (N) does not at all affect the absorption or fluorescence spectra. The pK_a for this equilibrium was determined potentiometrically. No changes in the absorption or fluorescence spectra above pH 10 would thus be expected, and in fact, no changes in the absorption spectra were observed with increasing pH, above pH 10. However, at pH 10 the fluorescence of chloroquine was quenched, vanishing completely at pH 14. The midpoint of this quenching occurred at pH 11.7. A similar phenomenon was observed in 4-aminoquinoline[3] and was attributed to proton abstraction in the fluorescent state, from the amino group. Presumably, this is also occurring in chloroquine as represented in scheme 2.

Scheme 2

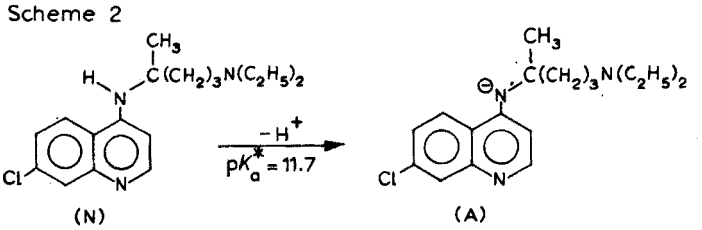

The inflection point in the quenching curve of chloroquine fluorescence with increasing pH may be assigned to the dissociation constant for the excited state equilibrium represented in scheme 2 and has the value 11.7. The corresponding dissociation cannot be observed in the absorption spectra, because the anion (A) is much too basic in the ground state to exist in water. That (A) can be generated in the excited state in the accessible pH range indicates that in the excitation of (N) from the ground state to the excited state, the amino group of (N) loses electronic charge to the aromatic ring, rendering (N) a stronger acid (or conversely, A a weaker base) in the excited state.

The relative quantum yields of fluorescence of each species derived from chloroquine were estimated from the integrated area under the fluorescence peak divided by the molar absorptivity at the wavelength of excitation. Comparison of these relative quantum yields permits the identification of the most intensely fluorescing species and therefore the species most desirable for the most sensitive fluorimetric analysis. The relative quantum yield of (T) was measured at Hammett acidity $H_0 - 10$ (96% H_2SO_4), that of (D) at pH 1.0 and that of (M) or (N) at pH 9.8. The relative quantum yields of (T), (D) and (M) or (N) were found to be in the ratio 1:1:100 indicating that the mono-cation or neutral species are certainly the most desirable for fluorimetry.

All of this leads to the original point of this paper. Because of the excited-state ionization which quenches the fluorescence of (N) at high pH and which could not be detected by ordinary chemical means, the fluorimetric assay of chloroquine, carried out by monitoring the fluorescence of the neutral species (N) at pH 13, is about 14 times less sensitive than if the solution which is measured fluorimetrically for chloroquine is adjusted to pH 9.8–10.0 and the fluorescence then monitored. Therefore, it is suggested that the procedure of Rubin *et al.*[1] be modified by neutralizing the 0.1 *M* hydrochloric acid extract of the methylene chloride extract with an equal volume of 0.1 *M* sodium hydroxide and then adjusting to pH 9.8–10.0 carefully with phosphate or borate buffer before fluorescence is measured. The standard solution should also, of course, be measured at the same pH.

Since the metabolites of chloroquine are simply dealkylated derivatives[1], the same pH considerations are presumably also applicable to their analysis.

REFERENCES

1 M. Rubin, N. Zvaifler, H. N. Bernstein and A. Mansour, *Proc. Int. Pharmacol. Meeting, 2nd*, Pergamon Press, Oxford, 1965, p. 467; and references contained therein.
2 M. J. Jorgenson and D. R. Hartter, *J. Amer. Chem. Soc.*, 85 (1963) 878.
3 P. J. Kovi, A. C. Capomacchia and S. G. Schulman, *Anal. Chem.*, 44 (1972) 1611.
4 S. G. Schulman, *Revs. Anal. Chem.*, 1 (1972) 85.

Analytica Chimica Acta, 70 (1974) 233–236

SHORT COMMUNICATION

The development of a reproducible dialysis system for the investigation of protein binding

ERIK J. OLSON

Department of Pharmacology, Meharry Medical College, Nashville, Tennessee 37208 (U.S.A.)

(Received 26th September 1973)

The understanding of enzyme reactions may make it advisable to investigate the binding of inhibitors and co-factors to enzymes[1]. The use of sephadex chromatography or filtration for such investigations may be undesirable because the enzyme surface may be disturbed when such techniques are employed. To avoid this complication one could resort to equilibrium dialysis. However, with equilibrium dialysis, the loose binding of a compound to an enzyme will have only a small influence on the distribution of the compound. For these reasons, it was considered advisable to develop a reproducible dialysis system which can be used to assess accurately the degree of binding of a compound to a protein without disturbing the enzyme surface. Because this dialysis system can detect differences in initial rates of dialysis, the degree of binding of compound to enzyme can be estimated with some accuracy.

Experimental

Reagents. Disodium adenosinetriphosphate (ATP; Sigma Chemical Co., St. Louis, Mo.) and bovine serum albumin (Armour Pharmaceutical Co., Chicago) were used.

Apparatus. The rotary dialyzer is illustrated in Fig. 1. The rack is rotated or rocked so that the reagent solution flows back and forth over the dialysis bags. All the chambers are positioned at a fixed angle to the rack with the center of the chamber at the center of the rotation.

Procedure. After the reaction mixture has been pipetted into the dialysis bag, air is expelled from the bag which is then tied. To ensure that all the dialysis bags are the same length, a measuring gauge made from a glass rod with two right-angle bends is used as a reference. When tying the knots, care should be taken to avoid causing stress throughout the length of the dialysis tubing. The dialysis bags are then immersed immediately in the appropriate reaction mixture to keep the tubing wet. It seems best to place dialysis bags in test tubes filled with the appropriate dialyzing reagent solution.

When all the dialysates have been prepared, each bag is taken individually, after its tails have been trimmed off completely and its knots immersed briefly in water, and placed in a reaction chamber with the appropriate dialysing reagent solution. The chamber, which is 15.0 cm long and has a 20-ml capacity, is then

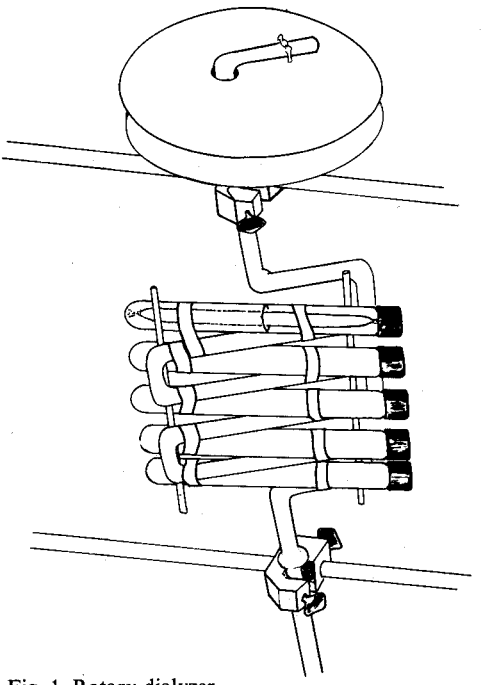

Fig. 1. Rotary dialyzer.

capped securely and placed on its side so that the dialysis bag is completely submerged with its flat surface parallel to the dialyzing solution surface; 10 ml is considered to be the minimal volume of solution for complete immersion of the bag. The last bag is allowed to equilibrate with the dialysing solution for 1–2 min before rotation or rocking of the rack is started. Rubber gloves are worn to minimize the possibility of chemical or bacterial contamination.

To demonstrate the reproducibility of the dialysis, 2-ml aliquots of a solution containing 7.3 μmol of disodium ATP per ml were added to five dialysis bags of 13.5 cm length. The dialysis bags were then immersed in test tubes filled with water. After all the dialysis bags had been prepared, they were placed in 10 ml of distilled water (dialyzing solution). The chambers were rotated at room temperature at a rate of one rev s^{-1} or rocked once every 2 s for 20 min.

The washing of dialysis tubing. To remove contaminants from the dialysis tubing, a modification of a procedure developed by Segall[2] was used. A 6-ft. length of dialysis tubing (0.25 in. diameter) was tied at one end, and mounted on a glass rack. The tubing was then immersed in 1.2 l of distilled water at 80° and stirred for at least 4 h. If bubbles formed in the dialysis tubing, the tubing was removed from the rack and cut open to let the bubbles escape. The tubing was then retied and remounted on the glass rack before being immersed in the hot distilled water, for 4 h. The rack was then removed, placed in 1.2 l of 3% sodium sulfide at 90°C and stirred for 20 min. The rack was then placed in 1.2 l of distilled water at 90°C and stirred for 30 min. After this time, individual lengths were rinsed with a jet of distilled water (250 ml at 90–95°C) from a wash bottle in the direction of

initial drainage. The washed lengths of dialysis tubing were then submerged in test tubes of distilled water. The effectiveness of the washing procedure was checked by placing the lengths of dialysis tubing in the dialysis chambers with distilled water, the chambers being rotated for 20 min.

Results and discussion

Table I shows the results of a series of experiments where adenosine triphosphate was extracted into distilled water. After 20 min, *ca.* 17% of the ATP was extracted from the unwashed dialysis bags by rotating dialysis (Experiment 1) and about 21% of the ATP by rocking dialysis (Experiment 2). This difference observed with the unwashed tubing was statistically significant. Furthermore, the dialysis appeared to be less variable when the rocking motion was employed with unwashed dialysis tubing (Experiments 2 and 4). Rotating dialysis with washed dialysis tubing was also less variable than rotating dialysis with unwashed dialysis tubing. To ensure reproducibility within a run, the rate of rotation or racking of the dialysis chamber should not exceed the time required for the dialysing solution to flow from one end of the chamber to the other. Any difference in the flow rates of the reagent solution will be accentuated if the rate of rotation or rocking is too rapid.

TABLE I

THE EXTRACTION OF ADENOSINE TRIPHOSPHATE FROM DIALYSATES

(Absorbances were measured at 260 nm)

Run	*1*	*2*	*3*	*4*	*5*	*Ave.*
Experiment 1: Rotational dialysis, unwashed tubing						
Ave.	0.231	0.234	0.238	0.237	0.225	0.233[a]
$S^{b,c}$	0.0172	0.0106	0.0188	0.0210	0.0130	0.0161
Experiment 2: Rocking dialysis, unwashed tubing						
Ave.	0.285	0.279	0.261	0.284	0.264	0.275[a]
S^{b}	0.0116	0.0080	0.0132	0.0148	0.0093	0.0113
Experiment 3: Rotational dialysis, washed tubing						
Ave.	0.252	0.286	0.295	0.282	0.218	0.266
S^{c}	0.0084	0.0155	0.0133	0.0100	0.0115	0.0116
Experiment 4: Rocking dialysis, washed tubing						
Ave.	0.277	0.254	0.234	0.264	0.237	0.255
S	0.0222	0.0104	0.0123	0.0207	0.0090	0.0149

[a] P 0.01, Student t test, Mann Whitney U test (ref. 3).
[b] S/Ave. Experiment 1 > S/Ave. Experiment 2: P 0.025, Student t test, Mann Whitney U test (ref. 3).
[c] S/Ave. Experiment 1 > S/Ave. Experiment 3: P 0.025. Student t test, Mann Whitney U test (ref. 3).

Because of the limited volume of dialysing reagent solution used, this solution will contain higher concentrations of contaminants from the dialysis tubing than would normally be encountered. For this reason, it is necessary to wash and check the dialysis tubing before experiments. Figure 2 represents a comparison of dialyzing solutions that were exposed to unwashed and washed

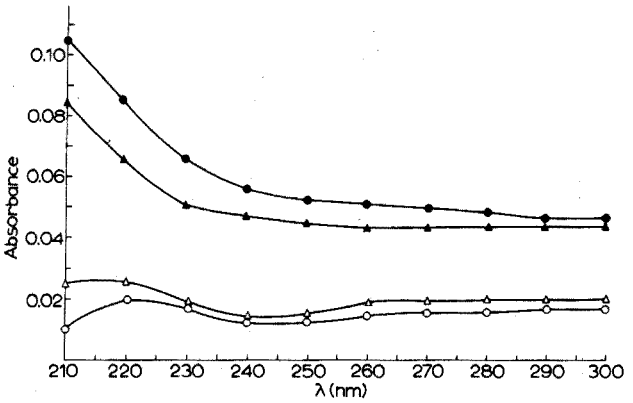

Fig. 2. Comparison of dialyzing solutions from washed and unwashed tubing. (●),(▲) Unwashed; (○),(△) washed.

dialysis tubing. It may be seen that the washing procedure reduced contamination to lower levels. According to analysis, the major contaminant of dialysis tubing is glycerol[2]; however, the absorbance in the region 210–300 nm is not due to glycerol.

While the washing procedure appears to be successful, the author has encountered rolls of dialysis tubing which have lengths spaced at regular intervals that cannot be successfully washed. Such lengths should be discarded.

Rotary dialysis failed to extract bovine serum from a dialysate when washed dialysis tubing was used.

This dialysis system has the following advantages: it is easy to assemble and does not require elaborate equipment; the motion required for the circulation of the dialyzing reagent can be easily reproduced. It may also be noted that the dialysate has a large contact area with the dialysis solution so that there can be an efficient solute exchange.

This reproducible dialysis system may also be used to provide continuous infusions and extractions of biological preparations. It may be possible to isolate biologically labile intermediates by extraction before they can be metabolized further. It is likely that the concentration of a given compound in the dialyzing reagent solution will be directly proportional to the integral summation $\int_0^T ct\,dt$ where ct equals the concentration gradient, $(ct_{\text{dialysate}} - ct_{\text{dialyzing reagent}})$ at time t, and T is the total dialysis time. In all probability this expression will not be proportional to the final concentration of this compound in the dialysate.

The ionic strengths of the solutions used in the dialysis should be sufficient to minimize any Donnan effects[4].

REFERENCES

1 J. S. Bond, A. H. Frances and J. H. Park, *J. Biol. Chem.*, 245 (1970) 1041.
2 H. Segall, Union Carbide, Chicago, personal communication.
3 S. Siegel, *Nonparametric Statistics for the Behavioral Sciences*, McGraw-Hill, New York, 1956, p. 116.
4 S. Glasstone, *Textbook of Physical Chemistry*, Van Nostrand, New York, 1943, p. 1234.

Analytica Chimica Acta, 70 (1974) 237–240

SHORT COMMUNICATION

The polarographic behaviour of uranyl ions in the presence of pyridine and hydrazine*

V. ALMAGRO, F. S. GARCÍA and J. SANCHO

Department of Chemistry, Universidad Autónoma de Madrid and Junta de Energía Nuclear, Madrid (Spain)

(Received 20th July 1973)

The complexes formed by pyridine and similar compounds with certain metallic ions, such as Cd(II), Zn(II), Fe(III) etc., are well known, as are the complexes formed with complex cations such as uranyl and vanadyl[1]. The species formed with uranyl ions have the general formula $B_2 \cdot UO_2^{2+}$, where B can be ethyl ether, pyridine, aniline, etc.

Sanwal[2] indicated that pyridine uranyl chloride can crystallize in two different forms; absorption spectra showed that the structures were similar whether pyridine or deuteropyridine was used.

Using uranyl perchlorate, Savant and Ramamurthy[3] studied the bond characteristics and stereochemistry of the complexes formed with antipyrine, assigning the formula $UO_2(ant)_5(ClO_4)_2$ to the uranyl complex. Joshi and Lal[4] studied complexes based on uranyl nitrate by conductimetric measurements, obtaining a uranium: antipyrine molar ratio of 1:3.

Various chemical species have also been described in which the uranyl ion and hydrazine participate. Thus, Volchkov[5] indicates several methods of preparing $UO_2C_2O_4 \cdot N_2H_4 \cdot 0.75\ H_2O$. Kalnins and Gibson[6] studied the complexes formed by uranyl chloride with hydrazine, ammonia and amines by X-ray diffraction, and concluded that the species formed is $UO_2Cl_2 \cdot 4\ N_2H_4$ in solid state.

A polarographic determination of uranyl ion in the presence of hydroxylamine has been recommended in order to eliminate some interferences[7]. Strubl[8] and Athavale[9] have made polarographic studies of the uranyl ion in hydrazine under different conditions. Athavale found a polarographic wave in the presence of perchloric acid, hydrochloric acid or EDTA, and stated that only a 1:1 uranium/acetate species was obtained in the presence of hydrazine.

The object of the work described here was to study the characteristics of the uranyl polarographic wave in pyridine and hydrazine media, and to describe the ionic species formed.

Experimental

Pyridine or hydrazine was used in all experiments with an equimolar quantity of perchloric or nitric acid; the pH was regulated with an appropriate extra amount of pyridine or acid.

* This paper was presented at the I.U.P.A.C. Congress held in Hamburg in September, 1973.

Triton-X100 was used as a maximum suppressor and lithium nitrate or perchlorate, depending on the system, was used as the inert electrolyte.

A Radiometer PO4G polarograph was used, with capillaries and other equipment from the same firm. A Beckman H-5 pH meter was also used. The height of the mercury column in the polarographic measurements was in all cases 40 cm, giving a drop time of 4 s and a mercury flow of 1.55 mg s^{-1} measured at −0.2 V.

The values of the half-wave potential, $E_{\frac{1}{2}}$, were corrected for the ohmic drop, iR.

Results and discussion

Pyridine. The uranyl ion produces a polarographic wave at *ca.* −0.210 V. This wave is best defined at pH 2–3, becoming deformed outside these limits; above pH 4, the solution becomes yellowish, and the diffusion current decreases noticeably. The characteristics of this wave are summarized in Table I.

TABLE I

VARIATION OF THE POLAROGRAPHIC WAVE OF THE URANYL ION WITH CONCENTRATION OF PYRIDINE

(Composition of the cell: $5 \cdot 10^{-4}$ *M* uranyl perchlorate; $5 \cdot 10^{-4}$% Triton-X100; equimolar amounts of C_5H_5N and $HClO_4$. Average ionic strength, 0.4; pH, 4.2. Within experimental error, the diffusion current was 1.40 μA in all cases)

(C_5H_5N) (*M*)	0.025	0.10	0.15	0.25	0.35	0.45
$E_{\frac{1}{2}}$(V)	−0.205	−0.197	−0.202	−0.213	−0.208	−0.210
$\Delta E/\Delta \log [i/(i_d - i)]$	−0.069	−0.071	−0.073	−0.073	−0.072	−0.072

After a certain concentration of pyridine, which is a function of the uranium concentration and of ionic strength, has been reached, the top of the wave becomes deformed; this occurs when the pyridine is *ca.* 0.6 *M* for $5 \cdot 10^{-4}$ *M* uranyl ion at an ionic strength of 0.4.

A perfectly linear relationship was found between the height of the polarographic wave and the concentration of uranyl ion in the range $0.25–1.00 \cdot 10^{-3}$ *M* in the presence of pyridine. There was no appreciable variation in the half-wave potential between pH 1 ($E_{\frac{1}{2}} = 0.24$ V) and pH 4 ($E_{\frac{1}{2}} = 0.21$ V) but there was a rapid decrease at higher values of pH, probably because of hydrolysis; the diffusion current decreased rapidly above pH 4. The value of the diffusion constant, *I*, was 1.312 in 0.1 *M* pyridine–0.1 *M* perchloric acid.

In order to make a comparative study of the nature of the ionic species in solution, in accord with Deford and Hume's method[10], the variation of the half-wave potential of uranyl ion was studied at different concentrations of pyridine in the presence of perchloric acid, the ionic strength and pH being kept constant. The variations found were insignificant in the range $10^{-3}–10^{-2}$ *M* pyridine.

Under the conditions used, the process was almost reversible, with a value of $0.817 \cdot 10^{-3}$ for the specific velocity constant of the electrode reaction, k_0, obtained by the method of Koutecky[11]. The value of the transfer coefficient, α, obtained by the same method and also by the method of Tamamushi and Tanaka[12], was 0.78. By means of a graphical representation of $\Delta(E_{\frac{1}{2}}^{f} - E_{\frac{1}{2}}^{c})$ *vs.* log [pyridine], as

discussed by Heyrovsky and Kůta[13], the ratio of the stability constants of the oxidized and reduced forms of the complexes with pyridine, β_p/β_q, can be obtained from the ordinate in the origin; the difference between the number of ligands $(p-q)$ can be obtained from the slope of the graph. The individual values of β_p, β_q, p and q cannot be obtained by this method, given that it is an almost reversible process. The values obtained were $\beta_p/\beta_q=3.08$ and $(p-q)=0.26$.

It can be concluded that, under the conditions described, the oxidized and reduced forms have the same structure which, if the structure given for the oxidized form[1] is accepted, will be $B_2 \cdot UO_2^{2+}$. The stability will be somewhat greater, however, for the oxidized form.

Hydrazine. The uranyl ion produces a polarographic wave at *ca.* -0.180 V in the presence of hydrazine. The variation of the height of this wave with the uranyl concentration was perfectly linear in the range $0.25–1.5 \cdot 10^{-3}$ *M*. The diffusion constant, *I*, was 1.731 in 0.15 *M* hydrazine–0.15 *M* perchloric acid medium. The $E_{\frac{1}{4}}$ value changed only from -0.20 to -0.18 V in the pH range 1.0–3.0, and the changes in $E_{\frac{1}{4}}$ value with ionic strength in the range 0.6–1.1 were similarly insignificant. The polarograms of the uranyl ion must be obtained at a pH less than 3.5, at which pH the medium takes on a yellowish color (it turns cloudy at pH 5.5), but the polarograms are best defined at the highest possible pH. The characteristics of this uranyl wave in the presence of hydrazine are summarized in Table II.

TABLE II

VARIATION OF THE POLAROGRAPHIC WAVE OF THE URANYL ION WITH CONCENTRATION OF HYDRAZINE

(Composition of the cell: $5 \cdot 10^{-4}$ *M* uranyl perchlorate; $5 \cdot 10^{-4}$% Triton-X100; 0.1 *M* lithium perchlorate; equimolar amounts of $HClO_4$ and N_2H_4. Average ionic strength, 0.5; pH, 3.5)

(N_2H_4) (*M*)	0.025	0.15	0.40	0.60	0.80
$E_{\frac{1}{4}}$ (V)	-0.205	-0.198	-0.183	-0.186	-0.171
i_d (μA)	1.40	1.40	1.37	1.37	1.35
$\Delta E/\Delta \log [i/(i_d-1)]$	-0.070	-0.070	-0.070	-0.060	-0.060

The possible ionic species which exist in solution were examined in a similar way to the study in pyridine medium, since the characteristics of the process are very similar: $k_0=1.079 \cdot 10^{-3}$, $\alpha=0.8$. Thus, the variation of $\Delta(E_{\frac{1}{4}}^{f}-E_{\frac{1}{4}}^{c})$ *vs.* log [hydrazine] was examined, and the values $\beta_p/\beta_q=2.3 \cdot 10^2$ and $(p-q)=0.3$ were obtained from the ordinate in the origin and the slope of the graph. This can be interpreted to mean that the oxidized and reduced forms have a similar structure. It was not possible to determine which of the ionic complexes proposed by different authors actually exist, but it is evident that the oxidized form is more stable.

REFERENCES

1 O. N. Srivastava and J. K. Gupta, *Indian J. Chem.*, 8 (1970) 302.
2 D. N. Sanwal, *Proc. Indian Acad. Sci., Sect. A*, 70 (1969) 221.
3 V. V. Savant and P. Ramamurthy, *J. Less-Common Metals*, 22 (1970) 479.
4 D. P. Joshi and K. Lal, *J. Indian Chem. Soc.*, 46 (1969) 484.

5 G. N. Volchkov, *Zh. Neorg. Khim.*, 15 (1970) 41.
6 I. Kalnins and G. Gibson, *J. Inorg. Nucl. Chem.*, 7 (1958) 55; 11 (1959) 115.
7 G. W. C. Milner, *The Principles and Applications of Polarography*, Longmans, London, 1957, p. 271.
8 R. Strubl, *Coll. Czech. Chem. Commun.*, 10 (1938) 466.
9 V. T. Athavale, *Indian J. Chem.*, 5 (1967) 424.
10 D. D. DeFord and D. N. Hume, *J. Amer. Chem. Soc.*, 73 (1951) 5323.
11 J. Koutecky, *Chem. Listy*, 47 (1953) 232; *Coll. Czech. Chem. Commun.*, 18 (1953) 597; 21 (1956) 836.
12 R. Tamamushi and N. Tanaka, *Bull. Chem. Soc. Japan*, 22 (1949) 227.
13 J. Heyrovsky and J. Kůta, *Principles of Polarography*, Academic Press, New York, 1966, Chap. VIII, p. 223.

Analytica Chimica Acta, 70 (1974) 241–244

SHORT COMMUNICATION

Determination of sub-micromolar concentrations of sulphonamides by differential pulse polarography after diazotization and coupling with 1-naphthol

A. G. FOGG and Y. Z. AHMED

Chemistry Department, University of Technology, Loughborough, Leicestershire LE 11 3TU (England)

(Received 26th October 1973)

Recent advances in instrument electronics have made available relatively inexpensive pulse polarographs. For this reason, and also because of the high sensitivities (10^{-9} *M*) attainable, there has been a renewed interest in polarography as a viable routine analytical technique. Examples of recent applications in the drug field are the determination of phenobarbital and diphenylhydantoin in blood[1], and of trimethoprim in blood and urine[2]; the sensitivities quoted for these procedures are about 1 μg ml^{-1}.

The present work was undertaken to study the suitability of pulse polarography for determining sulphonamides at levels below those that can be determined colorimetrically. Sulphonamides having a free aromatic group, can be determined colorimetrically after diazotization and coupling with, for example, N-(1-naphthyl)-ethylenediamine, to form an azo dye[3,4]. The molar absorptivities, at the wavelength of maximum absorbance (about 545 nm), of the azo dyes formed in these reactions are commonly about $5 \cdot 10^4$ l mol^{-1} cm^{-1}; thus, 10^{-6} *M* solutions have an absorbance of about 0.05 in 1-cm cells.

The direct polarography of sulphonamides is not straightforward. Heyrovský showed that several sulphonamides can be determined by oscillopolarography at the $6 \cdot 10^{-4}$ *M* level[5], and Voorhies and Adams[6] determined them at $0.4 \cdot 10^{-4}$ *M* concentrations by means of the anodic waves obtained at a rotating platinum electrode. The most comprehensive study of the conventional cathodic polarography of sulphonamides seems to have been made by Uno and Okazaki[7] who used dioxan–water mixtures and a quaternary ammonium supporting electrolyte. No polarographic waves were observed for sulphanilamide and sulphaguanidine, and other sulphonamides gave waves more negative (usually considerably more negative) than -1 V. In a brief study of the pulse polarography of sulphacetamide with this supporting electrolyte, the present authors experienced difficulty in obtaining satisfactory polarograms at concentrations of sulphacetamide less than 10^{-4} *M*. Even at higher concentrations, purification of the dioxan to remove all traces of peroxides was essential in order to obtain a good baseline.

To overcome these difficulties, and also in order to make the procedure more generally applicable, it was decided to polarograph azo dye derivatives of the sulphonamides, rather than the sulphonamides themselves.

N-(1-Naphthyl)ethylenediamine was tried initially as the coupling agent after diazotization of sulphanilamide. The optimal pH was found to be 4.1, but the polarographic wave obtained was too close to the steep baseline at 0 V, for use at very low concentrations. The waves obtained at the 10^{-5} and $10^{-6}M$ levels are shown in Fig. 1.

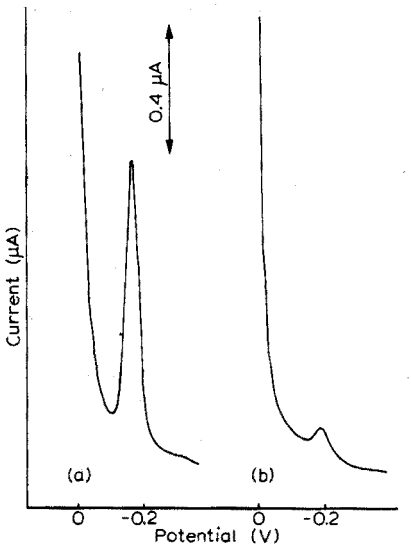

Fig. 1. Differental pulse polarograms obtained with diazotized sulphanilamide coupled with N-(1-naphthyl)ethylenediamine. Concentration of sulphanilamide: (a) $9.3 \cdot 10^{-6}$ *M*; (b) $9.3 \cdot 10^{-7}$ *M*.

An attempt was also made to use the polarographic waves of the diazonium salts formed without addition of a coupling agent. For sulphanilamide, the optimal pH was found to be 1.6, and two polarographic waves were obtained (at −0.10 and −0.45 V) at the $5 \cdot 10^{-5}M$ level. Unfortunately, at lower concentrations no waves were observed, presumably owing to the instability of the diazonium compound.

Satisfactory polarograms were obtained with 1-naphthol as the coupling agent. This also had an advantage over N-(1-naphthyl)ethylenediamine in that coupling can be effected in alkaline solution and the pH of the final solution can be controlled quite satisfactorily by adding a measured volume of sodium hydroxide solution. The polarographic wave of the azo dyes at −0.74 V occurred between two waves at −0.56 V and −0.88 V, which were due to 1-naphthol or an impurity in the 1-naphthol, and to sodium nitrite or an impurity in the sodium nitrite, respectively. After reaction conditions and reagent concentrations had been optimized, the procedure described below was adopted. The use of 2-naphthol, 1,8-diaminonaphthalene and 8-amino-1-naphthol-3,6-disulphonic acid as alternative coupling agents did not give useful polarographic waves at low concentrations.

Experimental

Polarograms were obtained with a PAR 174 Polarographic Analyzer

(Princeton Applied Research Corporation) in the differential pulse polarographic mode of operation (forced drop-time 2 s). The purest grades of reagent available were used, but no attempt was made to purify reagent solutions further by electrolysis. Instead it was found possible to reduce the reagent concentrations sufficiently to obtain a good baseline whilst maintaining complete chemical reaction. Traces of oxygen in the nitrogen gas used to deoxygenate the solutions were removed by means of a vanadium(II) scrubber. Two-electrode operation was used and all potentials were measured against a saturated calomel electrode.

Standard sulphonamide solutions, 10^{-5} M. Prepare sulphonamide solutions (10^{-3} *M*) by dissolving an appropriate amount of solid in dilute hydrochloric acid and diluting to volume; these solutions should contain the equivalent of 1 ml of (1+1) hydrochloric acid in 500 ml. Prepare standard sulphonamide solutions (10^{-5} *M*) by diluting these solutions with water.

Preparation of calibration graph. To 25-ml polarographic cells add aliquots (0–10 ml) of the standard sulphonamide solution. Then add by pipette, swirling between additions, 0.1 ml of hydrochloric acid (1+1), 0.5 ml of sodium nitrite solution (0.1% w/v) and an amount of deionized water to bring the total volume to 25 ml exactly. Place the polarographic cell in an ice bath. After 3 min add 1 ml of sulphamic acid solution (0.5% w/v), and, after a further 1 min add 2 ml of sodium hydroxide solution (4% w/v). After 5 min add 0.4 ml of 1-naphthol solution (0.005% w/v, in methanol, prepared by dilution of a 0.5% solution). Polarograph this solution after standing for a further 30 min to allow complete azo dye formation. During this final standing period deoxygenate the solution by bubbling vanadium(II)-treated nitrogen gas through it; during polarography pass nitrogen over the surface of the solution.

Obtain polarograms by scanning (differential pulse polarographic mode) at a rate of 2 mV s^{-1} from −0.6 V to −0.9 V. In the present work, the forced drop-rate was 2 s and the modulation amplitude (pulse height) was 50 mV. For the lowest concentrations the sensitivity was 0.5 μA full-scale.

Results

Typical polarograms obtained for a calibration graph are shown in Fig. 2. As can be seen the sensitivity is increased slightly by offsetting part of the current. Calibration curves are given in Fig. 3, which also illustrates the difference in sensitivities for the sulphonamides studied. The lower limit of detection was about $5 \cdot 10^{-8}$ *M* for sulphanilamide, sulphathiazine and sulphacetamide, and about $1.2 \cdot 10^{-7}$ *M* for sulphaguanidine (all concentrations quoted for the polarographed solution). The coefficient of variation on 10 solutions at the $2.3 \cdot 10^{-7}$ *M* level of sulphanilamide was 4%.

Discussion

At concentrations above about $2 \cdot 10^{-6}$ *M*, the polarographic method has no outstanding advantage over the traditional colorimetric method. The differential pulse polarographic procedure described here, however, is useful in the range $5 \cdot 10^{-8}$ *M*–$2 \cdot 10^{-6}$ *M* in the case of sulphanilamide, sulphathiazole and sulphacetamide, and $1.2 \cdot 10^{-7}$ *M*–$2 \cdot 10^{-6}$ *M* for sulphaguanidine. The procedure will undoubtedly prove useful for the submicromolar determination of other sulphonamides and primary aromatic amines.

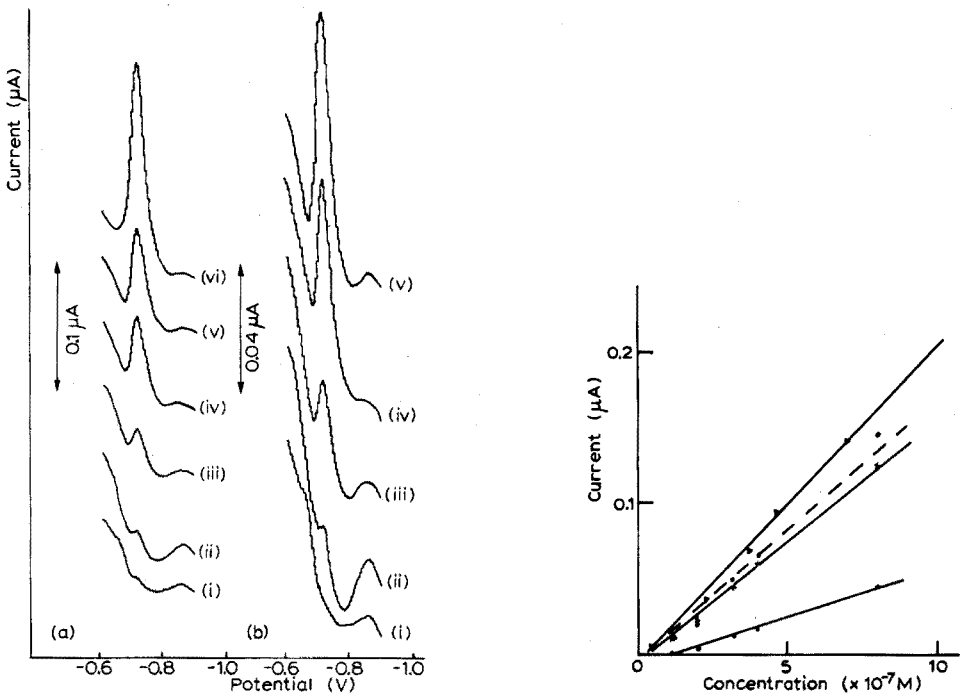

Fig. 2. Differential pulse polarograms of sulphathiazole obtained by the recommended procedure. (a) Sensitivity 0.5 μA; (b) sensitivity 0.2 μA (current offset 0.12 μA). Concentrations ($\cdot 10^{-8} M$): (i) 4, (ii) 12, (iii) 20, (iv) 32, (v) 40, (vi) 80.

Fig. 3. Calibration graphs for sulphonamides. (▲—▲), Sulphanilamide; (·---·), sulphathiazole; (×—×), sulphacetamide; (●—●), sulphaguanidine.

An advantage of polarographing azo dye derivatives rather than the sulphonamides themselves is that in the analysis of sample solutions which are subsequently found to be more concentrated than $2 \cdot 10^{-6} M$, the determination can be finished either colorimetrically or polarographically whichever is the more convenient. The polarographic method, however, does have the advantage that it can be applied to a very wide range of concentrations in the sample solution simply by altering the sensitivity control.

The authors wish to thank Dr. D. Thorburn Burns for his encouragement.

REFERENCES

1 M. A. Brooks, J. A. F. De Silva and M. R. Hackman, *Anal. Chim. Acta*, 64 (1973) 165.
2 M. A. Brooks, J. A. F. De Silva and L. M. D'Arconte, *Anal. Chem.*, 45 (1973) 263.
3 E. K. Marshall, Jr., *J. Biol. Chem.*, 122 (1937/8) 263.
4 A. C. Bratton, E. K. Marshall, Jr., D. Babbitt and A. R. Hendrickson, *J. Biol. Chem.*, 128 (1939) 573.
5 J. Heyrovský, *Anal. Chim. Acta*, 12 (1955) 600.
6 J. D. Voorhies and R. N. Adams, *Anal. Chem.*, 30 (1958) 347.
7 T. Uno and Y. Okazaki, *J. Pharm. Soc. Jap.*, 81 (1961) 1292.

Analytica Chimica Acta, 70 (1974) 245–247

SHORT COMMUNICATION

A study of pH glass electrode drift in acetonitrile buffer solutions

R. S. FARINATO, R. P. T. TOMKINS and P. J. TURNER
Rensselaer Polytechnic Institute, Department of Chemistry, Troy, New York 12181 (U.S.A.)
(Received 16th August 1973)

Glass electrodes have been used for pH measurements in many mixed and nonaqueous solvents with few difficulties[1]. Such pH measurements do not necessarily represent an equilibrium state and long periods of equilibration have shown variations in potential. Several investigators have reported systematic drifts of potentials in nonaqueous solutions, in mixed solvents and in concentrated solutions[2]. This drift has been discussed in terms of exchange of solvent or ions at the glass surface, with a corresponding change in acid–base properties of the glass.

On initial soaking, the approach of the glass electrode to a pseudo-equilibrium state, representing its most stable potential, is governed by the uptake of solvent by the electrode, accompanied by swelling of the surface. The investigation of surface swelling of the pH glass electrode has been confined largely to aqueous solutions, and the exact role of "imbibed" solvent is still unclear[3]. The dissolution of water and other solvents in glass has not been adequately investigated[4].

A recent paper[5] has illustrated that the performance of an electrode glass depends on the structure of its surface layers, and that this is frequently sharply different from the bulk glass structure. The effects of imbibed solvent were not discussed. In the present communication, the drift patterns obtained by soaking glass electrodes in two solvents with widely differing acid–base properties, namely water and acetonitrile, are described.

Experimental

Glass electrodes were Beckman general purpose pH electrodes (4-1263 or equivalent). They were soaked in twice-distilled water for 7 days and the pH response in aqueous solution was verified by measurement in buffers[6] at pH 2.0, 4.0, 6.0, 6.8, 7.0, 7.2, 8.0 and 10.0. Buffer temperature was recorded to ± 0.1°C and the pH response was, in all cases, within 2 mV of the theoretical value. E.m.f. measurements were made with either a Leeds–Northrup Model 7401 pH meter or a Lear–Siegler Model 6753 digital multimeter, against a Corning saturated calomel reference electrode. Acetonitrile (Fisher, Cert. A.C.S., reagent grade) was purified as described previously[7]. The cell and the buffer solutions in acetonitrile were essentially the same as those described by Kolthoff and Chantooni[8]. The cell was filled under nitrogen in a controlled atmosphere and

measurements were carried out in a silicone–oil thermostat maintained at 25 ± 0.01°C.

Electrode drift in the acetonitrile buffers was followed for 2–3 days, after which the electrodes were removed and recalibrated in the aqueous buffers. The electrodes were then stored in acetonitrile for several weeks and soaked in water for periods up to 5 days before recalibrating again in water. No significant change in pH response was found in either case. The drift in acetonitrile of glass electrodes stored in water was followed several times for each electrode, and the pH response in acetonitrile buffers examined.

Results and discussion

The general features of electrode drift in the acetonitrile buffers are summarized in Fig. 1. This refers to electrodes soaked for one week each in water, acetonitrile, and water, in sequence. The period of drift to more negative potentials, AB in Fig. 1, occurred regardless of the detailed history of the electrode, and implies an increased basicity of the cell solution relative to the glass. If the buffer solution can be regarded as having a fixed pH, it can only be concluded that the proton activity in the glass is being increased either by dehydration or by an exchange of solvent between the glass lattice and the buffer which makes the glass behave as a less basic mixed solvent. This drift can be represented by a Nernst equation involving proton exchange between glass electrode and solutions, *viz.*,

$$E = E^0 + RT/F \ln [a_{H^+(\text{solution})}/a_{H^+(\text{glass})}] \quad (1)$$

where E, R, T, and F have their usual significance, and E^0 is a combination of reference electrode potentials on both sides of the glass, and includes the liquid junction potentials and the asymmetry potential at the inside surface of the glass.

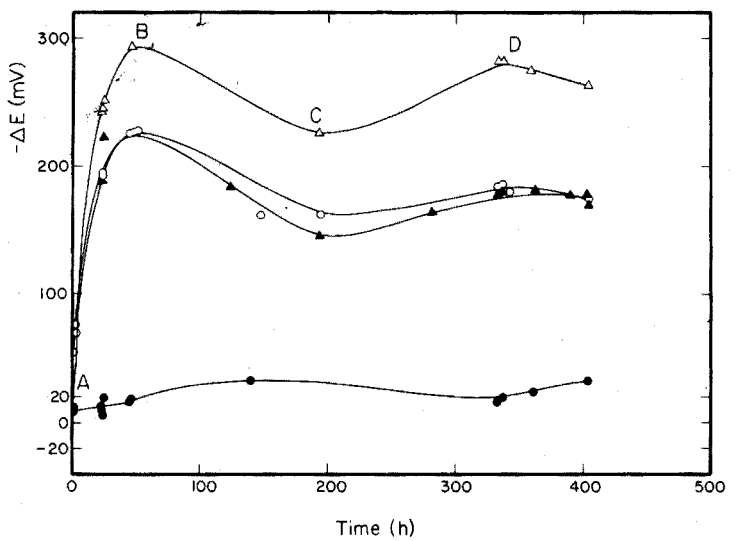

Fig. 1. Drift curves for Beckman glass electrodes in acetonitrile buffers. The curves drawn through the points (○), (●), (△), and (▲) represent drift patterns for four different electrodes.

When $a_{H^+\,(solution)}$ is fixed, the typical drift of 210–300 mV in the section AB represents a change in the pH of the glass of 3.5–5 pH units.

Boundaries within the glass can be treated in the same way as the glass–solution boundary[4]; if the proton is the most mobile species in the glass, which can be expected for a region saturated with solvent, eqn. (1) can be applied. A boundary of the type

$$\begin{array}{c|c} \text{(inside) glass sat.} & \text{glass sat. (outside)} \\ \text{with MeCN} & \text{with } H_2O \end{array}$$

will be influenced by removal of water from the right-hand side and its replacement by acetonitrile: a_{H^+} is raised if the overall solvent basicity decreases and the proton concentration remains essentially the same. This theory embodies the assumption that the solvents are more readily moved through the glass structure than protons. The above accounts for the section BC of the graph. The section CD can be interpreted as either a further solvent–solvent boundary in the reverse sense, or the disappearance of the in-glass boundary suggested above, when most of the water has been removed or redistributed over a larger volume of glass.

The authors are indebted to the U.S. Department of Defense, Project Themis for support with this project.

REFERENCES

1 G. J. Hills, in D. J. G. Ives and G. J. Janz (Eds.), *Reference Electrodes*, Academic Press, New York, 1960, Ch. 10.
2 W. H. Beck and W. F. K. Wynne-Jones, *J. Chim. Phys.*, 49 (1952) C97.
3 R. G. Bates, in D. J. G. Ives and G. J. Janz (Eds.), *Reference Electrodes*, Academic Press, New York, 1960, Ch. 5.
4 R. H. Doremus, in G. Eisenman (Ed.), *Glass Electrodes for Hydrogen and Other Cations*, Dekker, 1967, p. 130.
5 B. Csákvári, Z. Boksay and G. Bouquet, *Anal. Chim. Acta*, 56 (1971) 279.
6 *Langes' Handbook of Chemistry*, Handbook Publishers, Sandusky, Ohio, 7th edn., 1949, 1127–28.
7 E. J. Andalaft, R. P. T. Tomkins and G. J. Janz, *Trans. Faraday Soc.*, 65 (1969) 1906.
8 I. M. Kolthoff and M. K. Chantooni, *J. Amer. Chem. Soc.*, 87 (1965) 4428.

Analytica Chimica Acta, 70 (1974) 248–250

BOOK REVIEWS

Indicators, Edited by E. Bishop, International Series of Monographs in Analytical Chemistry, Vol. 51, Pergamon Press, Oxford, 1972, x + 746 pp., Price £ 12.00.

The use of indicators is so widespread that it is not easy to imagine analytical chemistry existing without them, and yet they are often taken for granted and virtually ignored in considering analytical reactions. There are very few textbooks which deal with indicators in any depth, and those that do are either outdated or restrict themselves to a consideration of one or two types of indicators.

This book is essentially a collection of monographs each dealing with some aspect of the field. They are up-to-date and extensive; indeed in one chapter that deals with metallochromic indicators, there are approximately 200 pages listing colour changes involved and the solution conditions necessary for the optimal use of the indicator. In another section, over 1,000 dyestuffs are listed for redox use. This will surely be the source book and standard reference book on indicators for some time. It is well presented, has a very useful index and covers the entire working range of visual indicators. There are very few books which deserve the commendation "Should be in every analytical laboratory"—this however is one such book.

L. S. Bark (Salford)

Instrumentation in Applied Nuclear Chemistry, Edited by Jan Krugers, Plenum, New York, 1973, xiv + 383 pp., Price $ 29.00.

This book makes an interesting and generally successful attempt to explain in non-mathematical terms the mode of action of some commonly used systems for the measurement of radiation from radioactive substances. Three introductory chapters survey the basic phenomena of radioactivity and its instrumentation. These are followed by chapters each devoted to a particular topic, such as detectors, preamplifiers, main amplifiers, single and multi-channel analysers, and timing circuits: there are also chapters on statistics, the Nuclear Instrument Module specifications, and the use of computers. Each of the chapters is reasonably complete in itself. There is a good index.

On the whole, the editor has managed to steer a nice course between unnecessary duplication of material and omission of essential information within the bounds of the topics dealt with. It seems inevitable, however, that one finds in a "multi-author" book a few sections written in a jargon which could often mystify or even mislead the novice. Perhaps a more serious criticism is that there is no section on scalers and ratemeters *per se*, nor on radiation monitoring equipment. This is, of course, an American book and readers in the U.K. should bear in mind that NIM equipment is available from British suppliers, as indeed is stated in one

place (p. 156). There are very few misprints; the diagrams and tables are generally adequate and some are very good. Each chapter concludes with a list of references which cover the important books and definitive articles published in the last two decades.

The blurb on the dust cover particularly commends to the reader the chapters on amplifiers and on the use of computers. These are indeed well written. Of the others, the chapters on the NIM standard and Krugers' own chapter on Statistics are of particular interest and usefulness. Altogether this is a book to be very highly recommended to all those whose work depends in any way on the measurement of radiation from radioactive isotopes.

K. F. Chackett (Birmingham)

Milton J. Rosen and Henry A. Goldsmith, *Systematic Analysis of Surface-Active Agents*, 2nd edn. (Vol. 12 of Chemical Analysis ed. by I. M. Kolthoff and P. J. Elving), Wiley-Interscience, New York, 1972, xxvi + 591 pp., Price £ 10.80.

Many of the rapid developments in analytical chemistry are reflected in this new edition of the original 1960 text. In particular, infra-red and nuclear magnetic resonance spectrometry are of great value in the elucidation of molecular structure, and chromatography of all types has greatly facilitated the separation and identification of the various surfactants. Both these aspects are included in the new edition and a table of g.l.c. packings and representative i.r. spectra are included in an Appendix. Another addition is a section dealing with the separation and identification of raw materials and non-surfactant additives. Various other minor changes and re-arrangements have been made, including updating of tables of surfactants and their properties, so that the overall book presents a comprehensive, logical account of current methods of surfactant analysis. The text is essentially a working manual, and as such will be especially welcomed by all surfactant chemists working at the bench.

A. Townshend (Birmingham)

Organometallic compounds. Methods of synthesis, Physical Constants and Chemical Reactions, Vol. 2, First Supplement, Edited by M. Dub, Springer Verlag, Berlin, 1973, xxv + 1116 pp., price DM 112,90; $ 50.80.

This volume covers methods of synthesis, physical constants and chemical reactions of the compounds of germanium, tin and lead which have been published during the period 1965–1968. The output of literature has increased to such an extent that this four-year supplement covers more references than the respective main volumes contained for the period 1937–1964. Accordingly, additional assistance has been required and Dr. R. W. Weiss of Lemgo, Germany, is responsible for this invaluable compilation. The coverage is thorough and is based mainly on American Chemical Abstracts. In addition, references to patents and articles from

Soviet journals are included. Apart from the aspects mentioned in the title, biological properties have been included.

The format of this book is good, and production is of the usual high standard. The latest reference in the book is now, however, five years old, and one feels that some of its usefulness has been lost by the long delay in publishing.

E. J. Forbes (Birmingham)

RECENT N.B.S. PUBLICATIONS

Space Groups and Lattice Complexes, W. Fisher, H. Burzlaff, E. Hellner and J. D. H. Donnay, N.B.S. Monograph 134, May 1973, 184 pp., price $4.10.

Reactivity of the Hydroxyl Radical in Aqueous Solutions, L. M. Dorfman and G. E. Adams, NSRDS-NBS 46, June 1973, 72 pp., price 65 cents.

Method for Determining the Resolving Power of Photographic Lenses, F. E. Washer and I. C. Gardner, N.B.S. Special Publ. 374, June 1973, 32 pp., price $3.00.

Selected Specific Rates of Reactions of Transients from Water in Aqueous Solution. I. Hydrated Electrons, M. Anbar, NSRDS-NBS 43, May 1973, 67 pp., price 90 cents.

Standard Reference Materials. Development of the NBS SRM No. 1579: Powdered lead-based paint, B. Greifer, E. J. Maienthal, T. C. Rains and S. D. Rasberry, N.B.S. Special Publ. 260–45, March 1973, 31 pp., price 50 cents.

Liquid Densities of Oxygen, Nitrogen, Argon and Parahydrogen, H. M. Roder, R. D. McCarty and V. J. Johnson, N.B.S. Technical Note 361, October 1972, 142 pp., price $1.50.

Standard Reference Materials: Preparation and Use of Superconductive Fixed Point Devices, SRM 767, J. F. Schooley, R. J. Soulen, Jr. and G. A. Evans, Jr., N.B.S. Special Publ. 260–44, December 1972, 35 pp., price 75 cents.

Low-Temperature Thermometry: Interim Report, G. Cataland and H. H. Plumb, N.B.S. Technical Note 763, May 1973, 23 pp., price 40 cents.

Selected Values of Chemical Thermodynamic Properties: Tables for the Lanthanide Elements (Elements 62–76), R. H. Schumm, D. D. Wagman, S. Bailey, W. H. Evans and V. B. Parker, N.B.S. Technical Note 270–7, April 1973, 93 pp., price $1.25.

A New Method for Generating Water Drops of Specified Mass. J. E. Potzick, N.B.S. Technical Note 776, May 1973, 12 pp., price 35 cents.

Accuracy in Spectrophotometry and Luminescence Measurements, Proceedings of the Conference held at N.B.S., Gaithersburg, March 1972, edited by R. Mavrodineanu, J. I. Schulz and O. Menis, N.B.S. Special Publ. 378, May 1973, 268 pp., price $4.85.

Platinum Resistance Thermometry, J. L. Riddle, G. T. Furukawa and H. H. Plumb, N.B.S. Monograph 126, April 1973, 129 pp., price $2.10.

All these publications can be obtained (prepaid in $) from the Superintendent of Documents, U.S. Government Printed Office. Washington, D.C. 20402. Foreign remittances must include 25% of the purchase price to cover mailing costs.

Analytica Chimica Acta, 70 (1974) 251

ANNOUNCEMENTS

2nd International Symposium on Mass Spectrometry in Biochemistry and Medicine

The Istituto di Ricerche Farmacologiche "Mario Negri" is organizing the 2nd International Symposium on Mass Spectrometry in Biochemistry and Medicine, from Monday 24th June to Wednesday 26th June 1974, at the Institute in Milan, Italy.

The Symposium will be devoted to topics such as gas chromatography–mass spectrometry, mass fragmentography, stable isotope measurements, field ionization, field desorption, chemical ionization, high resolution studies, data acquisition and processing, and the areas of application will include biochemistry, medicine, toxicology, drug research, forensic science, clinical chemistry and pollution.

The Symposium will consist of presentations from invited speakers and free communications.

It is intended to publish the Proceedings of the Symposium. The Final Program will be mailed to all participants in May 1974. The official language will be English.

An instrument and book exhibition and displays of manufacturers' literature on mass spectrometers and related instrumentation will be staged for the whole period of the Symposium.

The registration fee, including a copy of Abstracts of papers to be given at the Symposium, is 15,000 Italian Lire.

Further information can be obtained from Dr. Alberto Frigerio, Istituto di Ricerche Farmacologiche "Mario Negri", 20157 Milano, Via Eritrea 62, Italy.

5th EUCHEM Conference on Molten Salts, September 1974

The 5th EUCHEM Conference on Molten Salts will take place on 9–13 September, 1974, at Freising/Obb. (BRD). Prof. Dr. A. Klemm, Mainz, will be Chairman of the Conference.

The Conference will cover: (1) Computer simulation, (2) Short time dynamics, (3) Reactions, (4) Transport properties, (5) Spectroscopy, (6) Thermodynamics, (7) Applications, (8) Recent advances.

The provisional program as well as the preliminary registration forms may be obtained from Dr. W. Fritsche, Gesellschaft Deutscher Chemiker, D-6000 Frankfurt/M 90, Post Office Box 90 04 40 (BRD).

Analytica Chimica Acta, 70 (1974) 252

ERRATA

Takayoshi Yoshimori and Tatsuhiko Tanaka, Preparation of sulphamic acid single crystals and their assay by precise coulometric titration, *Anal. Chim. Acta*, 66 (1973) 85–91.

Tables I and II of this paper should have read as follows:

TABLE I

LOSS IN WEIGHTS OF FOUR CRYSTALS DRIED SUCCESSIVELY BY VARIOUS METHODS

(Weight in mg)

Method of drying	*1*	*2*	*3*	*4*	*Average of weight loss (%)*
In atmosphere	840.038	790.043	551.045	882.492	—
Stored in conc. H_2SO_4 desiccator	840.037	790.041	551.045	882.491	0.000_1
In vacuo over conc. H_2SO_4 — 2 h	840.036	790.038	551.044	882.489	0.000_4
In vacuo over conc. H_2SO_4 — 48 h[a]	840.034	790.038	551.044	882.490	0.000_4
Heated at 60° for 4 h	840.038	790.041	551.046	882.493	0
Heated at 140° for 1 h	840.088	790.057			

[a] JIS method.

TABLE II

PURITIES OF SINGLE CRYSTALS

Sample	*Method of drying*	*Weight before breaking (g)*	*No. of detns.*	*Average purity (%)*	*s (%)*
Small crystal 200–400 mg	A[a]		6	99.882_3	0.090_2
	B[b]		5	99.899_1	0.097_7
Medium crystal 1–2 g	A		12	99.927_1	0.047_0
	B		5	99.896_3	0.056_3
Large crystal 4.5 g	A	7.0	4	99.979_1	0.004_1
		5.5	7	99.967_0	0.016_3
		4.8	6	99.972_8	0.013_8
	B	6.1	6	99.984_7	0.016_8
		8.5	6	99.984_5	0.019_9
		5.4	5	99.951_7	0.009_3
		7.9[c]	11	99.978_4	0.017_6
		7.0[d]	8	99.977_2	0.013_5

[a] *In vacuo* over concentrated sulphuric acid for 48 h. [b] In the atmosphere. [c] Crystal prepared from an unguaranteed reagent. [d] Crystal grown at room temperature.

Analytica Chimica Acta, 70 (1973) 253–263

SIMULTANEOUS DETERMINATION OF SILICON AND ALUMINIUM IN FERROSILICON BY INSTRUMENTAL NEUTRON ACTIVATION ANALYSIS WITH THE AID OF AN ^{227}Ac–Be ISOTOPIC NEUTRON SOURCE

L. ALAERTS*, J. P. OP DE BEECK and J. HOSTE

Institute for Nuclear Sciences, Rijksuniversiteit Gent, Proeftuinstraat 86 B-9000 Gent (Belgium)

(Received 20th December 1973)

Many chemical and physicochemical methods have been described for the determination of silicon in silicate rocks and silicon-containing alloys with a relative precision ranging from 0.2 to 0.6% (refs. 1–5). All these methods include the tedious decomposition of the sample by digestion with strong mineral acids or by fusion with a suitable flux. The most commonly used absolute method is the gravimetric determination, based on the weighing of silica obtained by dehydration, in strong acids of freshly precipitated silicic acid; differences of 1% or more have, however, been observed between analytical results from different laboratories[6]. Furthermore, silicon determinations in six U.S. Geological Survey standard rocks show relative discrepancies ranging from 0.6 to 1.2% if results obtained by different analysts using different techniques are compared[7].

In earlier publications[8,9], it was shown that neutron activation analysis with an isotopic neutron source can be made competitive with classical wet chemical methods. Indeed, precision and accuracy are comparable, if not better, provided that some potential sources of systematic errors are carefully evaluated and eliminated or corrected for. These errors are geometry effects arising from sampling and pellet preparation, neutron self-shielding, γ-attenuation, the presence of strong neutron absorbers, and the reproducibility of geometry during irradiation and counting.

Silicon and aluminium can be determined simultaneously by a double irradiation technique with different ratios of fast to thermal neutron flux. This method has already been used in prospecting and refining of bauxite in the aluminium industry[10]; in that work the simplicity and speed were mainly emphasized, and the precision obtained was satisfactory for field applications only.

In the following paragraphs, it will be shown that the precision of the method can be made similar to that obtained from the chemical or physicochemical methods used hitherto for the determination of silicon and aluminium in ferrosilicon. The accuracy of the method is believed to be better than that of the classical chemical methods used previously, since systematic errors can be easily predicted and corrected for.

The neutron source and counting equipment

An annular ^{227}Ac–Be isotopic neutron source with a total neutron output

* Aspirant of the N.F.W.O.

of 10^8 n s^{-1} was used. The characteristics of this irradiation facility have been described elsewhere[8]. Figure 1 shows the flux gradients for fast, epithermal and thermal fluxes in the vicinity of the source as well as the two irradiation positions used for activation.

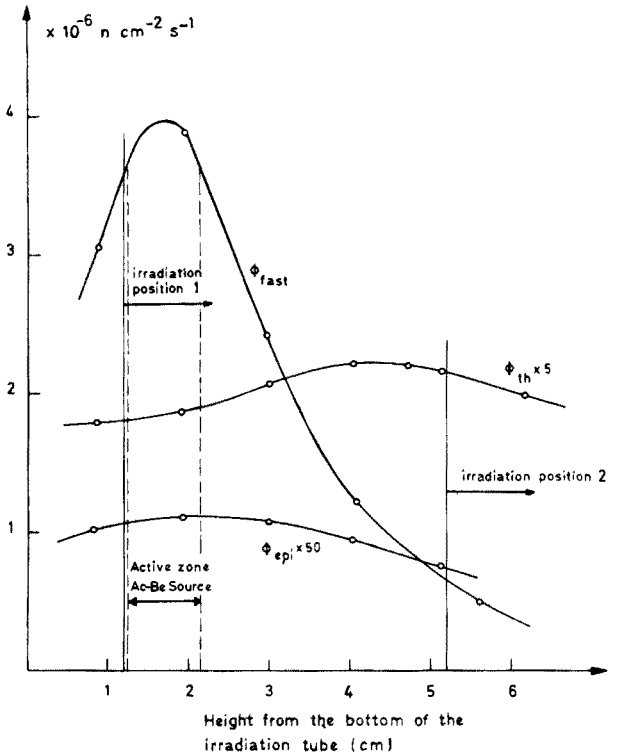

Fig. 1. Flux gradients for fast, epithermal and thermal fluxes in the vicinity of the source and the two irradiation positions used for activation.

As can be seen, the design of the source and irradiation facility results in rather well-separated thermal and fast flux maxima. This allows consecutive irradiation at two positions with a strongly different $\phi_{fast}/\phi_{thermal}$ ratio, without making use of cadmium covers.

The consecutive irradiation of the same sample at the two different irradiation positions was preferred to the simultaneous irradiation of two different samples, in order to avoid small systematic errors arising from slight differences in sample preparation.

Principle of the method

If ferrosilicon is exposed to a flux of both fast and thermal neutrons, only a few reactions give rise to measurable activities. They are due to the presence of silicon (70–80%), iron (*ca.* 20%), aluminium (1–4%) and manganese (up to 0.1%). The nuclear reactions of interest are listed in Table I, whilst Fig. 2 shows the spectrum of a typical irradiated sample.

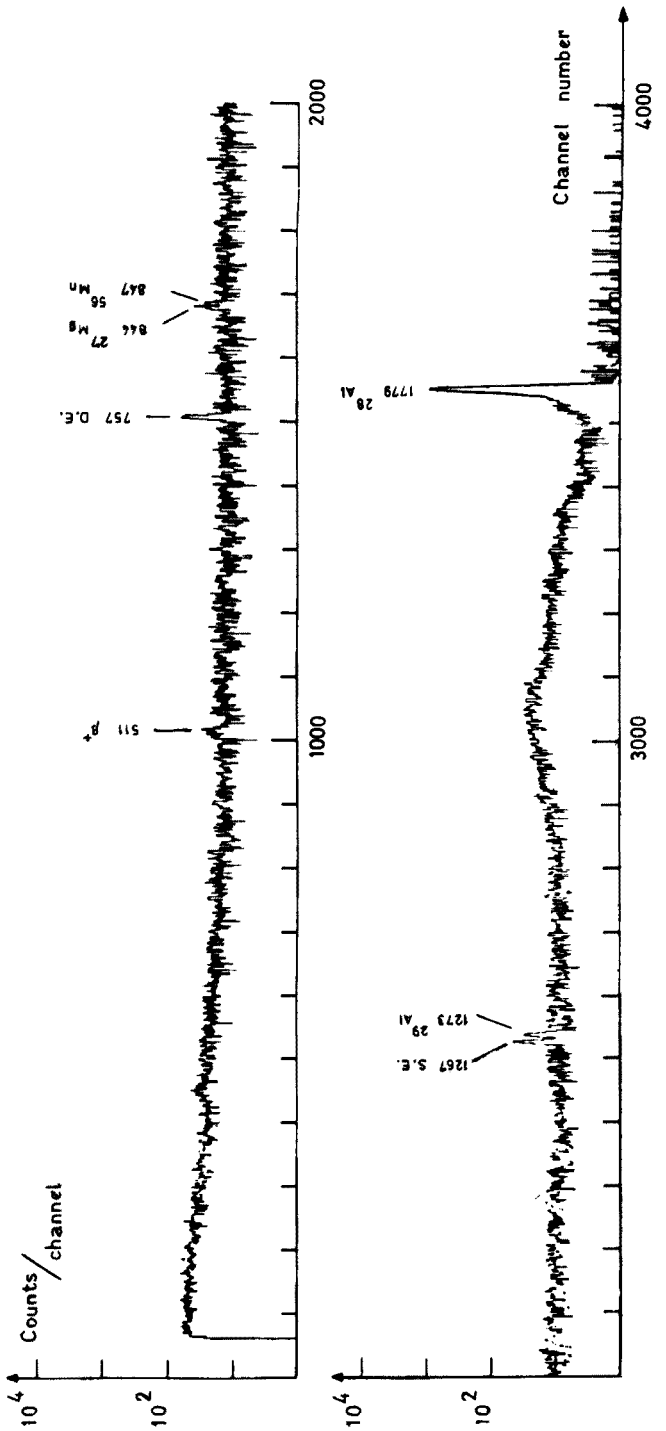

Fig. 2. Ge(Li) spectrum of a pellet of sample 0972/200; irradiation time, 200 s; cooling time, 40 s; counting time, 300 s.

TABLE I

NUCLEAR REACTIONS AND DATA

Reaction	*Abundance of parent isotope (%)*	*Cross section (mb)*	*Half-life (ref. 12)*	*γ-Energies (keV) (ref. 13)*
$^{28}Si(n, p)^{28}Al$	92.21	2.0 (11)	2.240 min	1778.8
$^{29}Si(n, p)^{29}Al$	4.7	0.6 (11)	6.52 min	1273.3
$^{30}Si(n, \alpha)^{27}Mg$	3.09	0.1 (11)	9.45 min	843.8, 1014.4
$^{27}Al(n, \gamma)^{28}Al$	100	231 (12)	2.240 min	1778.8
$^{27}Al(n, p)^{27}Mg$	100	4.3 (11)	9.45 min	843.8, 1014.4
$^{27}Al(n, \alpha)^{24}Na$	100	0.65 (11)	15.02 h	1368.5, 2754.0
$^{56}Fe(n, p)^{56}Mn$	91.7	0.9 (11)	2.582 h	846.8, 1811.0;
$^{55}Mn(n, \gamma)^{56}Mn$	100	13300 (12)	2.582 h	2112.8

As can be seen, ^{56}Mn is the only isotope which has been obtained from neither silicon nor aluminium. Correction for it is therefore necessary. This can be done by a single measurement after complete decay of ^{28}Al, ^{29}Al and ^{27}Mg. The remaining ^{24}Na activity can be neglected even for the highest aluminium concentrations used in this work, as can be deduced from Fig. 3, which gives the decay curves of a pure (99.99%) aluminium sample of 6.8 g after irradiation in positions 1 and 2.

In the integral counting mode, after correction for ^{56}Mn, the activities measured after irradiation at two different irradiation positions (having different $\phi_{fast}/\phi_{thermal}$ ratios) are represented by the following set of equations:

$$A_1 = aw_{Si} + bw_{Al} \quad (1)$$

$$A_2 = cw_{Si} + dw_{Al} \quad (2)$$

where A_1 or A_2 is the activity after irradiation at posn. 1 or 2 after correction for ^{56}Mn; a or c is the total specific activity caused by silicon only, after irradiation in posn. 1 or 2; b or d is the total specific activity caused by aluminium only, after irradiation in posn. 1 or 2; w_{Si} is the weight of silicon in the sample; and w_{Al} is the weight of aluminium in the sample. Positions 1 and 2 are the irradiation positions as shown in Fig. 1.

The coefficients a, b, c and d are determined once and for all, for a given irradiation and counting set-up and timing sequence, with the aid of at least two samples of accurately known silicon and aluminium concentrations. The contents of silicon and aluminium in unknown samples can then be determined by solving the set of two equations for w_{Si} and w_{Al}, without the use of standards, provided that counting is carried out with highly stable counting equipment and that a correction for neutron source decay is included (*ca.* 0.01% per day).

Determination of the coefficients

The coefficients a, b, c and d in eqns. (1) and (2) are determined by carrying out the analytical sequence described below (Table III) with four synthetic samples of known composition pressed from a mixture of powdered high-purity semiconductor silicon, non-hygroscopic spectrographically pure alumina, carbonyl iron and a finely powdered wax (Hoechst wachs C pulver) as a pelletiz-

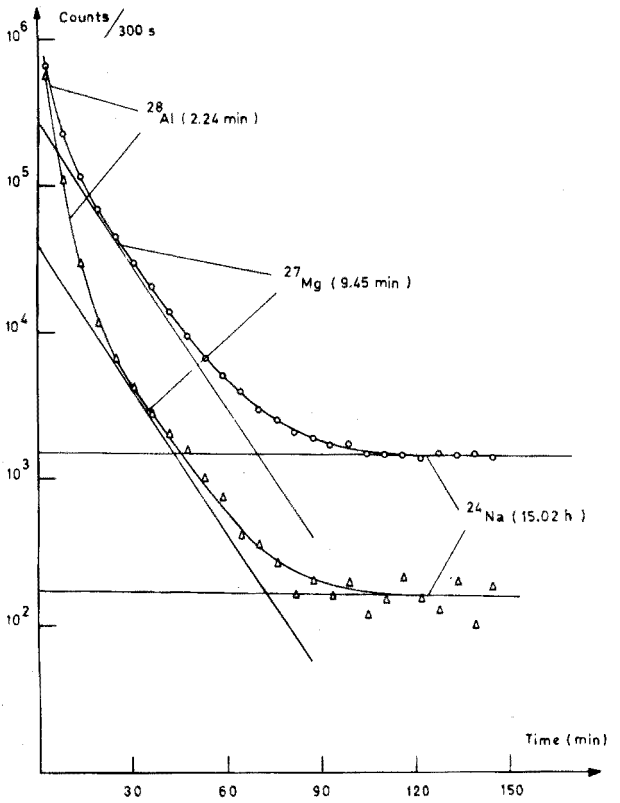

Fig. 3. Decay curves of a pure (99.99%) aluminium sample of 6.8 g, (○) after irradiation in position 1; (△) after irradiation in position 2.

ing agent. Three of the samples have approximately the same silicon and aluminium contents. They are combined one by one with the fourth, which differs considerably, in order to obtain optimal conditions for the determination of the coefficients.

The compositions of these synthetic ferrosilicon samples were as follows:

Samples 1–3: *ca.* 3.4 g of Si, *ca.* 1 g of Fe, *ca.* 0.3 g of Al_2O_3 and *ca.* 0.88 g of wax;

Sample 4: *ca.* 2.2 of Si, *ca.* 0.9 g of Fe, *ca.* 1.2 g of Al_2O_3 and *ca.* 0.87 g of wax.

Each of the four pellets was irradiated three times at every irradiation position and the mean of activities was used in the calculations. The weighted mean of the coefficients obtained and the standard deviation on that mean were as follows (counts per 300 s g^{-1}): $a = 78{,}039 \pm 180$, $b = 94{,}136 \pm 769$, $c = 10{,}494 \pm 23$, $d = 79{,}517 \pm 186$.

These coefficients were used to calculate the contents of the four synthetic pellets; the results are shown in Table II. The close agreement between the activation results and the true contents for all of these samples proves that the method is internally consistent and that no systematic errors occur in this group of samples.

No systematic errors from γ-attenuation are to be expected in using the obtained coefficients for the analysis of true ferrosilicon samples, since there is a

TABLE II

COMPARISON BETWEEN NEUTRON ACTIVATION RESULTS AND ACTUAL CONTENTS OF FOUR SYNTHETIC SAMPLES

Sample no.	*Silicon content (%)*		*Aluminium content (%)*	
	Actual	*N.A.A.*	*Actual*	*N.A.A.*
Synth 1	74.90	74.93±0.50	2.74	2.78±0.09
Synth 2	72.78	73.00±0.53	3.52	3.46±0.07
Synth 3	71.16	70.91±0.38	3.39	3.46±0.08
Synth 4	51.52	51.58±0.41	14.68	14.62±0.10

great similarity in composition and in pellet weight between ferrosilicon pellets and the synthetic samples used above.

SAMPLE PREPARATION AND SEQUENCE OF ANALYSIS

Samples were made from a mixture of powdered material and the wax. The mixture was pressed, at 400 kg cm^{-2}, into pellets of constant dimensions (diameter 2.00 cm; height 0.82 cm±0.03 cm). The ferrosilicon samples contain *ca.* 4.58 g of ferrosilicon and *ca.* 0.88 g of wax. Table III shows how nine pellets (3 different samples) go through a sequence of analysis with a total duration of 3 h and 39 min.

TABLE III

SEQUENCE OF ANALYSIS

Pellet no.	*Start time irradn. in position 1*	*Start time 2nd counting (^{56}Mn)*	*Start time irradn. in position 2*	*Start time 2nd counting (^{56}Mn)*
I_1	0 h 00	0 h 58	1 h 48	2 h 46
I_2	0 h 06	1 h 04	1 h 54	2 h 52
I_3	0 h 12	1 h 10	2 h 00	2 h 58
II_1	0 h 18	1 h 16	2 h 06	3 h 04
II_2	0 h 24	1 h 22	2 h 12	3 h 10
II_3	0 h 30	1 h 28	2 h 18	3 h 16
III_1	0 h 36	1 h 34	2 h 24	3 h 22
III_2	0 h 42	1 h 40	2 h 30	3 h 28
III_3	0 h 48	1 h 46	2 h 36	3 h 34

At position 1 each pellet is irradiated for 200 s and then transferred from the irradiation container to the detector. A counting time of 300 s starts exactly 40 s after the end of the irradiation. The second sample is irradiated while the first is being counted. After the ninth pellet has been counted, the whole series is counted a second time in order to provide a correction for ^{56}Mn activity for each pellet during the first counting period.

During the second count of the last pellet after irradiation in position 1, an identical series of irradiations and double countings is started for irradiation in position 2.

As can be seen from Table III, there is a decay period of 54 min between the first and second counting period for the same pellet in each of the two irradiation positions. At the end of this period, the ^{28}Al and ^{29}Al have completely decayed, but a small ^{27}Mg activity is counted together with the ^{56}Mn activity. The systematic error resulting from this is less than 0.1% relative to the silicon and aluminium determinations, provided that the silicon content is larger than 55% and the aluminium content is lower than 5%. These limits are never exceeded in commercial ferrosilicon samples. If synthetic samples with lower silicon or higher aluminium content are used, or if less than 9 pellets in one sequence are analysed, a sufficient waiting time between the first and the second measurement of each pellet has to be included in order to allow the ^{27}Mg activity to decay to a negligible level.

Corrections

Decay of the neutron source. In addition to the correction for ^{56}Mn activity which is included in the sequence of analysis, a correction for the decay of the ^{227}Ac-Be neutron source has to be carried out. Indeed, by solving two equations with two unknowns, even a simultaneous change in the two activities measured after irradiation at the two positions results in a systematic error in the calculated silicon and aluminium contents.

In a previous publication[8], it was shown that after the end of the growth period the neutron output of the source can be represented by the following equation:

$$n = n_0 \cdot e^{-\lambda t} \tag{3}$$

where n = neutrons s^{-1}; $n_0 = 1.147 \cdot 10^8$; $\lambda = 8.7145 \cdot 10^{-5}$ (days^{-1}); and t = time in days.

This corresponds to 0.0088% per day.

Geometrical errors during irradiation. Even when pellets are pressed from the same amounts of ferrosilicon and wax at exactly the same pressure, differences of 0.3 mm on a total pellet thickness of 8.2 mm can still be observed. In view of the sharp flux gradients at the two irradiation positions for the thermal and especially for the fast neutron flux, each of the coefficients determined above needs a different correction, since pellets of different thickness are not exposed to the same average flux. The position of the cylindrical pellets at the two irradiation positions is defined and reproduced by fixing the distance of the base of the pellets relative to the neutron source. As the correction for slight differences in pellet height is small, it can be estimated graphically with sufficient precision and accuracy. Starting from the accurately determined curves for flux gradient (Fig. 1), the average flux for a series of pellet thicknesses varying from 5 to 10 mm, was calculated by graphical numerical integration. The integration was carried out by applying the trapezium rule after each pellet had been divided into ten equal parts.

For each of the four flux gradients (two gradients at each of the irradiation positions), a curve was thus obtained giving the average thermal or fast flux in a pellet, as a function of its thickness. Each curve provides a correction for one of the four coefficients defined above. The curves are represented in Fig. 4.

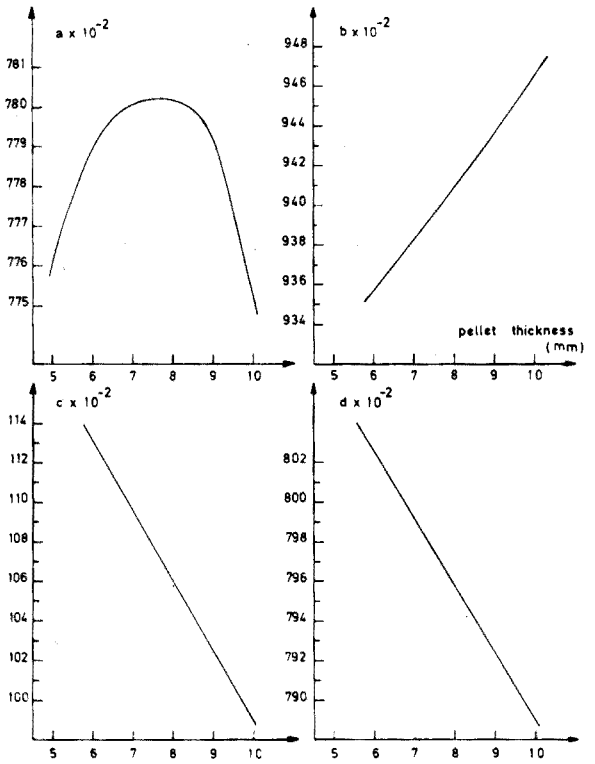

Fig. 4. Coefficients of eqns. (1) and (2) as functions of pellet thickness.

RESULTS AND DISCUSSION

The method of analysis was tested by applying it to two industrial standards, certified respectively by B.C.S. and by I.R.S.I.D., and to a synthetic pellet prepared in this Institute by pressing a mixture of high-purity aluminium filings, high-purity semiconductor silicon and wax. This last sample contained a large amount of aluminium (32%). Finally four samples of ferrosilicon analysed gravimetrically on a routine basis in a steel producing factory were analysed by the proposed method.

Each time three pellets were analysed in an analysis sequence involving 2×9 irradiations, as explained above. From the three counting results, corrected for ^{56}Mn activity, that were obtained for each pellet at each irradiation position, the mean and the standard deviation on the mean, taking into account Student's t-factor for 70% confidence level, were calculated. With these net results, eqns. (1) and (2) were solved. The resulting contents for silicon and aluminium were expressed in percent and a standard deviation was calculated by means of the common error propagation quations, taking into account the standard deviations on the activities as well as on the coefficients. The results are summarized in Table IV.

As can be seen from Tables II and IV, for all of the five synthetic samples, as well as for the B.C.S. and I.R.S.I.D. standards and sample 0972/200, the differences between the results obtained by activation and classical chemical

methods lay practically within the range of the standard deviation for both silicon and aluminium. For the other three industrial samples the activation method gave higher results for silicon and lower results for aluminium. It is interesting in this respect that a tendency to systematically low results for silicon and high results for aluminium is known to occur commonly for gravimetric silicon and aluminium determinations[14].

TABLE IV

COMPARISON OF RESULTS OBTAINED BY NEUTRON ACTIVATION AND CLASSICAL METHODS

	Si content		*Al content*	
	Chem. (%)	*N.A.A. (%)*	*Chem. (%)*	*N.A.A. (%)*
1071/735	74.80	77.15±0.52	1.62	1.38±0.13
1071/386	75.00	75.71±0.54	2.20	1.98±0.13
0372/340	74.97	78.09±0.65	3.22	1.96±0.12
0972/200	76.20	75.85±0.56	2.14	2.14±0.09
IRSID 501/1[a]	79.30	79.90±0.67	—	1.50±0.08
BCS 305/1[b]	75.00	75.45±0.43	1.38	1.47±0.05
Synth 5	67.62	68.15±0.73	32.37	32.31±0.27

[a] Only two pellets were analysed.
[b] Six pellets were analysed.

The relative precision obtained for the silicon determination in ferrosilicon containing approximately 75% Si was ±0.7%, 80% of which is due to counting statistics on the activities and on the coefficients, for an analysis based on double irradiation of three pellets.

For the aluminium determination, the relative precision is strongly dependent on the aluminium content and varies from ±2% for a content of 3.5% to ±7% for a content of 1.5%. From the results for the samples Synth 4 and Synth 5, it can be seen that the relative precision becomes 0.8% for an aluminium content of 15% or higher. Because of the methods of calculation and correction, the precision for both silicon and aluminium depends on their relative ratio as well as on their absolute concentration, and even to a lesser extent, on the amount of iron present.

CONCLUSION

A method has been developed for the simultaneous determination of silicon and aluminium in ferrosilicon, with high precision and accuracy. An isotopic neutron source is used as a highly stable, safe and relatively cheap irradiation facility. The counting equipment consists of standard, commercial, simple, relatively cheap integral counting mode plug-in units, coupled to a well-type NaI(Tl) scintillation detector.

The technique requires two consecutive irradiations of 200 s and two countings of 300 s per irradiation for each sample. Time is most economically used in a semi-automatic analytical sequence involving nine samples with overlapping counting and irradiation periods.

Evaluation of the analytical results requires the solving of a set of two linear equations. The coefficients for these equations can be determined once and for all, with the aid of two or more ferrosilicon samples of accurately known composition or with synthetically made samples, provided that the following conditions are fulfilled: (1) the irradiation positions must be carefully reproduced by always using the same rabbit and by using the same massive polyethylene separator inside the rabbit to fix the position of the sample; (2) the pellets must be carefully reproduced by using always the same amount of ferrosilicon (regardless of its composition) combined with the same amount of wax, and by using the same pressure; (3) a large volume well-type detector (7.5 × 7.5 cm) must be used to insure reproducible counting geometry; (4) the electronic counting equipment must be stable; in the present case, the shift was only *ca.* 0.4% over a 3-month period.

Practically, two corrections are required. The first is a simple correction for decay of the neutron source (21.77 years half-life) and should be done every week. The second correction is required to compensate small, practically unavoidable discrepancies in thickness between pellets. This correction is obtained by applying a correction factor from a graph because the required corrections depend only on the flux gradients and can be determined once and for all.

The precision of the proposed technique is similar to that obtained for silicon determinations by means of classical chemical methods. The method is relatively fast since three samples can be analyzed in threefold within 3.5 h. Because systematic errors can be easily predicted, calculated or measured, and corrected, the activation method has inherently a better accuracy than other methods used hitherto.

The irradiation facility, counting apparatus, calculation and correction procedure are sufficiently safe and foolproof to allow the method to be used in an industrial environment without the necessity for highly qualified personnel.

Thanks are due to the Nationaal Fonds voor Wetenschappelijk Onderzoek for partial financial support and to Dr. D. De Soete for providing the ferrosilicon samples.

SUMMARY

A method has been developed for the accurate determination of silicon and aluminium by instrumental neutron activation analysis with the aid of an ^{227}Ac–Be isotopic neutron source. The samples are pellets made of 4.6 g of ferrosilicon and 0.9 g of a pelletizing agent. Each pellet is irradiated twice at two different fast-to-thermal neutron flux ratios. Each irradiation is followed by two integral mode countings. This allows correction for manganese activities and calculation of the fraction of the aluminium activity induced in silicon and aluminium. The method has been tested with laboratory-prepared synthetic samples as well as commercially certified ferrosilicon. For ferrosilicon containing 75% Si, a relative precision of 0.7% for the results of the silicon concentration has been obtained. For aluminium the relative precision varied from 2 to 7% for concentrations of 3.5 to 1.5%.

REFERENCES

1 A. Ringbom, P. E. Ahlers and S. Siitonen, *Anal. Chim. Acta*, 20 (1959) 78.
2 P. G. Jeffery and A. D. Wilson, *Analyst (London)*, 85 (1960) 478.
3 F. J. Langmyhr and P. E. Paus, *Anal. Chim. Acta*, 43 (1968) 397.
4 F. J. Langmyhr and P. E. Paus, *Anal. Chim. Acta*, 45 (1969) 173.
5 W. Dobner, G. Wronka and W. Becker, *Arch. Eisenhuetten.*, 42 (1971) 643.
6 H. W. Fairbairn, *Geochim. Cosmochim. Acta*, 4 (1953) 143.
7 F. J. Flanagan, *Geochim. Cosmochim. Acta*, 33 (1969) 81.
8 L. Alaerts, J. P. Op de Beeck and J. Hoste, *Anal. Chim. Acta*, 69 (1974) 1.
9 L. Alaerts, J. P. Op de Beeck and J. Hoste, *Proc. Int. Conf., Mod. Trends Activ. Anal., Saclay, France, 2nd–6th Oct. 1972; J. Radioanal. Chem.*, 15 (1973) 601.
10 F. Dugain and J. Tatar, *Ann. Inst. Geol. Publici Hung.*, 54 (1970) 375.
11 J. C. Roy and J. J. Hawton, *AECL-1181 (CRC-1003) 1960.*
12 N. E. Holden and F. W. Walker, *Chart of the Nuclides*, General Electric Company, Schenectady, N.Y., 1972.
13 R. Dams and F. Adams, *J. Radioanal. Chem.*, 7 (1971) 127.
14 I. M. Kolthoff and P. J. Elving, *Treatise on Analytical Chemistry*, Part II, Vol. 2, Wiley, New York, 1962, p. 156.

Analytica Chimica Acta, 70 (1973) 265–274

DETERMINATION OF NIOBIUM, TITANIUM AND ZIRCONIUM BY HIGH-FREQUENCY PLASMA TORCH EMISSION SPECTROMETRY AND ITS APPLICATION TO STEEL

RYOZO NAKASHIMA, SHOZO SASAKI and SHOZO SHIBATA

Government Industrial Research Institute, Nagoya, Hirate-machi Kitaku, Nagoya (Japan)

(Received 8th November 1973)

High-frequency plasma torches for analytical emission spectrometric purposes have been developed in the last few years[1–3]. Dickinson and Fassel[3] studied the detection limits of 26 metals with an induction-coupled plasma having a 30-MHz frequency and a 2.5-kW output, and showed that the limits were superior by 2–4 orders of magnitude to those obtained by atomic absorption or emission methods. Because of its better detection limits and easier introduction of samples, the method has been utilized not only for solution samples, but also for powdered[4,5], metallic[6] and molten samples[7]. However, only two reports have dealt with applications to steel analysis[8]. The present paper describes the analytical conditions for the determination of niobium, titanium and zirconium with a high-frequency plasma torch emission method and an application in steel analysis.

EXPERIMENTAL

Apparatus

A Hitachi UHF Plasma Spectrascan, Model 300, the plasma excitation source of which has been reported elsewhere[9,10], was used. This apparatus is composed of four parts: a plasma torch flame and sample introduction facility, a spectrometer, a programmer for measurement and a high-voltage source.

The sample introduction facility used is schematically represented in Fig. 1. The nebulizer is pneumatic and is provided with an impact bead, of 5-mm diameter, separated by 10 mm from the nozzle tip, in order to eliminate and destroy any large droplets of sample solution. The flow rate of liquid (as distilled water) at a gas flow rate of 2.5 l min^{-1} for nebulizing, was 2.4 ml min^{-1}. The heating chamber is 45 cm long, 6.5 cm in diameter at the entrance, and 3.0 cm in diameter at the exit. The temperature was held at $180 \pm 10°C$ for all experiments. The cooling tube for eliminating water mist in the sample aerosol is 32 cm long and 5.5 cm in diameter.

The high-frequency generator was operated at 2450 MHz and had a 450-W nominal output at maximum.

The spectrometer is a scanning dual-wave type having a Czerny–Turner mounting (focal length, 120 mm), a grating blazed at 200.0 nm, and a reciprocal linear dispersion of 0.6 nm mm^{-1} at 300.0 nm. Entrance and exit slits were set at 30 μm and 50 μm, respectively, in all the experiments. Argon was used as the plasma

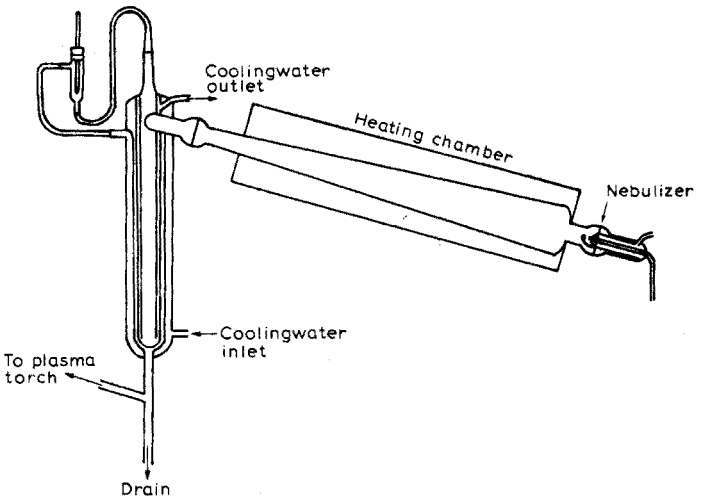

Fig. 1. Schematic diagram of sample introduction facility.

gas for nebulizing and as the sheath gas for thermal pinching at flow rates of 2.0–5.5 l min^{-1}

Reagents

Stock solution of niobium (10^{-2} M). Niobium pentoxide (Johnson Matthey; 0.1329 g) was weighed in a platinum dish, and dissolved with 10 ml of 40% hydrofluoric acid and 20 ml of concentrated sulphuric acid on a sand bath. After dissolution, the solution was evaporated to dense fumes of sulphur trioxide. Concentrated sulphuric acid (20 ml) was added, and the solution was transferred to a 100-ml volumetric flask and then diluted to the mark with water.

Stock solution of titanium (1000 p.p.m.). An aqueous solution of titanium oxysulphate which was 0.5 *M* in sulphuric acid was used.

Stock solution of zirconium (1000 p.p.m.). Zirconium oxychloride (Johnson Matthey; $ZrOCl \cdot 8H_2O$; 0.3532 g) was dissolved in 1.0 *M* hydrochloric acid and the solution was diluted to 100 ml with this acid.

All other reagents used were analytical-grade chemicals.

Measurement

In order to measure the spectral pattern and intensity, an aliquot of stock solution was adequately diluted with water.

In measurements of niobium, hydrolytic dissociation occurred within 30 min of dilution and the line intensity decreased gradually, hence a small amount of hydrogen peroxide was added to prevent the dissociation. Under these conditions the intensity of the niobium line (405.89 nm) was unchanged for a long period (*ca.* 2 h) and the addition of hydrogen peroxide did not affect the intensity.

RESULTS AND DISCUSSION

Spectral pattern and measuring conditions

In order to compare the relative intensities of several strong lines of the three

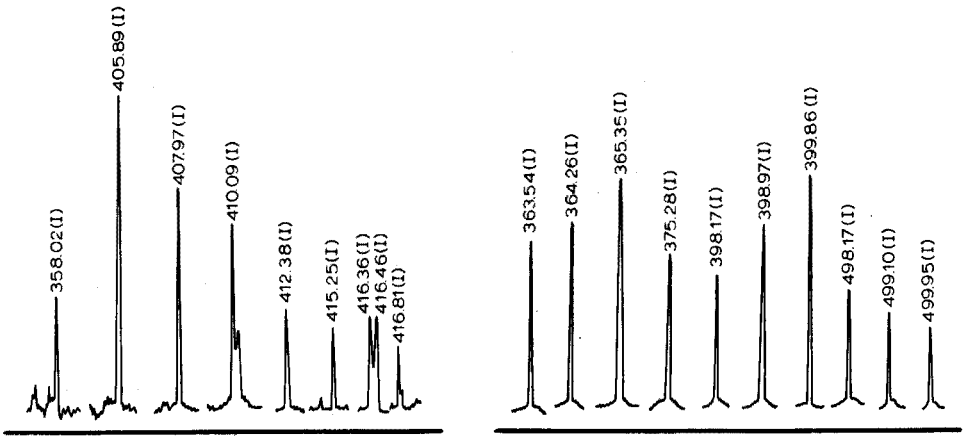

Fig. 2. Spectral pattern of niobium. Niobium, 18.6 p.p.m., 0.14 *M* H_2SO_4 solution. Photomul. voltage, 500 V; plasma gas, 3.5 l min^{-1}; sheath gas, 4.0 l min^{-1}; anode current, 300 mA; field current, 350 mA; slit, 30 μm (entrance), 50 μm (exit); cooling water, 15°C.

Fig. 3. Spectral pattern of titanium. Titanium, 40 p.p.m., 0.02 *M* H_2SO_4 solution. Other conditions as in Fig. 2.

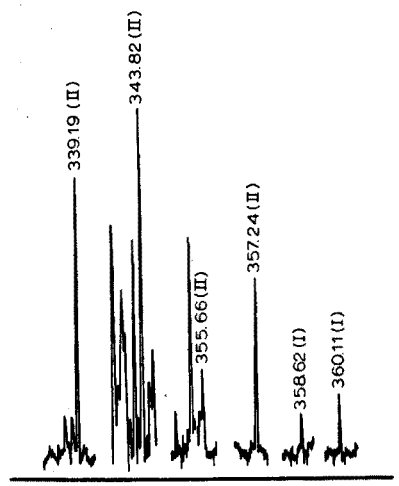

Fig. 4. Spectral pattern of zirconium. Zirconium, 20 p.p.m., 0.02 *M* HCl solution. Other conditions as in Fig. 2.

elements, the spectral line intensities were scrutinized. The results are shown in Figs. 2–4. The strongest lines were 405.89 nm for niobium, 334.94 nm for titanium and 343.82 nm for zirconium. The zirconium 343.82-nm line had more noise in the vicinity of the line than the 339.19-nm line, hence subsequent experiments were performed with the latter line. The experiments with titanium were done at the 365.35-nm line for the same reason as in the case of zirconium.

Since the distribution of the line intensity in the plasma flame differs characteristically for various elements, the measuring position in the circular cone

of the plasma may affect the intensity. In all cases here, the maximal intensity was found in the flame axis at a fixed distance of 15–30 mm from the electrode tip.

Although the present experiments were carried out at flow rates of 3.5 l min^{-1} for the plasma gas and 4.0 l min^{-1} for the sheath gas, the spectral line intensities of all three elements were enhanced by increase of flow rate up to at least 5.5 l min^{-1}. As an increase of high-frequency out-put also enhanced the intensities, subsequent experiments were carried out at maximal power (450 W) in all cases.

Calibration curves were linear and passed through the origin, at least in the ranges 1–50 p.p.m. niobium at 405.89 nm, 0.5–100 p.p.m. titanium at 365.35 nm, and 5–100 p.p.m. zirconium at 339.19 nm.

The detection limits (signal : noise = 2 : 1) for a plasma gas flow rate of 5.5 l min^{-1}, were 0.5, 0.1 and 2.0 p.p.m. for niobium, titanium and zirconium, respectively.

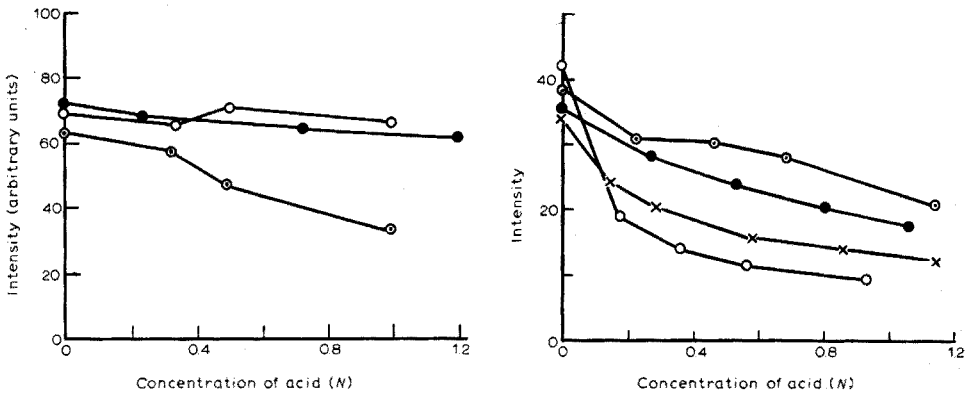

Fig. 5. Effect of acid concentration on niobium (18.58 p.p.m.) at 405.89 nm. (–○–) HCl, (–●–) $HClO_4$, (–⊙–) H_2SO_4.

Fig. 6. Effect of acid concentration on titanium (20 p.p.m.) at 365.35 nm. (–⊙–) HCl, (–●–) HNO_3, (–×–) H_2SO_4, (–○–) $HClO_4$.

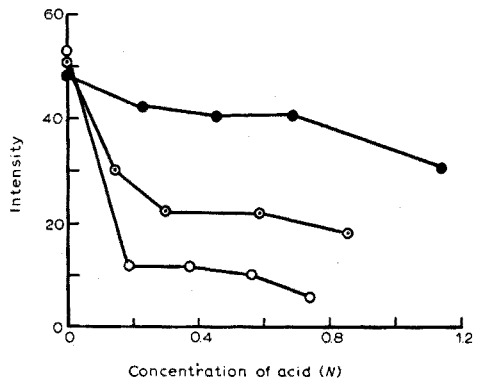

Fig. 7. Effect of acid concentration on zirconium (50 p.p.m.) at 339.19 nm. (–●–) HCl, (–⊙–) H_2SO_4, (–○–) $HClO_4$.

Influence of concentration of inorganic acids

The effects of the concentration of inorganic acids on the line intensities are shown in Figs. 5–7. In the case of niobium, as the concentration of hydrochloric acid was increased, the intensity was decreased only slightly; the decrease was only 10% when 1.2 *M* hydrochloric acid was present. Perchloric acid had virtually no effect up to at least 1.0 *M*, but sulphuric acid appreciably decreased the intensity. In the case of titanium, the intensity was appreciably decreased as the acid concentration was increased. The effect of the acids decreased in the order perchloric > sulphuric > nitric > hydrochloric acid. Similar tendencies were also shown in the case of zirconium.

Effect of alkali metals

When alkali metals were not present, the detection limit of zirconium worsened by one order of magnitude compared to niobium and titanium, since the fluctuation in the vicinity of the line was apparently larger than in the other cases. Murayama[11], in describing experiments with rare-earth elements by the high-frequency plasma torch emission method, mentioned that the spectral intensity of the samarium(II) 442.43-nm line was stronger in the circumference of the torch flame than at the central axis; however, as the concentration of sodium salt was increased, the region showing maximal intensity was altered to the center of the torch flame and the detection limit was improved.

In order to improve the detection limit in this work, the effect of addition of alkali metals on the intensity of zirconium was examined. In these experiments, the off-axis distance in the plasma flame showing maximal line intensity remained unchanged in the presence of alkali metals. The results are shown in Fig. 8; it can be seen that potassium had the greatest effect. The sensitivity was improved about 2.5 times in the presence of 27 p.p.m. of potassium.

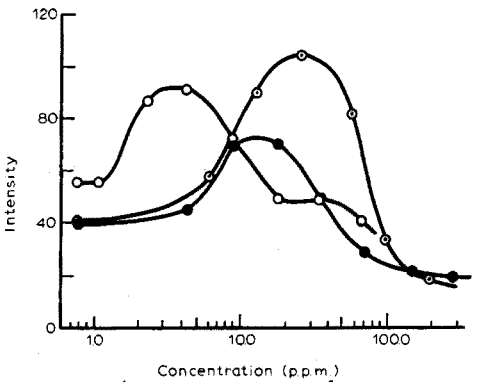

Fig. 8. Effect of alkali metal salts on the 339.19-nm zirconium line. (-○-) Lithium, (-●-) sodium, (-⊙-) potassium (as chloride).

Effects of diverse metals

Elements at concentrations which showed overlapping spectra with intensities more than 5% compared to the signal heights of 10 p.p.m. titanium, 10 p.p.m. niobium and 20 p.p.m. zirconium were regarded as interfering. Sixteen elements in-

cluding antimony, bismuth, chromium, cobalt, copper, iron, manganese, molybdenum, nickel, niobium, silicon, tin, titanium, tungsten, vanadium and zirconium, which are commonly encountered in steel, were tested. Iron (200 p.p.m.) caused a 10% error for niobium, and the same amount of cobalt resulted in a 13% error for zirconium. The interference of cobalt on niobium was considerably larger on account of the 405.86-nm line, and the allowable amount was less than 20 p.p.m. Nickel showed a strong line at 339.29 nm, therefore the amount had to be restricted to less than 10 p.p.m. for determinations of zirconium. Manganese showed a fairly strong line at 405.89 nm; the presence of 10 p.p.m. manganese resulted in a 13% error for the determination of niobium. No interferences were observed in the presence of 200 p.p.m. of the other metals mentioned above.

APPLICATION TO STEELS

For the determination of niobium, titanium and zirconium in steels without prior chemical separation, lines which were not subject to interferences from iron in the 10^3–10^4 p.p.m. region were first sought experimentally over a wide range of wavelength. In the case of niobium and zirconium, it was impossible to find a line which did not suffer from interferences and still had sufficient sensitivity compared to the main analytical lines. In the case of titanium, only the 499.95-nm line did not suffer from the interferences; the relationship between the concentration of iron(III) as chloride and the intensity at this line are shown in Fig. 9, where each point is the average of five measurements, and the vertical bars indicate the range found. The intensity of the titanium line increased with increase of iron added up to 4000 p.p.m., and then decreased abruptly on further addition. This decrease may have been caused by a decrease of sample flow rate based on increase of viscosity. The maximal value of the intensity was nearly three times that found in the absence of iron. The intensity was also measured in the presence of other iron salts at a level of 10,000 p.p.m. as iron; no differences based on the salt species were observed. The effects of free acid concentration on the spectral intensity in the presence of large amounts of iron showed the same trends as in the absence of iron. The presence of elements such as molybdenum, nickel and tungsten, which showed weak spectra in the vicinity of 499.95 nm was permissible up to 1000 p.p.m.

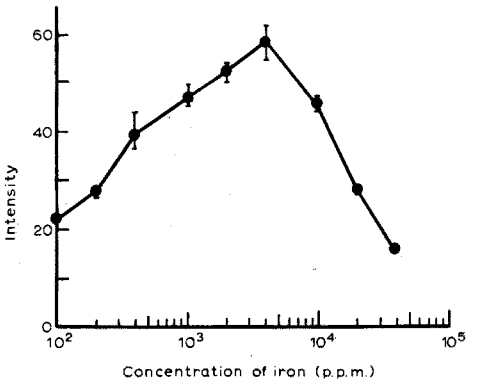

Fig. 9. Effect of concentration of iron on the titanium line intensity at 499.95 nm. Titanium, 10 p.p.m. Iron(III) added as chloride.

Procedure for titanium without separation

Decompose a 1.0-g sample in 5–8 ml of hydrochloric acid and 1–2 ml of nitric acid by gentle heating on a sand bath. If the sample decomposed completely, after cooling, transfer the solution to a 25-ml volumetric flask and dilute with water to the mark. Pipette 3 aliquots of 2.5 ml into 10-ml volumetric flasks, and add appropriate amounts of a standard solution of titanium to two of the flasks, before dilution the mark. Measure these solutions by the proposed method, and calculate the quantity of titanium on the basis of the standard addition method.

The method for the separation of zirconium was based on the use of cupferron, as reported by Maekawa *et al.*[12] for zirconium in steel, and on extraction of the iron with methyl isobutyl ketone. In this method, not only zirconium but also niobium and titanium are separated and the decomposed precipitate is used for the determination by the plasma emission technique.

Procedure for niobium, titanium and zirconium following separation

Decompose 1 g of sample in a 200-ml beaker with a mixture of concentrated acids (20 ml of perchloric acid, 2 ml of sulphuric acid and 2–3 ml of nitric acid) on a sand bath. If a sample weighing more than 1 g is necessary, another 5 ml of perchloric acid per 1 g of sample should be added.) Evaporate the solution until perchloric acid fumes appear. Cool the solution, and dissolve any salts by adding 50 ml of water with heating. Dilute to 100 ml. Add 5 g of sodium sulphite and reduce iron(III) by heating. Add 10 ml of hydrochloric acid and cool to below 10°C. Add 20 ml of cupferron solution (6% w/v), allow the precipitate to settle for about 30 min, and decant the solution through a dense filter paper. Transfer precipitate and filter paper to the original beaker, and decompose with 2 ml of concentrated sulphuric acid and 5 ml of nitric acid by heating on a sand bath, until dense fumes appear; add further 1-ml portions of nitric acid, with heating

TABLE I

RESULTS FOR SYNTHETIC SAMPLE AFTER SEPARATION

(1 g of iron present)

Metal	*Amount added (mg)*	*Amount found (mg)*	*Difference (mg)*
Titanium	1.00	1.08	+0.08
	1.00	1.03	+0.03
	2.00	1.90	−0.10
	2.00	1.93	−0.07
Niobium	0.93	0.93	±0.00
	0.93	1.00	+0.07
	1.86	1.70	−0.16
	1.86	1.70	−0.16
Zirconium	1.00	1.10	+0.10
	1.00	0.85	−0.15
	2.00	2.00	±0.00

to fumes until all the organic substance has decomposed. Cool the residue and transfer to a 50-ml separatory funnel. Rinse the beaker several times with small quantities of 6 *M* hydrochloric acid. Collect the rinsings in the same separatory funnel, and dilute to 25 ml with 6 *M* hydrochloric acid. Extract iron with two 25-ml portions of methyl isobutyl ketone. To the aqueous layer, add 1 ml of sulphuric acid and 5 ml of nitric acid, and heat on a sand bath until dense fumes of sulphur trioxide are evolved. If decomposition of organic substance is unsatisfactory, add another 1 ml of nitric acid and repeat the above treatment. Transfer the residue to a 10-ml volumetric flask and dilute to the mark. Determine niobium, titanium and zirconium by the standard addition method with aliquots of this final solution.

RESULTS

The results obtained for synthetic mixtures and for steels are summarized in Tables I–III. Since there was a large fluctuation in background noise in the vicinity of the zirconium line (339.19 nm), as observed in Fig. 4, and as sulphuric acid and contaminated salts were present, the detection limit of zirconium was less in these applications than was found in the preliminary studies. Consequently, the quantity of sample available is an important problem in obtaining reproducible results. The determinations of niobium and titanium presented fewer problems. Relative standard deviations for results obtained with standard solutions of niobium and titanium are shown in Table IV. From these results, the method should be satisfactory for steel analyses.

TABLE II

RESULTS FOR TITANIUM WITHOUT SEPARATION

Standard steel[a]	*Certificated value* (%)	*Titanium found* (%)
160-2	0.093	0.088
		0.098
		0.089
501-1	0.018	0.020
		0.017
		0.020
		0.021
655-3	0.050[b]	0.049
		0.050

[a] Japanese iron and steel standards.
160-2: C, 0.004; Mo, 0.16; V, 0.10; Co, 0.061; Al, 0.006; As, 0.051; Sn, 0.061; B, 0.062; Pb, 0.0020; Nb, 0.11%.
501-1: C, 0.33; Si, 0.27; Mn, 0.75; P, 0.024; S, 0.014; Cu, 0.10; Ni, 0.063; Cr, 1.04; Mo, 0.17%.
655-3: C, 0.056; Si, 0.60; Mn, 1.59; P, 0.033; S, 0.0060; Cu, 0.088; Ni, 11.50; Cr, 18.54; Mo, 0.052; Nb, 0.59; Ta, 0.030; N, 0.025%.
[b] Titanium added value.

TABLE III

RESULTS FOR NIOBIUM AND ZIRCONIUM AFTER SEPARATION

Standard steel	*Niobium (%)*		*Zirconium (%)*	
	Cert. value	*Found*	*Present*[a]	*Found*
160-2	0.11	0.11 0.11		
501-1			0.030	0.029 0.024 0.038

[a] Zirconium added.

TABLE IV

RELATIVE STANDARD DEVIATION IN REPEAT DETERMINATIONS

(The statistical treatment is based on 15 determinations at each step. Measurements for titanium were done in the presence of 10,000 p.p.m. iron, while those for niobium were done, with a synthesized sample, after separation of iron.

Metal	*Concentration (p.p.m.)*	*Average signal (mm)*	S_r *(%)*
Ti	2.0	23.8 ± 1.4	6.0
	7.0	80.4 ± 4.0	5.0
	9.0	23.3 ± 1.3	3.8
	29.3	114.4 ± 2.5	2.2
Nb	11.0	33.5 ± 1.4	4.1
	31.0	106.5 ± 3.1	2.9

SUMMARY

The basic conditions for the determination of niobium, titanium and zirconium with an argon plasma and a Hitachi UHF Plasma Spectrascan operated at 2450 MHz and 450 W maximum output, have been established. The niobium 405.89-nm, titanium 365.35-nm and zirconium 339.19-nm lines gave detection limits of 0.5, 0.1 and 2.0 p.p.m., respectively, when pure solutions were used. Effects of gas flow rates, high-frequency output and concentration of acids were examined. In applications to steel, titanium was determined without prior chemical separation from iron at the 499.95-nm line, whereas niobium and zirconium could not be determined in the presence of large amounts of iron. When a cupferron precipitation method followed by extraction of iron with methyl isobutyl ketone was applied, satisfactory results were obtained.

REFERENCES

1 S. Greenfield, I. W. Jones and C. T. Berry, *Analyst (London)*, 89 (1964) 713.

2 R. H. Wendt and V. A. Fassel, *Anal. Chem.*, 37 (1965) 920.
3 G. W. Dickinson and V. A. Fassel, *Anal. Chem.*, 41 (1969) 1021.
4 H. C. Hoare and R. A. Mostyn, *Anal. Chem.*, 39 (1967) 1153.
5 R. M. Dagnall, D. J. Smith and T. S. West, *Anal. Chim. Acta*, 54 (1971) 397.
6 S. Murayama and H. Matsuno, *Bunko Kenkyu*, 18 (1970) 149.
7 V. A. Fassel and G. W. Dickinson, *Anal. Chem.*, 40 (1968) 247.
8 M. Suzuki, *Jap. Anal.*, 17 (1968) 1529; 19 (1970) 207.
9 S. Murayama, *J. Appl. Phys.*, 39 (1968) 5478.
10 S. Murayama, H. Matsuno and M. Yamamoto, *Spectrochim. Acta, Part B*, 23 (1968) 513.
11 S. Murayama, *Spectrochim. Acta, Part B*, 25 (1970) 191.
12 S. Maekawa, Y. Yoneyama and E. Fujimori, *Jap. Anal.*, 10 (1961) 341.

Analytica Chimica Acta, 70 (1974) 275–282

ANALYSE DÜNNER SCHICHTEN VON TETRAMETHYLEN-DITHIOCARBAMIDATEN AUF METALLOBERFLÄCHEN MITTELS F.M.I.R.-SPEKTROSKOPIE IM INFRAROTEN BEREICH

R. KELLNER

Institut für Analytische Chemie und Mikrochemie, Technische Hochschule, Wien (Österreich)

(Eingegangen den 29. Oktober 1973)

Die Analyse dünner organischer Überzüge auf anorganischen Trägermaterialien hat besonders bei der Aufklärung von Korrosionsfällen sowie bei der Produktionskontrolle von Metall–Kunststoff-Verbundfolien grosse Bedeutung. Zum Studium eventueller Oberflächenreaktionen an der Grenzschicht zwischen Metall und organischer Substanz ist eine Erfassungsgrenze im Bereich weniger Molekülllagen erforderlich. Von den heute zur direkten Untersuchung von Oberflächenreaktionen herangezogenen physikalischen Analysenmethoden eignet sich für organische Substanzen besonders die I.R.-Spektroskopie, da die in der Praxis angewandte empirische Spektreninterpretation erprobt ist und grosse Spektrenkarteien zur Referenz vorhanden sind. Speziell zum Studium von Elektrodenvorgängen bei Redoxreaktionen unter Teilnahme organischer Systeme wurde die F.M.I.R. (frustrated multiple internal reflectance) – Methode im I.R.-Bereich erfolgreich eingesetzt[1–3].

Die folgende Arbeit beschreibt die Durchführung von Modellversuchen zum Problemkreis Korrosion der Gebrauchsmetalle Fe, Ni, Cu, Zn, Cd, Pb in einer wässrigen Lösung von Ammonium–Tetramethylendithiocarbamidat (TMDTC), da dieses unterschiedliche Affinität zu den genannten Metallen aufweist und die I.R. Spektren der jeweiligen Metallchelate bereits genau studiert wurden. Die I.R.-Spektren der TMDTC weisen mehrere Banden auf, deren Lage besonders strukturempfindlich und abhängig von der Elektronenverteilung im Molekül sind (1400–1500 cm^{-1}, 300–400 cm^{-1} sowie besonders unter 200 cm^{-1}, refs. 4 und 5. Es war zu prüfen, ob und bis zu welcher Schichtdicke diese Absorptionsbanden mit Hilfe von Reflexions- oder F.M.I.R.-Einheiten erfassbar sind und inwiefern eventuelle Bandenverschiebungen auf Grund von Redox-Reaktionen, Assoziationen oder Einflüssen der Probenpräparation die Verwendung von Standardspektren erschweren.

EXPERIMENTELLES

Die untersuchten TMDTC-Schichten wurden in der in Abb. 1 gezeigten Versuchsanordnung hergestellt. Die Reinigung der Bleche (Grösse $5 \times 1{,}2$ cm) erfolgte mit Ausnahme von Blei durch Polieren mit einer Schleifpaste und nachfolgendes Entfernen der organischen Rückstände mit Aceton und Chloroform. Blei wurde durch Abziehen der Oberfläche mit einer Ziehklinge gereinigt.

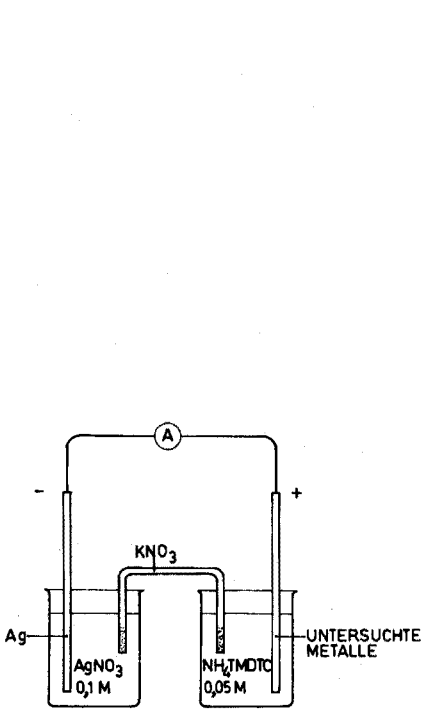

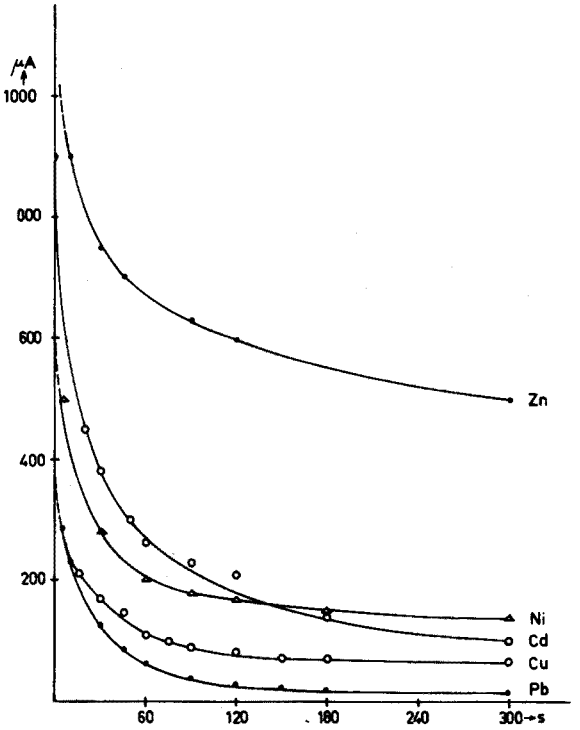

Abb. 1. Versuchsanordnung zur Herstellung der Chelatschichten (Daniell-Element).

Abb. 2. Strom–Zeit-Kurven, aufgenommen während des Ablaufs der Reaktionen in der Anordnung nach Abb. 1.

Je nach Affinität des TMDTC-Liganden zum untersuchten Metall kommt es zu einer mehr oder weniger raschen Passivierung der Anode, was sowohl in der Form der Strom–Zeit-Kurve, als auch in der Restleitfähigkeit zum Ausdruck kommt (Abb. 2). Der Stromfluss wurde jeweils zu verschiedenen Zeiten unterbrochen, die Bleche wurden mit destilliertem Wasser abgespült (Blei mit Methanol) und im Vakuum bei Raumtemperatur getrocknet.

Zur Aufnahme der I.R.-Spektren der erzeugten Chelatschichten wurde wegen der erforderlichen Messgenauigkeit ein Gitterspektrophotometer des Typs 180 der Firma Perkin-Elmer mit geeichter Wellenzahlmarkierung sowie mit F.M.I.R.- und Mikroreflexionseinheiten verwendet. Als Kristallmaterialien wurden KRS-5 und Ge mit jeweils 25 Reflexionen eingesetzt.

DISKUSSION

Prinzipiell lassen sich beide unter Experimentelles genannten Präparationsmethoden zur Untersuchung von organischen Schichten auf Metallen heranziehen. Welcher Methode der Vorzug zu geben ist, hängt vom jeweiligen Problem, von der Schichtdicke der Überzüge, vom Reflexionsvermögen des Untergrundes und von der Grösse und Form der Probe ab (Tab. I).

TABELLE I

ANWENDUNGSBEREICHE VON F.M.I.R.- UND REFLEXIONSEINHEIT[a]

(10 fache Ordinatendehnung)

Probe	*F.M.I.R. (45°)*	*Reflexion*
Probe eben	+	+
Probe uneben	−	+[b]
Mindestgrösse	4 × 8 mm	ϕ 1 mm
Reflexionsvermögen des Trägermaterials		
Gut	+	+
Schlecht	+	−
Dicke der Überzüge		
Minimal	10–100 nm (Kristall beidseitig bedeckt)	1 μm
Maximal	bis auf apparative Momente unbegrenzt	*ca.* 100 μm
Nutzbarer Spektralbereich im Gerät PE 180	KRS-5 4000–280 cm^{-1} Ge 4000–800 cm^{-1}	4000–32 cm^{-1}

[a] +, Anwendbar; −, nicht anwendbar.

[b] Fokussierende Reflexionszusätze gestatten auch die Untersuchung stark konkaver Materialien mit schlechtem Reflexionsvermögen[6].

Wie in früheren Arbeiten gezeigt werden konnte[4,5], ist das F.I.R.-Gebiet vom Standpunkt der dort auftretenden überaus starken Bandenverschiebungen in Abhängigkeit von der Molekülstruktur her gesehen für die Lösung der hier zu untersuchenden Probleme am besten geeignet. Die Bandenintensität ist im F.I.R. jedoch auf Grund der geringen Übergangswahrscheinlichkeit klein[7]. Daher reicht die Empfindlichkeit der besten Gittergeräte nicht aus, um F.I.R.-Spektren von Schichten dünner als 1 μm mit der Reflexionseinheit zu erhalten. Man ist derzeit gezwungen, F.M.I.R.-Einheiten zur Erzielung von Mehrfachreflexion einzusetzen und den durch das Kristallmaterial bedingten eingeengten Messbereich in Kauf zu nehmen (KRS-5: 4000–280 cm^{-1}, Ge: 4000–800 cm^{-1}).

Wegen der relativ hohen Affinität des Tl im KRS-5 zum hier verwendeten Chelatbildner NH_4TMDTC kommt es während der Aufnahme des F.M.I.R.-Spektrums zu einer teilweisen Reaktion der Chelatschicht mit dem Reflexionskristall, was weitere Messungen durch Auftreten eines starken Blindwertes unmöglich macht. Dagegen reagiert Ge nicht mit den TMDTC-Schichten und ermöglicht die wiederholte störungsfreie Aufnahme der ν C≡≡N im Bereich 1400–1500 cm^{-1}

Als Nachweisgrenze für die Untersuchung der Chelatschichten mit der angegebenen Versuchseinrichtung wurden in Übereinstimmung mit der Literatur[1,2] sowohl durch Auswägen der aufgebrachten Chelatschichten als auch aus der Extinktion der ν C≡≡N Schichtdicken von 10–50 nm entsprechend *ca.* 10 Monolagen ermittelt (die Dicke einer Monolage wird zu 10 Å angenommen). Bei diesen Schichtdicken erhält man mit einem 45° F.M.I.R.-Kristall noch eine ν C≡≡N mit einer Extinktion von mindestens 0.01. Die Bande ist bei einer 10-fachen Ordinatendehnung noch einwandfrei auswertbar.

Die folgenden Abb. 3 sowie Abb. 5–8 zeigen die auf die beschriebene Weise erhaltenen I.R.-Spektren der untersuchten Chelatschichten. Die Modellversuche zur Schichterzeugung wurden jeweils zu verschiedenen Zeitpunkten nach Beginn des Experiments abgebrochen (zwischen 10 s und 12 min). Wegen deren grosser Affinität zu dem hier angewendeten Liganden konnten die Systeme Blei–TMDTC und Kupfer-TMDTC besonders ausführlich studiert werden (Abb. 2).

Die zu den Zeiten 15, 30 und 300 s aus der Versuchsanordnung genommenen Blei-Bleche zeigen I.R.-Spektren, die sich sowohl in der Intensität, als

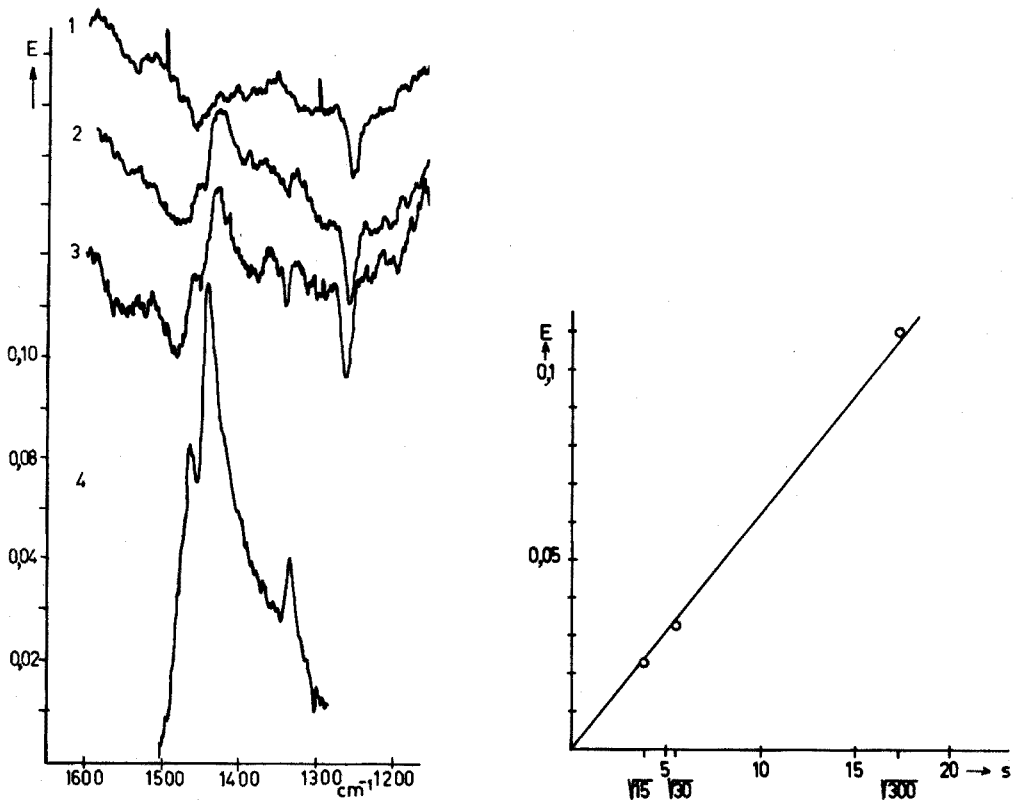

Abb. 3. Blei-Blech, F.M.I.R.-Spektren: (1) 0 s, (2) 15 s, (3) 30 s und (4) 300 s nach Reaktionsbeginn (KRS-5, 45°, OD 10×).

Abb. 4. Abhängigkeit der Änderung der E_{max} bei *ca.* 1430 cm^{-1} (Abb. 3) von der Reaktionszeit.

auch in der genauen Lage der Banden unterscheiden (Abb. 3). Die Intensitätsänderung gehorcht der Beziehung $E = \text{prop } \sqrt{t}$ (t...Zeit) geringe Abweichungen erklären sich durch den Einfluss des nicht konstant zu haltenden Anpressdruckes in der F.M.I.R.-Einheit (Abb. 4).

Die geringe Verschiebung der Lage der intensivsten Bande im untersuchten Gebiet in Richtung höhere Wellenzahlen wird dadurch verursacht, dass zu Beginn der Reaktion hauptsächlich das Oxidationsprodukt Thiuramdisulfid mit einer starken Absorption bei 1426 cm^{-1} entsteht, während sich im Laufe der weiteren Reaktion mit zunehmender Dicke der entstehenden organischen Sperrschicht auf dem Blech bevorzugt ein Blei–TMDTC-Komplex bildet (starke Absorption bei 1436 cm^{-1}). Ein Beweis für das Vorliegen des Blei-Chelates ist eine nicht aufgespaltene Bande bei 1325 cm^{-1} im Spektrum.

Im System Kupfer-TMDTC ist der Bildungsvorgang der Isolatorschicht auf Grund der stark unterschiedlichen Bandenlagen von Kupfer–TMDTC und Thiuramdisulfid wesentlich klarer zu erkennen (Abb. 5). Durch Ermittlung der Extinktionsverhältnisse der beiden Schlüsselbanden bei 1505 cm^{-1} (Cu–TMDTC) und bei 1440 cm^{-1} (hauptsächlich vom Thiuramdisulfid stammend) kann direkt eine bevorzugte Bildung des Oxidationsproduktes zu Beginn der Reaktion unter den angegebenen Bedingungen nachgewiesen werden. Das charakteristische Extinktionsverhältnis E_{1505}/E_{1440} steigt von 1,25 (Probe A, Reaktionsdauer 10 s) über 1,60 (Probe D, Reaktionsdauer 8 min) auf 2,28 für das reine Kupfer(II)–TMDTC. Bei den kurz exponierten Proben treten Abweichungen vom $\sqrt{t}$-Gesetz auf, die noch nicht erklärt werden können. Das Problem ist Gegenstand weiterer Arbeiten.

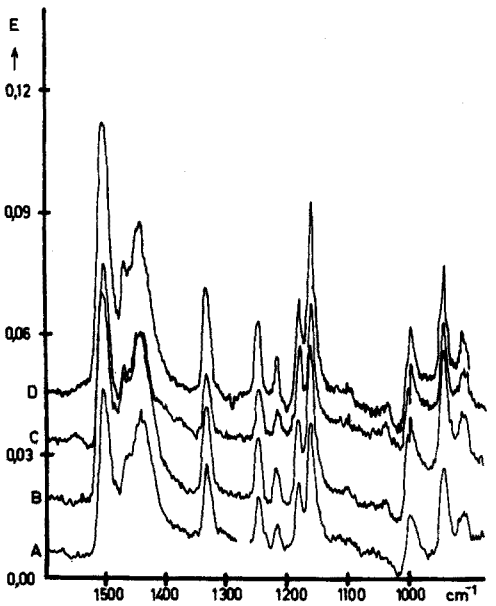

Abb. 5. Kupfer-Blech, F.M.I.R.-Spektren: (A) 10 s, (B) 20 s, (C) 210 s und (D) 480 s nach Reaktionsbeginn (Ge, 45°, OD 10×).

Wie aus Abb. 2 ersichtlich, reagierten die übrigen in dieser Arbeit untersuchten Metalle auf Grund deren geringerer Affinität zum TMDTC-Liganden langsamer und unvollständig. F.M.I.R.-Spektroskopie erlaubt jedoch auch in diesen Fällen Aussagen über die Natur der entstehenden Schichten zu treffen. Im Falle des Nickel (Abb. 6) entsteht nach 5 min eine gerade messbare Schicht, die sich auf Grund des I.R.-Spektrums eindeutig als Gemisch von Thiuramdisulfid und Nickel–TMDTC erweist.

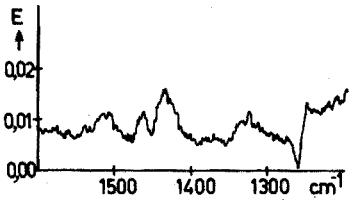

Abb. 6. Nickel-Blech, F.M.I.R.-Spektrum; 300 s nach Reaktionsbeginn (Ge, 45°, OD 10×).

Cadmium bildet unter den angegebenen Bedingungen bereits nach 1 min einen gut analysierbaren Überzug. Infolge der Überlagerung der dem Cadmium-Chelat eigenen starken Absorption bei 1433 cm^{-1} mit der Thiuramdisulfidbande bei 1436 cm^{-1} ist auf ein Vorhandensein des Oxidationsproduktes in der Isolatorschicht wieder nur durch Intensitätsvergleich der Banden bei 1433 cm^{-1} und 1477 cm^{-1} abzuschätzen (s. Pb). Das Verhältnis E_{1433}/E_{1477} beträgt in der gemessenen Schicht 2,1, dagegen im Cadmium-Chelat 1,7. Nach 3 min nähert sich das Verhältnis diesem Grenzwert an 1,9 (Abb. 7).

Dagegen lassen sich im Spektrum der Zink-Bleche Oxidationsprodukte nicht mit Sicherheit nachweisen. Lediglich die Intensitätsunterschiede der Bande

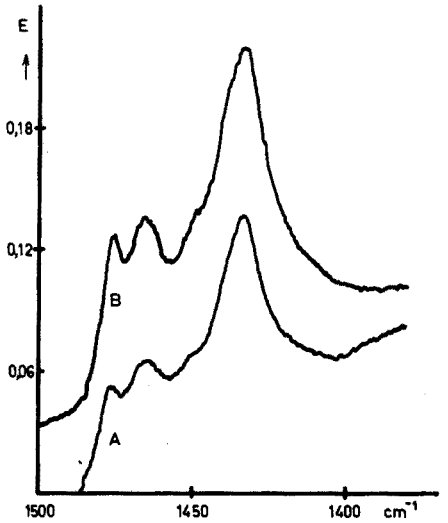

Abb. 7. Cadmium-Blech, F.M.I.R.-Spektren: (A) 60 s und (B) 180 s nach Reaktionsbeginn (Ge, 45°, OD 5×).

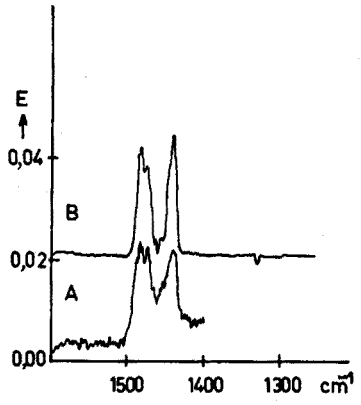

Abb. 8. Zink-Blech, F.M.I.R.-Spektren: (A) 300 s und (B) 600 s nach Reaktionsbeginn (Ge, 45°, OD 10×).

bei 1438 cm^{-1} in den Spektren A und B bilden einen Anhaltspunkt für das Auftreten von Thiuramdisulfid (Abb. 8).

Eisen bildet unter den gleichen Versuchsbedingungen auch nach 12 min. keine I.R.-spektroskopisch nachweisbare auf dem Blech festhaftende Isolatorschicht aus. Dementsprechend kommt es auch nicht zu einem Stromabfall mit fortschreitender Reaktionsdauer und zu keiner Einstellung eines konstanten Reststromes wie bei den übrigen hier besprochenen Metallen.

Endgültige Erklärungen für dieses Verhalten stehen zwar noch aus, doch können Affinität zwischen TMDTC-Liganden und Eisen(III), sowie sterische Faktoren für die "Anomalie" verantwortlich sein (Eisen ist als einziges der untersuchten Metalle oktaedrisch koordiniert). Die hier beschriebenen Ergebnisse zeigen, dass die F.M.I.R.-Spektroskopie vorteilhaft zum Studium von chemischen Vorgängen in organischen Schichten mit einer grössenordnungsmässigen Dicke von 10 nm eingesetzt werden kann. Bei Vorhandensein einer Probe in der Grösse

TABELLE II

ABHÄNGIGKEIT DER LAGE DER MESSBANDE VON DER PROBENPRÄPARATION

	KBr (cm^{-1})	*F.M.I.R. (Ge-Kristall, 45°)* (cm^{-1})	
		aufgedunstet	*chemisorbiert*
Fe	1484	1484	—
Ni	1508	1512	1515
Cu	1498	1502	1505
Zn	1483	1485	1483
Cd	1432	—[a]	1433
Pb	1435	1430[b]	1435[b]
Thiuram-disulfid	1437	1436	1435

[a] Nicht löslich.
[b] KRS-5-Kristall.

eines Standard-F.M.I.R. Reflexionskristalles können somit Korrosionsprozesse verfolgt und Korrosionsprodukte identifiziert werden. Es stellte sich heraus, dass die üblichen Referenzspektren nach Probenpräparation in KBr oder durch Aufbringen von Kristallen auf den F.M.I.R.-Kristall aus einer Chloroform-Lösung im Bereich der ν C---N für genaue Messungen nicht herangezogen werden können. Es treten in Abhängigkeit von der Affinität der untersuchten Metalle zum TMDTC-Liganden Bandenverschiebungen bis zu 7 cm^{-1} auf (Tab. 2).

Diese Beobachtung kann auch bei der I.R.-Analyse von dünnen Kunststoffschichten auf Aluminium-Folien und Verwendung von Spektrenkarteien zur Interpretation von grosser Bedeutung sein.

Herrn Prof. Dr. H. Malissa möchte ich auch an dieser Stelle für die wertvolle Förderung dieser Arbeit herzlich danken. Weiters danke ich Herrn Doz. Dr. P. Ettmayer für die freundliche Bereitstellung einiger Metallproben sowie dem Fonds zur Förderung der wissenschaftlichen Forschung für das zur Verfügung gestellte Infrarotspektrophotometer Perkin-Elmer 180.

ZUSAMMENFASSUNG

Es wird über die Möglichkeiten und Grenzen der F.M.I.R.-Spektroskopie im mittleren Infrarot zur Analyse von organischen Korrosionsprodukten auf Metalloberflächen berichtet. Als Modellsubstanzen wurden in simulierten Korrosionsprozessen (anodische Oxidation) die Tetramethylendithiocarbamidate von Fe, Ni, Cu, Zn, Cd und Pb als dünne Schichten auf den jeweiligen Metallblechen hergestellt. Mit 45° Ge-Kristallen (25 Reflexionen) und zehnfacher Ordinatendehnung können Schichten bis herab zu 10 nm Dicke spektroskopiert und deren Aufbau verfolgt werden.

SUMMARY

The possibilities and limitations of the application of frustrated multiple internal reflectance spectroscopy in the mid-infrared region for the analysis of organic corrosion products are described. As model substances, the tetramethylenedithiocarbamates of Fe, Ni, Cu, Zn, Cd and Pb, prepared as thin layers on the corresponding metal sheets in a simulated corrosion process, have been investigated. Chelate layers down to a thickness of 10 nm can be analyzed with 45° Ge internal reflection plates (25 reflections).

LITERATUR

1 H. B. Mark Jr. und B. S. Pons, *Anal. Chem.*, 38 (1966) 119.
2 J. S. Mattson, *Anal. Chem.*, 45 (1973) 1473.
3 G. W. Poling, *Corros. Sci.*, 10 (1970) 359.
4 R. Kellner, *Anal. Chim. Acta*, 63 (1973) 277.
5 R. Kellner, *Anal. Chim. Acta*, 68 (1974) 49.
6 R. Kellner, *Mikrochim. Acta*, im Druck.
7 A. Finch, P. N. Gates, K. Radcliffe, F. N. Dickson und F. F. Bentley, *Chemical Application of Far-Infrared Spectroscopy*, Academic Press, London, 1970.

Analytica Chimica Acta, 70 (1974) 283–289

THE DETERMINATION OF VANADIUM IN SEA WATER BY HOT GRAPHITE ATOMIC ABSORPTION SPECTROMETRY ON CHITOSAN AFTER SEPARATION FROM SALT

R. A. A. MUZZARELLI

G. Ciamician Chemical Institute, Faculty of Sciences, University of Bologna, Via Selmi 2, 40126 Bologna (Italy)

R. ROCCHETTI

Laboratory of Chemistry, Faculty of Medicine, University of Ancona, Via Posatora, 60100 Ancona (Italy)

(Received 1st November 1973)

Vanadium is an essential micronutrient involved, at the p.p.b. level, in the photosynthesis of certain algae, in the growth stimulation of crop plants, and in the nutrition of chicks. The blood of certain ascidians, molluscs, holoturians and other marine organisms contains important amounts of vanadium, a high proportion of which is the vanadium protein hemovanadin.

While vanadium is not particularly toxic to man, the toxicity to chicks and rats has been evidenced by both growth depression and mortality, from 25 p.p.m. V fed as ammonium metavanadate or vanadyl sulphate. The mechanism of vanadium toxicity in animals is poorly understood, and furthermore the estimate of the intakes of vanadium by living organisms is made difficult by doubts about the validity of many of the reported methods.

The concentration of vanadium in sea water can surely affect the growth of various organisms and therefore the survey of the vanadium concentration should be based on reliable analytical methods in order to detect pollution and assess its importance.

The analytical methods so far developed are rather cumbersome or difficult to apply to sea water: for instance, a colorimetric method based on the oxidation of N,N-diethyl-*p*-phenylenediamine by potassium chlorate with vanadate as catalyst is satisfactory for vanadium concentrations as high as 12–120 μg V l^{-1} but is of no use in research on sea water[1]. Another colorimetric method has been developed for vanadium in the concentration range usually found in sea water; however, it is not clear from the paper whether analyses were actually carried out on sea water or were limited to pure saline solutions; the method is based on the use of 1,2-cyclohexanediaminetetracetic acid, potassium cyanide and PAR solutions, with extraction by zephiramine and chloroform[2]. Vanadium in lake waters has been determined by extraction with 0.1% dichloro-oxine in butyl acetate followed by conventional atomic absorption spectrometry[3].

Unsuccessful attempts have been made to determine vanadium in sea water by atomic absorption spectrometry with a graphite furnace; the volatilization of the large

amount of salt in the graphite atomizer prevented a sensitive and accurate determination of vanadium[4].The separation of vanadium from salt has been done by chromatography on the chelating resin Dowex A-100: 3 l of filtered sea water acidified with nitric acid to pH 5.0 were passed through a 10×60 mm column; after washing with 200 ml of water, vanadium was eluted with 2 *M* ammonia solution, and eventually determined spectrophotometrically with 3,3'diaminobenzidine[5]. This method has been applied in oceanographic research[6]. The use of an anion-exchange resin has also been proposed: ammonium thiocyanate was added to 1 l of sea water but extensive manipulations were further required to destroy thiocyanate by oxidation, and to destroy the excess of oxidant[7].

Atomic absorption spectrometry with a graphite furnace and a deuterium background corrector is today a powerful analytical tool for carrying out, easily and accurately, vanadium determinations on both liquid and solid samples. The high salt content of sea water, however, does not permit the direct determination of vanadium and other trace elements, and a separation step is mandatory.

Chitosan, a natural chelating polymer that has been characterized only recently[8], is suitable for the separation of transition elements from alkali and alkaline-earth salts, and can collect vanadium from saline waters. Light absorption by its smoke during the atomization period can be efficiently compensated by the deuterium background compensator. By combining the high sensitivity, reproducibility and accuracy of the instrumental technique with the separation of vanadium from salt on chitosan, a new and relatively simple method has been developed for the determination of vanadium.

EXPERIMENTAL

Columns

Chitosan (Food, Chemical & Research Laboratories, Ltd., 4900 Ninth ave. N.W., Seattle, Wash.) was used to prepare columns in 6×40-mm plastic syringes which were filled with 500 mg of 100–200 mesh powder, which had been previously conditioned with sulphuric acid solution at pH 4.0.

Instrumentation

A Perkin-Elmer 305 atomic absorption spectrometer equipped with a hot graphite atomizer HGA-70, a deuterium background corrector and a Hitachi Perkin-Elmer 56 Recorder was used.

Standard vanadium solutions

The vanadium solutions were prepared by appropriate dilution of a stock solution containing 0.78533 g of sodium metavanadate dihydrate in 100 ml of distilled water. All reagents were of analytical-reagent grade.

Sea-water

The surface sea-water samples were collected a few km offshore of Capo Conero, Ancona, Italy. Samples were filtered on 0.45-μm Millipore membranes on a 12-cm teflon support, and the pH adjusted to 4.0 with 0.1 *M* sulphuric acid. It is inadvisable to leave the sea water in the sun and preferable to store it in a refrigerator.

Procedure

After the sea water sample (usually 1 l) had been passed at a flow rate of 10 ml min^{-1}, the columns were dried by suction and extruded by means of the plastic piston into porcelain crucibles. The chitosan was then stirred with absolute ethanol and dried at 60°C to constant weight. Aliquots (5 mg) of this powder, which was sufficiently homogeneous with respect to vanadium, were weighed into special tantalum spoons (Perkin-Elmer) and deposited in the central position of the graphite atomizer.

The HGA-70 programme was as follows: No. 7 with 40-s drying at 100°C, 50-s charring at 700°C and 20-s atomization at 2600°C, voltage 10 V. Wavelength 318.4 nm, damping 1, chart speed 10 mm min^{-1}. Ultrapure nitrogen was used for both the deuterium compensator and the graphite atomizer. The atomization time was maintained for as long as 20 s in order to ensure complete purging.

RESULTS AND DISCUSSION

Analyses of the polymer itself showed no absorption signal, which indicated that the deuterium accessory was efficient in compensating the signal arising from smoke, and that no vanadium was present in chitosan. During preliminary experiments, 5 mg of chitosan were introduced in the graphite atomizer, and 20 μl of 1 p.p.m. vanadium solution were added with an Eppendorf pipette before the determination was carried out; the same procedure was repeated with progressively diluted solutions. Linear responses for the determination of vanadium were obtained when 5, 10 and 15-mg quantities of chitosan were used with 20 μl of different vanadium solutions.

The straight-line calibration graph obtained with vanadium in the presence of chitosan was coincident with that obtained with vanadium alone.

The determination of vanadium in a matrix of chitosan is feasible because the physicochemical characteristics of vanadium (melting and boiling points, resistance to carbide formation) and chitosan (thermal degradation, absence of aromatic rings, absence of sulphur) are such as to ensure that the atomization of vanadium occurs after the maximum smoke evolution, so that the smoke particles do not drag vanadium out of the atomizer.

Figure 1 shows the recordings of five 5-mg fractions of chitosan powder from one column. The above-mentioned instrumental conditions, and the treatment of the chromatographic support with ethanol permit a good reproducibility of the results. The polymer grains carrying vanadium are uniformly distributed after suspension in ethanol, and smoke interferences are compensated.

The results obtained with 100 ml of 3% sodium chloride solutions containing 1.6 μg of vanadium on columns preconditioned with sulphuric acid or ammonia at different pH values, are presented in Fig. 2. They show that the maximum 80% recovery is obtained at pH 4.0. When the same solutions are made 0.1 *M* with ammonium sulphate, the yield at pH 4.0 is depressed to 55% but in the interval of pH 5.5–7.0, it remains constant at 55%. From the shape of the latter curve, it is evident that two phenomena are superimposed; one of these is that the presence of ammonium sulphate favours the interaction of the metal ion with chitosan in the interval of pH 5.5–7.0, probably by acting on the polymer, whose capacities for

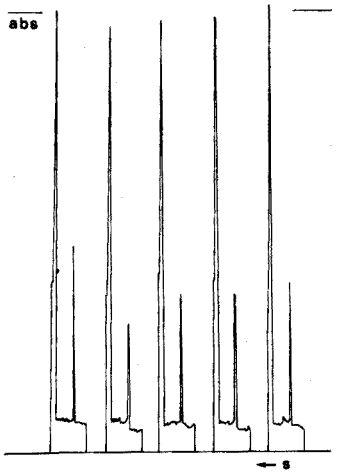

Fig. 1. Readings for vanadium on 5-mg aliquots of chitosan from a 500-mg homogenized column.

transition metal ions are generally enhanced by a preliminary treatment with ammonium sulphate[9].

Figure 2 shows also that vanadium can be eluted with sulphuric acid solutions below pH 2.0 or ammonia solutions above pH 9.0. Vanadium was actually eluted by both methods with overall yields of 80%, on the basis of analyses performed on both solid and liquid fractions, as reported in Table I.

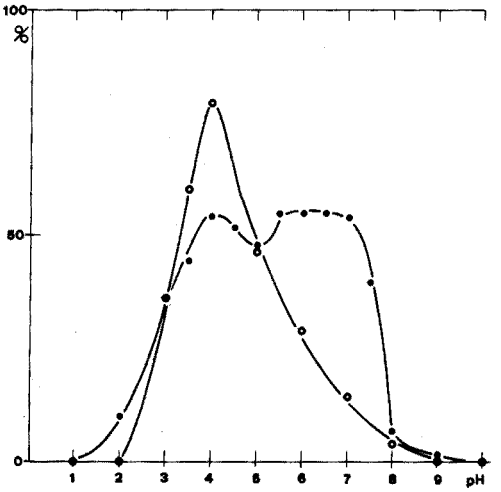

Fig. 2. Recoveries of vanadium (1.6 μg in 100 ml 3% NaCl solutions) at different pH values, after passing through a 500-mg chitosan column conditioned at the desired pH with 0.1 *M* sulphuric acid or 0.1 *M* ammonia. (○) 3% NaCl, (●) 3% NaCl–0.1 *M* $(NH_4)_2SO_4$.

The interactions of vanadium with chitosan can be indicated as follows:

$$-NH_2 + H^+ + SO_4^{2-} \rightleftharpoons -NH_3^+\ SO_4^{2-}$$

$$-NH_3^+\ SO_4^{2-} + VO_3^- \rightleftharpoons -NH_3^+\ VO_3^- + SO_4^{2-}$$

TABLE I

PERCENTAGE RECOVERY OF VANADIUM FROM SALINE SOLUTIONS

(100 ml of 3% NaCl solution containing 5 μg of vanadium was passed through a 500-mg chitosan column; vanadium was eluted with four 5-ml fractions of 0.1 *M* sulphuric acid or 0.1 *M* ammonia. Four samples were tested with each eluant.)

Fraction	*Percentage recovery*							
	0.1 M Sulphuric acid				*0.1 M Ammonia*			
1	2	7	6	10	3	22	4	20
2	50	40	46	45	50	45	49	47
3	25	30	21	20	17	10	18	9
4	5	2	5	5	11	2	10	3
	82	79	78	80	81	79	81	79

The chelating polymer behaves in this case as an anion exchanger and the interaction is not so strong as in the case of transition metal cations or Group VIB oxyanions[8]. The chromatographic band itself is probably rather extended. Figure 3 and Table II show the decrease in percentage recoveries for increasing volumes of the 3% NaCl solution at pH 4.0, in the absence (A) and presence (B) of ammonium sulphate. Curve (A) in Fig. 3 was taken into account when measurements were made on proportional volumes of sea water, in order to assess the general validity of the method. For sea water samples of 1, 2 and 3 l, the respective corrected results were 0.52 ± 0.04, 0.57 ± 0.05 and 0.52 ± 0.04 μg V l^{-1}.

The vanadium determinations were carried out on 1-l sea-water samples, for which the percentage recovery was 60%. The results for waters from two different locations are presented in Table III. These were obtained on freshly collected

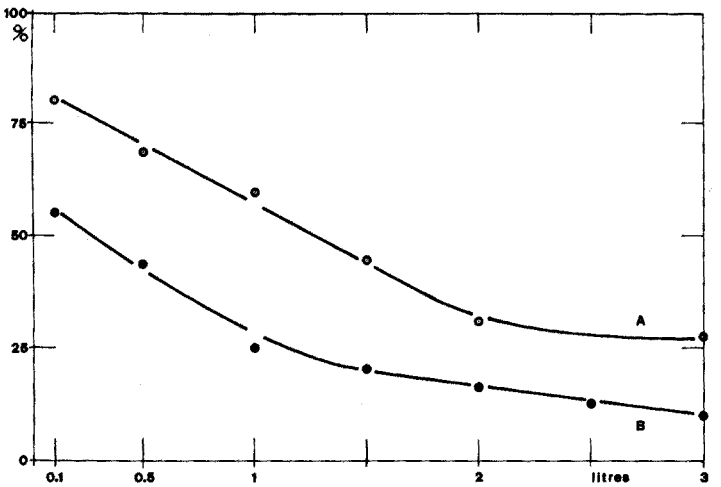

Fig. 3. Recoveries of vanadium *versus* the volumes of 3% NaCl solution (50 μg V l^{-1}). (A) pH 4.0, ammonium sulphate absent; (B) pH 4.0 or 6.5, with 0.1 *M* ammonium sulphate.

TABLE II

PERCENTAGE RECOVERIES FOR DIFFERENT SAMPLE VOLUMES

(1.6 μg V in 3% NaCl solutions at pH 4.0 determined on 5-ng chitosan aliquots from a homogenized 500-mg column.)

Sample volume (ml)	*Recovery (%)*					*Mean (%)*
100	74	80	84	84	73	79
1000	66	58	61	63	56	61

TABLE III

DETERMINATIONS OF VANADIUM IN TWO SEA-WATER SAMPLES

(1-l samples were used 5-mg chitosan fractions were taken from a homogenized 500-mg column.)

Sample I ($\mu g\ V\ l^{-1}$)	*Sample II* ($\mu g\ V\ l^{-1}$)
0.85	0.55
0.70	0.52
0.70	0.50
0.63	0.50
0.57	0.60
0.78	0.46
0.75	0.54
mean value: 0.71	mean value: 0.52
s: ±0.09	*s*: ±0.04

waters; when the sea water was not stored as recommended, the results were lower, and after twenty days, vanadium could no longer be detected, except after oxidative treatment with persulphate.

CONCLUSIONS

The main feature of the proposed method for the determination of vanadium in sea water is that, except for a little acid, no chemicals are required. The method is based on the anion-exchange behaviour of chitosan toward the metavanadate ion. Chitosan, as currently produced, contains no vanadium, and its smoke does not affect the base line when the hot graphite atomizer is used in conjunction with the deuterium compensator. This method requires very few manipulations; only acidification of the sea water to pH 4.0, conditioning a 500 mg column, drying and weighing are needed. Elution is unnecessary, though feasible, and this simplification avoids contamination risks. The procedure is suitable for use on board ships, as many samples can be handled by one technician; the columns can run unattended and can be sealed and stored for later analysis. Only a small aliquot of the polymer from a column is used for a determination, so that replicate analyses can be done on the same column, and the residue can be stored indefinitely.

Vanadium can be eluted from a chitosan column with sulphuric acid or ammonia, and the column can then be used again for many cycles. In order to carry out vanadium determinations on the eluate, the absolute amount of vanadium in the 10–15-ml eluate should be high enough to make it possible to read vanadium signals on 20 μl.

This research was carried out under the auspices of the National Research Council of Italy, Rome, (Contract No. 72-00165-03).

SUMMARY

The anion-exchange behaviour of chitosan toward metavanadate was studied in salt solutions at different pH values. Filtered and acidified sea water was passed through a 500-mg chitosan column. Vanadium was determined by atomic absorption spectrometry with a graphite furnace and a deuterium background corrector on 5-mg aliquots of the homogenized column. The method was assessed for the 0.2–12.0 μg V l^{-1} interval on the basis of the linear response for proportional amounts of vanadium in saline solutions and sea water and in the absence of interferences from smoke during atomization. Two sea-water samples gave 0.71 ± 0.09 and 0.52 ± 0.04 μg V l^{-1}

REFERENCES

1 J. Vrbsky and J. Fogl, *Sb. Vys. Sk. Chem.-Technol. Praze, Anal. Chem.*, (1969) 25.
2 M. Nishimura, K. Matsunaga, T. Kudo and F. Obara, *Anal. Chim. Acta*, 65 (1973) 466.
3 Y. K. Chau and K. Lum-Shue-Chan, *Anal. Chim. Acta*, 50 (1970) 201.
4 D. A. Segar and J. G. Gonzales, *Anal. Chim. Acta*, 58 (1972) 7.
5 J. P. Riley and D. Taylor, *Anal. Chim. Acta*, 41 (1968) 175.
6 J. P. Riley and D. Taylor, *Deep-Sea Res.*, 19 (1972) 307.
7 T. Kiriyama and R. Kuroda, *Anal. Chim. Acta*, 62 (1972) 464.
8 R. A. A. Muzzarelli, *Natural Chelating Polymers*, Pergamon, Oxford, 1973, p. 144.
9 R. A. A. Muzzarelli, Italian Patent Application 3329 A-74, 6th February, 1974.

Analytica Chimica Acta, 70 (1974) 291–298

THE DETERMINATION OF TIN BY CARBON FILAMENT ATOMIC ABSORPTION SPECTROMETRY

G. L. EVERETT* and T. S. WEST

Chemistry Department, Imperial College of Science and Technology, London SW7 2AY (England)

R. W. WILLIAMS

B.P. Research Centre, Sunbury-on-Thames, Middlesex (England)

(Received 16th November 1973)

Tin is very rarely found in any quantity in crude oils and fuels, but it has considerable importance within the petroleum industry as a wear metal. The official ASTM method[1] involves gravimetric determination of tin by volatilization of SnI_4, but Schallis and Kahn[2] have determined tin in lubricating oils by atomic absorption measurements in a nitrous oxide–acetylene flame, obtaining a sensitivity of 3 p.p.m. at the 286.3-nm tin resonance line, for 1% absorption.

The main problem with the determination of tin by atomic spectrometric methods arises from the formation of SnO. This has a decomposition energy of 5.7 eV, and the air–acetylene and nitrous oxide–acetylene flames commonly used in atomic flame spectrometry do not have the requisite reducing or thermal properties to break down SnO completely. The fuel-rich hydrogen flame diluted with an inert gas or with air as support has a far greater reducing power and improved sensitivity has been obtained when it is used.

The most widely used tin resonance line is that at 286.3 nm, although there is a more sensitive line at 224.6 nm. However, this latter line has a very high background and is difficult to utilize unless high-brightness hollow-cathode lamps or electrodeless discharge lamps are employed as sources.

Kahn and Schallis[3], using a high-brightness hollow-cathode lamp and a fuel-rich air–hydrogen flame, reported a sensitivity of 0.15 p.p.m. at the 224.6-nm line. The best sensitivity reported in this flame for the 286.3-nm line is 0.7 p.p.m. (ref. 4) but, with the nitrogen–hydrogen or argon–hydrogen flame, Rubeska and Miksovsky[5] obtained sensitivities of 0.3 or 0.5 p.p.m., respectively, at 286.3 nm. The lack of a reducing atmosphere also limited the sensitivity for the HGA-70 carbon furnace[6], a figure of $1.5 \cdot 10^{-9}$ g being obtained at 224.6 nm.

With tin(II) chloride as standard, the most likely processes that the species can undergo in a flame[4] are:

$$SnCl_2 \rightarrow SnCl \begin{cases} \xrightarrow{[O]} SnO \xrightarrow{5.7\ eV} Sn + O \\ \longleftrightarrow Sn + Cl \\ \xrightarrow{[H]} SnH \xrightarrow{2.7\ eV} Sn + H \end{cases}$$

*Present address: Johnson-Matthey Chemicals Ltd., Royston, Herts., England.

The better sensitivity of hydrogen-rich flames for tin may, therefore, be attributed to the relative thermal instability of tin hydride, as well as the low oxygen concentration.

EXPERIMENTAL

Apparatus

This was basically the same as that described previously[7]. The collimator used was a 3×0.5-mm slit cut in a copper sheet mounted in a copper tube. The source was an "Intensitron" hollow-cathode lamp (Perkin-Elmer Ltd., Beaconsfield, Bucks) but for the investigation of the 224.6-nm line, an SnI_4 electrodeless discharge lamp was used. This was placed in an air-cooled Broida-type ($\frac{3}{4}$-wave) cavity which received power from a 2450 MHz generator (Electro-Medical Supplies Ltd., London). The experimental parameters used were as follows: monochromator slit-width, 0.1 mm (*ca.* 0.3 nm bandpass); hollow-cathode lamp current, 29 mA; electrodeless discharge lamp power, 50 W; EHT, -1100 V; atomic line, 286.3 nm or 224.6 nm as appropriate.

Calibration solutions

Aqueous standards were prepared from A.R. tin (1 g) dissolved in *ca.* 100 ml of concentrated hydrochloric acid and made up to 1 l with glass-distilled deionized water. Calibration solutions were made up by dilution of this stock; those of $\leqslant 10$ p.p.m. were not kept for longer than 12 h. Organic standards were prepared from tin octoate dissolved in either reagent-grade xylene or a metal-free SAE 10 base oil. No blank readings were observed from these solvents when the sample size was 1 μl. Disposable Drummond glass micropipettes (Shandon Scientific Ltd.) were used for sample placement.

Measurement technique

The basic technique was to first dry the liquid sample by application of low power to the carbon filament. When all visible signs of liquid had disappeared, the power was turned off and the Variac setting was raised. The organic solutions were then distilled off at an intermediate voltage to remove the bulk organic matrix, to break down any organotin compounds and ensure maximal atomic absorption of tin. The sample was then atomized by applying a high voltage for *ca.* 2 s. The following sequences were used: Aqueous: Dry, 1.2 V for 10 s. Atomize, 8.4 V for 60 s cycle. SAE 10 oil: Dry, 3.36 V for 15 s. Distil, 4.8 V for 5 s. Atomize, 8.4 V for 90 s cycle. Xylene: Dry by extrusion from the micropipette on to the filament. Distil, 4.8 V for 5 s. Atomize, 8.4 V for 60 s cycle. It was found that all tin was removed at the atomization stage and there were no memory effects.

RESULTS AND DISCUSSION

Effect of sheathing gas on signal

It was absolutely necessary to have hydrogen in the nitrogen sheathing gas in order to reduce the SnO formed. The hydrogen was ignited automatically by

the glowing filament and its presence increased the sensitivity ten-fold. The optimal flow rate of nitrogen was 2.8 l min^{-1} for all standards, but the optimal for hydrogen differed for organic and aqueous standards, these two values being 1.65 l min^{-1} and 1.3 l min^{-1}, respectively. This higher value for organic tin is required because the tin octoate, having a direct tin–oxygen bond, is more difficult to reduce than tin(II) chloride.

Effect of atomization conditions on signal

As already mentioned, the effect of hydrogen in the sheathing gas was considerable, but the physical state of the filament was found to have an even greater effect. When the filament was new, the sensitivity was very low, but this increased with increasing porosity of the used filament until an optimum was reached. This optimum was equivalent to two or three "burns" of the filament in air. The atomization voltage was then optimized at 8.4 V and at this power the filament was good for over 500 "burns" before a reduction in sensitivity and reproducibility was observed.

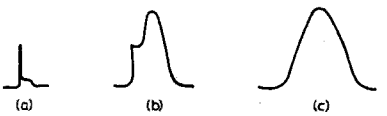

Fig. 1. Peak shapes for atomic absorption of tin in aqueous solution. (a) Impervious filament, (b) porous filament, (c) porous filament + interferent.

This phenomenon can probably be accounted for by loss of tin as tin(II) chloride before the hydrogen ignites. With the increasing porosity of the filament and penetration of the sample, this volatilization is slowed down until all the tin comes off together. This appears to be upheld by investigation of the peak shape (Fig. 1). There was a very fast "pre-peak" which is attributed to the reduction of this initial loss of tin(II) chloride, the main peak being the bulk of the tin. As the filament porosity increased, the relative height of the pre-peak decreased to a steady value. Investigation of the nearby Mn 280.11-nm resonance line showed no peak and it was, therefore, concluded that both peaks were due to true atomic absorption of tin.

When organic standards were atomized, unless a pyrolysis or distillation step of 4.8 V for 5 s was included, multiple absorption peaks were seen. This is thought to be due to the incomplete breakdown of tin octoate and the differing atomization and reduction rates of the tin species present. When the high-temperature preheat was included in the heating sequence, only one peak was seen, indicating that the breakdown of the octoate was complete.

Effect of filament height on signal

The effect of the height of the light beam above the filament is shown in Fig. 2. The optimal position involved grazing incidence of the light on the filament surface. It is here, close to the filament, that the atomic population will be at a maximum and interferences at a minimum. It is apparent that, apart from increasing the sensitivity, the presence of hydrogen maintains the atomic population to a

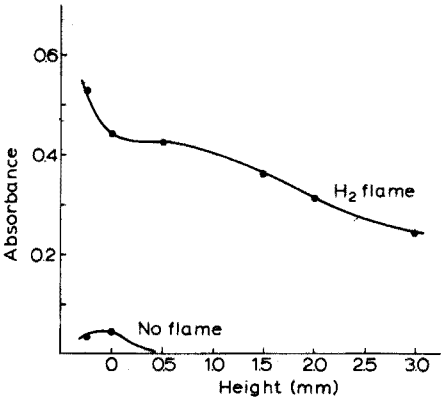

Fig. 2. Dependence of tin absorbance on height of light beam above filament.

considerable extent, quite high above the filament. This agrees with the conclusions of Reeves *et al.*[8].

Calibration curves and sensitivity

Several wavelengths were investigated from the point of view of sensitivity and the results are shown in Table I. Figures obtained for tin absorption in an air–hydrogen flame are given for comparison.

The actual values of sensitivity for 1% absorbance are listed in Table II. For absorption at 286.3 nm, the aqueous tin solutions were found to give smaller signals, at high levels of tin (>20 ng), than xylene solutions. This is undoubtedly due to the prior loss of tin(II) chloride from the aqueous solutions. Working curves for xylene and oil solutions are shown in Fig. 3.

TABLE I

SENSITIVITY FOR TIN AT DIFFERENT WAVELENGTHS

Transition[9]	*Wavelength (nm)*	*Absorbance*		*Sensitivity*[a] *CFAR (g)*
		CFAR (100 ng or 1 p.p.m.)	*Flame*[10] *(200 p.p.m.)*	
$5p^2\ ^3P_0$–$5d\ ^3D_1$	224.6	1.364	0.821	$6.7 \cdot 10^{-11}$
$5p^2\ ^3P_1$–$5d\ ^3D_1$	235.5	0.602	0.398	$7.3 \cdot 10^{-10}$
$5p^2\ ^3P_2$–$5d\ ^1F_3$	242.95	0.198	—	$2.2 \cdot 10^{-9}$
$5p^2\ ^3P_0$–$6s\ ^1P_1$	254.66	0.693	0.178	$6.4 \cdot 10^{-10}$
$5p^2\ ^3P_1$–$6s\ ^1P_1$	266.1	0.076	0.028	$5.8 \cdot 10^{-9}$
$5p^2\ ^3P_1$–$6s\ ^3P_2$	270.65	0.788	0.202	$5.6 \cdot 10^{-10}$
$5p^2\ ^3P_2$–$6s\ ^3P_2$	284.0	0.326	—	$1.35 \cdot 10^{-10}$
$5p^2\ ^3P_0$–$6s\ ^3P_1$	286.3	1.330	0.492	$9 \cdot 10^{-11}$
$5p^2\ ^3P_1$–$6s\ ^3P_1$	300.9	0.333	0.087	$1.3 \cdot 10^{-9}$
$5p^2\ ^3P_1$–$6s\ ^3P_1$	303.4	0.441	0.148	1.10^{-9}
$5p^2\ ^3P_2$–$6s\ ^3P_1$	347.5	0.191	—	$2.3 \cdot 10^{-9}$

[a] Weight of Sn equivalent to 0.0044 absorbance.

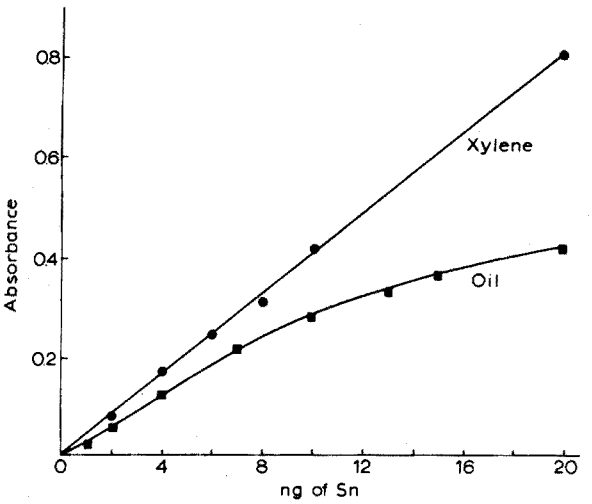

Fig. 3. Working curves. 1-μl samples at 286.3 nm.

TABLE II

SENSITIVITIES, DETECTION LIMITS AND LINEAR RANGES OF CALIBRATION

Solvent	*Wavelength (nm)*	*Sensitivity (g)*	*Detection limit (g)*	*Linear range (ng)*
Water	224.6	$6.7 \cdot 10^{-11}$	10^{-10}	0–8
	286.3	$9 \cdot 10^{-11}$	$1.3 \cdot 10^{-10}$	0–10
			$7 \cdot 10^{-11}$ [a]	
Xylene	286.3	$1.1 \cdot 10^{-10}$	$1.5 \cdot 10^{-10}$	0–20
SAE 10 Oil	286.3	$1.3 \cdot 10^{-10}$	$1.8 \cdot 10^{-10}$	0–6

[a] With electrodeless discharge lamp.

By choice of the appropriate wavelength, linear calibration curves may be constructed for a wide range of concentrations.

Detection limits are also shown in Table II. The detection limit is that concentration where the mean signal from ten replicates is equal to twice the standard deviation of peak height of those ten replicates. The effect of a more intense source may be seen by the improvement in detection limit with an electrodeless discharge lamp.

The relative standard deviation (s_r) of peak height was calculated from replicates of solution at approximately twenty times the detection limit. For aqueous solutions, the s_r value was 5.3% for six results; for SAE 10 base-oil, s_r was 9.4% for thirteen results; and for xylene solutions, s_r was 6.5% for eight results.

Origin of the signal

Signals for 100 ng of tin were measured at the following lines: tin non-resonance 226.6 and 276.3 nm, cadmium 228.8 nm and manganese 280.11 nm. In

no case was any absorption seen and, therefore, signals at 224.6 nm and 286.3 nm were confirmed as being due to absorption by tin atoms.

Interference studies

Reagents used for aqueous studies were A.R.-grade metal chlorides, sulphuric acid and phosphoric acid. Organic reagents used were naphthenates (Cr, Ca, Fe, Ni), Cerechlor 42 (Cl) and a special British Petroleum additive (Al).

Interferences in aqueous solution were examined for a range of ions at 10- and 100-fold levels (Table III). For the elements Cr, Ca, Ni, Al, Fe and Cl, the study was made for 10–100-fold amounts in both aqueous and xylene solutions (Figs. 4 and 5).

TABLE III

EFFECTS OF DIVERSE IONS IN AQUEOUS SOLUTIONS

(Percent change of absorbance for 5 ng of tin.)

Interferent	*10-Fold amount (50 ng)*	*100-Fold amount (500 ng)*
Mg	+40	+10
Co	+30	0
Ba	+15	0
Pb	+10	−25
Zn	0	0
Cu	−20	−20
Na	−40	−65
SO_4^{2-}	0	0
PO_4^{3-}	0	0

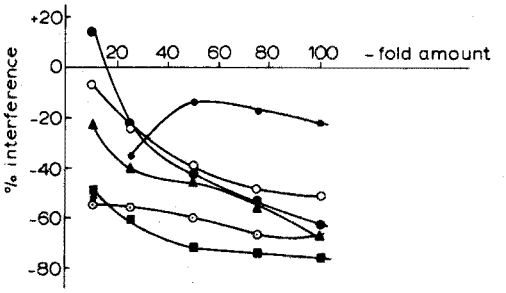

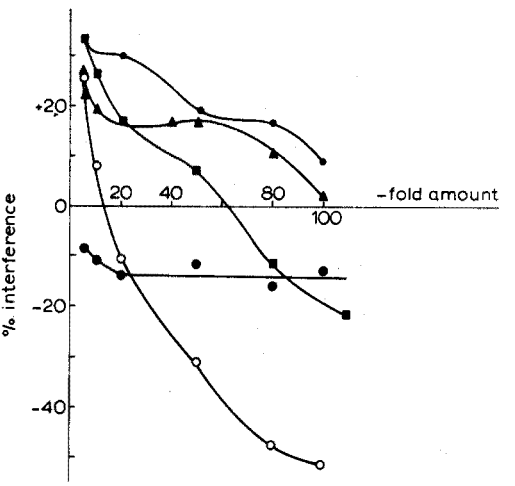

Fig. 4. Interferences in xylene solutions. (•) Ni, (○) Cr, (●) Cl, (▲) Al, (⊙) Fe, (■) Ca.

Fig. 5. Interferences in aqueous solutions. (•) Al, (▲) Cr, (●) Fe, (■) Ca, (○) Ni.

In aqueous media, many metals enhance tin absorption and it was observed that the peak shape was improved (Fig. 1), by disappearance of the pre-peak. When no interferent was present, a small amount of tin(II) chloride was lost, the reduction of which caused these peaks. When an interferent was present, the volatilization of the standard was altered so that this $SnCl_2$ was held back and all the tin came off in one step, thus "smoothing" the peaks and enhancing the absorption. As the concentration of interfering ion increased, the peaks broadened, because the volatilisation rate was reduced. Probably, there was some vapour-phase interaction between interferent and analyte, causing reduced signals, but the presence of the hydrogen flame should minimize this effect compared to the "atomization" interference.

For those metals which did not show such enhancements, the analytical signal was unchanged in shape from the standard. Here the major cause of interference was vapour-phase interaction, as is normally the case with the carbon filament technique.

In organic solution, the signal was also "smoothed" and although the curve shapes (Figs. 4 and 5) for organic and aqueous solutions were similar in most cases, the magnitudes of interference were very different.

Enhancement of tin atomic absorption signals in both inert gas–hydrogen[5] and air–hydrogen[11] flames has been reported for aqueous solutions. The explanation offered[5] is that there is augmented heat transfer from interferent to analyte, presumably within the clotlet in the flame, which causes increased atomization. Work by Bulewicz and Padley[12] supports this explanation; they found that in hydrogen–oxygen–nitrogen flames, chromium particles were *ca.* 500°C hotter than the ambient flame gases, probably because of free radical recombination on the particle surface. This theory is not relevant to the results obtained on the carbon filament since particles are not introduced into the flame. Instead the sample is volatilized by the hot carbon filament which is at a much higher temperature than the flame. The interference processes on the filament are more probably due to atomization differences of standards and vapour phase interactions between interferent and the analyte atoms.

We are grateful to the SRC for the award of a CAPS studentship to G.L.E. and to the British Petroleum Co, Sunbury, for the provision of the organic reagents and the SAE 10 base-oil.

SUMMARY

The atomic absorption characteristics of tin on a carbon filament atom reservoir are described. The behaviour of tin in aqueous solution as tin(II) chloride, in xylene as tin octoate and in oil solutions is studied. The interference effects of a selected range of seven cations, added as chlorides in aqueous solution or as naphthenates in non-aqueous media, and of sulphate and phosphate were examined. In all cases, the signals were measured in the filament reservoir with a surrounding hydrogen diffusion flame. The 1% absorption sensitivity in the organic media at the 286.3-nm line was 10^{-10} g and $9 \cdot 10^{-11}$ g in aqueous solution. In the latter medium, the corresponding sensitivity at 224.6 nm was $6.7 \cdot 10^{-11}$ g. The linear analytical range lay in the region 0 to 20 ng.

REFERENCES

1 *ASTM Standards, Part 17*, Philadelphia, Pa., 1970.
2 J. E. Schallis and H. L. Kahn, *At. Absorption Newslett.*, 7 (1968) 84.
3 H. L. Kahn and J. E. Schallis, *At. Absorption Newslett.*, 7 (1968) 5.
4 T. Nakahara, M. Munemori and S. Musla, *Anal. Chim. Acta*, 62 (1972) 267.
5 J. Rubeska and M. Mikovsky, *At. Absorption Newslett.*, 11 (1972) 57.
6 T. J. Fernandez and D. C. Manning, *At. Absorption Newslett.*, 10 (1971) 65.
7 G. L. Everett, T. S. West and R. W. Williams, *Anal. Chim. Acta*, 66 (1973) 301.
8 R. D. Reeves, B. M. Patel, C. J. Molnar and J. D. Winefordner, *Anal. Chem.*, 45 (1973) 246.
9 R. Mavrodineanu and H. Boiteux, *Flame Spectroscopy*, Wiley, New York, 1965.
10 L. Capacho-Delgado and D. C. Manning, *Spectrochim. Acta, Part B*, 22 (1966) 1505.
11 B. Moldan, I. Rubeska, M. Mikovsky and M. Huka, *Anal. Chim. Acta*, 52 (1970) 91.
12 E. M. Bulewicz and P. J. Padley, *Proc. Roy. Soc., Ser. A*, 323 (1971) 377.

Analytica Chimica Acta, 70 (1974) 299–310

THE APPLICATION OF ELECTRODEPOSITION TECHNIQUES TO FLAMELESS ATOMIC ABSORPTION SPECTROMETRY

PART I. THE DETERMINATION OF CADMIUM WITH A TUNGSTEN FILAMENT

WALTER LUND and BJØRN VIGGO LARSEN
Department of Chemistry, University of Oslo, Blindern, Oslo 3 (Norway)
(Received 12th November 1973)

The introduction of flameless techniques has greatly improved the detection limits of atomic absorption spectrometry. Flameless cells are now commercially available, the two most popular designs being the graphite furnace and the carbon rod atomizer. Both these cells make use of a high-voltage power supply with water cooling of the electrical terminals, and automated temperature programming. The use of a thin metal wire instead of a furnace or rod obviously simplifies the technical approach, as only a low current and voltage are then needed for the electrical heating of the filament. However, only a few papers have appeared in the literature discussing the applications of such filaments.

Thin metal wires were first used for the determination of mercury by spontaneous amalgamation onto copper[1] or silver[2]. Later, tantalum[3–7], tungsten[8] and a tungsten–rhenium alloy[9–10] were used as filament materials for the determination of various elements. Platinum and tungsten wires have also been used in atomic fluorescence analysis[11–13]. Except for the determination of mercury, the solution to be analyzed is always placed directly on the filament by means of a microsyringe, and the solvent is then vaporized completely at a low temperature before the atomization of the element takes place. In order to avoid interferences from the matrix, the matrix should also if possible be removed by vaporization before the determination of the element. However, this is not possible when elements with low boiling points are determined. In this case some chemical separation, such as solvent extraction, must be used in combination with the flameless technique[14].

A separation technique which seems to be particularly well suited for the metal wire flameless atomic absorption analysis is electrolytic deposition. By such a deposition most of the common interferences from the matrix can be eliminated. At the same time, the electrolytic deposition on the metal wire represents a powerful preconcentration step, which improves the sensitivity of the method. Also the usual drying and charring sequences would no longer be necessary. Of course, only those metals which are electrochemically reduced or oxidized in the accessible potential region can be determined. However, the metals which are most frequently mentioned in toxicological discussions today, *e.g.* mercury, cadmium, lead, are all easily deposited electrochemically from aqueous solutions. These metals are normally

present only in ultratrace amounts (at the p.p.b. level), so that only a method with very high sensitivity, such as flameless atomic absorption, can be employed.

The determination of mercury mentioned above[1,2] represents a special application of the electrolytic deposition technique, which in this case is based on the spontaneous amalgamation of mercury on the metal wire. A similar technique, which is also based on a spontaneous chemical reaction, has recently been described by Newton *et al.*[9]. However, for the technique to be generally applicable the deposition should be carried out electrochemically. This approach was suggested by Brandenberger[15]. The electrodeposition should, however, be performed by means of a potentiostat, where the deposition potential is controlled. The only paper describing the use of controlled potential electrolysis in combination with flameless atomic absorption analysis seems to be a recent work by Fairless and Bard[16]; these authors used a carbon rod atomizer in their work.

This series of papers will investigate the application of controlled potential electrolysis for metal wire flameless atomic absorption analysis. In the present paper the determination of cadmium with a tungsten filament is studied.

EXPERIMENTAL

Apparatus

A double-beam atomic absorption spectrophotometer, Perkin-Elmer 403, and a Hitachi Perkin-Elmer 165 recorder were used. The cadmium hollow-cathode lamp was operated at a current of 12 mA, and the signal was measured at 228.8 nm. The instrument was used in the concentration mode, with the Recorder Response (noise suppression) in position 2. The burner head was replaced by the absorption cell shown in Fig. 1. The cell is made of glass, with quartz windows. It is held in the correct position by means of two clips mounted on a metal plate which is in turn mounted on the commercial burner body. Joints were sealed on the top of the cell to allow the passage of a stream of highly purified nitrogen through the cell. The flow rate of the gas was controlled by a flowmeter. The electrode with the tungsten filament is placed in the centre of the absorption cell through a B14 ground-glass joint. The details of this electrode are shown in Fig. 2. The filament itself is a rigid spiral of tungsten wire from a commercially available light bulb, Osram (Germany) 8100, 6 V, 5 A. The tungsten wire, which has a diameter of 0.20 mm, is welded onto thick support wires of platinum with a diameter of 1.0 mm. The platinum wires are sealed into a B14 male joint. Inside the joint, where an inert metal is no longer necessary, the platinum wires are replaced by copper wires of the same diameter. This is done purely for economic reasons. The total length of the electrode is chosen so that the electrode fits into the electrolytic cell, which is described below.

The way the tungsten spiral is welded onto the thick support wires proved to be of great importance. The following procedure was found to be satisfactory: thin holes, 0.30 mm in diameter and 2 mm deep, were drilled into the ends of the platinum wires, the ends of the tungsten spiral were placed in the holes, and the platinum was melted around the ends of the spiral by spot welding. This procedure also explains why the support wires were made of platinum, and not tungsten.

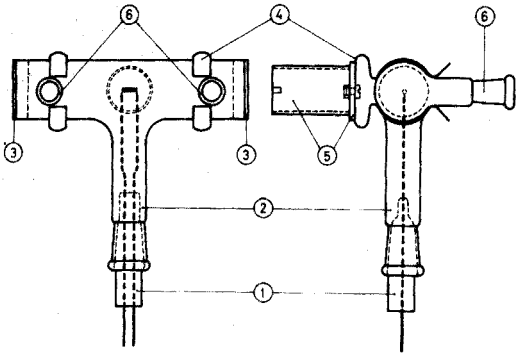

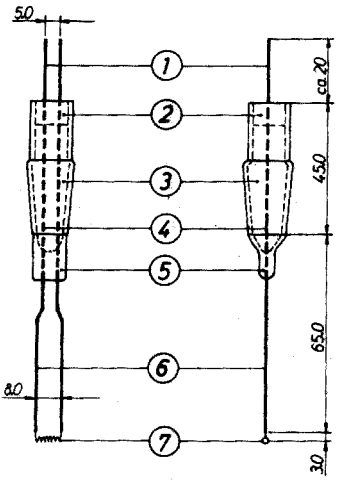

Fig. 1. Absorption cell with filament electrode. Top view to the left, side view to the right. 1, electrode with filament; 2, absorption cell; 3, quartz windows, 30-mm diameter; 4, metal clips; 5, metal plate and stem; 6, B9 joints.

Fig. 2. Electrode with filament. Dimensions are given in mm. 1, Copper support wires, 1 mm diameter; 2, teflon stopper; 3, B14 joint; 4, point where the Cu and Pt wires are melted together; 5, glass seal; 6, platinum support wires, 1 mm diameter; 7, tungsten filament.

The tungsten filament was electrically heated by connecting the ends of the support wires to a power supply. This was either a d.c. source, such as four 1.5-V alkali batteries connected in series, or a Variac with a 6-V a.c. transformer. The inert gas in the absorption cell prevents oxidation of the filament during the heating period. The temperature of the filament was measured with an optical pyrometer.

The controlled-potential electrolysis was performed by means of a potentiostat built in this laboratory. The electrochemical measurements of charge were done by means of an electronic integrator also built in this laboratory. A Metrohm EA 880-20 vessel was used as electrolytic cell. An Ag/AgCl reference electrode (Metrohm EA 427), with a salt bridge filled with the solution to be analyzed, and a platinum counter electrode were used in combination with the working electrode described above (Fig. 2). The solution was stirred during the electrolysis by means of a steady flow of highly purified nitrogen gas through the cell. The flow-rate was controlled by means of a flowmeter. This flow of nitrogen gas also removed dissolved oxygen from the solution.

Reagents and solutions

All reagents were of analytical grade, except the potassium chloride used as supporting electrolyte, which was of Suprapure quality (Merck). The water was de-ionized with an ion-exchange resin and distilled. Solutions for analysis were prepared just before use.

General procedure

For ultratrace analysis, an adequate cleaning of all the equipment is of

utmost importance. To prevent adsorption of metals on the glass walls of the electrolytic cell, the cell was treated with a silicone repellent. This was done in the following way: the electrolytic cell was first cleaned with (1+1) nitric acid and dried. Dimethyldichlorsilane was then placed in a cup inside the cell and the cell was kept closed for 10 h. After this treatment, the cell could be used for weeks without further treatment, except simple cleaning with dilute nitric acid.

A typical analysis is carried out in the following manner. Place 20 ml of the solution to be analyzed in the electrolytic cell and electrolyze for 2 min at -1.0 V *vs.* Ag/AgCl with a nitrogen flow of 100 cm^3 min^{-1}. Lift the filament electrode out of the cell without disconnecting the electrical circuit (if the electrical terminals are disconnected while the electrode is still in the solution, the metal deposited will immediately be oxidized), rinse the filament with water and dry it with acetone. Place the electrode in the absorption cell, which already has been purged with nitrogen gas, and record the atomic absorption peak during the application of a voltage of 4 V to the tungsten filament for 5 s. Some typical absorption peaks are shown in Fig. 3.

An oxide film is occasionally formed on the filament wire. This film can be removed by dipping the filament in molten sodium nitrite. The sodium nitrite is rinsed off with water.

All the experiments described in this paper were carried out with solutions containing 0.1 *M* potassium chloride. Unless otherwise stated, the concentration of cadmium was 50 p.p.b. The experimental points indicated in the different Figures always represent the mean values of 3–5 determinations.

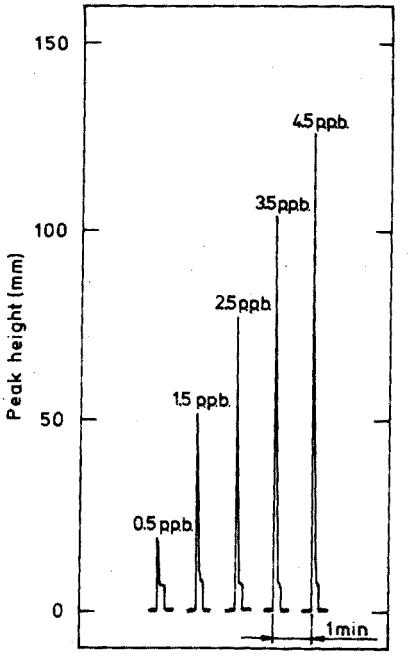

Fig. 3. Some typical atomic absorption peaks for cadmium. The concentrations (in p.p.b.) are indicated in the figure.

RESULTS AND DISCUSSION

Choice of filament material

The shape and dimensions of the filament are of importance for the sensitivity and reproducibility of the method. The filament wire should be spiral-wound to obtain maximal electrode area while preserving reasonable dimensions of the filament. The wire should also be so thin that only a low current is needed for the electrical heating of the wire. However, too thin wires should be avoided, as the filament must be sufficiently rigid to be handled without changing its form. It was found that a wire diameter of 0.20 mm provided the best compromise. With this diameter, the wire can be heated to a white glow even with ordinary torch batteries.

If tungsten is chosen as filament material, a wire of the correct shape and dimensions is easily obtained from a commercially available light bulb. For this work the filament wires were taken from Osram 8100 light bulbs. Another advantage of choosing tungsten as filament material is the high melting point of tungsten, which makes the analysis of less volatile metals feasible. Tungsten was also found to be a suitable filament material from an electrochemical point of view. Because of the low overvoltage of hydrogen on many electrode materials, hydrogen evolution often interferes with the electrochemical reduction of metal ions in aqueous solution. This is especially true for cadmium, as a reduction potential of -0.8 to -1.0 V *vs.* Ag/AgCl must be used. However, no evolution of gas was noticed on the tungsten filament during the deposition at -1.0 V from neutral solutions, in spite of the expected low overvoltage for hydrogen on tungsten[17]. Because of the high overvoltage for hydrogen on cadmium, an increase in the overvoltage would not have been surprising, if the filament wire was completely covered with cadmium during the electrolysis. However, in most cases only a very small fraction of the electrode was covered with cadmium.

During the electrolysis, cadmium is also deposited on that part of the filament support wires which dips into the solution. However, the support wires are so much thicker than the filament wire, that only the cadmium on the tungsten filament is atomized during the electrical heating of the wire. One is therefore, with this electrode, guaranteed a well-defined, reproducible filament area, which is independent of the solution volume in the electrolytic cell.

Effect of deposition potential

To determine the optimal reduction potential for cadmium, the amount of cadmium deposited on the filament was studied as a function of the potential. The amount of cadmium deposited was determined electrochemically, by integrating the current measured during the oxidation of cadmium at 0 V. The resulting charge *vs.* potential curve is shown in Fig. 4. As can be seen, the curve has a maximum in the region -0.9 to -1.0 V *vs.* Ag/AgCl. The decrease in charge above -1.0 V is probably due to the onset of the evolution of hydrogen. The experiments described below were all carried out with a deposition potential of -1.0 V.

Effect of stirring of the solution

For a given deposition period, the sensitivity of the method depends on the

rate of the mass transport to the electrode during the electrolysis. This rate is affected by cell geometry, electrode design and stirring rate of the solution. The stirring can be done in different ways. A magnetic stirrer can be used, or a vertical stirring bar which is rotated by means of a synchronous motor placed above the cell. The stirring can also be effected by simply passing nitrogen through the solution at a constant flow rate. The last approach was chosen in the present investigation, because it has the advantage that dissolved oxygen is simultaneously removed. Also the hydrogen and oxygen gas, which can be formed at the working and counter electrodes during the electrolysis, are removed. Stirring by nitrogen gas is effective and reproducible, provided that a flowmeter is used to control the flow rate. A linear relationship between the atomic absorption signal and the flow rate was observed in the region 40–200 cm^3 min^{-1}, but the increase in the absorption signal was only 20% when the flow rate was increased from 40 to 200 cm^3 min^{-1}. Flow rates above 200 cm^3 min^{-1} caused splashing of the solution. For the present work, a flow rate of 100 cm^3 min^{-1} was always used.

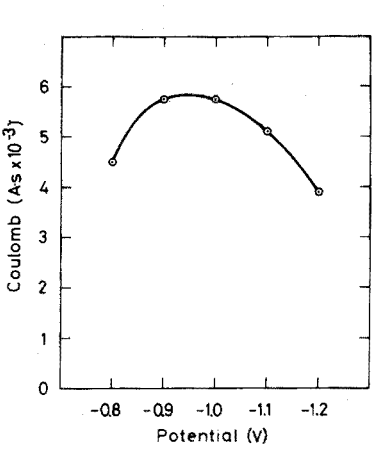

Fig. 4. Effect of deposition potential on amount of cadmium deposited for 5 p.p.m. cadmium.

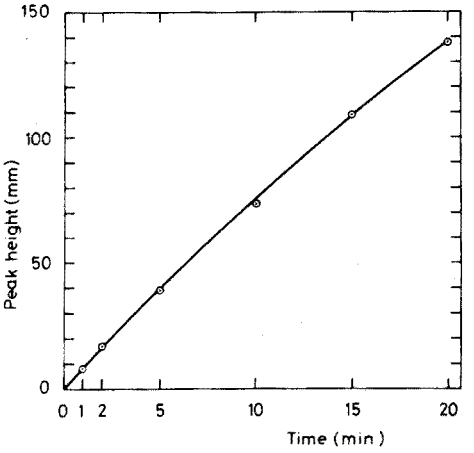

Fig. 5. Effect of deposition time on signal for 1 p.p.b. cadmium.

Effect of deposition time

The sensitivity of the method can be increased by increasing the electrolytic deposition period. The variation of the absorption signal with deposition time is shown in Fig. 5 for 1 p.p.b. cadmium. As can be seen, there is an approximately linear dependence between the height of the signal and the deposition time. However, at higher concentrations of cadmium the deviation from linearity becomes pronounced. Thus, for 50 p.p.b. cadmium the absorption signal is almost independent of the deposition time for deposition periods above 5 min (Fig. 6).

Effect of filament position

The effect of the filament position relative to the light beam from the hollow-cathode lamp was studied by varying the position of the absorption cell.

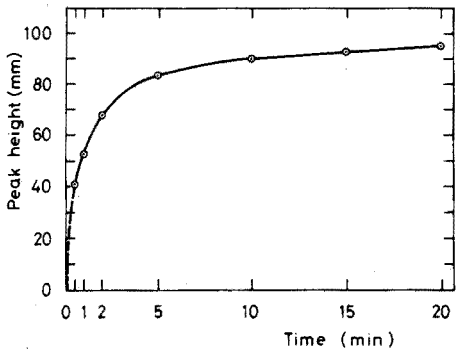

Fig. 6. Effect of deposition time on signal for 50 p.p.b. cadmium.

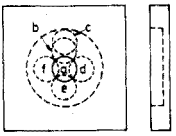

Fig. 7. Positions of the light beam relative to the filament. The filament is in the center (not shown). See Figs. 8 and 9.

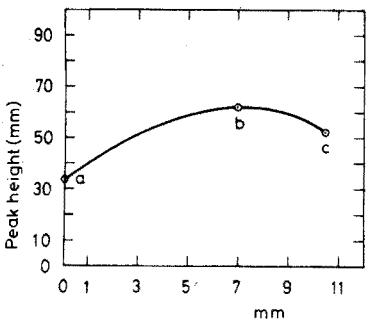

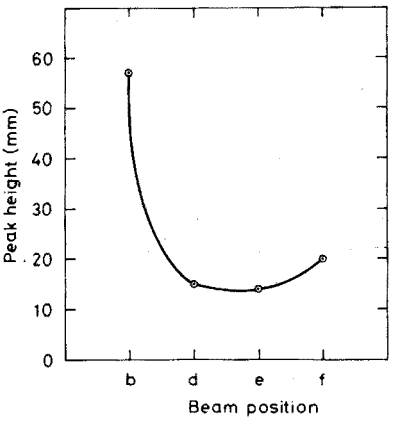

Fig. 8. Effect of the position of the light beam relative to the filament. The letters refer to the positions indicated in Fig. 7. The *x*-axis represents the height of the light beam center above the filament center. The concentration of cadmium is 50 p.p.b.

Fig. 9. Effect of the position of the light beam. See Figs. 7 and 8.

The positions indicated in Fig. 7 were studied. The resulting peak heights for 50 p.p.b. cadmium are drawn in Fig. 8 and 9. In Fig. 8 the *x*-axis represents the height of the center of the light beam above the filament. Of the six positions studied, the b-position, with the light beam center 7 mm above the filament, gave the best sensitivity. This position was used in all other experiments.

Effect of inert-gas flow rate

Nitrogen was used to provide an inert atmosphere around the filament. The absorption signal was not much influenced by the passage of nitrogen through the absorption cell during the atomization step. The effect is illustrated in Fig. 10. The signal was lowered only 30% when the flow rate was increased from 0 to 900 cm^3 min^{-1}. To ensure an inert atmosphere in the cell it is recommended that a slow continuous flow of nitrogen is always maintained.

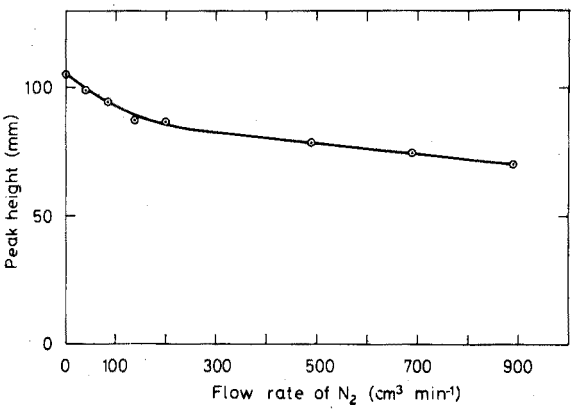

Fig. 10. Effect of inert-gas flow rate on signal for 50 p.p.b. cadmium.

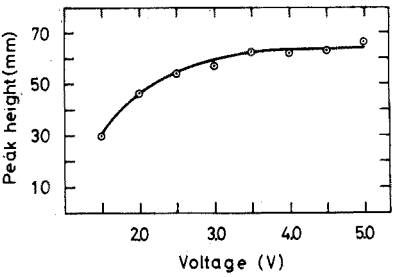

Fig. 11. Variation of signal with filament voltage for 50 p.p.b. cadmium.

Effect of filament voltage and temperature

The variation in absorption signal with filament voltage is shown in Fig. 11. Little improvement in signal was obtained above 3.5 V. Too high voltages should be avoided, as this will lead to premature ageing of the filament.

The relationship between the atomization voltage and the filament temperature is given in Table I. From this Table and Fig. 11 it can be seen that the optimal atomization temperature for cadmium with the present technique is 1400–1500°C. This is in good agreement with the temperature given by L'vov (1500°C)[18] for flameless atomization of cadmium. However, the manufacturer of a commercially available graphite furnace recommends a somewhat higher temperature (1800°)[19].

TABLE I

RELATIONSHIP BETWEEN FILAMENT VOLTAGE AND TEMPERATURE

Voltage (V)	2.0	2.5	3.0	3.5	4.0	4.5	5.0
Temperature (°C)	940	1050	1230	1430	1650	1780	1940

The voltages given in Fig. 11 and Table I were supplied from a Variac and an a.c. transformer. Four 1.5-V batteries connected in series gave a peak height corresponding to *ca.* 1400° (or 3.5 V).

Calibration curves and detection limit

A calibration curve for the concentration range 0–5 p.p.b. is shown in Fig. 12 for a 2-min deposition period; as can be seen, there is a slight curvature of the line. At higher concentrations, the non-linearity becomes more pronounced. When the concentration reaches 200 p.p.b. the curve is almost parallel with the *x*-axis. This is in accordance with the results obtained for the dependence of the signal of the deposition time (Fig. 5 and 6). Here it was also found that the absorption

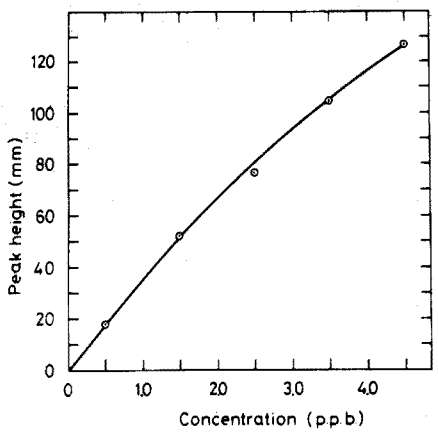

Fig. 12. Calibration curve for low concentrations of cadmium. Deposition time 2 min.

signal becomes almost independent of the amount of cadmium deposited on the filament for too high concentrations of cadmium. Calculations show that this upper concentration limit, 200 p.p.b. for a deposition time of 2 min, corresponds approximately to a complete monolayer coverage of cadmium on the filament.

The detection limit of the present method, given in terms of concentration, depends on the deposition time, and to a smaller extent also on parameters such as electrode design and stirring rate. With a 2-min deposition period, the detection limit (signal:noise 2:1) was found to be 0.1 p.p.b. cadmium. With a deposition time of 20 min, the detection limit should be 0.01 p.p.b. cadmium.

The absolute detection limit of the method, given in grams, is not so easily determined. In this case, an estimate must be made of the fraction of cadmium which is deposited on the filament during the electrolysis. This again is a function of experimental parameters such as electrode and cell design, stirring rate and sample volume. From separate experiments, where the decrease in the concentration of cadmium during electrolysis was studied as a function of time, it was concluded that approximately 1% of the cadmium was deposited on the filament wire per min during the electrolysis. With a sample volume of 20 ml, the absolute detection limit was then calculated to be $4 \cdot 10^{-11}$ g.

Reproducibility

The reproducibility of the method was determined by repetitively measuring standard solutions under optimized conditions. For the concentration range 0.5–50 p.p.b. cadmium, the relative standard deviation was 5–10%.

Typically, a relative standard deviation of 5.6% was obtained for 25 determinations, carried out on five standard solutions, all containing 1 p.p.b. cadmium.

Interference studies

Owing to the electrochemical deposition step, there should be no interference from most metals when cadmium is determined by the present technique. This was verified by adding a 1000-fold amount of the cations of sodium, magnesium, calcium, strontium, manganese, iron, cobalt, nickel and aluminium to

a cadmium solution. The metals, which were added as the chlorides, had no effect on the atomic absorption signal for 1 p.p.b. cadmium. None of the metals mentioned above is deposited on the filament at −1.0 V. However, it was also found that a 1000-fold excess of copper could be present without causing a change in the absorption signal. This is interesting, as it indicates that not even the simultaneous deposition of a large excess of a metal on the filament interferes with the determination of cadmium when the proposed technique is used.

The effect of the anions nitrate, sulphate and phosphate was also studied. No change in the signal for cadmium was observed in the presence of 1000-fold amounts of these anions. The anions were added as the sodium or potassium salts.

In the experiments mentioned above, the various ions were added in 1000-fold amounts. In fact, the concentrations of these ions can be much higher without causing interferences in the determination of cadmium. It should be kept in mind that all the experiments described here were carried out with solutions containing 0.1 *M* potassium chloride. This indicates that the presence of a high concentration of salts does not in itself give rise to any interference effects. This is important, considering the well-known non-specific absorption by light-scattering commonly encountered in atomic absorption spectrometry, in the presence of high concentrations of salts.

However, the present method was not completely without interference effects. In the presence of a 1000-fold amount of lead, the absorption signal for cadmium was decreased by 90%. The reason for this interference has not yet been found.

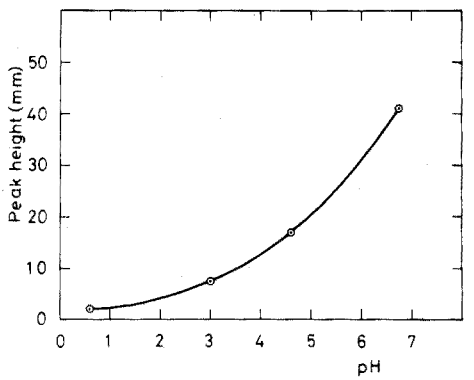

Fig. 13. Dependence of the signal on the concentration of nitric acid for 1 p.p.b. cadmium.

Serious interference effects were also observed in the presence of mineral acids. In acidic solutions the surface of the tungsten filament seems to undergo some chemical reaction, giving rise to a marked decrease in the absorption signal with time. The change in the signal is a function of the pH of the solution. The effect was particularly marked when nitric acid was added to the solution, as shown in Fig. 13.

Further work is in progress in order to study, and if possible overcome. the interferences mentioned above.

APPLICATIONS

The proposed method should be eminently suited for trace and ultratrace analysis of cadmium in samples with a complex matrix, such as for instance sea-water samples. In contrast to most other flameless techniques, the analysis of such samples should be quite feasible without the introduction of a chemical separation, such as solvent extraction, before the flameless atomization.

It should also be pointed out that although small sample volumes (in the order of μl) cannot be analyzed directly by the present technique, a dilution of the sample to a more suitable volume (5–10 ml) should be quite acceptable in many cases, owing to the high sensitivity of the method.

The technique is of course not restricted to the determination of cadmium. Work is in progress for the determination of other heavy metals, such as mercury, lead and copper. The application of the technique to the analysis of sea water for heavy metals is also under investigation.

We are grateful to cand. real. Ingvar Dahl and the National Institute of Public Health for the use of their atomic absorption instrument, and to siv. ing. Sverre Grimnes and cand. real. Nils Gundersen for valuable discussions.

SUMMARY

The use of controlled-potential electrolysis as a separation and preconcentration technique for metal wire flameless atomic absorption analysis has been studied. The metal to be determined is electrolyzed onto a thin tungsten wire, and then atomized by electrical heating of the filament in an inert atmosphere within an absorption cell. A detailed study of the effect of various experimental parameters on the determination of cadmium is presented. The detection limit was found to be 0.1 p.p.b. cadmium, for a 2-min electrolysis period. The absolute detection limit was $4 \cdot 10^{-11}$ g. The method appears to be well suited for the determination of cadmium in samples with a complex matrix.

REFERENCES

1 H. Brandenberger and H. Bader, *Helv. Chim. Acta*, 50 (1967) 1409.
2 M. J. Fishman, *Anal. Chem.*, 42 (1970) 1462.
3 J. Y. Hwang, P. A. Ullucci, S. B. Smith and A. L. Malenfant, *Anal. Chem.*, 43 (1971) 1319.
4 J. Y. Hwang, C. J. Mokeler and P. A. Ullucci, *Anal. Chem.*, 44 (1972) 2018.
5 T. Takeuchi, M. Yanagisawa and M. Suzuki, *Talanta*, 19 (1972) 465.
6 T. Maruta and T. Takeuchi, *Anal. Chim. Acta*, 62 (1972) 253.
7 T. Maruta and T. Takeuchi, *Anal. Chim. Acta*, 66 (1973) 5.
8 M. Williams and E. H. Piepmeier, *Anal. Chem.*, 44 (1972) 1342.
9 M. P. Newton, J. V. Chauvin and D. G. Davis, *Anal. Lett.*, 6 (1973) 89.
10 J. V. Chauvin, M. P. Newton and D. G. Davis, *Anal. Chim. Acta*, 65 (1973) 291.
11 M. P. Bratzel, Jr., R. M. Dagnall and J. D. Winefordner, *Anal. Chim. Acta*, 48 (1969) 197.
12 M. P. Bratzel, Jr., R. M. Dagnall and J. D. Winefordner, *Appl. Spectrosc.*, 24 (1970) 518.
13 J. W. Winefordner, *Pure Appl. Chem.*, 23 (1970) 35.
14 D. Clark, R. M. Dagnall and T. S. West, *Anal. Chim. Acta*, 63 (1973) 11.

15 H. Brandenberger, *Chimia*, 22 (1968) 449.
16 C. Fairless and A. J. Bard, *Anal. Lett.*, 5 (1972) 433.
17 P. Ruetschi and P. Delahay, *J. Chem. Phys.*, 23 (1955) 195.
18 B. V. L'vov, *Spectrochim. Acta*, 24B (1969) 53.
19 Perkin-Elmer, HGA Method book.

Analytica Chimica Acta, 70 (1974) 311–317

ISOCEIN—A NEW FLUORESCENT REAGENT FOR CALCIUM

GERALDINE M. HUITINK

Department of Chemistry, Indiana University at South Bend, Indiana 46615 (U.S.A.)

(Received 6th September 1973)

Metal ion indicators composed of a chromophore and half an EDTA molecule were first studied by Schwarzenbach *et al.*[1–3]. Subsequent variations on these studies led to combination of an assortment of fluorophores with half an EDTA molecule, the resulting metallofluorescent indicators proving more sensitive to metal ions than metallochromic indicators. Calcein, a Mannich condensation product of fluorescein, formaldehyde and iminodiacetic acid, is such a fluorescent metal ion indicator[4,5]. Another is calcein blue, a benzo-α-pyrone, which, because it is excited by light near the principal emission line of the mercury vapor lamp, has been deemed superior to calcein.[6].

Determinations of calcium in the presence of magnesium with metallofluorescent indicators are performed at pH 13 and higher. In this pH range the indicators do not fluoresce, but the calcium–indicator compounds are fluorescent and magnesium, present as the hydroxide, does not interfere. Unfortunately, benzo-α-pyrones undergo ring opening in solutions of high alkalinity and the higher the pH the faster the rate of ring opening. A direct result of ring opening is loss of indicator activity.

Taking advantage of the reduced susceptibility to ring opening exhibited by benzo-γ-pyrones, Scheppers[7] prepared methyleneiminodiacetic acid derivatives of 2-methyl-7-hydroxychromone, 7-hydroxyflavone and 4'-methoxy-7-hydroxyflavone. The compounds are more stable in alkaline solution than calcein blue but their calcium complexes proved to be weakly fluorescent. In general benzo-γ-pyrones are less fluorescent in alkaline solution than benzo-α-pyrones. A benzo-α-pyrone that exhibits relatively high fluorescence in alkaline solution is 2-methyl-7-hydroxyisoflavone[8]. Its methyleneiminodiacetic acid derivative, henceforth termed isocein, has an excitation maximum at 339 nm in alkaline solution, satisfactory stability, and good sensitivity to calcium.

EXPERIMENTAL

Reagents

7-Hydroxy-2-methylisoflavone was prepared by the method of Baker and Robinson[9]. (M.p. 253–255.5°; reported 240°C)

Iminodiacetic acid was prepared from disodium iminodiacetate monohydrate (Eastman Organic Chemicals).

Versatrol serum calibration references were used (General Diagnostics Division, Warner–Chilcott Laboratories).

Isocein stock solution, $3.11 \cdot 10^{-3}$ *M*, was prepared by mechanically shaking its aqueous suspension and adding the minimal amount of potassium hydroxide needed for dissolution.

Stock solutions of magnesium nitrate, calcium nitrate, strontium nitrate and barium nitrate prepared from reagent-grade chemicals were standardized against EDTA and were $3.0 \cdot 10^{-3}$ *M*, $3.2 \cdot 10^{-3}$ *M*, $3.3 \cdot 10^{-3}$ *M*, and $3.3 \cdot 10^{-3}$ *M*, respectively.

All reagent chemicals used were of reagent-grade quality.

All water was distilled and deionized by passage through Amberlite MB-1 ion-exchange resin.

Apparatus

Measurements of pH were made with a Corning Model 10 pH meter. equipped with a Corning No. 476022 glass electrode and a Corning No. 476002 fiber type calo mel electrode.

Fluorescence spectra were obtained on an Aminco–Keirs spectrophosphorimeter that had been converted to a spectrofluorimeter. The slit widths used were in order: excitation monochromator $\frac{1}{8}$, $\frac{1}{16}$, and $\frac{1}{8}$ in.; emission monochromator $\frac{1}{8}$, $\frac{1}{16}$, $\frac{1}{8}$, and $\frac{1}{16}$ in. A 1-cm quartz cell was used. Spectra were recorded on an Aminco XY recorder and are uncorrected for variations in the emission characteristics of the lamp and response characteristics of the photomultiplier.

A G.K. Turner Associates Model 10 fluorimeter (primary filter, 7–60; secondary filters, Wratten 2A plus a 1% neutral density filter) was used for routine fluorescence readings and for fluorescence *versus* time studies.

A Micrometric Model SB2 microburet and Model S5Y syringes were used to deliver appropriate volumes of reagent stock solutions for fluorescence work.

Synthesis of isocein

To 50 ml of deionized water containing 0.06 mole (3.36 g) of potassium hydroxide, were added 0.03 mole (3.99 g) of iminodiacetic acid, 0.03 mole (7.58 g) of 7-hydroxy-2-methylisoflavone and 0.045 mole (4.44 ml) of 37% formaldehyde solution. The reaction was allowed to proceed for 10 h at 60–65°C with mechanical stirring. After cooling to room temperature, the reaction mixture was filtered and the pH of the filtrate was adjusted to 4 by dropwise addition of dilute hydrochloric acid (1 + 3). The resulting gelatinous material was filtered through a sintered glass funnel of medium porosity. The filtrate was evaporated to about 3 ml and 200 ml of acetone subsequently added. After 5 h a white residue was isolated by filtration. This was dissolved in water by adding potassium hydroxide. The solution was filtered and the material recrystallized by adjusting the pH of the filtrate to 3 by dropwise addition of dilute hydrochloric acid. The precipitate was filtered, washed with acetone and recrystallized twice in the same manner. The product melts at 179–181°C with decomposition. Neutralization equivalent found: 208.0. Analysis (Spang Microanalytical Laboratory): found 60.3% C, 5.2% H, 3.1% N; $C_{21}H_{19}NO_7 \cdot H_2O$, eq. wt. 207.7, requires 60.2% C, 5.1% H, 3.4% N.

Potentiometric titration

The neutralization equivalent of isocein was obtained by adding 0.0779 g

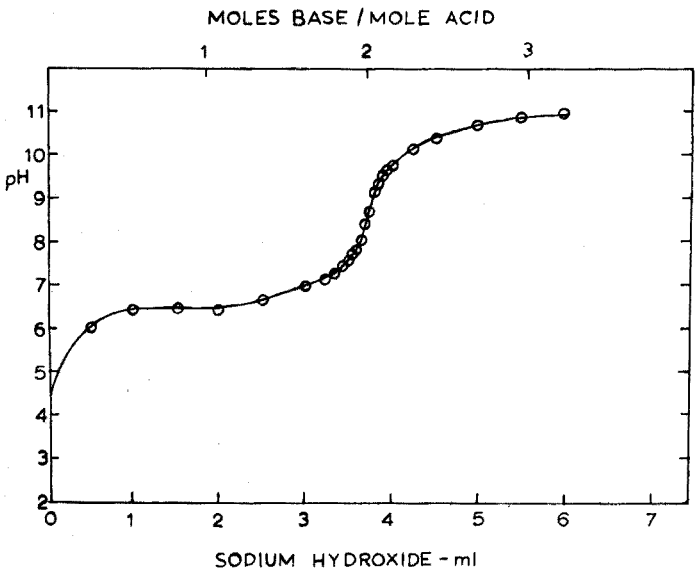

Fig. 1. Titration of isocein with sodium hydroxide. Solvent, 0.1 *M* potassium nitrate; sodium hydroxide, 0.1008 *M* in 0.1 *M* potassium nitrate; sample, 0.0779 g.

of the compound to 75 ml of 0.1 *M* potassium nitrate and titrating with 0.1008 *M* sodium hydroxide. The titration curve obtained is shown in Fig. 1.

Effect of pH on fluorescence

Fluorescence excitation and emission spectra of isocein were obtained at 0.5 pH unit intervals ranging from 3 to 13. Solutions on which spectra were run contained 15 μl of $1.46 \cdot 10^{-2}$ *M* EDTA to sequester any metal ions present and 5 ml of buffer solution. Just before the spectra were recorded, 50 μl of isocein was added and the volume adjusted to 25 ml by addition of 0.1 *M* potassium nitrate. The pH was checked after the spectra were recorded. Fluorescence excitation and emission spectra of isocein at pH 4 and 8.5 are shown in Fig. 2. The relative fluorescence of each of the buffered solutions, measured at the excitation and emission maxima found at pH 4 and 8.5, was plotted against the pH of that solution (Fig. 3).

Effect of alkaline earths on fluorescence

The effect of magnesium, calcium, strontium and barium on the fluorescence of isocein was studied by measuring the relative fluorescence of solutions containing the alkaline earth–isocein compounds at pH values ranging from 7 to 13 (Fig. 3). Solutions were prepared as described above, adding 125 μl of metal ion stock solution.

Fluorescence intensity of calcium–isocein as a function of time

Variation in the relative fluorescence of solutions of the calcium–isocein compound in 0.8 *M* potassium hydroxide (30 μl of 1.46×10^{-2} *M* EDTA, 500 μl

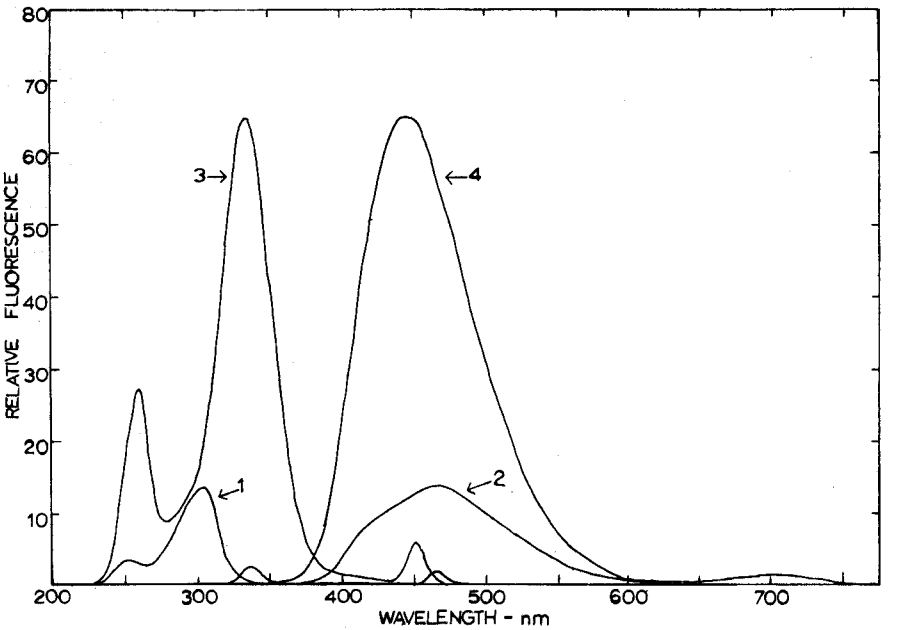

Fig. 2. Fluorescence spectra of isocein. (1) Excitation, emission monochromator set at 470 nm, pH 4; (2) emission, excitation monochromator set at 302 nm, pH 4; (3) excitation, emission monochromator set at 441 nm, pH 8.5; (4) emission, excitation monochromator set at 339 nm, pH 8.5.

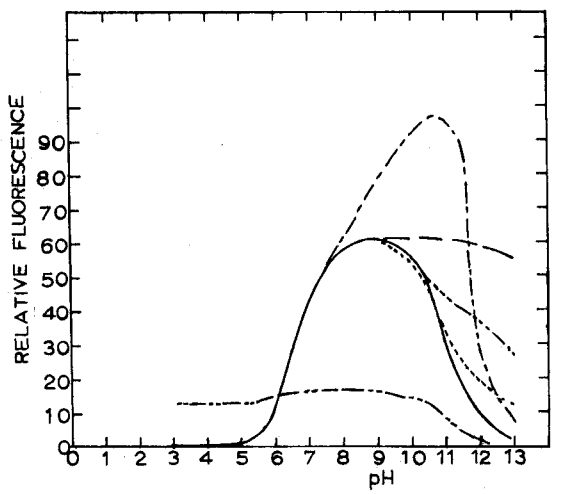

Fig. 3. Variation in intensity of fluorescence of isocein and its magnesium, calcium, strontium and barium derivatives with pH. (——) Free indicator, excitation 302 nm; (——) free indicator, excitation 339 nm; (——) magnesium derivative, excitation 339 nm; (——) calcium derivative, excitation 339 nm; (——) strontium derivative, excitation 339 nm; (------) barium derivative, excitation 339 nm.

of calcium stock solution and 190 μl of isocein stock solution in 50 ml of 0.8 *M* potassium hydroxide) was determined as a function of time. In one study the fluorescence of a continuously irradiated solution as monitored. In the other study the fluorescence of portions of a solution stored in the dark was measured at various times.

Determination of calcium in blood serum

Calibration curves for the spectrofluorimetric determination of serum calcium were prepared by measuring the relative fluorescence of solutions containing 100 μl of a Versatrol serum calibration reference in 25 ml of 0.8 *M* potassium hydroxide that was also $2.8 \cdot 10^{-5}$ *M* in isocein and contained sufficient EDTA to sequester metal ions present in the potassium hydroxide. Analysis of blood serum was performed by measuring the fluorescence of solutions prepared in the same manner but substituting 100 μl of serum for the calibration reference. After mixing, the solutions were allowed to stand for at least 20 min before the fluorescence was measured. Fluorescence readings were taken 15 s after samples had been placed in the fluorimeter.

RESULTS AND DISCUSSION

Synthesis of isocein is straightforward. A pure product consisting of one molecule of 7-hydroxy-2-methylisoflavone, one methyleneiminodiacetic acid group and one molecule of water is obtained from the Mannich condensation. This was verified by elemental analysis, by potentiometric titration data exhibiting one break at the point corresponding to 2 moles of base added per mole of isocein, and by examination of the fluorescence emission spectrum which remains unchanged upon excitation of isocein with light of different wavelengths[10]. In keeping with substitution patterns exhibited by coumarins[11], chromones and isoflavones[7,12] the methyleneiminodiacetic acid group is assigned to position 8.

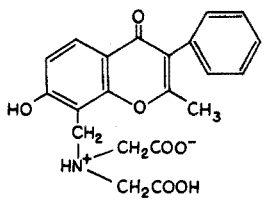

Isocein, like other amino acids, exists as a zwitterion in aqueous solution. As the pH is raised first the carboxylic acid proton, next the phenolic proton, and then the imino proton is neutralized. Complete dissolution of the material does not occur until the pH reaches about 6.7, *i.e.*, before the break in the titration curve corresponding to neutralization of the phenolic proton.

Fluorescence studies showed that below pH 6 isocein is excited primarily by light of 302 nm and emits light of 470 nm. These wavelengths shift, as the pH is increased, to 339 and 441 nm, respectively. The shift in the excitation maximum from shorter to longer wavelength is attributed to neutralization of the ground state phenolic proton. Fluorescence emission at 441 nm is attributed to the

phenolate form of isocein and is approximately five times as intense as the emission at 470 nm which is attributed to the tautomerized form of the excited state phenol.

A plot of relative fluorescence *versus* pH when isocein was excited by light of 339 nm contained an inflection point at pH 6.4. Fluorescence continued to increase as pH was raised above 6.4, reached a maximum at pH 8.9 and then decreased. This decrease corresponds to neutralization of the imino proton. At pH 13 isocein was virtually non-fluorescent; however, addition of alkaline earths restored, to varying degrees, the fluorescence of isocein (Fig. 3). Magnesium, present as undissociated magnesium hydroxide, exerted only a minimal effect on fluorescence at pH 13. Barium caused a slight increase in fluorescence, strontium restored approximately half the fluorescence that the free indicator exhibited at pH 8.9 and calcium, to the largest extent, restored the fluorescence of the indicator.

The stoichiometry of the calcium–isocein compound, as determined by the method of continuous variations in 0.8 *M* potassium hydroxide, is 1.09 calcium:1 isocein, or 1:1. This compound is a great deal more stable in alkaline solution than the calcium–calcein blue compound which loses half of its fluorescence intensity in 37 min[13]. A constantly irradiated solution of calcium–isocein in 0.8 *M* potassium hydroxide showed its greatest fluorescence decrease during the first 10 min; the fluorescence loss was less dramatic after this. Solutions of calcium–isocein in 0.8 *M* potassium hydroxide irradiated only long enough to take a fluorescence reading and otherwise stored in the dark, also showed a decrease in relative fluorescence, the time required for half the fluorescence to be lost being 24 h. Products of this decomposition are a deoxybenzoin and formaldehyde[14].

TABLE I

FLUORIMETRIC DETERMINATION OF CALCIUM IN BLOOD SERUM

Sample	*Calcium (mg/100 ml)*	
	Present method	*Clinical results*[a]
1	9.6±0.1	9.6
2	10.0±0.1	10.0
3	10.2±0.2	10.3
4	9.9±0.1	9.7
5	9.6±0.2	9.5

[a] Clinical results were obtained by atomic absorption at the South Bend Medical Foundation.

Table I lists results of determinations of serum calcium. All results obtained fluorimetrically with isocein are reported for a minimum of three determinations per sample and precision is reported as standard deviation. The results agree with those obtained by atomic absorption analysis and verify the efficacy of this indicator. Because the Versatrols used for preparing the calibration curve contained varying amounts of constituents found in blood serum including magnesium, inorganic phosphorus, and protein, it can be concluded that these substances do not interfere in this analysis. Frothing occurs when the solutions are shaken

and it is necessary to wait for about 20 min after mixing, before a fluorescence reading can be taken. Calibration curves should be prepared daily, because of decomposition of isocein in alkaline solution.

Support for this research was obtained from the Indiana University Foundation in the form of Summer Faculty Fellowships and Grant-in-Aid of Research funds. The author thanks Dr. H. Diehl, Iowa State University, and Dr. N. Mhatre, Ames Company Division of Miles Laboratories, for making instruments available for this work. She also thanks Miss M. Winsted, South Bend Medical Foundation, for providing analyzed blood serum.

SUMMARY

A metallofluorescent indicator, isocein, has been synthesized from 7-hydroxy-2-methylisoflavone, iminodiacetic acid and formaldehyde. It is readily obtained in pure form and in alkaline solutions is excited by light of 339 nm. It is recommended for use as a spectrofluorimetric reagent for calcium.

REFERENCES

1 G. Schwarzenbach, G. Anderegg and R. Sallmann, *Helv. Chim. Acta*, 35 (1952) 1785.
2 G. Schwarzenbach, G. Anderegg and R. Sallmann, *Helv. Chim. Acta*, 35 (1952) 1794.
3 G. Anderegg, H. Flaschka, R. Sallmann and G. Schwarzenbach, *Helv. Chim. Acta*, 37 (1954) 113.
4 H. Diehl and J. L. Ellingboe, *Anal. Chem.*, 28 (1956) 882.
5 B. M. Tucker, *Analyst*, 82 (1957) 284.
6 D. H. Wilkins, *Talanta*, 4 (1960) 182.
7 G. J. Scheppers, Ph.D. dissertation, Iowa State University, 1967.
8 S. Rangaswami and T. R. Seshadri, *Proc. Indian Acad. Sci., Sect. A*, 12 (1940) 375.
9 W. Baker and R. Robinson, *J. Chem. Soc.*, 1925 (1925) 1981.
10 I. B. Berlman, *Handbook of Fluorescence Spectra of Aromatic Molecules*, Academic Press, New York, 1965, p. 18.
11 G. M. Huitink, Ph.D. dissertation, Iowa State University, 1967.
12 D. V. Joshi, J. R. Merchant and R. C. Shah, *J. Org. Chem.*, 21 (1956) 1104.
13 J. H. Eggers, *Talanta*, 4 (1960) 38.
14 in T. A. Geissman (Ed.), *The Chemistry of Flavonoid Compounds*, Macmillan, New York, 1960, p. 94.

Analytica Chimica Acta, 70 (1974) 319–326

SPECTROPHOTOMETRIC DETERMINATION OF COBALT(II) WITH 2,2′-DIPYRIDYL-2-PYRIDYLHYDRAZONE

G. S. VASILIKIOTIS, Th. KOUIMTZIS, C. APOSTOLOPOULOU and A. VOULGAROPOULOS
Laboratory of Analytical Chemistry, University of Thessaloniki, Thessaloniki (Greece)
(Received 12th November 1973)

In recent years, many nitrogen-containing heterocyclic hydrazones, derived from 2-pyridylhydrazine, have been prepared and tested as possible analytical reagents. Lions *et al.*[1,2] first reported the analytical properties of these compounds.

An evaluation of some similar substituted hydrazones, as analytical reagents, has been given by Zatka *et al.*[3]. Going and Pflaum[4] described the synthesis of 2-benzoylpyridine-2-pyridylhydrazone and introduced it as a useful and extremely sensitive reagent for certain cations. Later, Pflaum and Tucker[5] proposed benzil-(2-pyridyl)hydrazone for determination of cobalt in selected samples.

In a continuation of studies in this laboratory on hydrazones as analytical reagents, Vasilikiotis and Alexaki[6,7] synthesized a new compound, 2,2′-dipyridyl-2-pyridylhydrazone(DPPH, I), which is a very sensitive reagent for zinc(II), palladium(II), copper(II) and vanadium(V). This reagent also forms intensely coloured complexes with a number of other cations. A detailed study of these reactions has been undertaken for possible analytical application.

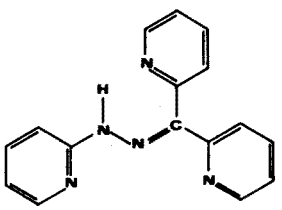

I

In the work presented here, the analytical properties of the Co–DPPH complex were studied. It was found that this reagent is very sensitive and selective for the spectrophotometric determination of cobalt(II). It seems to be unique in the sense that it is suitable for the microdetermination of cobalt(II) ions in the presence of large quantities of other ions.

In aqueous solutions of pH 2–11, DPPH reacts instantly with cobalt(II) to form an orange-yellow coloured complex. This complex is water-soluble and by adding a strong acid (perchloric acid), the colour changes from orange-yellow to pink. This new complex is stable even in the presence of 30 or 50% of perchloric acid, while in this strongly acidic medium other transition metal–DPPH complexes are decomposed. In 20% perchloric acid solution, the Co–DPPH complex shows

maximal absorption at 500 nm with a molar absorptivity of $4.2 \cdot 10^4$ l mol^{-1} cm^{-1}. Beer's law is obeyed over the range 0.15–2.00 μg Co ml^{-1}. By utilizing these properties, a selective and accurate determination of cobalt(II) has been developed.

EXPERIMENTAL

Reagents

2,2'-Dipyridyl-2-pyridylhydrazone. DPPH was prepared by refluxing equimolar quantities of 2-pyridylhydrazine with di-(2-pyridyl)-ketone in ethanolic solutions[6]. Both compounds were commercial products (Aldrich Chemical Co. Inc.). The crude product was purified by recrystallization from ethanol. The purity was checked by m.p. (138°C) and by t.l.c. on silica gel G (Merck, Darmstadt).

Solutions of DPPH were prepared by dissolving the required weight in ethanol. The ethanolic solution was stable and could be kept for several weeks in an amber glass bottle.

Standard cobalt solution. Standard solutions of cobalt(II) were prepared by dissolving the appropriate amount of cobalt(II) perchlorate (K and K Laboratories, U.S.A.) in doubly distilled water. The solutions obtained were standardized by EDTA titration.

All other solutions of cations and anions were prepared by dissolving analytical-reagent grade chemicals in doubly distilled water.

Ethanol and perchloric acid (70%) were AnalaR reagents (B.D.H.).

Apparatus

Absorbance measurements were made in 10-mm quartz cells with a Zeiss M4QII spectrophotometer. pH measurements were performed with a Pusl ACL-112 pH meter, calibrated by NBS pH standards at 25 ± 0.5°C.

Recommended procedure

Take 2–5 ml of the sample solution, which should contain 5–50 μg of cobalt. Adjust the pH to 3–8, by using dilute solutions of ammonium hydroxide or perchloric acid. Transfer the solution to a 25-ml volumetric flask, add 2 ml of an ethanolic 10^{-2} *M* solution of DPPH reagent and mix well. Add 5 ml of perchloric acid (70%) and dilute to volume with doubly distilled water. Measure the absorbance of the complex at 500 nm against a reagent blank. From the standard graph, calculate the amount of cobalt in the unknown sample.

If palladium(II) is present, heat the solution for 20 min at 80°C or add 10 ml of perchloric acid instead of 5 ml and allow the solution to stand for 20 min at room temperature.

If copper(II), iron(III) or nickel(II) is present in a concentration of 100-fold over cobalt, add an increased amount of DPPH, *e.g.* 4 ml of an ethanolic 10^{-1} *M* solution.

RESULTS AND DISCUSSION

Absorption spectra

Absorption spectra of DPPH at different pH values (0.2–12.8) have been

reported previously[6]. This reagent exists as a neutral molecule at pH 7.0–11.8, while at lower pH values (4.0–5.5) it is protonated by one hydrogen ion, and below pH 2.5 by two hydrogen ions. Above pH 12, diprotonation of the hydrazone nitrogen atom proximal to the pyridine ring takes place[3,6]. A representative absorption spectrum of DPPH, at a concentration of $1.0 \cdot 10^{-5}$ *M*, in 20% perchloric acid medium, is shown as curve (1) of Fig. 1. The absorption spectra of solutions of the cobalt–DPPH complex at pH 5 and in 20% perchloric acid, are also shown in Fig. 1, as curves (2) and (3), respectively. In both cases, the final concentrations of cobalt(II) and DPPH were $1.0 \cdot 10^{-5}$ *M* and $1.0 \cdot 10^{-4}$ *M*, *i.e.* a 10-fold excess of reagent was used.

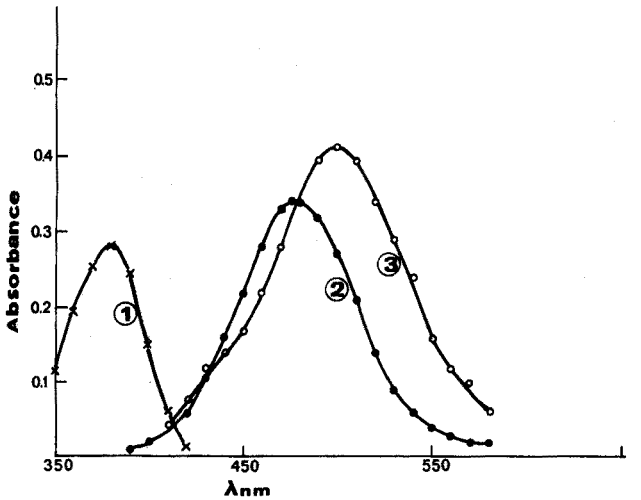

Fig. 1. Absorption spectra. (1) DPPH, $1.0 \cdot 10^{-5}$ *M*, in 20% of perchloric acid. (2) Co–DPPH complex, $1.0 \cdot 10^{-5}$ *M* Co and $1.0 \cdot 10^{-4}$ *M* DPPH at pH 5. (3) Co-DPPH complex (concentrations as for 2) in 20% perchloric acid.

By comparison of the two absorption spectra of the cobalt–DPPH complex, it can be seen that on adding a strong acid (perchloric acid) to the originally formed complex, the wavelength of maximal absorption is increased from 480 nm to 500 nm. The same results were obtained with hydrochloric acid and sulfuric acid. The system is reversible and can be represented as follows.

$$\text{Orange-yellow complex} \underset{OH^-}{\overset{H^+}{\rightleftharpoons}} \text{pink complex.}$$

The reagent itself does not absorb at the wavelength of maximal absorption of its cobalt complex in either case. This is advantageous because the excess of reagent is not critical and a blank is necessary only to check the purity of the reagents used to adjust the conditions for the reaction. The colour intensity of the complex, in both cases, was stable over a measured period of 24 h.

Effect of acidity

A pH study was carried out over the pH range 2–11. The results indicated that the formation reaction is independent of pH in this range, and the maximal

absorbance shows no shift between pH 3 and 10. Since the complex is kinetically stable to protons, it can be used for a specific determination of cobalt, as the reaction of DPPH with other transition metal cations is pH-dependent. Most of these complexes are destroyed by the addition of a strong acid, because of the protonation of the ligand.

The maximal absorbance of the cobalt–DPPH complex shows a bathochromic shift on the addition of a strong acid and then remains stable even in the presence of 30 or 50% of perchloric acid. This shift, from 480 nm to 500 nm is probably due to a characteristic protonation of the complex with a simultaneous redistribution of electrons.

The spectral similarity of the transition metal complexes at higher pH values has been explained by the deprotonation of the imino-hydrogen of the ligand molecule[3]. This deprotonation and redistribution of the previously shared electron pair gives rise to a new stable resonating system between the separated heterocyclic π-systems, which is, in some way, independent of the chelated cation.

In the case of the cobalt–DPPH complex, probably an oxidation of Co(II) to Co(III) occurs, and then the cobalt(III) complex once formed, remains inert to the hydrogen ion concentration.

The absorbance of the pink complex, measured at 500 nm, remains constant in media containing 20%–30% of perchloric acid, and decreases only very gradually in the ranges 30–50% and 20–5% of perchloric acid. In subsequent work on the determination of cobalt, solutions containing 20% of perchloric acid were used. At this concentration of acid, the transition metal complexes are completely destroyed and do not interfere, hence any further increase in the concentration of the acid is futile (unless palladium is present, see below).

Reaction conditions and Beer's law

The formation of the cobalt–DPPH complex takes place only in the pH range 2–11. If the reagent is added to a highly acidic medium of cobalt ions or vice versa, then no reaction is observed, probably because of strong protonation of the reagent molecule, which does not allow the formation of the complex.

Maximal colour development takes place immediately at room temperature.

Beer's law is obeyed at pH 5 in the range 0.25–3.75 p.p.m. of cobalt. The Sandell sensitivity index for this case is 0.0018 $\mu g\ cm^{-2}$ and the molar absorptivity is $3.2 \cdot 10^4\ l\ mol^{-1}\ cm^{-1}$ at 480 nm.

In 20% perchloric acid media, Beer's law is obeyed from 0.15 to 2.00 p.p.m. of cobalt. The Sandell sensitivity index for this medium is 0.0014 $\mu g\ cm^{-2}$ and the molar absorptivity is $4.2 \cdot 10^4\ l\ mol^{-1}\ cm^{-1}$ at 500 nm. In both cases the calibration plots are straight lines, passing through the origin.

Composition of the complex

The composition of the coloured complexes at pH 5 and in a 20% solution of perchloric acid was determined by Job's method of continuous variations and the mole ratio method. Job plots obtained from measurement at 480 and 500 nm, respectively, are shown in Fig. 2. The mole ratio method applied for both complexes (Fig. 3) confirmed that both at pH 5 and in 20% perchloric acid medium, the ratio of metal ions to ligand molecules is 1:2.

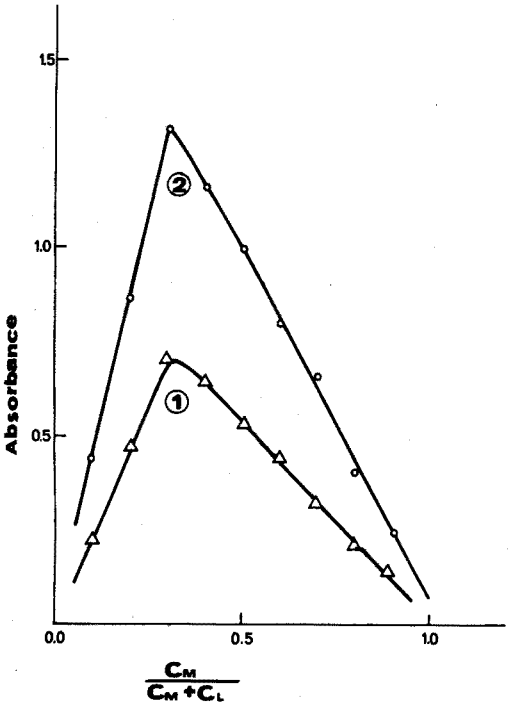

Fig. 2. Determination of the composition of the complex formed between cobalt(II) and DPPH by Job's continuous variations method. C_M, concentration of cobalt(II). C_L, concentration of DPPH. $C_M + C_L = 1.0 \cdot 10^{-4}$ *M*. Curve (1) at pH 5 and 480 nm, curve (2) in 20% perchloric acid at 500 nm.

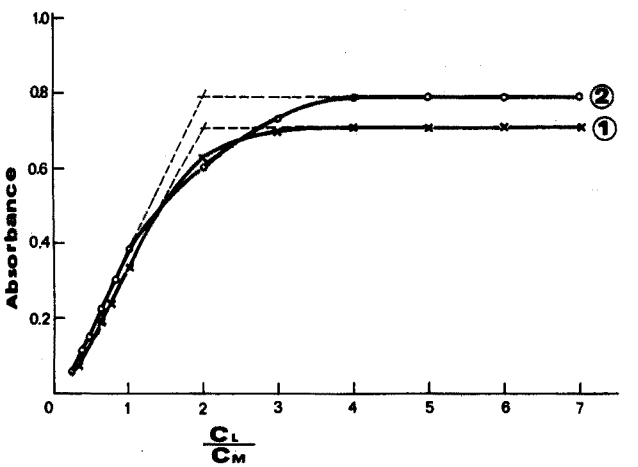

Fig. 3. Mole ratio method for the determination of the cobalt–DPPH complex composition. C_M, $2.0 \cdot 10^{-5}$ *M*. Curve (1) at pH 5 and 480 nm; curve (2) in 20% perchloric acid at 500 nm.

Effect of diverse ions

Various ions were tested for possible interference. The criterion for significant interference was taken to be a $\pm 2\%$ difference in absorbance from that found with

cobalt ions alone (measured at 500 nm in 20% perchloric acid media).

Of the tested ions, zinc(II), cadmium(II), lead(II), manganese(II), silver(I), mercury(II), chromium(III), aluminium(III), indium(III), gallium(III), sodium, potassium, calcium, strontium and barium did not interfere even at a high ratio of 1:500. Ions such as nickel(II), iron(III) and copper(II) did not interfere up to a ratio of 1:100. When greater than 100-fold concentrations were present, an increased excess of the reagent was added to eliminate their interference. This type of interference is due to complex formation of these ions with the reagent, so that the reagent is consumed, leaving unreacted cobalt ions. Otherwise, these complexes are labile in highly acidic medium and do not interfere.

An increased amount of reagent in the sample solution does not interfere as the reagent does not absorb at the analytical wavelength of 500 nm. The use of DPPH thus offers a considerable advantage over the group of nitrosonaphthol ligands.

In the presence of palladium(II), there was some interference, as the palladium–DPPH complex is almost stable in 20% perchloric acid medium. To eliminate this interference, either the solution must be heated for 20 min at 80°C, or the concentration of perchloric acid must be increased to 50% and the solution allowed to stand for 20 min at room temperature. In both ways, the palladium–DPPH complex can be destroyed while the corresponding cobalt complex remains stable.

When iron(II) was present, interference was caused by the formation of the stable iron(II)–DPPH complex. This interference can be eliminated either by heating the solution for 20 min at 80°C, or even better, by oxidizing iron(II) to iron(III) before the reagent addition.

Common anions like fluoride, chloride, bromide, sulphate, nitrate, acetate, oxalate, citrate and tartrate did not interfere.

Typical results for cobalt(II) in the presence of other cations are shown in Table I.

TABLE I

DETERMINATION OF COBALT

Co taken (p.p.m.)	*Cation present (p.p.m.)*	*Co found (p.p.m.)*	*Co taken (p.p.m.)*	*Cation present (p.p.m.)*	*Co found (p.p.m.)*
0.59	Ni(II) 100	0.58	0.59	Fe(III) 100	0.61
1.18	Ni(II) 200	1.17	1.18	Fe(III) 200	1.20
0.59	Cu(II) 100	0.60	0.59	Fe(II) 100	0.62
1.18	Cu(II) 200	1.20	1.18	Fe(II) 200	1.21
0.59	Zn(II) 100	0.59	0.59	Pd(II) 100	0.61
1.18	Zn(II) 200	1.17	1.18	Pd(II) 200	1.22

Comparison with some other reagents

Table II presents a comparison of the most sensitive reagents for the spectrophotometric determination of cobalt. The use of DPPH as a reagent for cobalt compares favourably in respect of sensitivity and selectivity with these reagents. It

TABLE II

COMPARISON WITH SOME OTHER REAGENTS FOR COBALT

Reagent	*Complex with cobalt(II)*		*Ref.*
	λ_{max} *(nm)*	*($10^3 \cdot l\ mol^{-1}\ cm^{-1}$)*	
Thiocyanate (isoamyl alcohol)	620	1.0	8
Thiocyanate (cyclohexane)	620	20.0	9
Nitroso R salt	520	15.0	9
Nitroso R salt	420	31.0	8
2-Nitroso-1-naphthol($CHCl_3$)	530	15.0	8
1-Nitroso-2-naphthol($CHCl_3$)	317	26.5	8
BPPH (50% ethanol, pH 4–12)	478	29.3	4
PAQH (50% ethanol, pH 3.0)	480	30.0	10
DPPH (pH 3.0–11.0)	480	32.0	Present work
DPPH (20% $HClO_4$)	500	42.0	Present work

is the most sensitive and highly selective reagent. The spectrophotometric determination can be carried out over a wide pH range, between 3 and 11, if there are no interfering elements or in strongly acidic medium without any prior separation. There is no need for extraction, the reaction takes place immediately and both reagent and complex are stable for a long period of time. Large amounts of reagent do not interfere, which is an advantage over the nitrosonaphthol reagents. The high molecular absorptivity of the complex allows the accurate determination of cobalt in the range 0.15–2.00 p.p.m.

SUMMARY

A spectrophotometric study of the cobalt(II) complex of a new reagent, 2,2′-dipyridyl-2-pyridylhydrazone (DPPH) is presented. A water-soluble yellow-orange complex is formed in the pH range 3–11, and shows maximal absorbance at 480 nm with a molar absorptivity of $3.2 \cdot 10^4$ l mol^{-1} cm^{-1}; Beer's law is obeyed over the range 0.25–3.75 p.p.m. of cobalt. This complex is very stable and on addition of perchloric acid only a bathochromic shift takes place from 480 nm to 500 nm. This complex is stable even in the presence of 20% perchloric acid and shows a molar absorptivity of $4.2 \cdot 10^4$ l mol^{-1} cm^{-1}; Beer's law is obeyed over the range 0.15–2.00 p.p.m. of cobalt. A new method of determining trace amounts of cobalt is proposed, which possesses the advantages of high sensitivity and very high selectivity.

REFERENCES

1 F. Lions and K. V. Martin, *J. Amer. Chem. Soc.*, 80 (1958) 3858.
2 J. F. Geldard and F. Lions, *J. Amer. Chem. Soc.*, 84 (1962) 2262; *Inorg. Chem.*, 2 (1963) 270; 4 (1965) 414.
3 V. Zatka, J. Abraham, J. Holzbecher and D. E. Ryan, *Anal. Chim. Acta*, 54 (1971) 65.
4 J. E. Going and R. T. Pflaum, *Anal. Chem.*, 42 (1970) 1098.

5 R. T. Pflaum and E. S. Tucker, *Anal. Chem.*, 43 (1971) 458.
6 G. Vasilikiotis and H. Alexaki-Tzivanidou, in press.
7 H. Alexaki-Tzivanidou, Doctoral Thesis, University of Thessaloniki, May 1972.
8 E. B. Sandell, *Colorimetric Determination of Traces of Metals*, Interscience, New York, 3rd edn., 1965, p. 414.
9 G. Charlot, *Colorimetric Determinations of Elements*, Elsevier, London, 1964, p. 232.
10 S. R. Singal and D. Ryan, *Anal. Chim. Acta*, 37 (1967) 91.

Analytica Chimica Acta, 70 (1974) 327–339

NOUVELLE MÉTHODE DE DOSAGE PHOTOMÉTRIQUE AUTOMATIQUE DES PROTÉINES DANS LE LAIT ENTIER

PARTIE I. BASES THÉORIQUES ET OPTIMISATION DES PRINCIPAUX PARAMÈTRES DE LA RÉACTION

J. BOSSET et B. BLANC

Station fédérale de recherches laitières, 3097 Liebefeld-Bern (Suisse)

E. PLATTNER

Institut de génie chimique de l'Ecole Polytechnique Fédérale de Lausanne, 1025-Lausanne (Suisse)

(Reçu le 15 novembre 1973)

D'une étude récente et bien documentée[1] tendant à faire le point des méthodes les plus couramment utilisées pour déterminer la teneur en protéines du lait entier frais, il s'avère que l'une des méthodes les plus avantageuses, celle dite "du biuret", n'a pas trouvé en chimie laitière le développement et l'emploi généralisé qu'elle a rencontré dans un domaine voisin, la chimie clinique[2]. Malgré sa grande simplicité (méthode colorimétrique directe ne nécessitant dans son principe ni séparation préalable — *cf.* méthodes au dye-binding — telle que dialyse, filtration ou centrifugation, ni minéralisation), sa sensibilité (quelques μl suffisent), sa relativement bonne spécificité (la réaction fait intervenir les ponts peptidiques, éléments constitutifs par excellence des chaînes protéiniques), son excellente reproductibilité, sa stabilité (quelques $^0/_{00}$ de dérive/h), cette méthode analytique a été jusqu'ici presque complètement délaissée au profit d'autres méthodes[1] bien plus compliquées et laborieuses. Cette situation a vraisemblablement pour origine les deux causes principales suivantes:

la méthode du biuret n'est pas utilisable, sous sa forme habituelle, pour le dosage des protéines du lait entier à cause de l'extrême turbidité de ce milieu.

le lactose interfère par son caractère réducteur et par le complexe bleu qu'il forme avec le cuivre(II) engagé comme réactif.

La littérature ne fait mention que de quelques essais d'utilisation de la réaction du biuret pour le dosage de protéines lactiques[3–7], mais il ne s'agit pourtant que de travaux isolés qui n'ont jamais donné lieu à des applications pratiques sur une grande échelle.

Le présent travail propose une solution simple, rapide et efficace permettant de parer à ces deux inconvénients majeurs par l'emploi d'un solvant puissant capable de dissoudre intégralement et simultanément les caséines et la matière grasse (le lait devenant ainsi une solution vraie), et l'emploi d'un chélateur assez puissant pour stabiliser (vis-à-vis du lactose) l'excès de cuivre(II) à engager, sans entraver pour autant la réaction colorimétrique avec les protéines. Pour obtenir une valeur plus exacte, il est encore possible de corriger par le calcul les erreurs dues aux variations de la teneur en lactose, si ce dernier fait parallèle-

ment l'objet d'un dosage par une autre méthode.

C'est dans ce but qu'a été développé, au cours d'une étude antérieure, le mélange dissolvant: soude (2 volumes; 0,1 à 0,2 *M*) + n-butylamine (3 volumes; pure), capable de dissoudre quasi instantanément le colloïde qu'est le lait entier. Parallèlement, cette amine complexe l'excès de cuivre(II) engagé, affaiblissant le complexe Cu(II)–ose, sans empêcher le complexe du biuret de se former (Cu(II)–protéines). Quant à l'action réductrice du lactose sur le cuivre(II), on peut l'inhiber ou la rendre négligeable en jouant sur les diverses cinétiques des réactions en compétition (influence surtout de la température).

THÉORIE ET PRINCIPE DE LA MÉTHODE

La méthode est basée sur la propriété du cuivre(II) de former de manière reproductible un complexe coloré et stable avec les ponts peptidiques des protéines[8]. Il faut au moins un tripeptide (2 ponts –CO–NH–) pour que la réaction puisse se produire. Le composé le plus simple qui soit capable de donner une réaction positive est le biuret produit de condensation à chaud de l'urée. La réaction est spécifique aux (poly)peptides et aux protéines. Les autres composés azotés du lait, tels que l'ion ammonium, les acides aminés libres en général, *etc.*, sont en concentrations suffisamment faibles pour qu'ils n'interfèrent pas ou de manière constante. Il faut néanmoins rappeler que cette réaction a lieu avec toutes les substances contenant deux groupes $-CONH_2$ liés soit directement, soit par l'intermédiaire d'un autre atome. Il en est de même[9] pour les composés contenant les groupes $-CH_2NH_2$, $-CH(NH)NH_2$, $-CSNH_2$, *etc.* au lieu de $-CONH_2$.

La coloration violette observée en milieu très alcalin est très probablement due à la formation d'un complexe de coordination des ions cuivriques avec les doublets électroniques libres des atomes d'azote et même d'oxygène dans certains cas. Suivant le pH du milieu et le rapport N (peptidiques)/Cu(II), on connaît actuellement trois types de complexes différents (solides cristallisés):

(a) le chlorure de bis (biuret) cuivrique, vert pâle, $[Cu(C_2H_5N_3O_2)_2]Cl_2$ obtenu à partir d'une solution dont les concentrations molaires en biuret, en cuivre(II) et en soude sont dans le rapport 2:1:0 (abrégé BT: Cu: OH = 2:1:0). Dans ce type de complexe, à caractère de cation bivalent, le cuivre(II) est lié par coordination aux oxygènes des 4 fonctions amides provenant de 2 molécules de biuret, chacune d'elles fonctionnant comme un ligand neutre. Les 4 oxygènes se situent aux sommets d'un carré légèrement distordu (configuration non rigoureusement coplanaire), admettant le cuivre(II) comme centre[10–12]:

BT : Cu : OH = 2 : 1 : 0

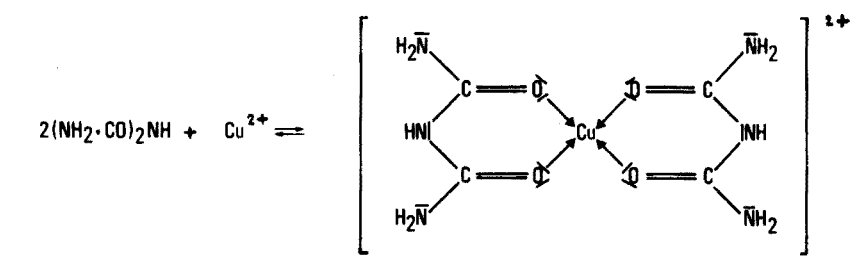

(b) le di-μ-hydroxyle-bis(biureto)dicuprate(II) de potassium tétrahydraté, $K_2[Cu(C_2H_3N_3O_2)(OH)]_2 \cdot 4\ H_2O$, violet, obtenu à partir d'une solution où BT:Cu:OH$\simeq$2:2:6, semble ne contenir qu'un reste biuret par atome de cuivre; ce complexe se comporterait dans son ensemble comme un anion bivalent et aurait une structure de dimère avec 2 groupes hydroxyles servant de ponts entre les 2 Cu(II); en outre, les 2 molécules de biuret sont coordinées à 2 atomes de Cu(II) par l'intermédiaire des azotes de leurs fonctions amides[10,13–15].

BT : Cu : OH = 2 : 2 : 6

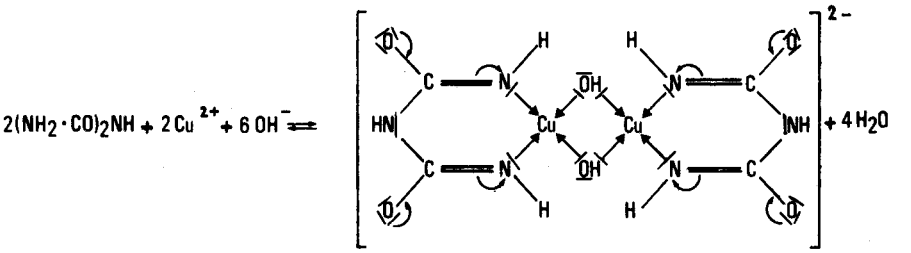

(c) le bis(biureto)cuprate(II) de potassium tétrahydraté, $K_2[Cu(C_2H_3N_3O_2)_2] \cdot 4\ H_2O$, rouge, obtenu à partir d'une solution où BT:Cu:OH$\simeq$2:1:4, se comporte aussi dans son ensemble comme un anion bivalent. Dans ce nouveau complexe, le cuivre(II) serait cette fois-ci coordiné dans une configuration de plan carré directement par les azotes des 4 fonctions amides de 2 molécules de biuret, fonctionnant chacune à nouveau comme un ligand dianionique en suite de l'ionisation de leurs hydrogènes[10–15].

BT : Cu : OH = 2 : 1 : 4

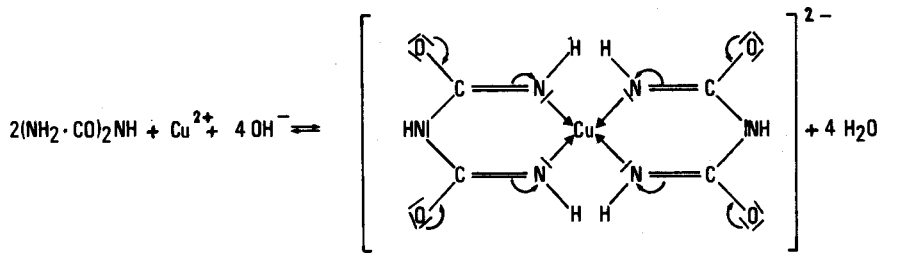

On trouve encore quelques informations intéressantes[10] concernant la position des maxima (λ_{max}) obtenus par spectroscopie de réflexion dans l'u.v. et le visible, soit: à 279 nm (35,800 cm^{-1}) et à 541 nm (18,500 cm^{-1}) pour le complexe b; à nouveau à 279 nm (35,800 cm^{-1}), et à 495 nm (20,200 cm^{-1}) pour c.

Les couleurs indiquées pour les trois types de complexes considérés (a, b et c) peuvent être interprétées selon la théorie spectrochimique qui indique une augmentation du champ ligand[16] pour les coordinations suivantes: $[CuO_4] < [CuO_2N_2] < [CuN_4]$.

Les quelques indications qui précèdent sont valables pour les complexes

à l'état solide. En milieu aqueux, on assiste à un déplacement hypsochrome de 495 à 505 nm[13,14,17] pour le complexe c et de 541 à 560–570 nm[13,14] pour le complexe b.

Ce qui a été vu précédemment pour les complexes cuivre(II)–biuret doit encore être vrai pour les complexes cuivre(II)–protéines en tant que polypeptides. Il faut néanmoins noter une différence entre ces deux classes de complexes: dans les premiers, le cuivre(II) est lié aux atomes d'azote des amides dans une structure cyclique hexagonale; dans les seconds, on ne peut qu'envisager une structure cyclique pentagonale, les atomes d'azote considérés n'étant séparés que par deux atomes dans les protéines au lieu de trois dans le biuret[14].

Dans la méthode proposée, il se forme compétitivement au moins un autre complexe coloré, celui que forme la n-butylamine, engagée comme dissolvant des protéines et des lipides du lait, avec l'excès de cuivre(II). La n-butylamine forme, comme toutes les autres amines, des complexes colorés avec le cuivre(II). Avec l'ammoniaque en milieu aqueux, on connaît la série des complexes analogues suivants: $[Cu(NH_3)_x(H_2O)_{6-x}]^{2+}$, où x peut varier[18] entre 0 et 5 suivant la teneur en NH_3. Il va donc s'établir un équilibre entre le(s) complexe(s) cuivre(II)–protéines et le(s) complexe(s) cuivre(II)–n-butylamine. Malgré cette seconde réaction colorée (parasite puisqu'elle diminue dans une certaine mesure la sensibilité de la méthode), la réaction du biuret, même réalisée dans de telles conditions, reste encore valable pour le dosage des protéines, puisque: le spectre d'absorption du complexe violet cuivre(II)–protéines, dans le visible et dans le proche u.v., est suffisamment décalé par rapport à celui du complexe bleu cuivre(II)–n-butylamine (vraisemblablement $[Cu(BTA)_4(H_2O)_2]^{2+}$) (*cf.* Fig. 1); et l'équilibre existant entre le(s) complexe(s) cuivre(II)–n-butylamine et cuivre(II) protéines est très déplacé en faveur de ces dernières (*cf.* ci-dessous, *Influence de la concentration en cuivre(II)*).

Finalement il se forme un troisième type de complexe, le(s) complexe(s) cuivre(II)–lactose. Ce point sera repris ultérieurement et traité de façon indépendante.

ÉTUDE DE LA RÉACTION DE COLORATION

Le réactif du biuret comporte: (1) un sel de cuivre(II). On prend généralement le $CuSO_4 \cdot 5\ H_2O$. Il semble que le $Cu(EDTA)Na_2 \cdot \sim 2\ H_2O$, qui présente une sensibilité bien moindre à l'hydrolyse alcaline, assure parallèlement une meilleure reproductibilité (cette constatation a été faite avec une méthode très semblable, celle de Folin-Ciocalteu[19]). Lors de l'étude de la dissolution du lait, il s'est avéré que la fonction EDTA favorisait également la dissolution des caséinates de métaux alcalinoterreux. C'est donc sous cette forme qu'a été engagé le cuivre(II) dans cette étude; (2) un complexant empêchant la précipitation du cuivre(II) sous forme d'hydroxyde. On utilise ordinairement le tartrate double de sodium et de potassium. Avec le sel d'EDTA, ce composant n'est plus indispensable; (3) une solution aqueuse très alcaline (NaOH ou KOH).

Le rapport optimal des concentrations en ces trois constituants ne semble pas être connu avec certitude. Il dépend d'abord du complexe recherché (a, b ou c), mais même pour un type donné, on trouve pour chaque auteur des concentrations différentes.

Il s'ensuit que l'on commencera par rechercher les meilleures conditions de mesure (λ_{max}) en étudiant les spectres d'absorption de ces composés, puis l'influence de chacun des composants du réactif sur le système global, permettant de définir ainsi un rapport optimal de composition. On étudiera encore les conditions de réaction, soit l'influence du temps et de la température de réaction. Cette optimisation des divers paramètres devra respecter les "contraintes" que représentent les conditions optimales définies pour la dissolution du lait, à savoir: 0,1 vol. de lait entier (0,2 vol. à la limite), 2,0 vol. de solution aqueuse de NaOH (0,1 à 0,2 *M*), 3,0 vol. de n-butylamine (éventuellement plus); temps et température de réaction, si possible 1 min à 60°C.

Le mode opératoire consiste à former le complexe violet cuivre(II) protéines en milieu alcalin en ajoutant les réactifs mentionnés à un échantillon de lait entier frais ou correctement conservé. Le cuivre(II) doit être en excès par rapport aux protéines. Suit l'adjonction de n-butylamine pour dissoudre la matière grasse (les caséines étant déjà presque complètement dissoutes). L'expérience a montré qu'il est même possible d'ajouter en une seule fois tous les réactifs préalablement mélangés (y compris la n-butylamine), ce qui simplifie beaucoup le dosage.

Les mesures d'extinction ont été effectuées à l'aide des spectrophotomètres suivants, équipés de cuvettes Hellma OS 110; un Perkin Elmer 124 muni d'un enregistreur PE 165 pour les mesures où le spectre d'absorption est intéressant; ou un Zeiss PMQII pour les mesures à une longueur d'onde donnée (meilleure précision de lecture).

Étude des spectres d'absorption

Les Figures 1(a) et (b) montrent les parties les plus intéressantes des spectres d'absorption, à savoir: E_A, spectre des complexes cuivre(II)–protéines et cuivre(II)–n-butylamine*; E_R, spectre du complexe cuivre$(II)_{total}$–n-butylamine (du réactif); $\Delta E = E_A - E_R$, spectre différentiel (apparent); E_A/E_R, rapport signal/bruit de fond.

Les spectres sont pris après 15 minutes (temps de réaction) à température ambiante. Pour les 100 μl de lait entier (respectivement d'eau pour la référence) engagés, le réactif est composé du mélange suivant: 1,0 ml d'une solution aqueuse de NaOH (0,4 *M*); 1,0 ml d'une solution aqueuse de $Cu(EDTA)Na_2 \cdot 2H_2O$ (19,2 g l^{-1}) et de KNa tartrate $\cdot$ 4 H_2O (12,2 g l^{-1}); et 3,0 ml de n-butylamine (puriss). Les 2 volumes de soude 0,2 *M* indiqués précédemment comme nécessaires pour la dissolution du lait sont remplacés ici par 1 volume de soude de concentration double (0,4 *M*) et 1 volume de solution de cuivre(II) et de tartrate.

Le spectre d'absorption du réactif E_R (avec la n-butylamine), enregistré contre de l'eau, est extrêmement large. Il présente un maximum au voisinage de 705 nm. Ce maximum se déplace vers des longueurs d'onde plus courtes, soit à 685 nm environ lors de l'addition du lait (lactose et surtout protéines). La déformation importante que l'on observe alors dans le "flanc gauche" du nouveau pic d'absorption ainsi obtenu, E_A, toujours enregistré contre de l'eau, révèle sous la forme d'une épaule la formation du complexe dit du biuret.

* Bien qu'on l'omette en première approximation, le complexe Cu(II)–lactose est également une composante de E_A. (A = Analyse; R = Référence).

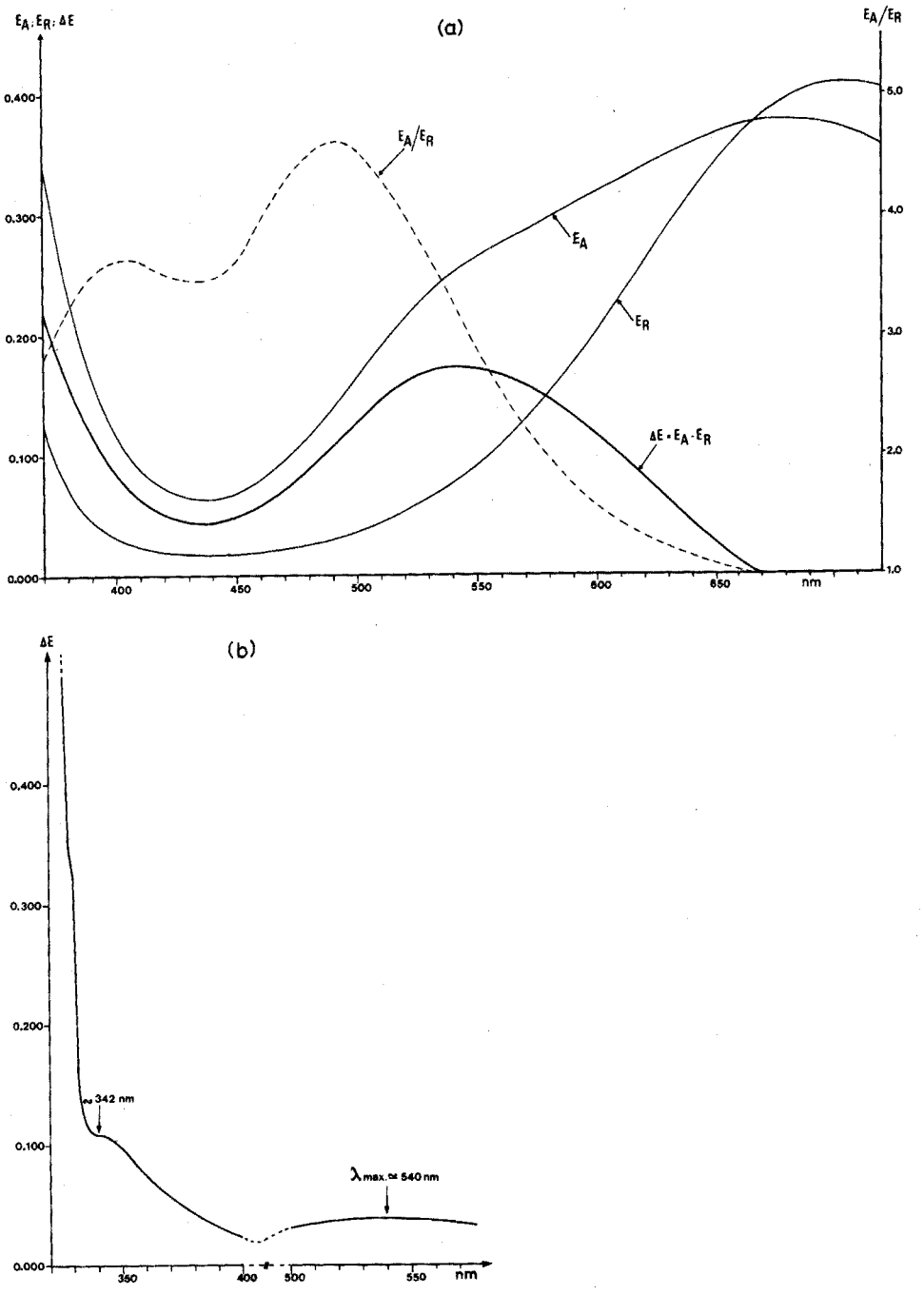

Fig. 1. (a) Spectres dans le visible du complexe dit du biuret E_A et du réactif E_R, de leur différence AE et de leur rapport E_A/E_R. (b) Spectre différentiel ΔE du complexe dit "du biuret" dans le visible et l'u.v.

Le spectre différentiel ΔE (double faisceau) indique un maximum au voisinage de 535–540 nm. Ce maximum ne correspond pourtant pas au rapport optimal E_A/E_R qui se situe au voisinage de 493 nm.

La position de ce maximum d'absorption à 540 nm, valeur intermédiaire entre $\lambda_{max} \simeq 505$–515 nm (complexe c) et $\lambda_{max} \simeq 560$–570 nm (complexe b) ne permet pas de se décider catégoriquement pour l'un ou l'autre type de complexe. Le type c est néanmoins le plus vraisemblable; il existe certainement un équilibre entre les formes b et c.

Dans l'u.v. proche, le complexe du biuret présente également un pic d'absorption, beaucoup plus intense que dans le visible. Dans les conditions expérimentales choisies, il serait possible de travailler à $\simeq 340$ nm (λ_{max} se situe encore en-dessous de cette valeur), où l'on dispose encore d'une énergie transmise suffisante pour effectuer de bonnes mesures, comme le montre la figure complémentaire 1(b).

Influence de la concentration en soude

Les équations chimiques régissant la formation des complexes a, b et c indiquent théoriquement déjà que la concentration en ions hydroxyles joue un rôle primordial. Il est avantageux de travailler en milieu très alcalin puisque

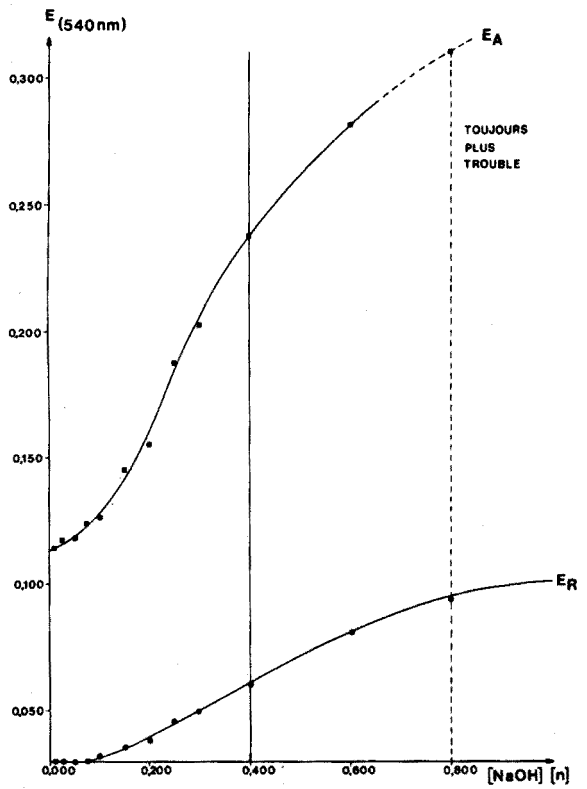

Fig. 2. Influence de la concentration en NaOH sur E_A et E_R (1 ml engagé).

les équilibres sont déplacés en faveur des complexes colorés b ou c, à la condition de rester dans certaines limites. La Figure 2 montre l'influence de la concentration de la soude engagée sur la coloration de l'échantillon E_A et de la référence E_R. Pour cet essai, la composition du mélange (lait ou eau, réactifs) est la même que précédemment, à la concentration de la soude près, qui varie cette fois de 0,000 à 1,000 *M*. Les mesures sont effectuées à 540 nm, contre de l'eau, au moyen du PMQII, après 30 min à température ambiante.

A concentrations égales en protéines et en cuivre(II), la concentration en soude augmente la coloration obtenue pour l'échantillon E_A et pour la référence E_R. Les faibles pentes des graphes de E_A et E_R à l'origine peuvent s'expliquer ainsi: en présence d'un gros excès de n-butylamine, les faibles concentrations en soude n'ont que peu d'effets sur le pH, donc sur la coloration. Au-delà du domaine de concentration optimal (0,4 à 0,6 *M* environ pour 1 ml engagé)*, on retrouve le phénomène de précipitation des protéines (déjà observé lors de l'étude de la dissolution du lait), entraînant une augmentation de la turbidité du milieu, puis la démixtion du mélange dissolvant (eau/soude/n-butylamine).

Une étude parallèle des spectres enregistrés avec le PE124 indique que dans le domaine envisagé la position des sommets des pics n'est pas fonction de la concentration de la soude engagée. On retrouve l'optimum entre 535 et 540 nm (pic à sommet relativement aplati).

Influence de la concentration en cuivre(II)

Tout comme la concentration en soude, la concentration en cuivre(II) favorise la réaction (équilibre, cinétique, *etc.*). C'est ce que montre la Fig. 3. Le mélange réactionnel est le même que précédemment, à ceci près que la concentration en $Cu(EDTA)Na_2 \cdot 2H_2O$ varie cette fois de 0,00 à 19,2 g l^{-1} (1 ml engagé). On fera abstraction du lactose dont l'influence sera étudiée plus loin.) La lecture des extinctions des échantillons et des références est effectuée à 535 nm contre de l'eau au moyen du PMQII, après 15 min de développement de la couleur à température ambiante.

Le graphe obtenu présente une partie médiane à forte courbure (approximativement entre 1,92 et 11,52 g de $Cu(EDTA)Na_2 \cdot 2\ H_2O$ par litre) et deux branches "asymptotiques", l'une à forte pente (Cu en défaut), l'autre à pente faible (Cu en excès). Leur point d'intersection est le point d'équivalence cuivre(II)–protéines comme pour une titration.

La partie médiane de la courbe disparaît lorsque l'essai est réalisé sans n-butylamine (on prend alors du lait écrémé). Il ne subsiste alors que les parties latérales rectilignes, les asymptotes, qui forment un point anguleux au point d'équivalence.

Un tel comportement est significatif de la compétition de deux équilibres:

(a) Cu(II) + protéines $\rightleftharpoons$ Cu(II)–protéines (complexe I)

(b) Cu(II) + n-butylamine $\rightleftharpoons$ Cu(II)–n-butylamine (complexe II)

---

* Pour la réaction de coloration proprement dite, on pourrait engager des concentrations en soude beaucoup plus élevées, comme c'est le cas dans les méthodes proposées en chimie clinique ne nécessitant aucun dissolvant des lipides.

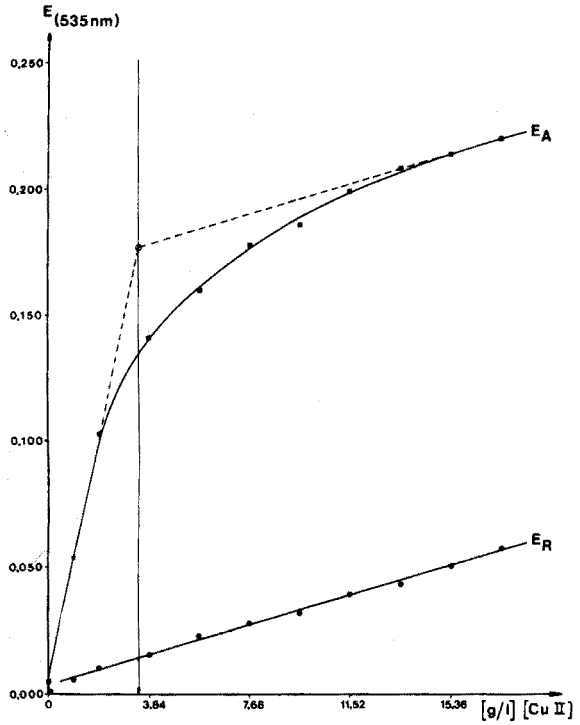

Fig. 3. Influence de la concentration en cuivre(II) sur E_A et E_R (1 ml engagé).

Le complexe I étant plus stable que le II, les protéines complexent presque complètement les premières portions de cuivre(II) ajoutées. Puis progressivement, pour des teneurs croissantes en cuivre(II), s'établit le double équilibre que dictent les équations (a) et (b). La courbe s'infléchit et quitte la première asymptote. Il faut engager un excès de cuivre(II) relativement important pour retrouver une croissance linéaire, la seconde asymptote. Dans ce cas, on peut considérer que l'équilibre (a) est pratiquement complètement déplacé vers la droite, au profit du complexe I. La concentration de $Cu(EDTA)Na_2 \cdot 2\,H_2O$ utilisée jusqu'ici ($19{,}2\ g\ l^{-1}$) était donc justifiée.

Cette seconde symptote est approximativement parallèle à la droite des E_R (solutions de références), ce qui confirme encore l'interprétation donnée à la forme du graphe des E_A.

En déterminant l'abscisse du point d'intersection des deux asymptotes, on obtient l'équivalence pour 3,46 g de $Cu(EDTA)Na_2 \cdot 2\,H_2O$ (P.M.=433,8 par litre); le volume engagé étant 1 ml pour ce réactif, la stoechiométrie est donc réalisée avec *ca.* 8 microatome-g de cuivre(II). En travaillant avec 19,2 g de $Cu(EDTA)Na_2 \cdot 2\,H_2O$ par litre, on dispose donc d'un excès (dans le rapport cuivre(II)–protéines) au moins égal à 5, ce qui est pourtant juste suffisant à cause de la n-butylamine. Dans les conditions de travail choisies, on pourrait admettre encore une concentration 25 à 50% plus élevée. Cet ion donnant un(des) complexe(s) fortement coloré(s) avec l'amine en milieu aqueux, il n'est pourtant

pas souhaitable de l'engager en beaucoup plus gros excès: si $\Delta E = E_A - E_R$ ne peut plus croître, E_A/E_R par contre décroît en tendant vers 1.

Pour calculer le nombre de microatome-g d'azote peptidique engagé dans cet essai, on dispose des données de base suivantes: volume de lait engagé, 0,1 ml; poids spécifique, 1,03 [g ml^{-1}]; teneur en azote total (TN) selon Kjeldahl, 0,52 g % (g d'azote pour 100 g de lait frais); et teneur en azote peptidique (PBN), 89% du TN*. On obtient ainsi *ca.* 34 μat-g d'N peptidique. Pour les conditions expérimentales choisies, on en déduit donc que le rapport N (peptidique)–cuivre(II) vaut en moyenne 4, ce qui est en parfait accord avec la conclusion de Mehl et coll.[20] et confirmerait bien l'hypothèse précédente, à savoir qu'il doit s'agir du complexe type c.

Si l'on effectue le même calcul avec la n-butylamine engagée, dont tous les azotes peuvent être ligands, on obtient *ca.* 30.350 μat-g d'N, soit en gros 10^3 fois plus que précédemment. Quel que soit le type de complexe Cu–n-butylamine envisagé $[Cu(C_4H_9 \cdot NH_2)_x]^{2+}$, où $1 < x < 6$, l'excès de l'amine est énorme pour le cuivre(II) comparativement à l'azote peptidique présent (calcul effectué pour 3 ml de n-butylamine, de densité = 0,740 et de poids moléculaire = 73,14). La formation prioritaire du complexe I dans de telles conditions prouve donc que le pouvoir complexant des peptides est bien supérieur à celui de l'amine. Il n'est néanmoins pas possible de diminuer la concentration de la n-butylamine à engager, cette dernière étant requise pour obtenir une dissolution du lait suffisante: d'où l'importance de la différence des constantes de dissociation des deux complexes, sans laquelle la méthode proposée serait à rejeter.

Influence du temps et de la température de réaction

Dans la méthode du biuret utilisée pour le dosage des protéines sériques[2], il est recommandé d'effectuer la mesure après un temps de réaction de 30 min à température ambiante. Ces deux paramètres ont été étudiés simultanément comme suit: à 0,1 ml de lait, respectivement d'eau pour la référence, on ajoute rapidement les 5 ml du mélange de réactifs décrit précédemment pour l'étude des spectres d'absorption. Immédiatement après le mélange (temps zéro), on verse aussi rapidement que possible la solution à mesurer dans la cuvette du spectrophotomètre PE-124 et l'on enregistre l'évolution de la coloration de l'échantillon en fonction du temps et à différentes températures (20°, 30°, 40° et 50°C). Les mesures, effectuées à 535 nm contre E_R sont présentées par la Fig. 4, en % de la coloration ou de l'extinction finale (= 100%). Cette dernière est atteinte approximativement en 30 min, quelle que soit la température.

La température jusqu'à 40°C ne joue pratiquement aucun rôle dans le développement de la couleur, ce qui prouve que l'énergie d'activation pour la formation de ce complexe est très faible. A partir de 50°C, les mesures deviennent instables et décroîssent irrégulièrement, avec une perte de sensibilité, ce qui est en accord avec les résultats de Zak et Cohen[19]. Il faut peut-être attribuer cet effet à la réduction du cuivre(II) en cuivre(I) par le lactose, le milieu étant suffisamment

* Le PBN est déterminé colorimétriquement par la réaction des groupes $-NH_2$ avec la ninhydrine avant et après hydrolyse alcaline; cette valeur de 89% tient compte également du NPN (déterminé par Kjeldahl).

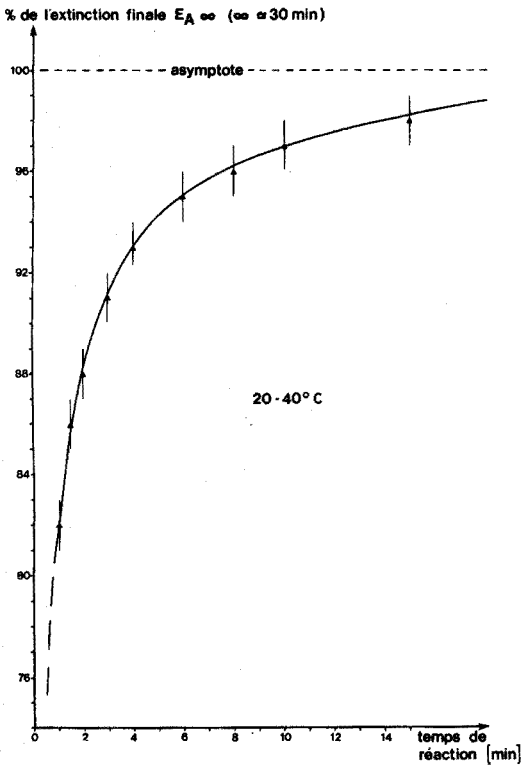

Fig. 4. Étude de la vitesse de réaction (développement de la coloration).

alcalin. De toute façon, ce domaine de température n'est pas à envisager ou ne peut l'être que pour un laps de temps très court vu la forte tension de vapeur du milieu (point d'ébullition de la n-butylamine = 70–78°C) et les risques d'une variation du volume de l'échantillon à mesurer.

Il faut néanmoins rappeler qu'une courte élevation de la température (30 à 60 s à *ca.* 60°C) s'avère des plus bénéfiques pour la dissolution proprement dite des laits très gras ou légèrement altérés par la conservation. Il y a donc un compromis à trouver en fonction du système d'analyse automatique adopté.

Comme le montre la Fig. 4, la coloration croît très rapidement au début de la réaction. Après 2,5 min, on atteint déjà 90% de la coloration finale: après 10 min 97%. Puis il faut attendre encore *ca.* 20 min pour obtenir l'extinction finale. Pour l'analyse manuelle ou dans un système automatique discontinu, où un tel temps d'attente ne pose pas de problème particulier, on peut attendre 30 min (15 min au minimum) avant d'effectuer la mesure. Dans un système à flux continu, on se contentera d'un temps de développement plus court de l'ordre de 5 à 10 min pour éviter l'emploi d'une bobine d'attente exagérément longue (risques de diffusion et de contamination accrus, perte de charge inutile, *etc.*).

CONCLUSION

La présente étude montre qu'il est possible d'adapter au dosage des protéines

du lait entier la méthode du biuret utilisée jusqu'ici avec succès en chimie clinique pour d'autres liquides biologiques (sérum, liqueur cérébro-spinale *etc.*). Si le principe de la méthode reste le même, les conditions expérimentales sont fondamentalement différentes en raison de la nature colloïdale du lait qui doit être dissous. Vu sa très grande simplicité, cette méthode se prête particulièrement bien à une automatisation intégrale, tant en discontinu automatique qu'en flux continu: elle ne nécessite aucune opération de séparation (filtration, centrifugation ou dialyse) ou de digestion. Afin d'augmenter la sensibilité de la méthode, on fixera les diverses grandeurs qui définissent la réaction à leurs valeurs maximales admissibles pour la solubilité des divers composants.

La réaction de coloration n'étant que faiblement dépendante de la tempé rature, on la laissera se développer à température ambiante pendant 15 à 30 min, ce qui d'une part simplifie la méthode et d'autre part limite la réduction du cuivre(II). Le léger échauffement nécessaire au début de réaction pour faciliter la dissolution du lait peut être obtenu soit par un court préchauffage (en flux continu) soit par la chaleur de réaction du mélange (exothermique) butylamine–soude.

RÉSUMÉ

Le présent travail propose une nouvelle méthode pour le dosage photométrique des protéines dans le lait entier. Après une dissolution rapide et complète des composants responsables de la turbidité du lait (graisses et caséines) par addition de n-butylamine, on fait réagir les ponts peptidiques avec un excès de Cu(II) pour former le complexe dit "du biuret". La simplicité de cette méthode, qui ne nécessite aucune opération de digestion ou de séparation (filtration, centrifugation ou dialyse), la rend idéale pour une automatisation intégrale tant en discontinu qu'en flux continu. Après une étude des structures et des spectres d'absorption des divers complexes possibles avec le Cu(II), les principaux paramètres de la réaction sont optimisés, à savoir la concentration en réactif (soude et Cu(EDTA)Na_2), le temps et la température de réaction.

SUMMARY

A new method for the spectrophotometric determination of the protein content of whole milk is proposed. The fat and caseins, which render the milk turbid, are dissolved rapidly and completely by addition of n-butylamine. The peptide bonds are then reacted with an excess of copper(II) in a strong alkaline solution to form the so-called "biuret complex". The simplicity of this method, which requires no separation or digestion, is adequate for full automation either with continuous flow or with discontinuous (automatic) analyzers. After a study of structure and absorption spectra of the different possible copper complexes, the main parameters are investigated, *i.e.* the concentration of the reagents (NaOH and Cu(EDTA)Na_2), the time and the temperature of the reaction.

RÉFÉRENCES

1 E. Renner et S. Ömeroglu, *Z. Lebensm. Unters.-Forsch.*, 149 (1972) 267; 149 (1972) 329; 150 (1972) 295; 150 (1972) 338.

2 R. Richterich, *Clinische Chemie (Theorie und Praxis)*, Karger Vrlg., Basel–New York, 1965, pp. 207–209.
3 M. Molnar, *Magy. Kem. Lapja*, 3 (1948) 428.
4 R. Schober, W. Niclaus et W. Christ, *Milchwissenschaft*, 19 (1964) 75.
5 R. Schober, W. Niclaus et W. Christ, *Milchwissenschaft*, 10 (1955) 238.
6 H. Salwin, *Food Res.*, 19 (1954) 235.
7 B. C. Johnson et A. M. Swanson, *J. Dairy Sci.*, 35 (1952) 823.
8 W. Autenrieth et F. Mink, *Münch. Med. Wochenschr.*, 62 (1915) 1417.
9 P. B. Hawk, B. L. Oser et W. H. Summerson, *Practical Physiological Chemistry*, Blakiston, Philadelphia, 14th ed., 1965, p. 180.
10 A. W. McLellan et G. A. Melson, *J. Chem. Soc. A*, (1967) 137.
11 H. C. Freeman et J. E. W. L. Smith, *Acta Crystallogr.*, 20 (1966) 153.
12 H. C. Freeman, J. E. W. L. Smith et J. C. Taylor, *Nature*, 184 (1959) 707; *Acta Crystallogr.*, 14 (1961) 407.
13 K. Aida, Y. Musya et S. Kinumaki, *Inorg. Chem.*, 2 (1963) 1268.
14 M. Kato, Y. Komuro et K. Sone, *J. Chem. Soc. Japan, Pure Chem. Sect.*, 75 (1954) 1134; 76 (1955) 1034; 77 (1956) 308; 78 (1957) 896.
15 M. Kato, *Z. Anorg. Chem.*, 300 (1959) 84; *Z. Phys. Chem. (Frankfurt am Main)* 23 (1960) 375; *Z. Phys. Chem., (Frankfurt am Main)* 23 (1960) 391.
16 P. A. Kober et A. B. Haw, *J. Amer. Chem. Soc.*, 38 (1916) 457.
17 F. A. Cotton et G. Wilkinson, *Advanced Inorganic Chemistry.*, Interscience, New York, 2nd ed., 1968, pp. 905, 906.
18 F. A. Cotton et G. Wilkinson, *Advanced Inorganic Chemistry*, Interscience, New York, 2nd ed., 1968, p. 680.
19 B. Zak et J. Cohen, *Clin. Chim. Acta*, 6 (1961) 665.
20 J. W. Mehl, E. Pakovska et R. J. Winzler, *J. Biol. Chem.*, 177 (1949) 13.

Analytica Chimica Acta, 70 (1974) 341–350

SPECTROPHOTOMETRIC DETERMINATION OF TRACES OF BORON IN SILICON BY MEANS OF SOLVENT EXTRACTION

PIETRO LANZA
Chemical Institute "G. Ciamician", University of Bologna, Bologna, (Italy)
PIER LUIGI BULDINI
Lamel CNR, Bologna, (Italy)
(Received 2nd January 1974)

Because of the strong influence of traces of boron on the electrical properties of silicon used in semiconductor devices, much interest has been shown in sensitive and reliable analytical methods for boron. Available chemical methods of analysis are still not satisfactory enough for the determination of microgram quantities of boron in silicon. The extraction–spectrophotometric method with methylene blue introduced by Ducret[1] seemed the most promising one and it has been investigated by many authors for the determination of boron in various materials, such as steel[2–7], plant and soil samples[8], rocks[9], natural water[10], uranium[11], uranium tetrafluoride[12] and aluminium and its alloys[13].

This method is based on the conversion of boron to tetrafluoroborate, followed by the formation of a colored complex with methylene blue which is extracted into dichloroethane; the absorbance is measured at 660 nm.

On applying the procedure described by Ducret[1], the present authors encountered many difficulties and did not succeed in obtaining reproducible and reliable results. Difficulties were essentially due to the high blank absorbance and to the poorly reproducible efficiency of washing.

Considering the promising characteristics of the method, it seemed interesting to examine carefully its essential features.

PRELIMINARY STUDIES

Extraction of methylene blue from boron-free solutions

As indicated by several authors[1,14], methylene blue forms extractable salts with various acids, such as nitric, perchloric, hydrochloric and hydrofluoric, whereas sulphuric and phosphoric acid give only poorly extractable salts. Methylene blue can, therefore, be extracted even from solutions which do not contain boron.

In our preliminary research, the investigation was limited to the effects of hydrofluoric, fluorosilicic and sulphuric acids. There is no agreement in the literature regarding the effects of hydrofluoric acid and fluoride ions.

Ducret[1] indicated the extractability of the methylene blue–fluoride complex and the effect of its concentration in the organic phase on the extraction coefficient of the methylene blue–fluoroborate complex. The addition of fluoride ions to the aqueous phase decreases the extraction of the fluoroborate complex. The high value

of the absorbance of the organic phase, in the conditions chosen by Ducret, is mostly due to the extracted fluoride complex.

The great effect of the hydrofluoric acid concentration on the extraction of the fluoroborate complex was also recognized by Pasztor *et al.*[2], who observed that, in order to obtain a good reproducibility, the amount of hydrofluoric acid added must be carefully controlled and the final concentration of the acid in the aqueous phase must be maintained below 0.30 *M*. Recently, Vernon and Williams[7] found that "the blank value is virtually independent of fluoride concentration but is influenced by the sulphuric acid concentration".

In order to check the behaviour of fluoride and hydrofluoric acid in relation to the extractability of the methylene blue, increasing volumes of 1 *M* hydrofluoric acid or sodium fluoride solution were diluted to 25 ml with water, mixed with 5 ml of methylene blue and extracted with dichloroethane, following the described procedure. The results are shown in Fig. 1, where the absorbance is plotted versus the concentration of various acids in the solution (before the addition of methylene blue). It is clear that fluoride ions have little effect, while increasing hydrofluoric acid concentration aids the methylene blue extraction.

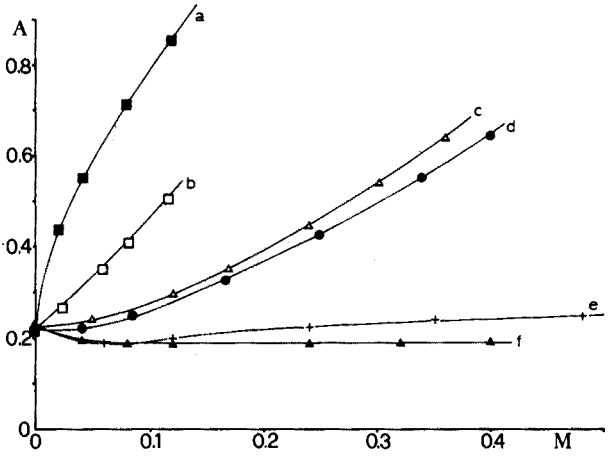

Fig. 1. Effects of acids on the methylene blue extraction. (■) H_2SiF_6, (□) fluoride solution of silicon, (△) HF + NH_4F (fluoride solution; see Experimental), (●) HF, (+) H_2SO_4, (▲) F^-

In Fig. 1, the effects of sulphuric and fluorosilicic acids and "fluoride solution" are also given. Curve (a) was obtained from commercial reagent-grade fluorosilicic acid and curve (b) was obtained by dissolving pure silicon in the smallest necessary quantity of the specified "fluoride solution" (see Experimental). The high absorbance obtained with commercial fluorosilicic acid is due, probably, to boron being present as an impurity.

The effect of sulphuric acid on the extraction of the compounds which methylene blue forms with various inorganic acids and salts seems to be rather complex. It was studied in some detail in view of its importance in determining the absorbance of the blank. For this purpose, increasing quantities of sulphuric acid were added to solutions containing a constant amount of the various reagents to be

studied; then, the methylene blue complexes were extracted under the given conditions. In this way, the effects of sulphuric acid, sodium fluoride, "fluoride solution", and "fluoride solution" containing fluoroborate were investigated. A solution containing fluorosilicate ions, formed by dissolution of pure silicon in the smallest quantity of "fluoride solution" necessary (see *Procedure*), was also checked. The results of these experiments are shown in Fig. 2.

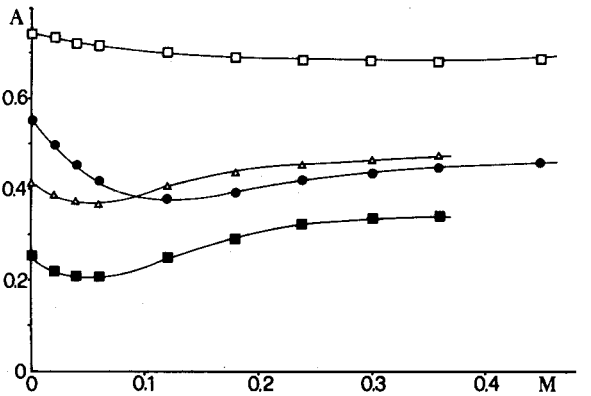

Fig. 2. Effect of H_2SO_4 on: (□) fluoride solution containing fluoroborate ions ($1.2 \cdot 10^{-5}$ *M* B), (△) fluoride solution of silicon, (●) 0.32 *M* HF, (■) fluoride solution ([HF]+[F^-]=0.1 *M*).

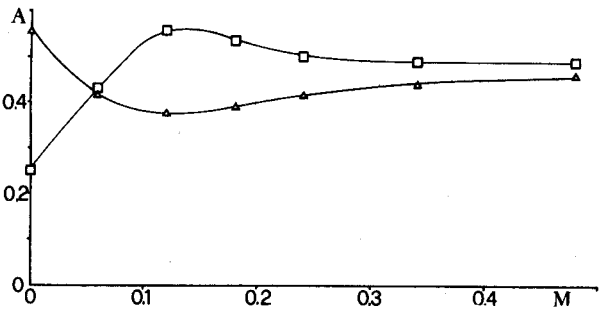

Fig. 3. Effect of H_2SO_4 on: (□) 0.32 *M* F^-, (△) 0.32 *M* HF.

It is interesting to observe the change in the absorbance of 0.30 *M* hydrofluoric acid or 0.30 *M* sodium fluoride solutions as a function of added sulphuric acid (Fig. 3). The addition of sulphuric acid initially increases the absorbance of the sodium fluoride solution, while it lowers that of the hydrofluoric acid solution. This fact supports the hypothesis that HF_2^- ions are the complexing agents for methylene blue. From a practical point of view, it appears that a small amount of sulphuric acid can be useful for lowering the blank absorbance of the "fluoride solution" of the sample.

To define the effect of the pH on the extraction, as has been tried by some authors[1,2], is a difficult problem, because it is not a simple matter to distinguish the true effect of the pH from the possibly more selective effect of anions. The following experiments were carried out: 25 ml of 0.2 *M* hydrochloric acid or 0.1 *M*

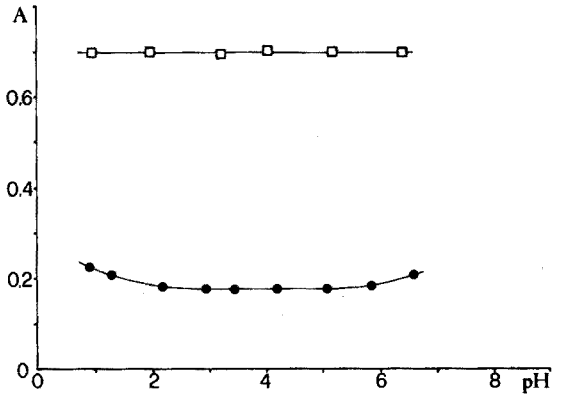

Fig. 4. pH effect on the methylene blue extraction. (□) pH adjusted with HCl and NH_3, (●) pH adjusted with H_2SO_4 and NH_3.

sulphuric acid solutions adjusted to the required pH value by addition of ammonia (added with methylene blue) were extracted in the usual way with dichloroethane. The results are given in Fig. 4. The curves clearly indicate that the behaviour of chloride, sulphate and hydrogensulphate ions greatly affects the value of the absorbance.

Formation and extraction of the fluoroborate ion

It is known that fluoroboric acid is formed when boric acid reacts with hydrofluoric acid, according to the reactions:

$$H_3BO_3 + 3\,HF \rightarrow HBF_3OH + 2\,H_2O \quad \text{(very fast)} \tag{1}$$

$$HBF_3OH + HF \rightarrow HBF_4 + H_2O \quad \text{(slower)} \tag{2}$$

Wamser[15] studied the equilibria and the kinetics involved in this system; he found that reaction (2) is acid-catalyzed. The relation between the rate constant and hydrogen ion concentration is given by:

$$k = k_0 + k_H[H^+] \tag{3}$$

in which $k_0 = 0.064$ l mol^{-1} min^{-1} is the constant of the "spontaneous reaction", and $k_H = 7.35$ (at 25°C).

When, as in conditions useful for analytical purposes, the hydrofluoric acid is present in very great excess compared to the boron of the sample, the pseudo first-order constant of reaction (2) is given by:

$$k' = (0.064 + 7.35[H^+])[HF] \tag{4}$$

On the basis of these data, one can calculate that for practical analytical conditions ($[H^+] = 0.1$ and $[HF] = 0.2$, about) at 25°C, the formation of the fluoroboric acid is almost complete in less than 1 h.

The results of an experimental check are shown in Fig. 5. The measurements quoted were obtained by analyzing at various times a solution consisting of 0.25 *M* hydrofluoric acid and 0.072 *M* sulphuric acid containing 0.2 μg of boron (as boric acid) per ml. At recorded time intervals, 50-ml aliquots were withdrawn and analyzed

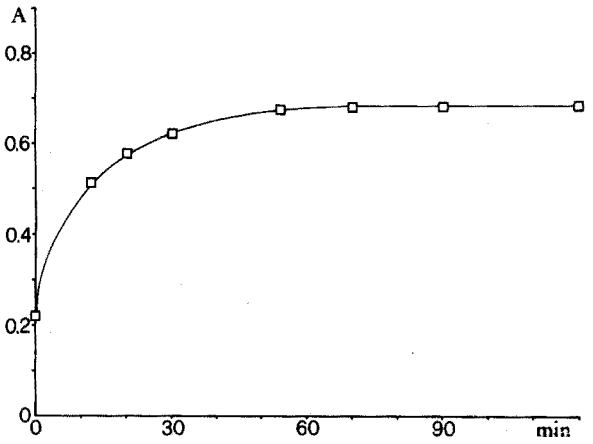

Fig. 5. Formation of fluoroborate as a function of time.

for fluoroboric acid by adding 10 ml of 0.001 *M* methylene blue and extracting with 25 ml of dichloroethane. After the layers had separated completely, 5 ml of the organic layer were pipetted out and diluted to 25 ml with dichloroethane in a volumetric flask. The absorbance of the solution was measured at 660 nm against dichloroethane in a 10-mm cell.

In order to check the relation between the absorbance and the boron content of the solutions under practical work conditions, a calibration curve was prepared. For this purpose, known quantities of boron as boric acid or fluoroboric acid were added to 4.0 ml of *M* hydrofluoric acid, 3.0 ml of 0.05 *M* sulphuric acid, 1 ml of hydrogen peroxide (120 vol.) and 1 drop of 1% copper chloride solution. After standing for about 1 h at 60°C, the solutions were diluted to 25 ml with water. Then, 5 ml of a 0.001 *M* methylene blue solution were added, and the mixture was extracted with 5 ml of dichloroethane. The extract was diluted to 25 ml with dichloroethane and the absorbance was measured at 660 nm against dichloroethane. The results are shown in Fig. 6.

This plot indicates that the Lambert-Beer law fails even at relatively low concentrations of 4 μg of boron; the results, however, are quite reproducible. It has been claimed[3,7] that the use of more concentrated methylene blue solutions allows Beer's law to be obeyed. The lack of linearity of the calibration curve can be related however, both to deficiency of methylene blue, as well as to the colloidal character of these solutions[1,2].

The described working conditions were chosen in order to minimize the value of the reagent blank and to avoid the washing of the organic extracts with water, as Ducret[1] and other authors prescribe.

Dissolution of silicon

The decomposition of the sample is performed by treatment with a mixture of hydrofluoric acid and ammonium fluoride in the presence of hydrogen peroxide, according to the reaction:

$$Si + 4HF + 2F^- + 2H_2O_2 \rightarrow SiF_6^{2-} + 4H_2O \qquad (5)$$

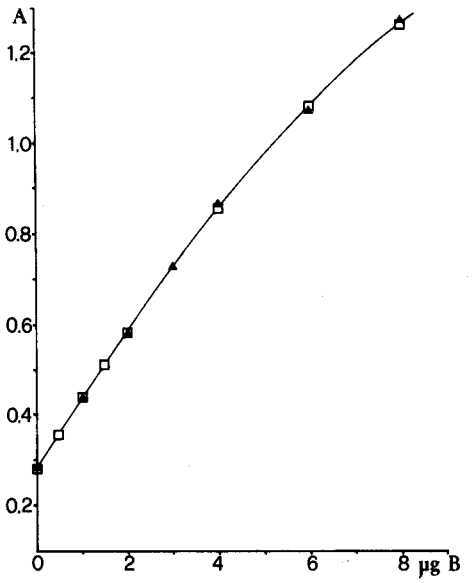

Fig. 6. Calibration curve: (▲) from boric acid, (□) from fluoroboric acid.

The process is catalyzed by copper(II). Silver, platinum and gold(III) salts were also shown to have a considerable catalytic activity. Silicon dissolves very readily in this mixture, even at room temperature. The reaction is exothermic and rather vigorous, but it is easily controlled by adding hydrogen peroxide dropwise. If, instead of the mixture, one uses hydrofluoric acid alone, *i.e.* without ammonium fluoride, the dissolution proceeds more slowly.

Suitable experiments showed that the dissolution of silicon does not need an excess of reagent. This allows the blank absorbance to be maintained within acceptable values.

In addition, the use of "fluoride solution" leads to the formation of fluoroboric acid during the dissolution of the sample, so that the time of analysis is reduced. For practical use, the quantity of "fluoride solution" to be used for dissolving the samples is quoted in Fig. 7. One must realize that even if boron is present in the sample in very small quantities in comparison with the silicon, some excess of the fluoride solution is necessary for the kinetics of the fluoroborate formation. The "practical quantity" quoted in Fig. 7 corresponds to a final concentration of 0.16 *M* of the total fluoride content ($HF + F^-$) in the solution to be extracted.

EXPERIMENTAL

Apparatus

A Spectronic 505 Bausch & Lomb spectrophotometer was used.

Reagents and standard solutions were prepared in boron-free glassware. All solutions containing hydrofluoric acid were prepared and stored in polyethylene bottles. Dissolution of silicon samples was carried out in polypropylene test tubes (Kartell, 24 mm diam. and 95 mm long) with polyethylene covers. Extractions were

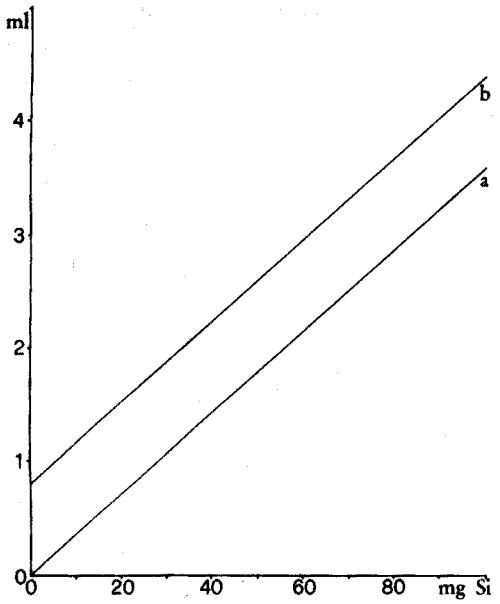

Fig. 7. Theoretical (a) and practical (b) quantity of "fluoride solution" for dissolving silicon samples.

made in polyethylene bottles of suitable size.

Polypropylene pipets and volumetric flasks were used throughout. Small volumes were precisely measured with an SB-2 Syringe Microburet having a capacity of 1 ml (division 0.001 ml; Micrometric Instrument Co., Cleveland).

Reagents

Standard boron solution (10 μg B ml^{-1}). Dissolve 0.571 g of reagent-grade boric acid in 1 l of water and dilute this solution ten times with water.

0.001 M Methylene blue. Merck solution; C.I. No. 52015, S No. 1038.

Fluoride solution (4 *M* HF, 2 *M* NH_4F). Baker BAR ACS 48% hydrofluoric acid and C. Erba RSE 32% ammonia (for electronic use) were used. Mix in a polypropylene volumetric flask 6 moles of hydrofluoric acid with 2 moles of ammonia and dilute to 1 l with water.

1,2-Dichloroethane was RPE grade from C. Erba.

Procedure

(A) Samples containing 1–500 p.p.m. of boron. Place three accurately weighed portions of the sample of suitable size (10–100 mg), containing no more than 5 μg of boron, in three polypropylene test tubes. Place four samples of boron-free silicon of the same size ($\pm$1 mg) as the sample in four other test tubes. Add. 3 drops of aqueous 1% (w/v) copper chloride solution to each test tube. Shake gently in order to wet the silicon with the solution.

Add suitable quantities of the standard solution of boron with a microsyringe to three of the four test tubes containing pure silicon. Select the boron quantities so as to include, in the concentration range, that expected in the unknown sample.

Add the prescribed volume of "fluoride solution", indicated by Fig. 7, to each test tube. Add 2 drops of hydrogen peroxide (120 vol.) to each portion; the reaction starts at once with development of oxygen. Keep the test tubes covered, and add dropwise 10–15 drops of hydrogen peroxide for those samples up to 40–50 mg, and 20–30 drops for samples up to 100 mg of silicon.

After the peroxide addition, heat the covered test tubes at 60–70°C in a thermostated bath for 2 h; this allows a complete dissolution of the sample and a careful washing of the walls and covers of the tubes by reflux of the condensed water.

After this period, add 1 ml of 1.5 *M* sulphuric acid to each test tube and store the solutions for about 1 h at room temperature. This time is necessary to transform into fluoroborate ion any traces of boron present in the sulphuric acid. Then transfer the solutions to 25-ml polyethylene graduated cylinders and, by washing the tubes with small quantities of water, dilute to 25 ml.

Place the solutions in polyethylene flasks, and add 5 ml of 0.001 *M* methylene blue solution and 5 ml of dichloroethane. Stopper the flasks and shake for 2 min. After the layers have separated completely, remove 2.0 ml of the organic layer with a polypropylene graduated pipet and dilute to 10.0 ml with dichloroethane in a volumetric flask. Read the absorbance of the extract at 660 nm against dichloroethane.

Prepare a calibration graph from the points obtained with the standard solution, and read the boron content of the unknown samples in the usual way.

Table I gives the results of a typical experiment.

TABLE I

RESULTS OF A TYPICAL EXPERIMENT

(1.20 ml of the "fluoride solution" was added.)

Test tube	*Nature of sample*	*Weight* (*mg*)	*B added* (*μg*)	*A*	*B found* (*μg*)
1	B-free Si	09.80	0.00	0.370	—
2	B-free Si	10.25	1.00	0.520	—
3	B-free Si	10.53	2.00	0.655	—
4	B-free Si	10.02	3.00	0.815	—
5	Unknown	09.90	0.00	0.588	1.50[a]
6	Unknown	10.54	0.00	0.595	1.54[a]
7	Unknown	10.19	0.00	0.590	1.51[a]

[a] These results correspond to 152, 146 and 148 p.p.m. B, respectively, with a mean value of 149 p.p.m.

(B) Samples with more than 500 p.p.m. of boron. The above procedure is applied to about 10-mg portions of the sample and of boron-free silicon. Add known quantities of boron to three of the four portions of pure silicon so that the standards cover a range which includes the presumed amount of boron in the unknown. After the addition of 1 ml of 1.5 *M* sulphuric acid, dilute the fluoride solutions of the samples with water to 25 ml. Take aliquots of these solutions, containing no

more than about 5 μg of boron, and dilute to 25 ml with water. Transfer these solutions to polypropylene flasks, and add methylene blue and dichloroethane for extraction.

RESULTS AND DISCUSSION

Table II shows the results obtained for boron in some samples, with an indication of the precision. A degree of familiarity with the procedure is required before highly precise results can be achieved.

TABLE II

DETERMINATION OF BORON CONTENT IN SILICON SAMPLES

Sample	*Resistivity (ohm cm)*	*No. of detns.*	*[B] p.p.m.*	*s*	*S_r (%)*
Schuchardt SI 172	—	10	10.3	±0.24	2.3
Wacker Chemitronic Burghausen	$2.18 \cdot 10^{-2}$	8	22.1	±1.57	7.1
Wacker Chemitronic Burghausen	$2.28 \cdot 10^{-2}$	8	19.3	±1.63	8.5
Wacker Chemitronic Burghausen	$4.45 \cdot 10^{-3}$	9	162	±8.72	5.4
Montedison spa Milano	$3.91 \cdot 10^{-4}$	6	2116	±55	2.6
Montedison spa Milano	$3.93 \cdot 10^{-4}$	11	2120	±136	6.4
Montedison spa Milano	$2.76 \cdot 10^{-4}$	10	3430	±164	4.8

The sensitivity of the method is essentially limited by the relatively high absorbance of the blank. Impurities in the reagents and distilled water can obviously contribute to the blank absorbance. Even if the optimal conditions are used, the boron present is only partially extracted during one extraction; this incomplete extraction does not affect the accuracy of the determination, but it is another factor in limiting the sensitivity.

In practical applications, it is convenient to adopt the technique of analyzing standards during each analysis, instead of using a single calibration curve. This is preferred because it is difficult to obtain a satisfactory reproducibility of the blank absorbance. This procedure has been recommended by other authors[1,3], but Pasztor *et al.*[2] subtracted the average of two reagent blanks from the absorbance value of the solutions, before using a calibration curve.

In spite of this and other minor disadvantages, the methylene blue method for determining microquantities of boron in silicon appears to be one of the most practical of the available colorimetric methods for the determination of boron. It is highly selective and highly sensitive, and requires little working time.

The authors wish to thank Prof. Dario Nobili for his helpful discussions and suggestions, the staff of the Lamel – CNR for supplying and checking standards and samples, and Prof. Giovanni Semerano, Director of the Chemical Institute "G. Ciamician", for his encouraging remarks and friendly criticism.

SUMMARY

A spectrophotometric method for the determination of boron in silicon based

on the extraction of the methylene blue–fluoroborate complex has been improved. Some important points, such as the dissolution of silicon with hydrofluoric acid and hydrogen peroxide, the effect of various anions on the blank absorbance and the best working conditions for forming and extracting the complex, have been studied. The method is applied to the determination of boron in silicon containing at least 1 p.p.m. of boron, with a relative standard deviation of $\pm 5\%$.

REFERENCES

1 L. Ducret, *Anal. Chim. Acta*, 17 (1957) 213.
2 L. Pasztor, I. D. Bode and Q. Fernando, *Anal. Chem.*, 32 (1960) 277.
3 R. Rosotte, *Chim. Anal.*, 44 (1962) 208.
4 N. Fukushi and Y. Kakita, *Jap. Analyst*, 15 (1966) 553.
5 J. Mrozniski, *Chem. Anal. (Warsaw)*, 15 (1968) 2003.
6 O. P. Bhargawa and W. G. Hines, *Talanta* 17 (1970) 61.
7 F. Vernon and J. M. Williams, *Anal. Chim. Acta*, 51 (1970) 533.
8 C. C. Weir and R. L. Jones, *Trop. Agr. (Trinidad)*, 47 (1970) 261.
9 A. Isozaki and S. Utsumi, *J. Chem. Soc. Japan*, 88 (1967) 741.
10 S. Utsumi and A. Isozaki, *J. Chem. Soc. Japan*, 88 (1967) 545.
11 Commissariat a l'energie atomique, *C.E.A. Report No. 66*, (1961).
12 Z. K. Karalova and A. A. Nemodruk, *Z. Anal. Khim.*, 18 (1963) 615.
13 A. Gomez Coedo and J. L. Jimenez, *Rev. Met. (Madrid)*, 4 (1968) 447.
14 O. B. Skaar, *Anal. Chim. Acta*, 28 (1963) 200.
15 C. A. Wamser, *J. Amer. Chem. Soc.*, 70 (1948) 1209; 73 (1951) 499.

Analytica Chimica Acta, 70 (1974) 351–357

KINETIC STUDY AND ANALYTICAL APPLICATION OF THE IODATE–ARSENITE REACTION IN STRONGLY ACIDIC SOLUTIONS

M. I. KARAYANNIS, S. M. TZOUWARA-KARAYANNI and T. P. HADJIIOANNOU
Laboratory of Analytical Chemistry, University of Athens, Athens (Greece)
(Received 22nd October 1973)

It is well known[1–4] that the iodate–arsenite reaction (Dushman reaction) takes place in two main steps as follows:

$$3\,AsO_3^{3-} + IO_3^- \xrightarrow{k_1} 3\,AsO_4^{3-} + I^- \quad (1)$$

$$5\,I^- + IO_3^- + 6\,H^+ \xrightarrow{k_2} 3\,I_2 + 3\,H_2O \quad (2)$$

If the arsenite reagent is in excess, a third reaction takes place simultaneously with reactions (1) and (2), in which the iodine formed by reaction (2) reacts with the excess of arsenite and vanishes from the reaction mixture:

$$AsO_3^{3-} + I_2 + H_2O \xrightarrow{k_3} AsO_4^{3-} + 2\,I^- + 2\,H^+ \quad (3)$$

The above series of reactions which shows analogy to the well-known Landolt reaction[5] has been studied by many investigators[6–8], under conditions where the reaction is relatively slow, so that the Landolt effect can be followed with a stop watch. Bognar and Sarosi[4] used the catalytic action of iodide on the iodate–arsenite reaction to determine concentrations of iodide in the range 1–50 μg.

In the work described here, this reaction was studied under conditions where the appearance of iodine, after mixing of the reagents, is much faster (ms range). The concentration of arsenite used was small compared to the iodate and hydrogen ion concentrations, so that the iodine consumption described by eqn. (3) could not be observed. Under such conditions, the overall reaction of the consecutive reactions (1) and (2) can be described by the equation

$$5\,AsO_3^{3-} + 2\,IO_3^- + 2\,H^+ \xrightarrow{k} 5\,AsO_4^{3-} + I_2 + H_2O \quad (4)$$

Arsenite could be determined in the range $5.0 \cdot 10^{-4}$ *M*–$1.0 \cdot 10^{-2}$ *M* with an average error of about 3%.

EXPERIMENTAL

Apparatus

A commercial spectrophotometer for the study of fast reactions (Durrum-Gibson Stopped-Flow Spectrophotometer, Model D-131) was used. The signal from the photomultiplier was fed to the differential amplifier A263 of a Tektronix storage oscilloscope and the course of the transmittance of the reacting system was followed on the screen of the storage scope and photographed with a polaroid camera.

Solutions

All solutions were prepared in doubly distilled water from reagent-grade chemicals.

Potassium iodate solution, 0.150 M. Dissolve 32.10 g of reagent in 1 l of water. Prepare more dilute solutions by appropriate dilution.

Arsenite solution, 0.1000 M. Dissolve 19.78 g of As_2O_3 in 1 *M* sodium hydroxide, neutralize and dilute to 1 l with sulfuric acid to a final concentration of 0.500 *M* acid.

The final concentrations of the reagents in the reaction mixture are half of those given in the Figures and Tables, because of the mixing of the reagents in a ratio of 1:1. All runs were performed at 28°C, unless otherwise stated, with the reagents well thermostated before mixing. The formation of iodine was followed at 460 nm.

Procedure

Switch the unit on at least 30 min before the measurements are started, and turn the lamp selector knob at the TUNGSTEN position. Set the wavelength selector knob at the 330–1000 nm position and the filter-slide control at the 360–550 nm position. Turn the wavelength dial at 460 nm and the slit-width control at 0.5 mm. Fill the two 20-ml reservoir syringes and two 2-ml drive syringes with the iodate and arsenite solutions. Push the ACTUATE button once for each measurement. For better precision push the ACTUATE button at least twice before each measurement, to ensure thorough cleaning of the reaction cell from traces of iodide produced; the latter acts catalytically on the iodate–arsenite reaction.

RESULTS AND DISCUSSION

In order to study the effect of reagent concentration on the reaction rate, the concentration of each substance taking part in the reaction was changed in turn, keeping the concentration of the other substances constant and measuring the reaction rate (for example, from the slope of the curve of voltage against

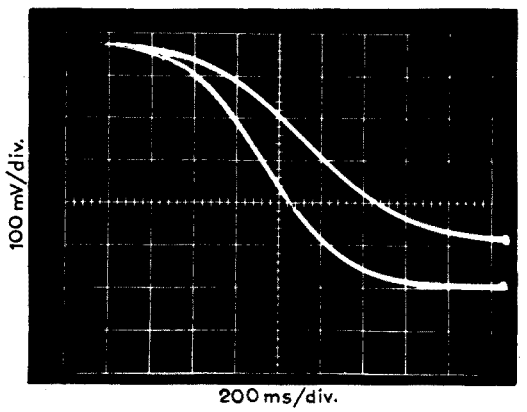

Fig. 1. Typical oscilloscope picture of the iodate–arsenite reaction in strongly acidic solutions 0.150 *M* KIO_3. AsO_3^{3-}: A, $2.5 \cdot 10^{-3}$ *M*, B, $4.0 \cdot 10^{-3}$ *M*, in 0.500 *M* H_2SO_4.

time). Thus to study the effect of arsenite, the potassium iodate concentration and the pH were kept constant at 0.150 M and 1.00 M, respectively, and the arsenite concentration was varied from $1.00 \cdot 10^{-4}$ M to $1.00 \cdot 10^{-2}$ M. A typical oscilloscope picture is shown in Fig. 1. The two curves correspond to two different arsenite concentrations. The slope of the linear part of such curves, dV/dt, is proportional to the arsenite concentration in the range $5 \cdot 10^{-4}$–$1 \cdot 10^{-2}$ M (Table I) and is used

TABLE I

REACTION RATE DATA FOR WORKING CURVE

Concentration of AsO_3^{3-} ($M \cdot 10^4$)	*Reaction rate dV/dt ($mV\ s^{-1}$)*	*Final absorbance (Abs. units)*
1	2.8	—
3	16.4	—
5	40.7	—
7	69.5	0.111
10	142.0	0.147
20	335	0.285
30	510	0.438
40	750	0.577
50	960	0.699
60	1160	0.823
70	1420	—
80	1560	—
90	1690	—
100	1900	—

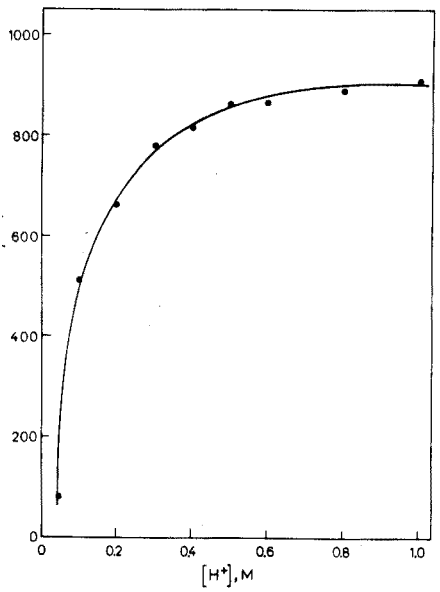

Fig. 2. Effect of iodate concentration on reaction rate.

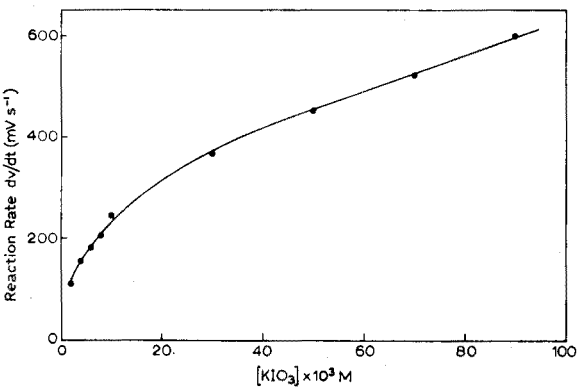

Fig. 3. Effect of hydrogen ion concentration on reaction rate.

for the plotting of the working curve, which is linear in the above range. Figures 2 and 3 illustrate the effects of iodate and hydrogen concentrations on the rate of the reaction.

The molar absorptivity $\varepsilon(I_2)$ for iodine solutions under the conditions used was calculated from the data of Table I. First, it was necessary to prove that the known stoichiometry of reaction (4), as the overall reaction, is also valid for the applied experimental conditions, *i.e.* in strongly acidic solutions.

If it is assumed that the coefficients are x, y and z for AsO_3^{3-}, IO_3^- and H^+, respectively, the initial rate (rate of formation of iodine) can be expressed as:

$$\frac{d[I_2]}{dt} = k[AsO_3^{3-}]^x[IO_3^-]^y[H^+]^z \tag{5}$$

For constant concentrations of iodate and hydrogen ion:

$$\frac{d(I_2)}{dt} = k_{obs}[AsO_3^{3-}]^x \tag{6}$$

where

$$k_{obs} = k[IO_3^-]^y[H^+]^z \tag{7}$$

From Beer's law, $A = \varepsilon b[I_2]$, and by differentiation we have

$$\frac{d(I_2)}{dt} = \frac{1}{\varepsilon b} \cdot \frac{dA}{dt} \tag{8}$$

By combining eqns. (6) and (8):

$$\frac{dA}{dt} = k_{obs}(\varepsilon b)[AsO_3^{3-}]^x = K[AsO_3^{3-}]^x \tag{9}$$

or

$$\log \frac{dA}{dt} = \log K + x \log[AsO_3^{3-}] \tag{10}$$

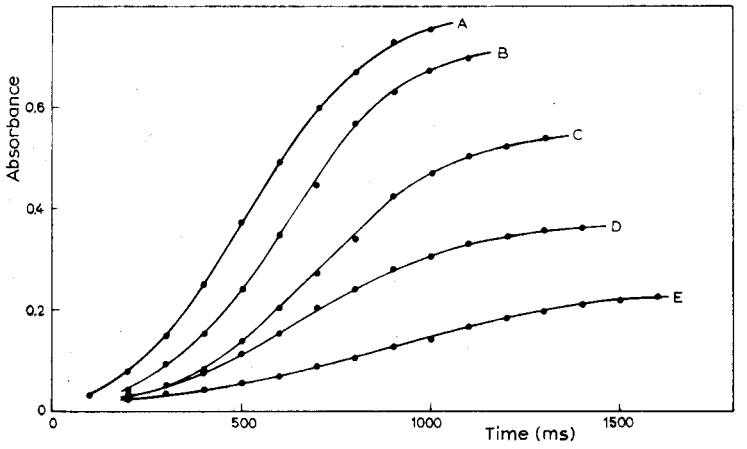

Fig. 4. Reaction curves (absorbance *versus* time) calculated from oscilloscope photographs. 0.150 *M* KIO_3. AsO_3^{3-}: A, $5.0 \cdot 10^{-3}$ *M*; B, $4.5 \cdot 10^{-3}$ *M*; C, $3.5 \cdot 10^{-3}$ *M*; D, $2.5 \cdot 10^{-3}$ *M*; E, $1.5 \cdot 10^{-3}$ *M*.

By calculating absorbance from the scope photographs (by calibration, 800 mV on the scope was equivalent to 100% transmittance) and plotting absorbance *versus* time, the group of curves given in Fig. 4 was obtained.

The initial values of dA/dt can be determined from the slopes of the linear parts of the curves of Fig. 4. By plotting $\log(dA/dt)$ *vs.* $\log[AsO_3^{3-}]$, a straight line was obtained, from the slope of which x was calculated to be 1.01. By the same technique, it was found that $y=z=0.42$. Thus it was proved that the stoichiometry of eqn. (4) is also valid for strongly acidic solutions.

According to eqn. (4), 1 mole of iodine is obtained from 5 moles of arsenite, so that with the 1:1 dilution:

$$[I_2]_{(final)} = 0.1\,[AsO_3^{3-}]_{(original)} \tag{11}$$

The final absorbances corresponding to each concentration of arsenite, as taken from the oscilloscope photographs, are given in column (3) of Table I. From the data of Table I and Beer's law, it was found that the molar absorptivity $\varepsilon(I_2)=710$ l mol^{-1} cm^{-1}. This value is in good agreement with the value 746 given in the literature[9] for aqueous solutions at 460 nm.

Temperature effect

The effect of temperature on the rate of the reaction is shown in Fig. 5. From Arrhenius plots of $\log(dV/dt)$ *versus* reciprocal of absolute temperature, the activation energy was calculated to be 5.9 kcal mol^{-1}.

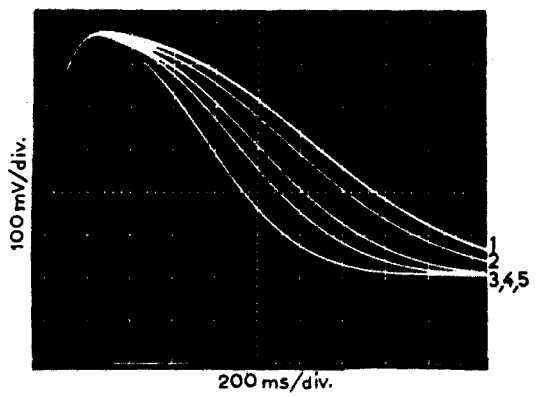

Fig. 5. Effect of temperature on reaction rate. 0.150 *M* KIO_3. $4\cdot10^{-3}$ *M* AsO_3^{3-} in 0.5 *M* $HClO_4$. 1, 14°C; 2, 18°C; 3, 22°C; 4, 25°C; 5, 29°C.

The use of $\log(dV/dt)$ instead of $\log k$ for the Arrhenius plots can be explained as follows:

$$A = -\log T = -\log(V/800) \tag{12}$$

where A=absorbance, T=transmittance and V=voltage in mV (800 mV are equivalent to $T=1.000$). By differentiating eqn. (12):

$$\frac{dA}{dt} = \frac{2.303}{T}\cdot\frac{dT}{dt} = -\frac{2.303}{V}\cdot\frac{dV}{dt} \tag{13}$$

By combining eqns. (9) and (13):

$$K[AsO_3^{3-}] = -\frac{2.303\,\frac{dV}{dt}}{V} \tag{14}$$

By taking the slopes of the curves in Fig. 5 at the same potential V, eqn. (14) becomes:

$$K = \Theta\left(\frac{dV}{dt}\right) \tag{15}$$

or

$$\log K = \log \Theta + \log \frac{dV}{dt} \tag{16}$$

The activation energy was determined for three different acids, sulfuric, perchloric and hydrochloric, and was found to be 5.9 kcal, 6.3 kcal and 4.1 kcal, respectively. The smaller value with hydrochloric acid can be attributed to the catalytic effect of chloride on the reaction rate.

Analytical application

The iodate–arsenite reaction was used for the kinetic determination of arsenite in aqueous solutions. Analyses of aqueous arsenite solutions of known concentrations gave the results shown in Table II. The data indicate that arsenite in the concentration range $5.0 \cdot 10^{-4}$ M–$1.0 \cdot 10^{-2}$ M could be determined with relative errors of about 3%. The relative standard deviation for a $4 \cdot 10^{-3}$ M arsenite solution was about 2%.

TABLE II

RESULTS FOR AQUEOUS ARSENITE SOLUTIONS

AsO_3^{3-} ($M \cdot 10^4$)		%Error
Taken	Found	
10	10.4	+4.0
30	28.5	−5.0
50	50.5	+1.0
60	60.4	+0.7
70	68.0	−2.8
90	86	−4.4
100	96.5	−3.5
		Mean error 3.1%

The deviation from linearity for concentrations larger than 10^{-2} M arsenite can be explained as follows. At higher concentrations of arsenite, the effect of reaction (3) on the consumption of iodine is significant and therefore the rate of formation of iodine is decreased. In such cases, the arsenite concentration should be brought by dilution to the measurable range.

The final transmittance of the reaction mixture can give an indication of the concentration range of the unknown sample. A concentration of 10^{-2} M arsenite gives a final concentration of 10^{-3} M iodine or a final transmittance equivalent to about 30 mV in the oscilloscope (3,8 $T\%$).

This research was supported in part by NATO research grants No 225 and 548.

SUMMARY

The iodate–arsenite reaction in strongly acidic solutions was studied by stopped-flow spectrophotometric techniques. The molar absorptivity of iodine and the activation energy of the reaction were determined. A method for determining arsenite was developed on the basis of this reaction. The method was checked in the concentration range $5.0 \cdot 10^{-4}$–$1.0 \cdot 10^{-2}$ M, the mean error being about 3%.

REFERENCES

1 J. Eggert, *Helv. Chim. Acta*, 32 (1949) 692.
2 J. Eggert and T. Rohr, *Helv. Chim. Acta*, 36 (1953) 855.
3 J. Eggert, *Helv. Chim. Acta*, 36 (1953) 868.
4 J. Bognar and S. Sarosi, *Anal. Chim. Acta*, 29 (1963) 406.
5 H. Landolt, *Ber.*, 19 (1886) 1317; 20 (1887) 745.
6 J. Eggert and B. Scharnow, *Z. Elektrochem.*, 27 (1921) 457.
7 R. P. Sanyal and N. R. Dhar, *Z. Anorg. Allgem. Chem.*, 139 (1924) 169.
8 S. Dushman, *Zh. Fiz. Khim.*, 8 (1904) 481.
9 A. D. Awtrey and R. E. Connick, *J. Amer. Chem. Soc.*, 73 (1951) 1842.

Analytica Chimica Acta, 70 (1974) 359–364

KONTINUIERLICHE KATALYTISCH-KINETISCHE BESTIMMUNG VON SILBER UND SULFID IM P.P.M.-BEREICH UNTER VERWENDUNG EINER DURCHFLUSSZELLE

H. LUDWIG, H. WEISZ und T. LENZ

Lehrstuhl für Analytische Chemie, Chemisches Laboratorium, Universität Freiburg i.Br. (Bundesrepublik Deutschland)

(Eingegangen den 1. Dezember 1973)

In einer vor kurzem veröffentlichten Arbeit wurde eine kinetische Strömungsmethode unter Verwendung katalysierter Reaktionen beschrieben[1]. Dabei wird eine Durchflusszelle zugleich als Mischkammer, Reaktionsgefäss und Messzelle verwendet. Der zu bestimmende Katalysator sowie die beiden Reaktionspartner der katalysierten Reaktion fliessen gesondert in drei Strömen mit konstanter Geschwindigkeit in die Durchflusszelle und werden dort möglichst augenblicklich und vollständig durchmischt; die resultierende Lösung verlässt hernach kontinuierlich die Zelle. In diesem strömenden System stellt sich für jede Katalysatorkonzentration ein entsprechender stationärer Zustand in Bezug auf die Konzentrationen aller Reaktionspartner und Reaktionsprodukte ein. Die stationäre Konzentration eines geeigneten Reaktionspartners wird photometrisch gemessen und daraus die zu bestimmende Konzentration der katalytisch aktiven Substanz ermittelt. Auf diese Weise lassen sich indirekt auch Inhibitoren und Reaktivatoren bestimmen[1].

In der vorliegenden Arbeit wird als weiteres Anwendungsbeispiel für diese Strömungsmethode die Bestimmung von Silber und Sulfid beschrieben.

Silber vermag die Oxidation von Sulfanilsäure durch Kaliumperoxodisulfat zu einem farbigen Reaktionsprodukt (Absorptionsmaximum bei 425 nm) stark zu beschleunigen[2,3]. Durch 2,2'-Bipyridin als Aktivator wird die katalytische Wirksamkeit von Silber noch beträchtlich erhöht[3].

Die stationäre Konzentration des Oxidationsproduktes der Sulfanilsäure[2] wird photometrisch gemessen. Je höher die Konzentration des katalytisch aktiven Silbers ist, je schneller also die Reaktion abläuft, desto höher ist naturgemäss die stationäre Konzentration des Oxidationsproduktes, und umgekehrt. Sulfid hemmt die katalytische Aktivität von Silber in definierter Weise (Bildung von Silbersulfid) und lässt sich somit indirekt bestimmen.

EXPERIMENTELLES

Die verwendete Versuchsanordnung wurde bereits ausführlich beschrieben[1]

Sulfanilsäurelösung, Kaliumperoxodisulfatlösung und die Probelösung werden mittels einer Schlauchpumpe (Buchler Instruments, Fort Lee, Modell 2-6200) kontinuierlich mit jeweils gleicher Strömungsgeschwindigkeit in die Durchflusszelle (Schichtlänge 10 mm, äussere Höhe 22 mm, äussere Breite 12,5 mm, siehe Abb. 1)

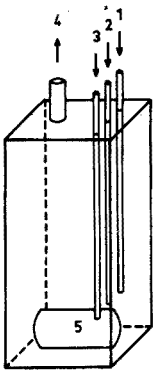

Abb. 1. Schematische Darstellung der Durchflusszelle. (1) Schlauch für Sulfanilsäure/2,2'-Bipyridin-Lösung, (2) Schlauch für Probelösung, (3) Schlauch für Kaliumperoxodisulfatlösung, (4) Abfluss, (5) Magnetrührstab.

gepumpt und dort mit einem Magnetrührer durchmischt. Die drei in die Pumpe eingelegten Schläuche bestanden aus Tygon (Innen-∅ 0,79 mm, Wandstärke 0,79 mm). Daran schloss sich jeweils ein in einem Thermostatmantel befindliches Stück Polyäthylenschlauch (Länge 210 mm, Innen-∅ 1 mm) an, das mit einem kurzen, in die Durchflusszelle eintauchenden Schlauchstück (Polyäthylen, Innen-∅ 0,5 mm, siehe Abb. 1) verbunden war.

Die kontinuierliche photometrische Messung erfolgte mit dem Spektralphotometer PMQ II (Fa. Zeiss, Oberkochen), an das ein Schreiber angeschlossen war. Die Durchflusszelle befand sich in einem temperierten Aluminumblock, welcher nach den Massen der Küvette und des temperierbaren, mit einem Magnetrührer ausgestatteten Küvettenhalters des Spektralphotometers angefertigt wurde.

Lösungen

Alle Lösungen wurden aus entsprechenden Reagenzien (*pro analysi*) mit bidestilliertem Wasser angesetzt.

Sulfanilsäure/2,2'-Bipyridin-Lösung. 1,039 g Sulfanilsäure + 0,375 g 2,2'-Bipyridin mit Citratpufferlösung (siehe unten) ad 500 ml. Die Lösung ist im Dunkeln bis zu einer Woche haltbar.

Kaliumperoxodisulfat-Lösung. 30 g $K_2S_2O_8$ werden unter leichtem Erwärmen auf 30–35°C in nahezu 500 ml Wasser gelöst und anschliessend auf 500 ml aufgefüllt. Die Lösung ist 2 Tage haltbar.

Natriumcitrat–Schwefelsäure-Puffer, pH 4,4. 320 ml 0,05 *M* Schwefelsäure + 680 ml 0,1 *M* Natriumcitratlösung. (21,01 g Citronensäure + 200 ml 1 *M* Natronlauge mit bidestilliertem Wasser ad 1000 ml.)

Alle hochverdünnten, zur Aufnahme der Eichkurve verwendeten Silberlösungen und die Silber-Standardlösung zur Sulfidbestimmung (6 μg Ag ml^{-1}) wurden in Messkolben hergestellt und aufbewahrt, welche mit konzentrierter Salpetersäure gereinigt wurden und mindestens zwei Tage mit den verdünnten Silberlösungen in Berührung waren. Diese Lösungen wurden selbstverständlich hernach verworfen. Auf diese Weise werden bei nachfolgender Benützung der Gefässe Substanzverluste durch Adsorption von Silber an Glas[4] vermieden, welche insbesondere

bei verdünnten Lösungen eine Fehlerquelle darstellen können.

Verdünnte Sulfidlösungen wurden aus einer Sulfid-Stammlösung ($Na_2S \cdot 9\ H_2O$, etwa 0,7 mg S ml^{-1}) hergestellt, deren Gehalt täglich iodometrisch bestimmt wurde. Der Titer der im Dunkeln aufbewahrten Stammlösung nahm innerhalb von 24 Stunden um etwa 1–3% ab. Die verdünnten Sulfidlösungen wurden nicht länger als 2 Stunden aufbewahrt.

Bestimmung von Silber

Nach Einschalten des Photometers (420 nm) wartet man so lange, bis sich am Gerät eine konstante Anzeige eingestellt hat; auch soll zwischen den Messreihen das Gerät ständig betriebsbereit gehalten werden. Die Raumtemperatur soll möglichst konstant sein, da eine Störung des thermischen Gleichgewichts des Gerätes zu Fehlern in der Anzeige führt.

Vor jeder längeren Messreihe wird bidestilliertes Wasser durch die Zelle gepumpt und die Grundlinie (= 100% Transmission) bei 420 nm eingeregelt. Diese Einstellung wird nach etwa 2,5 Stunden überprüft. Die Messungen werden bei einer Durchflussgeschwindigkeit in der Zelle von 1,8 ml min^{-1} (1 Schlauch = 0,6 ml min^{-1}) durchgeführt. Sulfanilsäure 2,2'Bipyridin-Lösung und Kaliumperoxodisulfatlösung befinden sich im Bad des Thermostaten (30,0 ± 0,1°C).

Nach Erreichen des stationären Zustandes im System wird die Transmission vor dem nächsten Probenwechsel noch 2–3 Minuten gemessen (Abb. 2). Der Mittelwert der Transmission wird aus der registrierten Kurve entnommen und in die Extinktion (E_s) umgewandelt.

Die Konzentration der Probe wird unter Verwendung einer Eichkurve

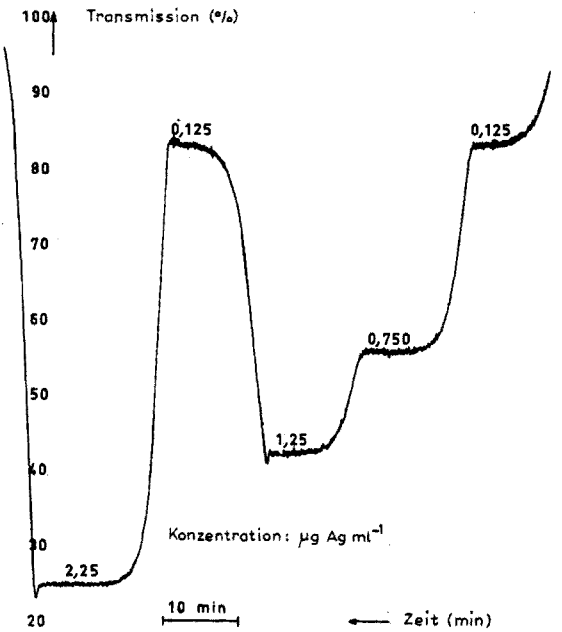

Abb. 2. Ausschnitt aus einer vom Schreiber registrierten Kurve. Bestimmung von Silber.

(Abb. 3) ermittelt, welche mit Lösungen folgender Konzentrationen aufgenommen wird: 0,1; 0,25; 0,5; 0,75; 1,0; 1,5; 2,0; 2,5; 3,0; 3,5 und 4,0 μg Ag ml^{-1}.

Bestimmung von Sulfid

Bei der Bestimmung von Sulfid wird die Probelösung mit Silber-Standardlösung (6 μg Ag ml^{-1}) in einem T-Stück aus kapillarem Glasrohr (Innen-$\varnothing$ 1 mm, Schenkellänge 20 mm) kontinuierlich zusammengeführt und durchmischt. Die resultierende Lösung durchströmt hernach eine Verzögerungsstrecke (Polyäthylenschlauch, Länge 750 mm, Innen-$\varnothing$ 1 mm, Verzögerungszeit etwa 0,5 min), um eine möglichst vollständige Reaktion von Sulfid mit Silber zu erreichen, und gelangt anschliessend in die Durchflusszelle. Die Strömungsgeschwindigkeit in der Zelle beträgt 2,0 ml min^{-1} (1 Schlauch = 0,5 ml min^{-1}). Die Eichkurve für Sulfid wird mit Lösungen folgender Konzentrationen aufgenommen: 0,2; 0,3; 0,4; 0,5; 0,6; 0,7; 0,8 und 0,9 μg S ml^{-1} (Abb. 4).

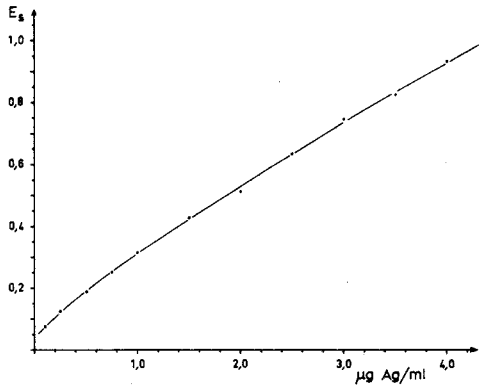

Abb. 3. Eichkurve zur Bestimmung von Silber.

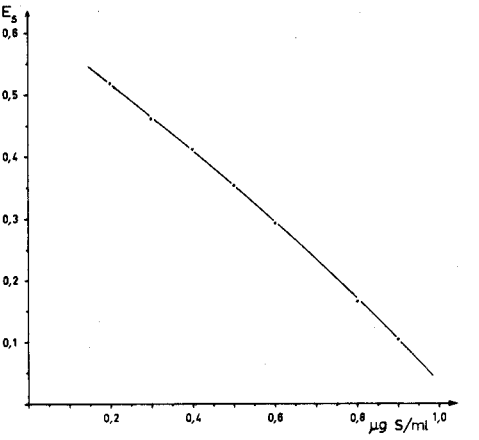

Abb. 4. Eichkurve zur Bestimmung von Sulfid.

Ansonsten erfolgt die Bestimmung von Sulfid in der gleichen Weise wie diejenige für Silber.

ERGEBNISSE UND DISKUSSION

Einige Resultate von Einzelbestimmungen sind in Tabelle 1 wiedergegeben.

Untersuchungen über den störenden Einfluss einiger Ionen auf die Bestimmung des Katalysators Silber wurden bereits von Bontchev *et al.*[3] unter Anwendung der Tangentenmethode[5] durchgeführt. Wir haben die störende Wirkung einiger Ionen auf die Bestimmung des Inhibitors Sulfid mit der kontinuierlichen kinetischen Methode untersucht. Es wurden dabei Ionen berücksichtigt, die insbesondere bei der Wasseranalyse von Interesse sind[6].

Zwei Messreihen wurden hierzu durchgeführt. Zur ersten Messreihe wurden Lösungen verwendet, die 0,3 μg S ml^{-1} und zusätzlich das zu untersuchende

TABELLE I

BESTIMMUNG VON SILBER UND SULFID

Silber ($\mu g\ ml^{-1}$)		*Standardabweichung*[a]	*Sulfid ($\mu g\ ml^{-1}$)*		*Standardabweichung*[a]
Gegeben	*Gefunden*		*Gegeben*	*Gefunden*	
0,125	0.120	±0,0100	0,200	0,190	±0,0228
0,250	0,250	±0,0141	0,300	0,287	±0,0147
0,750	0,750	±0,0245	0,400	0,415	±0,0116
1,25	1,22	±0,022	0,500	0,505	±0,0165
1,75	1,67	±0,048	0,600	0,570	±0,0239
2,75	2,86	±0,047	0,700	0,745	±0,0234
3,50	3,35	±0,108	0,800	0,839	±0,0461
4,00	3,90	±0,173	0,900	0,895	±0,0282

[a] Berechnet aus 5 Messergebnissen.

Fremdion enthielten. Als zulässige Konzentration an Fremdion wurde diejenige definiert, welche bei einer Einzelbestimmung einen relativen Fehler kleiner als 15% verursacht. Die zweite analoge Messreihe wurde mit Lösungen durchgeführt, die 0,7 μg S ml^{-1} und das Fremdion enthielten. Hier wurde als zulässige Fremdionenkonzentration diejenige definiert, die einen relativen Fehler kleiner als 7,5% verursacht. Die auf diese Weise ermittelten Fremdionenkonzentrationen, welche also in beiden Fällen nicht stören, sind in Tabelle II wiedergegeben. Das molare

TABELLE II

ZULÄSSIGE KONZENTRATION AN FREMDION

Fremdion	*Zulässige Konzentration an Fremdion ($\mu g\ ml^{-1}$)*	*Verhältnis der molaren Konzentrationen ([Fremdion]/[Sulfid])*
NO_3^-	500	$8{,}6 \cdot 10^2$
SO_4^{2-}	500	$5{,}6 \cdot 10^2$
F^-	100	$5{,}6 \cdot 10^2$
CrO_4^{2-}	7	6,4
HCO_3^-	3	5,3
$H_2PO_4^-$	3	3,3
Cl^-	1	3,0
$HAsO_4^{2-}$	0,3	$2{,}3 \cdot 10^{-1}$
CN^-	0,1	$4{,}1 \cdot 10^{-1}$
$S_2O_3^{2-}$	0,1	$9{,}5 \cdot 10^{-2}$
Mg^{2+}	500	$2{,}2 \cdot 10^3$
Ca^{2+}	250	$6{,}7 \cdot 10^2$
Cu^{2+}	3	5,0
Mn^{2+}	1	2,0
Pb^{2+}	1	$5{,}2 \cdot 10^{-1}$
Zn^{2+}	0,3	$4{,}9 \cdot 10^{-1}$
Hg^{2+}	0,1	$5{,}3 \cdot 10^{-2}$
Fe^{3+}	0,4	$7{,}7 \cdot 10^{-2}$

[a] Berechnet für die Sulfidkonzentration $9{,}4 \cdot 10^{-6}$ *M*.

Verhältnis der Konzentrationen Fremdion: Sulfid wurde für die Sulfidkonzentration 0,3 μg ml^{-1} ($=9.4 \cdot 10^{-6}$ M) berechnet.

ZUSAMMENFASSUNG

Die Bestimmung von Silber und Sulfid im p.p.m.-Bereich mit einer katalytisch–kinetischen Strömungsmethode wird beschrieben. Bei dieser Methode wird eine Durchflusszelle als Mischkammer, Reaktionsgefäss und Messzelle verwendet. Die Bestimmung von Silber beruht auf seiner beschleunigenden Wirkung auf die Oxidation von Sulfanilsäure durch Kaliumperoxodisulfat mit 2,2′-Bipyridin als Aktivator. Sulfid hemmt die katalytische Aktivität von Silber und kann daher indirekt bestimmt werden. Der Einfluss von 18 Kationen und Anionen auf die Sulfidbestimmung wird ebenfalls beschrieben.

SUMMARY

The determination of silver and sulphide in the p.p.m. range by a catalytic–kinetic flow method is described. A flow-through cell is used as the mixing and reaction vessel as well as for measurement. The determination of silver is based on its catalytic action on the oxidation of sulphanilic acid by potassium persulphate in the presence of 2,2′-bipyridine. Sulphide retards the catalytic activity of silver and so can be determined indirectly. Interfering ions are studied.

LITERATUR

1 H. Weisz und H. Ludwig, *Anal. Chim. Acta*, 62 (1972) 125.
2 A. Alexiev und P. R. Bontchev, *Mikrochim. Acta*, (1970) 13.
3 P. R. Bontchev, A. Alexiev und B. Dimitrova, *Talanta*, 16 (1969) 597.
4 F. K. West, P. W. West und F. A. Iddings, *Anal. Chem.*, 38 (1966) 1566.
5 K. B. Yatsimirskii, *Kinetic Methods of Analysis*, Pergamon Press, Oxford, 1966, S. 39.
6 J. E. Zajic, *Water Pollution, Vol. 1*, Marcel Dekker, New York, 1971, p. 7.

Analytica Chimica Acta, 70 (1974) 365–374

A PHOTOMETRIC AND POTENTIOSTATIC INVESTIGATION OF THE COMPLEX FORMATION BETWEEN FLUORIDE AND LANTHANUM–ALIZARIN COMPLEXONE

T. ANFÄLT and D. JAGNER

Department of Analytical Chemistry, University of Gothenburg, Fack, S-402 20 Göteborg 5 (Sweden)

(Received 5th November 1973)

In 1959 Belcher *et al.*[1] suggested that the blue complex formed between fluoride and lanthanum–alizarin complexone (alizarin fluorine blue) could be exploited for the determination of fluoride. Since then, several investigations have shown this method to be both accurate and precise and it has found application in, for example, the analysis of fluoride in sea water. Several attempts have been made, by means of spectrophotometric measurements, to elucidate the composition of the blue complex and to suggest a possible mechanism for its formation. The most generally accepted reaction for its formation is

$$\mathrm{MHA(red)} + \mathrm{F^-} \rightleftarrows \mathrm{MFA^{2-}(blue)} + \mathrm{H^+} \qquad (1)$$

where M can be cerium or praseodymium[2] instead of lanthanum. Ingman[3] has determined a conditional stability constant for this reaction for M = La, while Leonard and West[4] have proposed a mechanism for the formation of the cerium alizarin complex. According to this mechanism, the fluoride ion displaces one of the water molecules coordinated to the metal whereupon the strong electrophilic effect of the fluoride ion causes removal of proton 4 in alizarin complexone (I), protons 1–3 having, of course, been removed during the formation of the metal–alizarin complexone complex. Whereas it could seem possible that the initial step in the mechanism ought to be the displacement of a water molecule by a fluoride ion, the strong electrophilic nature of the fluoride ion is indeed debatable.

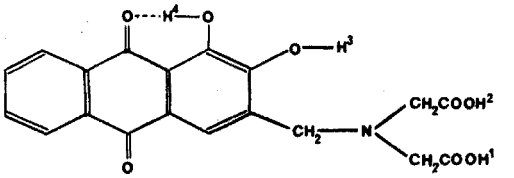

I

From Job plot techniques. Jeffery and Williams[5] have suggested the formula $Ce_5F_4A_4$ for the blue cerium complex. The Job plot technique does not, however, yield results of very high precision in ternary systems and, moreover, the results are difficult to interpret at high fluoride concentrations where it is likely that the metal is coordinated to more than one fluoride ion.

Langmyhr *et al.*[6] have suggested the formula $(MA)_2F_2$ for the complex or, rather, $(MHA)_2F_2$, according to Fig. 4 of their paper. The latter formula, however, seems improbable.

Owing to the development of the lanthanum trifluoride membrane electrode, the formation of the lanthanum–fluoride–alizarin complexone complex can now be studied potentiometrically as well as photometrically. Moreover, with computer-processed titration equipment, it is possible to undertake titration procedures which would be extremely difficult, if not impossible, to carry out manually. It was hoped that the results of such an investigation might, besides providing more information concerning the blue complex itself, also help to explain the interference of carboxylate with the lanthanum fluoride membrane electrode[7–9].

THEORY

The composition of the lanthanum–fluoride–alizarin complexone complex was investigated by means of potentiometric and photometric titrations in which increments of lanthanum titrant were added to solutions containing different total concentrations of fluoride, alizarin complexone and protons. Two different sets of experimental data were collected, one at constant pH and the other at constant pH and pF.

Titrations at constant pH

The net titration reaction is assumed to be

$$x\mathrm{La} + z\mathrm{H}_{4-c}\mathrm{A} + b\mathrm{F} \rightarrow \mathrm{La}_x\mathrm{H}_y\mathrm{A}_z\mathrm{F}_b + (z(4-c)-y)\mathrm{H} \qquad (2)$$

where c denotes the number of moles of hydroxide ions which must be added to one mole of alizarin complexone in order to obtain the pH value under consideration. The addition of titrant increments of lanthanum nitrate to a solution containing fluoride and alizarin will result in the liberation of hydrogen ions as long as the ratio of the total amount of lanthanum to the total amount of alizarin is less than $x:z$. Once this value is reached, further addition of lanthanum will not liberate any appreciable amounts of hydrogen ions, *i.e.* it is no longer necessary to add sodium hydroxide after each increment of lanthanum titrant in order to keep the pH constant. Consequently, if the total amount of hydroxide ions which must be added in order to maintain a constant pH is plotted against v ml of lanthanum titrant added, a break-point curve with two linear legs will be obtained. The slope of the leg after the break-point will be close to zero provided, of course, that eqn. (2) describes the complex formation. The total concentrations of lanthanum, alizarin complexone, fluoride and protons are known for each titration point, as are the free fluoride and proton concentrations. Consequently, it is possible to compute the ratios $x:y:z:b$ at the break-point. The free lanthanum and alizarin complexone concentrations in the break-point can be assumed to be negligible compared with their total concentrations.

Titrations at constant pH and pF

The interpretation of the titration data according to the net reaction given in eqn. (2) is particularly difficult at low and high total fluoride concentrations. At low fluoride concentrations complexes of composition $\mathrm{La}_x\mathrm{H}_y\mathrm{A}_z$ may interfere. At high fluoride concentrations only a minor fraction of the total amount of fluoride enters the blue complex and, consequently, the potentiometric fluoride

measurements will be poor in precision. In order to overcome these difficulties, titrations were carried out at constant pF, *i.e.* the total fluoride concentration was increased after each increment of lanthanum nitrate added. Moreover, constant pF considerably simplifies the equilibrium calculations.

EXPERIMENTAL

Reagents

All reagents were of analytical grade and the total concentrations of the stock solutions are specified in Table I. Alizarin complexone (Sigma, lot 1 18B-0410) was purified by extraction with methylene chloride as described by Ingman[10]. The elemental analysis showed a composition of 54.0% C, 4.5% H, 3.5% N and 38.0% O (calculated for $C_{19}H_{15}O_8N \cdot 2H_2O$: 54.2% C, 4.5% H, 3.3% N and 38.0% O). Weighed amounts of purified sample were standardized against sodium hydroxide of accurately known concentration by a potentiometric titration procedure. The equivalence volumes evaluated by the Gran plot technique[11] yielded a molecular weight of 421.3 (theoretical 421.15). The stability constants for the two most acidic protons were determined, the potentiometric data being evaluated by means of the computer program HALTAFALL[12,13]. The values of the constants, 2.54 and 5.47 respectively, were in good agreement with those determined by Ingman[10].

TABLE I

CONCENTRATIONS OF STOCK SOLUTIONS

Stock solution	*Concentration*
HCl	$5.00 \cdot 10^{-3}$ *M* in 0.1 *M* NaCl
NaOH	$4.93 \cdot 10^{-3}$ *M* in 0.1 *M* NaCl
$La(NO_3)_3$	$9.95 \cdot 10^{-3}$ *M* (with respect to lanthanum)
NaF	0.0100 M
NaF[a]	$5.00 \cdot 10^{-3}$ *M* in 0.1 *M* NaCl
Alizarin complexone (A)	$8.47 \cdot 10^{-3}$ *M* H_4A in $1.75 \cdot 10^{-2}$ *M* NaOH
NaCl	1.00 *M*

[a] Used in titrations in which pF was kept constant.

Lanthanum nitrate stock solutions were prepared by dissolving the salt in triply distilled water and the solutions were standardized against EDTA with xylenol orange as indicator. The primary standard for EDTA was zinc metal.

Fluoride solutions were prepared by dissolving the sodium salt in triply distilled water. The concentrations of the solutions were checked by precipitation titrations with the standard lanthanum solutions in unbuffered media, the fluoride electrode being used as sensor.

Sodium hydroxide solutions were prepared by dilution of concentrated sodium hydroxide (PH Tamm) with carbonate-free triply distilled water. These solutions were standardized against potassium hydrogenphthalate.

The hydrochloric acid solutions were standardized against the standard sodium hydroxide solutions.

Apparatus

All titrations were performed with a computer-processed titrator[14] The experimental set-up around the titrator is illustrated in Fig. 1.

The filter photometer (EEL Quantitrator) was equipped with an interference filter with a peak wavelength of 600 nm, connected to the digital voltmeter of the titrator *via* a current amplifying operational amplifier (Fairchild A 720)[15]. The arrangement yielded a linear relationship between concentration and absorb-

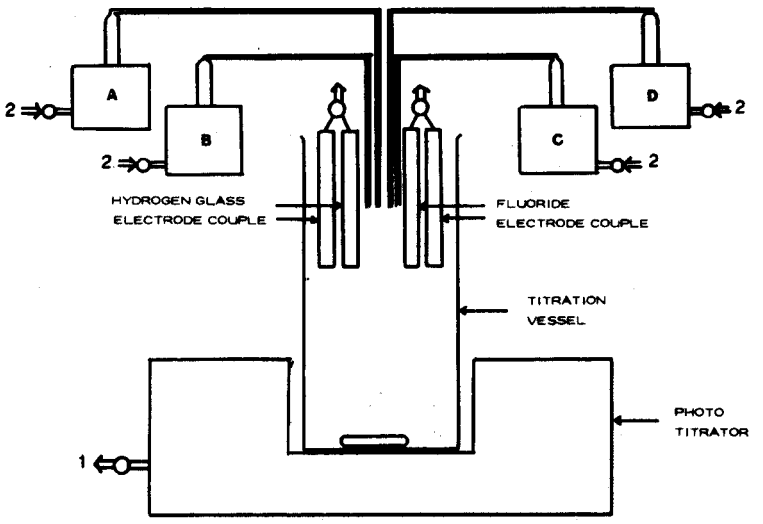

Fig. 1. The experimental set-up around the titrator. A, B, C and D are syringe burets containing hydrochloric acid, sodium hydroxide, lanthanum nitrate and sodium fluoride, respectively. The symbol numbered 1 indicates an analog signal which is fed into the computerized titrator, whereas the symbols numbered 2 indicate a control signal from the computer processing the burets.

TABLE II

VOLUMES OF STOCK SOLUTIONS USED IN TITRATIONS

(For each titration 2 ml of alizarin complexone solution and 25 ml of 1.00 *M* NaCl were taken)

Titration no.	*v ml of stock solution*		*Initial volume*	*pF*
	NaF	*HCl*		
1	0	4.8	282	—
2	0.5	4.9	282	—
3	1	5	283	—
4	1.3	5	283	—
5	1.7	4.8	284	—
6	2.4	4.8	284	—
1′	—	4.6	282	4.95
2′	—	4.8	282	4.75
3′	—	4.5	283	4.45
4′	—	4.8	285	3.97
5′	—	4.7	286	3.85

ance up to one absorbance unit. The glass electrode (Radiometer G 202 B) was connected to the titrator *via* an operational amplifier coupled as a voltage follower. A calomel (Radiometer K 401) reference electrode was used. The fluoride electrode (Orion 94-09) was used together with a single-junction reference electrode (Orion 90-04).

Gel filtrations were performed with Sephadex G 25 (fine) and G 50 (fine), and light-scattering experiments with a photogoniodiffusometer (ARL 42000).

Titration procedures

The computer-processing flow-scheme for the titrations at constant pH and

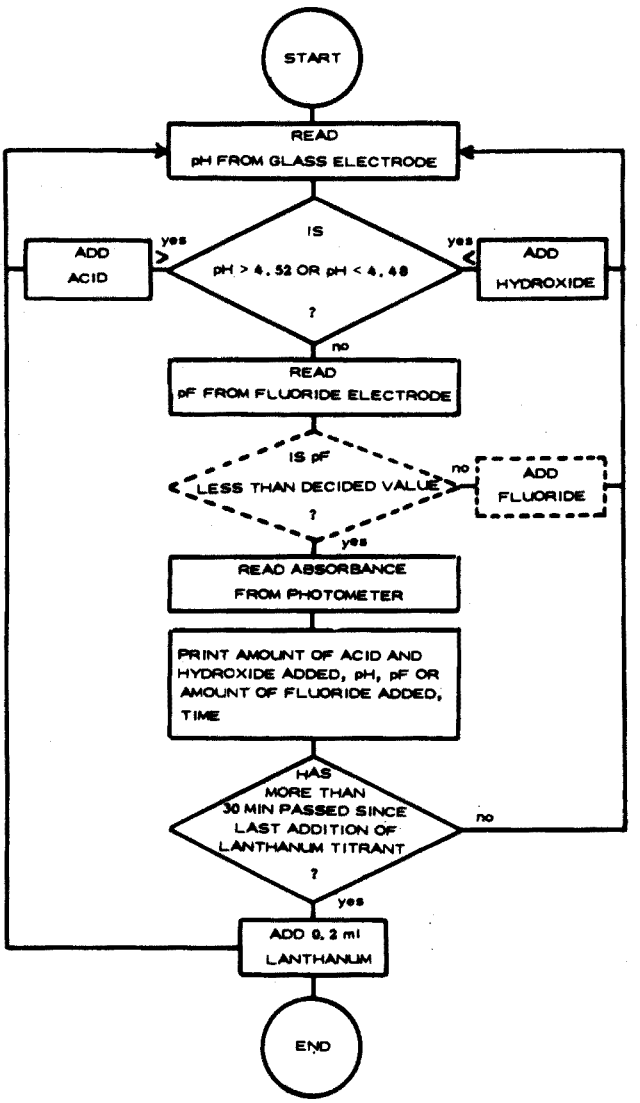

Fig. 2. A flow-scheme of the BASIC program. Dashed lines indicate a routine used only when the fluoride concentration was held constant.

at constant pF and pH is shown in Fig. 2. The glass and fluoride electrodes were calibrated before and after each titration and the duration of a single titration was 24 h, including the time required for calibration.

The total concentrations of the components in the titration vessel for the titration at pH 4.5, and at pH 4.5 for different constant pF values, may be derived from the volumes specified in Table II.

RESULTS

Titrations at constant pH

The results of titrations 1–6 at pH 4.5 are summarized in Table III and Figs 3 and 4.

In Fig. 3, n_H, defined as

$$n_H = ([H]_{tot} - [H^+])/[A]_{tot} \quad (3)$$

is plotted against $[La]_{tot}/[A]_{tot}$, where $[La]_{tot}$ and $[A]_{tot}$ denote the total concentrations of the two components in the titration vessel. As can be seen, the value of n_H decreases linearly with increasing $[La]_{tot}/[A]_{tot}$ down to a break-point after which

TABLE III

n_H AND n_F VALUES AT THE BREAK-POINTS IN TITRATIONS 1–6

Titration no.	$[F]_{tot}/[A]_{tot}$	$[La]_{tot}/[A]_{tot}$	$\bar{n}_H$	$\bar{n}_F$
1	0	1.00	0.56	0
2	0.29	1.03	0.46	0.25
3	0.59	1.12	0.35	0.44
4	0.77	1.19	0.25	0.53
5	1.00	1.25	0.10	0.53
6	1.42	1.25	0.14	0.57

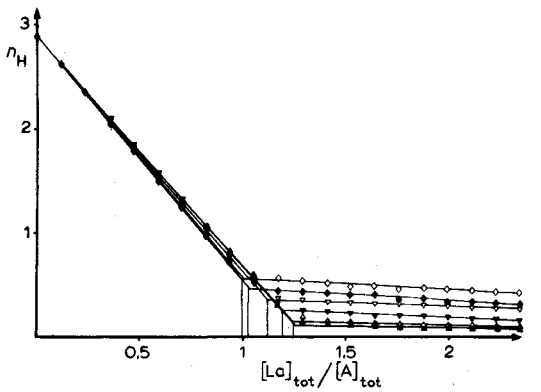

Fig. 3. n_H plotted against $[La]_{tot}/[A]_{tot}$ for different total concentrations of fluoride. Titration no. (*cf.* Table II): (◇) 1, (◆) 2, (▽) 3, (▼) 4, (▲) 5, (△) 6.

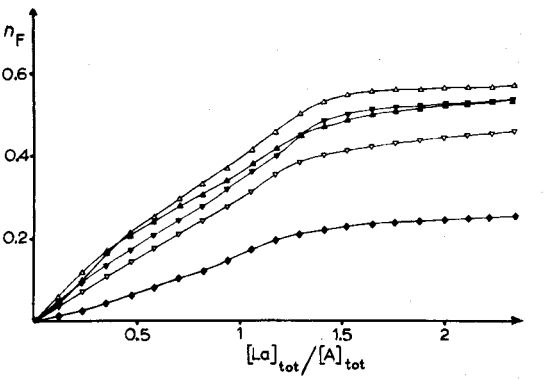

Fig. 4. n_F plotted against $[La]_{tot}/[A]_{tot}$ for different total concentrations of fluoride. Titration no. (*cf.* Table II): (◆) 2, (▽) 3, (▼) 4, (▲) 5, (△) 6.

n_H is almost constant. Moreover, the value of $[La]_{tot}/[A]_{tot}$ at the break-point varies with the total fluoride concentration in the titration vessel. In titration no. 1, where the total fluoride concentration is zero, $[La]_{tot}/[A]_{tot} = 1$ at the break-point, *i.e.* lanthanum and alizarin complexone only form complexes in which the lanthanum–alizarin complexone ratio is 1:1. However, when the total fluoride concentration is increased sufficiently to permit formation of the "blue complex" (this was confirmed photometrically), the $[La]_{tot}/[A]_{tot}$ value at the break-point increases until it reaches a limiting value of 1.25. After this, a further increase in the total fluoride concentration does not increase the $[La]_{tot}/[A]_{tot}$ value at the break-point. The photometric measurements, *i.e.* plots of absorbance *vs.* $[La]_{tot}/[A]_{tot}$, give very similar break-point curves.

The obvious interpretation of these results is that the lanthanum: alizarin complexone ratio in the blue lanthanum–fluoride–alizarin complexone complex is not 1:1 but 1.25:1. Moreover, the value of n_H at the break-point at higher fluoride concentrations is close to zero which indicates that the A:H ratio in the blue complex is, as expected, 1:0. An interesting feature of Fig. 3 is that in titration curve no. 1, *i.e.* in the absence of fluoride, the n_H value at the break-point is 0.56 and not 1.00 as expected. This supports the suggestion made by Langmyhr *et al.*[6] that the lanthanum–alizarin complexone system contains at least one other complex than LaHA.

The fluoride content of the blue complex was determined by plotting n_F:

$$n_F = ([F]_{tot} - [F^-](1 + \beta_{HF}[H^+]))/[A]_{tot}$$

against $[La]_{tot}/[A]_{tot}$, as shown in Fig. 4. Because of the low total fluoride concentrations the precision of the potentiometric measurements was poor. Despite this, it may be seen that the A:F ratio at the break-point is approximately 2:1. The same result was obtained from the photometric data. The relative absorbance at $[La]_{tot}/[A]_{tot} = 1.25$ (*cf.* Fig. 5) is plotted against $[F]_{tot}/[A]_{tot}$ in Fig. 6 and the asymptotes are seen to intersect one another at an $[F]_{tot}/[A]_{tot}$ value of approximately 0.5.

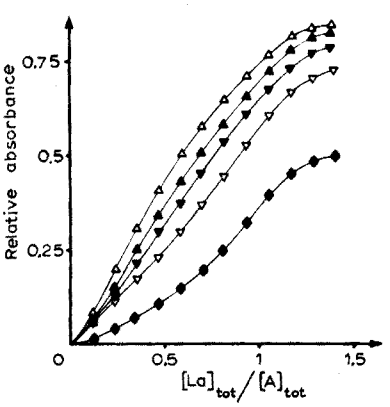

Fig. 5. The relative absorbance plotted against $[La]_{tot}/[A]_{tot}$ for different concentrations of fluoride. Titration no. (*cf.* Table II): (◆) 2, (▽) 3, (▼) 4, (▲) 5, (△) 6.

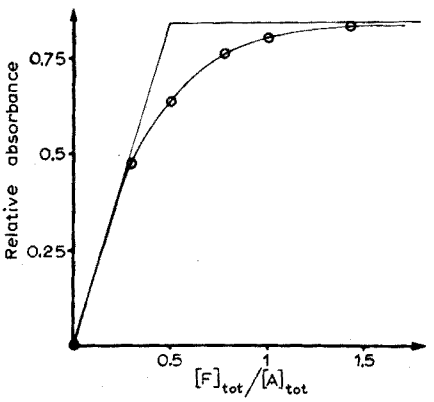

Fig. 6. The relative absorbance for $[La]_{tot}/[A]_{tot} = 1.25$ plotted against $[F]_{tot}/[A]_{tot}$ for titrations 1–6.

The composition of the lanthanum–fluoride–alizarin complexone complex can thus be written

$$(La_5A_4F_2H_0)_n$$

where n is an integer.

Titrations at constant pH and pF

The titration data for titrations 1′–5′ were interpreted as above by plotting n_H and n_F *vs.* $[La]_{tot}/[A]_{tot}$, and the results obtained at the break-point are summarized in Table IV. As can be seen, the results obtained at constant pH and pF confirm those obtained at constant pH.

TABLE IV

n_H AND n_F VALUES AT THE BREAK-POINTS IN TITRATIONS 1′–5′

Titration no.	*pF*	$[La]_{tot}/[A]_{tot}$	$\bar{n}_H$	$\bar{n}_F$
1′	4.95	1.20	0.10	0.40
2′	4.75	1.22	0.16	0.46
3′	4.45	1.25	0.06	0.52
4′	3.97	1.25	0.05	0.54
5′	3.85	1.25	0.02	0.57

Light scattering measurements

Light scattering measurements using the Zimm[16] plot technique were performed on solutions containing *ca.* $5 \cdot 10^{-6}$ *M* of the blue complex, in order to attempt to determine the molecular weight. Owing to the low total concentration and strong self-absorption, this was not, however, possible. It was, nevertheless, apparent that the molecular weight was less than 10–20000.

Gel filtration

Solutions containing approximately equal amounts of the lanthanum–alizarin complexone complex (red) and the lanthanum–fluoride–alizarin complexone complex (blue) were eluted through a 30-cm Sephadex G 25 (fine) column (molecular weight range for dextrans 100–5000 and peptides 1000–5000). A very satisfactory separation between the red and blue complexes was obtained, the latter passing rapidly through the column. A slight dissociation of the inert blue complex was observed as a red tail behind the blue front. Measurements of the elution volumes showed that the blue complex had a molecular weight of 3–5 times that of the red complex. The same procedure was carried out on a Sephadex G 50 (fine) column (molecular weight range for dextrans 500–10000 and for peptides 1500–30000); since it was not possible to separate the blue and red complexes on this column it could be concluded that the formula of the blue complex was $(La_5A_4F_2)_n$, where $n=1$.

DISCUSSION

A possible structure for $La_5A_4F_2$ is shown by formula II. According to the

suggested structure, the fifth lanthanum in $La(LaA)_4F_2$ is coordinated to four LaA units through oxygen atoms. For the sake of clarity, only two of the four LaA units are shown; a third A ligand is coordinated to La^4 and to La^5 through O^4, while the fourth is coordinated to La^2 and to La^5 through O^3. The whole complex is held together by La–F–La bridges between the fifth central lanthanum ion and the four lanthanum ions in the LaA units. The fluoride atoms have been assumed to have the same La-coordination as in lanthanum trifluoride.

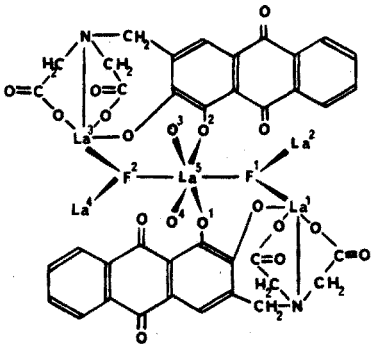

The suggested structure has some attractive features. First, it provides a simple explanation for the removal of the fourth hydrogen in alizarin complexone (*cf.* formula I) *i.e.* coordination to the fifth lanthanum. Secondly, it gives a reasonable explanation of the role of the fluoride ions in the formation of the blue complex *viz.* the formation La–F–La bridges. A scale model of the proposed structure shows that the distances and angles of LaA fit well into the lanthanum trifluoride skeleton and that the structure ought to be free from steric hindrance. Finally, the formula, $La(LaA)_4F_2$, explains why an excess of lanthanum over alizarin complexone is always recommended in the spectrophotometric determination of fluoride.

The authors are indebted to the head of the department, Professor David Dyrssen for many valuable discussions. Financial support from Swedish Natural Science Research Council, Alice och Knut Wallenbergs Fond and Carl Tryggers Stiftelse, the two latter grants to cover the costs of the computerized titrator, are gratefully acknowledged.

SUMMARY

The composition of the blue complex formed between fluoride and the lanthanum complex of alizarin complexone (H_4A) has been studied by photometric and potentiometric methods with glass and fluoride electrodes. The suggested composition of the complex, $La(LaA)_4F_2$, is supported by molecular weight estimations. A possible structure of the complex is given.

REFERENCES

1 R. Belcher, M. A. Leonard and T. S. West, *Talanta*, 2 (1959) 92.

2 R. Belcher and T. S. West, *Talanta*, 8 (1961) 853.
3 F. Ingman, Det. 13. Nordiske Kemikermøde, aug. 1968, København.
4 M. A. Leonard and T. S. West, *J. Chem. Soc.*, (1960) 4477.
5 P. G. Jeffery and D. Williams, *Analyst*, 86 (1961) 853.
6 F. J. Langmyhr, K. Klausen and M. Nouri-Nekoui, *Anal. Chim. Acta*, 57 (1971) 341.
7 T. Anfält, D. Dyrssen and D. Jagner, *Anal. Chim. Acta*, 43 (1968) 487.
8 T. Anfält and D. Jagner, *Anal. Chim. Acta*, 47 (1969) 483.
9 T. Anfält and D. Jagner, *Anal. Chim. Acta*, 50 (1970) 23.
10 F. Ingman, *Talanta*, 20 (1973) 135.
11 G. Gran, *Analyst*, 77 (1952) 661.
12 N. Ingri, W. Kakolowicz, L. G. Sillen and B. Warnqvist, *Talanta*, 14 (1967) 1261.
13 D. Dyrssen, D. Jagner and F. Wengelin, *Computer Calculation of Ionic Equilibria and Titration Procedures*, Almqvist & Wiksell, Stockholm, 1968.
14 T. Anfält and D. Jagner, *Anal. Chim. Acta*, 57 (1971) 177.
15 D. Jagner, *Anal. Chim. Acta*, 68 (1974) 83.
16 B. Zimm, *J. Chem. Phys.*, 16 (1948) 1093.

Analytica Chimica Acta, 70 (1974) 375–381

SEPARATION OF AROMATIC COMPOUNDS ON PELLICULAR ANION-EXCHANGE RESINS

JAN REXFELT and OLOF SAMUELSON

Department of Engineering Chemistry, Chalmers Tekniska Högskola, S-402 20 Göteborg 5 (Sweden)

(Received 11th December 1973)

Chromatographic studies on anion-exchange resins have shown that phenolic compounds are held very strongly in aqueous solutions. Successful separations were obtained by Sherma and Rieman[1] with styrene–divinylbenzene resins containing quaternary ammonium ions. In that study, as well as in the study of Halmekoski and Hyle[2], 1–6 *M* acetic acid was used as the eluent. Separations of hydroxybenzoic acids in acetic acid–methanol have also been reported[3]. More recently, phenolic compounds have been separated in a copper(II) chloride–organic solvent medium[4]. All these separations were very lengthy.

The application of a pellicular anion-exchange resin for the separation of aromatic acids and various phenols in mixed nitrate–borate media permitted a rapid separation of several species[5,6]. The purpose of the work described here was to study the separation of a large number of aromatic compounds including phenols, carboxylic acids and aldehydes on a pellicular anion-exchange resin in the acetate form.

EXPERIMENTAL

The acetate form of a quaternary ammonium-substituted methacrylate polymer, coated 1% by weight on spherical silicious particles (Zipax, SAX, 25–37 μm), was used throughout this work. The experiments were made in jacketed glass columns (990 × 2.6 mm) filled by slurrying an aqueous resin suspension into the column. Sodium acetate was used as the eluent, and the amounts of added solutes were 0.1–10 μg of each compound. The pressure drop in the column was about 25 atm and the temperature 30°C. The nominal linear flow was about 15 cm min^{-1}. Analyses of compounds with large peak elution volumes were carried out on a smaller column (350 × 2.0 mm) at a nominal linear flow of 35 cm min^{-1}. The eluate was analyzed spectrophotometrically (Chromatronix, model 220) at 280 nm. (Benzene was recorded at 254 nm).

RESULTS AND DISCUSSION

Influence of the eluent composition

The retention data in 0.1 *M* sodium acetate, given in Table I, show that all investigated solutes were retained more or less effectively by the pellicular anion exchanger. The lowest retention volume was recorded with benzaldehyde;

TABLE I

THE ADJUSTED RETENTION VOLUME (V_R') CALCULATED IN COLUMN VOLUMES AND THE RELATIVE RETENTION (r) IN 0.1 *M* SODIUM ACETATE AT pH 8.1 AND 5.7

	pH 8.1		*pH 5.7*	
	V_R'	r^a	V_R'	r^a
Benzene	0.87	0.90	0.87	0.89
Methoxybenzene	0.98	1.01	0.99	1.01
Phenol	0.97	1.00	0.98	1.00
1,2-Dihydroxybenzene	—	—	2.19[b]	2.23
1,3-Dihydroxybenzene	1.45	1.49	1.36	1.39
1,4-Dihydroxybenzene	0.53	0.55	0.53	0.54
1,3,5-Trihydroxybenzene	1.46[b]	1.51	1.18	1.20
2-Methylphenol	2.16	2.23	2.27	2.32
3-Methylphenol	2.05	2.11	2.19	2.23
4-Methylphenol	2.00	2.06	2.12	2.16
2,4-Dimethylphenol	4.5	4.6	4.9	5.0
3,4-Dimethylphenol	4.0	4.1	4.2	4.3
2,6-Dimethylphenol	2.92	3.01	3.3	3.4
2,4,5-Trimethylphenol	8.6	8.9	9.1	9.3
2-Methoxyphenol	0.71	0.73	0.64	0.65
3-Methoxyphenol	1.48	1.53	1.45	1.48
4-Methoxyphenol	0.83	0.86	0.86	0.88
2,6-Dimethoxyphenol	0.42	0.43	0.39	0.40
2-Methoxy-4-propylphenol	8.5	8.8	8.5	8.7
2-Methoxy-4-allylphenol	4.7	4.8	4.7	4.8
Benzoic acid	1.81	1.87	3.1	3.2
2-Hydroxybenzoic acid	37	38	53	54
3-Hydroxybenzoic acid	3.3	3.4	5.1	5.2
4-Hydroxybenzoic acid	2.10	2.16	3.2	3.3
2,5-Dihydroxybenzoic acid	33	34	44	45
4-Hydroxy-3-methoxybenzoic acid	1.98[b]	2.04	1.74	1.78
3,5-Di-tert-butyl-4-hydroxybenzoic acid	>60	>60	>60	>60
Benzaldehyde	0.33	0.34	0.34	0.35
2-Hydroxybenzaldehyde	3.3	3.4	0.94	0.96
3-Hydroxybenzaldehyde	1.43	1.47	1.14	1.16
4-Hydroxybenzaldehyde	2.62	2.70	1.41	1.44
2,4-Dihydroxybenzaldehyde	16	16	6.0	6.1
4-Hydroxy-3-methoxybenzaldehyde	2.03	2.09	1.25	1.28
2,7-Dihydroxynaphthalene	34	35	34	35
4-Hydroxybiphenyl	>60	>60	>60	>60

[a] Retention relative to phenol.
[b] Severe tailing.

a recalculation of the observed retention volume to a specific retention volume, calculated on unit weight of the active polymer, showed that even this compound was held very strongly by the resin. Evidently, benzaldehyde which has very weak acidic properties ($pK_a = 12.3$) exhibited a pronounced affinity for the resin. The elution behaviour was independent of the eluent composition.

In sodium acetate solutions, benzoic acid and the hydroxybenzoic acids

are dissociated almost completely, thus benzoate and hydroxybenzoate ions should be held as counter ions by the anion exchanger. This was confirmed when the influence of the sodium acetate concentration on the adjusted retention volume (Table II) was studied. About a five-fold decrease in retention volume was obtained when the eluent concentration was increased by a factor of five.

Among the compounds lacking carboxylic acid groups, the hydroxybenzaldehydes were the strongest acids. Their retention volumes were affected in the same direction as those of the carboxylic acids by changes in the sodium acetate concentration, which indicates that the ionization of these species also contributed markedly to their sorption. For the other compounds (Table II),

TABLE II

NFLUENCE OF THE SODIUM ACETATE CONCENTRATION ON THE RETENTION VOLUME

	Adjusted retention volume, calculated in column volumes (V_R')					
	0.25 M NaAc	*0.05 M NaAc*	*0.01 M NaAc*	*0.002 M NaAc*	*0.0004 M NaAc*	*H_2O*
Phenol	0.97	0.95	0.95	1.01	3.3[a]	5.3[a]
,3-Dihydroxybenzene	1.35	1.48	1.44	1.75	6.0[a]	>12
-Methylphenol	2.07	1.98	1.97	2.01	2.81	8.1[a]
,4-Dimethylphenol	4.8	4.5	4.4	4.4	5.8	>12
-Methoxyphenol	0.86	0.82	0.82	0.82	1.40	3.6
enzoic acid	0.69	3.0	>12	>12	>12	>12
-Hydroxybenzoic acid	0.70	3.6	>12	>12	>12	>12
enzaldehyde	0.34	0.33	0.32	0.32	0.32	0.32
-Hydroxybenzaldehyde	1.75	4.4	5.3[a]	7.8[a]	>12	>12
-Hydroxybenzaldehyde	1.11	1.48	1.70	2.31	>12	>12
-Hydroxybenzaldehyde	1.11	3.8	9.3	>12	>12	>12

[a] Severe tailing.

changes in the eluent concentration within the range 0.01–0.25 *M* sodium acetate had only a slight influence on the retention volume. Thus, these solutes were largely unionized and not held as counter ions by the resin. However, at lower concentrations, and in pure water, the retention volumes of these other compounds increased. This behaviour was expected, since according to the Donnan theory, the pH in the resin phase increases at low external acetate concentrations and reaches a level at which very weak acids such as phenol, are dissociated and held as counter ions. It is worth mentioning that most of the investigated species were held so strongly in pure water that they could not be eluted within a reasonable time.

Advantage can be taken of the fact that different types of compounds are influenced differently by changes in the eluent concentration. Some species which, in one medium, exhibit a very similar behaviour, *e.g.* 2,4-dimethylphenol and 2-hydroxybenzaldehyde in 0.05 *M* sodium acetate, can be very easily separated in another, *e.g.* in 0.25 *M* solution. With several species, a tailing was observed in both pure water and in sodium acetate solutions of extremely low concentrations. The preferred concentration range is 0.05–0.25 *M*.

Since the uptake of phenols by an ion-exchange mechanism is negligible in, for instance, 0.1 *M* sodium acetate, it is expected that a decrease in pH would have little influence upon the sorption, unless the added acid interfered with some other sorption mechanism. The results shown in Table I, which were obtained in 0.1 *M* sodium acetate with acetic acid added to pH 5.7, show that the retention of all studied compounds, except for the carboxylic acids and the hydroxybenzaldehydes, was only slightly affected. The results show that no competition between acetic acid and the phenolic compounds for any sorption sites was detected under the applied conditions.

The hydroxybenzaldehydes, which as already mentioned are held as counter ions at high pH, showed a marked decrease in sorption with a decrease in pH since the ions are converted into undissociated acids. This behaviour is typical of very weak acids whereas stronger acids, such as the hydroxyacids[7], should hardly be affected by a decrease in pH within the studied range. It was therefore expected that, unless other factors interfered, the hydroxybenzoic acids would not be affected by a decrease in pH whereas the retention volume of benzoic acid should decrease slightly. The results given in Table I show that, on the contrary, the retention volume of these species increased markedly when acetic acid was added. Controls showed that the results were reproducible and not due to any irreversible change of the stationary phase. The following explanation is offered. As demonstrated previously[8], carboxylic acids (HA) are held by an anion-exchange resin in the acetate (Ac^-) form by a sorption mechanism based on the formation of associated anions of the type ($HAAc^-$). Moreover, the solubility of benzoic acid is much higher in sodium acetate than in water[9] which suggests that associated ions of high stability are formed. Thus, a probable explanation of the observed effect is that associated species exhibit a larger affinity for the resin than the non-associated anions.

Influence of the structure on the retention volume

In ion-exchange systems in which only polar carboxylate ions are involved, the ion-exchange affinities increase with decreased ionic size and with increased strength of the parent acid[10]. Experiments with the pellicular anion exchanger showed that aromatic carboxylic acids were retained effectively (Table I), whereas strongly polar aliphatic acids, such as gluconic and lactic acids, appeared at an elution volume which was only slightly larger than the interstitial volume. The results show that the aromatic ring contributes markedly to the ion-exchange affinity. It is noteworthy that aromatic substituents contribute markedly to the affinities of cations for cation-exchange resins[11]. The acid strength increases with the introduction of a hydroxyl group at C-2 in benzoic acid and, as expected, the retention volume of 2-hydroxybenzoic acid was much larger than that of its isomers and also of the unsubstituted acid. Likewise, 2,5-dihydroxybenzoic acid, which is a strong acid, was held very firmly, whereas 4-hydroxy-3-methoxybenzoic acid, which is a weaker acid, exhibited an ion-exchange affinity very similar to that of 4-hydroxybenzoic acid.

With non-polar aliphatic carboxylic acids, the exchange affinities of the carboxylate anions increase when the length of the non-polar part is increased, *e.g.* from CH_3CH_2- to $CH_3CH_2CH_2-$ (ref. 10). It was therefore expected that the

introduction of aliphatic side-chains in the aromatic acids would lead to increased retention values. It was found, for example, that 3,5-di-tert-butyl-4-hydroxybenzoic acid was held so strongly that it could not be eluted with a reasonable volume of eluent.

Contributions of aliphatic substituents to the sorption were recorded also with the phenols. One of the studied phenols containing a propyl group at C-4 was found to exhibit an adjusted retention volume about 12 times larger than the compound (2-methoxyphenol) lacking this substituent. Similar types of interactions have been discussed in detail by Feitelson[11].

The observation that all methylphenols exhibited retention volumes about twice that of phenol, even though the acid strength is lowered, shows that even a single methyl group exerts a significant effect. An increase in the number of methyl groups strengthens this effect; 2,6-dimethylphenol with the hydroxyl group located between two methyl groups was held less strongly than the isomeric dimethylphenols. This may be explained by both a weakening of the non-polar interactions by the hydroxyl group and to a shielding of the hydroxyl group.

It is interesting to note that, among the methoxyphenols, the compound with symmetrical positions of the substituents (2,6-dimethoxyphenol) exhibited the lowest retention. The methoxyphenols with the substituents at C-2 and C-4 were held less strongly than phenol, whereas 3-methoxyphenol was held more strongly and in fact exhibited a retention volume very similar to that of 1,3-dihydroxybenzene.

One possible effect of the phenolic hydroxyl would be a hydrogen bond formation in which the proton is donated to some proton-accepting group in the resin, *e.g.* to the acetate ions. Although hydrogen-bond formation seems to be a key mechanism as far as the sorption of phenolic compounds onto polyvinylpyrrolidone-type resins[12] is concerned, it is probably of little or no importance with the anion exchanger in the acetate form, since the retention volume of methoxybenzene was about the same as that of phenol. Moreover, 4-methoxyphenol was held more firmly than 1,4-dihydroxybenzene.

As already mentioned, the aromatic ring contributes markedly to the ion-exchange affinity of the carboxylic acids. The fact that benzene is held more strongly than several of the compounds containing polar substituents, shows that interactions with the benzene ring have a great influence on the sorption. As can be seen from Table I, 4-hydroxybiphenyl and 2,7-dihydroxynaphthalene with two benzene nuclei, exhibits much higher retention volumes than most compounds containing one benzene nucleus.

Applications

The clean-cut separation of six phenolic compounds in 0.1 *M* sodium acetate is demonstrated by the chromatogram given in Fig. 1; the compounds were eluted within 40 min. Figure 2 demonstrates the separation of benzaldehyde and the three isomeric monohydroxybenzaldehydes in the same medium. The last compound was eluted within less than 30 min. As previously mentioned, other eluent compositions offer advantages in certain separations. The retention data reported in the Tables may facilitate the choice of suitable conditions. It should also be remembered that many phenolic compounds are oxidized in alkaline

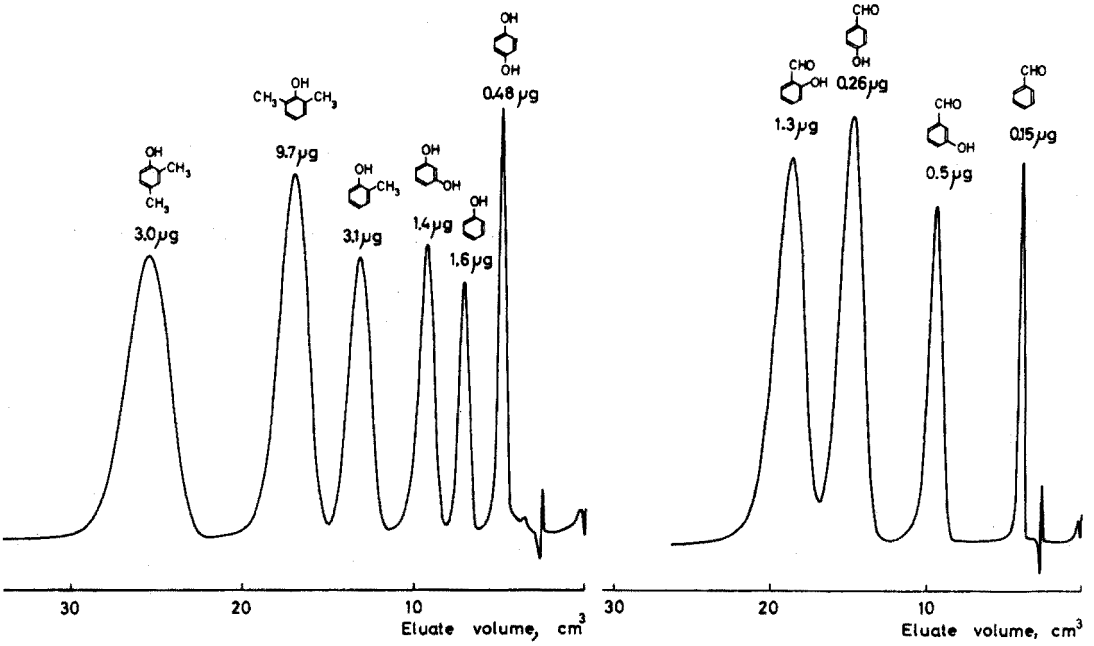

Fig. 1. Separation of six phenolic compounds in 10 μl of water by elution with 0.1 *M* sodium acetate. Column dimensions 2.6 × 990 mm. Flow rate 0.735 cm^3 min^{-1}.

Fig. 2. Separation of benzaldehyde and hydroxybenzaldehydes in 5 μl of water by elution with 0.1 *M* sodium acetate. Column dimensions 2.6 × 990 mm. Flow rate 0.806 cm^3 min^{-1}.

solutions. With such species, *e.g.* 1,2-dihydroxybenzene, it is therefore preferable to make the elution in acidic medium.

The method is well suited for the analysis of very dilute solutions of phenolic compounds. Organic contaminants such as polymers, sugars and aliphatic carboxylic acids, do not interfere, because they appear at elution volumes very close to the interstitial volume. The reproducibilities of the peak elution volumes and of the peak areas were within ±2% from the mean in repeated runs carried out during the same day. With the phenolic compounds, the retention data differed by less than 3% after the column had been used for about one week, whereas the values recorded with the carboxylic acids were lowered by about 5%.

The authors are much indebted to the Swedish Board for Technical Development for financial support.

SUMMARY

Aromatic compounds including phenols, carboxylic acids and aldehydes, can be rapidly separated on pellicular anion-exchange resins in the acetate form by elution with a sodium acetate solution. Like the aromatic carboxylic acids, hydroxybenzaldehydes are held as counter ions in the resin. The affinity of the resin for corresponding anions as well as that for sorbed non-electrolytes is largely influenced by the aromatic ring and non-polar aliphatic substituents. Formation of hydrogen bonds between the resin and phenolic groups is less important.

REFERENCES

1 J. Sherma and W. Rieman III, *Anal. Chim. Acta*, 18 (1958) 214.
2 J. Halmekoski and M. Hyle, *Suom. Kemistilehti B*, 35 (1962) 162.
3 N. Skelly and W. Crummett, *Anal. Chem.*, 35 (1963) 1680.
4 K. S. Lee, D. W. Lee and Y. S. Chung, *Anal. Chem.*, 45 (1973) 396.
5 R. A. Henry and J. A. Schmit, *Chromatographia*, 3 (1970) 116.
6 K. Bhatia, *Anal. Chem.*, 45 (1973) 1344.
7 O. Samuelson and L. Thede, *J. Chromatogr.*, 30 (1967) 556.
8 L. Löwendahl, O. Samuelson and D. Thornton, *Chem. Scripta*, 1 (1971) 227.
9 E. Larsson, *Z. phys. Chem.*, 3 (1927) 233.
10 E. Martinsson and O. Samuelson, *Chromatographia*, 3 (1970) 405.
11 J. Feitelson in J. Marinsky (Ed.), *Ion Exchange*, Dekker, New York, 1969, p. 135.
12 L. Olsson and O. Samuelson, *J. Chromatogr.*, in press.

Analytica Chimica Acta, 70 (1974) 383–389

DIFFERENTIAL THERMOMETRIC KINETIC ANALYSIS. A NEW GENERAL TECHNIQUE OF INTERPRETING THE DATA OBTAINED IN KINETIC ANALYSES

WALACE A. DE OLIVEIRA and LOUIS MEITES

Department of Chemistry, Clarkson College of Technology, Potsdam, New York 13676 (U.S.A.)

(Received 1st November 1973)

The simplest and most frequently discussed kind of kinetic analysis is that in which: (1) the sample contains two substances, A_1 and A_2, that react simultaneously with a reagent R; (2) each of these reactions obeys pseudo-first-order kinetics, implying that the concentration of R is large and constant; and (3) the products P_1 and P_2 of these reactions contribute to the measured signal S in proportion to their concentrations. When these conditions are satisfied the dependence of S on time is described by the equation

$$S = s_1 c_1^0(1-e^{-k_1 t}) + s_2 c_2^0(1-e^{-k_2 t}) \quad (1)$$

where s_1 and s_2 are the constants of proportionality relating the concentrations of P_1 and P_2 to their respective contributions to S, c_1^0 and c_2^0 are the initial concentrations of A_1 and A_2, and k_1 and k_2 are the pseudo-first-order rate constants under the conditions of measurement.

Mark and Rechnitz[1] have summarized the techniques most widely used for evaluating c_1^0 and c_2^0. These include the logarithmic extrapolation[2–4] and "tangent"[5] methods and the single-point[6] and double-point[7,8] or "proportional-equations" methods. The first two of these methods employ only data for the mixture being analyzed, but the other two also require values of k_1 and k_2 or equivalent information obtained with pure solutions or known mixtures, and the same thing is true of the two-parameter linear-regression technique devised by Willis *et al.*[9]. There are of course many cases in which the rate constant for each reactant is unaffected by the presence and simultaneous reaction of the other and is independent of the composition of the mixture, as is required for the success of a method of the latter type. However, in oximations of mixtures of carbonyl compounds, Siggia and Hanna[10] found the rate constant of a slower reaction to be increased by the simultaneous occurrence of a faster one. In any such situation the values of k_1 and k_2 obtained from prior experiments with pure solutions or known mixtures will be useless.

The present paper describes a new technique, which is based on the simultaneous evaluation of all four of the parameters ($s_1 c_1^0$, $s_2 c_2^0$, k_1 and k_2) appearing on the right-hand side of eqn. (1). From these the values of c_1^0 and c_2^0 are easily obtained if the constants of proportionality s_1 and s_2 are known, while concordance of the values of k with those for the individual compounds in pure solutions can serve either for the identification of the compounds or for the elucidation of complications that arise with mixtures of reactants.

The technique is illustrated by means of differential thermometric data obtained in reactions of mixtures of propanal and cyclohexanone with excess of hydroxylamine. The results confirm the reality of the effect reported by Siggia and Hanna[10] on the basis of different experimental procedures and data-handling techniques.

The only application of thermometry in kinetic analysis heretofore recorded was that of Papoff and Zambonin[11], who analyzed mixtures of methyl and isopropyl acetates by recording temperature–time curves for base-catalyzed hydrolyses in 1 *F* sodium hydroxide. The work reported here involves a smaller ratio of rate constants, compensation for heats of dilution and other adventitious thermal effects by means of a differential apparatus, and the application of corrections for heat exchange.

EXPERIMENTAL

Propanal and cyclohexanone were purified by distillation under nitrogen and were stored under dry nitrogen; all other chemicals were ordinary reagent grade. The apparatus has been described by Meites *et al.*[12]. It is a constant-temperature-environment calorimeter containing two identical vessels, one for the reaction mixture and the other for a reference solution. At the start of an experiment, 80 cm^3 of a stock reagent solution, containing 0.100 *F* hydroxylammonium chloride and *ca.* 0.05 *F* hydrochloric acid together with enough sodium chloride to yield an ionic strength of 1.00 *M*, was placed in each of these vessels. A syringe containing *ca.* 1.1 cm^3 of an aqueous solution of carbonyl compound was partially submerged in the solution in the reaction vessel, and an identical syringe containing an equal volume of water was similarly placed in the reference vessel. The difference between the temperatures of the two solutions was monitored by means of matched 10^5-ohm thermistors connected to a d.c. Wheatstone bridge whose unbalance voltage was presented to a strip-chart recorder. When thermal equilibrium had been reached the plungers of the syringes were actuated simultaneously. The recorded difference of temperature then increased at first as the exothermic oximation proceeded, passed through a flat maximum, and finally decayed exponentially toward zero as Newtonian heat exchange equalized the temperatures of the reaction mixture and the surroundings. Differences of temperature are expressed here in arbitrary units for convenience; the total change of temperature of the reaction mixture was usually about 0.002°C. All experiments were performed at 25.7 ± 0.3°C and the pH of the reaction mixture at the end of an experiment was always 1.36 ± 0.01.

Computations

All of the computations were performed on a PDP8/I computer (Digital Equipment Corp., Maynard, Massachusetts) operated in a multi-user configuration that made 4096 words of core memory available for this work. They employed a general multiparametric curve-fitting program that has been used for a number of other purposes in this laboratory*[,12]. This was combined with the coordinates

* Paper-tape listings, in BASIC, of this program and a related one, VARPAR, used to evaluate the variances of the parameters obtained, together with hardcopy listings and a manual of explanation and discussion may be obtained by remitting $5.00, to cover the cost of duplication and mailing, to the Computing Laboratory, Department of Chemistry, Clarkson College of Technology, Potsdam, N.Y. 13676.

of 20–30 data points and with a short subroutine written to compute ΔT at each point from eqn. (13). The standard deviation of the points from the best fits to this equation corresponded to a standard error of almost exactly ± 0.1 mm in the measurement of a single deflection on the recorded chart.

THEORY

The occurrence of heat exchange during a differential thermometric experiment necessitates the use of an expression more complicated than eqn. (1). If the reaction

$$A_1 + R \xrightarrow{k_1} P_1$$

occurred alone and followed pseudo-first-order kinetics in the presence of a large and constant concentration of R, the rate of change of the difference of temperature between the reaction mixture and its surroundings (or between the reaction mixture and the contents of the reference vessel) would be given by

$$\frac{d(\Delta T)}{dt} = \frac{(\Delta H_1)V}{Q}\frac{dc_1}{dt} - \varepsilon(\Delta T) \tag{2}$$

where ΔH_1 is the enthalpy change accompanying the reaction, Q is the thermal equivalent of the reaction vessel and its contents (cal deg^{-1}), $V dc_1/dt$ is the rate of reaction (mol s^{-1}), and ε is the Newtonian heat-exchange constant (s^{-1}). Since

$$c_1 = c_1^0 e^{-k_1 t} \tag{3}$$

the overall change of temperature in the absence of heat exchange is given by

$$\Delta T_{\text{corr. }\infty.1} = -(\Delta H) V c_1^0 / Q \tag{4}$$

By combining these equations it can be shown that

$$\Delta T = k_1(\Delta T_{\text{corr. }\infty.1})(e^{-k_1 t} - e^{-\varepsilon t})/(\varepsilon - k_1) \tag{5}$$

Similarly, for a mixture of two reactants A_1 and A_2, each of whose reactions obeys pseudo-first-order kinetics,

$$\Delta T = k_1(\Delta T_{\text{corr. }\infty.1})(e^{-k_1 t} - e^{-\varepsilon t})/(\varepsilon - k_1) + k_2(\Delta T_{\text{corr. }\infty.2})(e^{-k_2 t} - e^{-\varepsilon t})/(\varepsilon - k_2) \tag{6}$$

and this is the fundamental equation of differential thermometric kinetic analysis. It becomes identical with eqn. (1) in the hypothetical limiting case where $\varepsilon = 0$, whereupon $S = \Delta T$ and $S_i = \Delta T_{\text{corr. }\infty.i}/c_i^0 = -(\Delta H_i)V/Q$.

RESULTS AND DISCUSSION

Following the general procedure of Meites *et al.*[12], a value of ε was first obtained by analyzing the data obtained at long times, where both reactions are complete and the observed variations of ΔT are due to heat exchange alone. As this portion of the curve conforms to the equation

$$\Delta T = \Delta T^* e^{-\varepsilon(t - t^*)} \tag{7}$$

where ΔT^* represents the difference of temperature at an arbitrarily chosen instant t^* s after the initiation of the reaction, a two-parameter fit employing about a dozen points was performed to obtain the values of ΔT^* and ε. The value of ΔT^* is unimportant, but that of ε was used in the computing subroutine based on eqn. (13).

Modification of this general equation was necessitated in the present case by the fact that there is a small contribution to ΔT from some prior reaction that occurs almost instantaneously on mixing either propanal or cyclohexanone with hydroxylamine[14]. This contribution does not arise from heats of dilution, for these are nearly exactly compensated by the differential arrangement employed, and it must instead reflect the attainment of an equilibrium involving the carbonyl compound, the hydroxylamine, and the reactive carbinolamine adduct:

$$\rangle C{=}O + NH_3OH^+ = \rangle C\begin{matrix}OH\\ NHOH\end{matrix} + H_2O + H^+$$

This was confirmed by separate experiments in which the absorbance of the unreacted carbonyl compound was recorded as a function of time at each of a number of wavelengths during the reaction with excess hydroxylammonium ion under conditions (0.1 *F* hydroxylammonium chloride, 0.1 *F* hydrochloric acid, $\mu = 1.1$ *M*) substantially identical with those used in the differential thermometric experiments. The data at each wavelength were analyzed to evaluate the absorbance at the instant of mixing, and the resulting value was compared with that measured directly for the same concentration of the same compound in the absence of hydroxylamine but under otherwise identical conditions. The ratio of these two values, which is equal to

$$[\rangle C{=}O]/([\rangle C{=}O] + [\rangle C\begin{matrix}OH\\ NHOH\end{matrix}]),$$

was independent of wavelength and equal to 0.79 ± 0.12 for propanal and to 0.67 ± 0.06 for cyclohexanone; these values correspond to values of 0.25 and 0.50 for the equilibrium constants of the reaction given above. A substantial fraction of either carbonyl compound is thus consumed in the attainment of the initial equilibrium.

Consequently, eqns. (5) and (6) must be rewritten for the present application as follows:

$$\Delta T = k_1(\Delta T_{\text{corr.}\infty.1})(e^{-k_1 t} - e^{-\varepsilon t})/(\varepsilon - k_1) + \Delta T_1^0 e^{-\varepsilon t} \tag{8}$$

$$\Delta T = k_1(\Delta T_{\text{corr.}\infty.1})(e^{-k_1 t} - e^{-\varepsilon t})/(\varepsilon - k_1) + \\ + k_2(\Delta T_{\text{corr.}\infty.2})(e^{-k_2 t} - e^{-\varepsilon t})/(\varepsilon - k_2) + (\Delta T_1^0 + \Delta T_2^0)e^{-\varepsilon t} \tag{9}$$

Equation (8) pertains to the reaction of a single carbonyl compound and eqn. (9) to that of a mixture; ΔT_i^0 denotes the rapid initial temperature rise due to the presence of the *i*th carbonyl compound and $\Delta T_{\text{corr.}\infty.i}$ denotes the corresponding slow further rise, which is attributable partly to the loss of water from the carbinolamine intermediate and partly to the consumption of the carbonyl compound that survives the initial equilibration. In this range of pH values, ΔT_i^0 is small for either of these compounds, for the corresponding enthalpy changes are only about -200 cal mol^{-1}, and hence it was the values of $\Delta T_{\text{corr.}\infty.i}$ that were of most interest.

Nevertheless, the necessity of taking ΔT_i^0 into account by employing eqns. (8) and (9) would have made the computations lengthier and introduced an undesirable additional degree of freedom, and therefore it was circumvented by numerical evaluation of the integral $\int_0^t \varepsilon(\Delta T)\mathrm{d}t$ at each experimental time t. The value of this integral is equal to the difference between the value of ΔT that would be obtained in the absence of heat exchange and the one actually measured, so that the sum $\Delta T+\int_0^t \varepsilon(\Delta T)\mathrm{d}t$ approaches a constant limit, denoted by ΔT_∞, as the reactions approach completion. Since, if only one reactant is present, this limit corresponds to:

$$\Delta T_\infty = \Delta T_1^0 + \Delta T_{\mathrm{corr.}\,\infty.1} \tag{10}$$

or, for a mixture of two reactants, to:

$$\Delta T_\infty = (\Delta T_1^0 + \Delta T_2^0) + \Delta T_{\mathrm{corr.}\,\infty.1} + \Delta T_{\mathrm{corr.}\,\infty.2} \tag{11}$$

eqns. (8) and (9) may finally be written in the forms

$$\Delta T = k_1(\Delta T_{\mathrm{corr.}\,\infty.1})(\mathrm{e}^{-k_1 t}-\mathrm{e}^{-\varepsilon t})/(\varepsilon-k_1)+(\Delta T_\infty-\Delta T_{\mathrm{corr.}\,\infty.1})\mathrm{e}^{-\varepsilon t} \tag{12}$$

and

$$\begin{aligned}\Delta T = {} & k_1(\Delta T_{\mathrm{corr.}\,\infty.1})(\mathrm{e}^{-k_1 t}-\mathrm{e}^{-\varepsilon t})/(\varepsilon-k_1) \\ & + k_2(\Delta T_{\mathrm{corr.}\,\infty.2})(\mathrm{e}^{-k_2 t}-\mathrm{e}^{-\varepsilon t})/(\varepsilon-k_2) \\ & + (\Delta T_\infty-\Delta T_{\mathrm{corr.}\,\infty.1}-\Delta T_{\mathrm{corr.}\,\infty.2})\mathrm{e}^{-\varepsilon t}\end{aligned} \tag{13}$$

in which there are two unknown parameters to be evaluated for each reactant present, as is also true of the general equation (eqn. 6) given above.

Table I gives the results obtained in four-parameter fits to eqn. (13). The values of k obtained from similar experiments with the individual compounds were 0.174 s^{-1} for propanal and 0.028 s^{-1} for cyclohexanone. The average values obtained with mixtures were 0.161 ($\pm$0.021) s^{-1} for propanal and 0.0359 ($\pm$0.0019) s^{-1} for cyclohexanone; values in parentheses are standard deviations. There is no significant difference between the values for propanal alone and in the mixtures, but the value for cyclohexanone is nearly 30% higher in the mixtures. This is in agreement with the results of Siggia and Hanna[10] and proves that the effect is not an artefact of experimental technique or computational procedure. Siggia has suggested[15] that it results from an exchange reaction of the form

$$\mathrm{R_2CO} + \mathrm{R'_2C{=}NOH} \rightleftarrows \mathrm{R_2C{=}NOH} + \mathrm{R'_2CO}$$

where R_2CO is the more slowly reacting compound and R'_2CO the more rapidly reacting one; since this reaction would be followed by the relatively rapid conversion of R'_2CO back to the oxime by direct reaction with hydroxylamine, it would tend to accelerate the consumption of R_2CO, but this is not conclusively proven by the data available.

The constants of proportionality relating the values of $\Delta T_{\mathrm{corr.}\,\infty}$ given in the third column of Table I to the concentrations given in the fourth could be evaluated either from the average of the values of $\Delta T_{\mathrm{corr.}\,\infty}/c^0$ obtained with mixtures or from data obtained with the separate compounds. These two procedures gave results concordant within a few per cent and the averages were used to compute the "concentrations found" in the fourth column.

TABLE I

RESULTS OBTAINED IN DIFFERENTIAL THERMOMETRIC KINETIC ANALYSES OF MIXTURES OF PROPANAL AND CYCLOHEXANONE

(The first two columns give the concentrations initially present in the reaction mixture, the next two give the values of k and $\Delta T_{corr.\infty}$ obtained from a four-parameter fit of the data to eqn. (13), the fifth gives the concentrations calculated from $\Delta T_{corr.\infty}$ as described in the text, and the last gives the relative errors of these results. The experiments are listed in the order of the ratios of the initial concentrations)

Compound	*Concentration taken (mM)*	$k(s^{-1})$	$\Delta T_{corr.\infty}$ *(arbitrary units)*	*Concentration found (mM)*	*Relative error (%)*
EtCHO	0.238	0.153	2.10	0.231	−2.8
$C_6H_{10}O$	2.387	0.0358	29.51	2.105	−11.8
EtCHO	1.372	0.138	11.44	1.260	−8.2
$C_6H_{10}O$	1.404	0.0331	19.30	1.376	−2.0
EtCHO	2.476	0.162	20.92	2.304	−6.9
$C_6H_{10}O$	1.930	0.0360	26.46	1.887	−2.2
EtCHO	2.748	0.197	24.50	2.698	−1.8
$C_6H_{10}O$	1.753	0.0386	26.28	1.874	+6.9
EtCHO	3.062	0.167	27.64	3.044	−0.6
$C_6H_{10}O$	1.533	0.0358	21.59	1.540	+0.5
EtCHO	3.590	0.146	35.95	3.959	+10.3
$C_6H_{10}O$	1.167	0.0328	15.90	1.134	−2.8

The standard errors of the parameters calculated from the data of a single experiment were typically of the order of ± 0.5 arbitrary units in either value of $\Delta T_{corr.\infty}$, corresponding to a relative variance of about $\pm 3\%$ for the values in Table I, and about $\pm 2\%$ in either rate constant. As Table I shows the rate constants to be much less reproducible from one experiment to the next than these estimates of their errors would suggest, it is plain that, as is well known to be true in most kinetic work, most of the overall variation arises from unrecognized differences among the conditions in replicate experiments. Nevertheless, the precisions of the concentrations and rate constants obtained are comparable to those obtained by other techniques of kinetic analysis, and both the fact that the ratio of rate constants is only about 4 and the necessity of correcting for heat exchange make this a rather unfavorable test case.

This research was supported by grant number GM-16561 from the Institute of General Medical Sciences of the National Institutes of Health. We are grateful to the Eastman Kodak Company and the National Science Foundation for Departmental grants that made possible the purchase and maintenance of the computer system employed.

SUMMARY

The concentration–time data obtained in kinetic analyses may be easily and

conveniently interpreted by multiparametric curve-fitting. A new technique of kinetic analysis, in which the overall extent of reaction is monitored by following the variation with time of the difference between the temperature of a reaction mixture and that of a reference solution, is described. Both these techniques are illustrated with data obtained in oximations of mixtures of propanal and cyclohexanone. The results confirm the existence of the synergic effect reported by Siggia and Hanna.

REFERENCES

1 H. B. Mark, Jr. and G. A. Rechnitz, *Kinetics in Analytical Chemistry*, Interscience, New York, 1968, pp. 78–92.
2 G. Hevesy and F. A. Paneth, *A Manual of Radioactivity*, Oxford University Press, 1938.
3 H. C. Brown and R. S. Fletcher, *J. Amer. Chem. Soc.*, 70 (1948) 1845; 73 (1951) 1317.
4 B. E. Saltzman and N. Gilbert, *Anal. Chem.*, 31 (1959) 1914.
5 H. A. Laitinen, *Chemical Analysis*, McGraw-Hill, New York, 1960, pp. 456–457.
6 T. S. Lee and I. M. Kolthoff, *Ann. N. Y. Acad. Sci.*, 53 (1951) 1093.
7 R. G. Garmon and C. N. Reilley, *Anal. Chem.*, 34 (1962) 600.
8 L. J. Papa, H. B. Mark, Jr. and C. N. Reilley, *Anal. Chem.*, 34 (1962) 1443.
9 B. G. Willis, J. A. Bittikoffer, H. L. Pardue and D. W. Margerum, *Anal. Chem.*, 42 (1970) 1340.
10 S. Siggia and J. G. Hanna, *Anal. Chem.*, 33 (1961) 896.
11 P. Papoff and P. G. Zambonin, *Talanta*, 14 (1967) 581.
12 T. Meites, L. Meites and J. N. Jaitly, *J. Phys. Chem.*, 73 (1969) 3801.
13 L. Meites, *The General Multiparametric Curve-Fitting Program CFT3*, Computing Laboratory, Department of Chemistry, Clarkson College of Technology, Potsdam, N.Y., 1973.
14 W. A. de Oliveira, M. S. Report, Clarkson College of Technology, 1972.
15 S. Siggia, personal communication, 1970.

Analytica Chimica Acta, 70 (1974) 391–400

KATALYTISCH-KINETISCHE BESTIMMUNG VON KATALASE, KUPFER, MOLYBDÄN UND JODID MIT HILFE EINES BIAMPEROSTATEN

SIEGBERT PANTEL und HERBERT WEISZ

Lehrstuhl für Analytische Chemie, Chemisches Laboratorium der Universität, 78-Freiburg i.Br. (Deutschland)

(Eingegangen den 2 November, 1973)

Eine wichtige Gruppe katalytisch-kinetischer Analysenmethoden beruht auf der Anwendung "offener Systeme", bei denen während des Reaktionsablaufs Reaktionspartner zugeführt oder Reaktionsprodukte abgeführt werden oder auch beides. Dazu gehören die sogenannten "Stat"-Methoden[1].

Bei diesen "Stat"-Methoden wird ein stationärer Zustand im System dadurch aufrecht erhalten, dass ein geeignetes Reagens in eben dem Masse von aussen zugeführt wird, wie es nötig ist, die durch die katalysierte Reaktion auftretende Veränderung der Konzentration eines Reaktionspartners, eines Reaktionsproduktes oder des Verhältnisses beider zueinander gerade wiederum auszugleichen. Irgendeine geeignete physikalische Eigenschaft des Systems, die proportional ist der Konzentration jener Substanz, welche eben stationär gehalten werden soll, wird nach entsprechender Umwandlung des Messeffektes zur Steuerung der Reagenszugabe verwendet. Dieses Prinzip wurde zuerst bei den "pH-Staten" angewendet (z.B. Malmstadt und Piepmeier[2], Møller[3]). Hier steuert das Potential einer Messkette mit einer protonenselektiven Elektrode die Zugabegeschwindigkeit für eine Säure oder Base in dem Masse, wie in der Reaktionslösung Protonen verbraucht werden oder entstehen, d.h. es wird innerhalb der Reaktionszeit ein vorwählbarer pH-Wert konstant gehalten.

Auf gleiche Weise kann auch ein Redoxpotential im Reaktionssystem konstant gehalten werden, indem man eine Messkette mit einer auf dieses Redoxsystem ansprechenden Elektrode zur Steuerung des Reagenszuflusses benützt; auf diese Weise erhält man einen "Potentiostaten"[4,5].

Da in einem lichtelektrischen Photometer eine Änderung der Extinktion einer gemessenen Lösung eine Änderung der resultierenden Spannung bewirkt, ist es möglich, nach entsprechender elektronischer Anpassung einen "Staten" mit einem Photometer auszusteuern. So kann man die Konzentration eines gefärbten Reaktanten der katalysierten Reaktion durch Hinzufügen der Lösung des entsprechenden Reaktionspartners konstant halten. Eine solche Versuchsanordnung wird als "Extinktiostat" bezeichnet[1,6].

In dieser Arbeit wird gezeigt, dass auch die Konstanthaltung einer vorwählbaren Stromstärke, wie sie z.B. in der Biamperometrie auftritt[7,8], durch Steuerung der Reagenszugabe möglich ist. Dazu muss ein Strom-Spannungs-Wandler vorgeschaltet werden. Auch eine derartige, wohl am besten als "Biamperostat" zu bezeichnende Versuchsanordnung kann also zur Bestimmung von Katalysatoren verwendet werden.

EXPERIMENTELLES

Mess- und Regelanordnung

Für die vorliegende Arbeit ist ein Gerät erforderlich, das die Konstanthaltung eines vorwählbaren Sollwertpotentials durch entsprechende Reagenszugabe zum Reaktionsmedium ermöglicht. Wir haben den "Combi-Titrator 3 D" (Metrohm, Herisau-Schweiz) verwendet, der aus pH-mV-Meter, "Impulsomat" (Regeleinheit) und "Multidosigraph" (Automatbürette + Schreiber) besteht.

An den Elektrodeneingang des "Impulsomaten" wird der in Abb. 1 wiedergegebene Strom-Spannungs-Wandler angeschlossen. Dieser wandelt den zwischen den beiden Platin-Elektroden in der Messzelle (Abb. 1, M) fliessenden geringen Strom in eine ihm proportionale Spannung um ("Istwert"). Die Potentialdifferenz zwischen dem so erhaltenen Istwert und dem vorgegebenen Sollwert wird vom Impulsomaten in einen entsprechenden Dosierbefehl an die Automatbürette ("Dosimat") umgewandelt und der Reagensverbrauch in Abhängigkeit von der Zeit aufgezeichnet. Je nach Geräteeinstellung schaltet die Motorkolbenbürette bei Über- oder Unterschreitung des vorgewählten Potentials ab. Das Gerät wurde in Verbindung mit dem "Mikro-Dosimaten" (wirksames Volumen 1 ml) benutzt.

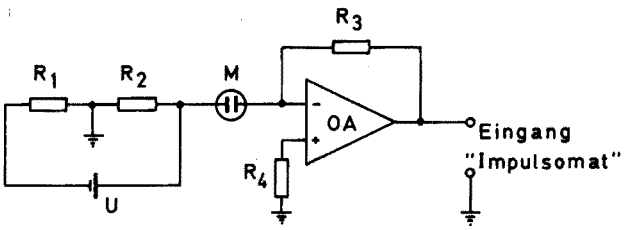

Abb. 1. Schaltschema des Strom-Spannungs-Wandlers zum Anschluss an den Elektrodeneingang des "Combi-Titrators 3 D". OA, Philbrick-Nexus Q 200; M, Doppel-Pt-Elektrode Pt 020 (Schott u. Gen., Mainz); U, Mallory RM 42 R (1.35 V).

Als Messgefäss dient ein 50 ml-Becherglas (Hochformat), welches sich in einem an einen Umlaufthermostaten angeschlossenen Aluminium-Hohlblock befindet. In einen auf dieses Becherglas passenden Teflon-Deckel sind ein Rührer, die Doppel-Pt-Elektrode (Typ Pt 020, Schott u. Gen., Mainz), der zur Kapillare ausgezogene Bürettenausgang des "Dosimaten" und der Auslauf einer 3 ml-Startpipette mit Hahn eingebaut. Das Messgefäss wird von unten gegen den fest am Stativ montierten Deckel gesetzt.

Der Papiervorschub am Schreiber betrug jeweils 15 mm min^{-1}.

BESTIMMUNG VON KATALASE IN RINDERBLUT DURCH MESSEN DER ZERFALLSGESCHWINDIGKEIT VON WASSERSTOFFPEROXID

Wasserstoffperoxid ist sowohl oxydierbar als auch reduzierbar und fungiert daher in der Biamperometrie als Depolarisator[9]. Da die Katalase den Zerfall von Wasserstoffperoxid aktiviert[10], lag es nahe, mit der oben beschriebenen Versuchsanordnung deren Enzymaktivität zu bestimmen.

Legt man nacheinander verschieden grosse Mengen von Katalase (z. B. 0.1–1 ml einer Lösung von Rinderleber-Katalase in Wasser/Thymol mit einer Enzymaktivität von 5 U ml^{-1}; Boehringer, Mannheim) in einem geeigneten Puffergemisch vor, so ist zur Aufrechterhaltung eines definierten Stromes (d.h. aber eines definierten Überschusses an Wasserstoffperoxid!) eine mehr oder weniger schnelle Zugabe von Wasserstoffperoxid mit dem Dosimaten erforderlich. Da der Schreiber den Reagensverbrauch in Abhängigkeit von der Zeit direkt registriert, kann aus der Schreiberkurve die jeweils erforderliche Zugabegeschwindigkeit für Wasserstoffperoxid als Tangens α abgelesen werden. In Abb. 2 ist eine einzelne derartige "Titrationskurve" wiedergegeben.

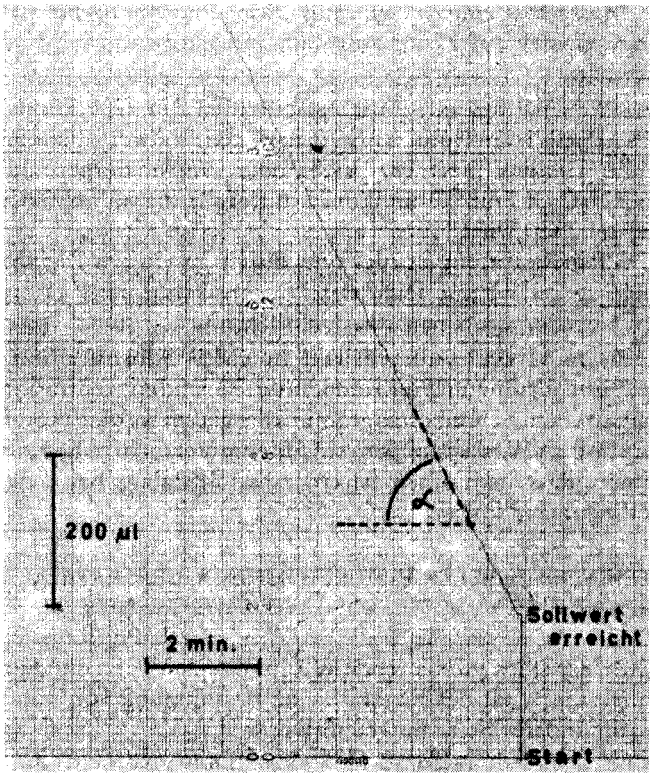

Abb. 2. Schreiberdiagramm für die Reaktion von 0.8 ml Katalase-Lösung (2.75 U ml^{-1} bei 50 µg H_2O_2-Überschuss in 27 ml Probelösung) mit Wasserstoffperoxidlösung der Konzentration 500 µg ml^{-1}

Verwendet man statt der reinen Katalase eine Suspension von Blut (z.B. Rinderblut) in physiologischer Kochsalzlösung, so kann bei bekannter, vorgegebener Blutmenge die spezifische Katalase-Aktivität dieses Blutes bestimmt werden. Hierzu ist es günstig, nach einem Vorschlag von Damaschke und Tödt[11] das Blut zunächst durch etwa halbstündiges Einleiten eines langsamen Luftstromes zu hämolysieren, damit auf maximale Aktivität zu bringen und anschliessend zu messen. Für eine Aktivitätsbestimmung sind etwa 30 µl Blut erforderlich. Ein linearer Zusammenhang zwischen Blutmenge (0–50 µl Blut) und Katalaseaktivität (tg α:

0–1.25) besteht. Bei der hier angegebenen Methode zur Bestimmung der Katalaseaktivität bleibt das Enzym mindestens 30 Min unverändert erhalten.

Messanordnung

Schaltschema Abb. 1:

$R_1 = 100$ KOhm; $R_2 = 3.9$ KOhm; $R_3 = 1.8$ MOhm; $R_4 = 33$ KOhm.

Durchführung

Das zu untersuchende Rinderblut wird zunächst mit physiologischer Kochsalzlösung 1+9 verdünnt und in einer Waschflasche mit Luftsauerstoff gesättigt, indem etwa 30 Min lang ein langsamer Luftstrom hindurchgesaugt wird. Nun werden 0.3 ml dieser Lösung in das Messgefäss einpipettiert, mit 10 ml Phosphatpuffer, pH 7.2 (0.15 *M*) versetzt und mit Wasser auf 27 ml aufgefüllt. Anschliessend wird 10 Min bei 25.0±0.3° thermostatiert.

Unter diesen Bedingungen beträgt das Ausgangspotential am Operationsverstärker (=Eingangspotential am Impulsomaten!) 10 mV; das Sollwertpotential wird auf 27.5 mV eingestellt. Diesem Wert entspricht eine Wasserstoffperoxid-Konzentration von etwa 50 μg H_2O_2/27 ml("Grundkonzentration"), die während der gesamten Messzeit konstant gehalten wird.

Die eigentliche Aktivitätsbestimmung erfolgt nun durch gesteuerte Zugabe von Wasserstoffperoxid (500 μg ml^{-1}) mit Hilfe des "Combi-Titrators 3 D" in Verbindung mit der in Abb. 1 wiedergegebenen Zusatzeinrichtung.

Die entsprechende Enzymaktivität—ausgedrückt in μMol Substratumsatz pro Min bei definierten Reaktionsbedingungen (Temperatur, Grundkonzentration an H_2O_2)—kann unmittelbar aus dem Schreiberdiagramm abgeglesen werden (vergl. Abb. 2). Die Grundkonzentration an Wasserstoffperoxid für eine Versuchsreihe lässt sich exakt dadurch bestimmen, dass man einen Ansatz ohne Katalase bei sonst völlig gleichen Reaktionsbedingungen "titriert".

BESTIMMUNG VON AZID-IONEN IM μg-BEREICH DURCH MESSEN DER KATALASE-INHIBIERUNG

Da Azid-Ionen auf Katalase stark inhibierende Wirkung zeigen[10], ist auf dem Wege über die Messung der Restaktivität der Katalase eine Bestimmung von Azid-Ionen möglich, wie bereits von anderer Seite mitgeteilt wurde[12]

Diese Azid-Bestimmung lässt sich auch mit Hilfe des "Biamperostaten" ausführen.

Durchführung

In das Messgefäss der oben beschriebenen Apparatur werden jeweils 0.5 ml einer Katalase-Lösung in physiologischer Kochsalzlösung mit einer konstanten Enzymaktivität von etwa 5 U ml^{-1} einpipettiert und mit 0.2–2 ml Natriumazid-Lösung (1.3 μg N_3^- ml^{-1}) zur Aufstellung der Eichkurve bzw. einem entsprechenden Volumen der zu bestimmenden neutralisierten Probelösung versetzt. Nach Zugabe von 10 ml Phosphatpuffer pH 7.2 und Auffüllen mit Wasser auf 27 ml wird 10 Min auf 25.0±0.3° thermostatiert und anschliessend Wasserstoffperoxid-Lösung (500 μg ml^{-1}) mit dem Dosigraphen zugesetzt.

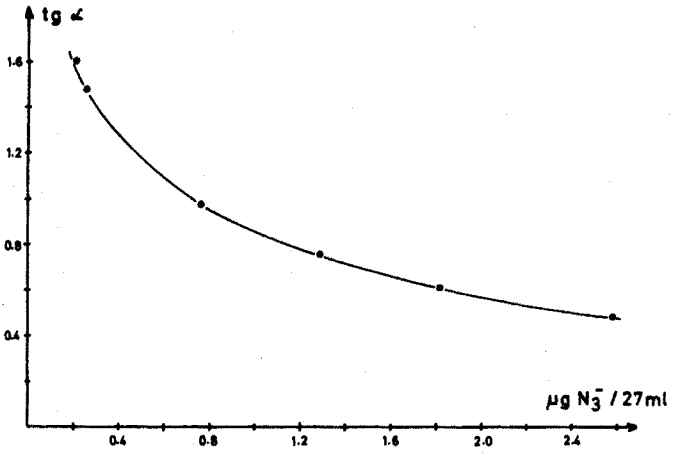

Abb. 3. Eichkurve für die Bestimmung von Azid-Ionen.

TABELLE I

BESTIMMUNG VON AZID-IONEN DURCH MESSEN DER KATALASE-RESTAKTIVITÄT AUF DEN ZERFALL VON WASSERSTOFFPEROXID

µg N_3^-/27 ml		*Fehler (µg)*	*µg N_3^-/27 ml*		*Fehler (µg)*
Gegeben	*Gefunden*		*Gegeben*	*Gefunden*	
0.20	0.19	−0.01	1.30	1.22	−0.08
0.40	0.40	±0.0	1.50	1.52	+0.02
0.60	0.62	+0.02	1.80	1.80	±0.0
0.80	0.79	−0.01	2.00	1.90	−0.10
1.00	1.02	+0.02	2.60	2.62	+0.02

Eine entsprechende Eichkurve ist in Abb. 3 wiedergegeben. Tabelle I bringt einige Ergebnisse.

BESTIMMUNG VON KUPFER(II) IM µg-BEREICH MIT HILFE DER KUPFER-KATALYSIERTEN OXYDATION VON JODID MIT PEROXIDISULFAT

Ebenso wie Wasserstoffperoxid wirkt auch das Redoxpaar Jodid/Jod bei biamperometrischen Messungen als Depolarisator[9]. Es ist daher möglich, auch solche katalysierte Reaktionen mit der oben beschriebenen Technik zu verfolgen, bei denen im Verlauf der Reaktion elementares Jod in Freiheit gesetzt wird. In diesem Falle gibt man zur Konstanthaltung des Stromes eine sehr verdünnte Thiosulfatlösung mit dem Dosimaten zu. Als Beispiel für die Anwendung dieser Methode soll die Kupfer-katalysierte Oxydation von Jodid mit Peroxidisulfat[13,14] dienen.

Messanordnung

Schaltschema Abb. 1:

$R_1 = 260$ KOhm; $R_2 = 3.9$ KOhm; $R_3 = 680$ KOhm; $R_4 = 1$ KOhm.

Durchführung

Da Jodid mit Peroxidisulfat auch ohne Anwesenheit eines Katalysators relativ rasch reagiert, wurde eine Versuchsdurchführung gewählt, bei der das Oxydationsmittel erst unmittelbar vor Beginn des Messvorganges zugegeben wird.

In das Messgefäss werden nacheinander 1–10 ml Kupfer-Standardlösung (10 μg Cu ml^{-1} als Kupferacetat) zur Aufstellung der Eichkurve bzw. ein entsprechendes Volumen der zu bestimmenden neutralisierten Probelösung, 2 ml 0.1 *M* Kaliumjodid-Lösung und 10 ml Phosphatpuffer pH 6.0 (0.3 *M*) einpipettiert und mit Wasser auf 27 ml aufgefüllt. Anschliessend wird 10 Min bei 25.0±0.3° thermostatiert. Unter diesen Bedingungen (also ohne Peroxidisulfat!) beträgt das Ausgangspotential etwa 20 mV; das Sollwertpotential wird auf 80 mV eingestellt.

Nun werden aus der Startpipette 3 ml Kaliumperoxidisulfat-Lösung (10 mg $S_2O_8^{2-}$ ml^{-1}) zugegeben und sofort anschliessend die automatische Zugabe von 0.005 *M* Natriumthiosulfat-Lösung aus dem Dosimaten gestartet.

In Abb. 4 ist eine auf diese Weise erhaltene Eichkurve wiedergegeben; in Tabelle II sind einige Messergebnisse zusammengestellt.

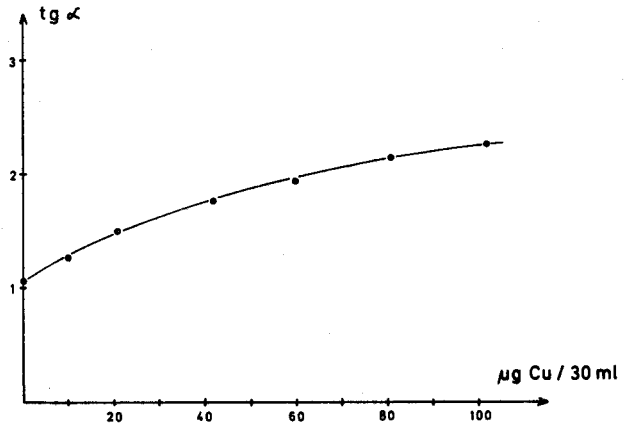

Abb. 4. Eichkurve für die Bestimmung von Kupfer(II).

TABELLE II

BESTIMMUNG VON KUPFER(II) MIT HILFE DER KUPFER-KATALYSIERTEN OXYDATION VON JODID MIT PEROXIDISULFAT

µg Cu/30 ml		*Fehler (µg)*	*µg Cu/30 ml*		*Fehler (µg)*
Gegeben	*Gefunden*		*Gegeben*	*Gefunden*	
1.0	1.5	+0.5	51.0	48.5	−2.5
5.0	4.6	−0.4	60.0	57.0	−3.0
10.0	10.5	+0.5	78.0	81.0	+3.0
21.0	22.0	+1.0	90.0	88.5	−1.5
30.0	28.5	−1.5	100.0	105.0	+5.0

BESTIMMUNG VON MOLYBDÄN(VI) IM μg-BEREICH MIT HILFE DER MOLYBDÄN-KATALYSIERTEN OXYDATION VON JODID MIT WASSERSTOFFPEROXID

Am Beispiel der Molybdän(VI)-katalysierten Oxydation von Jodid mit Wasserstoffperoxid[15–18] lässt sich zeigen, dass das Redoxpaar Jodid/Jod auch in Gegenwart von Wasserstoffperoxid selektiv erfasst werden kann, da die Depolarisationsspannung für Jodid/Jod wesentlich niedriger liegt (etwa 20 mV) als für Wasserstoffperoxid (etwa 50 mV).

Messanordnung

Schaltschema Abb. 1:

$R_1 = 260$ KOhm; $R_2 = 3.9$ KOhm; $R_3 = 680$ KOhm; $R_4 = 1$ KOhm.

Durchführung

Auch in diesem Falle verläuft die Oxydation von Jodid bereits ohne Katalysator relativ rasch, so dass das Oxydationsmittel ebenfalls erst unmittelbar vor der Bestimmung zugesetzt wird. In das Messgefäss werden nacheinander 5 ml 0.01 *M* Kaliumjodidlösung, 1–10 ml Molybdän-Standardlösung (5 μg Mo ml^{-1} als Natriummolybdat) zur Aufstellung der Eichkurve bzw. ein entsprechendes Volumen der zu bestimmenden neutralisierten Probelösung und 10 ml Acetatpuffer pH 3.6 (0.2 *M*) einpipettiert und mit Wasser auf 27 ml aufgefüllt. Anschliessend wird 10 Min bei $25.0 \pm 0.3°$ thermostatiert.

Unter diesen Bedingungen beträgt das Ausgangspotential 10 mV; dass Sollwertpotential wird auf 30 mV eingestellt.

Nach Zugabe von 3 ml Wasserstoffperoxid (500 μg ml^{-1}) aus der Startpipette wird sofort die Messung mit dem Biamperostaten begonnen. Als Reagens dient 0.005 *M* Natriumthiosulfat-Lösung. In Abb. 5 ist eine so erhaltene Eichkurve wiedergegeben; in Tabelle III werden einige Messergebnisse zusammengefasst.

Kupfer(II) stört bei dieser Bestimmung von Molybdän(VI) in vergleichbarer Konzentration nicht.

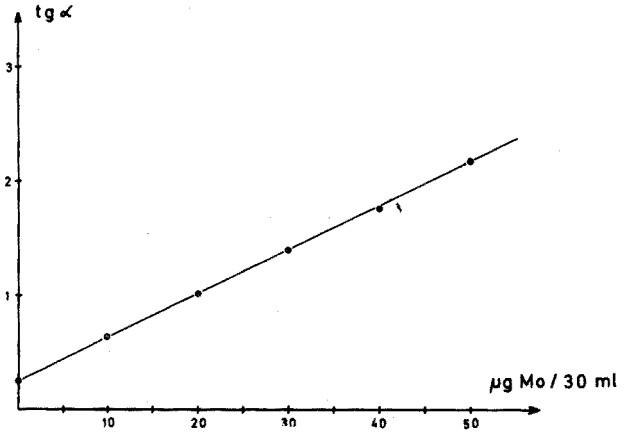

Abb. 5. Eichkurve für die Bestimmung von Molybdän(VI).

TABELLE III

BESTIMMUNG VON MOLYBDÄN(VI) MIT HILFE DER Mo-KATALYSIERTEN OXYDATION VON JODID MIT WASSERSTOFFPEROXID

µg Mo/30 ml		*Fehler (µg)*	*µg Mo/30 ml*		*Fehler (µg)*
Gegeben	*Gefunden*		*Gegeben*	*Gefunden*	
1.0	1.2	+0.2	20.0	20.0	±0.0
5.0	5.2	+0.2	29.0	28.0	−1.0
8.0	8.0	±0.0	30.0	29.7	−0.3
10.0	10.5	+0.5	40.0	39.0	−1.0
19.0	18.0	−1.0	50.0	50.5	+0.5

BESTIMMUNG VON JODID IM µg-BEREICH MIT HILFE DER JODID-KATALYSIERTEN OXYDATION VON ARSEN(III) MIT CER(IV)

Das Redoxpaar Cer(III)/Cer(IV) kann ebenfalls biamperometrisch erfasst werden, die Depolarisationsspannung beträgt etwa 100 mV. Als Beispiel für die Anwendung dieser Methode wurde von uns die Jodid-katalysierte Oxydation von Arsen(III) mit Cer(IV)[19,20] gewählt. Da die Reaktionsgeschwindigkeit auch hier stark pH-abhängig ist, wurden die Bestimmungen von Jodid in einer mit Glycin/Schwefelsäure gepufferten Lösung von pH 1.5 durchgeführt.

Messanordnung

Schaltschema Abb. 1;

$R_1 = 49$ KOhm; $R_2 = 3.9$ KOhm; $R_3 = 680$ KOhm; $R_4 = 1$ KOhm.

Durchführung

In das Messgefäss werden nacheinander 2 ml Arsen(III)-Lösung (5 g As_2O_3 in wenig 5 *M* Natriumhydroxid gelöst, mit Schwefelsäure auf pH 7.0 neutralisiert und mit Wasser auf 250 ml aufgefüllt), 1–10 ml Kaliumjodid-Standardlösung (2 µg J^- ml^{-1}) zur Aufstellung der Eichkurve bzw. ein entsprechendes Volumen der zu bestimmenden Probelösung und 10 ml Glycin/Schwefelsäurepuffer pH 1.5 (0.2 *M*) einpipettiert und mit Wasser auf 27 ml aufgefüllt. Anschliessend wird 10 Min bei 25.0 ± 0.3° thermostatiert.

Unter diesen Bedingungen beträgt das Ausgangspotential etwa 100 mV; das Sollwertpotential wird auf 400 mV eingestellt. Die katalysierte Reaktion beginnt mit der automatischen Zugabe von Cer(IV)-Sulfat-Lösung (0.005 *M* in 0.5 *M* Schwefelsäure) aus dem Dosimaten. Ein linearer Zusammenhang zwischen Jodidmenge (0–20 µg I^-/27 ml) und tg α (0–3.5) besteht; Tabelle IV enthält eine Auswahl von Messergebnissen.

Da die unkatalysierte Reaktion in diesem Falle nur sehr langsam abläuft, kann die Bestimmung von Jodid auch im Bereich von 0.2–2 µg/27 ml erfolgen, wenn die Vorschubgeschwindigkeit des Schreibers zum Dosimaten von 15 mm min^{-1} auf 2 mm min^{-1} gesenkt wird. Dabei wird gleichsam die Reaktionszeit und damit

TABELLE IV

BESTIMMUNG VON JODID MIT HILFE DER JODID-KATALYSIERTEN OXYDATION VON ARSEN(III) MIT CERIUM(IV)

$\mu g\ J^-/27\ ml$		*Fehler* (μg)	$\mu g\ J^-/27\ ml$		*Fehler* (μg)
Gegeben	*Gefunden*		*Gegeben*	*Gefunden*	
2.00	2.05	+0.05	10.00	10.10	+0.10
2.25	2.20	−0.05	12.50	12.40	−0.10
4.75	5.00	+0.25	15.00	14.90	−0.10
5.00	5.20	+0.20	17.00	17.10	+0.10
9.00	8.70	−0.30	20.00	19.80	−0.20

der Steigungswinkel α erhöht. Die Tangens-Werte liegen dann für den hier angegebenen Bereich zwischen 0.6 und 3.2.

ZUSAMMENFASSUNG

Biamperometrisch erfassbare Reaktionen können durch Verwendung eines Strom-Spannungs-Wandlers mit Hilfe der "Potentiostat"-Methode ausgewertet werden. Die durch Katalase katalysierte Zersetzung von Wasserstoffperoxid, die Kupfer-katalysierte Oxydation von Jodid mit Peroxidisulfat, die Molybdän(VI)-katalysierte Oxydation von Jodid mit Wasserstoffperoxid und die Jodid-katalysierte Oxydation von Arsen(III) mit Cer(IV) werden zur Illustration dieser Möglichkeit verwendet. Es werden die Katalysatoren Katalase, Kupfer, Molybdän-(VI) und Jodid sowie Azid als Inhibitor für Katalase im p.p.b.–p.p.m.-Bereich bestimmt.

SUMMARY

Biamperometrically observable reactions may be evaluated by the "potentiostat"-method with the application of a current-to-voltage transducer. The catalase-catalyzed autodecomposition of hydrogen peroxide, the copper-catalyzed oxidation of iodide with peroxydisulfate, the molybdenum(VI)-catalyzed oxidation of iodide with hydrogen peroxide, and the iodide-catalyzed oxidation of arsenic(III) with cerium(IV) are used to illustrate this concept. The catalysts, catalase, copper(II), molybdenum(VI) and iodide, as well as azide as an inhibitor for catalase, can be determined in the p.p.b.–p.p.m. range.

LITERATUR

1 D. Klockow, H. Weisz und K. Rothmaier, *Z. Anal. Chem.*, 264 (1973) 385.
2 H. V. Malmstadt und E. H. Piepmeier, *Anal. Chem.*, 37 (1965) 34.
3 K. M. Møller, *Biophys. Acta*, 16 (1955) 162.
4 H. Weisz, D. Klockow und H. Ludwig, *Talanta*, 16 (1969) 921.
5 D. Klockow, H. Ludwig und M. A. Giraudo, *Anal. Chem.*, 42 (1970) 1682.
6 H. Weisz und K. Rothmaier, Unveröffentl. Studie, Freiburg, 1972.

7 E. Michalski, K. Czarnecki und K. Pietrucha, *Chem. Anal. (Warschau)*, 8 (1963) 713; *Z. Anal. Chem.*, 237 (1968) 379.
8 H. Weisz und S. Pantel, *Anal. Chim. Acta*, 62 (1972) 361.
9 K. G. Stone und H. G. Scholten, *Anal. Chem.*, 24 (1952) 671.
10 H. U. Bergmeyer, *Methoden der Enzymatischen Analyse*, Bd. I, Verlag Chemie, Weinheim, 2. Aufl., 1970, S. 636ff.
11 K. Damaschke und F. Tödt, *Z. Naturforsch.* B, 11 (1956) 621.
12 J. Brad, E. Dobrescu und Z. Marcu, *Chim. Analit.*, 2 (1972) 62; *Anal. Abstr.*, 24 (1973) 3339.
13 Th. S. Price, *Z. Phys. Chem.*, 27 (1898) 474.
14 A. v. Kiss und L. v. Zombory, *Rev. Trav. Chim.*, 46 (1927) 230.
15 J. Bode, *Z. Phys. Chem.*, 37 (1901) 257.
16 K. B. Yatsimirskii und L. P. Afanaseva, *Zh. Anal. Khim.*, 11 (1956) 319; *Chem. Abstr.*, 50 (1956) 15333 g.
17 K. B. Yatsimirskii, *Catal. Chem. Kinet.*, (1964) 201; *Chem. Abstr.*, 66 (1967) 61514.
18 C. F. Garcia und L. J. Gomez, *Rev. Soc. Quim. Mex.*, 13 (1969) 222A; *Chem. Abstr.*, 72 (1970) 115232.
19 E. B. Sandell und J. M. Kolthoff, *J. Amer. Chem. Soc.*, 56 (1934) 1426.
20 G. Knapp und H. Spitzy, *Talanta*, 16 (1969) 1353.

Analytica Chimica Acta, 70 (1974) 401–410

A POTENTIOMETRIC AND CALORIMETRIC STUDY OF THE POLYNUCLEAR AND MONONUCLEAR COMPLEXES OF NICKEL(II) WITH THIOGLYCOLIC ACID

H. F. DE BRABANDER, L. C. VAN POUCKE and Z. EECKHAUT
Department of General and Inorganic Chemistry, University of Ghent, Ghent (Belgium)
(Received 2nd November 1973)

Thioglycolic acid forms very stable complexes with many metal ions. The replacement in complexiметry of potassium cyanide by thioglycolic acid as a masking agent has been thoroughly discussed by Přibil and Vesely[1]. However, it would be very interesting to know which types of complexes are formed and why these complexes are so stable. In this study, particular attention is paid to the nickel(II) complexes. In the first papers devoted to this subject, the system was considered as mononuclear. Stability constants were calculated from one formation curve only[2]. Later Leussing *et al.*[3] showed that polynuclear complexes are formed as well as mononuclear complexes; they claimed that a good description of the system was obtained by considering the complexes B_4A_6 and BA_2, B being the metal ion and A the ligand. Perrin and Sayce[4] repeated the experiments of Leussing, and treated the experimental data with a GAUSS computer programme. They found, in addition to the above-mentioned complexes, the complexes B_3A_4, B_2A_2 and BA_3, and also some evidence for the complex BA. Below pH 5.5, the complex B_3A_4 predominates; in neutral medium, B_4A_6 is the main compound, and in basic medium the complex formation is mononuclear with BA_2 as the most important species. In this study, an attempt was made to determine the enthalpy and entropy changes accompanying the complex formation from calorimetric experiments.

Therefore it was necessary to study the system again and to search for those regions where one complex largely predominates or where several complexes are simultaneously present in almost equal amounts, since only under these conditions can significant enthalpy changes be obtained. Furthermore, it was necessary to have sufficiently high concentration of the complexes, otherwise the heat liberated was too small for precise measurements.

EXPERIMENTAL

Apparatus

pH measurements were performed with a Radiometer pHM4 pH-meter, equipped with a G202c glass electrode and a saturated calomel electrode as reference. The glass electrode was standardized against a 0.01 *M* borax buffer solution as described by Bates[5]. All solutions were maintained at 25 ± 0.1°C.

Calorimetric measurements were carried out with an LKB 8700-2 Precision Calorimeter.

Reagents

Thioglycolic acid (Fluka) was redistilled before use. Aqueous solutions were prepared with oxygen-free water and regularly flushed with pure nitrogen gas. Under these conditions, the solutions were stable for a long period[6]. A stock solution of 0.2 *M* nickel nitrate was prepared and standardized gravimetrically as bis(dimethylglyoximato)nickel[7]. In order to keep the activity coefficients as constant as possible, all solutions were made up to an ionic strength of 0.5 with potassium nitrate (Merck *p.a.*). Before use, all solutions were abundantly flushed with pure nitrogen gas.

Procedure for pH titration

A mixture of metal ion and thioglycolic acid was titrated with potassium hydroxide. Four titrations were performed with total metal ion concentrations of respectively 0.032 *M*, 0.008 *M*, 0.002 *M* and 0.0005 *M* and an initial concentration of total ligand equal to five times the concentration of the metal ion. The total metal ion concentration was kept constant by adding, after each addition of potassium hydroxide, an equal volume of metal ion solution with concentration twice that of the total metal ion in the cell. During titration, the solution was protected from air by vigorously bubbling a stream of nitrogen gas through it.

Procedure for calorimetric titration

Four thermometric titrations were performed. In each titration, the total volume pipetted into the reaction vessel was 80 ml; the mixtures were composed as shown in Table I. To these solutions a 1 *M* potassium hydroxide solution was added in 0.25-ml portions. After each addition the heat capacity of the solution was determined by quantitative electrical heating. From this and from the change in temperature during the addition, the heat effect in calories was obtained as described by Wadso[8]. Before closing the reaction vessel, air was removed by a stream of pure nitrogen.

TABLE I

COMPOSITION OF TITRATED MIXTURES

Titration number	*Vol. 0.032 M $Ni(NO_3)_2$ (ml)*	*Vol. 0.128 M ligand (ml)*	*Vol. 0.5 M KNO_3 (ml)*
1	0	30	50
2	40	40	0
3	30	30	20
4	20	20	40

RESULTS AND MATHEMATICAL TREATMENT

The symbols used here are the same as in the papers of Sillén[9,10,11] and are listed below:

B total concentration of Ni^{2+}

b concentration of free Ni^{2+}

A total ligand concentration
h_2a concentration of $SH–CH_2–COOH$
ha concentration of $SH–CH_2–COO^-$
a concentration of $^-S–CH_2–COO^-$
$pa = -\log a$
h activity of hydrogen ion
c_{base} concentration of base added
Z average number of ligands bound per Ni^{2+} ion
t number of ligands in a link
n variable integer: number of links in a core + links complex
$\bar{n}$ average number of links in a core + links complex
K_{Hi} mixed protonation constants of the ligand, defined as $K_{Hi} = h_i a/h \cdot h_{i-1} a$
β_{pq} overall stability constant for a B_qA_p complex, defined as $\beta_{pq} = (B_qA_p)/b^q \cdot a^p$
$\log F = \log B/b$
$u = a^t b$
β_i overall stability constant for a complex $B(A_tB)_i$
$g = \sum_{i=1}^{n} \beta_i u^i$
$y = Z/t$
$x = t \log a + \log B$
N maximum number of hydrogen ions that the ligand can take up

Potentiometric study

The formation function $Z(a)$ was calculated from eqns. (1) and (2) by means of a general computer programme[12]. The results were printed, plotted and punched on cards for further use.

$$a = \frac{NA - c_{base} - [H^+] + [OH^-]}{\sum_{n=1}^{N} nh^n a \prod_{i=1}^{n} K_{Hi}} \tag{1}$$

$$Z = \left[A - a\left(1 + \sum_{n=1}^{N} h^n \prod_{i=1}^{n} K_{Hi}\right)\right]/B \tag{2}$$

In the pH range investigated (3–9), the terms $[H^+]$ and $[OH^-]$ can be neglected. As can be seen, the protonation constants K_{Hi} for the carboxyl and mercapto groups are needed to start the calculation of the formation function. These constants were obtained as described by Thiers *et al.*[13] and found to be, respectively, 3.548 and 10.048.

The formation curves $Z(pa)_B$ obtained by these calculations are shown in Fig. 1. As can be seen, a set of parallel curves was found for Z values lower than 1.3. Since a was small over the range investigated, we can assume that b is not negligible in comparison with B. According to Sillén[9,10,11], systems which give such curves in these conditions are polynuclear and form a so-called "core + links" system of general formula $B(A_tB)_n$. The value of t can be determined from the spacing of the curves with the aid of eqn. (3):

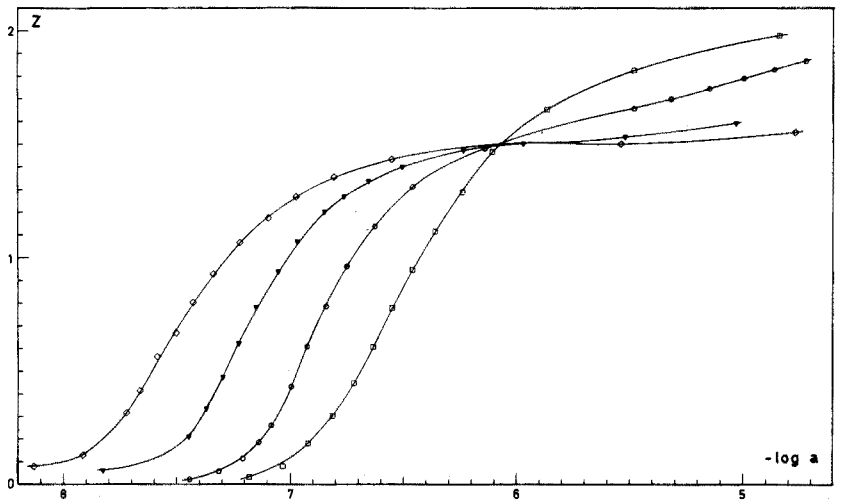

Fig. 1. The formation curves of the system nickel(II)– and thioglycolic acid. *B*: (◇) 0.032 *M*, (▼) 0.008 *M*, (○) 0.002 *M*, (□) 0.0005 *M*.

$$t = -\left(\frac{\partial \log B}{\partial \log a}\right)_Z \tag{3}$$

A plot of log *B* versus log *a* at a given *Z* below 1.3 gives a straight line of slope $t=2$. The complexes present can therefore be represented by the general formula $B(A_2B)_n$. It can be observed (Fig. 1) that for larger values of *B*, the curve $Z(pa)_B$ tends to a value of $Z=1.5$, which indicates that a very stable complex is formed. As can be seen from eqn. (4), for $Z \leqslant 1.5$, the highest possible value of *n* is 3:

$$Z = \frac{p}{q} = \frac{2n}{n+1} = 1.5 \tag{4}$$

Accordingly, three polynuclear species can be formed, namely B_2A_2, B_3A_4 and B_4A_6. This was confirmed by calculating the function $y(x)$, which is shown in Fig. 2. As *y* and *x* are both functions of the same variable *u*, all $y(x)$ curves must coincide. For *y* values below 0.6, this criterion was satisfied but for higher values deviations were observed. These deviations are due to the conversion of polynuclear to mononuclear species. During the titration the colour of the solution suddenly changed from brown to pink. As Z_{max} is 2 (Fig. 1), mononuclear species BA and BA_2 could be formed. To summarize, it can be stated that below $Z=1.5$ polynuclear species were formed, which were converted to mononuclear in the range $Z=1.5$–2.0.

In order to determine the stability constants of the polynuclear species, $\bar{n}$ can be calculated from eqn. (5):

$$\bar{n} = \frac{y}{1-y-F^{-1}} \tag{5}$$

F was found by calculating the following integral

$$\log F = 0.434y + \int_{-\infty}^{x} y\,dx \tag{6}$$

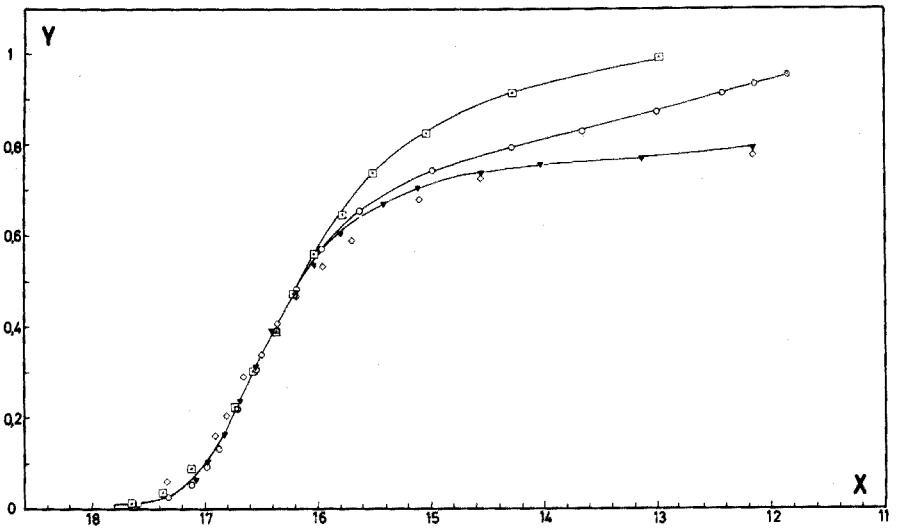

Fig. 2. The y,x curve of the system nickel(II)– and thioglycolic acid. *B*: As for Fig. 1.

TABLE II

CALCULATION OF $\bar{n}$

y	$\bar{n}$	y	$\bar{n}$
0.015	2.004	0.605	2.870
0.07	2.112	0.645	2.901
0.095	2.037	0.685	2.923
0.175	2.176	0.705	2.966
0.285	2.475	0.720	3.008
0.385	2.572	0.730	3.027
0.485	2.854	0.750	3.088
0.555	2.889		

Integration was started at a finite value of x, and the residual integral could be neglected. The results are given in Table II. $\bar{n}$ varies between 2 and 3, indicating that the complex B_2A_2 will not be formed.

The functions g and u were calculated. The successive extrapolation method of Fronaeus[14] and Leden[15] is used to obtain the stability constants.

The function $f_1 = g/u = \beta_1 + \beta_2 u + \beta_3 u^2$ was extrapolated for $u = 0$ in order to obtain a value for β_1. Another function $f_2 = (f_1 - \beta_1)/u$ was calculated and again extrapolated for $u = 0$. This extrapolation procedure was repeated until the function $f_n = (f_{n-1} - \beta_{n-1})/u$ was constant. This was found for $n = 3$, as expected. The results are given in Table III. The complex B_2A_2 was found not to be present.

For the calculation of the stability constants of the mononuclear species, the following points should be noted. As polynuclear species were assumed to predominate in the Z area $0 \rightarrow 1.5$, the stability constant of the mononuclear BA could not be determined. The stability constant of the mononuclear BA_2 could be

TABLE III

STABILITY CONSTANTS OF COMPLEXES

Log	*Extrapolation procedure*	*After modification*	*PNUC*	*Leussing et al.*[3]
$\beta_{3.4}$	32.079	32.699	32.219	33.845
$\beta_{4.6}$	49.643	49.301	49.157	49.845
$\beta_{1.2}$	12.809	12.666	12.759	13.040

determined from the data of the Z area 1.5→2, where a mixture of B_4A_6 and BA_2 was considered; the presence of B_3A_4 in that region could be neglected.

The following equations can be written:

$$B = b + \beta_{1.2} ba^2 + 4\beta_{4.6} b^4 a^6 \tag{7}$$

$$BZ = 2\beta_{1\ 2} ba^2 + 6\beta_{4\ 6} b^4 a^6 \tag{8}$$

Since data for $Z(a)_B$ are known, the two unknown factors are $\beta_{1.2}$ and b. Elimination of b from eqns. (7) and (8) yields:

$$a^8(2-Z)\beta_{1.2}^4 + 2a^6(4Z-9)\beta_{1.2}^3 + 18a^4(3-Z)\beta_{1.2}^2 + 54a^2\beta_{1.2} + 27Z - 2\beta_{4.6} a^6 B^3 (3-2Z)^4 = 0 \tag{9}$$

This fourth-power equation in $\beta_{1.2}$ can be solved by the method of Newton, to give $\log \beta_{1.2} = 12.809$.

The formation curves were recalculated and plotted from eqns. (10) and (11) with the aid of an IBM 360/30 computer

$$Z = \frac{2\beta_{1,2} ba^2 + 4\beta_{3,4} b^3 a^4 + 6\beta_{4,6} b^4 a^6}{b + \beta_{1,2} ba^2 + 3\beta_{3,4} b^3 a^4 + 4\beta_{4,6} b^4 a^6} \tag{10}$$

$$B = b + \beta_{1,2} ba^2 + 3\beta_{3,4} b^3 a^4 + 4\beta_{4,6} b^4 a^6 \tag{11}$$

It was found that the stability constants needed to be modified. The final results are given in Table III.

Later, the data of this experiment were treated by means of a PNUC computer programme, with a least-squares procedure. The square error sum U is given by

$$U = (Z_{exp} - Z_{calc})^2 \tag{12}$$

Z_{calc} was calculated with estimated values for β_{qp} from eqns. (10) and (11). The function U was minimized by the variable metric method, described by Davidon[16] The standard deviation $s(Z)$ was calculated from:

$$s(Z) = [U_{min}/(n_{exp} - n_{par})]^{\frac{1}{2}} \tag{13}$$

where U_{min} is the value for U at the minimum, n_{exp} the number of experimental points and n_{par} the number of parameters. The values of β_{qp} corresponding with U_{min} are the "best" parameters. These results are also given in Table III.

Other possible species present in solution are the complexes BA and B_2A_2. Perrin and Sayce[4] even found evidence for the presence of BA_3. Each of these three complexes was added to the system and the minimum U_{min} was again calculated. As no better minimum was found, these three species were rejected.

Calorimetric study

From titration 1 (Table I), the heats and entropies of protonation for the carboxylate and the mercaptan group were calculated with the aid of eqns. (14) and (15):

$$Q - Q_{dil} = -(\Delta H_{H_2O} - \Delta H_{Hi})[OH^-] \quad (14)$$

$$\Delta G_{Hi} = -RT \ln K_{Hi} = \Delta H_{Hi} - T\Delta S_{Hi} \quad (15)$$

ΔH_{H_2O} was taken to be -13.34 kcal mole^{-1}, as established by Vanderzee and Swanson[17], Hale *et al.*[18] and the present experiments. The results are given in Table IV.

TABLE IV

HEAT AND ENTROPY OF COMPLEX FORMATION

	log K_{Hi}/*log* β	ΔG (*kcal mole*$^{-1}$)	ΔH (*kcal mole*$^{-1}$)	ΔS (*cal mole* K^{-1})
–COOH	3.548	−4.84	+0.11	+16.6
–SH	10.084	−13.75	−6.52	+24.3
BA_2	12.759	−17.39	−3	+48
B_3A_4	32.219	−43.91	−21	+75
B_4A_6	49.157	−67.00	−31	+118

The heats and entropies of formation of the complexes were calculated from titrations 2,3 and 4 with the aid of the equation:

$$\Delta H_{1.2}(-\beta_{1.2}ba^2) + \Delta H_{3.4}(-\beta_{3.4}b^3a^4) + \Delta H_{4.6}(-\beta_{4.6}b^4a^6) + (\Delta H_{H1} + \Delta H_{H2})(a + 2\beta_{1.2}ba^2 + 4\beta_{3.4}b^3a^4 + 6\beta_{4.6}b^4a^6) + \Delta H_{H1}haK_{H2} - Q + Q_{dil} = 0 \quad (16)$$

The values for b, a and h were calculated from the stability constants and the total concentrations in the titration cell with the aid of the computer program BDTV[19]. The final values of $\Delta H_{1.2}$, $\Delta H_{3.4}$ and $\Delta H_{4.6}$ were obtained with the aid of a computer program THER. The results are given in Table IV.

DISCUSSION

As can be seen from Table II the nickel(II)–thioglycolic acid system can be represented by the formation of three complexes: BA_2, B_4A_6 and B_3A_4. The contribution of B_3A_4 to the system can be considered as small. These results are in good agreement with the work of Leussing *et al.*[3]. In contrast to the results of Perrin and Sayce[4], no evidence for the existence of the species BA, B_2A_2 or BA_3 was found.

From the formation function at different temperatures, Leussing *et al.* derived the enthalpy of formation of the complexes BA_2 and B_4A_6 and found -3.5 kcal mole^{-1} and -31 kcal mole^{-1}, respectively. The present calorimetric results (Table IV) confirm these values, and in addition a value for $\Delta H_{3.4}$ was deter-

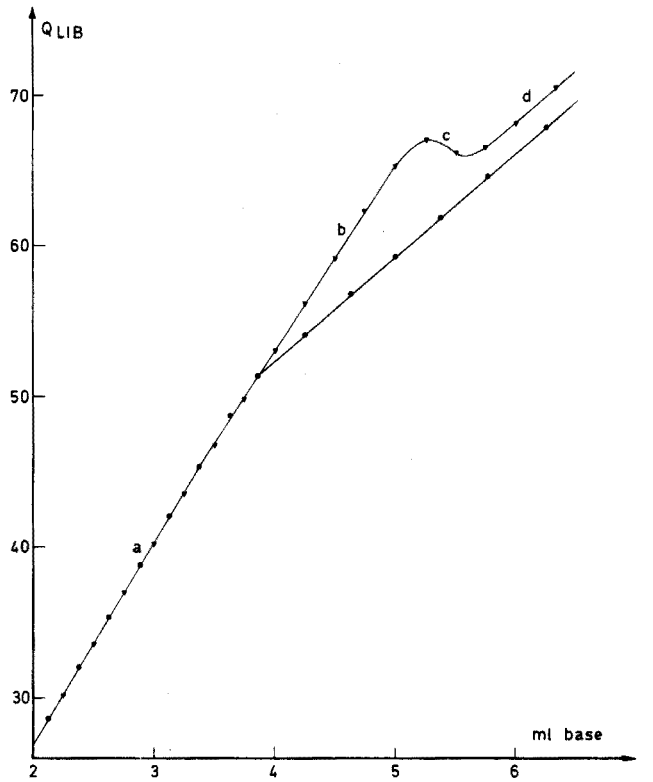

Fig. 3. Calorimetric curves for thioglycolic acid and for a mixture of nickel(II) and thioglycolic acid with potassium hydroxide. (●) Titration 1, (▼) titration 3.

mined as -21 kcal mole^{-1}. It is obvious that more heat is liberated per nickel ion when polynuclear complexes are formed than for mononuclear species. This is illustrated in Fig. 3, where two plots of the heat liberated during a titration *versus* the amount of added base are given. The first plot is related to titration 1 (Table I); two straight lines are obtained for the neutralization of the carboxylic and the mercaptan group, respectively.

The data obtained from titration 3 are shown in the second plot; the curve obtained can roughly be divided in four parts: (a) the carboxylic group is neutralized but no complexes are formed; (b) mainly polynuclear complexes are formed; (c) the polynuclear complexes are converted to mononuclear ones, the reaction being endothermic; (d) all metal ions are bound as BA_2, the heat liberated being due to the neutralization of the mercaptan group.

If it is accepted that the structures of the complexes proposed by Leussing *et al.*[3] are correct and that there are 6 double (Ni–S) and 4 (Ni–O) bonds for the B_4A_6 complex, 4 double (Ni–S) and 4 (Ni–O) bonds for the B_3A_4 complex, and 2 single (Ni–S) and 2(Ni–O) bonds for the BA_2 complex, then it can be calculated that a double (Ni–S) bond gives a contribution to the enthalpy of formation of about -5 kcal mole^{-1}. The heat liberated at the formation of a B_4A_6 complex will almost entirely be caused by the formation of six double (Ni–S) bonds.

As would be expected, the effect on enthalpy of a bonding carboxylate group is very small. It can also be shown that a single (Ni–S) bond gives an enthalpy effect less than one third of the effect of a double (Ni–S) bond. The stability of the mononuclear BA_2 is mainly caused by the entropy term; indeed, per nickel ion, the entropy contribution to the free energy is considerably higher than in the case of the B_3A_4 or B_4A_6 complex. The high entropy term could be caused by the chelating ability of the carboxylate group. This would explain why for analogous ligands such as 2-mercaptoethanol and 3-mercapto-1,2-propanediol, which lack a chelating group at the end of the aliphatic chain, the polynuclear chain formation is continued[20], polymeric complexes are formed, and no mononuclear species is found.

The fact that thioglycolic acid forms strong complexes can be ascribed to two different causes: in the first place the polynuclear complexes are very stable, which is mainly due to the favourable enthalpy change accompanying the linking of two metal ions by one sulphur atom; in the second place, when mononuclear complexes are formed, the stability is enhanced by chelate formation.

SUMMARY

The complex formation between nickel(II) and thioglycolic acid was studied by a potentiometric method at 25°C and in 0.5 *M* KNO_3. In solution two polynuclear complexes, B_3A_4 and B_4A_6, and one mononuclear complex, BA_2, were detected, and the following stability constants were determined: $\log \beta_{3,4} = 32.219$; $\log \beta_{4,6} = 49.157$; $\log \beta_{1,2} = 12.759$. The enthalpies of formation of the double (Ni–S–Ni) and single (Ni–S) bond were determined by calorimetric titration, and were found to be -5 kcal mol^{-1} and -1.5 kcal mol^{-1}, respectively. It was shown that the stability of the polynuclear complexes is due to the enthalpy term, whereas the stability of the mononuclear complexes can be ascribed principally to the entropy term.

REFERENCES

1 R. Přibil and V. Vesely, *Talanta*, 8 (1961) 743.
2 D. L. Leussing, *J. Amer. Chem. Soc.*, 80 (1958) 4180.
3 D. L. Leussing, R. E. Larahy and G. S. Alberts, *J. Amer. Chem. Soc.*, 82 (1960) 4826.
4 D. D. Perrin and I. G. Sayce, *J. Chem. Soc. A*, (1967) 82.
5 R. G. Bates, *Determination of pH*, Wiley, New York, 1954, p. 76.
6 E. Jacobsen and W. Lund, *Acta Chem. Scand.*, 19 (1965) 2379.
7 A. I. Vogel, *A text book of Quantitative Inorganic Analysis*, Longmans, London, p. 479.
8 L. Wadso, *Sci. Tools*, 13 (1966) 33.
9 L. G. Sillén, *Acta Chem. Scand.*, 8 (1954) 299.
10 L. G. Sillén, *Acta Chem. Scand.*, 8 (1954) 318.
11 G. Biederman and L. G. Sillén, *Acta Chem. Scand.*, 10 (1956) 1011.
12 H. F. De Brabander and L. C. Van Poucke, *J. Coord. Chem.*, in press.
13 G. F. Thiers, L. C. Van Poucke and M. A. Herman, *J. Inorg. Nucl. Chem.*, 30 (1968) 1543.
14 S. Fronaeus, *Diss. Lund.*, (1948).
15 I. Leden, *Diss. Lund.*, (1943).
16 W. C. Davidon, *ANL-5990 Physics and Mathematics AEC.*, Research and Development Report, Argonne National Laboratory, 1966.

17 C. E. Vanderzee and I. A. Swanson, *J. Phys. Chem.*, 67 (1963) 2608.
18 I. D. Hale, R. H. Izatt and J. J. Christensen, *Proc. Chem. Soc.*, (1963) 240.
19 R. Arnek, L. G. Sillén and O. Wahlberg, *Ark. Kemi*, 31 (1968) 27.
20 H. F. De Brabander, L. C. Van Poucke and Z. Eeckhaut, *Inorg. Chim. Acta*, 6 (1972) 459.

Analytica Chimica Acta, 70 (1974) 411–416

INVESTIGATIONS ON THE REDOX CHARACTER OF DITHIZONE BY VOLTAMMETRIC METHODS

PART I. THE REDUCTION OF DITHIZONE IN AQUEOUS SOLUTIONS

L. TOMCSÁNYI

Research Institute for Non-Ferrous Metals, 1116-Budapest-XI (Hungary)

(Received 11th October 1973)

Dithizone (diphenylthiocarbazone, 3-mercapto-1,5-diphenylformazan, H_2Dz) was first used for the colorimetric determination of traces of various heavy metals by Fischer[1] in 1925, and has since been very widely applied. The great advances in the development of voltammetric methods provides new possibilities for studying the redox properties of dithizone–dithizonate systems.

Dithizone ($C_{13}H_{12}N_4S$) exists in two tautomeric forms. As the reagent has been generally used in non-aqueous or basic media, the present investigations were carried out in basic solutions, where dithizone exists almost quantitatively in the enol form. The enol form is dibasic, but as it loses only a single proton from the thiol group below pH 14, it behaves[2] as a monobasic acid with a pK_1 value of 4.86.

The electrochemical redox properties of dithizone are governed by its thiol group and the formazan structure:

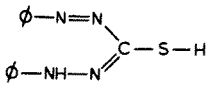

formazan thiol

Formazan can be either reduced or oxidized in a suitable medium at an appropriate redox potential[3], whereas the thiol group can only be oxidized:

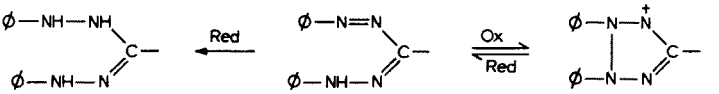

diphenylcarbazide colourless — diphenylformazan coloured — diphenyltetrazolium colourless

$$2\,\text{-SH} \overset{\text{Ox}}{\rightarrow} \text{-SS-}$$

disulphide

and

$$\text{-SH} \overset{\text{Ox}}{\rightarrow} \underset{\text{sulphinic acid}}{\text{-SOOH}} \overset{\text{Ox}}{\rightarrow} \underset{\text{sulphonic acid}}{\text{-SOOOH}}$$

The fact that dithizone is a weak reducing agent is well known; this behaviour and the results of spectrophotometric investigations of the oxidation products have been described by several authors[4,5].

As the mechanisms of redox processes can be investigated directly by different voltammetric methods, the redox properties of dithizone can be clarified further by applying this technique. The investigation was directed towards redox processes having an exact concentration function, so that polarographic techniques could be used for the determination of dithizone.

EXPERIMENTAL

The voltammetric measurements were carried out with a Radiometer PO4g polarograph connected to a Metrohm IR compensator E446. A Radelkis potentiostat combined with a current integrator (type OH404) was used for the coulometric macroelectrolysis. A Radiometer E65 dropping mercury electrode with a DLT 1 drop-life timer and an E69 hanging mercury drop electrode were used for the voltammetric measurements. For microcoulometry, a microcell (0.17 cm^3 volume) was constructed as described by Biondi and Bellugi[6]. A cell containing a large mercury pool electrode, a separate platinum foil counter electrode and a saturated calomel reference electrode was used for controlled potential macroelectrolysis. Generally, 100 ml of $5 \cdot 10^{-4}$ *M* dithizone solution was electrolysed. The pH of solutions was checked with a Radelkis OP205 meter and a Metrohm EA120U glass electrode.

All measurements were made at 25 °C and the chemicals used were of analytical grade.

The test solutions of dithizone were prepared and stored in deaerated solvents to protect them from air oxidation.

RESULTS AND DISCUSSION

Polarographic behaviour of dithizone

In the polarographic investigation of dithizone, one oxidation and two reduction waves were observed above pH 7 (Fig. 1). The first well-defined reduction

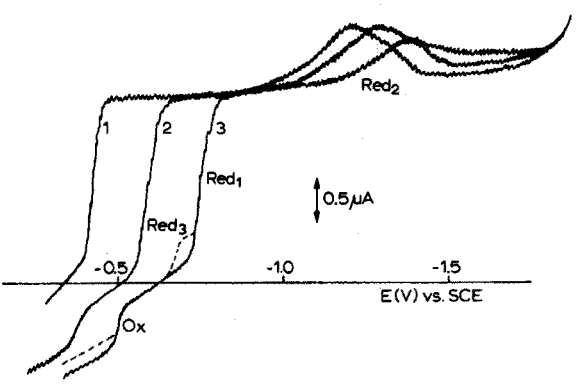

Fig. 1. Polarograms of $5 \cdot 10^{-4}$ *M* dithizone in buffer supporting electrolytes with different pH. Curve 1, pH 7.20; curve 2, pH 10.50; curve 3, pH 13.30.

TABLE I

THE TEMPERATURE COEFFICIENTS OF THE LIMITING CURRENTS OF THE Red_1 AND Red_2 ELECTRODE REACTIONS IN 1 *M* NH_4OH–NH_4Cl–20% ETHANOL SUPPORTING ELECTROLYTE

Temperature (°C)	i_d *(μA)*		*Temperature coefficients (%)*	
	Red_1	Red_2	Red_1	Red_2
20.0	11.3	0.70		
30.0	13.7	1.09	1.7	3.5
40.0	16.0	1.54	1.5	5.8
50.0	19.3		1.7	
60.0	22.5		1.5	
70.0	27.4		1.9	
80.0	32.4		1.8	

wave (Red_1) has a maximum of the first kind depending on the concentration of dithizone and the composition of the supporting electrolyte. The Red_1 wave is diffusion-controlled; this was proved by the linear dependence of the limiting current on the height of the mercury column (in the range $h^{\frac{1}{2}}=4$–8) in 1 *M* sodium hydroxide–0.2 *M* sodium sulphate–20% ethanol and 1 *M* ammonia–ammonium chloride–20% ethanol supporting electrolytes. The temperature coefficient of the limiting current also proves that this wave is diffusion-controlled, as can be seen from Table I.

In contrast, the Red_2 wave is not diffusion-controlled, but is probably a catalytic hydrogen wave caused by the sulphhydryl group of dithizone; however, further experimental work is needed to define the exact mechanism.

To estimate the number of electrons involved in the Red_1 reaction, log plot analyses and controlled-potential coulometry on the micro and macro scales were applied. The *n* values calculated from the slope of the log plot were found to be 1.8–2.2 in different supporting electrolytes. These *n* values give only rough information about the reaction, on the assumption that the charge transfer is reversible. The results of microcoulometry with a dropping mercury electrode as described by Biondi and Bellugi[6] were reproducible within 1%, and are summarized in Table II.

TABLE II

THE *n* VALUE OF THE Red_1 ELECTRODE REACTION IN DIFFERENT SUPPORTING ELECTROLYTES

pH	*n Value determined by*	
	Microcoulometry	*Controlled-potential electrolysis*
13.40	1.92	2.06
12.95	2.01	2.04
12.67	1.90	2.05
12.00	2.04	2.07

The most accurate n values are obtained by controlled-potential coulometry and these results confirm the value of $n=2$, unambiguously. The polarograms taken after complete reduction also proved that the redox couple is reversible, and that the product of the electrode reaction does not take part in any subsequent chemical reaction. The polarograms recorded during the electrolysis are shown in Fig. 2.

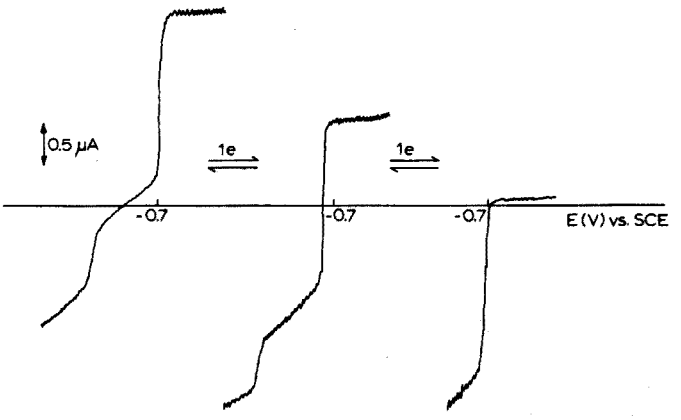

Fig. 2. The polarograms of $5 \cdot 10^{-4}$ M dithizone in buffered supporting electrolyte of pH 13.30 recorded during controlled potential electrolysis.

The reversibility of the Red_1 electrode reaction was also proved by cyclic voltammetric measurements. The half peak width $(E_p - E_{p/2})$ for a reversible system should[7] be equal to $0.057/n$. The cyclic polarogram of dithizone shown in Fig. 3 shows that E_p (the peak potential of the cathodic reaction) is 0.03 V more cathodic than $E_{p/2}$ (the half peak potential of the reaction). The fact that i_p (peak current) varied linearly with $V^{\frac{1}{2}}$ (sweep rate), and that the product of the electrode reaction could not be stripped anodically since it had not remained as a solid deposit on the electrode, were, because of the reversibility of this system, also expected.

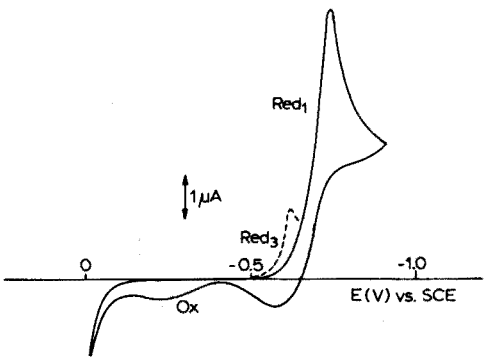

Fig. 3. Cyclic voltammogram of $5 \cdot 10^{-4}$ M dithizone in buffered supporting electrolyte of pH 13.30 on HMDE.

In detailed investigations of the effect of different supporting electrolytes over the pH range 2–14, the half-wave potential was shown to be a linear function of pH with a slope of 59.6 mV/pH. This shows that the number of protons involved in the electrode reaction must be equal to the number of electrons.

Mechanism of the reactions

As a result of the voltammetric investigation, the Red_1 electrode reaction can be considered as the reduction of the azo group of dithizone to a hydrazo group:

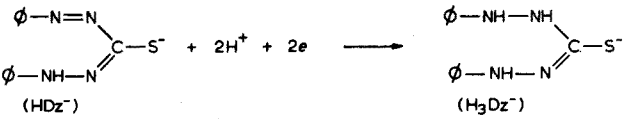

The $E_{\frac{1}{2}}$ *vs.* pH function should follow the conventional Nernstian expression[8] with a slope of -0.059 V at 25 °C and this was indeed found to be the case.

The azo–hydrazo reduction has already been investigated by polarographic methods[9,10]. Generally, the electrode reaction is reversible, although disproportionation of the products has sometimes been observed, depending on the substituents[10]. Hydrazobenzene and its derivatives may disproportionate to azo and amino compounds under the influence of heat effect or u.v. radiation. No disproportionation occurred with the hydrazo product, H_3Dz^-, under the conditions of the present measurements, for $n=2$; the symmetrical structure is probably unfavourable for disproportionation.

As the limiting current of the Red_1 electrode reaction is directly proportional to the concentration of dithizone in the range $1 \cdot 10^{-5}$–$1 \cdot 10^{-3}$ *M*, as shown in Fig. 4, it is possible to determine the concentration of dithizone polarographically with relative errors less than $\pm 3\%$.

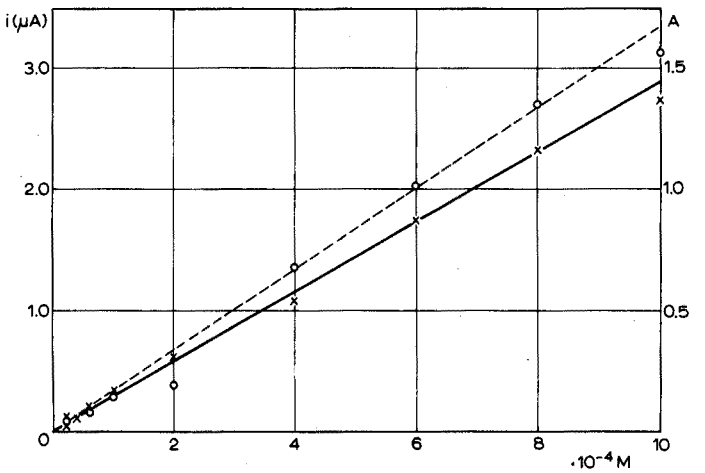

Fig. 4. The dependence of the limiting current (——) and the absorbance at 480 nm (– – –) on dithizone concentration in the concentration range 10^{-5}–10^{-3} *M* in 1 *M* NaOH–0.2 *M* Na_2SO_4–20% ethanol solution.

These results suggest valuable and versatile possibilities for the use of dithizone as an amperometric reagent for the determination of many heavy metals that form dithizonates.

Studies of the mechanism of the oxidation reaction of dithizone and various analytical applications of the voltammetric method are in progress.

The author thanks Dr. G. Farsang for his many helpful suggestions. The experimental assistance given by L. Magócsi and L. Adorján is gratefully acknowledged.

SUMMARY

The mechanism of the electrochemical reduction of dithizone to the corresponding hydrazo compound, diphenylthiocarbazide, has been examined in detail by polarographic and voltammetric techniques over a wide pH range. The reaction is reversible and dithizone can be determined polarographically in the range 10^{-3}–10^{-5} *M*. This polarographic behaviour suggests new applications of dithizone as an electroanalytical reagent.

REFERENCES

1 H. Fischer, *Wiss. Veröff. Siemens-Konzern*, 4 (1925) 158.
2 H. M. N. H. Irving and C. F. Bell, *J. Chem. Soc., London*, (1952) 1216.
3 I. T. Millar and H. D. Springall, *A Shorter Sidwick's Organic Chemistry of Nitrogen*, Calderon, Oxford, 1969, p. 386.
4 E. B. Sandell, *Colorimetric Determination of Traces of Metals*, Interscience, New York, 2nd edn., 1950, p. 106.
5 H. M. N. H. Irving, A. M. Kiwan, D. C. Rupainwar and S. S. Sahota, *Anal. Chim. Acta*, 56 (1971) 205.
6 C. Biondi and L. Bellugi, *J. Electroanal. Chem.*, 27 (1970) 431.
7 R. N. Adams, *Electrochemistry at Solid Electrodes*, Dekker, New York, 1969, p. 126.
8 J. O'M. Bockris and A. K. N. Reddy, *Modern Electrochemistry*, Plenum, New York, 1972, p. 1121.
9 I. M. Kolthoff and J. J. Lingane, *Polarography, Vol II*, Interscience, New York, 2nd edn., 1952, p. 767.
10 H. A. Laitinen and T. J. Kneip, *J. Amer. Chem. Soc.*, 78 (1956) 736.

Analytica Chimica Acta, 70 (1974) 417–423

SURFACTANT-SELECTIVE ELECTRODES

PART III. EVALUATION OF A DODECYL SULPHATE ELECTRODE IN SURFACTANT SOLUTIONS CONTAINING POLYMERS AND A PROTEIN

B. J. BIRCH, D. E. CLARKE, R. S. LEE and J. OAKES

Unilever Research, Port Sunlight Laboratory, Unilever Limited, Port Sunlight, Wirral, Cheshire L62 4XN (England)

(Received 18th December 1973)

The development of liquid membrane surfactant electrodes[1] in principle makes possible an *in situ* study of the binding of surfactants to polymers and proteins. These sensors, however, must give reliable data in micellar solutions, since the polymer–surfactant complex formed in solution is able to solubilize water-insoluble materials, indicating the presence of "micelle-like" regions[2]. Numerous techniques have been used to study the nature of this interaction process, *e.g.* viscosity, surface tension, dialysis, the results being generally used to construct a binding isotherm, *i.e.* a curve usually purporting to represent the amount of bound surfactant ion as a function of the concentration (activity) of non-bound surfactant ion[3]. However, none of these methods, even in principle, gives an unambiguous estimate of surfactant ion activity; instead concentrations of neutral surfactant or, in the case of equilibrium dialysis, mean ionic activities are obtained[4]. Binding studies with a surfactant electrode offer the advantage of fast *in situ* determinations of non-bound surfactant ion in solution.

Surfactant-selective electrodes operate satisfactorily in micellar solutions[1], and to ascertain the reliability of the liquid membrane surfactant electrode in sodium dodecyl sulphate (SDS) solutions containing nonionic polymers and proteins, the following comparisons are made here. For nonionic polymers, the data are compared with simultaneous pNa measurements, and with relevant results in the literature, whilst for the protein, data are compared with published equilibrium dialysis measurements.

EXPERIMENTAL

The nonionic polymers used were Dextran T-70 (mol. wt. *ca.* $7 \cdot 10^4$; Pharmacia), polyvinyl alcohol (PVA; mol. wt. *ca.* $12.5 \cdot 10^4$; BDH); polyvinyl pyrrolidone (PVP; mol. wt. *ca.* $4.4 \cdot 10^4$; BDH). The protein used was Bovine Serum Albumin (BSA; mol. wt. *ca.* $0.65 \cdot 10^4$; Koch-Light). All of these samples were used as supplied. Solutions were made up with water which had been singly distilled and passed through a mixed-bed ion-exchange column. Sodium dodecyl sulphate was BDH 'Specially Pure' grade.

The dodecyl sulphate (DS) selective electrode was constructed as described

previously[1]. A GEA33 sodium-selective glass electrode (E.I.L.) was used. Measurements of electrode potential, relative to a saturated KCl calomel electrode dipping into a 5 *M* ammonium nitrate salt bridge, were made with a Radiometer pHM 52 digital voltmeter. Simultaneous measurements of the electrode potentials were made at 25±0.2°C, with change in SDS concentration over the range 10^{-4}–10^{-1} *M*, in aqueous 1% solutions of each nonionic polymer. Measurements with the surfactant electrode with change in SDS concentration over the range 10^{-4}–10^{-2} *M*, in 0.1% BSA solution in a pH 5.6 phosphate buffer were made at 22±0.5°C. The high sodium content of this solution (*ca.* 0.03 *M*) precluded useful information being obtained from pNa measurements.

RESULTS

Figure 1 gives the data obtained with the dodecyl sulphate electrode in the 1% nonionic polymer solutions, presented as plots of electrode potential against concentration of SDS. The data for pure SDS are given for comparison.

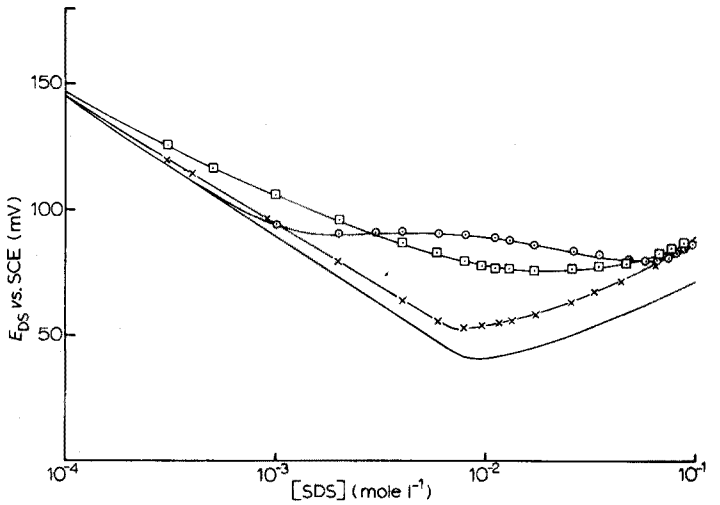

Fig. 1. Addition of 1% (w/v) polymers to SDS solutions: (×) Dextran, (⊡) PVA, (⊙) PVP, (——) SDS alone.

Concentration ranges over which differing interaction occurs between the polymers and surfactant are apparent. These ranges are much less apparent from pNa measurements—as expected—since it is the surfactant ion which interacts most strongly with the polymers. Similar data are given in Fig. 2 for solutions containing 0.1% BSA. The comparative data for SDS in the phosphate buffer solution are characterized by a lower critical micellar concentration (c.m.c.) caused by the buffer ionic strength[5], and a lowering in surfactant ion activity above the c.m.c. in a manner similar to that obtained with pure SDS.

DISCUSSION

The electrode potential values obtained are a direct function of the activities

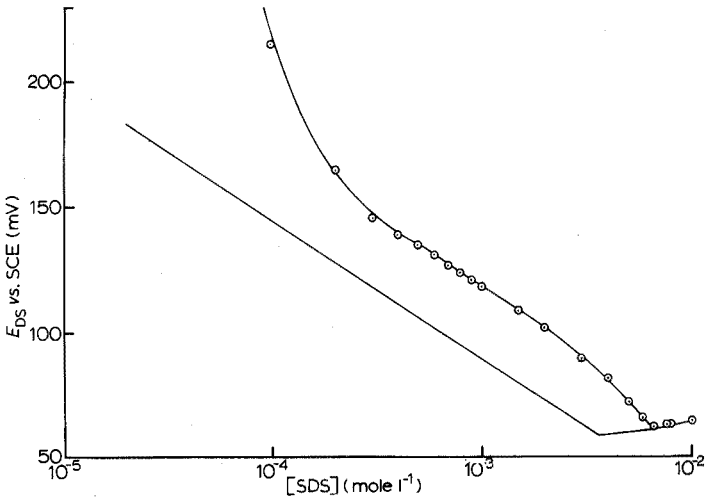

Fig. 2. Addition of 0.1% (w/v) BSA to SDS solutions: (——) pure SDS, (○) SDS + BSA.

of the corresponding ions. However, an assessment of the values of ionic activity coefficients in solutions containing both micellar and polymeric materials is of dubious value; accordingly, binding isotherms were constructed by comparing electrode potentials to the pre-micellar calibration obtained for pure SDS, plotted in terms of concentration. For the pNa data, concentrations of unbound ion in excess of those for the c.m.c. of pure SDS were obtained from the extrapolated pre-micellar slope. The results are therefore expressed in terms of unbound concentration of individual ions rather than activities. Any errors so involved are likely to be small—especially for the low concentrations of unbound DS ion found in these systems.

Binding isotherms obtained on this basis are presented in Figs. 3–6. The binding isotherms for surfactant ions are not of the classical Langmuir type and are extraordinary in that the unbound surfactant concentration begins to fall at some point along the isotherm. Such behaviour, by analogy with pure surfactant solutions, is characteristic of the presence of micelles in the bulk solution. This does not necessarily imply that a critical micellar concentration has been reached, but only that saturation of the polymer by surfactant ion has largely occurred, since micelle formation before saturation would not be unambiguously detected.

Binding to PVP

Inspection of Fig. 1 shows five regions of differing interaction, occurring over the SDS concentration ranges 0–0.0015 *M*, 0.0015–0.008 *M*, 0.008–0.03 *M*, 0.03–0.07 *M* and >0.07 *M*. These areas are also shown on the binding isotherm (Fig. 3), where SDS concentrations have been converted to unbound DS and Na concentrations.

The first four regions of interaction agree with the results of other workers[6–8] who used surface tension, viscosity and density measurements, and with our own pNa values. In the first region, little or no interaction occurs, *i.e.*, the unbound

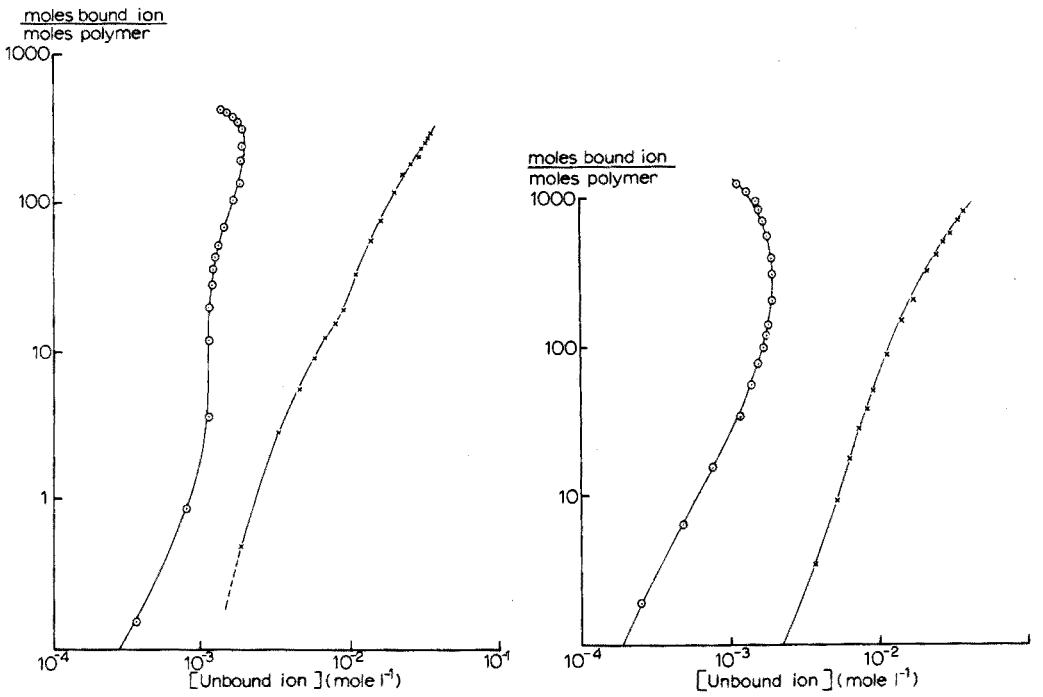

Fig. 3. Binding isotherm for PVP: (⊙) DS^- data, (×) Na^+ data.

Fig. 4. Binding isotherm for PVA: (⊙) DS^- data, (×) Na^+ data.

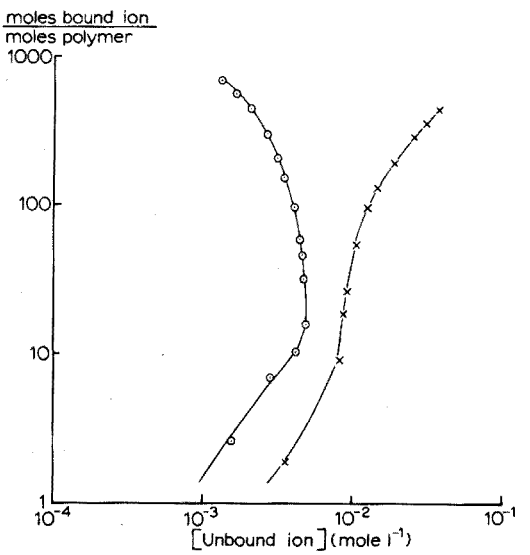

Fig. 5. Binding isotherm for Dextran: (⊙) DS^- data, (×) Na^+ data.

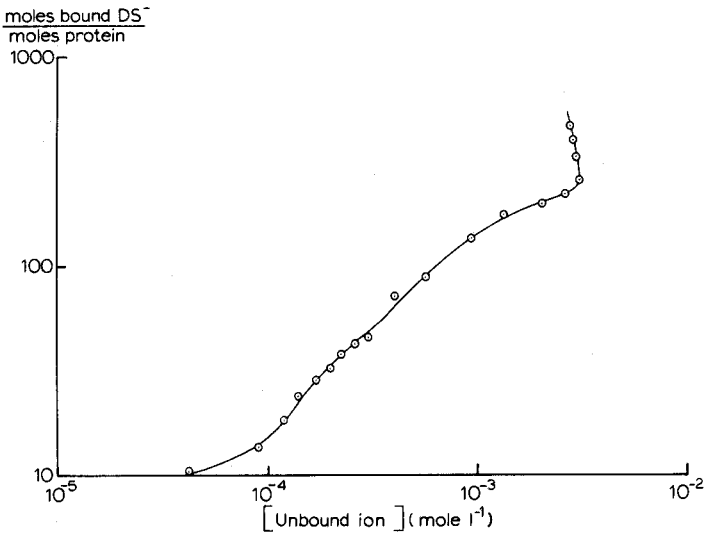

Fig. 6. Binding isotherm for BSA.

DS concentration is close to the total concentration. This is followed by an area of strong interaction, in which all added DS is bound to the polymer (Fig. 3). Such induced interaction has been accounted for by change in polymer configuration[9]. Further interaction (third region) is characterized by an increase in unbound DS in solution, which has been explained by the formation of surfactant clusters along the polymer chain[9]. Further increase in SDS concentration is said to result purely in formation of micelles in bulk solution[9]. However, the present electrode data clearly show that a further, fifth, region occurs at 0.07 *M* SDS, characterized by a sharp decrease in concentration of unbound DS. By analogy with pure SDS solutions, this region must contain micelles in bulk solution. It is possible that in the intermediate region, between 0.03 *M* and 0.07 *M* SDS, binding of surfactant to PVP and micelle formation in bulk solution occur together. This view is supported by sound velocity measurements which indicate the same five interaction regions[8].

Binding to PVA

Figures 1 and 4 indicate that binding of DS onto the polymer occurs even at low SDS concentrations. Above 0.02 *M* SDS (Fig. 1) or 0.0012 *M* DS (Fig. 4), micelle formation occurs, possibly together with binding. The absence of other pre-micellar binding regions indicates that no configurational changes occur during the interaction process. Similar conclusions may be drawn from pNa data.

Binding to Dextran

Surfactant electrode data are very similar to pure SDS (Figs. 1 and 5), indicating that little binding occurs. The c.m.c. value (0.007 *M*) may simply reflect a small amount of electrolyte impurity present in the polymer. pNa data give the same trends.

Comparison with equilibrium dialysis method

In dialysis experiments involving polymer and surfactant solutions, equilibrium was attained when the activities of neutral surfactant on either side of the dialysis membrane were equal[4]. This mean activity was then estimated on the non-polymer side of the dialysis cell, which is often equated to the unbound concentration of surfactant ion on the polymer side of the membrane. That these quantities are not equal in solutions containing micelles or polymer surfactant complexes is clear from Figs. 7 and 8. The unbound concentration of neutral SDS is calculated from the experimental unbound concentrations of ions, obtained as described earlier by means of the expression: Concentration of unbound neutral SDS = [(concentration of unbound Na^+) (concentration of unbound DS^-)]$^{\frac{1}{2}}$.

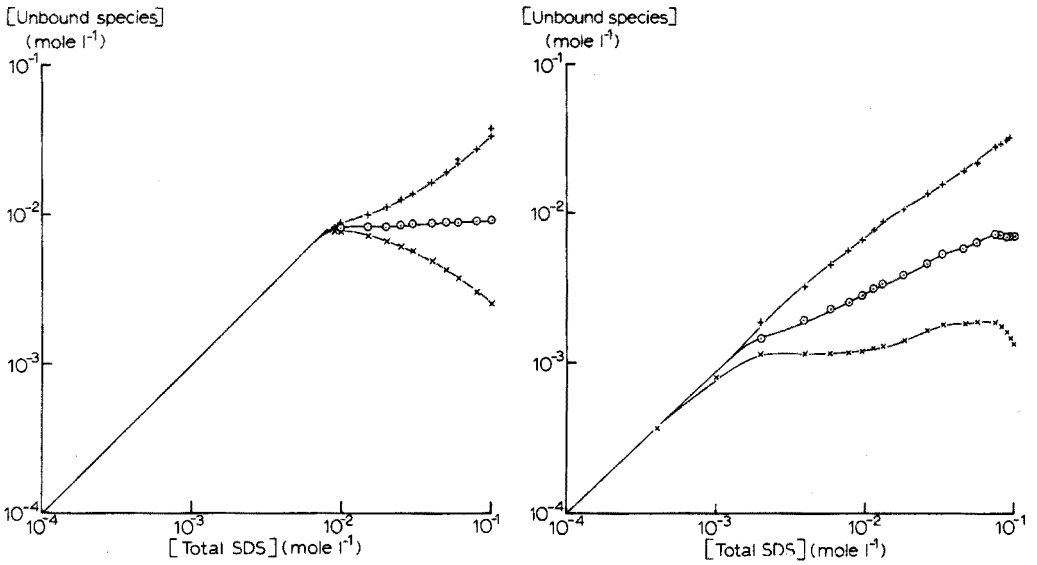

Fig. 7. Comparison of unbound concentrations of DS^-, Na^+ and neutral SDS in SDS solutions (no added polymer): (×) DS^- data, (+) Na^+ data, (⊙) SDS data (calcd.).

Fig. 8. Comparison of unbound concentrations of DS^-, Na^+ and neutral SDS in SDS solutions (1% w/v PVP added): (×) DS^- data, (+) Na^+ data, (⊙) SDS data (calcd.).

An exception to the above conclusion occurs when dialysis is performed in solutions of high ionic strength, *e.g.* pH buffers in biological systems. As these solutions are usually based on the sodium salts of weak acids, this ensures that the unbound sodium concentration is essentially constant during dialysis; hence the procedure is indeed a measure of unbound surfactant concentration in the system.

The DS binding isotherm to 0.1% BSA in pH 5.6 buffer (Fig. 6) agrees well with that for 1% BSA by the same technique[11]. The shape of the isotherm is similar to those obtained by equilibrium dialysis[12,13], as expected. Quantitative comparison was not possible, since it was shown that the isotherm depends upon batch variation of BSA[12], but the results obtained here did fall within these batch limits.

Micelles in bulk solution were detected at SDS concentrations greater than $6.5 \cdot 10^{-3}$ *M* (Figs. 2 and 6), indicating that protein saturation had been reached. This binding isotherm will be discussed more fully elsewhere[11].

Conclusion

The results and comparisons given show that the surfactant electrode gives reliable and rapid data in solutions containing polymer–surfactant complexes. It is probable that such electrodes provide the only present means of constructing binding isotherms for surfactant ions in the absence of swamping electrolyte.

We thank Dr I. D. Robb for helpful discussion.

SUMMARY

An electrode, selective to the dodecyl sulphate anion, has been evaluated for use in surfactant solutions containing polymers and a protein. Results obtained with the electrode have been used directly to construct surfactant ion binding isotherms which show similar regions of change to those previously established in the literature by indirect methods. It is shown that when equilibrium dialysis measurements are used to construct surfactant anion binding isotherms, it is only in the presence of a swamping amount of common cation that this method gives a true indication of the unbound surfactant ion concentration.

REFERENCES

1 B. J. Birch and D. E. Clarke, *Anal. Chim. Acta*, 69 (1973) 387.
2 M. M. Breuer and I. D. Robb, *Chem. Ind. (London)*, (1972) 530.
3 J. Steinhardt and J. A. Reynolds, *Multiple Equilibria in Proteins*, Academic Press, New York, 1969, p. 34.
4 E. F. Casassa and H. Eisenberg, *Adv. Protein Chem.*, 19 (1964) 287.
5 P. Mukerjee and K. J. Mysels, *Concentrations of Aqueous Surfactant Systems*, NBS Publication, NSRDS/NBS 36 (1971).
6 H. Lange, *Kolloid. Z. Z. Polym.*, 243 (1971) 101.
7 S. Saito, *Koll. Z.*, 154 (1957) 19.
8 I. D. Robb, unpublished work.
9 M. Fishman, Ph.D. Thesis, Polytechnic Institute, Brooklyn, N.Y., 1969.
10 P. Sams, personal communication.
11 J. Oakes, to be submitted for publication.
12 A. Ray, J. A. Reynolds, M. Polet and J. Steinhardt, *Biochemistry*, 5 (1966) 2606.
13 J. A. Reynolds, J. P. Gallagher and J. Steinhardt, *Biochemistry*, 9 (1970) 1233.

Analytica Chimica Acta, 70 (1974) 425–438

THE DETERMINATION OF LOSSES IN THE FIRE ASSAY OF GOLD

PART II. LOSSES IN THE COMPLETE ASSAY AND APPLICATION OF OPTIMAL PROCEDURES

S. G. WALL* and A. CHOW

Department of Chemistry, University of Manitoba, Winnipeg R3T 2N2 (Canada)

(Received 24th September 1973)

An examination of gold losses for a complete fire assay based on simulated samples[1], suggested that cupellation of silver and gold powders wrapped in lead foil was not truly analogous to cupelling the lead button normally obtained from the fusion process. In fact, under certain conditions, a complete fire assay involving fusion in addition to cupellation showed smaller losses than the simulated cupellation alone. It was therefore important to determine systematically the effect of varying assay conditions on the complete fire assay. In addition, a radiochemical procedure was used in an attempt to locate the total losses of gold.

Since this study of gold losses has dealt with samples containing 20–30 mg of gold, and since many economic ores may contain less than an ounce of gold per ton of ore, it was desirable to test the assaying of samples in which the concentration of gold was less than an ounce per ton. Since the quantity of ore taken is usually 0.5–1.0 assay ton (1 assay ton = 29.166 g), this would imply the presence of 500 μg of gold or less in the sample size commonly used in this research (*i.e.*, 0.5 assay ton). The approach in this study was to prepare synthetic ore samples of 15.0 g of silica salted with a known amount of gold. Once the procedure was established, it was tested with some actual gold ores which had been previously analyzed independently.

EXPERIMENTAL

The equipment and reagents used were those described in Part I[1] except for a solution of radioactive gold-195 ($t_{\frac{1}{2}} = 180$ d). This tracer was prepared by bombardment of platinum foil for 2 h, by 25 MeV protons in the University of Manitoba Cyclotron (Physics Department). The active gold was separated by appropriate radiochemical procedures and left unused for more than a year.

RESULTS

Effect of mixing procedure of ore and flux

Since fairly large crucibles are required for the fusion process, samples

* Present address: Department of Chemistry, University of Winnipeg, Winnipeg, Canada.

were prepared in groups of six. Initially, flux components were individually weighed out from a trip balance to the nearest 0.1 g, transferred directly to a cellophane sheet, and thoroughly mixed by tumbling back and forth for *ca.* 30 min. This procedure was found to be cumbersome and slow, and required the wearing of a dust mask for safety. In order to speed up this process and reduce the health hazard, the flux components were mixed in 12 × 12-in. polyethylene bags, by vigorous tumbling for 5 min.

Two experiments were performed. In one, the flux components were weighed and transferred directly to the fusion crucible. The accurately weighed gold was added to a slight central hollow in the flux mixture, and sufficient silver was added to give a silver–gold ratio of 6:1–7:1. The flux, silver and gold were mixed as thoroughly as possible with a spatula. No visible amounts of flux, silver or gold adhered to the spatula.

The other six samples, for the second test, were prepared by transferring the flux materials to a polyethylene bag (8 × 6.5-in.) weighing *ca.* 1.0 g. The gold and silver, in the same proportions as before, were transferred directly from the balance into this bag. The bags were tied off, and thoroughly mixed for 5 min. The bags and contents were then placed in the crucibles for fusion.

In this particular comparison, the assay samples were placed into the furnace at an initial temperature of 1950°F and heated as quickly as possible to 2100°F (about 1 h). The samples were allowed to remain in the furnace for 2.5 h, after which the crucibles were removed and their contents poured into a conical iron mold. After 1 h, the slag was separated from the lead button by gentle tapping with a metal bar.

The lead buttons were weighed to the nearest 0.1 g and cupelled at 1800°F as usual. After cooling, the beads were weighed on a milligram balance and parted as indicated previously[1]. The beads were not scraped to remove cupel material. The beads were washed three times with hot water, annealed and weighed accurately to obtain the weight of the parted bead. The silver content was determined as described for the cupellation studies[1] and the gold recovered was deduced in the usual way.

In the first test, without the use of polyethylene bags, the average gold loss was 1.51% ($s=0.62$), while with bags for mixing, the average gold loss was 1.04% ($s=0.28$). Thus both gold loss and deviations are reduced when plastic bags are used. In subsequent experiments this practice was adopted.

Effect of fusion temperature on gold losses

The basic procedure for preparation of samples and their fusion, cupellation and parting was the same as described above with polyethylene bags.

Since the initial temperature of the charge is always lower than the final temperature, it was thought that perhaps a change in furnace temperature during the process was an unnecessary refinement. A series of trials was therefore made for which furnace settings remained constant after the initial setting. Table I includes the results of these investigations.

The number of replicate samples varied somewhat throughout this study. In general, a repeat trial was performed whenever the number of rejected samples was more than one in six or when the results were contrary to expectations.

TABLE I

EFFECT OF FUSION TEMPERATURE ON GOLD LOSSES

Temperature (°F)	*Au loss (%)*	*s*	*n*	*Ag:Au*	*Weight lead button (g)*
1900	0.95	0.24	6	6.3:1.0	16.0
2000	0.81	0.15	6	6.5:1.0	16.9
2100	0.63	0.14	6	6.5:1.0	18.0
2200	0.70	0.16	10	6.4:1.0	17.5
2300	0.78	0.16	6	6.1:1.0	16.3
2400	0.88	0.19	9	6.3:1.0	16.0
2500	0.88	0.31	4	6.4:1.0	16.4

For the trial at 2500°F, this practice was not followed, because the process was visibly breaking down; the slag permeated through the crucible wall without any apparent breakage of the crucible itself, and two samples were entirely lost. This temperature was thus taken to be above the practical upper limit.

Table I indicates an optimal temperature of 2100°F. At temperatures above this, gold losses increase to 0.88% and at lower temperatures gold losses increase to 0.95%. The breakdown at the higher temperatures has already been explained. The losses at the lower temperatures may be due to the increased viscosity of the flux which militates against the settling of the gold particles which have not been collected by the lead. It may also be significant that 1900°F is the only temperature below the melting point of gold (1945°F); the significant decrease in precision here confirms that fusions should not be conducted below 2000°F. Charge used for this study was: 15.0 g SiO_2; 85.0 g PbO, 21.1 g Na_2CO_3; 4.5 g CaO, 0.9 g flour, 1 g polyethylene bag.

While statistical tests indicate a significant difference between the 2100°F trial and only one other (1900°F), and that only at the 95% confidence level, a fairly consistent trend towards a minimal gold loss at 2100°F does appear. Whether increased losses with increasing temperature can be attributed to increased losses to the pot wall as the gold viscosity decreases, or to increased volatility of the gold, cannot be decided. The overall average gold loss was 0.76% ($s=0.18$).

It should be noted that the weight of lead button passes through a maximum at the temperature where gold losses are minimized, so that the lead button weight might explain the observed trend.

Effect of lead button weight on gold losses

In these experiments the gold losses were determined exactly as discussed above. The charge used was, except for the weight of reducing agent, unchanged from the temperature study. The results are shown in Table II.

Statistical analysis indicated that variations in gold loss as a function of lead button weight were not significant at the 99% confidence level. In the development of an optimal procedure, the trial having a lead button weight of 18 g was chosen merely because the gold loss was then minimal.

The average gold loss was 0.73% ($s=0.14$), which is not significantly different

TABLE II

SUMMARY OF EFFECT OF LEAD BUTTON WEIGHT ON GOLD LOSSES

Weight flour[a] *(g)*	*Au loss (%)*	*s*	*Ag:Au*	*Weight lead button (g)*	*s*
nil	0.80	0.10	6.6:1.0	7.3	0.7
0.5	0.79	0.08	6.4:1.0	11.1	0.6
0.9	0.63	0.14	6.5:1.0	18.0	0.6
1.5	0.81	0.18	6.6:1.0	20.6	1.0
2.0	0.73	0.12	6.6:1.0	27.2	0.5
2.5	0.74	0.21	6.4:1.0	33.9	1.0

[a] The 1-g polyethylene bag also acts as a reducing agent.

from the average gold loss of 0.76% ($s=0.18$) for the temperature study, even at the 95% confidence level.

Effect of fusion time on gold losses

The objective here was to determine the shortest time required for the smallest gold losses. Fusion and cupellation temperatures were 2100°F and 1800°F, respectively. Samples were prepared as previously described with the charge indicated in Table III.

TABLE III

EFFECT OF FUSION TIME ON GOLD LOSSES

(Charge used: 15.0 g SiO_2, 85.0 g PbO, 21.1 g Na_2CO_3, 4.5 g CaO, 1.0 g flour)

Time (h)	*Au loss (%)*	*s*	*n*	*Ag:Au*	*Weight lead button (g)*
0.5	0.72	0.09	5	6.5:1.0	17.3
0.5	0.71	0.15	5	6.4:1.0	17.7
1.0	0.61	0.05	6	6.4:1.0	17.2
1.0	0.62	0.08	4	6.4:1.0	18.3
1.5	0.54	0.04	5	6.3:1.0	17.9
1.5	0.57	0.01	5	6.4:1.0	19.3
2.0	0.58	0.08	6	6.4:1.0	18.6
2.5	0.65	0.04	6	6.6:1.0	17.7
2.5	0.63	0.14	6	6.5:1.0	18.0
3.5	0.70	0.10	5	6.3:1.0	16.9
3.5	0.69	0.09	5	6.4:1.0	15.7

Since assays were done in groups of six, and since some samples had to be rejected, it was decided that each assay should be repeated in a duplicate trial, so that the reproducibility of the complete fire assay process could be estimated. The results (Table III) show that the difference between any two repeat trials was never greater than 0.03%, *i.e.* the reproducibility is about 3 parts in 10,000.

The results in Table III indicate a definite trend in gold losses. A statistical

analysis shows that the minimal gold loss, which occurred for a fusion time of 1.5 h, is significantly different from the losses in the 0.5-h and 3.5-h trials at the 99% confidence level, and also differs from that for the 2.5-h trial at the 95% confidence level. The optimal time of fusion would therefore seem to lie in the range 1–2 h with little to choose between those limits.

Effect of cupellation temperature on gold losses

The fusion temperature was maintained constant at 2100°F with a charge identical to that used for the fusion time study (Table III). The cupellation procedure involved initial heating for 5 min with the door and draft closed, a driving interval dependent on the size of the largest lead button, and a 5-min finishing period. The parting procedure involved two acid treatments with (1+4) and (1+1) nitric acid followed by three washings with hot water. The annealed bead was weighed and then analyzed for silver by atomic absorption. The results are shown in Table IV.

TABLE IV

EFFECT OF CUPELLATION TEMPERATURE ON GOLD LOSSES

Temperature (°F)	*Au loss (%)*	*s*	*n*	*Ag:Au*	*Lead weight (g)*
2000	0.86	0.16	12	6.5	15.0
1900	0.67	0.10	12	6.4	14.0
1800	0.56	0.03	10	6.3	18.7
1700	0.62	0.09	10	6.4	15.3

For the four temperatures studied, the highest standard deviation occurred at the highest temperature (2000°F) and the smallest deviations (3 parts in 10,000) at the two lowest temperatures. The minimal gold loss occurred at 1800°F, the usual temperature of cupellation throughout this research. This cupellation temperature produces a gold loss which is significantly different from all the other temperatures studied at the 95% confidence level, and differs significantly from the higher temperatures at the 99% confidence level.

The above results verify in part the generalization that increasing the temperature of cupellation increases gold losses, but contradict the idea that the best temperature of cupellation is the lowest temperature which prevents freezing of the cupelling buttons.

Effect of a cover

In order to test the effect of a cover, two trials, consisting of a dozen samples each, were run, one trial with, the other without, a cover. The cover consisted of 25 g of excess charge which was not salted with gold and silver. Since the results for the cupellation study had not been analyzed, the temperature of cupellation was 1700°F. Sample preparation and remaining aspects were as usual, with the charge the same as for the time study. The average gold loss without a cover was 0.62% (s=0.09) while with a cover it was 0.61% (s=0.08). Thus a cover is not worth the extra effort involved.

Miscellaneous considerations

While not strictly related to gold losses in fire assaying, a few points of interest to assaying are worth mentioning.

Effect of temperature on percentage silver retained by gold beads. Since all partings were performed on the same steam bath, it was assumed that the temperature of the parting acid(s) did not vary significantly. As more and more experiments were performed this did not prove to be the case; eventually an abrupt change in the percentage of silver retained by the parted beads was traced to a reduced steam flow rate through the steam bath. On measuring the temperature for a series of partings, variations as large as 25°C were observed over a period of time. Table V represents three partings chosen from a larger group, on the basis of a common silver-to-gold ratio and a common parting procedure. It is evident that the percentage of silver retained increases in a pronounced manner as the temperature decreases. Thus reports in the literature that a specified percentage of silver is retained by the gold beads are meaningless without stating the parting procedure and the temperature of the parting acid. Unfortunately this effect was not recognized at the time when the study of parting procedures was made .

Surcharge. As indicated earlier, the surcharge is the difference between the weight of the parted bead and the weight of gold added or taken. It is customary, especially in the assay of high-purity gold, to determine the surcharge by simultaneously assaying several standard samples with check gold. According to the literature[2], the weight of the parted bead is usually greater than the weight of gold taken, the gain in weight from incomplete parting being greater than the gold losses. Under the conditions of parting used here, the magnitude of the surcharge varied by as much as 0.400 mg within a single parting. When the results obtained for any three samples selected at random from a group of twelve were analyzed, an average surcharge yielded values ranging from 0.112 mg to 0.296 mg. If the average weight of gold taken were 24 mg, then the two possible results obtained with the extreme values of the surcharge would vary by about 0.8%, which is not a tolerable difference in view of the reproducibility attainable in fire assaying. While this particular example was chosen deliberately because of the large variations, it does show the limitations of simply applying the surcharge as a correction factor.

TABLE V

VARIATION IN SILVER RETAINED WITH PARTING TEMPERATURE

Temperature (°C)	*Ave. Ag retained*[a,b] *(%)*	*Ave. Ag:Au*	*Ave. Au added (mg)*
94.0	0.54 (±0.10)	6.6:1.0 (±0.1)	21.346
83.0	0.81 (±0.04)	6.6:1.0 (±0.2)	22.313
78.0	0.98 (±0.08)	6.6:1.0 (±0.3)	23.692

[a] Parting procedure: the bead was treated with 10-ml portions of (1+4) and (1+1) HNO_3, 15 min in each. The parting acid was poured off and the bead washed three times with 5 ml portions of hot water.

[b] Each result given is the average of 6 assays with the standard deviation in brackets.

A closer control of conditions such as temperature, thickness, weight of gold and silver–gold ratio reduces variations of the surcharge, but also greatly increases the time required for analysis. The determination of the silver content by routine atomic absorption should reduce the time involved. This was the practice throughout the present research.

Tracer techniques

Radioactive gold-195 was used in an attempt to locate the losses incurred during the fire assay. Aliquots of 3 ml of gold-195 solution giving about 2000 c.p.s., were taken for each sample and counted in test tubes which fitted exactly into the sodium iodide well-type detector. The background was determined before and after each series of measurements over 15 counting intervals. The activity of all samples was determined by counting for 5 counting intervals, averaging, and correcting for background. Two aliquots of the stock solution were retained throughout as calibration standards.

The preparation of the flux constituents and the carrier gold of about 20 mg was the same as before. After thorough mixing of the flux, the active gold was added to a hollow formed in the charge. The samples were allowed to dry overnight at about 50°C. The test tubes in which the active gold had been counted were counted again and were found to retain varying and significant amounts of activity. The activity actually added to the sample was calculated by difference.

After the samples had dried, they were mixed for about 5 min and any chunks were crushed. The samples were then placed in their appropriate crucibles, fused at 2100°F and poured into the iron mold as usual. After cooling, the slag and button were placed in a polyethylene bag and gently tapped to separate the slag and button dressing from the lead button. The lead button was weighed and cupelled as usual at 1800°F. The slags and associated button dressings, and the crucibles were kept for counting.

When the cupelled beads had cooled, each cupel was set aside for counting. The gold–silver beads were not weighed but were parted directly with a double acid treatment as outlined in Part I[1]. The parting acids were set aside for counting. The parted beads were then washed three times with hot water and the washings were collected for each sample and set aside for counting.

The parted beads were annealed and then directly placed in the original test tubes used for counting. In the interim the test tubes were cleaned with aqua regia and checked to ensure that no activity was retained. The beads were then dissolved in 3 ml of aqua regia in the usual way and set aside for counting.

The decay of the active gold was allowed for by measuring the activity of the standards each day and in the case of the dissolved beads, immediately after their measurement. The total activity decreased by only 2% over the time used for the complete study. In addition to the decay correction, the presence of 20–30 mg of carrier gold in the samples necessitated a correction for self-absorption. This amounted to about 3% of the total count as determined from duplicate evaluations.

Parted beads. After dissolution as outlined above, the beads containing more than 99% of the gold were counted in the same volume (3 ml) as the standards and in the same containers. After correction for decay and self-absorption these measurements should represent the gold recovered. The average gold recovery

TABLE VI

DISTRIBUTION OF GOLD-195 TRACER

(Charge used: 15.0 g SiO_2, 85.0 g. PbO, 21.1 g. Na_2CO_3, 4.5 g. CaO, 1.0 g. flour, 1.0 g. polyethylene bag)

Au added (mg)	*Activity (c/50 s)*	*Activity in parted bead*		*Activity in crucible*		*Activity in cupel*		*% Activity recovered*
		(c/50 s)	*(%)*	*(c/50 s)*	*(%)*	*(c/50 s)*	*(%)*	
26.247	137,694	137,270	99.7	870	0.63	32	0.023	100.3
20.501	137,418	135,863	98.9	758	0.55	35	0.025	99.4
30.029	136,733	137,989	100.9[a]	1060	0.77	41	0.030	101.7[a]
28.054	137,494	136,874	99.6	986	0.71	53	0.038	100.3
23.744	136,157	136,099	100.0	1074	0.78	37	0.027	100.8
23.486	137,326	137,032	99.8	1054	0.76	52	0.038	100.6
19.929	136,098	135,968	99.9	858	0.63	35	0.026	100.6
23.176	137,922	137,012	99.3	990	0.71	43	0.031	100.1
25.083	136,937	136,600	99.8	972	0.71	38	0.028	100.5
24.429	134,552	133,977	99.6	966	0.72	50	0.037	100.3
19.286	136,767	135,704	99.2	842	0.61	39	0.028	99.9
23.404	137,652	136,440	99.1	1196	0.86	33	0.024	100.0
			Ave.% = 99.5		Ave.% = 0.70		Ave.% = 0.030	100.2
			s = 0.3		*s* = 0.09		*s* = 0.005	0.4

[a] Rejected on statistical grounds.

(Table VI) of 99.5% ($s=0.3\%$) agrees very well with that obtained by direct weighing of the beads.

Crucibles. Initially the crucibles were counted whole. The crucible was inverted over the counting well and counted for five 100-s intervals. The background based on the average of 15 counting intervals before, and 15 intervals after, the crucible counts was 1010 ($s=18$). In view of the large size of the crucibles the lid of the counter could not be lowered; hence the background was determined with a used crucible which had contained no active gold. The average count for all the crucibles used with active gold ranged from 987–1045. The overall average of all twelve crucibles, 1006, was actually lower than the average background.

Since some of the crucibles had an average count higher than background, it was thought that the geometry might be significant, for the part of the crucible which according to autoradiographs was most likely to be active[4], was most remote from the counting well. Accordingly, one crucible was broken in a polyethylene bag so that no pieces were larger than would fit under the lowered lid of the counter. Each piece was counted either alone or together with smaller pieces; fines and very small pieces were counted together. In each case the side of the crucible which had been wetted by the charge was placed face down above the counting well. The result was surprising. In each case, the total activity was significant and averaged 0.70% ($s=0.09$) of the original bead activity. Of course, these results cannot be taken as exactly quantitative because of geometric effects; the face of the counting well on which the crucible pieces were counted was several centimeters above where the standards were counted.

Slag. The slag remained in one large piece except for a small quantity of button dressing. The whole slag pieces were counted along with the button dressing. That part of the slag which had been in contact with the lead button was placed closest to the counter well. The background, determined before and after the slag count, was obtained with a similar piece of slag from a previous non-active trial, and averaged 128 per 50-s counting interval. The range of activity for the slags from the "active" run was 109–130 counts for the same time, with an average activity of 122 counts. Within experimental sensitivity, the activity of the slag was considered to be insignificant.

Metal mold. The molds into which the fused samples were poured were checked. In order to obtain a background the mold was placed over the counting well with the unused side down. This was repeated three times with varying positions of the mold; the average count was 552 counts per 50-s interval. The counting was repeated with three different positions of the "active" side face down; the average count was then 540. The standard deviation in both cases was 30 counts. It was concluded that no significant activity was lost to the mold.

Parting solutions. The parting solutions were counted in test tubes placed directly in the counting well. For the first parting acid (1+4 nitric acid), the range of activity found corrected for background was 4–10 counts with an overall average of 7 counts ($s=2$) per 50-s interval. For the average sample this represents a loss of 0.01% gold. The second parting acid, counted in the same way, gave an average count of only 2 counts per 50 s. These losses were negligible.

Washing solutions. The combined wash solutions for each sample were counted in 30-ml beakers placed directly over the counting well. The corrected activity

averaged only 1 count per 50 s.

Cupels. The cupels were counted whole. According to autoradiographs[4], cupel absorption is mainly a surface effect with a maximum penetration less than 0.25 in. The cupels were therefore inverted over the counting well and counted for five 50-s intervals. The range of activity, corrected for background, was 32–53 with an overall average of 41 counts ($s=7$). This represents a gold loss of only 0.030% ($s=0.005$).

Microgram amounts of gold. The preparation of the samples containing microgram amounts of gold was a slight modification of that used for larger amounts. Standard solutions of gold and silver were prepared, and diluted to give working solutions from which various volumes of gold were pipetted into a hollow in the previously mixed flux constituents; in each case 2.0 ml of the 1000-p.p.m. silver solution was also added. The salted flux was placed in an oven at 65° and allowed to dry overnight or for at least 1 h for every ml of solution added. After drying, the mixture was agitated for 5 min in polyethylene bags.

The mixed samples were then placed in their crucibles and fused at 2100°F and cupelled at 1800°F. The bead obtained was weighed and then analyzed directly for gold without parting, by a procedure similar to that of Van Loon[5]. To each bead was added 0.5 ml of concentrated nitric acid in order to leach out the silver. The beads were heated at intervals until all action stopped and then treated with sufficient concentrated hydrochloric acid to make the final solution 50% (v/v) acid after dilution. Again the solution was heated to dissolve all the gold. Failure to leach the silver with nitric acid results in a silver chloride coating on the bead which hinders dissolution. After cooling and bringing the solution to volume in an appropriate volumetric flask, the gold content was determined by atomic absorption spectrometry.

Two blank determinations were made on the flux containing the usual amount of silver. In one case the litharge used was produced by Anachemia and in the other by Baker. The corresponding blanks were 0.98 μg ($s=0.37$) and 1.12 μg ($s=0.30$). Each blank was determined on 6 replicate samples.

In the atomic absorption determination of gold, scale expansion was used if the absorbance was less than 0.2, so that the absorbance reading could be obtained to one part in 200. Gold standards were aspirated after every other unknown. Instrumental drift was insignificant over such short periods. The aspirator used was corrosion-resistant, since difficulties involving the reduction of gold have been

TABLE VII

RECOVERY OF MICROGRAM AMOUNTS OF GOLD

Au added (μg)	*No. of samples*	*Au+Ag found*		*Au found*		*Recovery*	
		(μg)	*s*	*(μg)*	*s*	*(%)*	*s*
490	11	2536	21	494	4	101	0.7
245	11	2307	2	245	2	100	0.6
98	12	2119	24	99.1	2	101	1.5
24.5	11	2044	27	24.7	0.5	101	1.8

reported[6] in the aspiration of hydrochloric acid solutions with a steel aspirator.

The results for synthetic ores (Table VII) indicate complete recovery. Losses of gold are apparently less than can be observed by atomic absorption with the number of samples examined. These results compare favourably with those reported by Van Loon[5], who determined gold in the presence of platinum and palladium, with recoveries ranging from 97% to 105% depending on the amount of other noble metals.

Gold ores

Two gold ores were chosen, having a previously determined gold content[7] of less than an ounce per ton. The sample preparation was exactly as outlined in the previous section with the modification that the samples were only salted with silver and no silica was added.

The sampling procedure was as follows. The sample received consisted of a previously crushed and sieved ore. The entire ore passed through 100-mesh screen and 90–100% passed through a 200-mesh screen for both samples. About 1–2 pounds of the ore was placed on a large cellophane sheet and rolled or tumbled for 30 min by lifting alternate corners of the sheet. The ore had been previously inverted and shaken for about 20 min in its container. The sample was then spread out evenly on the cellophane and marked off into 1-in. squares. The sample was then obtained by taking a small portion on a spatula from each of the squares. The spatula was extended down to the bottom of the cellophane each time. The sample was weighed after each row of squares had been sampled.

After weighing the sample accurately in a polyethylene bag, the flux constituents were added in the usual way. In each case 2 ml of the standard silver solution (2 mg of silver) was added and the samples were dried for at least 2 h. The chunks which tended to develop were broken up and the ore, flux, and added silver were mixed for 5 min. Fusion, cupellation and analysis of the samples was then done as described above for microgram amounts of gold.

Each assay of six samples was duplicated. The gold content of the two ores examined was found to be 0.313 oz/ton ($s=0.034$) for ore 305 and 0.470 oz/ton ($s=0.012$) for ore 294. The relative standard deviations for the two ores were 10.9% and 2.9%, respectively, compared to 0.81% for a comparable assay of a synthetic gold ore. The precision of the method is thus a function not only of the sampling method, but also of the nature of the ore.

Since the particular ore samples used had been previously analyzed[7], a comparison of results was possible. The previous method involved parting of the silver from the gold, collection of the gold, ashing, dissolution and spectrophotometric determination of the gold content; the larger number of manipulations alone would be expected to lead to increased deviations and losses. The average results obtained previously[7] were 0.455 oz/ton ($s=0.026$) for ore 294 and 0.274 oz/ton ($s=0.031$) for ore 305. While the actual gold content of an ore is unknown, the application of the procedures developed here seems to have increased the gold recovery by 3.2% and 14.2% for ores 294 and 305, respectively. The precision of the analysis of ore 305 is essentially the same for the two procedures while the precision for ores 294 has increased considerably. As evidenced by a larger standard deviation, the analysis of ore 305 was not very satisfactory. While the

recovery was considerably increased, the separation of the lead button and the slag was not clean and this no doubt contributed to the increase in deviations. The difference between duplicate trials was found to be 6.5% *vs.* 0.85% (this study) for ore 294, and 12.0% *vs.* 7.6% (this study) for ore 305.

CONCLUSIONS

For the complete fire assay, the weight of lead button between the limits 7–34 g had no significant effect on gold losses. Excess charge used as a cover also had no effect. The use of polyethylene bags for mixing of the flux, silver and gold significantly reduced gold losses. The length of time used for the fusion process was important, with increased losses if either too short or too long a fusion time was used; the optimal time was found to be 1.5 h. Fusion and cupellation temperature both were significant variables, in terms of their effect on gold losses. For fusion, a maximal temperature of 2500°F was indicated, as the crucibles became porous to the slags above this temperature. A lower limit of 2000°F is desirable and an optimal temperature of 2100°F is recommended to minimize gold losses. The effect of varying cupellation temperature was not nearly so pronounced as expected from some statements in the literature. According to Hillebrand and Allen[3], gold losses due to increasing temperature from front to back of a gas-fired furnace ranged from 0.5% to 4.0%, for a temperature difference of about 100°C. In this study losses ranged from 0.56% to 0.86% for temperatures between 1700–2000°F.

In accurate gold assaying, the practice of estimating the surcharge on the basis of only three standard samples is highly suspect, unless extreme caution is exercised to maintain constant fusion, cupellation and parting conditions. In routine assaying, much better results can be obtained in a reasonably short time if the silver content is measured directly by some method such as atomic absorption, and proper correction made for the silver retained in the beads.

While variations in at least some of the conditions employed resulted in significant variations in gold losses, the overall impression obtained was that the fire assay for gold is remarkably insensitive to moderate changes in the conditions of assaying. Furthermore, even where gold losses did vary significantly, reproducible assaying was possible even with conditions other than those which minimized losses. Although small losses of gold of about 1% do occur, the use of a calibration factor obtained from standard samples under the same conditions provides for a very accurate determination of unknown samples. Perhaps these are some of the reasons why the fire assay for gold is considered to be one of the most reliable analytical methods known.

A consideration of Table VI which includes all the activity measurements for those sources contributing more than 0.01% of the total activity, indicates that the overall average recovery of the active gold, including losses, was 100.2% ($s=0.4$). In view of the differing counting techniques, this must be considered as being, at least partially, fortuitous. The major source of gold loss is undoubtedly due not to cupel absorption but to crucible losses. This statement contradicts the evidence obtained by "simulated cupellations", and it would appear that the cupellation of gold and silver powder encased in lead foil cannot be compared to the cupellation of the

lead button customarily obtained at the end of a fusion. The approximate equality of the gold losses to crucibles in the complete assay, and the gold losses to cupels for the abbreviated process, was fortuitous and misleading.

Losses to parting acids and wash solution were negligible as expected, since the beads remained nicely coherent under the conditions of parting.

It is to be expected that losses to slag in particular and crucible wall to a lesser degree would vary, both with variations in flux mixtures and hence in the nature of an ore. In the bulk of the work reported here, the flux components were known almost exactly (impurities excepted) and hence the losses reported should be viewed as characteristic of the conditions used and as an ideal situation which one would aspire to in the more real conditions of assaying ores.

The application of the optimal assay procedures developed for samples containing about 20 mg of gold, and samples containing 25–500 μg of gold is satisfactory. The recovery, as determined for synthetic gold ores, is quantitative within experimental error. The application of these procedures to real ores reflects the importance of sampling procedures and the kinds of variations which can be expected owing to sample differences.

There has been some intimation in the literature that the fire assay will be displaced by one of wet analysis with atomic absorption, emission or X-ray spectroscopy or activation analysis. At the present time it is impossible to see how any of these can match the ease and latitude of operation and the accuracy of the fire assay. Where only limited accuracy is required and only a few samples are to be analyzed, any of the above techniques may be applied but for rapid, accurate analysis of multiple samples on a routine basis, the fire assay remains the method of preference.

The authors wish to thank the National Research Council of Canada, the Research Board of the University of Manitoba, and Johnson Matthey and Mallory Ltd. (Toronto) for support.

SUMMARY

Losses in the complete fire assay for gold were found to be less than 1% under ideal conditions. The use of polythene bags for mixing each sample was shown to improve both the accuracy and the precision of the assay. Fusion temperatures of 1900°–2300°F and times from 0.5–3.5 h showed only small variations in gold recovery. The optimal conditions were fusion for 1.5–2 h at 2100°F, with a button weight of 18 g, and cupellation at 1800°F. However, the overall assay proved remarkably insensitive to variation in conditions. The need to determine the silver retained in the parted gold beads is emphasized. Gold losses in the procedural stages were established with tracers; the loss to the crucible was most significant. The use of lead foil as a simulated button gives misleading results. For synthetic samples containing 24.5–490 μg of gold, average recoveries were 100% (s=0.6–1.8). Application to two gold ores is discussed.

REFERENCES

1 S. G. Wall and A. Chow, *Anal. Chim. Acta*, 69 (1974) 439.
2 E. E. Bugbee, *A Textbook of Fire Assaying*, Wiley, New York, 3rd ed., 1940, p. 131.
3 W. F. Hillebrand and E. T. Allen, *U.S. Geol. Surv., Bull.*, 253 7.
4 M. Shima, *Radioisotopes*, 5 (1957) 1.
5 J. Van Loon, *Z. Anal. Chem.*, 246 (1969) 122.
6 S. Kallmann and E. W. Hobart, *Talanta*, 17 (1970) 845.
7 A. Chow and F. E. Beamish, *Talanta*, 14 (1967) 219.

Analytica Chimica Acta, 70 (1974) 439–442

SHORT COMMUNICATION

Determination of mercury in air by neutron activation analysis

H. A. VAN DER SLOOT and H. A. DAS
Stichting Reactor Centrum Nederland, Petten, N.H. (The Netherlands)
(Received 28th October 1973)

An important part of pollution studies is the determination of mercury in air. The method of analysis should meet three requirements: (a) the air should be freed from airborne particles; (b) both organically bound mercury and inorganic mercury compounds should be measured; and (c) the sensitivity should be at least 1 ng m^{-3} so that unpolluted air can be analysed.

Magos[1] reached a detection limit of 50 μg m^{-3} by an isotope exchange method. Moffitt and Kupel[2] used activated charcoal as an absorbent for mercury vapour; the mercury was determined by atomic absorption with a sampling boat system. The lower limit of the analysis (0.02 μg) is not sufficient for measurements in unpolluted air. Organic mercury compounds, if present in the sampled air, are fully absorbed on activated charcoal[3].

It was considered that concentration on previously purified activated charcoal followed by neutron activation analysis would produce a very sensitive method. In the procedure described here, the mercury is separated from the radioactive matrix by evaporation, followed by absorption on a second carbon absorbent. Concentrations down to 0.5 ng Hg m^{-3} can be determined in this way.

Experimental

Equipment and reagents. An electrical suction pump with variable capacity (0.05–2.8 m^3 h^{-1}), an integrating flowmeter with decimal reading (to 0.2 l), and an adsorption device (Fig. 1) were used.

Activated charcoal (20–35 mesh) was of chromatographic quality (E. Merck).

A 3 × 3-in. NaI well-type crystal connected to a 400-channel analyzer with an electrical typewriter was used for measurement.

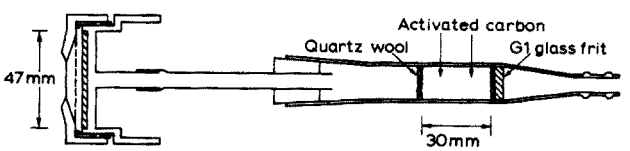

Fig. 1. The sampling system. The filter holder was a modified Swinnex 04700 model. The tube was 15 mm in diameter. The membrane filter had a 0.45 μm pore diameter.

Purification of activated charcoal and its absorption capacity. Commercially available activated charcoal contains *ca.* 20 ng Hg g^{-1}. For purification it was heated at 900°C in a small muffle furnace in the absence of oxygen by passing nitrogen through the glowing carbon. The nitrogen was purified by a carbon filter (at room temperature) before entering the furnace, thus removing any mercury. After this treatment, the mercury content of the charcoal was found to be *ca.* 0.1 ng g^{-1}. This concentration was established by the procedure described below. The absorption capacities of activated charcoal for metallic mercury and methylmercury(II) chloride at room temperature were found to be 2.9 mg g^{-1} and 3.1 g g^{-1}, respectively.

Sampling and irradiation. Fill the absorption device with 1.5 g of purified charcoal and place a clean filter (0.45 μm) in the filter holder (see Fig. 1). Connect the absorber to the suction pump. (No adsorption of mercury vapour on membrane filters or other parts of the absorption device was observed). Maintain the flow rate below 5 l min^{-1}. For unpolluted air, collect a sample of 1.5–2 m^3; for higher concentrations the minimal sample volume is smaller.

Transfer the charcoal with absorbed mercury to a quartz capsule (18 mm o.d., 40 mm long), and seal immediately. Homogenize by vigorous shaking. Prepare standards by putting 20-μl aliquots of a standard mercury(II) solution (2.649 μg Hg/20 μl) in similar quartz capsules, which already contain 1.5 g of purified charcoal. Irradiate standards and samples for 12 h in a thermal neutron flux of $5 \cdot 10^{12}$ cm^{-2} s^{-1}. Then cool for *ca.* 24 h.

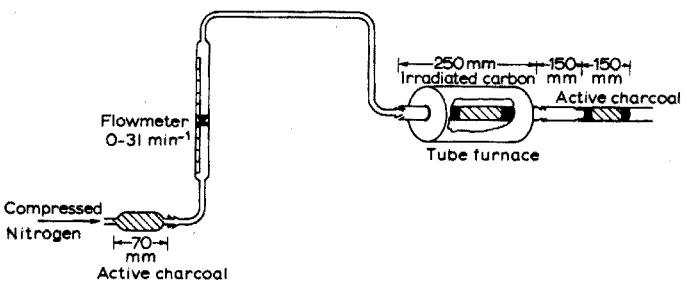

Fig. 2. Apparatus for the separation of mercury from a radioactive matrix. The initial scavenging tube (40 mm i.d., 70 mm long) contains activated charcoal. The final charcoal-containing tube has a 16 mm i.d.

Separation of the mercury. Maintain the tube furnace (35 mm i.d., 150 mm long; Fig. 2) at 900–950°C. Transfer the irradiated charcoal to the quartz tube (22 mm i.d., 250 mm long), placed inside the tube furnace. A second carbon absorber is placed outside the hot zone (Fig. 2). Pass nitrogen at a flow rate of 0.6 l min^{-1}. After 5 min remove the tube and collect the contents of the second absorber in a test tube (16 mm i.d., 160 mm long). Treat the standards in an identical manner.

Count samples and standards with the well-type crystal, connected to the 400-channel analyzer. The area under the 0.077-MeV photopeak of $^{197m-197}Hg$ ($t_{\frac{1}{2}} = 24$–66 h) is determined.

The specific count-rate under this photopeak is $1.58 \cdot 10^5$ counts min^{-1} μg^{-1} after a cooling period of two days.

Results

The distribution of mercury, methylmercury(II) and dimethylmercury in the initial carbon absorber is indicated in Fig. 3. It is clear that under the recommended conditions, collection was quantitative.

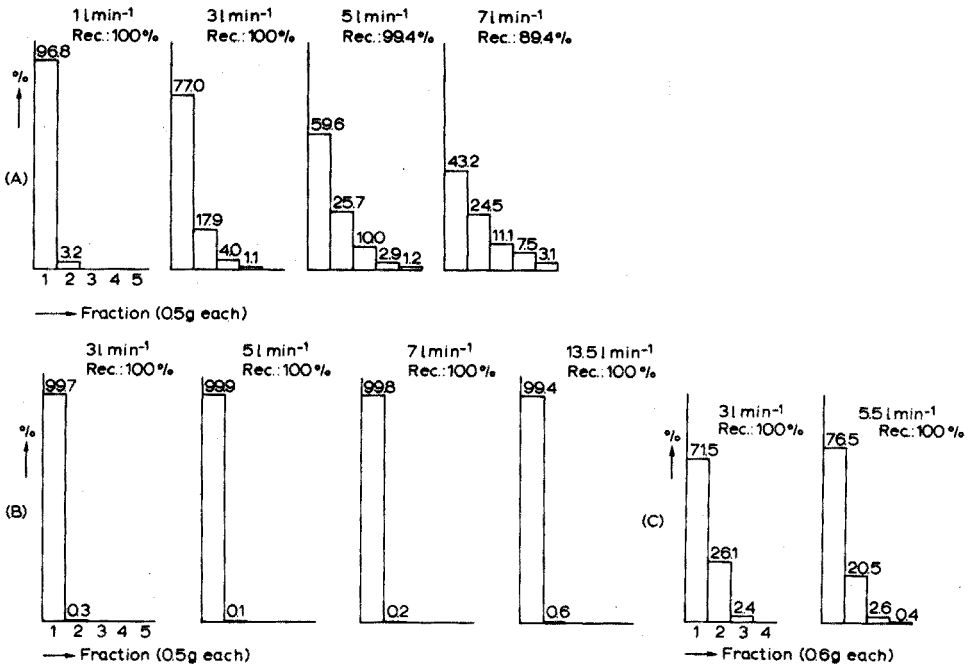

Fig. 3. The distribution of mercury species over the carbon adsorber at different flow rates. *A. Mercury metal.* The distribution was measured in the following way. About 30 mg of metallic mercury was irradiated for 24 h at a thermal neutron flux of $5 \cdot 10^{13}$ cm^{-2} s^{-1}. The mercury droplet was added to 1 l of water in a glass vessel, equipped with a glass sintered plate sealed to the vessel about 2 cm above the bottom, and with an aeration tube ending below the filter. An active carbon bed of 6 ml (*ca.* 2.5 g) in a polythene tube was connected to the outlet. The flow rate of the air was adjusted and, during 10 min, metallic mercury was removed from the solution by aeration (0.04 μg Hg^0 min^{-1}). The absorbent was extruded in 5 parts of *ca.* 0.5 g each. These fractions were measured with a $3 \times 3''$ NaI well-type crystal connected to a single-channel analyzer. *B. Methylmercury(II) chloride.* Methylmercury(II) chloride was labeled with ^{197}Hg by exchange with irradiated mercury(II) chloride in water[4]. The CH_3HgCl was separated by extraction with benzene. The benzene phase was washed three times with twice-distilled water to remove traces of mercury(II) chloride, and finally the benzene was evaporated. The labelled methylmercury(II) chloride was stored in a well sealed flask. About 4 mg of CH_3HgCl was transferred to a 10-ml weighing bottle inside a 1-l filtration flask. The small bottle was closed by a lid, which could be removed from outside. The filtration flask was flushed with air. A carbon absorber in a polythene tube was then mounted on the side arm, the flow rate of the air was adjusted and the cover of the weighing bottle was removed. (The saturated vapour concentration of CH_3HgCl is *ca.* 290 mg m^{-3} at 35°C (ref. 3). The experiment was completed as described for mercury metal. *C. Dimethylmercury.* This was formed by the reaction[5]: $2\ CH_3HgCl + 2\ Cu \xrightarrow{\text{pyridine}} (CH_3)_2Hg + CuCl_2 + Hg(Cu)$. By using labelled methylmercury chloride, radioactive dimethylmercury was obtained with a specific activity equal to that of methylmercury(II) chloride. The reaction was carried out in a filtration flask at 50°C, a carbon absorber being mounted on the side-arm. The flow rate of air was adjusted. The dimethylmercury escaping from the reaction mixture was slightly contaminated with metallic mercury. After 10 min, the carbon adsorber was removed and divided in fractions. Counting was performed as with mercury metal.

In tests of the method, four types of sample were analysed.

Laboratory air. Samples of 0.6–3 m^3 were taken in a chemical laboratory where mercury was used occasionally. Results obtained over a period of a few months varied between 40 and 68 ng m^{-3} with a standard deviation of 5% per measurement. After removal of the mercury storage bottle, the concentration in the air decreased within a week to 7.4 ng m^{-3} with the same relative standard deviation. The pressurized air system contained (5.5 ± 0.2)–(6.0 ± 0.2) ng m^{-3}.

Atmospheric air. Samples of 2–4 m^3 of air, taken in the vicinity of the Dutch Reactor Centre on various days, were analyzed. The observed range of mercury concentrations was (1.8 ± 0.2)–(2.3 ± 0.2) ng m^{-3}.

Natural gas. Natural gas may contain a considerable content of mercury. Concentrations of the order of 180 μg m^{-3} have been reported[6]. The mercury is partly removed in the purification step, and a further decrease may be caused by adsorption on the pipelines during transport. The concentration in the gas, as received in Petten, was found to be (7.0 ± 0.5) ng m^{-3}.

Offgas from the mud fermentation reservoir of a sewage plant. The methane gas evolving from a mud-cleaning installation may contain considerable amounts of mercury, owing to the reducing conditions existing in the fermentation tank and the methylation of mercury by bacteria. Values found during a fermentation at 32°C were for a 0.060-m^3 sample, 158 ng m^{-3} ($Sr = 12\%$), and for a 0.330-m^3 sample, 139 ng m^{-3} ($Sr = 4\%$).

REFERENCES

1 L. Magos, *Brit. J. Ind. Med.*, 23 (1966) 230.
2 A. E. Moffitt and R. E. Kupel, *Amer. Ind. Hyg. Ass. J.*, (1971) 614.
3 G. F. Phillips, B. E. Dixon and R. G. Lidzey, *J. Sci. Food Agr.*, 10 (1959) 604.
4 J. M. Cross and J. J. Pinajian, *J. Amer. Pharm. Ass.*, 40 (1951) 95.
5 Fr. Hein and K. Wagler, *Ber. Deut. Chem. Ges.*, 58 (1925) 1499.
6 A. Achterberg and J. J. Zaanen, *Chem. Weekbld.*, 68 (1972) 9.

Analytica Chimica Acta, 70 (1974) 443–447

SHORT COMMUNICATION

The direct determination of cadmium in biological samples by selective volatilization and graphite tube reservoir atomic absorption spectrometry

RALPH T. ROSS and JORGE G. GONZALEZ

Environmental Protection Agency, Pesticides and Toxic Substances Effects Laboratory, National Environmental Research Center, Research Triangle Park, North Carolina 27711 (U.S.A.)

(Received 2nd August 1973)

The biological influences of cadmium have been reviewed by Underwood[1] and Friberg *et al.*[2]. From an environmental point of view, the metal is one of the most dangerous of the atmospheric pollutants[3]. It has been shown that an estimated 100 human deaths have resulted from environmental cadmium poisoning[4]. In man, cardiovascular disease[5] and arterial hypertension[6] have been associated with inhaled doses of the metal toxicant. When administered to rats, the pollutant produces hypertension[7] and increased mortality[8].

As with mercury, very little is known about the fate and distribution of cadmium in the environment, but as greater quantities of the metal are refined, more of it becomes available to interact with man. Before the biological effects of cadmium can be completely understood, analytical methods which may be used to determine lengthy exposure of humans at low concentrations must be available. The method must be sensitive and relatively simple, in order to determine cadmium in large numbers of biological and environmental samples.

Several analytical methods for determining trace quantities of the metal have been reported[2]. Atomic absorption spectrometry (a.a.s.) is most widely used[9]. Extraction procedures for use with a.a.s. by conventional flame techniques for determining trace cadmium have been published[10,11]; because of the low concentrations found in biological matrices, direct determination is not feasible. In order to monitor human exposure to cadmium poisoning, it is important to have a method available in which the metal may be determined directly from biological samples thus eliminating the possibility for loss encountered in sample digestion and workup. Pulido *et al.*[10] achieved this by using flame a.a.s. interfaced with a vycor absorption cell, whereas Hauser *et al.*[11] developed a reagent-free method for the determination of both cadmium and lead in whole blood, employing a flame-purged tantalum sampling boat. The development of atom reservoirs for use with a.a.s., such as the graphite tube furnace (HGA) and the carbon rod atomizers, have increased the sensitivity of the technique by several orders of magnitude. The applications of these methods have been reviewed by Kirkbright[12]. A direct HGA method has been reported for the determination of low quantities of chromium in human urine samples[13]. It was the purpose of this investigation to adapt this system for the direct determination of cadmium in urine and serum.

Experimental

Apparatus. A Perkin–Elmer model 303 atomic absorption spectrophotometer equipped with a Graphicorder-10 (Dynatronic Instruments), a deuterium arc background corrector and a Perkin–Elmer heated graphite atomizer (HGA-2000) were used. The HGA-2000 provides variable temperature programs and controls which eliminate the need for voltage–temperature conversion tables and electronic modifications, and allows selective volatilization analyses to be performed for all samples[14]. The temperatures are also reported in voltages which are measured directly across the atomizer terminals. These corrected values are used throughout the paper because of the discrepancy between applied voltages and the actual temperatures achieved in the atomizer. The actual temperature obtained in the graphite tube is a function of the geometry and age of the tube[14].

The instrument was operated according to the standard conditions for cadmium recommended by the manufacturer. An inert atmosphere was maintained by purging the graphite tube with nitrogen at 1.5 l min^{-1}. Eppendorf microliter pipettes with disposable plastic tips were used for injections of the samples into the atomizer.

Reagents. Working standard solutions were prepared daily by diluting a 1000 p.p.m. cadmium reference solution (Fischer Scientific Co.) with doubly distilled deionized water which showed no cadmium absorption when analyzed by the HGA technique.

Urine samples were collected in polyethylene containers which had been pre-rinsed with quartz-distilled nitric acid. The samples were acidified and stored at 4°C. Serum samples were obtained from blood that had been collected in plastic syringes (which were checked for possible cadmium contamination) and allowed to coagulate in polyethylene centrifuge tubes.

Procedure. Aliquots (20 μl) of either urine or 20% solutions of serum in water were introduced into the graphite tube with disposable micropipettes. (Calibration curves were obtained by injecting cadmium working standard solutions and by fortifying cadmium-free urine or serum with identical amounts of cadmium.)

The HGA power supply was programmed as follows: drying, 30 s at 150°C (0.6 V); charring, 50 s at 450°C (1.2 V); atomizing, 8 s at 1300°C (2.0 V). The temperatures were read directly from the meter on the power supply unit, and the corresponding voltages were measured across the atomizer terminals by means of a voltmeter.

After each analysis, the graphite tube was heated to maximum temperature for 10 s; this was necessary because salts such as sodium chloride were not completely volatilized during the 8 s atomization step at 1300°C. No apparent aging of the graphite tube was found with up to 100 sample injections. The temperatures and times applied during the various steps are critical because many samples contain large amounts of dissolved salts which, if not removed by selective volatilization, would produce light scattering and higher apparent cadmium signals.

Samples were analyzed by direct injection into the graphite atomizer and by the chelation–extraction method described by Lehnert *et al.*[15,16].

The relative standard deviation (s_r) for peak signals calculated from ten injections of 20 μl of each urine, serum and aqueous standard solutions con-

taining 5 p.p.b. ($1 \cdot 10^{-10}$ g) of cadmium were 4.1%, 5.8% and 4.9%, respectively. This reproducibility is in close agreement with that cited in the literature[14,17,18].

The concentration of cadmium in urine or serum needed to produce a 1% absorption signal under the above conditions was found to be 0.25 $\mu g\ l^{-1}$ (0.25 p.p.b.).

Results and discussion

The initial application of the method for the measurement of cadmium in biological materials resulted in spectral and chemical interferences which were due to the formation of smoke produced from charring of the organic matter and inorganic salts such as sodium chloride in the matrix. This resulted in non-specific absorption and led to high cadmium readings. Elimination of these interferences was accomplished by using a deuterium arc background corrector. Figure 1 shows tracings from injections of 20-μl samples of urine fortified with 3 p.p.b. of cadmium both with and without the deuterium arc background corrector in the system. At 1700°C, cadmium was covolatilized with the matrix salts (A, Fig. 1). At higher temperatures light scattering due to salt volatilization resulted to an extent that precluded compensation, and the cadmium peak was only partly resolved. However, at 1300°C, the cadmium peak was clearly differentiated from the peak produced from light scattering even without the deuterium arc corrector (B, Fig. 1). At this temperature with the deuterium arc background corrector, a cadmium tracing essentially free of interferences was obtained (D, Fig. 1). Evidence

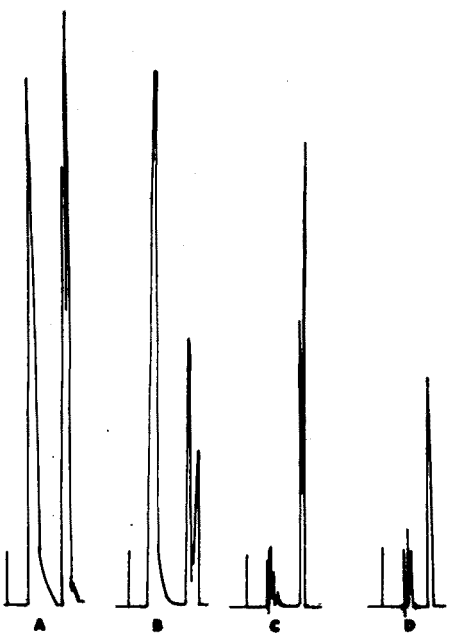

Fig. 1. Recorder tracings obtained from the HGA-2000 as a function of temperature and deuterium arc background correction. (A) 1700°C with deuterium background corrector off; (B) 1300°C with deuterium background corrector off; (C) 1700°C with deuterium background corrector on; (D) 1300°C with deuterium background corrector on.

for the authenticity of the cadmium signal was obtained by fortifying serum and urine samples with 100 p.p.b. of cadmium. The samples were then extracted with an excess of ammonium pyrrolidine dithiocarbamate (APDC) and methyl isobutyl ketone (MIBK) until the cadmium peak completely disappeared. Possible salt interferences from urine samples were also checked by adding to the samples 5 p.p.b. of cadmium. The samples were injected into the HGA, and the peak height recorded. The same samples were diluted to 2, 4, 8 and 16 times the original volumes, respectively, and the cadmium content was readjusted to its initial concentration of 5 p.p.b. The samples again were injected into the HGA, and the signal recorded. The cadmium peak heights for the diluted urine samples were the same as the cadmium peaks obtained in the original undiluted urine samples. These data illustrate that the response for cadmium is not affected by salt content in urine under the operating conditions described above. Pulido *et al.*[10] and Hauser *et al.*[11] have discussed the use of deuterium arc background correctors for the determination of cadmium in biological samples, using a.a.s. in conjunction with other sampling techniques. Their data is in close agreement with the data reported here.

Levels of cadmium found in the urine of nonexposed individuals are shown in Table I. The samples were analyzed by the proposed direct injection technique and also by an extraction method[15]. It can be seen that there is close agreement between the results obtained.

TABLE I

COMPARISON OF URINE CADMIUM LEVELS BY PROPOSED METHOD AND BY EXTRACTION METHOD

(Results in $\mu g\ l^{-1}$)

Sample	1	2	3	4	5	6	7	8	9
Proposed method	1.8	1.0	1.6	0.6	1.1	1.7	2.7	2.4	2.5
Extraction	1.8	1.0	1.9	0.9	1.1	1.6	3.0	2.0	2.5

TABLE II

DETERMINATION OF TRACE QUANTITIES OF CADMIUM IN URINE AND SERUM

Sample	*No. of samples*	*Range* $\mu g\ l^{-1}$	*Mean and std. deviation*
Urine	20	0.4–3.7	1.5 ± 0.7
Serum	5	7.5–9.5	8.8 ± 0.7

Table II illustrates applications to serum and urine. The levels of cadmium found in nonexposed urine samples are in agreement with those reported in the literature[11,15,16,19,20]. The values reported for serum are intermediate between the levels reported by Lehnert *et al.*[15] and Pulido *et al.*[10].

The data reported here for cadmium levels in urine and serum indicate a high potential for the direct application of a.a.s. in conjunction with the HGA and a deuterium arc background corrector to biological samples. Its sensitivity, simplicity and speed make this procedure by far superior to other previously reported analytical techniques for the determination of this element.

REFERENCES

1 J. E. Underwood, *Trace Elements in Human and Animal Nutrition*, Academic Press, New York, 3rd ed., 1971.
2 L. Friberg, M. Piscator and G. Nordberg, *Cadmium in the Environment*, CRC Press, Cleveland, Ohio, 1971, p. 16.
3 C. M. Christian II and J. W. Robinson, *Anal. Chim. Acta*, 56 (1971) 466.
4 N. Yamagata and I. Shigematsu, *Bull. Inst. Pub. Health, Tokyo*, 19 (1970) 1.
5 R. E. Carroll, *J. Amer. Med. Ass.*, 198 (1966) 267.
6 H. A. Schroeder, *Arch. Environ. Health*, 21 (1970) 798.
7 H. A. Schroeder and W. H. Vinton Jr., *Amer. J. Physiol.*, 202 (1962) 515.
8 H. A. Schroeder, W. H. Vinton Jr. and J. J. Balassa, *J. Nutr.*, 80 (1963) 48.
9 W. Slavin, *Atomic Absorption Spectroscopy*, Interscience, New York, 1968, p. 86, 87.
10 P. Pulido, K. Frena and B. L. Valla, *Anal. Biochem.*, 14 (1966) 393.
11 T. R. Hauser, T. A. Hinners and J. L. Kent, *Anal. Chem.*, 44 (1972) 1819.
12 G. F. Kirkbright, *Analyst*, 96 (1971) 609, 1146.
13 R. T. Ross, J. G. Gonzalez and D. A. Segar, *Anal. Chim. Acta*, 63 (1973) 205.
14 D. A. Segar and J. G. Gonzalez, *At. Absorption Newslett.*, 10 (1971) 94.
15 G. Lehnert, K. H. Schaller and T. Haas, *Z. Klin. Chem.*, 6 (1968) 174.
16 G. Lehnert, G. Klavis, K. H. Schaller and T. Haas, *Brit. J. Ind. Med.*, 26 (1969) 1156.
17 E. Norval and L. R. P. Butler, *Anal. Chim. Acta*, 58 (1972) 47.
18 M. D. Amos, D. A. Bennett, K. G. Brodie, P. W. Y. Lung and J. P. Matousek, *Anal. Chem.*, 43 (1971) 211.
20 H. M. Perry, *Trace Substances in Environmental Health—II*, University of Missouri, 1969, p. 101.
21 D. I. Hammer, J. F. Finklen, J. P. Creason, S. M. Sandifer, J. E. Keil, L. E. Priester and J. F. Stara, *Trace Substances in Environmental Health—II*, University of Missouri, 1969, p. 269.

Analytica Chimica Acta, 70 (1974) 448–452

SHORT COMMUNICATION

Direct determination of zinc in sea-bottom sediments by carbon tube atomic absorption spectrometry

DONALD V. BRADY, JOSEPH G. MONTALVO Jr., GREGORY GLOWACKI and ALEX PISCIOTTA

Department of Analytical Chemistry, Gulf South Research Institute, 5010 Leroy Johnson Drive, P.O. Box 26500; New Orleans, La. 70186 (U.S.A.)

(Received 20th September 1973)

The development of flameless atomic absorption techniques has considerably extended the detection limits for trace metals and allowed determinations to be made with very small samples[1–3]. Another potential advantage is the possible elimination of time-consuming sample pretreatment steps such as dry-ashing, etc.[4,5]. Yet, some types of samples have not been successfully analyzed by flameless atomic absorption procedures because of matrix interferences[6,7].

The U.S. Army Corps of Engineers requires trace metal analyses on bottom sediment samples before issuing dredging permits. Owing to the increasing number of permit applications, more rapid procedures for trace metals in sediments is essential. The Environmental Protection Agency procedure currently employed is time-consuming (wet digestion and dry ashing) and potentially subject to errors because of the number of steps involved in the sample preparation.

In this communication, the use of the flameless atomic absorption technique with the carbon tube for the direct and rapid determination of zinc in sediments is demonstrated with a sample obtained from a Mississippi coastal bay.

Experimental

Reagents. Analytical reagent-grade chemicals and redistilled or deionized distilled water were used.

Apparatus. A Beckman Atomic Absorption Spectrophotometer, Model 1301 was used for the standard EPA method.

Flameless atomic absorption spectrometry was done using two different instruments: (1) Perkin-Elmer 303 equipped with HGA 2000 Graphite Furnace; (2) Perkin-Elmer 306 equipped with HGA 70 Graphite Furnace. A Sargent Model SRLG recorder was used. Most experiments were run with the recorder on low speed of 0.2 in. min^{-1}.

EPA method (ref. 8). Pass the sample through a 2 mm (*ca.* 10 mesh) sieve by rubbing with a rubber stopper, if necessary; this removes large pieces of foreign material such as stones and twigs. Blend the sieved sample to a homogeneous mixture in a blender for 2 min at high speed. Place 2.5 g of the

sample in a 250-ml beaker, add 10 ml of metal-free concentrated nitric acid and 0.5 ml of 30% hydrogen peroxide and evaporate to dryness. Ash at 400–425°C for 1 h in a muffle furnace and cool. Add 25 ml of acid mixture (200 ml of concentrated nitric acid, 50 ml of concentrated hydrochloric acid and 750 ml of water), 20 ml of 10% ammonium chloride solution and 1 ml of 11.8% (w/v) calcium nitrate solution. Heat gently for 15 min and cool for 5 min or longer.

Transfer the sample to a centrifuge tube and centrifuge for 10 min at 20,000 rev min^{-1}. Transfer the supernate to a 250-ml volumetric flask. Rinse the residue in the centrifuge tube twice with redistilled water, add the washings to the supernate, and dilute to volume. Then transfer the sample to a small plastic bottle. Determine zinc by flame atomic absorption analysis using the procedures recommended in manufacturers' manuals. Air and acetylene gases are used.

Flameless atomic absorption procedure. Mix the wet sample as received thoroughly and dry a portion in an oven. Grind the dried sample finely in a mortar and mix thoroughly. Weigh out an appropriate sample (*ca.* 3 mg for the sediment sample employed here) and slurry in 10 ml of water in a Vortex mixer. After 20 s of slurrying, withdraw a 10-μl sample with an Eppendorf micropipette while mixing,, and inject it into the graphite furnace. Complete the analysis according to the manufacturer's instructions. The furnace conditions shown in Table I were used.

TABLE I

CONDITIONS USED WITH GRAPHITE FURNACES

	HGA 2000		*HGA 70*	
	Temperature (°C)	*Time (s)*	*Temperature (°C)*	*Time (s)*
Drying Cycle	100	20	100	60
Charring cycle	800	20	750	24
Atomizing cycle	1900	20	2000	18

Results and discussion

The analysis of a sediment sample by the EPA procedures and the EPA criteria for sediments are listed in Table II. The EPA will not approve a dredging permit if one or more of the given constituents exceeds the designated value.

The initial attempts to analyze the sediment sample consisted of weighing out very small samples on a microbalance and injecting the dry material onto the graphite tube. Although this method can be used, it was abandoned in favor of the slurry method, because the use of the microbalance is time-consuming and tedious, and it is difficult to accurately weigh the exact desired amount of sediment (as little as 3 μg) repetitively. A larger weight of sediment can be used with the slurry method and a standard analytical balance can be used. The concentration of zinc sediment in the aqueous slurry can be diluted simply by adding more water.

When a standard addition method (1.25, 2.5 and 5 p.p.b. Zn added) was used with either of the HGA instruments to determine the zinc concentration in the sediment (3.35 mg of sediment/10 ml of water), linear plots were obtained in both cases and the zinc concentration in the slurry was found to be 3.07 p.p.b. in each run. On a dry-weight basis this was equivalent to 9.16 p.p.m. zinc with the PE 306 AA–HGA 70 system and 9.30 p.p.m. zinc with the PE 303 AA–HGA 2000 system, which were of slightly different sensitivities. The average zinc concentration of 9.23 p.p.m. agrees reasonably well with the value of 11.1 p.p.m. obtained by the EPA method. The data obtained by the flameless method, which was used in different laboratories, should be more accurate than the value obtained by the flame procedure, because the former value was based on the method of standard additions, whereas the latter value was determined from a calibration line; moreover, the flame procedure is more susceptible to manipulative errors.

TABLE II

ANALYSIS OF SEDIMENT SAMPLE BY EPA METHODS AND EPA CRITERIA FOR SEDIMENTS

Constituent	*Dry weight basis*	
	Mississippi coastal bay sediment	*EPA criteria*
Volatile solids	2.99%	6.0%
Chemical oxygen demand	1.54%	5.0%
Total Kjeldahl nitrogen	0.055%	0.10%
Oil and grease	0.008%	0.15%
Mercury	<0.1 p.p.m.	1 p.p.m.
Lead	<5 p.p.m.	50 p.p.m.
Zinc	11 p.p.m.[a]	50 p.p.m.

[a] Average of two determinations.

The fact that essentially the same zinc value for the sediment sample was obtained with two different instruments in different places, provides more evidence of the validity of the flameless technique.

Linear calibration curves were obtained for aqueous zinc solutions in the range 3–20 p.p.b. Zn. A calibration curve was also prepared with varying concentrations of zinc in sediment slurries, which were obtained by mixing different weights of sediment in 10 ml of water; the average zinc value of 9.23 p.p.m. was used for calculation. The sediment curve could be superimposed on the aqueous curve, which indicates that the sediment matrix did not have an adverse effect on the zinc recovery. Thus the volatilization characteristics of zinc in sediment and water must be essentially the same when the instrument conditions described are used. This is probably because only μg-amounts of a sediment need be injected into the carbon tube, so that matrix effects are minimized.

The homogeneity of the mixed solid sample was demonstrated by the data for the above-mentioned calibration curve where 4 different weighed sediment samples gave values which all fell on a straight line. Homogeneity was also

confirmed by the reproducibility of the two above-mentioned determinations by the standard addition method.

The data points used for the calibration lines were average values of 3–7 runs. The standard deviations for the sediment samples are shown in Table III; very similar results were obtained for aqueous zinc solutions. Better precision could of course be obtained by further optimization of instrument operating conditions.

TABLE III

STANDARD DEVIATIONS OF ZINC IN SEDIMENT SLURRIES

Sediment in 10 ml H_2O (mg)	*Zinc in slurry (p.p.b.)*[a]	*Number of determinations*	*Average chart divisions*	*Std. deviation in chart divisions*
3.370	3.10	4	8.5	1.23
9.946	9.15	3	22.2	1.77
13.260	12.20	4	31.3	2.21
16.522	15.20	7	37.5	3.15

[a] Based on determination by Method of Standard Additions (zinc concentration in sediment = 9.2 p.p.m.).

A point near the middle of the sediment curve was chosen (24.0 chart divisions) and the confidence limits were calculated for this level. The value of s (standard deviation) for the sediment point nearest this value was 1.77 chart divisions. Calculations of the confidence limits for this level of zinc gave: for 66.7% confidence, 9.5 ± 0.7 p.p.b., and for 95.0% confidence, 9.5 ± 1.4 p.p.b. Similar calculations for zinc in water at a similar level gave: for 66.7% confidence, 9.5 ± 0.5 p.p.b.; and for 95.0% confidence, 9.5 ± 1.0 p.p.b.

Figure 1 compares identical runs with and without the Deuterium Background Corrector (DBC). Although the DBC eliminated almost all of the peak tailing, the peak heights were identical; accordingly the DBC is unnecessary for this type of work.

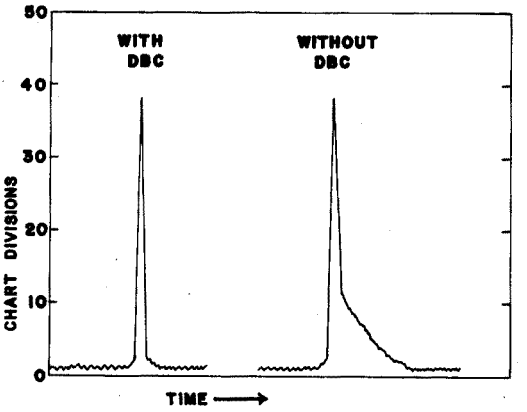

Fig. 1. Comparison of identical runs with and without deuterium background corrector (DBC).

The proposed procedure should also be applicable to other metals in sediments, as well as other types of soil, and possibly in the treatment of biological samples.

We would like to express our appreciation to Mr. Bud Brodtman of the Jefferson Parish Water Works for allowing us to utilize the Perkin-Elmer HGA 70 graphite furnace and the PE 306 AA.

REFERENCES

1 P. A. Ullucci, C. J. Mokeler and J. Y. Hwang, *Amer. Lab.*, 5 (1972) 63.
2 M. Glenn, J. Savory, L. Hart, T. Glenn and J. Winefordner, *Anal. Chim. Acta*, 57 (1971) 263
3 F. J. Fernandez and D. C. Manning, *At. Absorption Newslett.*, 10 (1971) 65.
4 J. P. Matousek, and B. J. Stevens, *Clin. Chem.*, 17 (1971) 363.
5 K. G. Brodie and J. P. Matousek, *Anal. Chem.*, 43 (1971) 1557.
6 I. W. F. Davidson and W. L. Secrest, *Anal. Chem.*, 44 (1972) 1808.
7 D. A. Segar and J. G. Gonzalez, *Anal. Chim. Acta*, 58 (1972) 7.
8 *Bottom Sediments*, Chemistry Laboratory Manual, compiled by Great Lakes Region Committee on Analytical Methods, EPA, FWQA, December 1969, pp. 1, 18–20.

Analytica Chimica Acta, 70 (1974) 453–456

SHORT COMMUNICATION

Photometric titration of chromium(VI) and vanadium(V) in a mixture

S. V. PARAB, S. SYAMSUNDAR* and T. K. S. MURTHY

Chemical Engineering Division, Bhabha Atomic Research Centre, Trombay, Bombay-400 085 (India)

(Received 10th November 1973)

Potentiometric titrations of mixtures of chromium(VI) and vanadium(V) with iron(II) solution do not yield separate end-points, marking their reduction to chromium(III) and vanadium(IV), respectively, because the oxidation potentals of the two systems are too close (1.33 V and 1.0 V). The advantages of photometric over potentiometric titrations for such mixtures have been demonstrated by Sweetser and Bricker[1]. Bricker and Schonberg[2] described a "photonometric titration" of chromium(VI)–vanadium(V) mixtures. Parab[3] studied the direct photometric titration of this mixture with iron(II). This method has been modified to improve its accuracy and reproducibility, and the results are summarized here.

Experimental

Reagents. Merck or Sarabhai-Merck guaranteed-grade reagents were used. Potassium dichromate was dried at 150°C before use. A 0.1 *M* solution of iron(II) ammonium sulphate in 0.25 *M* sulphuric acid was standardized against dichromate; cadmium powder was added as preservative[4]. A 0.1 *M* sodium vanadate solution was prepared from ammonium vanadate by boiling with a slight excess of sodium carbonate and standardized against the iron(II) solution[5].

A phosphoric acid–sulphuric acid mixture was made with 500 ml of phosphoric acid (s.g. 1.71), 100 ml of sulphuric acid (s.g. 1.84) and 2 l of distilled water; 15 g of potassium persulphate and 15 ml of 0.1 *M* silver sulphate were added, and the solution was boiled till its volume was reduced to about 1250 ml, and then cooled.

Apparatus. Absorption spectra were obtained with a Beckman Model-B spectrophotometer. For photometric titrations, the normal cell compartment was replaced by a laboratory-made titration assembly[6]. A 10-ml burette with 0.02 ml graduations was used for titration.

Procedure. Take an aliquot containing chromium(VI) and vanadium(V) in a 100-ml beaker (4-cm diameter), and add 50 ml of the acid mixture and sufficient water to make up the volume to 70 ml. Adjust the speed of the magnetic stirrer, avoiding vortex formation. Close the compartment and introduce the burette

* Present address: Nuclear Fuel Complex, Department of Atomic Energy, Hyderabad-500 040, India.

through the hole in the lid so that its tip touches the liquid. Set the wavelength at 760 nm and make the 100% transmittance adjustment. Start the titration with iron(II) solution and note the absorbance after each 0.2-ml addition. Correct the readings for the increase in volume and calculate the two end-points graphically.

Results

The best wavelength was selected by comparing the absorption spectra of vanadium(V and IV), iron(III and II) and chromium(VI and III) in 1–5 *M* sulphuric acid in the range 350–900 nm. At 760 nm, vanadium(IV) has an absorption maximum (molar absorptivity about 25), other species having negligible absorption. It was expected that on carrying out the titration at this wavelength, the absorbance would remain low and nearly constant until all chromium(VI) had been reduced, and would then show a gradual increase until all vanadium had been reduced, when it would once again remain constant.

When phosphoric acid was employed, negative errors were found for both metals; the error also increased with the standing time of the solutions. This was suspected to be due to slow action of reducing impurities like phosphorous acid, present even in the pure acid; several methods of overcoming the problem were tested and oxidation by persulphate was found satisfactory.

The titration curves obtained for Cr–V mixtures when the sulphuric acid and phosphoric acid concentrations were varied are shown in Fig. 1. In general, the sharpness of the end-point improved with increasing acid concentration but, for comparable acidity, phosphoric acid was more effective. Moreover, there was

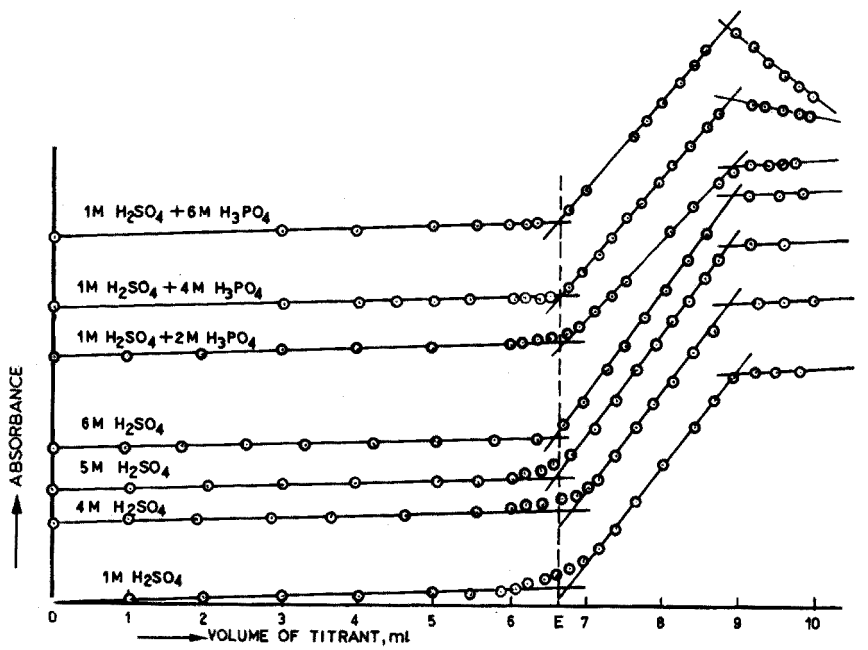

Fig. 1. Effect of acidity on spectrophotometric titration of chromium(VI)–vanadium(V) mixture with iron(II). E, calculated end-point for chromium(VI). For all curves, the initial absorbance was zero.

a positive error in the chromium results, and a corresponding negative error in those for vanadium, at low acidity; these errors decreased with increasing acidity. Concentrations of 1 *M* sulphuric acid and 4 *M* phosphoric acid were therefore selected. With more than 2 *M* phosphoric acid, there was a tendency for vanadium(IV) to be further reduced.

Known amounts of chromium (as dichromate) and vanadium (as 0.1 *M* vanadate) were mixed, and photometric titrations were plotted, as described above. The results are summarized in Table I.

TABLE I

PHOTOMETRIC TITRATION OF MIXTURE WITH IRON(II)

(Strength of iron(II): 0.0927 *M*)

Chromium(VI)				*Vanadium(V)*			
Taken (mg)	*Titrant added (ml)*	*Found (mg)*	*Relative error (%)*	*Taken (mg)*	*Titrant added (ml)*	*Found (mg)*	*Relative error (%)*
5.20	3.28	5.27	+1.4	48.24	10.12	47.87	−0.7
5.37	3.29	5.29	−1.5	48.24	10.18	48.14	−0.2
11.10	6.91	11.11	+0.1	33.77	7.09	33.54	−0.7
11.00	6.83	10.97	−0.3	33.77	7.12	33.68	−0.3
21.31	13.33	21.43	+0.6	19.30	4.09	19.35	+0.3
21.39	13.32	21.40	+0.1	19.30	4.05	19.17	+0.7
31.60	19.74	31.72	+0.4	9.65	2.05	9.70	+0.5
31.93	19.85	31.90	−0.1	9.65	2.05	9.70	+0.5

Discussion

In the titration of chromium(VI)–vanadium(V) mixtures, the following reactions are involved:

$$Cr(VI) + 3\ Fe(II) \rightarrow Cr(III) + 3\ Fe(III) \quad (1)$$

$$V(V) + Fe(II) \rightarrow V(IV) + Fe(III) \quad (2)$$

$$Cr(VI) + 3\ V(IV) \rightarrow Cr(III) + 3\ V(V) \quad (3)$$

The absence of a separate end-point in the potentiometric titration corresponding to the reduction of chromium(VI) can be attributed to the fact that reaction (2) has taken place, to an appreciable extent, before reaction (1) is complete. It was observed during titrations that after each addition of titrant, the absorbance increased and then decreased to a steady value, indicating the occurrence of the slow reaction (3). The photometric end-point was located by extrapolation of the absorbance readings obtained before the competing reactions became significant, and was quite sharp. The formal oxidation potentials of the Cr(VI)–Cr(III) (ref. 7) and V(V)–V(IV) (ref. 5) couples are influenced by acid concentration, and the difference between the potentials appears to increase with acidity. Phosphoric acid also lowers the redox potential of the Fe(III)–Fe(II) system. All these factors help to make the end-points sharp and accurate in the photometric titrations.

The proposed method is simpler than those reported earlier[2,8]. The phosphoric acid concentration prescribed is much lower than that suggested by Dikshitulu[9] and end-points for chromium are sharper.

REFERENCES

1 P. B. Sweetser and C. E. Bricker, *Anal. Chem.*, 24 (1952) 1107.
2 C. E. Bricker and S. S. Schonberg, *Anal. Chem.*, 30 (1958) 922.
3 S. V. Parab, *M.Sc. Thesis*, Bombay University, 1966.
4 S. Syamsundar and T. K. S. Murthy, *Curr. Sci. (India)*, 41 (1972) 503.
5 G. Gopala Rao and L. S. A. Dikshitulu, *Talanta*, 10 (1963) 295.
6 S. V. Parab and T. K. S. Murthy, *Atomic Energy Commission (India), Report B.A.R.C. 611*, (1972) 2.
7 G. F. Smith and F. P. Richter, *Ind. Eng. Chem., Anal. Ed.*, 16 (1944) 580.
8 J. W. Miles and D. T. Englis, *Anal. Chem.*, 27 (1955) 1996.
9 L. S. A. Dikshitulu, *Indian J. Chem.*, 9 (1971) 872.

Analytica Chimica Acta, 70 (1974) 457–461

SHORT COMMUNICATION

Microméthodes de caractérisation et de dosage des stéroïdes acétyléniques par formation d'acétylure d'argent

M. RIZK, J. J. VALLON et A. BADINAND

Laboratoire de Chimie Analytique, U.E.R. des Sciences Pharmaceutiques, Université Claude Bernard, 69008 Lyon (France)

(Reçu le 5 novembre 1973)

Les recherches effectuées en vue de produire des progrestatifs et oestrogènes, actifs par voie orale, ont conduit à l'obtention de structures parfois assez éloignées de celle de l'hormone naturelle: progestérone ou β-oestradiol. L'introduction du groupement éthinyle $-C\equiv CH$ en position α 17 favorise la résorption par voie orale; les stéroïdes éthinyliques constituent donc une importante classe de composés, particulièrement dans les contraceptifs oraux.

L'identification de ces composés par chromatographie en couche mince (c.c.m.) ou sur papier (c.p.) est effectuée habituellement par les procédés généraux de détection des stéroïdes[1,2,3]; ou bien par spectrophotométrie infra-rouge (i.r.) après élution du chromatogramme[3,4]. De même, plusieurs méthodes sont utilisées pour leur dosage: spectrophotométrie ultraviolette combinée à une séparation chromatographique[3,4,5,6], spectrophotométrie i.r.[7,8,9], chromatographie en phase gazeuse[10] et également colorimétrie[11,12].

Aucun de ces procédés n'utilise leur groupement éthinyle qui caractérise cependant cette famille de composés. Les éthinylstéroïdes sont des dérivés acétyléniques vrais; l'hydrogène fonctionnel est aisément remplaçable par un métal lourd[13,14,15]. La réaction la plus simple est celle avec l'argent:

$$R{-}C\equiv CH + Ag^+ \rightleftarrows R{-}C\equiv CAg + H^+ \qquad (1)$$

Cette réaction a été utilisée pour doser les composés acétyléniques vrais[16] et elle a été aussi adaptée pour doser des éthinylstéroïdes par acidimétrie[17] ou par potentiométrie[18].

Dans un article précédent[19], nous avons montré l'utilité de cette réaction (1) pour doser ces composés par colorimétrie à la dithizone; le travail que nous présentons décrit une sensibilisation du dosage grâce à l'extraction de l'acétylure d'argent formé par un solvant organique; une acidification libère ensuite une quantité équivalente d'ions argent dosés à l'état de dithizonate. Cette modification permet un dosage de quantités aussi faibles que $0{,}5\cdot10^{-4}$ M ($\equiv 15$ μg) des stéroïdes éthinyliques.

Nous proposons, de même, une identification de ces composés par c.c.m. ou c.p. selon la même réaction (1). On pulvérise successivement des solutions de

nitrate d'argent ammoniacal, puis d'un composé fluorescent tel que l'éosine ou le fluorescéinate de sodium; les stéroïdes sont ainsi révélés avec une grande sensibilité (de l'ordre de 0,1 μg sur chromatographie sur papier).

Étude qualitative

Stéroïdes. Norethistérone, acétate de norethistérone, lynostéronol, ethinyloestradiol, mestranol, norethynodrel et diacétate d'éthindiol.

Révélateurs. (a) Nitrate d'argent 0,1% p/v dans une solution d'ammoniac 0,5 *M*. (b_1) Eosine 0,02% p/v dans l'alcool. (b_2) Fluorescéinate de sodium 0,02% p/v dans l'alcool.

Procédé. La chromatographie en couche mince sur plaques de gel de silice G (Merck) a été faite suivant la méthode ascendante, la quantité déposée de 2 à 5 μg de stéroïde en solution dans le chloroforme–méthanol (1 + 1). Le solvant est un mélange de cyclohexane–acétate d'éthyle (1 + 1). Après migration, puis sèchage, la révélation des spots est obtenue par pulvérisation sur la plaque de la solution (a), puis sèchage à la température ambiante et pulvérisation de la solution b_1 ou b_2. Les éthinylstéroïdes, sauf l'éthinyloestradiol, sont aisément détectés par leur coloration rouge sur fond jaune fluorescent avec le fluorescéinate de sodium, ou bien rose violette sur fond rose pâle avec l'éosine. L'éthinyloestradiol donne une coloration rose foncé avec la fluorescéine et violette avec l'éosine.

Étude quantitative

Courbe d'étalonnage de Ag^+. Transférer dans des ampoules à décantation des volumes d'une solution de nitrate d'argent équivalent à 10, 20, 30, 40 μg; ajouter 10 ml d'eau, 1 ml d'acide sulfurique 2 *M*, et 5 ml de chloroforme; agiter vigoureusement en ajoutant goutte à goutte de solution chloroformique du dithizone (0,004% p/v) à la micro-burette. L'addition de dithizone est poursuivie ainsi que l'agitation jusqu'à ce que l'extrait chloroformique qui contient le dithizonate d'argent (jaune) ait une faible couleur verte, indiquant l'extraction totale de Ag^+. Les extraits chloroformiques sont dilués à 10 ml avec du chloroforme dans des fioles jaugées; on mesure l'absorbance de chacune à 472 nm, en utilisant une solution témoin contenant 2 gouttes de dithizone dans 10 ml de chloroforme; on trace la droite d'étalonnage.

Dosage des stéroïdes éthinyliques (éthinyloestradiol excepté). Transférer 1 ml d'une solution alcoolique de stéroïdes à 10–50 μg, dans une ampoule à décantation; ajouter d'abord 3 gouttes d'une solution ammoniacale (0,4% v/v), puis 5 ml d'une solution aqueuse de nitrate d'argent (0,002% p/v); agiter le mélange et abandonner environ 5 min; extraire l'acétylure d'argent deux fois en ajoutant des fractions de 3 ml de mélange chloroforme–benzène (4 + 1). L'extrait organique est lavé avec 3 ml d'eau distillée, puis on ajoute 1 ml d'acide sulfurique 2 *M* et 10 ml d'eau distillée; on agite vigoureusement et la dithizone est ajoutée. Terminer comme précédemment. En se reportant à la courbe d'étalonnage, on obtient la quantité d'argent équivalent à l'éthinylstéroide. 1 μg de $AgNO_3$ équivaut à: 1,828 μg de mestranol, 1,744 μg d'éthinyloestradiol 2,004 μg d'acétate de norethistérone, 1,756 μg de norethynodrel ou de norethistérone et 1,674 μg de lynostéronol.

Dosage de l'éthinyloestradiol. À cause de la présence du groupement phénolique libre, les résultats obtenus par le procédé précédent ne sont pas repro-

ductibles. En modifiant ce composé par acétylation du groupement phénolique, on peut le doser à l'état d'acétate.

Transférer 0,5 ml d'une solution alcoolique d'éthinyloestradiol équivalent à 0,5 mg dans un tube à essai bouché. Evaporer à sec sous azote, puis, au résidu, ajouter 0,3 ml de pyridine pure et 1,5 ml d'anhydride acétique, mélanger et fermer le tube fortement, laisser à 70°C au bain marie pendant 1 h. Évaporer à sec sous azote au bain marie bouillant. Transférer le résidu à l'aide de l'alcool dans une fiole jaugée à 25 ml, compléter jusqu'au volume avec l'alcool. Transférer 1 ml de cette solution dans une ampoule à décantation et procéder au dosage du stéroïde par la même méthode que précédemment.

Application au dosage des stéroïdes dans les comprimés (Gyn-Anovlar)^{R}.

Chaque comprimé se compose de 2,0 mg d'acétate de norethistérone et 0,05 mg d'éthinyloestradiol.

Mode opératoire. Transférer une prise d'essai des comprimés finement pulvérisés (équivalent à 10 comprimés) dans une ampoule à décantation (125 ml) contenant 50 ml de chloroforme. Extraire trois fois en ajoutant des fractions de 10 ml d'une solution aqueuse d'hydroxyde de sodium à 10%; agiter vigoureusement pendant 2 min pour chaque extraction; attendre également jusqu'à la séparation complète; conserver l'extrait chloroformique (A) afin de doser l'acétate de norethistérone. Réunir les extraits alcalins dans une autre ampoule à décantation. Acidifier avec 10 ml d'acide sulfurique (1+4), puis extraire en ajoutant trois fractions de 25 ml de chloroforme. Laver les extraits chloroformiques avec 15 ml d'eau distillée, rejeter l'eau distillée. Filtrer le chloroforme dans un entonnoir contenant de la laine de verre, recueillir le filtrat dans un bècher de 150 ml, laver la laine de verre avec 10 ml de chloroforme, évaporer jusqu'à 2–3 ml au bain-marie puis transférer quantitativement dans un tube à essai bouché à l'aide de 2 fois 3 ml de chloroforme, évaporer à sec, au bain marie, sous azote, ajouter les réactifs de l'acétylation et compléter pour doser l'éthinyloestradiol comme précédemment. L'acétate de norethistérone est dosé comme suit: la solution chloroformique (A) est filtrée et évaporée à sec au bain-marie bouillant; le résidu est redissous et transféré à l'aide de l'alcool dans une fiole jaugée à 100 ml et complété jusqu'au volume avec l'alcool; la solution est diluée dans l'alcool jusqu'à une concentration d'environ 20 $\mu g\ ml^{-1}$. 1 ml de cette solution finale est transféré dans une ampoule à décantation et le stéroïde est dosé avec la même méthode que précédemment.

Résultats et discussions

Étude qualitative. Pollard et coll.[20] ont montré que de nombreux anions, donnant des sels d'argent insolubles, peuvent être révélés sur les chromatogrammes par pulvérisation d'une suspension de fluorescéinate d'argent. Celui-ci est dépourvu de fluorescence et colore le chromatogramme en rouge; en présence des anions précipitants, la fluorescéine est libérée de son sel d'argent et une fluorescence apparaît.

Des essais d'application de cette méthode à la détection des acétyléniques nous ont donné des résultats négatifs, probablement parce que l'excès d'ions Ag^{+} nécessaire à la stabilisation du fluorescéinate d'argent dans le réactif entraîne la formation d'un complexe acétylénique soluble[3] ($RC \equiv CAg \cdot Ag^{+}$). Par contre, en milieu ammoniacal, on forme l'acétylure d'argent insoluble ($RC \equiv CAg$); une pulvérisation

ultérieure de fluorescéinate de sodium (ou d'éosine) fait apparaître des taches rosées non fluorescentes (fluorescéinate d'argent) sur un fond fluorescent. Ces faits indiquent que l'acétylure d'argent est déplacé par la fluorescéine, mais que les ions Ag^+ probablement précipités à l'état d'hydroxyde sur le fond du chromatogramme, ne réagissent pas avec la fluorescéine. La lecture est faite à l'oeil, à la lumière du jour.

La sensibilité est de l'ordre de 0,1 μg sur papier, et légèrement supérieure sur couche mince de silice. Une étude de sélectivité de la réaction a été faite; aucune réaction n'est obtenue avec les stéroïdes suivants: progrestérone, propionate de testostérone, estrone, β-oestradiol, 5 α cholestane, prégnenolone.

Étude quantitative. Des essais d'extraction de l'ammine argentique par le solvant chloroforme–benzène (4+1) en l'absence de stéroïdes ont montré l'insolubilité totale dans ce solvant (aucune coloration jaune en présence de traces de dithizone).

Une gamme étalon faite avec des quantités croissantes de stéroïde (lynostéronol) en présence d'excès d'argent, selon la technique décrite, montre une linéarité complète entre 0 et 60 μg de stéroïdes. Il est donc possible, soit d'étalonner par ce procédé avec des quantités croissantes de stéroïdes, soit de faire

TABLEAU I

RESULTATS POUR LES STÉROÏDES ÉTHINYLIQUES[a]

Stéroïde	*15 µg*		*30 µg*		*45 µg*	
	A	*B*	*A*	*B*	*A*	*B*
Norethynodrel	98.36±3.57	98.5±3	99.5±1.3	96.5±1.5	97.8±1.2	101.3±2.5
Lynostéronol	100.4±1.5	102.0±2	101.0±1.4	99.0±3.2	98.9±3.8	101.5±1.4
Norethistérone	100.6±2.3	96.5±1.0	103 ±1.5	98.0±2	101.0±2.0	98.5±1.8
Acétate de Norethistérone	103.0±3.5	98.6±1.5	104.0±3.0	94.3±3	101.5±2.0	96.5±2.3
Mestranol	99.8±1.6	101.0±2	99.6±1.9	96.2±1.7	98.2±2.1	97.5±2.2
Ethinyloestradiol (acétate)	94.0±2.0	97.2±3.0	104.3±3.2	101.5±3	103.8±2.8	98.6±3.3

[a] Moyenne de trois essais. A, pourcentage de récupération du stéroïde calculé en dosant l'Ag ayant reagi. B, pourcen de récuperation du stéroïde calculé en dosant l'excès d'Ag ajoute.

TABLEAU II

COMPRIMÉS GYN-ANOVLAR®

Stéroïde	*Théorique comp. (mg)*	*Trouvé (mg)*	*% Récup.*	*% Erreur*
Acétate de Norethistérone	2.0	2.044	102.2	±2.2
Ethinyl Oestradiol (après acétylée)	0.05	0.053	106.0	±6

une gamme étalon avec des quantités croissantes d'ions Ag^+. La première méthode évite d'appliquer un coefficient de corrélation entre stéroïdes et ions Ag^+ consommés.

Le tableau I montre les résultats obtenus pour les différents stéroïdes éthinyliques présents généralement dans les contraceptifs oraux. Les résultats expriment le % de récupération du stéroïde calculé soit en dosant l'Ag ayant réagi soit en dosant l'excès d'Ag. L'erreur est voisine de $\pm 3\%$. Le tableau II montre les résultats des dosages de l'acétate de norethistérone (erreur de $\pm 2\%$) et de l'ethinyloestradiol (erreur de $\pm 6\%$) dans des comprimés Gyn-Anovlar(R).

BIBLIOGRAPHIE

1 R. Neher, *Steroïd Chromatography*, Elsevier, Amsterdam, 1964, p. 259.
2 M. B. Simard et B. A. Lodge, *J. Chromatogr.*, 51 (1970) 517.
3 J. J. Thomas et LL. Dryon, *Proc. Int. Symp. Chromatogr. Electrophor. V*, 1969, 405.
4 G. R. Keay, *Analyst*, 93 (1968) 28.
5 R. A. Bastow, *J. Pharm. Pharmacol.*, 19 (1967) 41.
6 C. A. Brunner et M. F. Kunze, *J. Ass. Offic. Anal. Chem.*, 53 (1970) 234.
7 I. Akira et O. Amakaou, *J. Pharm. Soc. Japan*, 77 (1957) 1083.
8 A. L. Hayden et O. R. Sammul, *J. Amer. Pharm. Ass., Sci. Ed.*, 48 (1960) 489.
9 G. Bellomonte, *Ann. Ist. Super. Sanita*, 7 (1971) 102.
10 B. A. Lodge, *Can. J. Pharm. Sci.*, 5 (1970) 74.
11 R. V. Smith, T. H. Hassel et S. C. Liu, *J. Ass. Offic. Anal. Chem.*, 53 (1970) 1089.
12 J. F. Chissell, *J. Pharm. Pharmacol.*, 16 (1964) 490.
13 N. D. Cheronis et T. S. Ma, *Organic Functional Group Analysis*, Wiley-Interscience, New York, 1960, p. 385.
14 S. Siggia, *Quantitative Organic Analysis via Functional Groups*, Wiley, 2nd ed., New York, 1954, p. 86.
15 M. Miocque, *Lanalyse Chimique des Composés Acétyléniques. Mise au point de Chimie Analytique Pure et Appliquée*, Gautier, Paris, 7 Sér., 1959, p. 146.
16 M. Miocque et J. A. Gautier, *Bull. Soc. Chim. Fr.*, 5 (1958) 467.
17 S. Görög, *Acta Chim. Acad. Sci. Hung.*, 47 (1966) 1.
18 British pharmacopeia, (1968) 664.
19 M. Rizk, J. J. Vallon et A. Badinand, *Anal. Chim. Acta*, 65 (1973) 220.
20 F. H. Pollard, G. Nickless et K. W. C. Burton, *J. Chromatogr.*, 49 (1970) 317.

Analytica Chimica Acta, 70 (1974) 462–464

SHORT COMMUNICATION

Selective removal of germanium by retention on silica gel

P. LIEVENS and J. HOSTE

Institute of Nuclear Sciences, Rijksuniversiteit Gent, Proeftuinstraat 86, 9000 Gent (Belgium)

(Received 11th December 1973)

Neutron activation analysis for various trace impurities in germanium has been the subject of many studies. The standard ways of separating germanium from other elements are distillation of germanium tetrachloride, precipitation of germanium sulfide, hydrated germanium oxide or a metallic organic complex, solvent extraction of germanium(IV) halide and both anion and cation exchange[1]. From a review by Goryushima[2], it appears that most authors take advantage of the volatility of germanium tetrachloride. Moreover, most of the methods dealing with the preparation of carrier-free radioarsenic (^{73}As, ^{74}As, ^{77}As) are based on the fact that germanium tetrachloride and arsenic trichloride are volatile, whereas arsenic pentachloride is not[1]. It is difficult, however, to remove the last traces of germanium in this way. We have found that germanium can be removed much more easily by quantitative retention on silica gel from strong acidic media, with excellent selectivity. The behaviour of a number of elements in 7 *M* nitric acid on silica gel has already been reported by Girardi *et al.*[3]. They showed that most elements are not retained, whereas partial sorption takes place for Ge, Br, Zr, Nb, Sb, Hf, Ta and W.

Experimental

Germanium (0.15 g) was dissolved in 40 ml of a (1+1) mixture of 12 *M* hydrochloric acid and 14 *M* nitric acid by heating under reflux for 1 h. Afterwards the solution was diluted three-fold with 14 *M* nitric acid. The final chloride concentration appeared to be *ca.* 0.2 *M* and the nitric acid concentration about 9.5 *M*.

The silica gel was pretreated with 14 *M* nitric acid and then packed into a glass column of 9 mm diameter and 30 mm length (corresponding to 1 g of dry silica gel). In the chromatographic experiments, 10 ml of the radiotracer solution (9.5 *M* nitric acid and 0.2 *M* hydrochloric acid), obtained in the same way as for the dissolution of germanium, were passed through a column corresponding to 1 g of dry silica gel at a flow rate of 1.6 ml min^{-1} cm^{-2}. Subsequent elution was carried out with 1.5 ml of the same eluent. Radioactivity measurements were made with a 50-cm^3 Ge–Li detector and a 3 × 3-in NaI(Tl) well-type detector.

Retention capacity and decontamination factor

Figure 1 shows four elution curves obtained at flow rates of 0.5 and 1.6

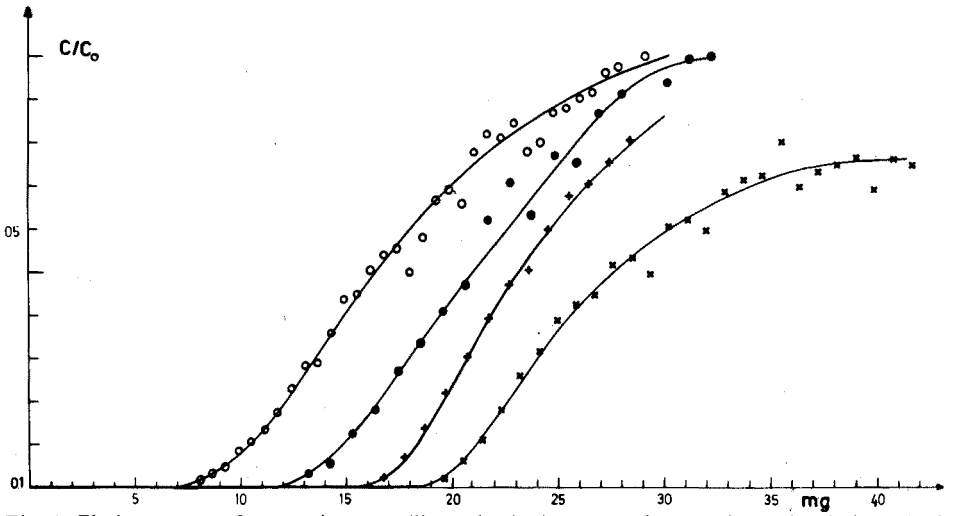

Fig. 1. Elution curves of germanium on silica gel; abscissa: mg of germanium passed through the column; ordinate: concentration ratio of effluent to input. (○) 1.6 ml of $9.33 \cdot 10^{-3}$ *M* Ge min^{-1} cm^{-2}/1 g of SiO_2 (Carlo Erba). (●) 0.5 ml of $9.33 \cdot 10^{-3}$ *M* Ge min^{-1} cm^{-2}/1 g of SiO_2 (Carlo Erba). (+) 1.4 ml of $8.21 \cdot 10^{-3}$ *M* Ge min^{-1} cm^{-2}/1 g of Kieselgel (Merck). (×) 0.6 ml of $8.21 \cdot 10^{-3}$ *M* Ge min^{-1} cm^{-2}/1 g of Kieselgel (Merck).

ml min^{-1} cm^{-2} on silica gel (Kieselgel für chromatographie 0.05–0.20 mm, from Merck; and silica gel from Carlo Erba). The breakthrough capacities were 6.8, 11.1, 15.8 and 18.4 mg of germanium per gram of silica gel. In the last case, 30 mg of germanium was adsorbed on the column after 42 mg of germanium had been passed. In column operation, a decontamination factor greater than $5 \cdot 10^5$ was obtained.

Selectivity of retention

The results expressed as the percent radiotracer eluted are shown in Table I. Germanium was quantitatively retained whereas silver and tungsten were partially retained. The other investigated elements were almost quantitatively eluted with the small eluent volume used (1.5 ml). Even with 40 ml of 1 *M* nitric acid or 30 ml of 6 *M* ammonia solution (which destroyed the column) it was not possible to elute germanium completely. The behaviour of most of these elements (except Ge and Ag) on silica gel seems to be quite similar in 7 *M* nitric acid, as reported by Girardi.

Applications

The selectivity, the high retention capacity and the decontamination factor fulfil all the requirements for applications in activation analysis. The method is of particular interest for the preparation of ^{77}As. After irradiation of germanium and sufficient waiting time to allow for the growth of the daughter activity ^{77}As from the ^{77}Ge parent (about 14 h for short irradiation times) the germanium is dissolved and passed through a silica gel column at a flow rate of about 1.5 ml min^{-1} cm^{-2} as described above. ^{77}As flows immediately through the column while ^{77}Ge and ^{75}Ge are completely retained.

TABLE I

RETENTION OF DIFFERENT ELEMENTS ON THE SILICA GEL COLUMN

Tracer	*Concentration* ($\cdot 10^{-5}$ *M*)	*% eluted*
^{110m}Ag	0.42	58
^{77}As	Carrier-free	95
^{198}Au	2.70	98
^{115}Cd	6.00	97
^{60}Co	1.10	100
^{51}Cr	400.0	96
^{134}Cs	0.72	99
^{64}Cu	48.0	99
^{59}Fe	859.0	96
^{72}Ga	2.50	97
^{77}Ge	820.0	0
^{203}Hg	7.40	97
^{115m}In	Carrier-free	98
^{140}La	1.80	97
^{54}Mn	Carrier-free	95
^{99}Mo	13.30	96
^{75}Se	69.00	99
^{46}Sc	9.00	97
^{99m}Tc	Carrier-free	93
^{65}Zn	51.10	99
^{187}W	0.28	4

In the same way, ^{73}As and ^{74}As can be prepared by proton or deuteron irradiation of a germanium target. This technique can obviously also be applied in activation analysis for trace impurities in germanium and for the determination of germanium in other matrices.

REFERENCES

1 J. A. Marinsky, *The Radiochemistry of Germanium*, NAS-NS 3043, 1961.
2 V. G. Goryushima, *Zavod. Lab.*, 37 (1971) 651.
3 F. Girardi, R. Pietra and E. Sabbioni, *Eur.*, (1969) 4287e.

Analytica Chimica Acta, 70 (1974) 465–468

SHORT COMMUNICATION

The behaviour of Srafion with transition metal ions

RICCARDO A. A. MUZZARELLI

"G. Ciamician" Chemical Institute, University of Bologna, Via Selmi 2, 40126 Bologna (Italy)

ROBERTO ROCCHETTI

Laboratory of Chemistry, Faculty of Medicine, University of Ancona, Via Posatora, 60100 Ancona (Italy)

(Received 15th August 1973)

Some years ago a new resin (Srafion; PITU; NMRR) carrying two resonating amino groups attached to a carbon atom on a styrene–divinylbenzene matrix was described as a chelating resin[1]. However, only a study of the separation of noble metals was reported. More recently, it was stated that Srafion can collect mercury in various chemical forms[2]. When Srafion was prepared, it was commonly believed that only a few chelating resins existed[3], Dowex A-100 (Chelex) being the most widely available of these, but it is now known that several natural chelating polymers also have useful analytical applications[4].

As no information is available on the general applicability of Srafion as a chelating resin, some transition metal ions were examined in order to reach a more general characterization of the polymer. Comparative measurements were carried on Dowex A-100.

Experimental

The metals tested were determined with a Perkin-Elmer 305 atomic absorption spectrometer, equipped with a three-slot air–acetylene burner, and the HGA-70 graphite atomizer. The latter was used for the determinations of vanadium and molybdenum, and for the determination of chromium at low concentrations[5].

The resin Srafion was purchased from Ayalon (Haifa, Israel). The metal ion solutions were 0.5 m*M*, unless otherwise stated, and 50 ml of each were shaken with 200 mg of wet polymer (moisture content, 70%). The columns were 0.5 × 3.0 cm, and were eluted with a mixture of 20 ml of ethanol and 80 ml of 36 m*M* sulphuric acid.

Results and discussion

Table I shows the collection percentages of several metal ions from slightly acidic solutions, and from 0.5 *M* EDTA solutions. Srafion does not collect the metal ions studied, from chromium(III) to lead(II). Silver, mercury, and possibly antimony, undergo precipitation as insoluble chlorides. The anions metavanadate,

TABLE I

COLLECTION PERCENTAGES FOR METAL IONS ON SRAFION[a]

	pH	*h*[b]	*Cr(III)*	*Cr(VI)*	*Mn(II)*	*Fe(II)*	*Ni(II)*	*Cu(II)*	*Zn(II)*	*As(V)*	*Mo(VI)*	*Ag(I)*	*Sn(II)*	*Sb(tart)*	*Hg(II)*	*Pb(II)*
Srafion																
	2.5	1	1	89	0	6	4	1	0	5	100	91	2	92	90	5
	2.5	12	13	95	5	2	5	15	0	—	—	96	70	—	74	0
0.5 *M* EDTA	2.5	1	17	82	4	6	2	0	7	5	—	97	—	3	30	10
	5.5	1	8	64	6	11	0	3	10	93	96	—	—	—	64	17
	5.5	12	20	100	11	3	5	18	—	—	97	—	—	—	74	12
0.5 *M* EDTA	5.5	1	21	93	22	2	13	0	5	14	—	—	—	—	10	6
0.05 *M* oxalic acid		1	2	10	0	50	14	77	30	7	—	—	—	87	44	—
Dowex A-100	2.5	1	66	15	8	0	68	52	46	5	0	78	98	0	20	87
	2.5	12	96	18	96	98	100	100	100	—	—	49	92	—	100	99
0.5 *M* EDTA	2.5	1	45	5	0	0	0	0	0	0	—	14	—	3	8	0
	5.5	1	79	0	94	92	100	98	94	0	20	—	—	—	96	82
	5.5	12	80	20	97	71	100	100	100	—	25	—	—	—	100	99
0.5 *M* EDTA	5.5	1	20	0	19	0	9	0	0	2	—	—	—	—	0	0
0.05 *M* oxalic acid		1	2	4	0	37	0	3	0	0	—	—	—	27	9	—

[a] Collection from 50 ml of 0.5 m*M* solutions on 200 mg (wet weight) of resin.
[b] Contact time.

chromate and molybdate are effectively collected at both pH 2.5 and 5.5, which indicates the cationic nature of the resin.

The results obtained with the chelating resin Dowex A-100 are in agreement with the very abundant literature data[6–10], and are in the opposite direction to those obtained with Srafion: the cations are collected whereas anions are not.

A column of Srafion became yellow on collection of vanadate, which could not be eluted with a solution of PAR even though the band became red. On attempted reduction of vanadate to VO^{2+} by hydrogen peroxide and sulphuric acid, the band became green and moved slightly, but the elution remained impracticable.

Srafion also became yellow on collection of chromate, but elution with diphenylcarbazide solution was impossible: the colour changed to violet but no trace of chromate could be detected in the eluates. On the basis of the results

TABLE II

DETERMINATION OF CHROMIUM ON ELUATE FRACTIONS FROM THE SRAFION COLUMNS

Cr taken[a] *(μg)*	*A.a.s. reading on four 5-ml eluates*[b]			*A.a.s. reading on original soln.*[b,c]			*Concn. of original soln. (μg ml⁻¹)*	*Chromatographic yield (%)*			*Mean value*
0.10	16	22	25								
	20	20	18								
	6	0	10								
	3	0	4								
	45	42	57	46	45	50	20	98	93	114	102
0.20	29	52	43								
	44	30	21								
	8	5	10								
	7	0	2								
	88	87	76	92	90	90	40	95	97	84	92
0.30	65	57	59								
	58	42	22								
	17	11	11								
	5	4	4								
	145	114	96	138	135	135	60	105	84	74	88
0.40	52	84	89								
	67	51	39								
	16	9	15								
	5	0	0								
	140	144	143	184	180	180	80	76	80	79	78

[a] This is the absolute amount in 5 ml of solution applied to the column.
[b] Readings are given as % absorption. Analyses were done in triplicate.
[c] Readings above 100% were obtained with lower scale expansion.

obtained with chromium(III) and chromium(VI), an attempt was made to reduce the chromate so that it could be eluted as chromium(III). Oxalic acid eluted only part of the chromate; a 20% hydrazine solution did not elute it at all. A 10% hydrogen peroxide–10% sulphuric acid solution eluted chromium with a yield between 10 and 93%, depending on the contact time, up to 12 h.

The ethanol–sulphuric acid mixture mentioned in *Experimental*, tested after a 4-h contact time, allowed satisfactory elution of chromium for the concentration range studied; the results did, however, tend to become low for more concentrated solutions (Table II).

In conclusion, the resin Srafion can be better described in terms of a basic resin, having a high affinity for oxyanions like metavanadate, chromate and molybdate, than as a general chelating resin.

The present work was carried out under the auspices of the National Research Council of Italy, (Contract No. 1952/03).

REFERENCES

1 G. Koster and G. Schmuckler, *Anal. Chim. Acta*, 38 (1967) 179.
2 S. L. Law, *Science*, 174 (1971) 285; *Intl. Lab.*, 5 (1973) 53.
3 G. Schmuckler, *Talanta*, 10 (1963) 745; 12 (1965) 281.
4 R. A. A. Muzzarelli, *Natural Chelating Polymers*, Pergamon Press, Oxford, 1973.
5 D. E. Leyden, R. E. Channel and C. W. Blount, *Anal. Chem.*, 44 (1972) 607.
6 R. Rossett, *Bull. Chem. Soc. France*, (1964) 1845; (1966) 59.
7 D. E. Leyden and A. L. Underwood, *J. Phys. Chem.*, 68 (1964) 2093.
8 D. G. Birney, W. E. Blake, P. R. Meldrum and M. E. Peach, *Talanta*, 15 (1968) 557.
9 J. P. Riley and D. Taylor, *Anal. Chim. Acta*, 41 (1968) 175.
10 C. W. Blount, D. E. Leyden, T. L. Thomas and S. M. Guill, *Anal. Chem.*, 45 (1973) 1045.

Analytica Chimica Acta, 70 (1974) 469–474

SHORT COMMUNICATION

Étude de la fixation des éléments de la première série de transition sur le dioxyde d'étain en milieu hydro–organique

N. RENAULT

Groupe de Recherche de Radiochimie Analytique, Laboratoire Pierre SUE – C.N.R.S. – C.E.N./SACLAY – B.P. no. 2, 91190 – Gif sur Yvette (FRANCE)

(Reçu le 5 novembre 1973)

Depuis quelques années, les "séparateurs minéraux"* ont vu leurs applications s'étendre en radiochimie[1,2]; le dioxyde d'étain, en particulier, a permis de réaliser une analyse systématique du fer[3].

Les mécanismes de rétention des oxydes amphotères, en milieu aqueux, ont été décrits par Amphlett[1,4]. Le dioxyde d'étain a été plus particulièrement étudié par Kraus *et al.*[5], Merz[6], Sykora et Kolarik[7], Brandone *et al.*[8], et Donaldson et Fuller[9–11].

Le mécanisme d'échange d'ions en milieu hydro–organique a fait l'objet de nombreux travaux, principalement pour les résines organiques[12,13] et a permis de mettre au point de nouvelles séparations[14].

Quelques recherches ont été menées à propos des séparateurs minéraux en milieu mixte; les zéolithes synthétiques[15–19], les gels de silice[20–22], les phosphate et tungstate stanniques[23], le phosphate de zirconium[24], l'alumine[25], le ferrocyanure de molybdène[26], les argiles[27] et le dioxyde d'étain[28]. Ces milieux doivent permettre de déterminer de nouvelles possibilités de séparations chimiques et d'étudier les mécanismes de rétention des séparateurs minéraux.

Cette étude porte sur l'influence des solvants organiques de faible constante diélectrique sur le mécanisme de rétention du dioxyde d'étain vis-à-vis des éléments de la première série de transition. Donaldson et Fuller[9] ont montré que le dioxyde d'étain adsorbe facilement des molécules d'eau par attraction ion-dipôle. Les cations seraient alors fixés sur l'oxyde hydraté par la réaction d'hydrolyse:

$$M^{n+} + H_2O \rightleftarrows MOH^{(n-1)+} + H^+ \qquad (1)$$

Ces auteurs ont remarqué que, dans les milieux aqueux faiblement acides, les coefficients de distribution des métaux de transition se classaient comme les constantes d'équilibre de la réaction d'hydrolyse[29], à savoir:

$$Cu(II) > Zn(II) > Co(II) \gg Fe(II) > Ni(II) > Mn(II)$$

Cette remarque est en accord avec le mécanisme proposé.

* Ce terme a été proposé par le Prof. Rollier lors du Colloque International du C.N.R.S. (Octobre 1972) C.E.N./SACLAY.

Nous avons fait une étude parallèle à celle de Donaldson et Fuller en étudiant la rétention des éléments [Fe(III), Cu(II), Zn(II), Co(II), Ni(II), Mn(II)] sur le dioxyde d'étain, dans des milieux contenant des solvants organiques de faible constante diélectrique; ceci nous a permis de savoir ans quelle mesure les conclusions de Donaldson et Fuller sont applicables dans ces solvants; nous avons mis au point quelques séparations chimiques possibles dans ces milieux.

Mode opératoire

Le dioxyde d'étain utilisé est un produit commercial (Carlo-Erba Italie), type cassitérite (structure tétragonale). Une analyse par diffraction-X a montré que ce produit est bien cristallisé.

Pour déterminer les rendements de fixation, nous avons employé les radio-isotopes suivants: ^{59}Fe, ^{64}Cu, ^{65}Zn, ^{60}Co, ^{65}Ni, ^{56}Mn. Tous nos essais ont été réalisés en agitant 25 ml de solution contenant l'élément étudié en présence de 500 mg d'oxyde d'étain; la concentration ionique des solutions est 1 μeq ml^{-1} pour fer(III) et 0,1 μeq ml^{-1} pour les autres. La solution contient des volumes variables de solvant organique.

Après centrifugation, la liqueur surnageante est prélevée et sa radioactivité A_x est comparée à la radioactivité initialement présente A_o, en tenant compte de la décroissance du radioisotope. Le coefficient de distribution est calculé suivant la relation:

$$K_D = \frac{(A_o - A_x)/\text{g de } SnO_2}{(A_x)/\text{ml de solution}}$$

Étude du mécanisme de rétention

Nous avons étudié l'influence de la concentration en acétone, la concentration en acide nitrique étant fixe (0.1 *M*; 0,05 *M*; 0,01 *M*). Les résultats sont présentés dans le Tableau I. Nous pouvons faire les remarques suivantes: quelle que soit la concentration en acétone, le classement des coefficients de distribution ne varie pas, il suit toujours les constantes de l'équilibre d'hydrolyse: $Fe(III) \gg Cu(II) > Zn(II) > Co(II) > Ni(II) > Mn(II)$; le mécanisme de fixation de ces ions, dans les milieux hydro–organique ne semble pas modifié par la présence du solvant.

Comme nous pouvons le prévoir après cette conclusion, pour un pourcentage donné en acétone, la fixation des éléments augmente lorsque la concentration en acide diminue: l'équilibre d'hydrolyse est déplacé:

$$M^{n+} + H_2O \rightleftarrows MOH^{(n-1)+} + H^+$$

Pour une concentration en acide donnée, l'acétone favorise la fixation des éléments; nous pouvons expliquer ce phénomène par l'abaissement de la constante diélectrique ($\varepsilon_{acetone} = 21$): les liaisons M–OH sont stabilisées et l'équilibre d'hydrolyse est déplacé favorablement.

Pour vérifier que la constante diélectrique est un paramètre influent, nous avons choisi d'étudier la fixation de ces éléments en présence de deux alcools aliphatiques; les phénomènes de solvatation seront alors similaires, seules les constantes diélectriques diffèrent: éthanol ($\varepsilon = 24$) et méthanol ($\varepsilon = 33$).

Nous pouvons alors prévoir que les ions seront plus retenus en milieu HNO_3 0,01 *M*–éthanol, de constante diélectrique plus faible.

Les résultats, présentés dans le Tableau II, confirment cette hypothèse: la constante diélectrique de la solution est un paramètre très influent pour ce mécanisme de fixation.

TABLEAU I

K_D DANS LES MILIEUX HNO_3-ACÉTONE

Ion	*v/v% Acétone*				
	0	*20*	*40*	*60*	*75*
HNO_3 0,1 M					
Fe(III)	50	66	125	230	335
Cu(II)	< 1	< 1	< 1	5	11
Zn(II)	< 1	< 1	< 1	3	11
Co(II)	< 1	< 1	< 1	2	4
Ni(II)	< 1	< 1	< 1	2	3
Mn(II)	< 1	< 1	< 1	2	3
HNO_3 0,05 M[a]					
Cu(II)	< 1	< 1	3	10	28
Zn(II)	< 1	< 1	< 1	6	19
Co(II)	< 1	< 1	< 1	4	12
Ni(II)	< 1	< 1	< 1	< 1	11
Mn(II)	< 1	< 1	< 1	< 1	5
HNO_3 0.01 M[a]					
Cu(II)	10	13	32	117	210
Zn(II)	10	11	27	55	210
Co(II)	< 1	< 1	< 1	12	28
Ni(II)	< 1	< 1	< 1	11	25
Mn(II)	< 1	< 1	< 1	8	17

[a] Fe(III) précipite partiellement dans ces milieux.

TABLEAU II

K_D DANS LES MILIEUX HNO_3 0,01 *M*-ÉTHANOL OU MÉTHANOL[a]

Ion	*v/v% Alcool*				
	0	*20*	*40*	*60*	*75*
Éthanol					
Cu(II)	10	24	44	89	188
Zn(II)	10	18	29	56	111
Co(II)	< 1	3	12	27	52
Ni(II)	< 1	1	3	11	18
Mn(II)	< 1	1	3	8	15
Méthanol					
Cu(II)	10	18	27	58	89
Zn(II)	10	14	22	35	46
Co(II)	< 1	< 1	5	12	18
Ni(II)	< 1	< 1	< 1	< 1	11
Mn(II)	< 1	< 1	< 1	< 1	5

[a] Fe(III) précipite partiellement dans ces milieux.

Pour confirmer que le mécanisme mis en évidence par Donaldson et Fuller est applicable dans les milieux HNO_3–acétone, nous avons mis en équation ce modèle; nos expériences ont porté sur la fixation de cuivre$^{(II)}$, en milieu 60% acétone, à force ionique constante.

L'équilibre de fixation s'écrit:

$$Cu^{2+}_{(sol)} + H_2O_{(SnO_2)} \rightleftarrows CuOH^{+}_{(SnO_2)} + H^{+}_{(sol)}$$

Nous pouvons appliquer la loi d'action de masse, et exprimer le coefficient de distribution K_D par

$$K = [CuOH^+]_{SnO_2}\,[H^+]_{sol}/[Cu^{2+}]_{sol}\,[H_2O]_{SnO_2}$$

et

$$K_D = [CuOH^+]_{SnO_2}/[Cu^{2+}]_{sol}$$

$$[H_2O]_{SnO_2} = q_0 - [CuOH^+]_{SnO_2}$$

où q_0 est la quantité maximale de cuivre$^{(II)}$ fixée par g de SnO_2. Dans ce cas, $[H_2O]_{SnO_2} \# q_0$. $[H^+]_{sol} \# c$ où c est la concentration initiale en HNO_3, acide fort dans ces milieux. La loi d'action de masse s'écrit: $K = K_D\,c/q_0$. L'expression logarithmique devient:

$$\log K_D = \log K + \log q_0 - \log c$$

Nous avons tracé la courbe $\log K_D = f(\log c)$. Nous obtenons une droite de pente -1, ce qui montre que la fixation suit bien le mécanisme proposé.

Séparations chimiques

Sur la colonne (7 mm de diamètre) contenant 2 g de dioxyde d'étain, nous versons au préalable 5 ml de solution S_1 de lavage de même composition que la solution S_2 contenant l'élément marqué (0,1 μ eq ml^{-1}). Le débit est de 1 ml min^{-1}. 5 ml de S_2 sont versés sur la colonne, puis celle-ci est lavée par S_1. Des fractions éluées de 5 ml sont recueillies et leur radioactivité $(A_x)_n$ est comparée à la radioactivité totale initiale A_0; le pourcentage R_n élué dans chaque fraction est calculé par la relation: $R_n = (A_x)_n/A_0$

La Figure 1 montre qu'en milieu HNO_3 0,1 M–40% acétone, fer$^{(III)}$ peut être séparé de Cu$^{(II)}$, Zn$^{(II)}$, Co$^{(II)}$, Ni$^{(II)}$ et Mn$^{(II)}$, à température ambiante. Il est à noter que Girardi *et al.*[2] proposait cette séparation sur SnO_2, en milieu HNO_3 0,1 M, à 60°C. La présence du solvant organique permet ici de faciliter la mise en oeuvre de la séparation. Le fer*(III)* ne peut être élué qu'en milieu réducteur, le SnO_2 étant alors détérioré.

En milieu HNO_3 0,01 M–50% acétone, le manganèse est élué alors que le cuivre reste fixé, comme le montre la Fig. 2. Le cuivre est élué rapidement en milieu HNO_3 0,1 M–40% acétone ($K_D < 1$); l'équilibre de fixation de Cu$^{(II)}$ peut être déplacé facilement en variant les concentrations en HNO_3 et en acétone.

Conclusion

Nous avons pu montrer que le mécanisme de rétention du SnO_2 pour les éléments de la première série de transition est le même en milieu aqueux et hydro-organique: les éléments bivalents sont fixés suivant l'équilibre d'hydrolyse (équilibre

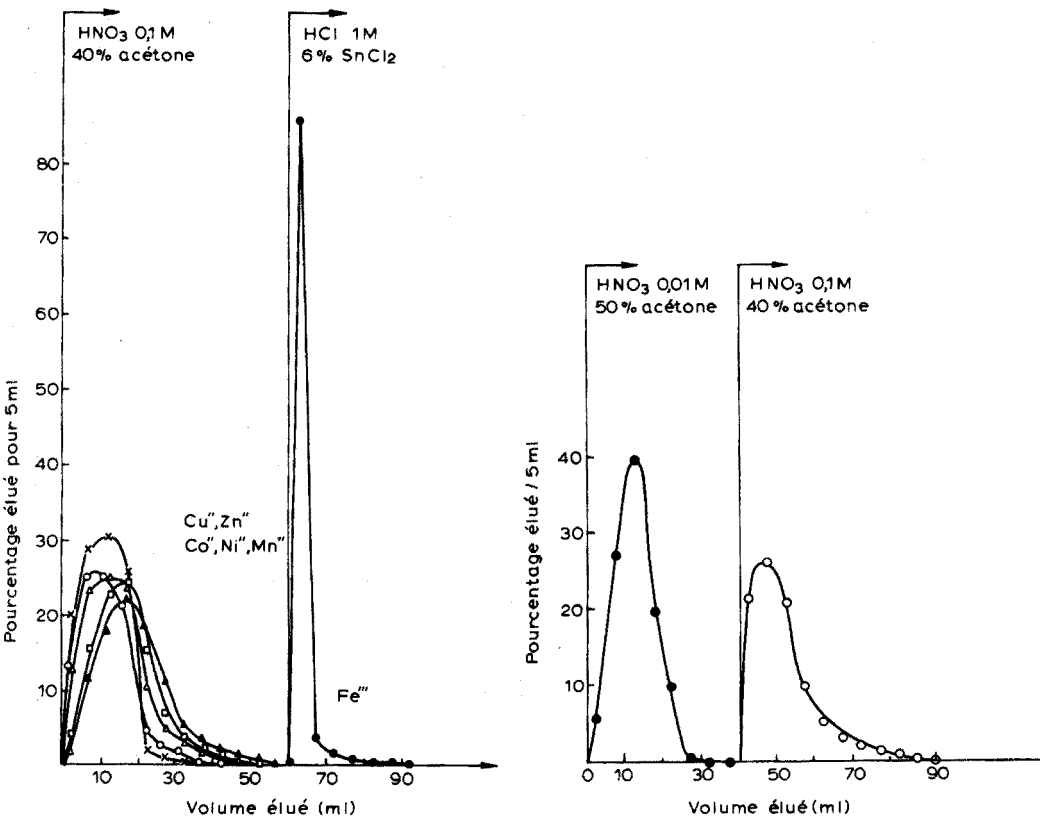

Fig. 1. Séparation Fe (●)/Cu (▲), Zn (□), Co (△), Ni (×), Mn (○).

Fig. 2. Séparation Mn (●)/Cu (○).

1). Le fer(III) semble être fixé plus fortement à la surface du dioxyde d'étain. La présence du solvant abaisse la constante diélectrique de la solution, ce qui favorise la fixation de ces cations en déplaçant l'équilibre d'hydrolyse.

Nous avons mis au point la séparation de Fe(III) des éléments Cu(II), Zn(II), Co(II), Ni(II), Mn(II), en milieu HNO_3 0.1 *M*–40% acétone; dans ce milieu cette séparation s'effectue à température ambiante. Le schéma d'analyse systématique du fer proposé par Cleyrergue[30] utilise la séparation Fe(III)/Cu(II), Zn(II), Co(II), Ni(II), Mn(II) proposée par Girardi *et al.*[2]; l'élévation de température rend difficile l'automatisation de la séparation, aussi le milieu que nous proposons permettra-t-il de nous affranchir de cet inconvénient.

BIBLIOGRAPHIE

1 C. B. Amphlett, *Inorganic Ion-Exchangers*, Elsevier, Amsterdam, 1964.
2 F. Girardi, R. Pietra and E. Sabbioni, *J. Radioanal. Chem.*, 5 (1970) 141.
3 Ch. Cleyrergue and N. Deschamps, Colloque International du C.N.R.S. sur l'Analyse par Activation, Saclay, France, 2–6 Octobre 1972.
4 C. B. Amphlett, *J. Inorg. Nucl. Chem.*, 6 (1958) 236.

5 K. A. Kraus, H. O. Philips, T. A. Careson and J. S. Johnson, *Proc. Int. Conf. Peaceful Uses At. Energy*, 2nd., 28 (1958) 3.
6 E. Merz, *Z. Elektrochem.*, 63 (1959) 288.
7 S. Sykora and Z. Kolarik, *Collect. Czech. Chem. Commun.*, 29 (1964) 1350.
8 A. Brandone, S. Meloni, F. Girardi and E. Sabbioni, *Analysis*, 2 (1973) 300.
9 J. D. Donaldson and M. J. Fuller, *J. Inorg. Nucl. Chem.*, 30 (1968) 1083.
10 J. D. Donaldson, M. J. Fuller and J. W. Price, *J. Inorg. Nucl. Chem.*, 30 (1968) 2841.
11 J. D. Donaldson and M. J. Fuller, *J. Inorg. Nucl. Chem.*, 32 (1970) 1703.
12 B. Tremillon, *Les Séparations par les Résines Échangeuses d'Ions*, Gauthier-Villars, Paris, 1965.
13 N. Renault, N. Deschamps and I. N. Bourrelly, *Anal. Chim. Acta*, 64 (1973) 19.
14 J. Korkisch, *Progress in Nuclear Energy*, Series IX, Analytical Chemistry, Vol. 6, Pergamon Press, Oxford, 1969.
15 P. C. Huang, A. Mizany and J. L. Pauley, *J. Phys. Chem.*, 68 (1964) 2575.
16 R. B. Barret and J. A. Marinsky, *J. Phys. Chem.*, 75 (1971) 85.
17 V. M. Radak, *J. Inorg. Nucl. Chem.*, 34 (1972) 1059.
18 Z. Dizdar, *J. Inorg. Nucl. Chem.*, 34 (1972) 1069.
19 Z. Dizdar and P. Popovic, *J. Inorg. Nucl. Chem.*, 34 (1972) 2633.
20 R. Maatman, A. Greertsema, H. Verhage, G. Baas and M. Du Mez, *J. Phys. Chem.*, 72 (1968) 97.
21 R. Caletka, *Radiochem. Radioanal. Lett.*, 2 (1969) 139.
22 R. Caletka, *Collect. Czech. Chem. Commun.*, 37 (1972) 1494.
23 M. Qureshi, I. Akhtar and K. N. Mathur, *Anal. Chem.*, (1967) 1766.
24 S. A. Marei, H. F. Aly and N. Zakareia, *Fresenius Z. Anal. Chem.*, 258 (1972) 282.
25 D. S. Gaibakyan and R. T. Egikyan, *Arm. Khim. Zh.*, 25 (1972) 394.
26 S. H. Kawamura and K. Kurotaki, *J. Chromatog.*, 45 (1969) 331.
27 A. K. Nag and A. Chatterjee, *J. Indian Chem. Soc.*, 49 (1972) 687.
28 N. Renault and N. Deschamps, *Radioanal. Radiochem. Lett.*, 13 (1973) 207.
29 L. G. Sillen et A. E. Mantell, *Stability Constants*, Special Publication no 17, 1964, p. 39.
30 Ch. Cleyrergue, Thèse, Paris, 1973.

Analytica Chimica Acta, 70 (1974) 475–477

SHORT COMMUNICATION

Behaviour of a carboxylic acid exchanger in the presence of 1,10-phenanthroline

S. GANAPATHY IYER, P. K. PADMANABHAN and CH. VENKATESWARLU
Analytical Chemistry Division, Bhabha Atomic Research Centre, Trombay, Bombay 400 085 (India)
(Received 1st September 1973)

Weak ion exchangers (cationic as well as anionic) are used much more rarely than the strong ones, as they function (mostly in their salt forms) only in a limited range of acidity. The uptake of bases like 1,10-phenanthroline (phen)[1,2] as well as the iron(II)–phenanthroline complex cation[3] by ion exchangers has been investigated only with strong sulphonic acid exchangers. This communication describes preliminary results on the uptake of phen by a carboxylic-acid exchanger (Zeo-karb 226) and its behaviour thereafter towards metal ions.

Experimental

Preliminary experiments indicated the retention of phen and its iron(II) complex on a column of Zeo-karb 226 (H^+ form). Hence the K_d of phen was studied in the absence and presence of iron(II) in the pH range 1.0–6.0 by the batch method, *i.e.* by equilibrating (continuously shaking for 2 h) a known quantity (0.25 g) of exchanger with a known volume of aqueous phase containing phen in the presence and absence of iron(II) at the desired pH (Table I). For comparison, the K_d values of some inorganic cations of different valencies at pH 1.0 and 4.0 were also studied.

Discussion

Carboxylic acid exchangers start functioning only around pH 4.0, exhibiting their maximal capacity above pH 7.0 (ref. 4). Inorganic cations of different valencies did, in fact, exchange against H^+ at pH 4.0, whereas at pH 1.0, only thorium(IV) exchanged to any extent (Table I). However, phen was taken up, at pH 1.0, to a greater extent (expt. 9) than thorium(IV); at pH 4.0 the take-up of phen increased to equal (expt. 10) that of lanthanum(III) when the exchanger was in the H^+ form. When the exchanger was in the NH_4^+ form, phen was not taken up at all from aqueous solution below pH 7. Accordingly, it seems more correct to attribute the uptake of phen to the affinity of its basic nitrogen for the proton in the exchanger, rather than to its distribution as a weak electrolyte or non-electrolyte[5].

The uptake of phen increased with pH (expts. 9, 10 and 15–18). However, the maximum phen taken up around pH 7.0 by the exchanger in the H^+ form (on saturation) was found to be only 0.3 mole per mole of exchanger.

TABLE I

K_d VALUES OF PHEN AND INORGANIC CATIONS ON ZEO-KARB 226 IN H^+ FORM[a]

Expt. no.	*Cation taken (mg)*	*pH*	K_d *of cation*	*Expt. no.*	*Phen taken (mg)*	*pH*	$K_d(phen)_{total}$
1	Na^+ (1.0)	1.0	nil	9	1.0	1.0	34
2	Na^+ (1.0)	4.0	5	10	1.0	4.0	300
3	Ca^{2+} (1.0)	1.0	nil	11	68.0	1.0	12
4	Ca^{2+} (1.0)	4.0	17	12	68.0	2.0	12
5	La^{3+} (1.0)	1.0	nil	13	68.0	4.0	123
6	La^{3+} (1.0)	4.0	312	14	68.0	6.0	738
7	Th^{4+} (1.0)	1.0	5	15[b]	68.0	1.0	43
8	Th^{4+} (1.0)	4.0	1900	16[b]	68.0	2.0	46
				17[b]	68.0	4.0	104
				18[b]	68.0	6.0	323
				19[b]	22.6	1.0	93
				20[b]	22.6	2.0	116
				21[b]	22.6	4.0	508
				22[b]	22.6	6.0	10,000

[a] K_d = [(mg phen/g resin)/(mg phen/ml solution)].

[b] In expts. 15–22, 5 mg of iron(II) was used. For expts. 15–18, $[phen] > 3 \cdot c_{Fe^{2+}}$ and for 19–22, $[phen] < 3 \cdot C_{Fe^{2+}}$.

[c] In expts. 1–10, the volume of the aqueous phase was 25 ml; in expts. 11–22, the volume was 100 ml.

At pH 1.0 and 2.0 there was no exchange of iron(II) with the exchanger, but there was significant exchange when phen was present in solution with iron(II), as can be seen from the increased K_d in expts. 15 and 16 compared to expts. 11 and 12. At pH values of 4.0 and 6.0, the K_d value of phen decreased in the presence of iron(II) (*cf.* expts. 17 and 18 with expts. 13 and 14); this is partly due to the reduced basicity of nitrogen after complexation. When the concentration of phen was less than three times that of iron(II) (expts. 19–22), the increase in K_d values showed that the iron(II) complex also exchanged more readily as the pH was raised. It may be mentioned that when an aqueous solution of tris(1,10-phenanthroline)-iron(II) chloride was passed through a column of RCOOH, two equivalents each of chloride and hydrogen ion per mole of complex were found in the effluent, which contained no phen. This indicates the exchange of $Fe(phen)_3^{2+}$. It may be mentioned that the adsorption of iron(II)–1,10-phenanthroline on filter papers[6], alumina[7–9] and other materials[10–13] has been reported.

In another set of experiments, the carboxylic acid exchanger was taken in two small columns, treated with 200 ml of 0.25% phen solution at pH 1.0 and 2.0, washed with water and air-dried. Then 0.25-g portions of the treated exchanger were equilibrated separately with iron(II), nickel and copper(II) ions at pH 1.0 and 2.0. The K_d values were 11, 11 and 8 at pH 1.0, and 108, 135 and 122 at pH 2.0 for the three metal ions, respectively; there was no exchange of these ions at these pH values by the untreated exchanger. It may be added that sorption of iron(II) was observed on a column of the exchanger which had been previously treated with phen at the same pH and washed.

It is evident from the above that the carboxylic acid exchanger in the H^+

form exchanges those metal ions which form complexes with phen, when the chelating ligand is present in solution or on the exchanger, in a similar manner to the Dowex chelating resin A-1 [14], the difference being that phen is not rigidly fixed on the resin like the iminodiacetic acid group on the chelating resin. It may be expected that weak cation exchangers will take up other organic reagents containing basic nitrogen and thereafter behave as chelating resins. Work is in progress with other types of compounds containing a basic nitrogen.

It is a pleasant duty of the authors to thank Dr. M. Sankar Das, Head, Analytical Chemistry Division, for his interest in the work.

REFERENCES

1 L. N. Tokareva, G. D. Galpern, A. V. Kotova, T. E. Kosonkhova and A. Ya. Lanchuk, *Zh. Prikl. Khim. (Leningrad)*, 43 (1970) 403.
2 V. Talašek and J. Eliasek, *Collect. Czech. Chem. Commun.*, 33 (1968) 3618.
3 A. Rusi and S. Ionescu, *Stud. Cercet. Fiz.*, 14 (1963) 127.
4 O. Samuelson, *Ion exchange separations in Analytical Chemistry*, Wiley, New York, 1963, p. 37.
5 O. Samuelson, *Ion exchange separations in Analytical Chemistry*, Wiley, New York, 1963, pp. 49 and 138.
6 E. Asmus, *Z. Anal. Chem.*, 122 (1941) 81.
7 L. H. Klemm, C. E. Klopfenstein and P. K. Heather, *J. Chromatogr.*, 23 (1966) 428.
8 L. R. Snyder, *J. Chromatogr.*, 17 (1965) 73.
9 Y. Nishimoto and S. Toyoshima, *Yakugaku Zasshi*, 85 (1965) 317.
10 H. Bartels and H. Erlenmeyer, *Helv. Chim. Acta*, 47 (1964) 1285; 48 (1965) 285, 301.
11 F. Vydra and V. Markhova, *Talanta*, 9 (1962) 449; 10 (1963) 339, 711.
12 C. A. Bower, *Soil Sci.*, 95 (1963) 192.
13 A. Jensen, F. Basolo and H. M. Neumann, *J. Amer. Chem. Soc.*, 81 (1959) 509, 512.
14 O. Samuelson, *Ion exchange separations in Analytical Chemistry*, Wiley, New York, 1963, p. 87.

Analytica Chimica Acta, 70 (1974) 478–481

SHORT COMMUNICATION

The determination of organic halogenomercury compounds by titration of halide

M. OLOMUCKI and G. ROURE
Laboratoire de Biochimie Cellulaire, Collège de France, 75231 Paris Cedex 05 (France)
(Received 30th October 1973)

A rapid and precise titrimetric method for the determination of organic halogenomercury derivatives is described. The compound to be analyzed is first treated with a thiol; the halogen, in a purely ionic form, and the organic derivative (containing the interfering mercury atom) thus formed can then be separated by partition between water and an organic solvent; the halide can be conveniently determined in the aqueous phase by Volhard titration.

Many aromatic and aliphatic halogenomercury derivatives were successfully analyzed by this method, which proved to be quite general.

Experimental

Halogenomercury derivatives. The alkyl mercury(II) bromides were prepared and converted to the corresponding chlorides and iodides as described by Slotta and Jacobi[1]. Phenylmercury(II) chloride (Aldrich) was recrystallized from benzene. The corresponding bromo and iodo derivatives were obtained by treating the chloride with hot methanolic 40% potassium hydroxide solution, filtering and adding hydrobromic or hydroiodic acid, respectively. The 2-chloro- and 2-bromomercuriphenols were prepared either as described by Whitmore and Hanson[2] or by Kaplan and Mellick[3], 4-Chloromercurianiline was obtained by the method of Dimroth[4]. 4-Chloromercuribenzoic acid (Nutritional Biochemical Co.) was purified three times by the procedure of Boyer[5]. 2-Chloromercuri-4-nitrophenol was prepared as described by McMurray and Trentham[6]. Halogenoesters of 2-halogenomercuriphenols are new compounds, the synthesis of which will be described elsewhere.

Solvents. In most cases, ethyl acetate was found to be a good solvent for dissolution of the sample and for the reaction. For *p*-chloromercuribenzoate, insoluble in ethyl acetate, ether containing 20% dimethylformamide was used.

Choice of mercaptan. Benzyl mercaptan was used in the first assays. It was later replaced, with equally good results, by octanethiol, another non-volatile hydrophobic mercaptan of less unpleasant smell.

Procedure. Weigh accurately a sample of *ca.* 0.5 mmole of the organomercurial and dissolve in 15 ml of ethyl acetate. Add 5 ml of a solution containing *ca.* 0.8 mmole of thiol in ethyl acetate followed, in some cases, (see *Results and discussion*) by 0.8 ml of alcoholic 1 *M* sodium hydroxide. Stir for

about 15 min, and then extract four times with separate 5-ml portions of distilled water*. Wash the water extracts with 5 ml of ethyl acetate and titrate the halide ions in the aqueous phase with standard 0.1 *M* solutions of silver nitrate and potassium thiocyanate.

Isolation of the organomercury derivatives formed. This was attempted in the case of the reaction of n-heptylmercury(II) bromide with n-octanethiol, chosen arbitrarily as an example. One equivalent of sodium hydroxide in alcoholic solution was added to a solution of 0.65 g (4.45 mmole) of octanethiol in 20 ml of ethyl acetate and this mixture was poured into a solution of 1 g (2.6 mmole) of n-heptylmercury(II) bromide in 50 ml of ethyl acetate. After 15 min, the solution was washed with water and the organic layer was evaporated. The residual oil, when treated with acetone, gave a white solid. [M.p. 72°C. N.m.r. in $CDCl_3$: δ (p.p.m.) 0.85, triplet, 6 H; 1.4, multiplet, 24 H; 3, triplet, 4 H. Found: 39.1%C, 7.2%H, 41.0% Hg, 13.2% S; $C_{16}H_{34}HgS_2$ requires: 39.1% C, 6.97% H, 40.84% Hg, 13.5% S. The yield was 0.3 g (25%).]

The mother liquor after evaporation of acetone yielded an oily uncrystallizable product. Its n.m.r. spectrum indicated *inter alia* the existence of two different methylene groups at δ 1.75 (CH_2–Hg?) and 3 (CH_2–S). When the oil was dissolved in ethyl acetate and re-treated at room temperature with octanethiol in the presence of alcoholic sodium hydroxide, the same white solid was obtained (m.p. and mixed m.p. 72°C).

The same product formed when *p*-chloromercurianiline was reacted with octanethiol.

Results and discussion

The compounds tested and the percentage recoveries for the halogens are listed in Table I.

Under the experimental conditions described, the reaction between mercaptans and halogenomercurials requires, in the case of aliphatic derivatives, the presence of sodium hydroxide; in the absence of base, much lower results were obtained. However, for aromatic derivatives, the addition of sodium hydroxide is unnecessary.

No interference was observed when the halogenomercurials contained another halogen atom in a haloalkyl group. The latter was not attacked by the thiol under the experimental conditions, and the second halogen could be detected only after prolonged refluxing.

The convenient and rapid Volhard titration of halides cannot be performed in the presence of mercury derivatives. However, when halogenomercury organic compounds are treated with hydrophobic mercaptans, the ionic halide and the mercury-containing organic derivative thus formed can be separated by extraction with water, rendering possible the titration of the halide in an aqueous phase.

In attempts to identify the organomercury compound formed in the reaction,

* The addition of water sometimes causes the precipitation of a solid which generally does not affect the extractions. In one case (analysis of *p*-chloromercuribenzoate) the abundant precipitate was filtered off and washed with water.

TABLE 1

TITRATION OF HALOGENS IN RHgX

R	*X*	*Halogen found (%)*	*R*	*X*	*Halogen found (%)*
$n\text{-}C_4H_9-$	Cl	99	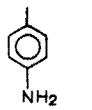	Cl	100
$n\text{-}C_4H_9-$	Br	100			
$n\text{-}C_4H_9-$	I	98			
$n\text{-}C_7H_{15}-$	Cl	100			
$n\text{-}C_7H_{15}-$	Br	100			
$n\text{-}C_7H_{15}-$	I	100	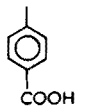	Cl	96
C_6H_5-	Cl	98			
C_6H_5-	Br	100			
C_6H_5-	I	99			
	Cl	98	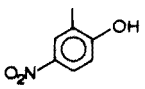	Cl	100
	Br	98	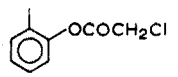	Cl	100
	Br	98	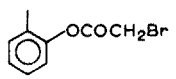	Cl	100
			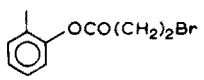	Cl	100

the only derivative which could be isolated in a pure form was bis(n-octylthio)mercury, $(n\text{-}C_8H_{17}S)_2Hg$. Compounds of this type, resulting from the reaction of mercaptans with halogenomercury derivatives, are known (see e.g. ref. 7).

The product which would normally be expected from the reaction of a thiol with an organic halogenomercury derivative

$$RHgX + R'SH \rightarrow RHg\text{–}SR' + HX$$

could not be obtained in a pure form. It seems, however, that the uncrystallizable oil which was obtained in the reaction of n-heptylmercury(II) bromide with octanethiol could correspond to more or less pure heptylmercurithiooctane as suggested by its n.m.r. spectrum and by its easy conversion to bis(n-octylthio)mercury after treatment with octanethiol.

The authors thank the Délégation Générale à la Recherche Scientifique et Technique (contract No 72.7.0736) and the Centre National de la Recherche Scientifique for their support. The collaboration of Mr. G. Bourges in the early stages of this work and the help of Mrs. H. Chwastek and Mr. J. Y. Le Gall in the preparation of the compounds tested is gratefully acknowledged.

REFERENCES

1 K. H. Slötta and K. R. Jacobi, *J. Prakt. Chem.*, 120 (1929) 249.
2 F. C. Whitmore and E. R. Hanson, *Org. Syn. Coll.*, 1 (1956) 161.
3 J. F. Kaplan and C. Mellick, *U.S. Patent 2,502, 382* (1950); *Chem. Abstr.*, 44 (1950) 5907.
4 O. Dimroth, *Ber. Deut. Chem. Ges.*, 35 (1902) 2032.
5 P. D. Boyer, *J. Amer. Chem. Soc.*, 76 (1954) 4331.
6 C. H. McMurray and D. R. Trentham, *Biochem. J.*, 115 (1969) 913.
7 S. Akerfeld, *Acta Chem. Scand.*, 13 (1959) 627.

Analytica Chimica Acta, 70 (1974) 482–484

SHORT COMMUNICATION

Microdetermination of manganese in airborne particulate samples by means of the ring-oven technique

MILTON MCDANIEL and PHILIP W. WEST

Environmental Sciences Institute, Coates Chemical Laboratories, Louisiana State University, Baton Rouge, La. 70803 (U.S.A.)

(Received 25th November 1973)

Manganese is one of the elements essential to the body. Inhalation of manganese, however, may induce manganic pneumonia or chronic manganese poisoning, a disease of the central nervous system[1]. Chronic poisoning is disabling and manganic pneumonia often results in death. Manganese may also be involved in catalytic oxidation[2,3] of other air pollutants to more undesirable compounds.

From the standpoint of air pollution, the oxides of manganese are the most important, particularly manganese dioxide[1]. Almost all of the manganese in the atmosphere enters as oxides, such as MnO, MnO_2, Mn_2O_3, or Mn_3O_4. Although these species may react with other pollutants to form water-soluble compounds, oxides are the predominant form.

Methods which have been applied to the determination of manganese in air pollution studies are atomic absorption[4–6], emission spectroscopy[5,7], flame photometry[7], neutron activation[8,9], laser techniques[10,11], and colorimetry[12]. Equipment requirements and sample preparation prohibit these methods from being useful to any degree outside the laboratory. For field studies, it is necessary to have a method which is rapid, sensitive, reliable and inexpensive. This has been accomplished by use of the ring-oven.

A semi-quantitative determination of manganese, using a combination of paper chromatography and the ring-oven, was reported by Ghose and Dey[13]. They isolated manganese by paper chromatography, precipitated it as $Mn(OH)_2$, air-oxidized it to $MnO_2 \cdot H_2O$, and subsequently reacted it with benzidine to give a blue product. The isolation step was very time-consuming, requiring about 7 h. The silver universal standard scale was used by Weisz *et al.*[14], to determine manganese, after converting it to $MnO_2 \cdot H_2O$. Neither of these methods is completely quantitative nor free of interferences. The method described below is quantitative and requires no prior separations.

Feigl was the first to report the use of benzidine as a spot test reagent for manganese[15]. The test was based on oxidation of the benzidine base or hydrochloride to benzidine blue with $MnO_2 \cdot H_2O$ in neutral solution. Ions which have two or more oxidation states, such as chromium, gold, copper and cobalt, would be potential interferences and should be made innocuous by complexation with suitable masking agents.

Experimental

Benzidine solution. Dissolve 0.05 g of benzidine base or its hydrochloride in 10 ml of glacial acetic acid, dilute to 100 ml with water and filter. The solution is stable for several weeks.

Apparatus and supplies. Ring-oven (trace-oven; Arthur H. Thomas Co., Philadelphia, Pa.); surface thermometer (Pacific Transducer Corp. model 311F); Whatman 41 filter paper; hair dryer; capillary tubes; micropipettes.

Sampling. Samples are collected from 0.5 to 2.0 m^3 of air, depending upon the dust level, using a sequential tape sampler. Sequential tape samplers of either 1-in. or 1.5-in. dust spots can be accommodated for the determination of manganese, with the ring-oven used.

Determination. The determinations can be performed directly on the sample spot on the collecting tape itself. Place the tape on a ring-oven maintained at 95–100°C, centering the dust spot exactly over the annular opening. Add 15 μl of hydrogen peroxide solution (2% w/v) in 2 *M* hydrochloric acid. Dry the paper *in situ*, then add another 15-μl portion of the hydrogen peroxide solution and wash to the ring zone with distilled water. Again dry the paper *in situ* and add 15 μl of ammonium acetate solution (15% w/v). Wash to the ring zone with water. Add 15 μl of sodium cyanide solution (0.5% w/v), wash to the ring zone with water and dry. Add enough 2 *M* hydrochloric acid to diffuse to the ring zone and dry the paper. Remove the paper from the ring oven, spray with 0.1 *M* sodium hydroxide and dry in a cool air current. Add the benzidine reagent to the ring zone; a blue color develops in 1–2 min. This color is stable for 5 min, but gradually fades. After 12 h, only 50% of the initial intensity remains; therefore, a set of permanent standards is mandatory. By using colored crayons, permanent standard rings can be made which give the same intensity as a known amount of manganese. To qualify as a standard, the intensity of the crayon ring must match that of three separate rings, each containing the same amount of manganese. The standard rings should range from 0.1 to 1.0 μg of manganese.

Analysis of the unknown. The usual methods of sampling are employed. The tape sampler is preferred because the test can be run on the tape itself. Acid-washed paper is used to insure reproducible results.

The orifice of the sampling device should be sufficiently small to ensure that the diameter of the dust spot is less than the inner diameter of the ring-oven orifice. This enables proper treatment of the sample *in situ*, with adequate washing to the ring zone.

Results and discussion

Selection of paper. Whatman 41 was used because of its purity and diffusion properties. Whatman 41 dust tapes are available and can be used on sequential tape samplers.

Interferences. Ammonium acetate is used to fix iron as the basic acetate, and to mask chromium and eliminate its interference. Sodium cyanide complexes the cobalt and copper. Silver or thallium is precipitated by hydrochloric acid.

The effect of interfering ions was investigated by preparing two rings for each ion. The first ring contained 20 μg of potential interfering ion, and the second 0.1 μg of manganese in the presence of 20 μg of potential interfering ion. The ion was

established as non-interfering, when the first ring was identical to the blank and the second identical to a ring containing 0.1 μg of manganese.

The following ions did not interfere at 20-μg levels:

Group I Li^+, K^+, Rb^+, Cs^+, Ag^+, Cu^{2+}, Au^{3+}
Group II Be^{2+}, Mg^{2+}, Ca^{2+}, Sr^{2+}, Ba^{2+}, Zn^{2+}, Hg^{2+}, Cd^{2+}
Group III BO_2^-, $B_4O_7^{2-}$, Al^{3+}, Ga^{3+}, Ce^{3+}
Group IV CO_2^{2-}, SiO_3^{2-}, Zr^{4+}, Sn^{2+}, Sn^{4+}, Pb^{2+}, Th^{4+}
Group V NO_2^-, NO_3^-, HPO_4^{2-}, VO_2^+, VO_3^-, $HAsO_3^{2-}$, $HAsO_4^{2-}$, Sb^{3+}, Sb^{5+}, Bi^{3+}
Group VI S^{2-}, SO_3^{2-}, $S_2O_3^{2-}$, SO_4^{2-}, SeO_4^{2-}, TeO_3^{2-}, TeO_4^{2-}, Cr^{3+}, CrO_4^{2-}, $Cr_2O_7^{2-}$, MoO_4^{2-}, WO_4^{2-}, UO_2^{2+}
Group VII F^-, ClO_3^-, ClO_4^-, Br^-, BrO_3^-, I^-, IO_3^-, SCN^-
Group VIII Fe^{3+}, Co^{2+}, Ni^{2+}

This work was supported in part by the National Science Foundation RANN Program Grant GP-35114X.

REFERENCES

1 H. E. Stockinger, in F. A. Patty (Ed.), *Industrial Hygiene and Toxicology*, Vol. II, Interscience, New York, 2nd edn., 1963, p. 1082.
2 J. M. Bracewell and D. Gall, *Proc. Symp. Physico-Chem. Transformation of Sulfur Compounds in Atmosphere and Formation of Acid Smogs*, Mainz, Germany, June 8–9, 1967.
3 K. C. Stein, J. J. Freeman, G. P. Thompson, J. F. Shultz, L. J. E. Hofer and R. S. Anderson, *Ind. Eng. Chem.*, 52 (1960) 671.
4 J. Y. Hwang and F. J. Feldman, *Appl. Spectrosc.*, 24 (1970) 371.
5 R. J. Thompson, G. B. Morgan and L. J. Purdue, *Analytical Instrument*, 7 (1969) 9.
6 S. Schadev, J. W. Robinson and P. W. West, *Anal. Chim. Acta*, 38 (1967) 499.
7 E. D. Prudnikov, *Zh. Prikl. Spektrosk.*, 14 (1971) 145.
8 H. Izhar and M. N. Cheema, *J. Radioanal. Chem.*, 5 (1970) 223.
9 K. K. Pillay, T. Sivasankara, C. Carlisle, Jr. and C. M. Hyche, *Nuclear Technology*, 10 (1971) 225.
10 H. Schreth, *Fresenius Z. Anal. Chem.*, 253 (1971) 7.
11 T. Yamane, S. Szuki and S. Matsushita, *Bunko Kenkyre*, 19 (1970) 147.
12 D. Suwalska and E. Balcerek, *Med. Pracy*, 21 (1970) 524.
13 A. K. Ghose and A. K. Dey, *Indian J. Appl. Chem.*, 31 (1968) 195.
14 H. Weisz, M. B. Celap and V. V. Almazan, *Mikrochim. Acta*, (1959) 36.
15 F. Feigl, *Chem. Ztg.*, 44 (1920) 689.

Analytica Chimica Acta, 70 (1974) 485–488

SHORT COMMUNICATION

Pneumatic voltammetry with a flow-through cell

J. TENYGL and D. G. LOVERING*

J. Heyrovský Institute for Physical Chemistry and Electrochemistry, Czechoslovak Academy of Sciences, Prague 110 00 (Czechoslovakia)

(Received 27th September 1973)

The principles of pneumatic voltammetry** have been fully elaborated elsewhere[1]. The method is based on monitoring the pressures of the gases evolved during constant-current electrolysis, against a separate reference electrolytic cell, the gaseous sections of the two cells being connected as a pneumatic equivalent of a Wheatstone bridge. Pressure changes resulting from electroactive depolarizer(s) in the test cell can be related to the depolarizer concentration. In the present communication, a new flow-through electrolytic cell, coupled to a sensitive electrical pressure transducer, is reported; this has permitted single-cell operation without the need for the complexities of a gas-phase bridge and reference cell. Thus, the equipment is suitable for automated continuous analysis, for example, in C.O.D. (chemical oxygen demand) determinations.

Essential features of "pneumatic" electrochemical analysis

Figure 1 illustrates the main features of the polarization curves, in the presence and absence of depolarizer, relevant to cell operation in the pneumatic mode. Curve 1 defines the limiting electrode processes for a supporting electrolyte at inert electrodes. Oxygen and hydrogen are evolved at the rates (V_{O_2}) s^{-1} and (V_{H_2}) s^{-1}, respectively. These rates will depend, at equilibrium, on the magnitude of the constant current applied, or under potentiostatic conditions, on the value of the chosen potential. If an electroactive species is introduced into the test cell (*e.g.* in Fig. 1 an electro-oxidizable solute), then the Faradaic efficiency with respect to gas evolution will diminish and the rate of gas evolution (oxygen, in this case) will fall to a new value (V'_{O_2}) s^{-1}, as shown by curve 2. The diminution in the oxygen evolution rate $(V_{O_2} - V'_{O_2})$ is measurable and can be directly related to the concentration of the oxidizable component by monitoring the difference in pressure between the test cell and the reference cell (or the ambient pressure in the case of the new design). In the original configuration[1], the

* Present address: Chemistry and Metallurgy Department, Royal Military College of Science, Shrivenham, Swindon, Wiltshire, England.

** "Pneumatic polarography" was coined in ref. 1. Although "pneumatic coulometry" would be appropriate in the present case, the term chosen now does not exclude the possibility for potentiostatic control.

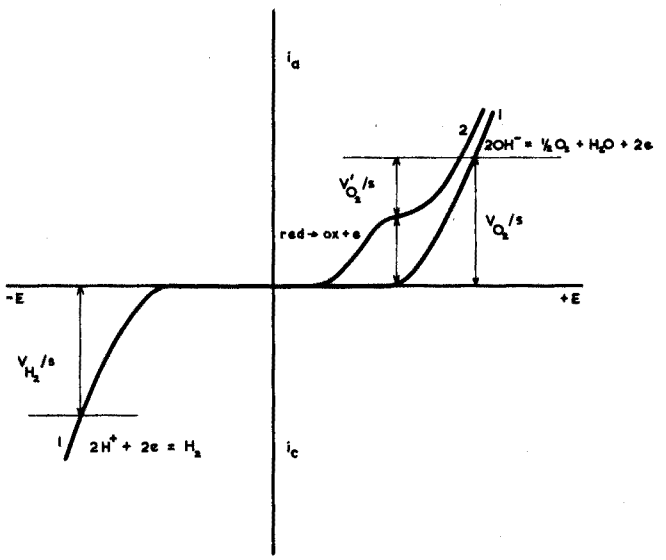

Fig. 1. Limiting electrode processes and the principles of the pneumatic polarographic method.

electrolysis was carried out under constant current, in a stirred cell with separate anode and cathode compartments, but alternative modes and designs are equally feasible. Similarly, reducible solutes are just as amenable to analysis by the pneumatic method simply by monitoring the rate of hydrogen evolution. Some of the advantages of the pneumatic mode include: (i) continuous cleaning of the electrode surfaces on an atomic scale and from within the double layer; and (ii) separate or simultaneous determination of species which are electroactive at very positive or very negative potentials.

The operating current density is selected so that the gas evolution rate does not fall to zero at the highest expected concentration of depolarizer to be determined. The gas evolution rate is determined by the pressure difference recorded in the absence and presence of the depolarizer; the range of working pressures is adjusted by venting a controlled portion of the liberated gases through a capillary of known dimensions.

Description of equipment

The equipment is shown diagrammatically in Fig. 2. The sample solution is metered at a constant rate (2–4 ml min^{-1}) by a Technicon Instruments proportioning pump(8) into the working electrode compartment of the electrolysis cell(7). The supporting electrolyte is simultaneously metered to the reference compartment at a lower rate (0.3–0.5 ml min^{-1}). Both solutions flow on parallel paths through the cell and pass to the gas–liquid separator (5). At the separator, the solution is pumped to waste at a rate about 5% greater than the combined rate of the liquids supplied to the cell. A constant proportion of the electrolytically generated gas is carried to waste with the spent solution; this is necessary to prevent liquid entering the measuring section and is compensated by initial calibration. The main gas flow is vented to the atmosphere via a capillary(4)

(thermometer tubing of 0.4–0.6 mm bore and 20 cm length) and tube(3). A constant fraction of the gas pressure in the system is thus continuously monitored with a pressure transducer(2) (Computer Instruments Corporation Model 6000; 0.1–0.5 p.s.i.; 0.07–0.35 atm). A small voltage of 1–10 mV is applied to the 10 Kohm track of the transducer operated in the gauge mode and the output is monitored with an EZ3 Laboratni Pristroje chart recorder(1). The magnitude of the pressure can be visually assessed from the manometer(6).

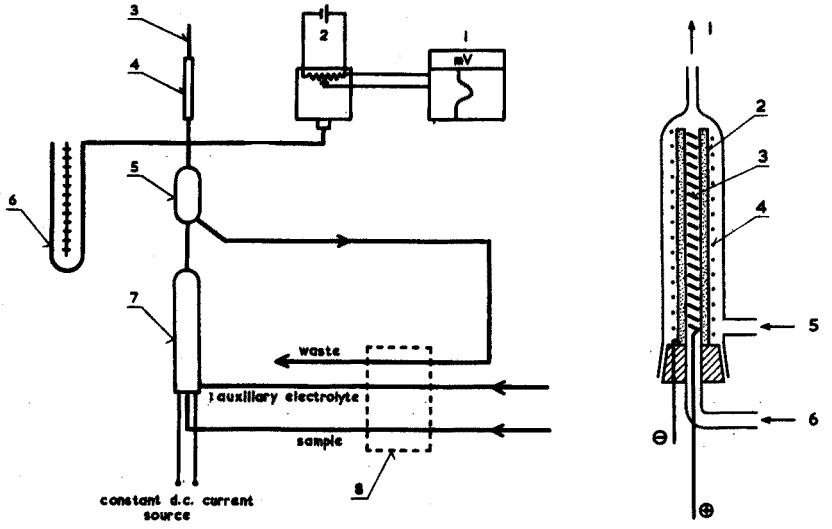

Fig. 2. Block diagram of apparatus for automated pneumatic voltammetry. See text for details.

Fig. 3. Construction of the flow-through electrolysis cell. See text for details.

The detailed construction of the electrolytic cell is shown in Fig. 3; other configurations were also used but the one shown proved most satisfactory. In this design, gas and electrolyte volumes are minimized and the whole cell is flushed rapidly; the solution *iR* drop is small and the anode–cathode separation is good. The working electrode(3) is disposed centrally inside the tubular porous PVC separator(2). Mass transfer of electroactive material to the electrode surface is enhanced by gas–liquid turbulence and liquid flow within the cell; further mixing or stirring is unnecessary. The simultaneous purging of the reference compartment by the electrolyte feed(5) prevents undesirable back-reactions of species in the working electrode compartment. The counter electrode material(4) can be chosen to suit the nature of the complementary electrode process: a platinum wire spiral or mesh is generally satisfactory. The working electrode(3), which may be an anode or a cathode, is preferably made of a material on which the gas evolution overpotential is large: lead, lead/lead dioxide, surface-amalgamated metals and the noble metals have proved satisfactory.

In this design, the hydrogen, which is produced at a constant rate, is mixed with oxygen, which is evolved at a rate depending on the amount of oxidizable species present in solution. The actual magnitude of pressure changes corresponding

to changes of depolarizer concentration is, therefore, attenuated according to the ratio of the rates of total gas evolution. However, the simplicity of the cell construction, which is capable of maintaining an equal gas pressure in both cell compartments, more than compensates for this disadvantage. Moreover, the very sensitive pressure transducer used was capable of measuring pressure changes beyond the sensitivity required here. The transducer effectively measured the pressure drop across the flow-restricting capillary, which was suitable for overpressures of about 0.1 atm. Active carbon and/or silica gel filters were interposed across the capillary to prevent blocking by dust particles or moisture. It was essential to maintain a laminar gas flow in the capillary, over the entire range of gas pressures used, in order to preserve linear pressure/flow-rate characteristics. Thus, the capillary bore must be uniform and the length must be at least 100 times its diameter. It is not permissible, therefore, to introduce a constriction into the capillary (*e.g.* by melting, pulling, etc.), because the flow-rate (q) would then be exponentially related to the pressure drop: $q = \Delta p^x$, where $x = 0.5$–1.0. For simplicity the gas tubes were not thermostatted; they were, however, lagged to protect them from draughts and sudden temperature changes. The constant current for electrolysis (about 200 mA) was derived from a Tesla BS452, 400 V stabilized power supply in series with standard resistances. Addition of a silicone anti-foaming agent to the supporting electrolyte (typically K_2SO_4, H_2SO_4, NaOH, etc.), prevented frothing and facilitated good gas–liquid partition.

This apparatus has been used for automated continuous determinations of industrially important species; details of these, as well as a self-calibrating device will be described elsewhere[2]. The equipment is particularly suitable for pollution control and monitoring, including river water analysis, for on-stream process control and C.O.D. estimations. Modifications to reduce the cell "dead volume" and the small, short-term pressure fluctuations are in progress.

We thank Computer Controls Ltd., London for their kind loan of the pressure transducer and the Czechoslovak Federal Ministry for Technology and Invention for arranging study-leave facilities at the J. Heyrovsky Institute for one of us (D.G.L.).

REFERENCES

1 J. Tenygl, *Collect. Czech. Chem. Commun.*, 33 (1968) 4141.
2 J. Tenygl, to be published.

Analytica Chimica Acta, 70 (1974) 489

ANNOUNCEMENTS

Fifth International Conference on Atomic Spectroscopy

At the Fourth International Conference, which was held at Toronto from 29th October to 2nd November 1973, it was decided that the Fifth Conference in this series will be held at Monash University near Melbourne, Australia, on 25th–29th August 1975. The Conference will be sponsored by the Australian Academy of Science, and, like other Conferences in the series, will be particularly concerned with the applications of atomic spectroscopy to spectrochemical analysis. Further details may be obtained from: Dr. J. B. Willis, Secretary, 5th International Conference on Atomic Spectroscopy, CSIRO Division of Chemical Physics, P.O. Box 160, Clayton, Victoria 3168, Australia.

Calendar of events of Gesellschaft Deutscher Chemiker, September–November 1974

8th–13th September	EUCHEM Conference on "Molten Salts" in Freising near Munich
9th, 10th September	Solid State Chemistry Division, meeting on "Basis of Epitaxy" in Bad Neuenahr
17th September	Chemistry day of GDCh on the occasion of 108th meeting of Gesellschaft Deutscher Naturforscher und Arzte in Berlin
18th–20th September	Food and Forensic Chemistry Division, German Food Chemistry Day in Wiesbaden
Between 18th–20th September	Independent Chemists Division, meeting on the occasion of German Food Chemistry Day in Wiesbaden
23rd–27th September	2nd International Symposium on the Chemistry of Nonbenzenoid Aromatic Compounds, in Lindau (Lake Constance)
2nd half of September	Chemical Education on the Secondary Level Division, symposium
10th, 11th October	Applied Electrochemistry Division, symposium on "Chloride electrolysis" in Leverkusen
24th, 25th October	Detergent Chemistry Division, inaugural meeting in Erlangen-Nürnberg
21st, 22nd November	Photochemistry Division, symposium in Konstanz (Lake Constance)

Details of the meetings listed above may be obtained from Gesellschaft Deutscher Chemiker, D-6000 Frankfurt (M), Federal Republic of Germany, Postfach 90 04 40.

AUTHOR INDEX

ANALYTICA CHIMICA ACTA, VOL. 70 (1974)

SUBJECT INDEX